

VOL. 449 NO. 1 SEPTEMBER 30, 1988

JOURNAL OF

## CHROMATOGRAPHY

INTERNATIONAL JOURNAL ON CHROMATOGRAPHY, ELECTROPHORESIS AND RELATED METHODS

EDITOR, Michael Lederer (Switzerland)

ASSOCIATE EDITORS, R. W. Frei (Amsterdam), R. W. Giese  
Boston, MA), J. K. Haken (Kensington, N.S.W.),

K. Macek (Prague), L. R. Snyder (Orinda, CA)

EDITOR, SYMPOSIUM VOLUMES, E. Heftmann (Orinda, CA)

## EDITORIAL BOARD

W. A. Aue (Halifax)  
 V. G. Berezkin (Moscow)  
 V. Betina (Bratislava)  
 A. Bevenue (Belmont, CA)  
 P. Boček (Brno)  
 P. Boulanger (Lille)  
 A. A. Boulton (Saskatoon)  
 G. P. Cartoni (Rome)  
 S. Dilli (Kensington, N.S.W.)  
 L. Fishbein (Washington, DC)  
 A. Frigerio (Milan)  
 C. W. Gehrke (Columbia, MO)  
 E. Gil-Av (Rehovot)  
 G. Guiochon (Knoxville, TN)  
 I. M. Hais (Hradec Králové)  
 S. Hjertén (Uppsala)  
 E. C. Horning (Houston, TX)  
 Cs. Horváth (New Haven, CT)  
 J. F. K. Huber (Vienna)  
 A. T. James (Harrold)  
 J. Janák (Brno)  
 E. sz. Kováts (Lausanne)  
 K. A. Kraus (Oak Ridge, TN)  
 E. Lederer (Gif-sur-Yvette)  
 A. Liberti (Rome)  
 H. M. McNair (Blacksburg, VA)  
 Y. Marcus (Jerusalem)  
 G. B. Marini-Bettolo (Rome)  
 A. J. P. Martin (Cambridge)  
 Č. Michalec (Prague)  
 R. Neher (Basel)  
 G. Nickless (Bristol)  
 N. A. Parris (Wilmington, DE)  
 R. L. Patience (Sunbury-on-Thames)  
 P. G. Righetti (Milan)  
 O. Samuelson (Göteborg)  
 R. Schwarzenbach (Dübendorf)  
 A. Zlatkis (Houston, TX)

## EDITORS, BIBLIOGRAPHY SECTION

Z. Deyl (Prague), J. Janák (Brno), V. Schwarz (Prague), K. Macek (Prague)

ELSEVIER

**Scope.** The *Journal of Chromatography* publishes papers on all aspects of chromatography, electrophoresis and related methods. Contributions consist mainly of research papers dealing with chromatographic theory, instrumental development and their applications. The section *Biomedical Applications*, which is under separate editorship, deals with the following aspects: developments in and applications of chromatographic and electrophoretic techniques related to clinical diagnosis or alterations during medical treatment; screening and profiling of body fluids or tissues with special reference to metabolic disorders; results from basic medical research with direct consequences in clinical practice; drug level monitoring and pharmacokinetic studies; clinical toxicology; analytical studies in occupational medicine.

**Submission of Papers.** Papers in English, French and German may be submitted, in three copies. Manuscripts should be submitted to: The Editor of *Journal of Chromatography*, P.O. Box 681, 1000 AR Amsterdam, The Netherlands, or to: The Editor of *Journal of Chromatography, Biomedical Applications*, P.O. Box 681, 1000 AR Amsterdam, The Netherlands. Review articles are invited or proposed by letter to the Editors. An outline of the proposed review should first be forwarded to the Editors for preliminary discussion prior to preparation. Submission of an article is understood to imply that the article is original and unpublished and is not being considered for publication elsewhere. For copyright regulations, see below.

**Subscription Orders.** Subscription orders should be sent to: Elsevier Science Publishers B.V., P.O. Box 211, 1000 AE Amsterdam, The Netherlands, Tel. 5803 911, Telex 18582 ESPA NL. The *Journal of Chromatography* and the *Biomedical Applications* section can be subscribed to separately.

**Publication.** The *Journal of Chromatography* (incl. *Biomedical Applications* and *Cumulative Author and Subject Indexes*, Vols. 401–450) has 37 volumes in 1988. The subscription prices for 1988 are:

*J. Chromatogr.* (incl. *Cum. Indexes*, Vols. 401–450) + *Biomed. Appl.* (Vols. 424–460):

Dfl. 6290.00 plus Dfl. 962.00 (p.p.h.) (total ca. US\$ 3537.50)

*J. Chromatogr.* (incl. *Cum. Indexes*, Vols. 401–450) only (Vols. 435–460):

Dfl. 5070.00 plus Dfl. 676.00 (p.p.h.) (total ca. US\$ 2803.00)

*Biomed. Appl.* only (Vols. 424–434):

Dfl. 2145.00 plus Dfl. 286.00 (p.p.h.) (total ca. US\$ 1185.75).

Our p.p.h. (postage, package and handling) charge includes surface delivery of all issues, except to subscribers in Argentina, Australia, Brasil, Canada, China, Hong Kong, India, Israel, Malaysia, Mexico, New Zealand, Pakistan, Singapore, South Africa, South Korea, Taiwan, Thailand and the U.S.A. who receive all issues by air delivery (S.A.L. — Surface Air Lifted) at no extra cost. For Japan, air delivery requires 50% additional charge; for all other countries airmail and S.A.L. charges are available upon request. Back volumes of the *Journal of Chromatography* (Vols. 1 through 423) are available at Dfl. 230.00 (plus postage). Claims for missing issues will be honoured, free of charge, within three months after publication of the issue. Customers in the U.S.A. and Canada wishing information on this and other Elsevier journals, please contact Journal Information Center, Elsevier Science Publishing Co. Inc., 52 Vanderbilt Avenue, New York, NY 10017. Tel. (212) 916-1250.

**Abstracts/Contents Lists** published in Analytical Abstracts, ASCA, Biochemical Abstracts, Biological Abstracts, Chemical Abstracts, Chemical Titles, Chromatography Abstracts, Current Contents/Physical, Chemical & Earth Sciences, Current Contents/Life Sciences, Deep-Sea Research/Part B: Oceanographic Literature Review, Excerpta Medica, Index Medicus, Mass Spectrometry Bulletin, PASCAL-CNRS, Referativnyi Zhurnal and Science Citation Index.

**See inside back cover** for Publication Schedule, Information for Authors and information on Advertisements.

All rights reserved. No part of this publication may be reproduced, stored in a retrieval system or transmitted in any form or by any means, electronic, mechanical, photocopying, recording or otherwise, without the prior written permission of the publisher, Elsevier Science Publishers B.V., P.O. Box 330, 1000 AH Amsterdam, The Netherlands.

Upon acceptance of an article by the journal, the author(s) will be asked to transfer copyright of the article to the publisher. The transfer will ensure the widest possible dissemination of information.

Submission of an article for publication entails the authors' irrevocable and exclusive authorization of the publisher to collect any sums or considerations for copying or reproduction payable by third parties (as mentioned in article 17 paragraph 2 of the Dutch Copyright Act of 1912 and the Royal Decree of June 20, 1974 (S. 351) pursuant to article 16 b of the Dutch Copyright Act of 1912) and/or to act in or out of Court in connection therewith.

**Special regulations for readers in the U.S.A.** This journal has been registered with the Copyright Clearance Center, Inc. Consent is given for copying of articles for personal or internal use, or for the personal use of specific clients. This consent is given on the condition that the copier pays through the Center the per-copy fee stated in the code on the first page of each article for copying beyond that permitted by Sections 107 or 108 of the U.S. Copyright Law. The appropriate fee should be forwarded with a copy of the first page of the article to the Copyright Clearance Center, Inc., 27 Congress Street, Salem, MA 01970, U.S.A. If no code appears in an article, the author has not given broad consent to copy and permission to copy must be obtained directly from the author. All articles published prior to 1980 may be copied for a per-copy fee of US\$ 2.25, also payable through the Center. This consent does not extend to other kinds of copying, such as for general distribution, resale, advertising and promotion purposes, or for creating new collective works. Special written permission must be obtained from the publisher for such copying.

No responsibility is assumed by the Publisher for any injury and/or damage to persons or property as a matter of products liability, negligence or otherwise, or from any use or operation of any methods, products, instructions or ideas contained in the materials herein. Because of rapid advances in the medical sciences, the Publisher recommends that independent verification of diagnoses and drug dosages should be made.

Although all advertising material is expected to conform to ethical (medical) standards, inclusion in this publication does not constitute a guarantee or endorsement of the quality or value of such product or of the claims made of it by its manufacturer.

## CONTENTS

(Abstracts/Contents Lists published in *Analytical Abstracts*, *ASCA*, *Biochemical Abstracts*, *Biological Abstracts*, *Chemical Abstracts*, *Chemical Titles*, *Chromatography Abstracts*, *Current Contents/Physical, Chemical & Earth Sciences*, *Current Contents/Life Sciences*, *Deep Sea Research/Part B: Oceanographic Literature Review*, *Excerpta Medica*, *Index Medicus*, *Mass Spectrometry Bulletin*, *PASCAL-CNRS*, *Referativnyi Zhurnal* and *Science Citation Index*)

Influence of silica surface chemistry and structure on the properties, structure and coverage of alkyl-bonded phases for high-performance liquid chromatography (Review) by J. Nawrocki (Poznań, Poland) and B. Buszewski (Lublin, Poland) (Received April 18th, 1988)	1
Prediction of band profiles in displacement chromatography by numerical integration of a semi-ideal model by A. M. Katti and G. A. Guiochon (Knoxville and Oak Ridge, TN, U.S.A.) (Received May 26th, 1988)	25
Experimental affirmation of the statistical model of overlap by J. M. Davis (Carbondale, IL, U.S.A.) (Received May 23rd, 1988)	41
Split peaks in non-linear chromatography and their effect on sample throughput in large scale separations by J. L. Wade and P. W. Carr (Minneapolis, MN, U.S.A.) (Received April 15th, 1988)	53
Absolute peak broadening calibration in size-exclusion chromatography using a polymer-bound chromophore by T. Q. Nguyen and H.-H. Kausch (Lausanne, Switzerland) (Received March 21st, 1988)	63
Solvent selectivity in the resolution of some regioisomeric and diastereomeric prostaglandin intermediates on silica by M. Lõhmus, I. Kirjanen, M. Lopp and Ü. Lille (Tallinn, U.S.S.R.) (Received May 19th, 1988)	77
Group contributions to hydrophobicity and elution behaviour of pyridine derivatives in reversed-phase high-performance liquid chromatography by F. Gago, J. Alvarez-Builla and J. Elguero (Madrid, Spain) (Received May 23rd, 1988)	95
Role of the alkyl chain length of the ion interaction reagent, flow-rate, column packing and detection in ion interaction reversed-phase high-performance liquid chromatography in separations of anions using amine salicylates by M. C. Gennaro (Torino, Italy) (Received May 24th, 1988)	103
Influence of bonding chemistry on the reordering/resolution of silica immobilized alkyl chains by S. S. Yang and R. K. Gilpin (Kent, OH, U.S.A.) (Received June 9th, 1988)	115
Separation of carotenol fatty acid esters by high-performance liquid chromatography by F. Khachik and G. R. Beecher (Beltsville, MD, U.S.A.) (Received May 4th, 1988)	119
Cross-axis synchronous flow-through coil planet centrifuge for large-scale preparative counter-current chromatography. I. Apparatus and studies on stationary phase retention in short coils by Y. Ito and T.-Y. Zhang (Bethesda, MD, U.S.A.) (Received May 26th, 1988)	135
Cross-axis synchronous flow-through coil planet centrifuge for large-scale preparative counter-current chromatography. II. Studies on partition efficiency in short coils and preparative separations with multilayer coils by Y. Ito and T.-Y. Zhang (Bethesda, MD, U.S.A.) (Received May 26th, 1988)	153
Solvent extraction clean-up for pre-treatment in amino acid analysis by gas chromatography. Application to age estimation from the D/L ratio of aspartic acid in human dentine by I. Abe, H. Tsujioka and T. Wasa (Osaka, Japan) (Received May 19th, 1988)	165

(Continued overleaf)

*Contents (continued)*

Modified method for analysis of C <sub>2</sub> -C <sub>5</sub> hydrocarbons in an aromatic-alkane matrix using an automated thermal desorber by A. Bianchi and H. A. Cook (Southampton, U.K.) (Received May 11th, 1988)	175
Gas chromatographic separation and chemometric analysis of mandarin essential oils by A. Cotroneo, G. Dugo (Messina, Italy), L. Favretto and L. Gabrielli Favretto (Trieste, Italy) (Received May 23rd, 1988)	183
Perfluorinated acids as ion-pairing agents in the determination of monoamine transmitters and some prominent metabolites in rat brain by high-performance liquid chromatography with amperometric detection by M. Patthy and R. Gyenge (Budapest, Hungary) (Received May 24th, 1988)	191
Optimizing copper-bicinchoninate carbohydrate detection for use with water-elution high-performance liquid chromatography: a technique to measure the major mono- and oligosaccharides in small pieces of wheat endosperm by T. D. Ugalde, J. P. M. Faber and C. F. Jenner (Glen Osmond, Australia) (Received May 16th, 1988)	207
High-performance liquid chromatographic determination of glucosides (glucose conjugates) with post-column reaction detection combining immobilized enzyme reactors and luminol chemiluminescence by P. J. Koerner, Jr. and T. A. Nieman (Urbana, IL, U.S.A.) (Received April 11th, 1988)	217
Preparative chromatography of oligogalacturonic acids by L. W. Doner, P. L. Irwin and M. J. Kurantz (Philadelphia, PA, U.S.A.) (Received May 11th, 1988)	229
Comparison of high-performance liquid chromatographic and atomic spectrometric methods for the determination of Fe(III) and Al(III) in soil and clay samples by M. Meaney, M. Connor, C. Breen and M. R. Smyth (Dublin, Ireland) (Received May 17th, 1988)	241
Determination of polycyclic aromatic compounds in fish tissue by D. A. Birkholz, R. T. Coutts and S. E. Hrudey (Edmonton, Canada) (Received May 20th, 1988)	251
Detection of trace levels of thiodiglycol in blood, plasma and urine using gas chromatography-electron-capture negative-ion chemical ionisation mass spectrometry by R. M. Black and R. W. Read (Salisbury, U.K.) (Received May 23rd, 1988)	261
* Determination of native folates in milk and other dairy products by high-performance liquid chromatography by D. L. Holt, R. L. Wehling and M. G. Zeece (Lincoln, NE, U.S.A.) (Received May 16th, 1988)	271
Detection and determination of common benzodiazepines and their metabolites in blood samples of forensic science interest. Microcolumn cleanup and high-performance liquid chromatography with reductive electrochemical detection at a pendent mercury drop electrode by J. B. F. Lloyd and D. A. Parry (Birmingham, U.K.) (Received May 16th, 1988)	281
Isotachopheresis of quaternary 4,4'-bipyridylium salts. Analytical control of synthesis and purification procedures by P. Stehle, P. Fürst, R. Ratz and H. Rau (Stuttgart, F.R.G.) (Received May 19th, 1988)	299
<i>Notes</i>	
Extraction chromatography of alkanethiols by Z. H. Kudzin and W. Kopycki (Łódź, Poland) (Received May 24th, 1988)	306
Characterisation of volatile oil constituents with relatively long gas chromatographic retention times on two stationary phases by T. J. Betts (Perth, Australia) (Received June 20th, 1988)	312

Analysis of tioconazole using high-performance liquid chromatography with a porous graphitic column by J. C. Berridge (Sandwich, U.K.) (Received June 7th, 1988) . . . . .	317
Difference in cell surface hydrophobicity of <i>Halobacterium salinarium</i> strains by J. L. Ochoa and F. Ascencio-Valle (La Paz, México) (Received June 1st, 1988) . . . . .	322
Comparison of volatile halogenated compounds formed in the chloramination and chlorination of humic acid by gas chromatography-electron-capture detection by M. P. Italia and P. C. Uden (Amherst, MA, U.S.A.) (Received May 24th, 1988) . . . . .	326
Detection of ligand-protein binding by direct electrophoresis of the complex by S. Nobile and J. Deshusses (Geneva, Switzerland) (Received June 6th, 1988) . . . . .	331
Validity of <i>post mortem</i> chest cavity blood ethanol determinations by R. D. Budd (Los Angeles, CA, U.S.A.) (Received June 28th, 1988) . . . . .	337
High-performance liquid chromatographic determination of loperamide hydrochloride in pharmaceutical preparations by C. P. Leung and C. Y. Au-Yeung (Hong Kong) (Received June 6th, 1988) . . . . .	341
<i>Letter to the Editor</i>	
Use of the term "detergent" in biochemistry by P. Lundahl and E. Mascher (Uppsala, Sweden) (Received June 7th, 1988) . . . . .	345
<i>Book Reviews</i>	
Chromatography — concepts and contrasts (by J. M. Miller) . . . . .	346
Ion-exchange chromatography of proteins (Chromatographic Science Series, Vol. 43) (by S. Yamamoto, K. Nakanishi and R. Matsuno) . . . . .	347

\*\*\*\*\*  
\*  
\* In articles with more than one author, the name of the author to whom correspondence should be addressed is indicated in the  
\* article heading by a 6-pointed asterisk (\*)  
\*  
\*\*\*\*\*



JOURNAL OF CHROMATOGRAPHY

VOL. 449 (1988)



# JOURNAL *of* CHROMATOGRAPHY

INTERNATIONAL JOURNAL ON CHROMATOGRAPHY,  
ELECTROPHORESIS AND RELATED METHODS

EDITOR

MICHAEL LEDERER (Switzerland)

ASSOCIATE EDITORS

R. W. FREI (Amsterdam), R. W. GIESE (Boston, MA), J. K. HAKEN (Kensington,  
N.S.W.), K. MACEK (Prague), L. R. SNYDER (Orinda, CA)

EDITORIAL BOARD

W. A. Aue (Halifax), V. G. Berezkin (Moscow), V. Betina (Bratislava), A. Bevenue (Belmont, CA), P. Boček (Brno), P. Boulanger (Lille), A. A. Boulton (Saskatoon), G. P. Cartoni (Rome), S. Dilli (Kensington, N.S.W.), L. Fishbein (Washington, DC), A. Frigerio (Milan), C. W. Gehrke (Columbia, MO), E. Gil-Av (Rehovot), G. Guiochon (Knoxville, TN), I. M. Hais (Hradec Králové), S. Hjertén (Uppsala), E. C. Horning (Houston, TX), Cs. Horváth (New Haven, CT), J. F. K. Huber (Vienna), A. T. James (Harrold), J. Janák (Brno), E. sz. Kováts (Lausanne), K. A. Kraus (Oak Ridge, TN), E. Lederer (Gif-sur-Yvette), A. Liberti (Rome), H. M. McNair (Blacksburg, VA), Y. Marcus (Jerusalem), G. B. Marini-Bettolo (Rome), A. J. P. Martin (Cambridge), Č. Michalec (Prague), R. Neher (Basel), G. Nickless (Bristol), N. A. Parris (Wilmington, DE), R. L. Patience (Sunbury-on-Thames), P. G. Righetti (Milan), O. Samuelson (Göteborg), R. Schwarzenbach (Dübendorf), A. Zlatkis (Houston, TX)

EDITORS, BIBLIOGRAPHY SECTION

Z. Deyl (Prague), J. Janák (Brno), V. Schwarz (Prague), K. Macek (Prague)



ELSEVIER

AMSTERDAM — OXFORD — NEW YORK — TOKYO

---

*J. Chromatogr.*, Vol. 449 (1988)

All rights reserved. No part of this publication may be reproduced, stored in a retrieval system or transmitted in any form or by any means, electronic, mechanical, photocopying, recording or otherwise, without the prior written permission of the publisher, Elsevier Science Publishers B.V., P.O. Box 330, 1000 AH Amsterdam, The Netherlands.

Upon acceptance of an article by the journal, the author(s) will be asked to transfer copyright of the article to the publisher. The transfer will ensure the widest possible dissemination of information.

Submission of an article for publication entails the authors' irrevocable and exclusive authorization of the publisher to collect any sums or considerations for copying or reproduction payable by third parties (as mentioned in article 17 paragraph 2 of the Dutch Copyright Act of 1912 and the Royal Decree of June 20, 1974 (S. 351) pursuant to article 16 b of the Dutch Copyright Act of 1912) and/or to act in or out of Court in connection therewith. **Special regulations for readers in the U.S.A.** This journal has been registered with the Copyright Clearance Center, Inc. Consent is given for copying of articles for personal or internal use, or for the personal use of specific clients. This consent is given on the condition that the copier pays through the Center the per-copy fee stated in the code on the first page of each article for copying beyond that permitted by Sections 107 or 108 of the U.S. Copyright Law. The appropriate fee should be forwarded with a copy of the first page of the article to the Copyright Clearance Center, Inc., 27 Congress Street, Salem, MA 01970, U.S.A. If no code appears in an article, the author has not given broad consent to copy and permission to copy must be obtained directly from the author. All articles published prior to 1980 may be copied for a per-copy fee of US\$ 2.25, also payable through the Center. This consent does not extend to other kinds of copying, such as for general distribution, resale, advertising and promotion purposes, or for creating new collective works. Special written permission must be obtained from the publisher for such copying.

No responsibility is assumed by the Publisher for any injury and/or damage to persons or property as a matter of products liability, negligence or otherwise, or from any use or operation of any methods, products, instructions or ideas contained in the materials herein. Because of rapid advances in the medical sciences, the Publisher recommends that independent verification of diagnoses and drug dosages should be made.

Although all advertising material is expected to conform to ethical (medical) standards, inclusion in this publication does not constitute a guarantee or endorsement of the quality or value of such product or of the claims made of it by its manufacturer.

CHROM. 20 611

## REVIEW

# INFLUENCE OF SILICA SURFACE CHEMISTRY AND STRUCTURE ON THE PROPERTIES, STRUCTURE AND COVERAGE OF ALKYL-BONDED PHASES FOR HIGH-PERFORMANCE LIQUID CHROMATOGRAPHY

JACEK NAWROCKI\*

*Faculty of Chemistry, Adam Mickiewicz University, Grunwaldzka 6, 60-780 Poznań (Poland)*  
and

BOGUSŁAW BUSZEWSKI

*Institute of Chemistry, M. Curie-Skłodowska University, 20-031 Lublin (Poland)*

(Received April 18th, 1988)

## CONTENTS

1. Introduction . . . . .	1
2. Chemical and physical properties of the silica surface . . . . .	2
2.1. Physical criteria of silica gel for chromatography . . . . .	2
2.2. Silanols as adsorption centres . . . . .	2
2.3. Apparent pH of silica surface, reactivity of silica silanols . . . . .	3
2.4. Trace amounts of metals and their influence on the properties of silica . . . . .	5
2.5. Heterogeneity of the silica surface . . . . .	6
2.6. Small populations of highly retentive silanols and their influence on retention data and properties of chromatographic columns . . . . .	8
2.7. Conclusions . . . . .	10
3. Chemically bonded phases for high-performance liquid chromatography . . . . .	11
3.1. Physical and chemical requirements for silica . . . . .	12
3.2. Dense coverage packings . . . . .	15
3.3. Models of bonded phase structure . . . . .	17
3.4. Residual silanols and their influence on retention . . . . .	19
4. Conclusions . . . . .	20
5. Summary . . . . .	21
References . . . . .	21

## 1. INTRODUCTION

The vast variety of commercially available bonded alkyl phases from various manufacturers is often blamed for the irreproducibility of chromatographic results. This happens when one compares, *e.g.*, C<sub>18</sub> bonded phases from various manufacturers and also various batches from the same manufacturer. Various methods for the preparation of the phases are used, various end-capping reactions are applied and various functionalities of the modifiers are introduced, which gives as a result a whole variety of “the same” phases. In this paper, we emphasize that the silica gel which is used in many methods can be a source of many differences among bonded phase materials. It has been generally assumed that silicas with the same physical characteristics such as surface area, pore radii and volume should be chemically the same, but this is not necessarily true.

## 2. CHEMICAL AND PHYSICAL PROPERTIES OF THE SILICA SURFACE

Silica is undoubtedly the most frequently used material in chromatography. It is utilized as an adsorbent in both gas and high-performance liquid chromatography (HPLC). The surfaces of modern fused-silica capillary columns have the same chemical nature and in reversed-phase (RP) HPLC silica is the basic material for synthesis of the packings. Silica seems to be one of the best known inorganic, polymeric materials<sup>1-3</sup>. Despite this new papers devoted to the chemistry of silica surfaces are still being published and new analytical techniques permit unknown structures, behaviours and reactions to be revealed.

### 2.1. *Physical criteria of silica gel for chromatography*

The parameters used most often to characterize silica are specific surface area, mean pore diameter, specific pore volume and mean particle size. Although those properties seem to be the most important with the current state of the art, they appear to be inadequate and it is postulated that other important features such as trace metal content<sup>4</sup> and surface pH<sup>5</sup> should be included to characterize the material satisfactorily. It is beyond the scope of this paper to discuss in detail the importance of specific surface area, pore diameter and volume; the comprehensive book by Unger<sup>2</sup> is recommended. A review by Majors<sup>6</sup> is a source of data for commercial silicas.

Another feature of silica is the average wall thickness. Verzele *et al.*<sup>4</sup> calculated the wall thickness for 250–400 m<sup>2</sup>/g silica as about 1–2 nm. They took a value of 1.9 g/cm<sup>3</sup> for the specific gravity of silica from papers by Berendsen and De Galan<sup>7</sup> and Strubert<sup>8</sup>; however, Unger<sup>2</sup> reported the specific gravity to be 2.2 g/cm<sup>3</sup>. The latter value would obviously increase the average wall thickness to about 2.2 nm for 450 m<sup>2</sup>/g silica. Hence we can say in general that the average silica wall consists of about 2–4 Si atoms. This illustrates the importance of trace metals in the silica network, as each metal atom can be located on the surface or just under the surface. In the latter instance such an atom has to interact with a surface silicon atom, which obviously would affect the surface properties of the silica. The influence of the trace metal activity on the properties of silica will be discussed below.

### 2.2. *Silanols as adsorption centres*

The surface of silica consists of various kinds of silanols and siloxane bonds. The silanols are considered as strong adsorption sites<sup>9</sup> and can easily be hydrated by adsorbing water molecules. Siloxane sites are usually considered as hydrophobic<sup>2</sup>. Silanols can exist on the surface in single, geminal or vicinal forms. A pair of vicinal silanols can form a so-called bonded pair, which was considered by Snyder<sup>10</sup> and Snyder and Ward<sup>11</sup> to be a “reactive” silanol. Miller *et al.*<sup>12</sup> postulated that geminal silanols can also form “reactive” centres. A variety of physical and chemical methods can be used to determine the surface concentration of silanols<sup>2</sup>. It is generally agreed that a fully hydroxylated surface contains about 8 μmol/m<sup>2</sup> of OH groups<sup>2,13-15</sup>.

The existence of various forms of silanols on a silica surface is generally accepted, but there is a tacit assumption that all silanols interact or react with the same strength. Only rarely one can find in the literature a differentiation between silanols. It is an essential question for chromatographers whether various silanols interact (react) similarly or not. Snyder<sup>10</sup> assumed that silanols should have various “retention

activities". However, Snyder and Poppe<sup>14</sup> neglected the interactions of other than single silanols, pointing out that single silanols comprise about 90% of the whole silanol population. Snyder and Ward<sup>11</sup> estimated "chromatographic-grade silica" to contain about 70% of all silanols in "reactive" form, whereas only 1% of hydroxyl groups would form "reactive" sites on a pyrogenic silica surface. In contrast to the "reactive" nature of the site as postulated by Snyder and Ward<sup>11</sup>, Hair and Hertl<sup>9</sup> considered bonded vicinal silanols to be capable of adsorbing water only, whereas free silanols were suggested to be the main adsorption or reaction sites, in agreement with earlier studies by Kiselev and co-workers<sup>16,17</sup>. Clark-Monks and Ellis<sup>18</sup> determined that about 10% of pyrogenic silica silanols can form "reactive" sites.

The silica surface can also bear very unusual adsorption sites, sometimes with a very high adsorption strength. Such sites were described in a series of papers by Low *et al.*<sup>19</sup>. Specially prepared silica contained about  $0.28 \mu\text{mol}/\text{m}^2$  (ref. 20) of strong adsorption sites capable of dissociative adsorption of hydrocarbons.

Another strange property of the silica surface was found by Krasilnikov *et al.*<sup>21</sup>. They described the ability of the dehydroxylated silica surface to adsorb oxygen molecules. The surface concentration of the sites was determined to be  $0.0001 \mu\text{mol}/\text{m}^2$  (ref. 21).

### 2.3. Apparent pH of silica surface, reactivity of silica silanols

Commercially available silicas for chromatographic purposes have properties that differ greatly from idealized or theoretically predicted properties. Theoretically, silica should have  $\text{p}K_a = 7.1 \pm 0.5$  (refs. 22 and 23). However, the literature values of  $\text{p}K_a$  for silica are 1.5 (ref. 24), 6–8 (ref. 25), 5–7 (ref. 26), 9.5 (ref. 27) and 10 (ref. 28). Surprisingly large differences in the apparent surface pH among silica packings for HPLC were first noted by Engelhardt and Müller<sup>5</sup>. A comparison of the pH values of HPLC silicas is given in Table 1.

The highest pH value was 9.9 for LiChrospher 500 and the lowest 3.9 for Zorbax-SIL<sup>5,29</sup>. It was also shown that the most acidic and the most alkaline pH values were found for spherical silica particles whereas relatively neutral pH values were characteristic of irregular packings<sup>29</sup>. This is probably connected with the methods of manufacture of the silicas<sup>29</sup>. The differences in pH values may be reflected in different chromatographic properties of the silicas<sup>29,30</sup>.

The variety of silica surface chemistry can probably also be reflected in the quality of alkyl-bonded phases for HPLC. Broadly observed ranges of  $\text{p}K_a$  and pH values may imply the existence of silanol groups differing in their acidity. It has been shown that the strength of hydrogen bonds of silanols depend on the acidity of the silanols<sup>22</sup>. One can easily imagine the existence of a broad range of hydrogen-bonded silanols on an amorphous silica surface having a whole variety of bond lengths, which would result in various acidities and reactivities of vicinal hydroxyl groups. The existence of such a broad range of hydrogen-bonded vicinal hydroxyls is shown by a broad and asymmetric IR band with a maximum at  $3640 \text{ cm}^{-1}$  (ref. 9).

Miller *et al.*<sup>12</sup> have shown that the silica surface contains a group of acidic, reactive silanols which are formed mainly by geminal and hydrogen-bonded species, *i.e.*, vicinal hydroxyls. However Bayer *et al.*<sup>34</sup> were not able to confirm the existence of geminal silanols by means of  $^{29}\text{Si}$  cross-polarization-magic angle spinning (CP-MAS) NMR spectroscopy. A higher reactivity of geminal silanols was also reported by

TABLE I

APPARENT SURFACE pH OF SELECTED SILICAS FOR HPLC

Silica		Reference				
		5, 29	30	31	32	33
LiChrosorb	Si 60	7.8/8.1*	7.4	7.2		7.12
	Si 100	7.0	7.5	6.7		6.9
LiChrospher	Si 100	5.3	5.8	4.6		
	Si 300	5.5	5.9	4.7		
	Si 500	9.9/8.8*	8.3	8.6		
	Si 1000	9.2	8.6	8.1		
Hypersil		9.0/8.1*	8.5			
Nucleosil 100			6.0		5.15	
	100V	5.7	8.7			
Polygosil 60		8.0	7.1	6.5		
Partisil 10		7.5	5.6	4.9		
Spherisorb S5W		9.5	9.0			
Zorbax-SIL		3.9	4.1			
	60			5.6	4.08	
	150			4.8	4.27	
	300			5.4	4.53	
Vydac 90			6.1	4.2		
TP				4.1	5.3	
Separon		4.5				4.5

\* Different batches.

Sindorf and Maciel<sup>35</sup>. Blockage of the acidic, reactive silanols appeared to have unexpectedly great effect on the efficiency of the packing. Marshall *et al.*<sup>36</sup> have shown that the initial partial deactivation of about 5% of the total silanol population before the synthesis of an octadecyl-bonded phase leads to a packing with higher efficiency. In a continuation of that work Marshall and co-workers<sup>37,38</sup> drew a similar conclusion to Miller *et al.*<sup>12</sup>, *i.e.*, that "on a silica surface a chemically distinct population of associated silanols of high reactivity remains". Marshall and co-workers<sup>36-38</sup> suggested that the reactive group of silanols is about 5% of the whole population of silica hydroxyls. All of the above studies<sup>12,35-38</sup> support in some sense the older concept of the "reactive silanols" of Snyder and Ward<sup>11</sup>, which emphasizes a higher reactivity of hydrogen-bonded silanols.

However, Mauss and Engelhardt<sup>39</sup> have shown by Fourier transform IR spectrometry that molecules with basic properties are adsorbed preferentially on acidic, isolated silanols, whereas solutes with hydroxyl groups are able to interact with vicinal hydrogen-bonded silanols and are adsorbed on these sites. Moreover, they found evidence that only isolated silanols react with chlorosilanes. The selectivity of the silica was said to depend on the concentration of surface silanol groups and on the ratio between isolated and vicinal silanols. At about the same time, Köhler and co-workers published two papers<sup>32,40</sup> in which they traced the source of an undesirable adsorption of basis compounds on the silica surface. They concluded that the existence of highly acidic isolated SiOH groups is responsible for the unwanted adsorption of organic bases and also for the low hydrolytic stability of alkyl-bonded

phases made of the silica containing such groups. This concept of a higher reactivity of isolated silanols<sup>32,39,40</sup> supports the earlier conclusions of Kiselev and co-workers<sup>16,17</sup> and those of Hair and Hertl<sup>9</sup>.

Now, it would be interesting to answer two questions: how many deleterious, isolated silanols exist on silica surface?; and what is the chemical reason for the higher acidity of some silanols or why are some silanols more acidic than others?

Marshall *et al.*<sup>36</sup> estimated that about 5% of the total silanol population should be deactivated before the synthesis of alkyl bonded phases in order to obtain a phase with higher efficiency. In light of Köhler *et al.*'s paper<sup>40</sup>, the population can be estimated as a much lower value, as 10 nmol of N,N-diethylaniline (N,N-DEA) were sufficient to deactivate the strongly adsorbing sites in an LC column. It was stated<sup>40</sup> that "NN-DEA is adsorbed on a relatively small concentration of high-energy sites...". This is in agreement with the findings of Nawrocki<sup>41-44</sup>, who used an amine to block the strongest adsorption sites in a gas chromatographic column. It seems that a very low concentration of silanols (about 0.3% of the total population) may be responsible for 20% of the retention of benzene. This value was found for a silylated silica surface<sup>41</sup>, but similar values have been found for bare silica<sup>42</sup> and trimethylsilylated silica surfaces<sup>43</sup>. It has also been shown that these few, deleterious silanols can considerably influence the column efficiency, which supports Marshall and co-workers<sup>36-38</sup> efforts to obtain more efficient LC phases by prior deactivation of the silica surface. In a subsequent study<sup>44</sup>, the concentration of strongly interacting silanols was found to be lower than 0.1  $\mu\text{mol}/\text{m}^2$  for three gas chromatography grade silicas.

There is still no answer to the second question, but the content of trace metals seems a likely reason.

#### 2.4. Trace amounts of metals and their influence on the properties of silica

The various acidities or reactivities of silanols may be caused by the structure of amorphous silica, *e.g.*, by variations in the distances of hydrogen-bonded silanols<sup>9,12</sup>. This, however, could apply if the strongly reactive silanols were hydrogen bonded as in the concept of Snyder and Ward<sup>11</sup>. It is much more difficult to explain the high acidity of single silanols.

Silica gels utilized in chromatography are not pure silicon dioxide. Chromatographic-grade silica usually contains 0.1–0.3% of metal oxides impurities. Verzele *et al.*<sup>45,46</sup> have shown that chromatographic materials may contain a whole variety of metals with Na, Ca, Al, Mg, Ti and Fe as the prevailing impurities. These traces of metals can obviously influence the chromatographic process<sup>47</sup>. One might expect that such low levels of impurities would not contribute substantially to the retention of solutes. However, taking into account the conclusions in earlier studies<sup>12,36-38</sup>, particularly those of Nawrocki<sup>41-44</sup>, even these low concentrations have to be considered. We believe that the properties of relatively pure pyrogenic silicas of the Cab-O-Sil or Aerosil type are attributed too often to chromatographic-grade silicas also (although, *e.g.*, Aerosil from Degussa, Frankfurt, F.R.G., has a guaranteed purity of *ca.* 99.8%<sup>48</sup>, it is not pure silicon dioxide). Such differences were observed by Hendra *et al.*<sup>49</sup>, who reported different behaviours of chromatographic-grade silica and Cab-O-Sil in the adsorption of pyrimidine bases. Similarly, Adams and Giam<sup>50</sup> did not expect localized adsorption of amines on Cab-O-Sil whereas adsorption took

place on chromatographic-grade silica. The difference was explained<sup>50</sup> by the presence of metal oxides in the silica matrix which could generate additional adsorption centres with Brönsted acidity capable of chemisorbing amines<sup>49,50</sup>.

An *ab initio* calculated of silanol model groups has shown that silanols with the highest absolute acidity are those which are associated with a Lewis acid like boron or aluminium atom<sup>51</sup>. A porous glass surface containing considerable amounts of boron was reported<sup>52</sup> to contain two types of acid centre. These centres differed in their  $pK_a$  values, which were 5.1 and 7. The  $pK_a = 7$  centres were identified as silanols whereas the  $pK_a = 5.1$  centres could not be identified as B–OH sites as these should have lower acidity. Magnesium atoms introduced into the silica structure form so-called “structural Lewis sites”, which enhance the acidity of adjacent silanols<sup>53</sup>. Recently Sadek *et al.*<sup>54</sup> described the influence of traces of metals in a silica matrix on the acidity and consequently the hydrogen-bond donating capability of neighbouring silanol groups. They also determined the amount of such strong silanol sites in an HPLC column and, although no surface concentration was given, the values seem to be similar to those published by us<sup>42,43</sup>. The results of Sadek *et al.*<sup>54</sup> confirm our supposition<sup>43</sup> that metal impurities influence the acidity of silanols. According to Sadek *et al.*<sup>54</sup>, silica can contain metals in three forms: surface species, internal and secluded. This can be confirmed by acid washing results<sup>45–47</sup>. According to Verzele and co-workers<sup>45–47</sup>, acid washing can remove only one third to two thirds of metals from the silica.

A number of interesting facts can be found in the literature concerning the adsorption of amines or furan on a silica surface. It has long been known that the heats of adsorption of such compounds are much higher at very low coverages (of the order of  $0.1 \mu\text{mol}/\text{m}^2$ ) than at higher coverages<sup>55–57</sup>. These high values were connected with traces of metals in the silica matrix<sup>56–58</sup>. Traces of aluminium were shown to increase the catalytic activity of silica, although some intrinsic activity of the pure gel was suspected<sup>58</sup>. Hydrocarbons, both saturated (hexane) and unsaturated (benzene), appeared to have much higher heats of adsorption at very low coverages (below  $0.1 \mu\text{mol}/\text{m}^2$ ) than at higher surface concentrations<sup>59</sup>. Similarly, higher heats of adsorption of *n*-hexane and benzene on fume (pyrogenic) and precipitated silicas were found in the low coverage region<sup>60</sup>. Papirer *et al.*<sup>60</sup> also emphasized the difference in the distribution of surface silanol groups on precipitated and fume silicas of identical surface area.

Cusumano and Low<sup>61,62</sup> have shown that the residence time of an adsorbed molecule of benzene calculated from the Frenkel equation at low coverages can approach *ca.* 100 s, which is expected for chemisorption, whereas for higher coverages the residence time decreases to  $10^{-8}$  s, *i.e.*, by ten orders of magnitude. Although this was calculated for the adsorption of benzene on porous glasses, the same must be true for porous silicas as the heats of adsorption of benzene are similar on both adsorbents.

## 2.5. Heterogeneity of the silica surface

Most known surfaces are heterogeneous. Heterogeneity of the surface is, in simple words the ability of some parts of the surface to interact more strongly with adsorbates than do other parts of the surface. The phenomenon of heterogeneity plays an important role in catalysis and chromatography. Acidity or basicity of the surface can be considered as a manifestation of the heterogeneity, as these phenomena are

directly connected with particular centres on the surface. Acidity or basicity can be investigated by both static<sup>63</sup> and dynamic<sup>64,65</sup> methods.

Rudziński and co-workers<sup>66,67</sup> have found five different adsorption centres on the silica surface. These sites were said to represent various silanol and siloxane centres and were ordered in terms of their strength of interaction with hydrocarbons as: reactive > geminal > free > bonded > siloxane. This reminds one of Snyder's<sup>10</sup> classification of the adsorption activity of silanols: reactive > free > bond. Rudziński and co-workers<sup>66,67</sup> found that the strongest adsorption centres on the silica surface comprise 1.5–13% of the total number of centres, depending on the silica gel and the solute chromatographed. It has been suggested<sup>66,67</sup> that a considerable part of hydrocarbon adsorption proceeds on siloxane centres, which cannot be supported by other (spectroscopic) data. Hair and Hertl<sup>9</sup> have shown that the silanols are the adsorption centres, particularly single or free types, while bonded species interact weakly with hydrocarbons. In another study applying the same model of Rudziński and co-workers<sup>66,67</sup>, only three adsorption sites were found on the silica surface, with strengths: reactive > free >  $\text{Si}^{4+}$  (ref. 68). The silica was thermally treated<sup>68</sup>; however, there is no spectroscopic evidence in the literature for adsorption on  $\text{Si}^{4+}$  sites on the silica surface. In another paper<sup>69</sup> from the same university it was stated that Rudziński and co-workers' method can be considered as a kind of approximation and the maxima on the energy curve cannot be ascribed to specific functional groups on the silica surface. The same theoretical model was applied to show how very small amounts of water block the strongest adsorption sites on a kaolinite surface<sup>70</sup>.

An older concept of heterogeneity, which allowed the site energy distribution to be estimated from the experimental adsorption isotherm and an arbitrarily chosen local isotherm function, was used by Sorrell and Rowan<sup>71</sup> to show that modification of silica can hardly remove the highest energy sites from the surface. They also showed<sup>72</sup> that modification of the silica surface increases the efficiency of a chromatographic column.

<sup>29</sup>Si CP-MAS-NMR has been applied to show that the silica surface can be considered to be heterogeneous, *i.e.*, consisting of separate regions resembling the 100 and 111 faces of  $\beta$ -cristobalite<sup>73</sup>.

In the view of Farin and Avnir<sup>74</sup>, the heterogeneity of adsorption sites originates from a homogeneous distribution on a geometrically irregular surface. They suggested that a concave zone increases the number of hydroxyl groups per unit whereas a convex zone decreases this number.

Deactivation was shown to eliminate sites with extremely high activity for an alumina surface<sup>75</sup>. The interactions with the sites were said to be the only mechanism that contributes to the  $c_k$  term in the plate-height equation for GSC capillary columns.

In high-performance adsorption chromatography, the presence of strong adsorption sites on an adsorbent (silica) surface requires the addition of water to the non-polar solvent to deactivate the sites. However, water was found to be inconvenient for such a purpose and organic modifiers were proposed instead<sup>76</sup>. Saunders<sup>76</sup> emphasized that the existence of these strongly adsorbing sites greatly affects the sample capacity. Generally, the chromatographic literature stresses the negative role of heterogeneity. However, it was found theoretically that energetically homogeneous surfaces may exhibit a lower selectivity than heterogeneous adsorbents having the same average adsorption energy in relation to the substances being chromatographed<sup>77</sup>.

### 2.6. Small populations of highly retentive silanols and their influence on retention data and properties of chromatographic columns

There is agreement that the strongest adsorption sites constitute only a small part of the total number of sites on the silica surface<sup>36,40,66,67</sup>. This was fully confirmed by a recently developed method for the determination of the concentration of the strongest adsorption sites<sup>41-44</sup>. First, it was noted that on relatively poorly deactivated silica surfaces a very small amount of amine blocking the adsorption sites drastically reduces the retention of benzene<sup>41</sup>. The method was developed further and its usefulness for the evaluation of the distribution of the strength of retention sites on bare silica surfaces was demonstrated<sup>42</sup>.

The principle of the method is very simple and is illustrated in Fig. 1. Although the experiments were carried out by means of gas chromatography, the method is

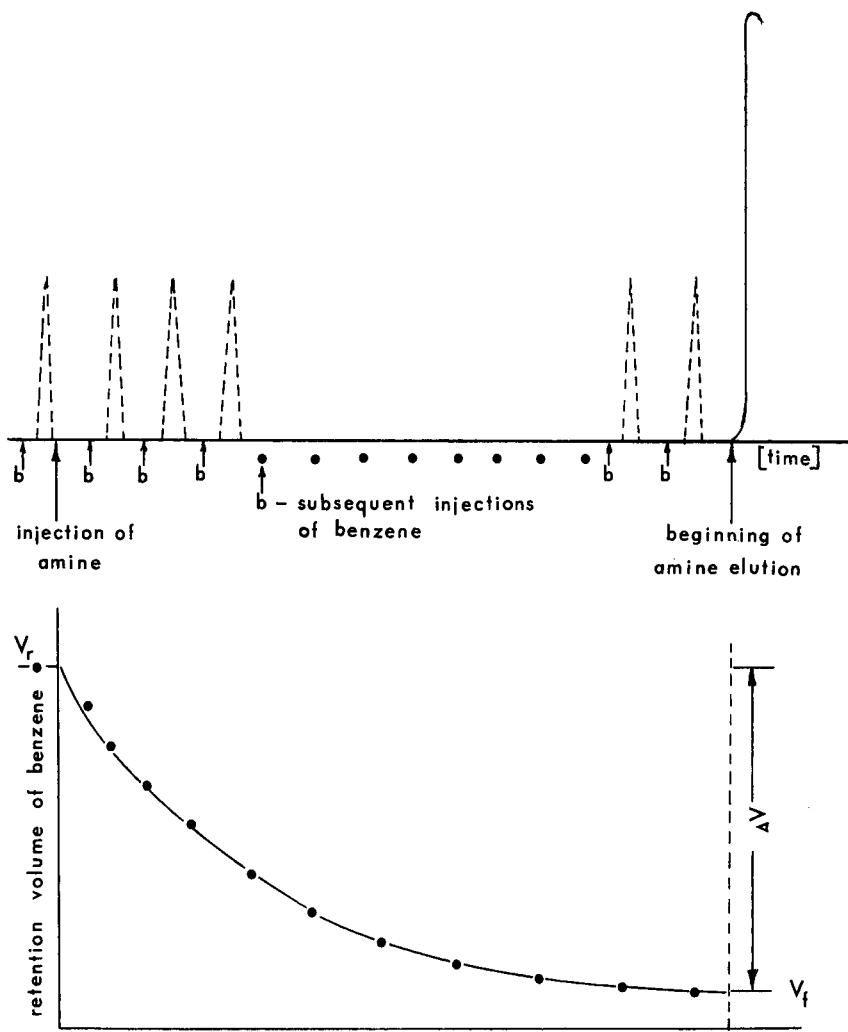


Fig. 1. Principle of the method.

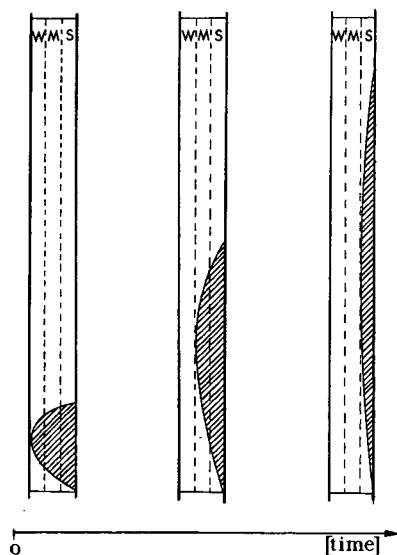


Fig. 2. Development of the amine band along the column. W, M, S = Weak, medium and strong adsorption sites, respectively, on the surface of the adsorbent.

generally chromatographic in nature and it can be performed using other chromatographic techniques. After measuring the retention volume of, *e.g.*, benzene or another hydrocarbon solute, a known amount of amine is injected into the column containing modified or bare silica. The amine is very strongly retained. Slowly a concentration profile is developed along the column. At the beginning the amine molecules will occupy the various, *i.e.*, weak (W), medium (M) and strong (S), adsorption sites. This is shown in Fig. 2. The desorption of the molecules will occur mainly from the weak (W) and medium (M) sites. Slowly the amine molecules will be adsorbed mainly on the strongest (S) adsorption sites available.

The very long retention time of the amine permits the retention of, *e.g.*, an unsaturated hydrocarbon to be measured in the presence of the amine in the column. Usually there is sufficient time to make several injections (up to tens) of the hydrocarbon before the amine begins to elute. Subsequent injections of the hydrocarbon reveal a decrease in retention time, as shown in Fig. 1. This gradual decrease in retention indicates that the amine blocks the strongest adsorption sites on the adsorbent surface.

According to Hair and Hertl<sup>9</sup> and Curthoys *et al.*<sup>78</sup>, silanols on a silica surface can be considered to be the main adsorption sites and the adsorbate-adsorption site ratio can be assumed as 1:1. As a known amount of amine is injected into the column, the observed decrease in the retention volume of the hydrocarbon,  $\Delta V$ , (Fig. 1) can be simply related to the blockage of a known number of adsorption centres. In other words, we can say that the amount of surface species blocked is responsible for the part which equals  $\Delta V$  in the hydrocarbon retention.

Now, on injecting various amounts of the amine we shall obtain different  $\Delta V$  values. These can be used for the evaluation of the distribution of the strength of the

surface sites. The distribution curve can be obtained by plotting the relative  $\Delta V$  values against the surface concentration of the blocking reagent, *i.e.*, amine. The relative  $\Delta V$  values are calculated by dividing  $\Delta V$  by the amount of the amine blocking agent,  $A$  ( $\mu\text{mol}$ ):

$$\Delta V_R = \frac{\Delta V}{A}$$

The physical meaning of  $\Delta V_R$  value is the decrease in the retention volume of the hydrocarbon caused by 1  $\mu\text{mol}$  of the blocking reagent at a given surface concentration of the reagent. Since the surface concentration of the reagent is simply equal to the surface concentration of the blocked sites, we obtain direct information on the surface concentration of strongly adsorbing sites.

For this method the term "gas-phase titration" was proposed<sup>43</sup> as the distribution curves form straight lines with characteristic deflection points. Such a point can be considered as a "titration end-point" and it probably indicates the surface concentration of a specific subset of strongly interacting sites. It was shown that one or two such points can be found for bare or modified silica surfaces<sup>42-44</sup>. The method can also determine the relative strengths of interactions of strongly retaining silanols among various adsorbents<sup>44</sup>. However, the most interesting aspect for chromatographers was evidence that these few silanols are responsible for substantial broadening of the chromatographic band<sup>43</sup>. It was shown<sup>43</sup> that the blockage of less than 0.1% of the available silanols on a trimethylsilylated silica surface can considerably increase the efficiency of the column. This directly supports Marshall and co-workers'<sup>36-38</sup> attempts to make more efficient columns for HPLC by prior deactivation of the small, reactive population of silanols. This also supports much earlier theoretical predictions by Giddings<sup>79</sup> that "a few active sites on the solid support may lead to tailing".

## 2.7. Conclusions

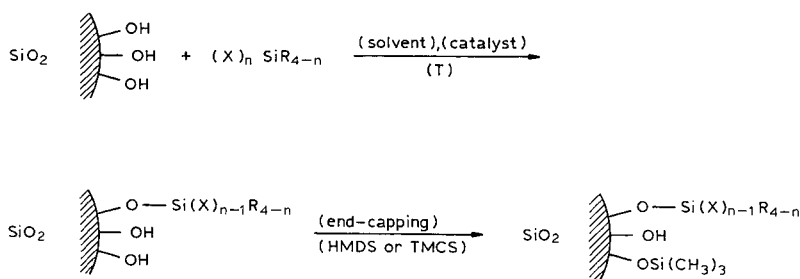
The above-described facts can be summarized in the form of the following conclusions:

- (i) the surface of chromatographic-grade silica differs from that of pyrogenic silica (Cab-O-Sil, Aero-Sil)<sup>49,50,60</sup>;
- (ii) there exists a small group of highly acidic, reactive silanols on the silica surface<sup>12,32,37,39-44</sup>;
- (iii) the reaction of silica surface silylation should proceed mainly on acidic sites<sup>35</sup>, but probably for steric reasons some of these highly acidic sites remain unreacted<sup>12,32,38</sup>;
- (iv) these few, highly reactive sites can have an important influence on column efficiency<sup>36-38,43</sup> and sample capacity<sup>76,79</sup>, which is particularly important in preparative chromatography;
- (v) metal impurities are the most likely reason for the enhanced acidity of some isolated silanols<sup>54</sup>.

### 3. CHEMICALLY BONDED PHASES FOR HIGH-PERFORMANCE LIQUID-CHROMATOGRAPHY

Bonded phases are widely used in HPLC and it is estimated that about 80% of chromatographic analyses are carried out with these phases<sup>80</sup>. However, widely differing capacity factors and selectivities are observed for the same solutes using various commercially available reversed-phase (RP) silica packings of the same type<sup>81</sup>. Thus, it seemed to be of interest to trace the possible sources of such differences. The aim of this section is to indicate the influence of various factors on the properties of reversed-phase silica packings.

Generally, the formation of an HPLC packing involves the reaction of an organosilane with a silica surface:



This scheme shows that the quality of the final result, *i.e.*, the RP packing, can depend on the following factors: silica surface, functionality of the silane, solvent, catalyst, temperature and end-capping reagent.

Statistical weighting<sup>82,83</sup> of the variables of the reaction has shown the following relative importance: functionality of the reagent, presence of acid scavenger (or catalyst as in the above scheme), number of silanizations with principal reagent, stoichiometry of silanizing reagent over the theoretical amount, hydroxylation of the silica surface, solvent pretreatment and type and functionality of the capping reagent. A further fourteen variables were said to be insignificant<sup>82</sup>. However, it must be stressed that carbon coverage was used for the judgement between good and poor results, which does not necessarily reflect the good or poor chromatographic quality of the phase. Moreover, only one kind of silica material was used<sup>82,83</sup>, which seems to be insufficient to draw conclusions about the importance of the variables.

Many papers have been devoted to the influence of the functionality of the reagents on the reaction. Functionality can mean here both the number of functional groups able to react with surface silanols or the chemical nature of the groups. Monofunctional silanes are said to result in well defined products whereas di- and trifunctional silanes can produce oligomer or polymer layers on the silica surface. Although monomeric phases are usually considered to have the most reproducible properties, manufacturers use mono-, di- and trifunctional silanes to produce bonded phases<sup>34,84</sup>. Oligomer or polymer phases can sometimes have better chromatographic selectivity than monomer phases<sup>31,85,86</sup>. The reactivities of various functional groups

were compared for *n*-octyldimethylsilanes by Lork *et al.*<sup>87</sup>, who found the following sequence:  $\text{N}(\text{CH}_3)_2 > \text{OCOCF}_3 > \text{Cl} \gg \text{OH} \approx \text{OCH}_3 \approx \text{OC}_2\text{H}_5 \gg \text{-O-}$  (siloxane).

Only limited studies have been carried out to establish the importance of the solvent<sup>82,83,88</sup>. The role of the solvent has probably been underestimated, and the solvent is probably much more important when a catalyst (amine) is used as an acid scavenger. Jones<sup>82,83</sup> proposed the application of a chlorinated solvent (1,1,2-trichloroethane) whereas Kinkel and Unger<sup>88</sup> found dichloromethane, dimethylformamide or acetonitrile to be the best choice. A similar recommendation of chlorinated hydrocarbons as solvents was made by Little *et al.*<sup>89</sup>. However, the densest coverages were obtained when *n*-hexane<sup>90-97</sup> or toluene<sup>98,99</sup> was applied as a diluent.

As the temperature of the reaction mainly depends on the solvent chosen, it will not be discussed in detail. The influence of temperature on the reactivity of various functional groups was reported by Lork *et al.*<sup>87</sup>. The role of amines and end-capping reactions will be discussed in section 3.2.

### 3.1. Physical and chemical requirements for silica

Silica is the base on which the silanization reaction proceeds, so it can obviously determine the resulting properties of bonded phase packings. It is obvious that silica should satisfy various requirements before it can be used efficiently for the preparation of phases, and these requirements are both physical and chemical in nature. Physical requirements can concern the silica macro- and micro-properties, and particle size, shape and distribution can be considered as macro-physical requirements. These parameters are usually well recognized by chromatographers and their influence on chromatographic efficiency is well known<sup>2</sup>. Apparent density, another macro-physical parameter, has been postulated to be important<sup>4</sup>. The apparent density of chromatographic-grade silica is usually between 0.4 and 0.6 g/cm<sup>3</sup> whereas the ideal value is said to be 0.45 g/cm<sup>3</sup><sup>4</sup>.

The influence of the micro-physical properties of silica on the quality of bonded-phases is not always realized and for this reason it will be reviewed below. Specific surface area, mean pore diameter, specific pore volume and pore size distribution will be taken into account. The first three of these parameters depend on each other. Hence the influence of one of these parameters on the quality of a bonded phase cannot be checked by keeping the other two parameters constant and changing only the one being investigated.

The specific surface area of the silica used for the synthesis of bonded phases usually lies in the range 150–400 m<sup>2</sup>/g, but it must be pointed out that for size-exclusion chromatography much lower values are required<sup>2,4</sup>. The mean pore diameter should be in the range 6–10 nm, with an ideal value of 8 nm according to Verzele *et al.*<sup>4</sup>. The specific pore volume of silica is usually higher than 0.2–0.3 ml/g and lower than 1.5 ml/g; Verzele *et al.*<sup>4</sup> consider 0.7 ml/g to be an ideal value. Pore size distribution seems to be one of the most important physical parameters. A homogeneous distribution of pore sizes, *i.e.*, resembling a Gaussian distribution, should be the main requirement. The narrower the distribution curve the better is the silica material, but it should be emphasized that the actual range of pore diameters usually spans an order of magnitude and the mean pore diameter which is given by the manufacturer is only an average. This means that on any silica surface a variety of pores exist.

Pores of diameter less than 2 nm (micropores) are particularly undesirable.

Berendsen *et al.*<sup>100</sup> have shown how the curvature of the pores can influence the final coverage of the bonded phase. This effect is of greater importance the longer is the alkyl chain anchored on the pore surface, *i.e.*, the effect has to be taken into account particularly for the most common octadecyl phases. Bearing in mind that an extended conformation of a  $C_{18}$  phase is 2.45 nm long, the maximum coverage cannot be obtained on silicas with narrow pores. Berendsen *et al.*<sup>100</sup> stated that for pore diameters smaller than 12 nm the pore curvature will decrease the coverage. Silicas with narrower pores would probably show a tendency to produce ink-bottle-shaped pores after silanization<sup>100</sup>, as the initial silanization of the cylindrical pores at the edges would prevent other molecules of ODS reagent diffusing inside the pores. Smaller pores existing in the structure will be only partly silanized, which is why an "end-capping" procedure is necessary to cover as many silanols as possible. Sander and Wise<sup>31,85,86</sup> tried to evaluate the bonded-phase selectivity differences for various pore diameters. For monomeric phases they observed a decrease in retention with increasing pore diameter. The observed decrease in retention was caused by the decrease in the specific surface area for packings with large pore diameters. However, it must be emphasized that the phases in question had much lower coverages than predicted theoretically. For polymeric phases synthesized on the same silicas, the selectivity was observed to change as a function of the pore diameter. The best separations were achieved on packings of large pore diameter.

Similar investigations were carried out by Engelhardt *et al.*<sup>101</sup>, who showed that wider pore silica permitted phases with higher coverage to be obtained. A packing obtained from narrow-pore silica (mean pore diameter 3.5 nm) was shown to be much less efficient than the wider pore materials.

Chemical requirements are considered much less often than physical requirements by most chromatographers. The most important chemical criteria are a fully hydroxylated silica surface, suitable pH of the silica surface and a low content of trace metal impurities.

It has been known for many years that silica used for the synthesis of bonded phases must be dry, *i.e.*, it must not contain physically adsorbed water. Water was shown to have a deleterious effect on the coverage of alkylsilyl groups on the silica surface<sup>87</sup>. For this reason, silica is always thermally and vacuum treated before the reaction in order to remove physically adsorbed water<sup>86,87,102-107</sup>. Thus it seems surprising that the preliminary dehydration of silica was not considered to be a significant variable in the statistical optimization of the silanization process, whereas hydroxylation of the silica surface appeared to be an important variable<sup>82</sup>. Extended investigations of various methods for the rehydroxylation of silica surfaces were recently carried out by Köhler and Kirkland<sup>32</sup>. In view of their findings, the hydroxylation of the surface seems previously to have been an underestimated parameter. They stated<sup>32</sup> that fully hydroxylated silica exhibits (1) a larger number of associated silanols, (2) a higher pH, (3) a markedly lower adsorptivity for basic compounds, (4) a significantly improved hydrolytic stability of bonded phase ligands and (5) increased mechanical stability. Köhler and co-workers<sup>32,40</sup> found that chromatographic-grade silicas often contain only 5–6  $\mu\text{mol}/\text{m}^2$  of silanols. Rehydroxylation has so far usually been accomplished by heating in aqueous acids or by extensive boiling in water. For example, Hennion *et al.*<sup>103</sup> and Kingston and Gerhart<sup>108</sup> boiled silica in concentrated nitric acid–sulphuric acid (1:1) to obtain a fully hydroxylated surface.

Gobet and Kováts<sup>109</sup> have proposed a reproducible method for obtaining a fully hydroxylated surface of fume silica (Cab-O-Sil). Their procedure consisted of thermal treatment at 1173 K for 120 h, then rehydration for 70 h in boiling water and subsequent freeze-drying of the wet silica. Such a procedure was sufficient to ensure maximum coverage with trimethyldimethylaminosilane of the order of  $4.75 \mu\text{mol}/\text{m}^2$ . Köhler and Kirkland<sup>32</sup> found this procedure to be inadequate to give total rehydroxylation of the silica surface, which again confirms our belief (section 2) that the surfaces of fume and chromatographic-grade silicas are not completely identical. Köhler and Kirkland<sup>32</sup> recommend rehydroxylation of the silica surface with certain basic activators, *e.g.*, treatment with dilute ammonia solution at room temperature, tetrabutylammonium hydroxide or ethylenediamine. They also found that treatment with 100 ppm of hydrofluoric acid for 24 h led to a support with a low adsorptivity for organic bases<sup>32</sup>.

A different concept concerning the silanol concentration was proposed by Scott and Kucera<sup>110</sup>, who employed a thermal treatment for reducing the silanol content on silica. Later it was found by Van de Venne<sup>111</sup> that thermal pretreatment up to 400°C reduces the number silanols but does not affect the carbon content.

Welsch and Frank<sup>112</sup> developed the so-called "high temperature silylation" at 250°C, which led to sufficient alkyl coverages (*ca.*  $3.6\text{--}3.8 \mu\text{mol}/\text{m}^2$ ) and simultaneously reduced the number of remaining silanols. The resulting materials were shown to be comparable to commercial bonded phase packings. Frank<sup>113</sup> also showed that asymmetry of phenol and benzyl alcohol peaks was highest for certain silanol surface concentrations (*ca.*  $3 \mu\text{mol}/\text{m}^2$ ) whereas higher or lower silanol concentrations greatly improved the symmetry of the peaks.

The next question to consider is the problem of surface pH. As discussed in section 2.3, different surface pH values can manifest themselves in various chromatographic properties when normal-phase chromatography is considered<sup>29,30</sup>. However, the surface pH was shown to affect the packing properties of alkyl bonded phases made of silica. Engelhardt *et al.*<sup>101</sup> have shown that bonded phases made of basic silica were more suitable for the separation of basic solutes, whereas the opposite was true and bonded phases based on acidic silica gave better efficiencies for the separation of acidic compounds.

Köhler and Kirkland<sup>32</sup> pointed out that the rehydration procedure usually increase the pH and a low adsorptivity of bases was observed for silicas with surface pH ranging from 4.80 to 6.89. However, these two extreme values seem to be exceptions as the remaining silicas have pH values in a much narrower range of 5.15–5.59. Trimethylsilylated silicas obtained from these rehydrated silicas were covered with  $3.47\text{--}5.43 \mu\text{mol}/\text{m}^2$  of TMS<sup>32,40</sup>. The last value seems surprising in view of the Van der Waal's radius of the trimethylsilyl group. The concentration of the densest trimethylsiloxy layer was calculated by Boksanyi *et al.*<sup>114</sup> to be of the order of  $4.7 \mu\text{mol}/\text{m}^2$  [trimethylsilyl enolate (enolate of pentane-2,4-dione) was used for the synthesis of the densest layer<sup>32,40</sup> and the same reagent was earlier shown to give an even higher density of  $6.6 \mu\text{mol}/\text{m}^2$  (ref. 115)]. Their "good" chromatographic properties were judged by chromatographic experiments rather than from the coverage values.

The final chemical requirement for silica is a low trace metal content. As discussed in section 2.4, traces of metals can seriously affect the chromatographic

process, as was shown by Verzele and co-workers<sup>45–47</sup> and Sadek *et al.*<sup>54</sup>. Boiling on an RP C<sub>18</sub> packing in hydrochloric acid was recommended for removal of the metals, whereas the application of EDTA was said to be ineffective<sup>45–47</sup>. In contrast, Köhler *et al.*<sup>40</sup> have shown that washing silica with 1% Na<sub>2</sub>EDTA solution can remove all the trace metals from the matrix. This seems surprising in view of Verzele and co-workers' attempts to remove traces of metals by extensive washing with acids<sup>45–47</sup>. Our experience<sup>116</sup> confirms Verzele and co-workers' results. As the procedures described above for the rehydration of a silica surface would be also effective in removing some metal traces, it is possible that the removable part of the trace metals is washed out during the rehydration process, which should obviously improve the chromatographic properties of the silica.

### 3.2. Dense coverage packings

The term "dense coverage" can be reasonably used only for chemically bonded phases prepared from monofunctional silanes. Attempts to make the densest possible organic layers bonded to a silica surface were begun in order to suppress the interactions of unreacted silanols. Colin and Guiochon<sup>117</sup> stated that "For extensive coverages ... the unreacted silanols do not have a critical role. Theoretically it is possible to change them into inactive species by reaction with DMCS or TMCS". This statement was made 11 years ago during the early development of chemically bonded phases. Today it is generally accepted that the unreacted silanols play an important role in the mechanism of retention<sup>118,119</sup> and for steric reasons the remaining silanols cannot be converted into inactive species with TMCS reagent and DMCS is no longer used for "end-capping". The maximum coverage on a silica surface can be calculated from the space requirements for a given molecule. This, however, needs a further assumption of a flat silica surface. This assumption can be true only for small molecules. The space requirement for a trimethylsilyl (TMS) group has been calculated to be 0.37, 0.35 or 0.43 nm<sup>2</sup>, depending on the equation or method applied<sup>2</sup>. From these data, an average value 0.38 nm<sup>2</sup> per TMS group gave a maximum surface concentration of 4.3 μmol/m<sup>2</sup> of TMS. A very close value, namely 4.2 μmol/m<sup>2</sup>, was obtained by Unger *et al.*<sup>104</sup>. The surface concentration of TMS groups calculated from the density of trimethylchlorosilane is about 4.7 μmol/m<sup>2</sup> and Boksanyi *et al.*<sup>114</sup> obtained 4.7 μmol/m<sup>2</sup> by the ammonia-catalysed reaction of trimethylsilanol with Cab-O-Sil M5. The space requirement calculated from such a coverage equals 0.32 or 0.28 nm<sup>2</sup> per group, depending on the arrangement of the groups on the surface<sup>114</sup>. These values, according to Berendsen's<sup>120</sup> calculations, would indicate a rigid position of the TMS group and an Si–O–Si angle of 110–150°. Berendsen<sup>120</sup> has shown that the cross-sectional area of the TMS group depends on the Si–O–Si angle and the rotation of the group. Taking into account the space requirements of the TMS group calculated for angles in the range 110–180° with and without rotation, he assumed the highest surface coverage with the group to be 3.82 μmol/m<sup>2</sup> (2.3 nm<sup>2</sup> per TMS group), despite the fact that the author<sup>20</sup> easily exceeded this value, obtaining 4.16 μmol/m<sup>2</sup>, in the same work. However, for longer alkyl radicals lower coverages were obtained, which was explained by hindered diffusion of the reactant into smaller pores. Unger *et al.*<sup>104</sup> considered prolonged heating at high temperature would ensure a dense surface coverage. However, attempts to obtain the dense coverages soon went in other directions, *i.e.*, a search for a silane with a more reactive functional group. A variety of

such groups were examined<sup>87,115</sup> and the most reactive seems to be the N,N-dimethylamino group, which was introduced into chromatography by Kováts and co-workers<sup>90,121</sup>. The application of N,N-dimethylaminotriorganysilanes permitted a number of densely silylated silica surfaces to be obtained with coverages above  $4 \mu\text{mol}/\text{m}^2$  (refs. 91, 109, 122, 123). Trimethyl(dimethylamino)silane applied at  $125\text{--}275^\circ\text{C}$  for 120–170 h gave a theoretically calculated<sup>114</sup> value of  $4.77 \mu\text{mol}/\text{m}^2$  of TMS<sup>91</sup>, whereas for longer radicals the values decreased as the alkyl chain length increased. The coverages obtained were  $4.52 \mu\text{mol}/\text{m}^2$  for ethyl,  $4.31 \mu\text{mol}/\text{m}^2$  for propyl,  $4.24 \mu\text{mol}/\text{m}^2$  for tetradecyl and  $4.20 \mu\text{mol}/\text{m}^2$  for octadecyl<sup>91</sup>. All of these results were achieved on Cab-O-Sil M5 fume silica hydrated according to the described procedure<sup>109</sup> and are much higher than the values predicted by Berendsen *et al.*<sup>100</sup>. No value for the pore volume of hydrated Cab-O-Sil silica was given by Kováts and co-workers<sup>48,91,109,122,123</sup>, but it can be calculated roughly from the nitrogen adsorption isotherm<sup>109</sup> to be *ca.*  $0.41 \text{ cm}^3/\text{g}$ . This value and specific surface area of  $179 \text{ m}^2/\text{g}$  allow the mean pore diameter ( $D$ ) to be calculated according to the Wheeler equation<sup>2</sup> as  $D = 9.2 \text{ nm}$ . This low value, according to Berendsen *et al.*<sup>100</sup>, would permit a coverage of  $\text{C}_{18}$  ligands lower than  $2.5 \mu\text{mol}/\text{m}^2$  to be obtained. Although hydrated and silanized samples of Cab-O-Sil were not used in HPLC, probably because of their low apparent density of  $0.15 \text{ g}/\text{cm}^3$ , very similar coverages with TMS groups were obtained on precipitated silica surfaces and on LiChrosorb Si 100 chromatographic-grade silica<sup>48</sup>.

Approximately at the same time, Serpinet's group started to investigate phase transitions in very compact octadecyl bonded phases. The phases were synthesized according to Kováts' procedure<sup>90</sup> on wide-pore silica gels<sup>92,93</sup>. Morel and Sepinet<sup>92,93</sup> showed that under gas chromatographic conditions the grafted alkyl chains undergo a melting-like phase transition and the transition for the octadecyl radical occurred at ambient temperature, which was said to change the retention characteristics of the phase. The coverages obtained were  $4.13\text{--}4.64 \mu\text{mol}/\text{m}^2$ , depending on the support. Subsequently the same authors<sup>94</sup> confirmed the occurrence of the phase transition under liquid chromatographic conditions for a  $\text{C}_{22}$  bonded silica. The work on densely covered phases was continued<sup>95–97</sup>, always using phases with surface concentrations higher than  $4 \mu\text{mol}/\text{m}^2$ . The authors<sup>97</sup> concluded that the widespread choice of the  $\text{C}_{18}$  ligand was probably unfortunate as the phase undergoes a transition over the entire laboratory temperature range. For that reason, Morel *et al.*<sup>97</sup> advocated a  $\text{C}_{16}$  phase instead of the  $\text{C}_{18}$  phase.

The same reagent, N,N'-dimethyloctadecyldimethylsilane, and the same procedure according to Kováts<sup>90</sup> were shown to produce a densely covered ODS phase for HPLC<sup>124</sup> on wide-pore silica. The packing obtained had much better chromatographic properties than sparsely covered phases obtained from chloro and methoxy derivatives<sup>124</sup>. A high-density ( $> 4 \mu\text{mol}/\text{m}^2$ ) of grafted alkyl ligands was shown to be relatively easily obtainable even with chloro derivatives on controlled porosity glasses<sup>125–128</sup>.

The application of basic catalysts seems to be another means of producing high-density reversed phases. Pyridine was used as a hydrochloric acid scavenger<sup>102,129</sup> in the reaction of trichlorosilanes with silica. Berendsen *et al.*<sup>100</sup> also used pyridine when bonding with monochlorosilanes. All of these reactions<sup>100,102,129</sup> were carried out in toluene. The coverages for the ODS phase obtained by Berendsen *et*

*al.*<sup>100</sup> were 3.04 and 3.28  $\mu\text{mol}/\text{m}^2$ . Kinkel and Unger<sup>88</sup> have shown that the role of both the amine and the solvent are much more complicated than had previously been believed. According to Kinkel and Unger<sup>88</sup>, the solvent can have a considerable effect on the Si–O bond strength, can also activate the silica atom of an organohalosilane and finally can influence the reactivity of the added base. However, in order to be able to predict an optimum solvent–base combination, much more work has to be done. It was shown also that the type of base does not cause substantial differences in the kinetics of the silanization reaction. The *n*-octyl ligand densities obtained were scattered around 3.01  $\mu\text{mol}/\text{m}^2$  for most of the bases. The best result of 3.53  $\mu\text{mol}/\text{m}^2$  was obtained when the reaction was catalysed by imidazole. Berendsen *et al.*'s values<sup>100</sup> for the *n*-octyl phase were 3.49 and 3.45  $\mu\text{mol}/\text{m}^2$ . A comparison of the results<sup>88,100</sup> favours Berendsen *et al.*'s methodology, especially as Kinkel and Unger<sup>88</sup> used wider pore silica. All of the results are much lower, however, than the “true” dense phase obtained via N,N'-dimethylaminoalkylsilanes<sup>92,94</sup>.

In contrast to Kinkel and Unger's<sup>88</sup> investigations of the role of base catalysts, Buszewski and co-workers<sup>98,99</sup> found a clear relationship between  $\text{p}K_{\text{a}}$  value of the base and the obtained bonded phase coverage obtained. Morpholine ( $\text{p}K_{\text{a}} = 8.33$ ) was shown to be the most efficient catalyst for the bonding reaction. The same activator was also used in the synthesis of densely covered controlled porosity glasses<sup>130</sup>. As the dense coverages of 4.24  $\mu\text{mol}/\text{m}^2$  obtained are higher than predicted from Berendsen *et al.*'s model<sup>100</sup>, Buszewski and Suprynowicz<sup>99</sup> criticized the model as unrealistic.

The importance of amines as catalysts and not as simple acid scavengers was shown by Boksanyi *et al.*<sup>114</sup>, who tried numerous compounds as catalysts of the reaction of triorganysilanols with silica and found amines to be the best.

### 3.3. Models of bonded phase structure

Since the initial experiments on surface-anchored groups, attention has been devoted to the explanation of the chromatographic behaviour of the bonded phases and for this purpose various models of the phases have been proposed. The first models were static whereas the later models assumed flexibility and mobility of the ligands.

Historically, Halász and Sebestian<sup>131</sup> were the first to introduce the static model of an esterified surface of Porasil. The model, well known now as a “bristle” or “brush”, dominated the thinking of chromatographers for about 10 years<sup>132</sup>. Hemetsberger *et al.*<sup>133</sup> noticed that the bonded alkyl radicals are not rigid rod-like structures but are rather folded or pressed into the surface. This description has been known since then as a “blanket” model. Another static model of “alkyl grass” was proposed by Scott and Simpson<sup>134</sup>. They noticed that hydrocarbon chains anchored on the silica surface can associate with themselves at low methanol or high water concentrations. They also showed that the phase needs a significant time to reach equilibrium with the mobile phase. In contrast to monomeric phases, polymeric bonded phases were said to be held fairly rigidly in the structure of the phase.

Scott and Simpson's findings were generally in agreement with Lochmüller and Wilder's<sup>135</sup> concept of microdroplets and Gilpin and Squires'<sup>136</sup> suggestion of considerable interactions of hydrocarbon chains among themselves under certain conditions. Lochmüller and Wilder's first concept of aggregation of alkyl chains to form “bundles”<sup>135</sup> was later confirmed in a study of the luminescence of pyrene molecules chemically bonded to microparticulate silica gel. That study resulted in the

“microdroplet” model<sup>137,138</sup>, which assumes a non-homogeneous distribution of silanols on a fully hydroxylated silica surface, which subsequently leads to clusters of covalently bonded molecules. Their conclusions were recently criticized by Farin and Avnir<sup>74,139</sup>, who pointed out that the silanols are homogeneously distributed on the silica surface but various curvatures of the surface may result in different accessibilities of the silanols. First, Lochmüller and Wilder’s assumption of a flat silica surface was said to be unrealistic, in addition to their view of the pore network, *i.e.*, with the silica being treated as a zeolite-like material with one typical pore size<sup>74,139</sup>, whereas in fact the pore diameters of silica are usually distributed over a fairly wide range. However, the idea of a non-uniform distribution of silanols and consequently of bonded alkyl chains was supported by a chromatographic study of the entrapment and release of solvent<sup>140</sup> and also by NMR<sup>141</sup> and infrared investigations<sup>142</sup>. On the other hand, taking into account Farin and Avnir’s<sup>74,139</sup> arguments and the pore size distribution in chromatographic-grade silica, it is still disputable whether the observed clustering of bonded alkyl groups occurs because of a non-homogeneous distribution of silanol or whether it occurs in pores of smaller diameters. To judge between these two possibilities one would have to have access to more detailed data on pore size distribution, *e.g.*, for Partisil 10, which was used by Lochmüller *et al.*<sup>137,138</sup>. Consequently, similar<sup>137,138</sup> experiments could be carried out on very wide-pore silica to avoid the influence of small diameter pores. The above discussion emphasizes again our belief of the importance of pore size distribution in the production and understanding of bonded phases for HPLC.

Another model was proposed by Gilpin and co-workers<sup>136,140</sup> in which both folded and bristle states are possible and transitions between the two take place with changes in temperature or solvent. Such a model was confirmed by Fourier transform IR spectrometry by Sander *et al.*<sup>143</sup>. According to their study, a disordered “folded” state is favoured when the packing is either dry or in the presence of a non-wetting mobile phase, and a more ordered “bristle” state is favoured when the chains are wetted with a mobile phase of high organic content. At that time it became increasingly clear that the alkyl chains possess a certain molecular mobility. Such a motion was confirmed mainly by numerous NMR studies. CP-MAS NMR investigations have shown an increase in motion towards the end of the chain<sup>144</sup>. Measurements of spin-lattice relaxation data for <sup>13</sup>C-labelled bonded alkyl chains indicated that rotation of the terminal methyl carbon atom is the dominant factor in the overall mobility of the chains in solvated conditions<sup>141,145</sup>. A decrease in end-group mobility was also observed to occur when a certain critical surface concentration of the alkyl groups was attained. These conclusions were in agreement with earlier suggestions by Sindorf and Maciel<sup>144</sup>. The results of <sup>29</sup>Si and <sup>13</sup>C CP-MAS NMR studies of RP-HPLC packings<sup>146</sup> have shown that under conditions typical of chromatographic separations the alkyl chains assume different conformations. There are several factors governing the behaviour of the chains: interactions of the chains with themselves, with neighbouring chains, with trimethylsilyl groups, with the mobile phase and with the solutes. The extended conformation of the chain appears to be more flexible while the increasing polarity of the mobile phase increases the rigidity of the bonded alkyl groups, *i.e.*, the collapsed structure appears to be more rigid. Bayer *et al.*<sup>146</sup> noticed that the process of end-capping reduces the mobility of long chains. This means that in uncapped packings the alkyl chains will be more extended whereas in capped packings

they will have a tendency to collapse. This indicates the importance of the unreacted silanols for interactions with solute and solvent molecules.

The investigations of densely grafted bonded phases by Serpinet and co-workers<sup>92-97,147</sup> led to the proposal of another model, a "solid condensed-liquid expanded" phase. Based mainly on gas chromatographic experiments, the model assumes the existence of two temperature-controlled states of the phase. At lower temperatures the "solid condensed" state is the most likely whereas an increase of the temperature causes a transition of the phase into a "liquid expanded" state. The transition results in an irregular retention behaviour of the phase, *i.e.*, an increase in the absolute retention volume with increase in temperature. The transition appears to be a sort of two-dimensional "melting" which gives the solute access to new retention sites. As for the C<sub>18</sub> bonded phase the phenomenon takes place at ambient temperatures, Serpinet's group is advocating the use of shorter or longer alkyl grafts instead of the octadecyl type.

Martire and Boehm<sup>148</sup> have proposed a "breathing" surface model, which describes mathematically the dynamic nature of the bonded layer. The surface layer can adjust itself depending on the mobile phase composition. The model assumes a swelling of the bonded phase in solvents compatible with *n*-alkanes, *i.e.*, promoting extension of the bonded alkyl chains ("brush" structure) and the collapse of the chains in fairly polar solvents. However, the "breathing" model involves some simplifications which do not allow the retention behaviour of some polar molecules to be predicted. The model assumes no interactions with residual silanols, but such interactions can play a major role particularly when an organic-rich mobile phase is used and molecules containing heteroatoms are chromatographed<sup>118,119</sup>.

### 3.4. Residual silanols and their influence on retention

Early attempts to explain the retention mechanism in HPLC on bonded alkyl phases mostly neglected any influence from unreacted silanols. Essentially three possibilities of the mechanism were considered: partition, adsorption and partition between the mobile phase and a new adsorbed, mixed stationary phase having a composition different to that of the mobile phase. The controversy regarding the retention mechanism deepened because of the difficulties encountered in preparing batches of modified silica gels with sufficient reproducibility. An interesting discussion of those early attempts can be found in the review by Colin and Guiochon<sup>117</sup>. The neglect of the participation of residual silanols in the chromatographic process led to the development of a solvophobic theory by Horváth *et al.*<sup>149</sup>. According to this theory, retention is governed by the formation of reversible complexes due to solvophobic interactions between solute molecules and chemically bonded organic chains on the surface of silica. The very important role of the mobile phase was emphasized. Although the theory appeared valid in numerous chromatographic systems, particularly when water-rich solvents were used, irregularities were noted by many workers<sup>150-152</sup>. Some of these irregularities could be explained by changes in the conformations of the chromatographed compounds<sup>153</sup>. However, more and more facts supported the idea of the availability of the residual silanols on the stationary phase surface for interaction with solute molecules<sup>154-156</sup>. Simple tests were proposed for the detection of silanophilic interactions<sup>157,158</sup>.

Generally, unreacted silanols are considered undesirable<sup>159-162</sup>. However, as

Nahum and Horváth<sup>118</sup> have emphasized, no detailed study has so far focused on their role in determining retention behaviour. On the basis of some recently published papers<sup>32,36-44,163</sup>, we believe that not all unreacted silanols are undesirable but only a very small population of highly acidic, isolated silanols. The role of this strongly interacting group of silanols was described in detail in section 2.3. The other silanols probably play a "positive" role in the separation mechanism. Bij *et al.*<sup>119</sup> have shown that blocking of silanols may sometimes lead to deterioration of a separation. A similar example was given by Gonnet *et al.*<sup>96</sup>. The silanols on the surface of the bonded phase generate some kind of heterogeneity and it was shown theoretically that heterogeneous surfaces may exhibit a higher selectivity than homogeneous surfaces with the same average adsorption energy<sup>77</sup>. Heterogeneity of alkyl bonded phases was recently confirmed by an investigation of sorption-desorption dynamics by means of a relaxation kinetic method<sup>164,165</sup>. On the other hand, the residual silanols produce a polar surface environment, which was detected by means of fluorescence spectroscopy of chemically modified surfaces<sup>166</sup>. If some of the silanols are considered "undesirable" than it becomes obvious that their influence on chromatographed solutes should be suppressed. Such a suppression can be achieved when the mobile phase contains a strongly adsorbing compound, usually an amine. This is advisable when chromatographed compounds have an unprotected nucleophilic function. The advantages of the silanol blockage were demonstrated by Wehrli *et al.*<sup>167</sup>, Wahlund and Sokołowski<sup>168</sup> and Moats<sup>169</sup>, who used an amine to block the active sites on the bonded phase surface. In supercritical fluid chromatography, dioxane was used for "on-column" silica surface modification, which improved the speed and efficiency of the separation<sup>170</sup>. Other advantages of silanol masking are a reduction of the dependence of retention on sample size and improvements in column efficiency and sample recovery<sup>109</sup>. Silanophilic retention can also be eliminated by protecting the function of the solute molecule<sup>109</sup>.

We believe that the above advantages of the partial masking of unreacted silanols confirm our idea of a small, highly retentive population of silanols<sup>43</sup>. We have already shown<sup>43</sup> that the blocking of a very few strongly adsorbing sites can dramatically improve the column efficiency. A similar phenomenon was observed by Marshall *et al.*<sup>38</sup> after treatment of a fully end-capped packing with a highly reactive reagent, trimethylsilylphosphine. The reagent did not increase the carbon coverage but it did greatly improve the column efficiency. As the blocking improves the solute peak shape<sup>43</sup> it will obviously reduce the dependence of retention on sample size<sup>119</sup>. Sample recovery also depends on the strong adsorption sites, so the blocking should improve the recovery<sup>119</sup>.

#### 4. CONCLUSIONS

We have shown that the properties of silicas may differ, despite them having the same surface area, mean pore diameter or pore volume, because of slight differences in the chemistry of the surface. Several reports<sup>32,36-44,54,163</sup> support the idea of a small population of silanols which can be blamed for the undesirable, strong adsorption of compounds with a nucleophilic character. Part of these silanols remain active even on octadecyl bonded phase surfaces and may reduce the efficiency of chromatographic separations of compounds with unprotected nucleophilic groups. The chemistry of this

population is still unknown, although traces of metals in the silica matrix are suspected to be a possible cause<sup>54</sup>. Blocking of these highly retentive sites can result in an improvement in column efficiency, a reduced dependence of retention on sample size, an improved sample recovery, an improved hydrolysis of the phase, a lower adsorptivity for basic compounds and an increased mechanical stability<sup>32,36-38,40,43,119</sup>. Three strategies have been adopted in the literature for avoiding adsorption on the strongly retentive sites:

- (1) rehydration of the silica surface to obtain a fully hydroxylated surface<sup>32,40</sup>;
- (2) synthesis of the bonded phase by a method that permits these strongly interacting sites to react<sup>36,37</sup>;
- (3) blocking of the sites in the chromatographic column with an amine in the mobile phase<sup>119,163,167-169</sup>.

We have also shown that the physical properties of silica may influence the coverage, and the importance of the pore size distribution is emphasized.

An excellent, recently published review on HPLC packing development can be recommended to the reader for other aspects of the synthesis and behaviour of packings<sup>171</sup>.

## 5. SUMMARY

This review does not pretend to cover all the achievements of the technology for the synthesis of bonded phases for HPLC. We have rather reviewed some selected topics connected with the preparation of alkyl bonded phases. Particular emphasis is put on the undesirable adsorption of nucleophilic compounds on both modified and unmodified silica surfaces. The advantages of reducing the number of strong adsorption sites are pointed out. A more detailed discussion is given of silanols as adsorption centres, metal impurities in the silica matrix and the highly retentive population of silanols.

## REFERENCES

- 1 R. K. Iler, *The Colloid Chemistry of Silica and Silicates*, Cornell University Press, New York, 1955.
- 2 K. K. Unger, *Porous Silica*, Elsevier, Amsterdam, 1979.
- 3 I. E. Neimark and R. Yu. Sheinfain, *Silikagel, Ego Poluchenie, Svoistva i Primenenie*, Naukova Dumka, Kiev, 1973.
- 4 M. Verzele, C. Dewaele and D. Duquet, *J. Chromatogr.*, 329 (1985) 351.
- 5 H. Engelhardt and H. Müller, *J. Chromatogr.*, 218 (1981) 395.
- 6 R. E. Majors, *Int. Lab.*, Nov/Dec. (1975) 11.
- 7 G. Berendsen and L. de Galan, *J. Liq. Chromatogr.*, 1 (1978) 403.
- 8 W. Strubert, *Chromatographia*, 6 (1973) 50.
- 9 M. L. Hair and W. Hertl, *J. Phys. Chem.*, 72 (1969) 4269.
- 10 L. R. Snyder, *Principles of Adsorption Chromatography*, Marcel Dekker, New York, 1968.
- 11 L. R. Snyder and J. W. Ward, *J. Phys. Chem.*, 70 (1966) 3941.
- 12 M. L. Miller, R. W. Linton, G. E. Maciel and B. L. Hawkins, *J. Chromatogr.*, 319 (1985) 9.
- 13 L. T. Zhuravlev and A. V. Kiselev, in D. H. Everett and R. H. Ottewill (Editors), *Proceedings of the IUPAC International Symposium on Surface Area Determinations*, Butterworths, London, 1970, p. 155.
- 14 L. R. Snyder and H. Poppe, *J. Chromatogr.*, 184 (1980) 363.
- 15 R. K. Iler, *J. Chromatogr.*, 209 (1981) 341.
- 16 V. Ya. Davydov, L. T. Zhuravlev and A. V. Kiselev, *Russ. J. Phys. Chem.*, 38 (1964) 2254.
- 17 A. V. Kiselev and V. I. Lygin, *Infrared Spectra of Surface Compounds*, Wiley-Interscience, New York, 1975.

- 18 C. Clark-Monks and E. Ellis, *J. Colloid Interface Sci.*, **44** (1973) 37.
- 19 M. J. D. Low, E. McNelis and H. Mark, *J. Catal.*, **100** (1986) 328.
- 20 C. Morterra and M. J. D. Low, *J. Catal.*, **28** (1973) 265.
- 21 K. G. Krasilnikov, V. F. Kiselev and E. A. Sysoev, *Dokl. Akad. Nauk SSSR*, **116** (1957) 990.
- 22 M. L. Hair and W. Hertl, *J. Phys. Chem.*, **74** (1970) 91.
- 23 D. N. Strazhesko, V. B. Strelko, V. N. Belyakov and S. C. Rubanik, *J. Chromatogr.*, **102** (1974) 191.
- 24 C. Walling, *J. Am. Chem. Soc.*, **72** (1950) 1164.
- 25 D. L. Dugger, J. H. Stanton, B. N. Irby, B. L. McConnell, W. W. Cummings and R. W. Maatman, *J. Phys. Chem.*, **68** (1964) 757.
- 26 B. N. Karger, J. N. LePage and N. Tanaka, in Cs. Horvath (Editor), *High Performance Liquid Chromatography — Advances and Perspectives*, Vol. 2, Academic Press, New York, 1980, p. 133.
- 27 R. E. Majors, in Cs. Horvath (Editor), *High Performance Liquid Chromatography — Advances and Perspectives*, Vol. 1, Academic Press, New York, 1980, p. 78.
- 28 T. Bernstein, H. Ernst, D. Freude, I. Juenger, B. Standte and J. Sauer, *Z. Phys. Chem. (Leipzig)*, **262** (1981) 1123.
- 29 H. Müller and H. Engelhardt, in I. Molnar (Editor), *Practical Aspects of Modern HPLC*, Walter de Gruyter, Berlin, New York, 1982, p. 25.
- 30 S. H. Hansen, P. Helboe and M. Thomsen, *J. Chromatogr.*, **368** (1986) 39.
- 31 L. C. Sander and L. A. Wise, *Adv. Chromatogr.*, **25** (1986) 139.
- 32 J. Köhler and J. J. Kirkland, *J. Chromatogr.*, **385** (1987) 125.
- 33 B. Buszewski, D. Berek, J. Garaj, I. Nowak and Z. Supryniewicz, *J. Chromatogr.*, **446** (1988) 191.
- 34 E. Bayer, K. Albert, J. Reimers, M. Nieder and D. Müller, *J. Chromatogr.*, **264** (1983) 197.
- 35 D. W. Sindorf and G. E. Maciel, *J. Phys. Chem.*, **86** (1982) 5208.
- 36 D. B. Marshall, K. A. Stutter and C. H. Lochmüller, *J. Chromatogr. Sci.*, **22** (1984) 217.
- 37 D. B. Marshall, C. L. Cole and D. E. Connolly, *J. Chromatogr.*, **361** (1986) 71.
- 38 D. B. Marshall, C. L. Cole and A. D. Norman, *J. Chromatogr. Sci.*, **25** (1987) 262.
- 39 M. Mauss and H. Engelhardt, *J. Chromatogr.*, **371** (1986) 235.
- 40 J. Köhler, D. B. Chase, R. D. Farlee, A. J. Vega and J. J. Kirkland, *J. Chromatogr.*, **352** (1986) 275.
- 41 J. Nawrocki, *J. Chromatogr.*, **362** (1986) 117.
- 42 J. Nawrocki, *J. Chromatogr.*, **391** (1987) 266.
- 43 J. Nawrocki, *J. Chromatogr.*, **407** (1987) 171.
- 44 J. Nawrocki, *Chromatographia*, **23** (1987) 722.
- 45 M. Verzele, M. DePotter and J. Ghysels, *J. High Resolut. Chromatogr. Chromatogr. Commun.*, **2** (1979) 151.
- 46 M. Verzele, *LC — Mag. Liq. Chromatogr. HPLC*, **1** (1983) 217.
- 47 M. Verzele and C. Dewaele, *J. Chromatogr.*, **217** (1981) 399.
- 48 J. Gobet and E. Sz. Kováts, *Adsorption Science & Technology*, **1** (1984) 111.
- 49 P. J. Hendra, J. R. Horder and E. J. Loader, *J. Chem. Soc. A*, (1971) 1766.
- 50 J. Adams and C. S. Giam, *J. Chromatogr.*, **285** (1984) 81.
- 51 D. Heidrich, D. Volkmann and B. Zurawski, *Chem. Phys. Lett.*, **80** (1981) 60.
- 52 I. Altug and M. L. Hair, *J. Phys. Chem.*, **71** (1967) 4260.
- 53 M. Kermarec, M. Briend-Faure and D. Delafosse, *J. Chem. Soc., Faraday Trans. 1*, (1974) 2180.
- 54 P. C. Sadek, C. J. Koester and L. D. Bowers, *J. Chromatogr. Sci.*, **25** (1987) 489.
- 55 A. V. Kiselev, B. V. Kuznetsov and S. N. Lanin, *J. Colloid Interface Sci.*, **69** (1979) 148.
- 56 S. G. Ash, A. V. Kiselev and B. V. Kuznetsov, *Trans. Faraday Soc.*, **67** (1971) 3118.
- 57 E. Robinson and R. A. Ross, *J. Chem. Soc. A*, (1970) 84.
- 58 P. B. West, G. L. Haller and R. L. Burwell, Jr., *J. Catal.*, **29** (1973) 486.
- 59 A. V. Kiselev, *Q. Rev. Chem. Soc.*, **15** (1961) 99.
- 60 E. Papirer, A. Vidal, Wang Meng Jiao and J. B. Donnet, *Chromatographia*, **23** (1987) 279.
- 61 J. Cusumano and M. J. D. Low, *J. Phys. Chem.*, **74** (1970) 792.
- 62 J. Cusumano and M. J. D. Low, *J. Phys. Chem.*, **74** (1970) 1950.
- 63 K. Tanabe, *Solid Acids and Bases, Their Catalytic Properties*, Kodansha, Tokyo, and Academic Press, New York, 1970; Russian edition, Mir, Moscow, 1973.
- 64 T. Paryczak, *Gas Chromatography in Adsorption and Catalysis*, Ellis Horwood, Chichester, 1986.
- 65 P. E. Eberly, *J. Phys. Chem.*, **65** (1961) 68 and 1261.
- 66 A. Waksmundzki, W. Rudziński, Z. Supryniewicz, R. Lebeda and M. Lasoń, *J. Chromatogr.*, **92** (1974)

- 67 W. Rudziński, A. Waksmundzki, R. Leboda, Z. Suprynowicz and M. Lasoń, *J. Chromatogr.*, 92 (1974) 25.
- 68 R. Leboda, S. Sokołowski, J. Rynkowski and T. Paryjczak, *J. Chromatogr.*, 138 (1977) 309.
- 69 J. Gawdzik, Z. Suprynowicz and M. Jaroniec, *J. Chromatogr.*, 131 (1977) 7.
- 70 W. T. Cooper and J. M. Hayes, *J. Chromatogr.*, 314 (1984) 111.
- 71 J. B. Sorrell and R. Rowan, Jr., *Anal. Chem.*, 42 (1970) 1712.
- 72 R. Rowan, Jr. and J. B. Sorrell, *Anal. Chem.*, 42 (1970) 1716.
- 73 D. W. Sindorf and G. E. Maciel, *J. Am. Chem. Soc.*, 105 (1983) 1487.
- 74 D. Farin and D. Avnir, *J. Chromatogr.*, 406 (1987) 317.
- 75 J. de Zeeuw, R. C. M. de Nijs and L. T. Henrich, *J. Chromatogr. Sci.*, 25 (1987) 71.
- 76 D. L. Saunders, *J. Chromatogr.*, 125 (1976) 163.
- 77 R. Leboda, A. Waksmundzki and S. Sokołowski, *J. Chromatogr.*, 124 (1976) 60.
- 78 G. Curthoys, Y. Ya. Davydov, A. V. Kiselev, S. A. Kiselev and B. V. Kuznetsov, *J. Colloid Interface Sci.*, 48 (1974) 54.
- 79 C. Giddings, *Anal. Chem.*, 35 (1963) 1999.
- 80 R. E. Majors, *J. Chromatogr. Sci.*, 18 (1980) 489.
- 81 A. P. Goldberg, *Anal. Chem.*, 54 (1982) 342.
- 82 K. Jones, *J. Chromatogr.*, 392 (1987) 1.
- 83 K. Jones, *J. Chromatogr.*, 392 (1987) 11.
- 84 S. D. Fazio, S. A. Tomellini, Hsu Shih-Hsien, J. B. Crowther, T. V. Raglione, T. R. Floyd and R. A. Hartwick, *Anal. Chem.*, 57 (1985) 1559.
- 85 L. C. Sander and S. A. Wise, *Anal. Chem.*, 56 (1984) 504.
- 86 L. C. Sander and S. A. Wise, *J. Chromatogr.*, 316 (1984) 163.
- 87 K. D. Lork, K. K. Unger and J. N. Kinkel, *J. Chromatogr.*, 352 (1986) 199.
- 88 J. N. Kinkel and K. K. Unger, *J. Chromatogr.*, 316 (1984) 193.
- 89 C. J. Little, A. D. Dale, J. A. Whatley and M. B. Evans, *J. Chromatogr.*, 171 (1979) 431.
- 90 E. sz. Kováts, *Ger. Pat.*, 2 930 516, 1979.
- 91 K. Szabo, Ngol Le Ha, P. Schneider, P. Zeltner and E. sz. Kováts, *Helv. Chim. Acta*, 67 (1984) 2128.
- 92 D. Morel and J. Serpinet, *J. Chromatogr.*, 200 (1980) 95.
- 93 D. Morel and J. Serpinet, *J. Chromatogr.*, 214 (1981) 202.
- 94 D. Morel and J. Serpinet, *J. Chromatogr.*, 248 (1982) 231.
- 95 P. Claudy, J. M. Letoffé, C. Gaget, D. Morel and J. Serpinet, *J. Chromatogr.*, 329 (1985) 331.
- 96 C. Gonnet, D. Morel, E. Ramamonjirinirina, J. Serpinet, P. Claudy and J. M. Letoffé, *J. Chromatogr.*, 330 (1985) 227.
- 97 D. Morel, K. Tabar, J. Serpinet, P. Claudy and J. M. Letoffé, *J. Chromatogr.*, 395 (1987) 73.
- 98 B. Buszewski, A. Jurasek, J. Garaj, L. Nondek, I. Novak and D. Berek, *J. Liq. Chromatogr.*, 10 (1987) 2325.
- 99 B. Buszewski and Z. Suprynowicz, *Chromatographia*, 24 (1987) 573.
- 100 G. E. Berendsen, K. A. Pikaart and L. de Galan, *J. Liq. Chromatogr.*, 3 (1980) 1437.
- 101 H. Engelhardt, B. Dreyer and H. Schmidt, *Chromatographia*, 16 (1982) 11.
- 102 H. Hemetsberger, W. Maasfeld and H. Ricken, *Chromatographia*, 9 (1976) 303.
- 103 M. C. Hennon, C. Picard and M. Caude, *J. Chromatogr.*, 166 (1978) 21.
- 104 K. K. Unger, N. Becker and P. Roumeliotis, *J. Chromatogr.*, 125 (1976) 115.
- 105 G. E. Berendsen, K. A. Pikaart and L. de Galan, *Chromatogr. Sci.*, 2 (1982) (Biol. Biomed. Appl. Liq. Chromatogr.) 97.
- 106 G. Schomburg, A. Deege, J. Köhler and U. Bien-Vogelsang, *J. Chromatogr.*, 282 (1983) 27.
- 107 B. Buszewski, L. Nondek, A. Jurašek and D. Berek, *Chromatographia*, 23 (1987) 442.
- 108 D. G. I. Kingston and B. B. Gerhart, *J. Chromatogr.*, 116 (1976) 182.
- 109 J. Gobert and E. sz. Kováts, *Adsorption Science & Technology*, 1 (1984) 77.
- 110 R. P. W. Scott and P. Kucera, *J. Chromatogr. Sci.*, 13 (1975) 337.
- 111 J. M. L. van de Venne, *Ph.D. Thesis*, Technische Hogeschool, Eindhoven, 1979.
- 112 T. Welsch and H. Frank, *J. Chromatogr.*, 267 (1983) 39.
- 113 H. Frank, *PhD Thesis*, Karl Marx Universität, Leipzig, 1985.
- 114 L. Boksanýi, O. Liardon and E. sz. Kováts, *Adv. Colloid Interface Sci.*, 6 (1976) 95.
- 115 G. Schomburg, A. Deege, J. Köhler and U. Bien-Vogelsang, *J. Chromatogr.*, 282 (1983) 27.
- 116 J. Nawrocki, in preparation.
- 117 H. Colin and G. Guiochon, *J. Chromatogr.*, 141 (1977) 289.

- 118 A. Nahum and Cs. Horváth, *J. Chromatogr.*, 203 (1981) 53.  
119 K. E. Bij, Cs. Horváth, W. R. Melander and A. Nanum, *J. Chromatogr.*, 203 (1981) 65.  
120 G. E. Berendsen, *Ph.D. Thesis*, Delft University Press, Delft, 1980.  
121 D. A. Fritz, A. Sahil, H. P. Keller and E. sz. Kováts, *Anal. Chem.*, 51 (1979) 7.  
122 J. F. Erard and E. sz. Kováts, *Anal. Chem.*, 54 (1982) 193.  
123 J. F. Erard, L. Nagy and E. sz. Kováts, *Colloids Surf.*, 9 (1984) 109.  
124 B. Buszewski and Z. Supryniewicz, *Anal. Chim. Acta*, 208 (1988) 263.  
125 A. Dawidowicz, J. Rayss and Z. Supryniewicz, *Chromatographia*, 17 (1983) 157.  
126 J. Rayss, A. Dawidowicz, Z. Supryniewicz and B. Buszewski, *Chromatographia*, 17 (1983) 437.  
127 A. L. Dawidowicz and J. Rayss, *Chromatographia*, 20 (1985) 555.  
128 Z. Supryniewicz, J. Rayss, A. L. Dawidowicz and R. Lodkowski, *Chromatographia*, 20 (1985) 677.  
129 I. Halász and I. Sebastian, *Chromatographia*, 7 (1974) 371.  
130 Z. Supryniewicz, R. Lodkowski, A. L. Dawidowicz and B. Buszewski, *J. Chromatogr.*, 395 (1987) 145.  
131 I. Halász and I. Sebastian, *Angew. Chem.*, 8 (1969) 453.  
132 R. K. Gilpin, *J. Chromatogr. Sci.*, 22 (1984) 371.  
133 H. Hemetsberger, P. Behrensmeyer, J. Henning and H. Ricken, *Chromatographia*, 12 (1979) 71.  
134 R. P. W. Scott and C. F. Simpson, *J. Chromatogr.*, 197 (1980) 11.  
135 C. H. Lochmüller and D. R. Wilder, *J. Chromatogr. Sci.*, 17 (1979) 574.  
136 R. K. Gilpin and J. A. Squires, *J. Chromatogr. Sci.*, 19 (1981) 195.  
137 C. H. Lochmüller, A. S. Colborn, M. L. Hunnicutt and J. M. Harris, *Anal. Chem.*, 55 (1983) 1344.  
138 C. H. Lochmüller, A. S. Colborn, M. L. Hunnicutt and J. M. Harris, *J. Am. Chem. Soc.*, 106 (1984) 4077.  
139 D. Avnir, *J. Am. Chem. Soc.*, 109 (1987) 2931.  
140 R. K. Gilpin, M. E. Gangoda and A. E. Krishen, *J. Chromatogr. Sci.*, 2 (1982) 345.  
141 R. K. Gilpin and M. E. Gangoda, *Anal. Chem.*, 56 (1984) 1470.  
142 B. E. Suffolk and R. K. Gilpin, *Anal. Chem.*, 57 (1985) 596.  
143 L. C. Sander, J. B. Callis and L. R. Field, *Anal. Chem.*, 55 (1983) 1068.  
144 D. W. Sindorf and G. E. Maciel, *J. Am. Chem. Soc.*, 105 (1983) 1848.  
145 R. K. Gilpin and M. E. Gangoda, *Talanta*, 33 (1986) 176.  
146 E. Bayer, A. Paulus, B. Peters, G. Laupp, J. Reiners and K. Albert, *J. Chromatogr.*, 364 (1986) 25.  
147 J. Serpinet, *Wiad. Chem.*, 36 (1982) 703.  
148 D. E. Martire and R. E. Boehm, *J. Phys. Chem.*, 87 (1983) 1045.  
149 Cs. Horváth, W. Melander and I. Molnár, *J. Chromatogr.*, 125 (1976) 129.  
150 H. Colin, N. Ward and G. Guiochon, *J. Chromatogr.*, 149 (1978) 169.  
151 S. Eksborg, *J. Chromatogr.*, 149 (1978) 225.  
152 S. Eksborg, H. Ehrsson and U. Lönnroth, *J. Chromatogr.*, 185 (1979) 583.  
153 W. R. Melander, A. Nahum and Cs. Horváth, *J. Chromatogr.*, 185 (1979) 129.  
154 K. Karch, I. Sebastian and I. Halász, *J. Chromatogr.*, 122 (1976) 3.  
155 N. Tanaka, H. Goodell and B. L. Karger, *J. Chromatogr.*, 158 (1978) 233.  
156 W. R. Melander, J. Stoveken and Cs. Horváth, *J. Chromatogr.*, 199 (1980) 35.  
157 L. Nondek, B. Buszewski and D. Berek, *J. Chromatogr.*, 360 (1986) 241.  
158 P. C. Sadek and P. W. Carr, *J. Chromatogr. Sci.*, 21 (1983) 314.  
159 J. J. Kirkland, *Chromatographia*, 8 (1975) 661.  
160 E. J. Kikta, Jr. and E. Grushka, *Anal. Chem.*, 48 (1976) 1098.  
161 J. H. Knox and J. Jurand, *J. Chromatogr.*, 142 (1977) 651.  
162 J. K. Baker, *Anal. Chem.*, 51 (1979) 1693.  
163 E. Bayer and A. Paulus, *J. Chromatogr.*, 400 (1987) 1.  
164 D. B. Marshall, J. W. Burns and D. E. Connolly, *J. Am. Chem. Soc.*, 108 (1986) 1087.  
165 D. B. Marshall, J. W. Burns and D. E. Connolly, *J. Chromatogr.*, 360 (1986) 13.  
166 C. H. Lochmüller, D. B. Marshall and D. R. Wilder, *Anal. Chim. Acta*, 130 (1981) 31.  
167 A. Wehrli, J. C. Hildebrand, H. P. Keller, R. Stampfli and R. W. Frei, *J. Chromatogr.*, 149 (1987) 199.  
168 K.-G. Wahlund and A. Sokołowski, *J. Chromatogr.*, 151 (1978) 299.  
169 W. A. Moats, *J. Chromatogr.*, 366 (1986) 69.  
170 F. P. Schmitz, D. Leyendecker and D. Leyendecker, *J. Chromatogr.*, 389 (1987) 245.  
171 L. C. Sander and S. A. Wise, *CRC Crit. Rev. Anal. Chem.*, 18 (1987) 299.

CHROM. 20 662

## PREDICTION OF BAND PROFILES IN DISPLACEMENT CHROMATOGRAPHY BY NUMERICAL INTEGRATION OF A SEMI-IDEAL MODEL

A. M. KATTI

*Department of Chemical Engineering, University of Tennessee, Knoxville, TN 37996 (U.S.A.); and Analytical Chemistry Division, Oak Ridge National Laboratory, Oak Ridge, TN 37831-6120 (U.S.A.)*

and

G. A. GUIOCHON\*

*Department of Chemistry, University of Tennessee, Knoxville, TN 37996 (U.S.A.); and Analytical Chemistry Division, Oak Ridge National Laboratory, Oak Ridge, TN 37831-6120 (U.S.A.)*

(First received February 25th, 1988; revised manuscript received May 26th, 1988)

---

### SUMMARY

A numerical solution for the semi-ideal model of chromatography, incorporating dispersion in the numerical integration scheme, has been developed for the prediction of intermediate and isotachic peak profiles of a multi-component mixture in displacement chromatography. The model was used here to study the effect of various operating parameters on the band shapes, production and yield for a binary mixture.

The effect of the displacer concentration and the column length on the yield and the production was investigated. Optimal concentrations can be found that maximize the yield or the production. Very low displacer concentrations lead to peak shapes identical with those in overloaded elution chromatography and extremely large displacer concentrations result in the lack of a separation. The band profiles obtained prior to the formation of the isotachic train are in agreement with profiles taken from the literature.

---

### INTRODUCTION

The differences between elution and displacement chromatography were recognized by Tswett in the early 1900s<sup>1</sup>; however, it was in 1942 that Tiselius<sup>2</sup> clearly defined and discussed the various possible modes of chromatography (elution, frontal and displacement). During the last 40 years the enormous growth of linear elution chromatography for analytical separations has overshadowed the use of displacement chromatography, in spite of the development of several important industrial applications that took place during this period. In the 1940s, the isolation of various rare earth oxides was accomplished in the displacement mode<sup>3</sup>, which proved to be more productive than elution chromatography<sup>4</sup>. Later, displacement chromatography was employed at the American Petroleum Institute<sup>5</sup> to fractionate petroleum distillates in 52.4 ft. × 3/4 in. I.D. columns. In the 1960s, Sorbex and several other

similar processes were developed at UOP, using various novel technologies to achieve what is essentially displacement chromatography on a moving bed column, without physically moving the column packing<sup>6</sup>.

For the last four decades, however, displacement chromatography has basically been ignored by analysts and separation chemists alike and no fundamental research was carried out in this area until in the late 1970s when Horváth and co-workers reintroduced the technique. They were able to capitalize on the various technological advances developed for elution chromatography, *e.g.*, microparticulate stationary phases, high-efficiency columns and fast high-performance liquid chromatography (HPLC) analyses to follow the band profiles at the column exit. They developed methods for separating small organic molecules<sup>7</sup>, polymyxin antibiotics<sup>8</sup>, steroids<sup>9</sup>, amino acids<sup>10</sup>, short peptides<sup>11-13</sup>, nucleotides<sup>14</sup> and, more recently, proteins<sup>15</sup>. The utility of this method has been confirmed by other results for the separation of insulins<sup>16</sup> and oligomycins<sup>17</sup>. Carrier displacement chromatography has been employed for the displacement of proteins using carboxymethyl dextrans as spacers as well as a displacer<sup>18-20</sup>. Other workers have investigated the separation of lithium isotopes<sup>21-24</sup> for either the enrichment or the isolation of pure isotopes by ion-exchange displacement chromatography. These studies demonstrated experimentally the utility of this technique for the separation of various mixtures and its capacity to achieve high yields and high purities.

On the theoretical front, various models have been proposed to describe the displacement process. Gluckauf<sup>25</sup> provided an analysis of displacement development and discussed the importance of the solute and displacer concentrations on the band development. The equations corresponding to ideal chromatography have been solved by Helfferich and Klein<sup>26</sup>, employing the H-transform, and in a similar approach by Rhee and Amundson<sup>27</sup>. Experimental studies showed good agreement between theory and experiment<sup>28</sup>. More recently, Basmadjian and Coroyannakis<sup>29</sup> proposed a model neglecting accumulation in the fluid phase and axial dispersion, and assuming infinitely fast mass transfer. They discussed the importance of the displacer adsorption strength and its concentration on the profiles of a two-component system (one solute and one displacer). However, in real systems one does not have an infinite column efficiency and one does not have vertical boundaries between the isotachic bands<sup>30</sup>. Guiochon and co-workers<sup>31,32</sup> developed a numerical solution of the system of partial differential equations accounting for the behavior of chromatographic systems under non-linear, non-ideal conditions. These results were used for the simulation of the separation of multi-component samples in overloaded elution chromatography<sup>33-36</sup>. We report here on the application of these theoretical results to the prediction of isotachic and non-isotachic band profiles in displacement chromatography. The model was extended to three components (two solutes in a binary mixture and the displacer) and the initial conditions were adjusted accordingly.

## THEORETICAL

Neglecting axial dispersion and assuming infinitely fast kinetics of radial mass transfer, we can write the following mass balance for each component involved in the process:

$$(1 + k'_i) \frac{\partial C_i}{\partial t} + u \cdot \frac{\partial C_i}{\partial z} = 0 \quad (1)$$

where  $t$  is time,  $z$  the column length,  $C_i$  the concentration of each species in the mobile phase,  $u$  the linear velocity of the mobile phase and

$$k'_i = \varphi \cdot \frac{\partial q_i}{\partial C_i} \quad (2)$$

where  $q_i$  is the concentration of each species in the stationary phase at equilibrium and  $\varphi$  is the stationary phase to mobile phase ratio<sup>31,32</sup>. This is the classical model of ideal chromatography<sup>26,27,31</sup>.

Competitive Langmuir isotherms were employed for each component in the solution and for the displacer. They have the form

$$q_i = a_i C_i / (1 + \sum b_i C_i) \quad (3)$$

Eqn. 3 corresponds to the simplest model of competitive adsorption behavior and its representativeness will be discussed later.

A mass balance equation (eqn. 1) and an isotherm equation (eqn. 3) must be written for each component of the sample and for the displacer. The carrier is inert in classical displacement chromatography, and therefore no mass balance was written for it. The system is solved numerically using a finite difference method<sup>31</sup>. It has been shown that a stable numerical solution is obtained if the space and time increments used for the calculations are chosen appropriately to meet the Courant–Friedrichs–Lewy condition<sup>37</sup>. The finite column efficiency can be accounted for by relating the space increment to the Courant number and the HETP of the chromatographic column used<sup>32</sup>. We have chosen a Courant number of 2 and the values of the respective space and time increments are given by

$$\delta z = H \quad (4)$$

$$\delta t = 2H/uz \quad (5)$$

where  $uz$  is the average velocity of the concentration profiles at infinite dilution. Comparison between experimental and theoretical results for the elution of large concentration bands of a pure compound showed excellent agreement between the recorded and predicted profiles<sup>38</sup>.

In displacement chromatography, the column is first equilibrated with a carrier stream, a mobile phase which elutes the solutes considered with large retention factors. Then the feed (the solute mixture, usually dissolved in the mobile phase) is injected or pumped into the column. Lastly, the displacer, a solution containing a species which is more strongly adsorbed than any of the feed components, is pumped continuously through the column until all the components of the feed have left the column. A typical batch process involves a final step of regenerating the column on completion of the displacement process and re-equilibration with a carrier stream. Then the column is ready for the next run. The regeneration process has not been modeled in this study.

The initial and boundary conditions for displacement chromatography (the displacer is component  $n$ ) are

$$t \leq 0: 0 < z < L, C_i = 0, i = 1, n \quad (6)$$

$$0 < t < R\delta t: z = 0, C_i = C_i^0, i = 1, n - 1, C_n = 0 \quad (7)$$

$$R\delta t < t < t_a: z = 0, C_i = 0, i = 1, n - 1, C_n = D_0 \quad (8)$$

where  $C_i^0$  is the concentration of component  $i$  in the stream entering the column,  $D_0$  is the displacer concentration,  $t_a$  is the analysis time and  $R\delta t$  is the time it takes for the sample to enter the column. In practice, the sample volume can be significant compared with the column volume and then the sample concentration is relatively dilute. However, the components are retained strongly by the packing material in the carrier. Moreover, it is practical to express the sample size as a fraction of the column saturation capacity<sup>39</sup>.

## RESULTS AND DISCUSSION

In displacement chromatography, the displacer plays an essential role in the separation process. It can be shown that provided the concentration of the displacer is large enough and the column is long enough, an isotachic train forms<sup>7,25</sup>. The profile of each zone is stable and its width depends on the amount of each solute in the sample. The concentration of the isotachic zone depends on the concentration of the displacer,  $D_0$ , and its isotherm, *i.e.*, on the characteristic speed of its front<sup>40</sup>. The concentrations of the individual solute species under isotachic conditions are given by the intersection of solute isotherms with the operating line. The operating line (Fig. 1) is the chord extending from the origin to the displacer isotherm and which has a slope  $q_1/D_1$ , where  $q_1$  is the equilibrium concentration of the displacer in the stationary phase corresponding to  $D_1$ .

Investigations of the role of the displacer in displacement development and the effect of its concentration on the height and the width of rectangular isotachic displacement bands have been carried out employing the ideal model of chromatography<sup>26</sup>. We used here a more realistic semi-ideal model which provides exact predictions of zone profiles as long as the kinetics of mass transfer between mobile and stationary phase are fast. This model provides an opportunity to view isotachic and non-isotachic peak profiles under non-ideal conditions and to investigate the effects of the experimental conditions on the yield, production and product purity. The effects of the displacer concentration and of the column length will be discussed in some detail here to demonstrate the utility of the model and to illustrate the importance of these two parameters in the optimization of the displacement process for a two-component separation problem.

In presenting the results of a computer simulation, the parameters of the model must have specific values. The results presented here consider the separation of a binary mixture (concentration ratio 1:3) with retention factors ( $k'$ ) for component 1, component 2 and the displacer of 5.75, 6.25 and 7.5, respectively. These values are reasonable and typical. We note that the relative retention of the displacer with respect

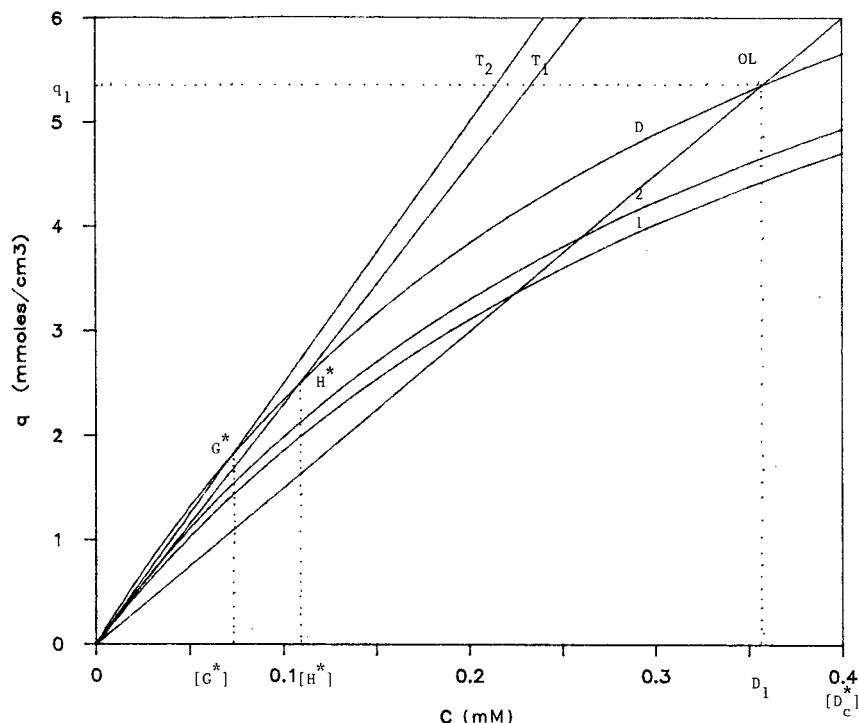


Fig. 1. Single-component adsorption isotherms for each component and the displacer. OL = operating line;  $T_1$  = tangent to component 1 isotherm;  $T_2$  = tangent to component 2 isotherm.

to component 2 is 1.2 and that it need not be too large. The column void fraction was assumed to be 0.8. The parameters of the ternary isotherm,  $b_1$ ,  $b_2$ ,  $b_3$ , are 2.38, 2.56 and 2.8  $\text{mmol}^{-1}$ , respectively. These three isotherms are slowly divergent (Fig. 1). The column HETP was 48  $\mu\text{m}$ , which corresponds to a well packed column with 15–20  $\mu\text{m}$  particles, a grade frequently used at present in preparative applications. Much lower values of  $H$  could be achieved with real columns. Such columns would take a longer CPU time to simulate than the columns used here.

The column lengths were varied from 5 to 50 cm and the displacer concentrations from 0.02 to  $> 6 \text{ mM}$ . The individual zone profiles and the total profiles presented can be considered to be the response of a specific detector and non-specific detector, respectively. In these simulations, unless stated otherwise, the injection simulates a Dirac injection pulse as a narrow rectangular band of width  $\delta t$ . The sample size is 0.2 mmol, which is 1.3% of the column saturation capacity.

#### *Effect of displacer concentration*

The effect of the displacer concentration on the shape of the band profiles on a 25-cm column with the parameters specified above is illustrated in Figs. 2 and 3. Fig. 2a shows that at low displacer concentrations the band shape corresponds to that obtained in overloaded elution chromatography. The velocity of the solute band is greater than that of the displacer and no interference occurs between the zones of the

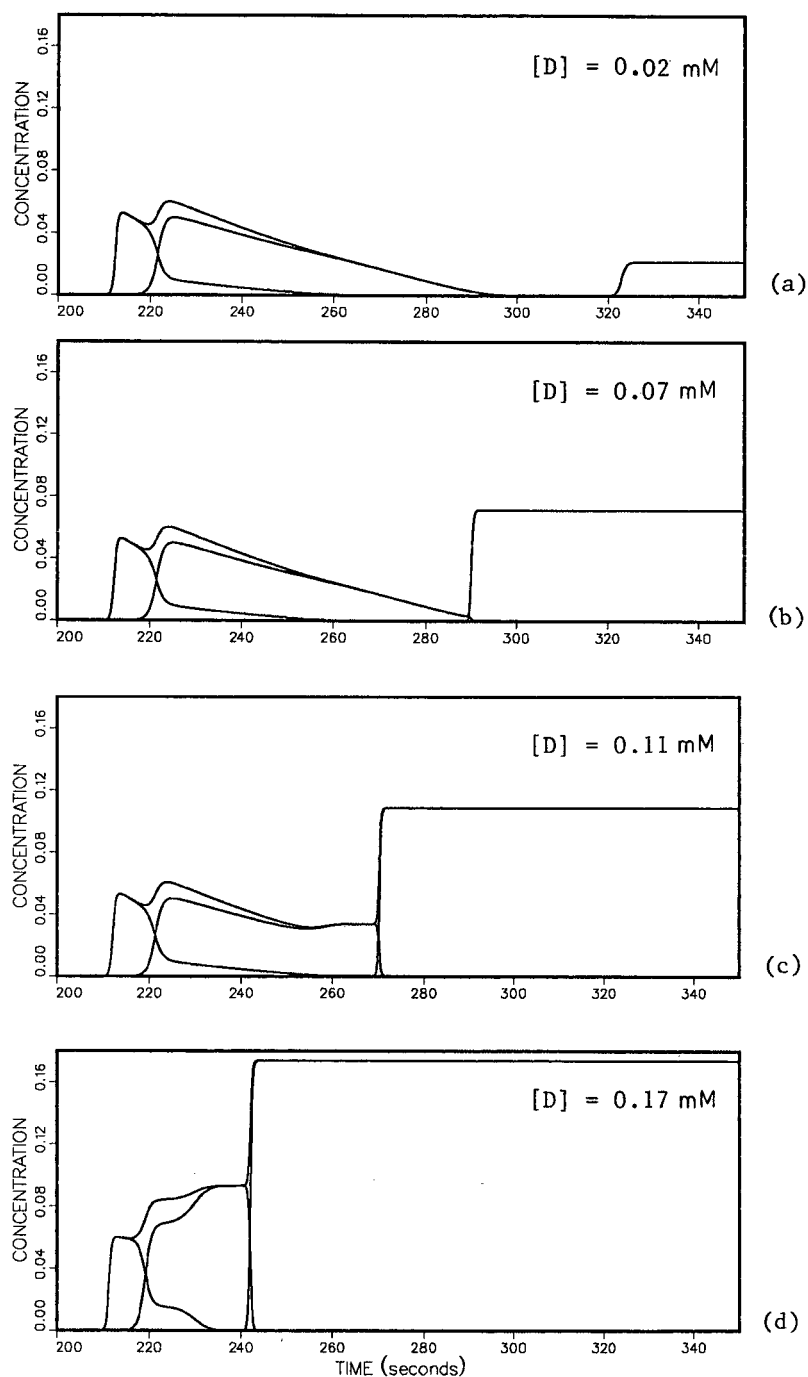


Fig. 2. Effect of the concentration of the displacer on the displacement profile at 25 cm (the abscissa scales are the same for all figures).  $[D]$ : (a) 0.02; (b) 0.07; (c) 0.11; (d) 0.17 mM.

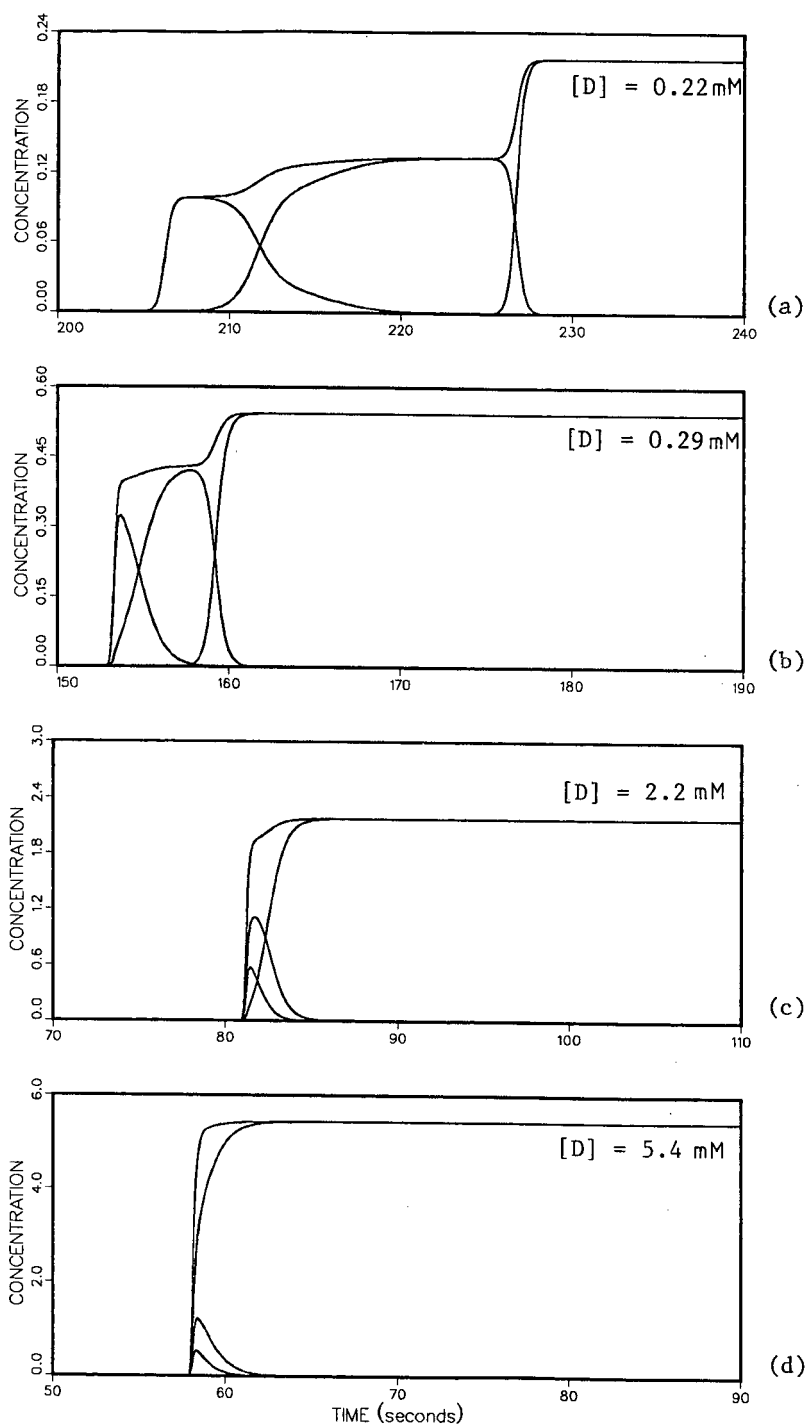


Fig. 3. Effect of the displacer concentration on the displacement profile at 25 cm (the width of the chromatogram is constant).  $[D]$ : (a) 0.22; (b) 0.29; (c) 2.2; (d) 5.4 mM.

displacer and the solute. As the displacer concentration is increased, the velocity of the displacer front increases; however, the retention time of the overload band remains unchanged until a critical displacer concentration,  $G^*$ , is reached. This critical concentration corresponds to the intersection of the initial slope of the second component  $[(n-1)\text{th component}]$  isotherm with the displacer isotherm, illustrated in Fig. 1. At this concentration the front of the displacer meets the tail of the second component just as it exits the column, hence with essentially no interference (Fig. 2b); at concentrations below  $G^*$ , components 1 and 2 propagate down the column as in overloaded elution chromatography.

As the displacer concentration is increased beyond  $G^*$ , interference occurs between the bands of the second component and the displacer, in addition to interference between the bands of the two solutes (Fig. 2c). The displacer front begins to push and sharpen the rear of the second component, giving rise to the early stages of displacement development as seen by the formation of a secondary front (Fig. 2c). When the operating line coincides with the tangent to the first component isotherm at zero concentration, the intersection is given by  $H^*$  and is illustrated in Fig. 1. Under isotachic conditions, displacer concentrations corresponding to  $H^*$  result in the first component eluting as an overloaded band or an elution band for concentrations in the linear region of the isotherm, as expected. Under non-isotachic conditions, however, Fig. 2c shows that after 25 cm the secondary front has reached the tail of the first component. For displacer concentrations higher than  $H^*$ , at 25 cm the secondary front has distorted the tail of the first component, giving rise to the displacement effect for the first component (Fig. 2d). For displacer concentrations higher than  $H^*$ , but lower than some critical value to be discussed later, isotachic displacement bands form with plateaux on both peaks on columns of sufficient length.

As the displacer concentration is increased further, beyond  $H^*$ , the tails of the bands sharpen, their width decreases and their height increases (Fig. 3a). Note that the time scales in Fig. 3 are much larger than those in Fig. 2. Moreover, in Fig. 2 the absolute scale is the same on the graphs whereas in Fig. 3 the absolute scale changes, but the relative scale is the same. However, as it is not physically possible to obtain an infinitely high concentration for an infinitely narrow band, nor would one expect to return to the initial injection conditions because of band broadening, something must occur at high displacer concentrations. As the displacer concentration is increased further, the displacer begins to squeeze components 1 and 2 whose bands interfere more and more strongly. The amount of band overlap equals the band width (Fig. 3b) and eventually neither product can be obtained with 99% purity. We call this critical displacer concentration  $D_c^*$  and define it as the displacer concentration for which the yield of 99% pure component 1 becomes zero. Under the conditions studied here, this concentration is about 4 mM (see Figs. 1 and 4). Increasing the displacer concentration still further results in very strong band interference and in the displacer overtaking the rear boundaries of the first component, such that the front of the second component coincides with the front of the first component (Fig. 3c), and then to the displacer overtaking the peak maxima of the first and second components until all of the fronts coincide (Fig. 3d).

Fig. 2a-d shows no change in the breakthrough time of the first component at lower displacer concentrations. At higher displacer concentrations it can be seen that the breakthrough time decreases, as the velocity of the displacer front increases with

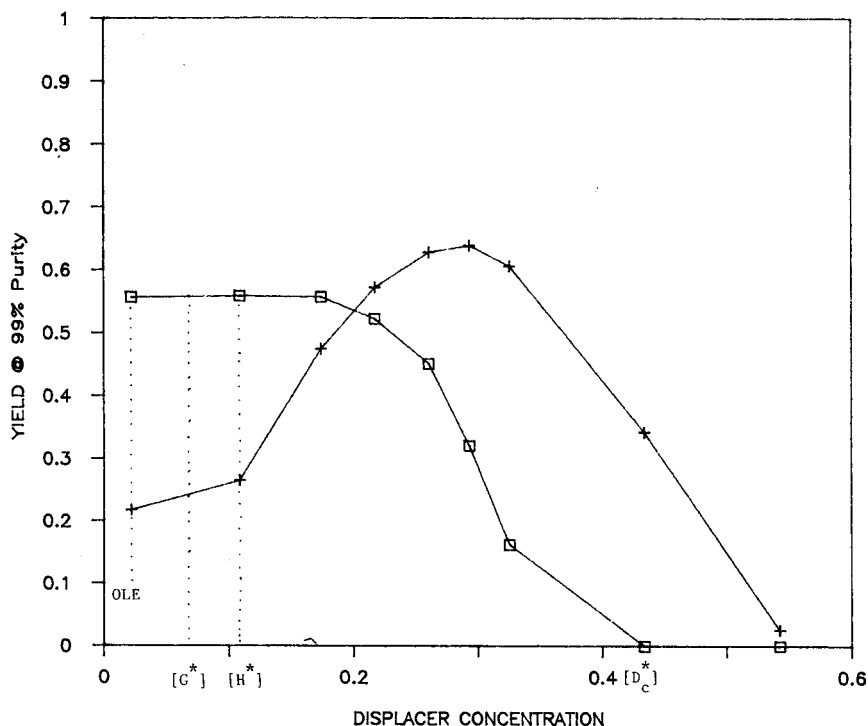


Fig. 4. Effect of the displacer concentration (mM) on the yield at 99% purity with a 25-cm column. □, Component 1; +, component 2. OLE = overloaded elution.

increasing concentration for a Langmuir isotherm. At the same time the degree of interference between neighboring bands increases and the yield decreases (Figs. 2d, 3a and 3b). There is an optimal concentration that lies between  $H^*$  and  $D_c^*$  that would lead to maximal production of the desired product(s). For the conditions in this investigation, the displacer concentration at  $G^*$ ,  $H^*$  and  $D_c^*$  are 0.071 mM (Fig. 2b), 0.109 mM (Fig. 2c) and 0.4 mM, respectively. Although the results presented here are for a specific set of conditions, similar peak profiles are seen at other values of the parameters. This specific problem is used to illustrate some of the basic stages in displacement development.

Investigation of the effect of the displacer concentration on the separation yields for components 1 and 2 at 99%, 98% and 95% purity shows that the yield of component 2 can always be increased with the use of a displacer (Figs. 4 and 5). This is not always true for component 1. The displacer concentration for which the yield of component 2 is a maximum is slightly higher when the required purity is higher. At 99% purity (Fig. 4), the yield of component 1 at first remains constant and equal to the yield achieved in overloaded elution, and then decreases with increasing displacer concentration. At 98% and 95% purity the yield of component 1 goes through a weak maximum (Fig. 5). The increase in yield at 98% purity is small but for 95% purity it is more pronounced. The result arises from the fact that component 1 has a tail and the amount to be recycled is reduced when the purity demanded is decreased.

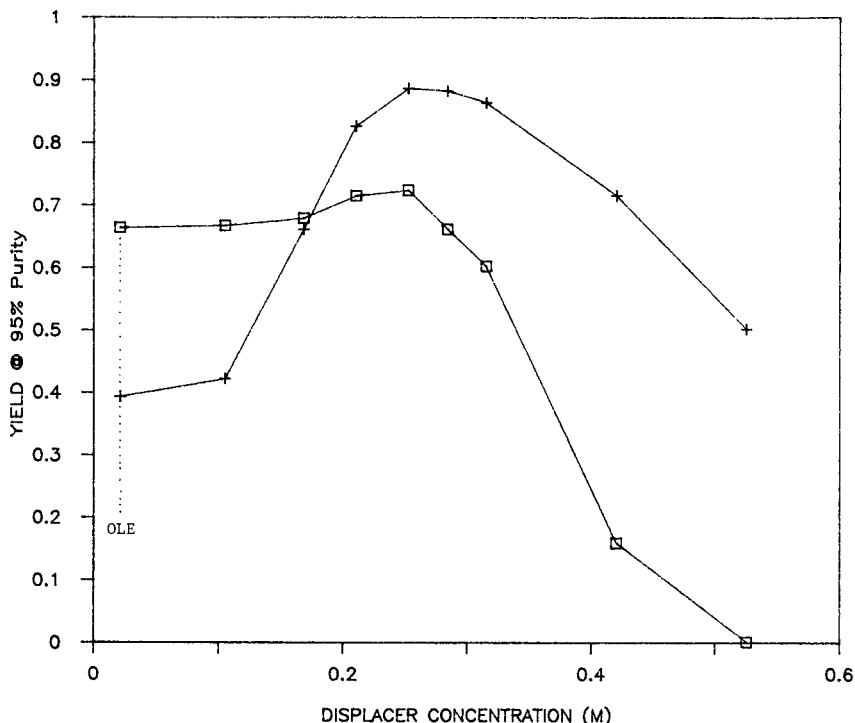


Fig. 5. Effect of the displacer concentration ( $mM$ ) on the yield at 95% purity with a 25-cm column. Symbols as in Fig. 4.

The effect of the displacer concentration on the production was also investigated for 99%, 98% and 95% purity for both components 1 and 2 (Fig. 6). In this work, production is defined as the amount of product at a specified purity recovered per run. A more realistic production rate would require an estimate of the time needed to regenerate the column. As the production is the product of the yield and the amount of feed, the trends are the same as for the yield. Fig. 6 illustrates the effect of production for components 1 and 2 at 98% purity. The key point is that the production of component 2 increases considerably with displacer concentration (more than 3-fold).

The effect of the displacer concentrations on the isotachic length (*i.e.*, the column length at which an isotachic train is formed) was studied semi-quantitatively by comparison of the peak profiles obtained at various column lengths. The results show that the length required to reach isotachic conditions decreases with increasing displacer concentration. For example, at displacer concentrations of 0.2, 0.3 and 0.5  $M$ , the isotachic lengths are approximately 45, 35 and 25 cm, respectively.

#### *Effect of column length*

The effect of column length, with all other parameters held constant, was investigated at the displacer concentration corresponding to the maximal production of component 2. Fig. 7 illustrates the effect of the column length on the peak profiles at a displacer concentration of 0.3  $M$ . In the first 5 cm, the rectangular injection plug

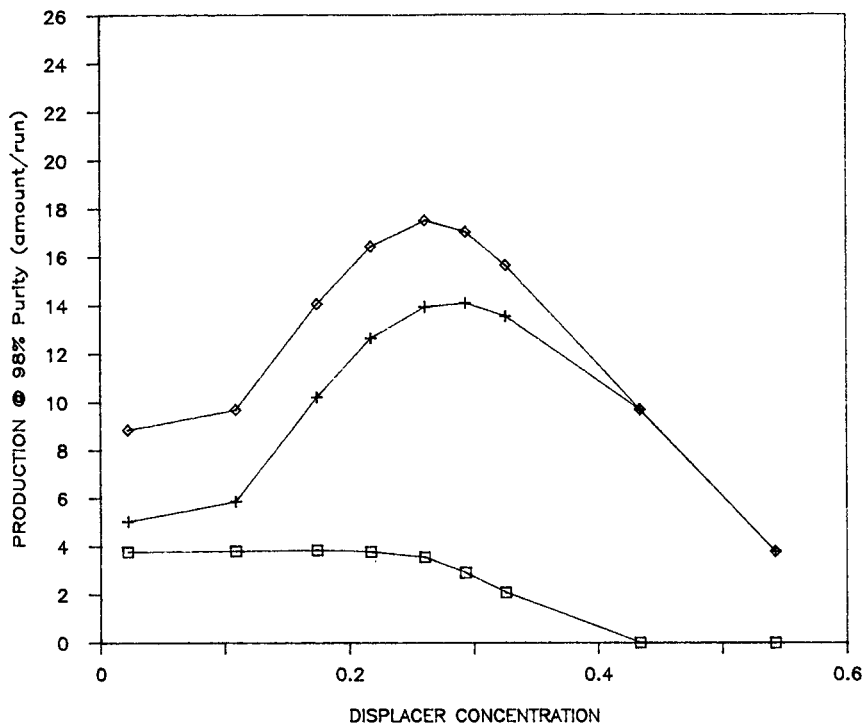


Fig. 6. Effect of the displacer concentration ( $mM$ ) on the production at 98% purity with a 25-cm column.  $\diamond$ , Total;  $\square$ , component 1; +, component 2.

having a height of 217 and a width of 0.11 s collapses to a band having a height of about 2 and a width of about 15 s (Fig. 7a). This illustrates the early stages of the displacement effect indicated by the formation of the secondary front on component 2 which begins to push the tail of component 1. At 15 cm (Fig. 7b), the rear boundary has already sharpened considerably, the tail of component 1 is less important and the fronts of the two zones are well separated. At 25 cm (Fig. 7c), the bands are almost totally resolved with increased sharpening of the rear boundary of the first component. At 35 cm (Fig. 7d), isotachic conditions have been reached, giving the maximum yield possible under the specified conditions. The band of component 2 exhibits a wide plateau, but not the band of component 1. The interference zone is reduced. The cut points corresponding to 99% purity are shown for the 25- and 35-cm columns (Fig. 7c and d). The area between the first two vertical lines represents the amount to be recycled.

The effect of column length on the yield and production at 99% purity for components 1 and 2 are shown in Figs. 8 and 9. As the column length increases, the yield increases and tends towards a limit reached for about 35 cm for 99% purity (Fig. 8). The same result is observed for production (Fig. 9) as a function of column length. When isotachic conditions are reached, there is no further increase in the production or the yield. It is clear from the Figs. 6 and 9 that there is an optimal column length and an optimal displacer concentration that will maximize the production at a specified

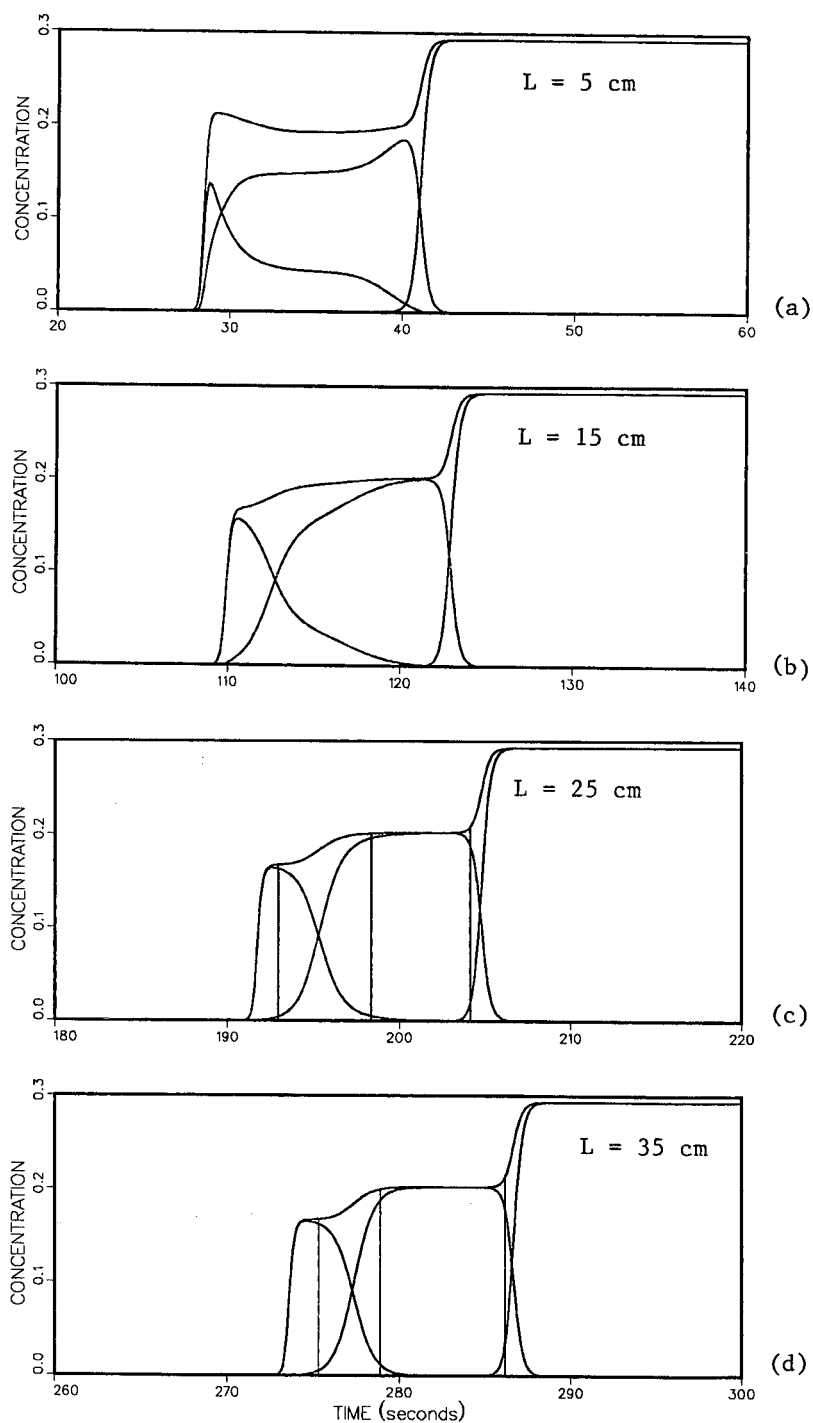


Fig. 7. Displacement profiles as a function of column length at maximal production for displacer concentrations of 0.3 mM. (a) 5; (b) 15; (c) 25; (d) 35 cm column.

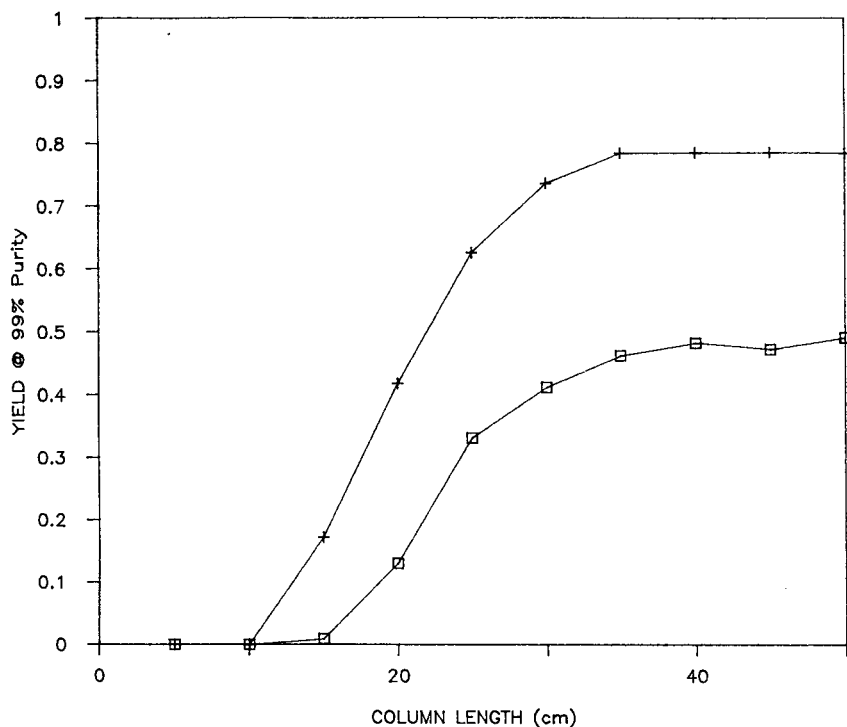


Fig. 8. Effect of column length on the yield at constant displacer concentration and 99% purity. Symbols as in Fig. 4.

purity. Obviously, these values depend on the sample size, velocity of the mobile phase, particle size and column efficiency, which will be discussed elsewhere<sup>41</sup>.

#### *Comparison with experimental results*

Semi-quantitative agreement can be found between the intermediate profiles predicted by the numerical solution and data in the literature. Horvath *et al.* (ref. 7, Fig. 12) have published intermediate profiles for the separation of 3,4-dihydroxyphenylacetic acid from 4-hydroxyphenylacetic acid with phenol as the displacer, together with the parameters of the single component isotherms of these two compounds. The single component isotherms for components 1 and 2 were employed in a competitive Langmuir model (eqn. 3) and an isotherm was assumed for the displacer. The experimental conditions for 2:1, 1:2 and 2:2 mixtures were used in our model and the peak profiles predicted are shown in Fig. 10a, b and c, respectively. Good agreement is seen between the chromatograms shown in Fig. 10 here and in Fig. 12 in ref. 7, with similar breakthrough times, similar values for the peak maxima and similar waves appearing on the tails of the bands. Slight discrepancies are seen, for example, in Fig. 10c, where the second component exhibits a plateau between the two humps, whereas in ref. 7 it rather shows a deep minimum and no plateau. This can be explained by the fact that our assumption of competitive Langmuir isotherms modeled

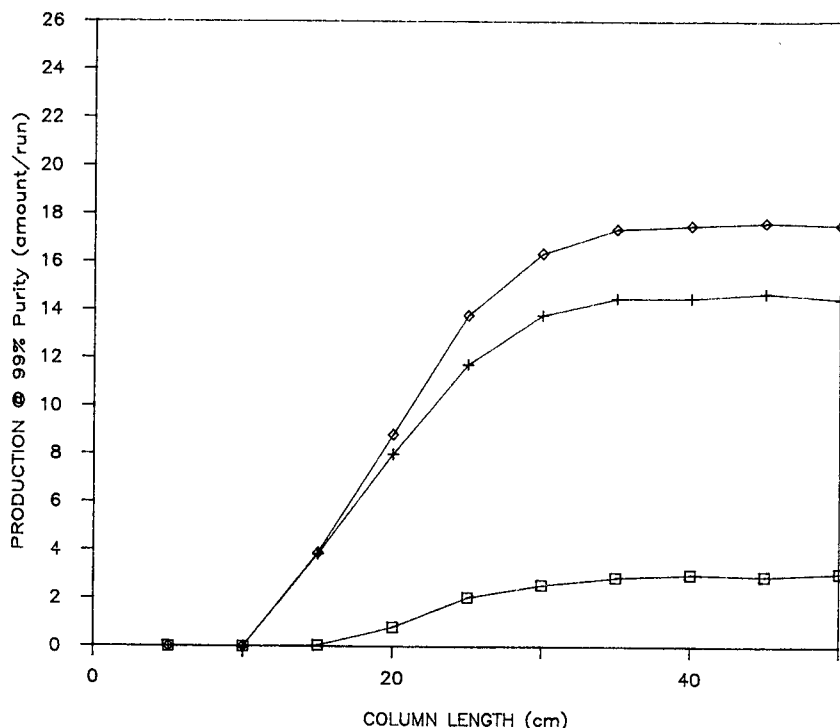


Fig. 9. Effect of column length on production at constant displacer concentration and 99% purity. Symbols as in Fig. 6.

by combining single component isotherms is very crude. It has been observed that competitive isotherms measured by frontal analysis are correctly accounted for by more complex equations<sup>42</sup>.

## CONCLUSIONS

It has been demonstrated that the proposed model allows the rapid optimization of the experimental conditions and a thorough investigation of the effect of the operating parameters on the separation. Preliminary results indicate that the prediction of experimental band profiles is satisfactory.

Finally, this work permits some comparison between overloaded elution and displacement chromatography. If in a two-component mixture the purification of the first component is of interest, then overloaded elution chromatography can achieve this goal satisfactorily and no significant gain in the recovery yield or production is brought by the use of a displacer. This is not the case if isolation of the second component is desired. The question is whether these gains are sufficient to compensate for the case of the displacer and the regeneration step. Work is in progress to investigate this problem<sup>41</sup>.

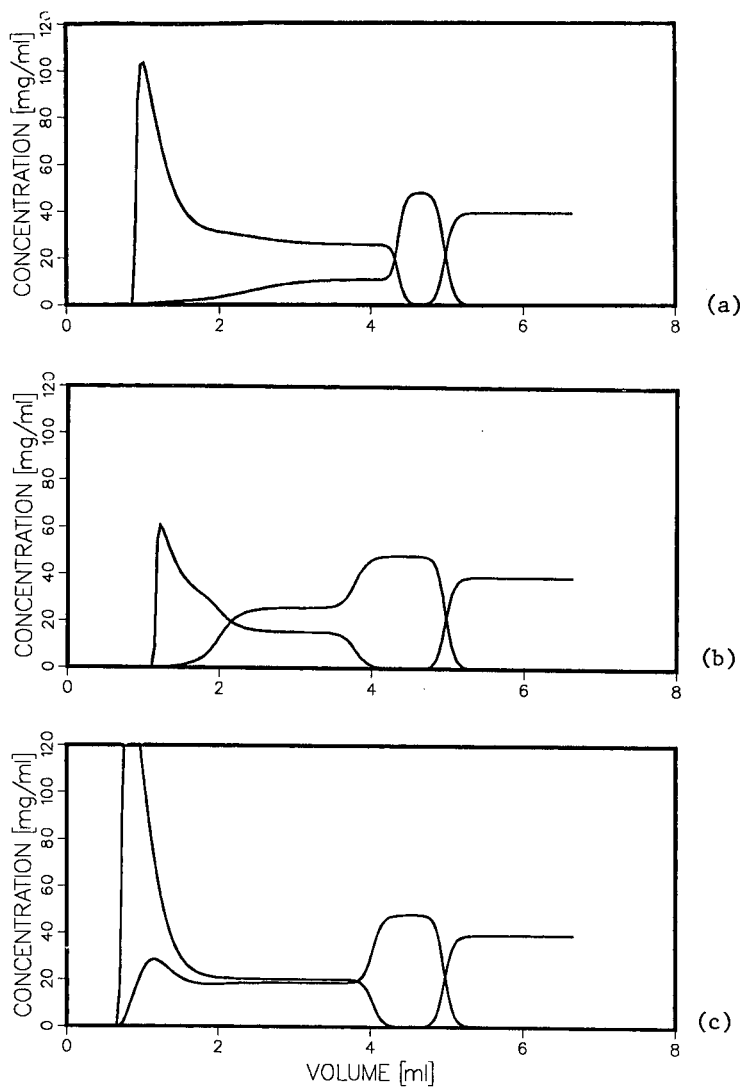


Fig. 10. Effect of sample concentration on the peak shape; comparison with experimental data in ref. 7. Ratio of amounts of components 1 and 2: (a) 114:57; (b) 57:114; (c) 114:114 (mg/mg).

#### ACKNOWLEDGEMENTS

This work was supported in part by Grant CHE-8715211 from the National Science Foundation and by a collaborative agreement between the University of Tennessee and Oak Ridge National Laboratories.

## REFERENCES

- 1 L. S. Ettre, in C. Horvath (Editor), *High Performance Liquid Chromatography: Advances and Perspectives*, Vol. 1, Academic Press, New York, 1980, p. 25.
- 2 A. Tiselius, *Ark. Kemi. Mineral. Geol.*, 16a (1943) 1.
- 3 F. H. Spedding, E. I. Fulmer, T. A. Butler and J. E. Powell, *J. Am. Chem. Soc.*, 72 (1950) 2349.
- 4 F. H. Spedding, *Discuss. Faraday Soc.*, 7 (1949) 38.
- 5 B. D. Mair, A. L. Gaboriault and F. D. Rossini, *Ind. Eng. Chem.*, 39 (1947) 1072.
- 6 D. B. Broughton, *Sep. Sci. Technol.*, 19 (1984) 723.
- 7 Cs. Horváth, A. Nahum and J. H. Frenz, *J. Chromatogr.*, 218 (1981) 365.
- 8 J. Frenz, Ph. Van der Schrieck and Cs. Horváth, *J. Chromatogr.*, 330 (1985) 1.
- 9 H. Kalász and Cs. Horváth, *J. Chromatogr.*, 215 (1981) 295.
- 10 H. Kalász and Cs. Horváth, *J. Chromatogr.*, 239 (1982) 423.
- 11 Cs. Horváth, J. Frenz and Z. El Rassi, *J. Chromatogr.*, 255 (1983) 273.
- 12 S. M. Cramer, Z. El Rassi and Cs. Horváth, *J. Chromatogr.*, 394 (1987) 305.
- 13 G. Viscomi, S. Lande and Cs. Horváth, *J. Chromatogr.*, 440 (1988) 157.
- 14 Z. El Rassi and Cs. Horváth, *J. Chromatogr.*, 266 (1983) 319.
- 15 A. W. Liao, Z. El Rassi, D. M. LeMaster and Cs. Horváth, *Chromatographia*, 24 (1987) 881.
- 16 Gy. Vigh, Z. Varga-Puchony, G. Szepesi and M. Gazdag, *J. Chromatogr.*, 386 (1987) 353.
- 17 K. Valkó, P. Slégel and J. Bárti, *J. Chromatogr.*, 386 (1987) 345.
- 18 A. R. Torres, S. C. Edberg and E. A. Peterson, *J. Chromatogr.*, 389 (1987) 177.
- 19 E. A. Peterson, *Anal. Biochem.*, 90 (1978) 767.
- 20 A. R. Torres, G. G. Krueger and E. A. Peterson, *Anal. Biochem.*, 144 (1985) 469.
- 21 R. Jacques, *Sep. Sci. Technol.*, 15 (1980) 533.
- 22 Y. Fujii, M. Aida, M. Okamoto and T. Oi, *Sep. Sci. Technol.*, 20 (1985) 377.
- 23 S. Fujine, *Sep. Sci. Technol.*, 17 (1982) 1049.
- 24 S. Fujine, K. Saito and K. Shiba, *Sep. Sci. Technol.*, 18 (1983) 15.
- 25 E. Gluckauf, *Proc. Soc. London*, 186 (1946) 35.
- 26 F. Helfferich and G. Klein, *Multicomponent Chromatography—Theory of Interference*, Marcel Dekker, New York, 1970.
- 27 H.-K. Rhee and N. R. Amundson, *AIChE J.*, 28 (1982) 423.
- 28 J. Frenz and Cs. Horváth, *AIChE J.*, 31 (1985) 400.
- 29 D. Basmadjian and P. Coroyannakis, *Chem. Eng. Sci.*, 42 (1987) 1723.
- 30 R. W. Geldart, Q. Yu, P. C. Wankat and N.-H. L. Wang, *Sep. Sci. Technol.*, 21 (1986) 873.
- 31 P. Rouchon, M. Schonauer, P. Valentin and G. Guiochon, *Sep. Sci. Technol.*, 22 (1987) 1793.
- 32 B. C. Lin and G. Guiochon, *Sep. Sci. Technol.*, in press.
- 33 G. Guiochon, S. Golshan-Shirazi, A. Jaulmes, *Anal. Chem.*, submitted for publication.
- 34 G. Guiochon and S. Ghodbane, *J. Phys. Chem.*, 92 (1988) 3682.
- 35 S. Ghodbane and G. Guiochon, *J. Chromatogr.*, 440 (1988) 9.
- 36 S. Ghodbane and G. Guiochon, *J. Chromatogr.*, in press.
- 37 R. Courant, K. O. Friedrichs and H. Lewy, *Math. Ann.*, 100 (1928) 32.
- 38 S. Golshan-Shirazi, S. Ghodbane and G. Guiochon, *Anal. Chem.*, in press.
- 39 J. E. Eble and R. L. Grob, P. E. Antle and L. R. Snyder, *J. Chromatogr.*, 384 (1987) 25.
- 40 G. Guiochon and L. Jacob, *Chromatogr. Rev.*, 14 (1971) 77.
- 41 A. Katti and G. Guiochon, in preparation.
- 42 J.-X. Huang and G. Guiochon, *J. Colloid Interface Sci.*, in press.

CHROM. 20 704

## EXPERIMENTAL AFFIRMATION OF THE STATISTICAL MODEL OF OVERLAP

JOE M. DAVIS

*Department of Chemistry and Biochemistry, Southern Illinois University, Carbondale, IL 62901 (U.S.A.)*  
(First received April 12th, 1988; revised manuscript received May 23rd, 1988)

---

### SUMMARY

This article briefly reviews the statistical model of overlap and reports results from its first application to a fully characterized experimental chromatogram in which the numbers of detectible components, singlet peaks, doublet peaks, and triplet peaks are known. The overall agreement between these numbers and their theoretically expected values, which were predicted by the model from the relative distribution of maxima in the chromatogram, is very good. Specifically, the absolute errors between the predicted and actual numbers are all less than or equal to three.

---

### INTRODUCTION

This article reports results from an application of the statistical model of overlap (SMO) to an experimental multicomponent chromatogram containing known numbers of detectible singlet and multiplet peaks. The SMO, proposed some years ago<sup>1</sup>, is a simple theory of peak overlap that rests on the assumption that the components of complex mixtures elute randomly from chromatographic columns or beds. In this case, the expected number of peaks in the chromatogram can be calculated from theory, if the number of detectible mixture components and the column peak capacity are known. Alternatively, and more importantly, the number of detectible mixture components can be estimated by a simple procedure reviewed below, if the number of peaks in the chromatogram and the peak capacity are fit as experimental data to the theory by least-squares methods. The basic validity of this procedure was confirmed by its extensive application to computer-generated chromatograms<sup>2–6</sup>. These applications furthermore established criteria (which are restated below) by which one can evaluate the accuracy of the component-number estimate. The procedure has been applied to several gas and liquid chromatograms<sup>4,6–8</sup>, with results that are apparently consistent with those obtained from computer-generated chromatograms. This work is only one of many studies of peak overlap and its probability in chromatograms<sup>9–16</sup>.

One can furthermore estimate with the SMO the expected numbers of singlet, doublet, triplet, etc., peaks in the chromatogram, once the number of detectible components is known<sup>1</sup>. Because a fundamental objective of chromatography is to resolve mixture components into singlet peaks, the estimation of these numbers enables one to gauge quantitatively the overall efficiency of separation.

Perhaps the most significant implication of the SMO is the surprising severity of overlap expected, even in ultrahigh-resolution chromatograms<sup>1</sup>. Specifically, the numbers of resolved peaks and singlet peaks are never expected to exceed 36.8 and 18.4%, respectively, of the peak capacity. These predictions raise grave questions about the accuracy of component concentrations determined from chromatograms of complex mixtures and the feasibility of isolating select components from such mixtures. The possible overestimation of component concentrations in forensic and environmental mixtures is especially serious, as complex legal issues may be decided erroneously by failure to consider properly the likelihood of overlap.

The reported applications of the SMO to experimental chromatograms have principally been diagnostic evaluations of partially characterized mixtures, in which the numbers of detectible components are unknown. No results have been reported from an application of the SMO to an experimental chromatogram in which the numbers of detectible components, singlet peaks, and multiplet peaks are known. The results from one such application are reported here, principally to enhance confidence in the model and the procedure reviewed below. The excellent agreement between experimental component and peak numbers and their predicted values should emphasize the basic statistical pitfalls one commonly encounters when resolving complex mixtures.

## THEORY

The actual number  $m$  of single component-peaks (SCPs), each of which corresponds to a detected mixture component, in a complex chromatogram is unknown, because some of the SCPs overlap with one another. Only the statistically expected number  $\bar{m}$  of SCPs in the chromatogram can be estimated with the SMO; fortunately, in most cases,  $m \approx \bar{m}$ . When  $m$  is large [*i.e.*,  $> 30$  (4)] and the components are randomly distributed along the elution axis, the number  $p$  of peaks expected in the continuous region  $X$  of the chromatogram is related to  $\bar{m}$  by<sup>1</sup>

$$p = \bar{m} e^{-\bar{m}/n_c} = \bar{m} e^{-\alpha} \quad (1)$$

where  $\alpha = \bar{m}/n_c$  is the component saturation of the chromatogram and  $n_c$ , the peak capacity, is the maximum number of uniformly spaced SCPs separable in region  $X$

$$n_c = \frac{X}{x_0} = \frac{X}{4\sigma R_s^*} \quad (2)$$

In eqn. 2,  $x_0$  is the span between adjacent SCPs resolved to the arbitrarily chosen resolution  $R_s^*$ , and  $\sigma$  is the standard deviation of any representative SCP in region  $X$ . Taking the logarithm of eqn. 1 and combining the result with eqn. 2, one obtains

$$\ln p = \ln \bar{m} - \bar{m}x_0/X = \ln \bar{m} - \bar{m}/n_c \quad (3)$$

Thus, a plot of  $\ln p$  vs.  $x_0/X$  or  $1/n_c$  is a line of slope  $-\bar{m}$  and intercept  $\ln \bar{m}$ . Two independent estimates of  $\bar{m}$  are consequently obtained, one (termed  $m_{sl}$ ) from the slope

and the other (termed  $m_{in}$ ) from the intercept. Although it is strictly incorrect to estimate independently these two  $\bar{m}$  values<sup>17</sup>, the requirement that  $m_{si}$  should equal  $m_{in}$ , at least within statistical error, is one of several useful criteria by which to evaluate the accuracy of the  $\bar{m}$  estimate<sup>2-5</sup>.

As noted in the introduction, one can also calculate from theory the expected numbers of singlet peaks  $s$ , doublet peaks  $d$ , triplet peaks  $t$ , and higher order multiplet peaks in the chromatogram, once  $\bar{m}$  is known. The first of these expected numbers are<sup>1</sup>

$$s = \bar{m} e^{-2\alpha} \quad (4a)$$

$$d = \bar{m} e^{-2\alpha} (1 - e^{-\alpha}) \quad (4b)$$

$$t = \bar{m} e^{-2\alpha} (1 - e^{-\alpha})^2 \quad (4c)$$

The resolution  $R_s^*$  one chooses to define  $n_c$ , and thus  $\alpha$ , clearly determines the numbers of peaks, singlets, and multiplets that one actually calculates from eqns. 1 and 4a-c. One arbitrary but useful convention is to equate  $R_s^*$  with 0.5, in which case peaks, singlets, and multiplets correspond to visually distinguishable chromatographic maxima<sup>2-4</sup>. This convention will be adopted here.

A common objective of chromatography is to resolve mixture components into singlet peaks of high purity. Usually the achievement of near-baseline resolution, characterized by  $R_s^* = 1.5$ , between the SCP of interest and its adjacent neighbors is adequate for this task. In this case the relative component saturation  $\alpha = 4\sigma R_s^* \bar{m}/X$  is three times greater than that based on  $R_s^* = 0.5$ . The expected number  $s_b$  of baseline-resolved singlets is consequently determined from eqn. 4a as

$$s_b = \bar{m} e^{-6\alpha} \quad (5)$$

where, as stated above,  $\alpha$  is defined by  $R_s^* = 0.5$ .

Several procedures, which differ only in the minimal resolution  $R_s^*$  that one requires between adjacent peaks, have been proposed to determine experimental peak numbers from chromatograms<sup>2-6</sup>. The procedure reviewed here permits one to determine several effective peak numbers and to estimate  $\bar{m}$  from the relative positions of the chromatographic maxima in a single chromatogram<sup>5</sup>. Furthermore, it eliminates the need to determine the peak capacity  $n_c$ , which is rigorously sample-dependent<sup>16</sup>. For any arbitrarily chosen spacing  $x_0$ , the number of spans between adjacent maxima that equal or exceed this spacing is equated to the experimental number  $p$  corresponding to that  $x_0$ . (Throughout the text, the symbols  $p$ ,  $s$ ,  $d$ ,  $t$ , etc., will be used to represent both theoretical and experimental quantities.) The inclusive span between the first and last maxima in the region is identified with the quantity  $X$ . The procedure is repeated with several different  $x_0$  values and a data set ( $x_0/X$ ,  $\ln p$ ) is generated. These arbitrary changes in  $x_0$  in effect correspond to arbitrary changes in the resolution  $R_s^*$  that formally resolves clusters of SCPs into peaks, as rigorously defined by theory<sup>2</sup>; these resultant peaks, however, have little in common with peaks in any traditional sense (e.g., chromatographic maxima). When  $x_0 > 2\sigma$ , the number  $p$  increases with decreasing  $x_0$ . When  $x_0 < 2\sigma$  (i.e., when  $R_s^* < 0.5$ ), however,  $p$  equals one less than the number  $p_m$  of chromatographic maxima, because adjacent SCPs

cannot be visually resolved when  $R_s^* < 0.5$ . These data are excluded from the data set, which is then fit to eqn. 3 by least-squares methods. Theoretical weights can be assigned to each point in the fit to estimate the uncertainties in  $m_{s1}$  and  $m_{in}$ . Details of the method<sup>5</sup> and previously reported applications<sup>7,8</sup> are given elsewhere.

## EXPERIMENTAL PROCEDURES

No original chromatography is reported here. Fig. 1 (reproduced with permission) is a high-resolution chromatogram of a composite mixture of 113 polynuclear aromatic hydrocarbon (PAH) standards first reported by Lee *et al.*<sup>18</sup> and kindly brought to the author's attention by M. Lee. These standards were fractionated on a 12 m  $\times$  0.29 mm I.D. glass capillary, which was coated with a 0.34- $\mu$ m film of SE-52 and temperature-programmed from 50 to 250°C at 2°C/min. The helium carrier flow-rate lay between 1 and 3 ml/min.

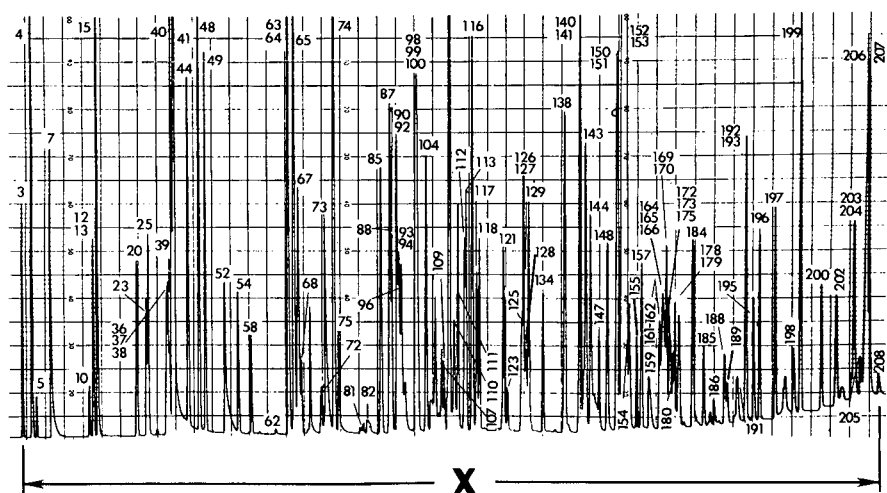


Fig. 1. Chromatogram of 113 PAH standards. Analytical conditions: column, 12 m  $\times$  0.29 mm I.D. glass capillary coated with a 0.34- $\mu$ m film of SE-52; temperature program, 50–250°C at 2°C/min; carrier, helium; flow-rate, between 1 and 3 ml/min. Reprinted with permission (ref. 18).

Each PAH standard was chromatographed several times to determine reliably a retention index<sup>18</sup>. Thus, the retention times of all standards were both accurately and precisely known, enabling the authors to identify the chromatographic maxima in Fig. 1 as singlets or multiplets. Each maxima is associated with one, two, or three numbers; singlets are associated with a single number (e.g., 3), doublets with two numbers (e.g., 12–13), and triplets with three numbers (e.g., 36–37–38). These numbers originally referred one to a table in reference 18, in which the identities of the mixture components corresponding to the numbered maxima are reported. (The maxima in the reprinted figure were actually renumbered by the author; the numbers reported in reference 18 are somewhat difficult to read, unless the figure occupies a full journal page, as it does in the reference.) A total of 92 maxima, comprised of 75 singlets, 13

doublets, and 4 triplets, are numbered in the chromatogram. Of the 75 singlets, 36 are also baseline-resolved, as judged by visual inspection. Four of these latter singlet types (44, 48, 49, and 54) actually reside on the tailing edges of the two maxima, 41 and 52. They were nevertheless counted as baseline-resolved singlets, because the tailing is highly unrepresentative of the chromatogram as a whole. These various singlet and multiplet numbers are reported in Table I. At least ten unnumbered maxima are also present in the chromatogram; their influence on the analysis is addressed below.

TABLE I

NUMBERS OF PEAK, SINGLET, AND MULTIPLET MAXIMA IN CHROMATOGRAM IN FIG. 1

Numbers in brackets identify numbered maxima in Fig. 1.

---

Detectable components: 113

Detectable (numbered) peak maxima: 92

Singlets *s*: 75

[3, 4, 5, 7, 10, 15, 20, 23, 25, 39, 40, 41, 44, 48, 49, 52, 54, 58, 62, 65, 67, 68, 72, 73, 74, 75, 81, 82, 85, 87, 88, 96, 104, 107, 109, 110, 111, 112, 113, 116, 117, 118, 121, 123, 125, 128, 129, 134, 138, 143, 144, 147, 148, 154, 155, 157, 159, 180, 184, 185, 186, 188, 189, 191, 195, 196, 197, 198, 199, 200, 202, 205, 206, 207, 208]

Doublets *d*: 13

[12-13, 63-64, 90-92, 93-94, 126-127, 140-141, 150-151, 152-153, 161-162, 169-170, 178-179, 192-193, 203-204]

Triplets *t*: 4

[36-37-38, 98-99-100, 164-165-166, 172-173-175]

Baseline-resolved singlets *s<sub>b</sub>*: 36

[3, 4, 5, 7, 10, 15, 20, 44, 48, 49, 52, 54, 58, 62, 81, 82, 85, 104, 134, 138, 148, 155, 157, 159, 184, 185, 186, 191, 195, 196, 197, 198, 199, 200, 202, 208]

---

## ANALYTICAL PROCEDURES

An enlarged copy of the chromatogram in Fig. 1 was prepared by careful xerography. The sequential relative positions of the numbered chromatographic maxima (which are analogous to relative retention times or volumes) were measured to a resolution of 0.005 in. with a True Grid 1011 Digitizer (Houston Instruments, Austin, TX, U.S.A.) and stored on an Apple IIe microcomputer. The digitization process was repeated to verify that the maxima positions could be determined reproducibly; the corresponding maxima positions in the two sets of numbers differed at most by 0.01 in. The positions of the unnumbered maxima were not digitized. Because these maxima are more or less randomly dispersed throughout the chromatogram, this small bias negligibly affects the analysis, as the results below will show.

The span *X* indicated in Fig. 1 was estimated as the difference, 10.100 in., between the first and last maxima. The data set ( $x_0/X$ ,  $\ln p$ ) was then determined as described above. No value of  $p < 16$  was considered, because of shortcomings in the SMO's development<sup>5</sup>. The data set was then graphed and inspected.

Only a subset of these data were fit to eqn. 3. Because the relative positions of any two adjacent maxima were both determined with a digitization error of 0.005 in., the relative error in small  $x_0$  values is considerable. If one demands that this relative error be less than 0.1, then

$$\frac{\sigma_{x_0}}{x_0} = \frac{\sqrt{(0.005)^2 + (0.005)^2}}{x_0} < 0.1 \quad (6)$$

where  $\sigma_{x_0}$  is the standard deviation of  $x_0$ . The span  $x_0$  must exceed 0.07 in. to satisfy this inequality. To minimize procedural errors, therefore, no data for which  $x_0/X < 0.07/10.100 \approx 0.007$  were fit to eqn. 3. These data include those for which  $x_0 < 2\sigma$ , which would normally be excluded anyway (see above).

The remaining data were fit to eqn. 3 by the theory of least squares<sup>19</sup>. The details of the fit are presented in the appendix.

## RESULTS AND DISCUSSION

As earlier work has demonstrated, a number of quantitative criteria must be satisfied, if one is to calculate  $\bar{m}$  accurately (*i.e.*, to within 10%) by the procedure detailed above. The first, as noted earlier, is that  $m_{sl} \approx m_{in}$ . Secondly, the relative saturation  $\alpha$  of the chromatogram must be less than 0.5, when  $R_s^* = 0.5$  (ref. 5). Finally, the distribution of distances between adjacent chromatographic maxima must be exponential, when  $x_0 > 2\sigma$  (ref. 5). One quantitative test for the existence of this distribution is the value of the reduced chi-square statistic  $\chi_v^2$ , defined by eqn. A15 in the appendix, which is a measure of the goodness of fit of the data set  $(x_0/X, \ln p)$  to eqn. 3. The test is inherently statistical, but when  $\chi_v^2 < 1$ , the distances are most likely exponentially distributed<sup>19</sup>.

Fig. 2 is the plot of  $\ln p$  vs.  $x_0/X$  generated by the procedures reported in the appendix. The solid line is a weighted least-squares fit of the indicated points to eqn. 3. As one would anticipate, these points are randomly scattered about the fit. The peak numbers for which  $2\sigma/X < x_0/X < 0.007$ , however, are systematically smaller than predicted by this fit, perhaps because of digitization error.

Table II reports, to the nearest whole number, the numbers of singlet peaks  $s$ , doublet peaks  $d$ , triplet peaks  $t$ , baseline-resolved singlet peaks  $s_b$ , and components  $m_{sl}$ , and  $\bar{m}$ , which were calculated as detailed in the appendix. Also reported, to the nearest whole number, are the standard deviations  $\sigma_s$ ,  $\sigma_d$ ,  $\sigma_t$ ,  $\sigma_{s_b}$ ,  $\sigma_{sl}$ ,  $\sigma_{in}$ , and  $\sigma_{\bar{m}}$  of these respective numbers, as evaluated from equations in the appendix. The saturation  $\alpha$  of the chromatogram, and the standard deviation  $\sigma_\alpha$  of the saturation, are also tabulated, for  $R_s^* = 0.5$ . The reported standard deviations are the statistical uncertainties in the estimates derived from the plot of  $\ln p$  vs.  $x_0/X$ .

In examining the data reported in Table II, one observes that  $m_{sl} \approx m_{in}$ . A simple Student's *t*-test indicates that these numbers are statistically equivalent. In addition,  $\alpha = 0.174$ , which is much less than the  $\alpha = 0.5$  limit above which  $\bar{m}$  cannot be reliably estimated. The reduced chi-square statistic for the fit is  $\chi_v^2 = 1.05$ , which suggests that the distances between adjacent maxima are indeed exponentially distributed. All the quantitative prerequisites to the calculation of accurate  $\bar{m}$  values stated above are

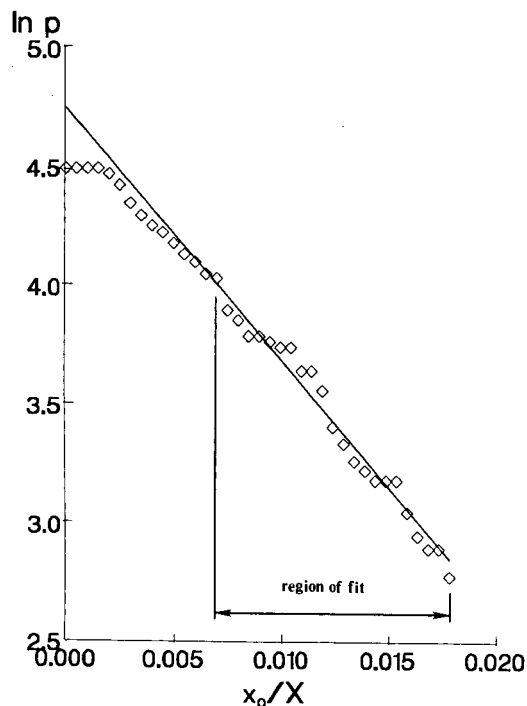


Fig. 2. Plot of  $\ln p$  vs.  $x_0/X$  derived from the chromatogram in Fig. 1. Solid line is least-squares fit of indicated points to eqn. 3.

consequently satisfied, and one would thus expect these predicted numbers to be fairly good estimates.

The predictions reported in Table II are, in fact, in very good agreement with the experimental peak and component numbers reported in Table I and parenthetically in Table II. Specifically, the experimental numbers  $m$ ,  $s$ ,  $d$ , and  $s_b$  all lie within, and usually well within, one standard deviation, and the number  $t$  within two standard deviations, of the predicted values. The absolute errors between the predicted and actual numbers are very small, and are all less than or equal to three.

TABLE II

RESULTS FROM SMO APPLICATION TO CHROMATOGRAM IN FIG. 1

Expected numbers (standard deviations) of components  $m_{sl}$  ( $\sigma_{sl}$ ) and  $m_{in}$  ( $\sigma_{in}$ ) from slope and intercept, respectively, of eqn. 3, SCPs  $\bar{m}$  ( $\sigma_{\bar{m}}$ ), singlets  $s$  ( $\sigma_s$ ), baseline-resolved singlets  $s_b$  ( $\sigma_{s_b}$ ), doublets  $d$  ( $\sigma_d$ ), and triplets  $t$  ( $\sigma_t$ ) are reported to the nearest whole number. Saturation  $\alpha$  and standard deviation  $\sigma_\alpha$  are reported to three significant figures. Experimental component and peak numbers are reported in parentheses below the theoretical results.

$m_{sl} \pm \sigma_{sl}$	$m_{in} \pm \sigma_{in}$	$\bar{m} \pm \sigma_{\bar{m}}$	$\alpha \pm \sigma_\alpha$ ( $R_s^* = 0.5$ )	$s \pm \sigma_s$	$d \pm \sigma_d$	$t \pm \sigma_t$	$s_b \pm \sigma_{s_b}$
$106 \pm 7$ (—)	$115 \pm 9$ (—)	$110 \pm 6$ (113)	$0.174 \pm 0.051$ (—)	$77 \pm 4$ (75)	$12 \pm 3$ (13)	$2 \pm 1$ (4)	$38 \pm 10$ (36)

Some interesting insights are obtained by examining the fraction of the peak capacity  $n_c$  utilized in this chromatogram to resolve peaks and singlets. Because the  $\alpha$  reported in Table II is defined with respect to chromatographic maxima (*i.e.*, with respect to  $R_s^* = 0.5$ ), the approximate peak capacity  $n_c$  of the chromatogram, in terms of maxima, is  $m/\alpha \approx 113/0.174 \approx 649$  components. In other words, 649 uniformly spaced maxima (of equal amplitude) could theoretically be resolved in space  $X$ , when  $R_s^* = 0.5$ . Only 92 maxima are actually resolved in this space, however, and the fraction of  $n_c$  utilized is only  $p_m/n_c = 92/649 = 0.142$ . The fraction of  $n_c$  utilized in resolving singlet maxima is somewhat less,  $s/n_c = 75/649 = 0.116$ . These  $p_m/n_c$  and  $s/n_c$  ratios are considerably smaller than their respective theoretical upper limits, 0.368 and 0.184<sup>1</sup>. The utilization of the available peak capacity for maxima separation is clearly far from optimized.

As shown by eqn. 2, the numerical value of  $n_c$  is determined by the resolution  $R_s^*$  that one chooses to discriminate between peaks. The peak capacity of any chromatogram, in terms of baseline-resolved peaks (defined by  $R_s^* = 1.5$ ), is consequently three times smaller than that based on chromatographic maxima (defined by  $R_s^* = 0.5$ ). Hence, the approximate baseline-resolved peak capacity of the chromatogram is  $649/3 \approx 216$ . The fraction of this capacity utilized in separating baseline-resolved singlets,  $s_b/n_c$ , is  $36/216 \approx 0.167$ . This ratio is only slightly less than the largest peak-capacity fraction, 0.184, that can be used for this purpose. This chromatogram therefore represents a highly optimal utilization of the available peak capacity for the baseline resolution of randomly spaced singlet peaks.

The peak and component numbers presented above clearly affirm that the SMO accounts quantitatively for peak overlap in this chromatogram. This analysis furthermore supports the hypothesis that the SMO accounts for overlap in many chromatograms, when certain well established criteria are met. As observed elsewhere, however, the SMO does not apply to all high-resolution chromatograms, especially when the mixture components exhibit order at the molecular level<sup>1</sup>. Furthermore, the agreement between experiment and theory, under one set of experimental conditions, does not imply that agreement will also be attained if the conditions are radically changed. For example, the careful optimization of multicomponent separations can, in some cases, introduce order and obviate the predictions of the SMO<sup>13,15</sup>. Other optimization procedures yield chromatograms in which peak overlap remains consistent with the SMO<sup>6</sup>. Each case must be addressed individually.

In conclusion, I note that additional studies of this type would provide useful data to test the reliability and universality of the procedures reviewed here or described elsewhere. A large set of experimental data is essential to the thorough testing and characterization of the SMO, because the effects on its predictions of many chromatographic variables, *e.g.*, mixture composition, mobile- and stationary-phase composition, and mobile-phase programming, cannot be deduced simply from analyses of computer-generated chromatograms. Because computer simulations furthermore are dismissed by some as idealistic approaches to the study of real-world problems, additional experimental confirmations of the SMO, and other theories of peak overlap, would build a solid experimental foundation on which to rest the sobering conclusions deduced from these theories.

## ACKNOWLEDGEMENT

The author thanks Southern Illinois University for the start-up funds with which this research was conducted.

## APPENDIX

*Least-squares fit of experimental data to eqn. 3*

The appropriate subset of the data set  $(x_0/X, \ln p)$  was fit to eqn. 3, as detailed below, to calculate  $m_{sl}$  and  $m_{in}$  and their respective standard deviations,  $\sigma_{sl}$  and  $\sigma_{in}$ . These numbers were evaluated from standard formulae for the least-squares fit of data to a straight line<sup>19</sup>

$$m_{sl} = \frac{1}{\Delta} \left[ \sum_{i=1}^j w_i \sum_{i=1}^j w_i \left( \frac{x_{0i}}{X} \right) \ln p_i - \sum_{i=1}^j w_i \left( \frac{x_{0i}}{X} \right) \sum_{i=1}^j w_i \ln p_i \right] \quad (A1)$$

$$m_{in} = \frac{1}{\Delta} \left[ \sum_{i=1}^j w_i \left( \frac{x_{0i}}{X} \right)^2 \sum_{i=1}^j w_i \ln p_i - \sum_{i=1}^j w_i \left( \frac{x_{0i}}{X} \right) \sum_{i=1}^j w_i \left( \frac{x_{0i}}{X} \right) \ln p_i \right] \quad (A2)$$

$$\sigma_{sl} = \frac{1}{\Delta} \sum_{i=1}^j w_i \quad (A3)$$

$$\sigma_{in} = \frac{1}{\Delta} \sum_{i=1}^j w_i \left( \frac{x_{0i}}{X} \right)^2 \quad (A4)$$

$$\Delta = \sum_{i=1}^j w_i \sum_{i=1}^j w_i \left( \frac{x_{0i}}{X} \right)^2 - \left[ \sum_{i=1}^j w_i \left( \frac{x_{0i}}{X} \right) \right]^2 \quad (A5)$$

In eqns. A1–A5,  $j$  is the number of data points in the fit (in this case, 23) and  $w_i$ ,  $x_{0i}$ , and  $p_i$  are the  $i$ th values of the theoretical weight  $w$ , arbitrary spacing  $x_0$ , and experimental number  $p$ . The weight  $w$  of each point was calculated as<sup>5</sup>

$$w = \frac{\bar{m} e^{-2\alpha'}}{f(\alpha') + (1 - \alpha')^2 e^{-2\alpha'}} \quad (A6)$$

where

$$f(\alpha') = \frac{0.099}{\alpha'} \exp \left[ -\frac{1}{2.341} \left( \ln \frac{\alpha'}{1.168} \right)^2 \right] \quad (A7)$$

and

$$\alpha' = \bar{m}x_0/X \quad (\text{A8})$$

Because the weights  $w$  depend on the unknown quantity  $\bar{m}$  (see eqns. A6–A8), the data set was fit iteratively to eqns. A1–A8 until the calculated results varied negligibly between iterations. Specifically, the arbitrary weight  $w = 1$  was initially assigned to all points, and the unknowns  $m_{sl}$ ,  $m_{in}$ ,  $\sigma_{sl}$  and  $\sigma_{in}$  were then evaluated from eqns. A1–A5. The statistical component number  $\bar{m}$  was then approximated as

$$\bar{m} = (m_{sl}/\sigma_{sl}^2 + m_{in}/\sigma_{in}^2)/(\sigma_{sl}^{-2} + \sigma_{in}^{-2}) \quad (\text{A9})$$

A series of new weights  $w$  was then computed from eqns. A6–A8 with the  $\bar{m}$  value estimated from eqn. A9, and the unknowns  $m_{sl}$ ,  $m_{in}$ ,  $\sigma_{sl}$ ,  $\sigma_{in}$ , and  $\bar{m}$  were again evaluated as detailed above. This iterative procedure was repeated until  $m_{sl}$ ,  $m_{in}$ ,  $\sigma_{sl}$ , and  $\sigma_{in}$  varied by less than 0.001% between successive iterations. The weighted standard deviation  $\sigma_{\bar{m}}$  of  $\bar{m}$  was then estimated from these data as

$$\sigma_{\bar{m}} = (\sigma_{sl}^{-2} + \sigma_{in}^{-2})^{-1/2} \quad (\text{A10})$$

The numbers  $m_{sl}$ ,  $m_{in}$ ,  $\sigma_{sl}$ ,  $\sigma_{in}$ ,  $\bar{m}$ , and  $\sigma_{\bar{m}}$  reported in Table II are the converged values determined as described above.

The relative saturation  $\alpha$  of the chromatogram in Fig. 1 was then calculated from eqn. 1 as

$$\alpha = -\ln(P_m/\bar{m}) \quad (\text{A11})$$

where  $p = p_m = 92$ , the number of chromatographic maxima, and  $\bar{m}$  is given by eqn. A9. With this choice, peaks, singlets, and multiplets are all identified with chromatographic maxima and  $R_s^* \approx 0.5^{2-4}$ .

The expected numbers of singlet, doublet, and triplet peaks were then calculated from  $\bar{m}$  (eqn. A9),  $\alpha$  (eqn. A11), and eqns. 4a–c. The standard deviations of these  $n$ -lets were estimated from a propagation of errors as<sup>19</sup>

$$\sigma_{n\text{-let}} = e^{-2\alpha} (1 - e^{-\alpha})^{n-1} \left[ \left( 1 - \frac{(n-1)e^{-\alpha}}{1 - e^{-\alpha}} \right)^2 \right]^{1/2} \sigma_{\bar{m}} \quad (\text{A12})$$

where  $n$  is the number of SCPs per maxima (*e.g.*,  $n = 2$  for a doublet). The standard deviations of the singlet  $s$ , doublet  $d$ , and triplet  $t$  peak numbers are designated  $\sigma_s$ ,  $\sigma_d$ , and  $\sigma_t$ , respectively, in Table II.

The number  $s_b$  of baseline-resolved peaks was calculated from  $\bar{m}$  (eqn. A9),  $\alpha$  (eqn. A11), and eqn. 5. The standard deviation  $\sigma_{s_b}$  of the number  $s_b$  of baseline-resolved singlets was determined from a propagation of error to be

$$\sigma_{s_b} = 5e^{-6\alpha}\sigma_{\bar{m}} \quad (\text{A13})$$

The standard deviation  $\sigma_\alpha$  of parameter  $\alpha$ , eqn. A11, was calculated as

$$\sigma_\alpha = \frac{\sigma_{\bar{m}}}{\bar{m}} \quad (\text{A14})$$

In eqns. A12–A14,  $\bar{m}$ ,  $\sigma_{\bar{m}}$ , and  $\alpha$  are given by eqns. A9–A11, respectively.

A reduced chi-square statistic  $\chi_v^2$  was calculated as<sup>19</sup>

$$\chi_v^2 = \sum_{i=1}^j \frac{w_i [\ln(\bar{m} e^{-\alpha'}) - \ln p_i]^2}{j - 2} \quad (\text{A15})$$

where  $w$ ,  $\alpha'$ , and  $\bar{m}$  are given by eqns. A6, A8, and A9, respectively. The value of  $\chi_v^2$  is a measure of the goodness of fit of the data set  $(x_0/X, \ln p)$  to eqn. 3.

#### LIST OF SYMBOLS

$d$	statistically expected or experimental number of doublet peaks
$f(\alpha')$	function defined by eqn. A7
$m$	number of detectible components in chromatogram
$m_{sl}$	component number estimated from slope of eqn. 3
$m_{in}$	component number estimated from intercept of eqn. 3
$\bar{m}$	statistically expected number of detectible components in chromatogram
$n_c$	peak capacity
$p$	statistically expected number of peaks in chromatogram, or experimental number of spans between adjacent maxima greater than $x_0$
$p_m$	number of chromatographic maxima
$R_s^*$	resolution that resolves adjacent SCPs into separate peaks
$s$	statistically expected or experimental number of singlet peaks
$s_b$	statistically expected or experimental number of baseline-resolved singlet peaks
SCPs	single-component peaks
$t$	statistically expected or experimental number of triplet peaks
$w$	statistical weight of point in $\ln p$ vs. $x_0/X$ plot
$x_0$	arbitrary spacing
$X$	span between first and last chromatographic maxima
$\alpha$	$\bar{m}/n_c$
$\alpha'$	$\bar{m}x_0/X$
$\Delta$	function defined by eqn. A5
$\sigma$	standard deviation of SCP
$\sigma_d$	standard deviation of doublet number $d$
$\sigma_{in}$	standard deviation of $m_{in}$
$\sigma_{\bar{m}}$	standard deviation of $\bar{m}$
$\sigma_{n\text{-let}}$	standard deviation of $n$ -let peak number
$\sigma_s$	standard deviation of singlet number $s$
$\sigma_{s_b}$	standard deviation of baseline-resolved singlet number $s_b$

$\sigma_{s1}$	standard deviation of $m_{s1}$
$\sigma_t$	standard deviation of triplet number $t$
$\sigma_{x_0}$	uncertainty in $x_0$ due to digitization error
$\sigma_\alpha$	standard deviation of $\alpha$
$\chi^2_v$	reduced chi-square statistic

## REFERENCES

- 1 J. M. Davis and J. C. Giddings, *Anal. Chem.*, 55 (1983) 418.
- 2 J. C. Giddings, J. M. Davis and M. R. Schure, in S. Ahuja (Editor), *Ultrahigh Resolution Chromatography (ACS Symposium Series 250)*, American Chemical Society, Washington, DC, 1984, p. 9.
- 3 J. M. Davis and J. C. Giddings, *J. Chromatogr.*, 289 (1984) 277.
- 4 D. P. Herman, M. F. Gonnord and G. Guiochon, *Anal. Chem.*, 56 (1984) 995.
- 5 J. M. Davis and J. C. Giddings, *Anal. Chem.*, 57 (1985) 2168.
- 6 F. Dondi, Y. D. Kahie, G. Lodi, M. Remelli, P. Reschiglian and C. Bighi, *Anal. Chim. Acta*, 191 (1986) 261.
- 7 J. M. Davis and J. C. Giddings, *Anal. Chem.*, 57 (1985) 2178.
- 8 S. Coppi, A. Betti and F. Dondi, *Anal. Chim. Acta*, submitted for publication.
- 9 D. Rosenthal, *Anal. Chem.*, 54 (1982) 63.
- 10 L. J. Nagels, W. L. Creten and P. M. Vanpeperstraete, *Anal. Chem.*, 55 (1983) 216.
- 11 M. Martin and G. Guiochon, *Anal. Chem.*, 57 (1985) 289.
- 12 M. Martin, D. P. Herman and G. Guiochon, *Anal. Chem.*, 58 (1986) 2200.
- 13 D. P. Herman, H. A. H. Billiet and L. de Galan, *Anal. Chem.*, 58 (1986) 2999.
- 14 W. L. Creten and L. J. Nagels, *Anal. Chem.*, 59 (1987) 822.
- 15 L. de Galan, D. P. Herman and H. A. H. Billiet, *Chromatographia*, 24 (1987) 108.
- 16 M. Z. El Fallah and M. Martin, *Chromatographia*, 24 (1987) 115.
- 17 J. M. Davis, *Ph.D. Thesis*, University of Utah, Salt Lake City, UT, 1985.
- 18 M. L. Lee, D. L. Vassilaros, C. M. White and M. Novotny, *Anal. Chem.*, 51 (1979) 768.
- 19 P. R. Bevington, *Data Reduction and Error Analysis for the Physical Sciences*, McGraw-Hill, New York, 1969.

CHROM. 20 673

## SPLIT PEAKS IN NON-LINEAR CHROMATOGRAPHY AND THEIR EFFECT ON SAMPLE THROUGHPUT IN LARGE SCALE SEPARATIONS

JAMES L. WADE\* and PETER W. CARR\*

*Department of Chemistry, Smith and Kolthoff Halls, University of Minnesota, Minneapolis, MN 55455 (U.S.A.)*

(Received April 15th, 1988)

---

### SUMMARY

The origin and mathematical properties of the split peak phenomenon are described for both linear and non-linear elution conditions. Through a series of computer calculations, the theoretical behavior of split peaks is predicted for a wide variety of conditions where chemical adsorption, as opposed to solute mass transfer, is the rate-limiting adsorption step. Our results, which derive from the fundamental solution of the non-linear chromatographic equations with an impulse input [ $\delta(t)$ ], are found to be in excellent agreement with the recent numerical simulations of Hage and Walters. The fraction of solute eluting at the dead volume ( $f$ ) is found to be a complex function of both the flow-rate and the amount injected ( $C_0$ ). Although it is theoretically possible to use the split peak mass to derive values for the adsorption rate constant and the density of binding sites, this methodology is difficult and time-consuming to apply. Split peak theory may be useful, however, in engineering design computations where it is desired to maximize solute throughput, yet keep the non-retained fraction below a certain percentage of the total mass of solute applied to the column. Universal working curves for this purpose are presented and discussed, and the optimum throughput is found for each of several specified split peak fractions.

---

### INTRODUCTION

One of the more curious phenomena in chromatography is the so-called "split peak". These occur when adsorption is so slow, or the density of binding sites is so small, that a significant fraction of the solute may traverse the length of the column without adsorbing even once<sup>1</sup>. The probability of a solute making this passage is enhanced by higher flow-rates, and is completely independent of the rate of solute desorption from the stationary phase; the amount of solute eluting at the dead volume depends only on its probability of *adsorbing* during its residence in the column.

Split peaks are found almost exclusively in protein and affinity chromatography, where both the solute and the immobilized ligand molecules tend to be large, and

---

\* Current address: Hercules Research Center, Hercules Incorporated, Wilmington, DE, 19894, U.S.A.

adsorption kinetics and mass transfer tend to be slow. Split peaks are not useful in quantitative analysis or in preparative scale work; indeed, they are undesirable artifacts. They have been used, however, to make physico-chemical measurements; their mass—a convenient and precisely measurable quantity—is directly related to the density of binding sites on a particular adsorbent, as well as to the adsorption kinetics of these sites<sup>2,3</sup>.

Sportsman and Wilson<sup>2</sup> were the first to make use of this fact in measuring the rate of formation of an antigen-antibody complex<sup>2</sup>. Recently, Hage *et al.*<sup>3</sup> used split peaks in an elegant study of the immobilization-dependent adsorption kinetics of Protein A<sup>3</sup>. They found that the chemical procedures used to immobilize the ligand had a significant effect on its adsorption kinetics. Their method of relating split peak mass to adsorption kinetics was, like Sportsman's, based on the assumption of linear ("infinite dilution") conditions. This has two undesirable consequences. First, linear elution conditions are all but unattainable in immobilized protein chromatography because ligand densities are simply too low; a detection system would not be able to measure precisely an "infinitely dilute" concentration of solute. Hence, experimental results need to be extrapolated to infinite dilution so that the linear theory may be properly applied. A further drawback to applying linear theory is that the density of binding sites must be known *a priori* in order to measure the adsorption rate constant. Each of these factors increases the number of experiments to be performed, thus diminishing the precision of the results.

Split peaks were first described in a theoretical way by Giddings and Eyring<sup>1</sup>, long before they were observed in affinity chromatography. In providing a stochastic description of the chromatographic process under linear conditions, they found that there was a finite probability, given sufficiently extreme chromatographic conditions, that an otherwise retained solute could travel the length of a column without adsorbing. DeLisi *et al.*<sup>4</sup> also examined linear split peak theory, and discussed its significance. It was only recently, however, that Hage and Walters<sup>5</sup> examined non-linear split peak theory for the first time. They used a finite element numerical analysis scheme to quantitatively simulate split peak behavior under two sets of conditions: (1) adsorption being limited by the rate of solute diffusion through the stagnant fluid, and (2) adsorption being limited by the rate of chemical adsorption. They also developed guidelines whereby non-linear effects in split peak behavior can be minimized, and "infinite dilution" behavior extrapolated from non-linear data.

In this article, we will examine the mathematical origin and behavior of split peaks in the adsorption-limited case, and discuss the difficulty of applying the appropriate theory to make physico-chemical measurements. If the physical parameters of a system have been accurately obtained by alternative means, however, split peak theory can prove to be useful. This is demonstrated by design calculations which provide a quantitative guide to optimizing solute throughput at a specified split peak fraction.

## THEORY

The non-linear system of equations which describes column overload under non-ideal conditions was solved for a delta function input to yield the following concentration-time relationship at the column exit<sup>6</sup>:

$$\frac{C}{C_0} = \left[ \frac{1 - \exp(-\gamma KC_0)}{\gamma KC_0} \right] \left[ \frac{[\gamma \sqrt{(k'/y)} I_1(2\gamma \sqrt{k'y}) + \delta(y)] \exp(-\gamma k' - \gamma y)}{1 - T(\gamma k', \gamma y) [1 - \exp(-\gamma KC_0)]} \right] \quad (1)$$

$$\frac{\tilde{q}}{C_0} = \left[ \frac{1 - \exp(-\gamma KC_0)}{\gamma KC_0} \right] \left[ \frac{\gamma k' I_0(2\gamma \sqrt{k'y}) \exp(-\gamma k' - \gamma y)}{1 - T(\gamma k', \gamma y) [1 - \exp(-\gamma KC_0)]} \right] \quad (2)$$

where:  $\tilde{q} = \varepsilon q$ ;  $\gamma = k_d t_0$ ;  $k' = (k_a/k_d) S_0 \varepsilon$ ;  $KC_0 = (k_a/k_d) C_0$ ;  $y = (t/t_0) - 1$ ;  $T(u, v) = \int_0^u e^{-t} I_0(2\sqrt{vt}) dt$ . The computation of the T function, a Bessel function integral, has been discussed elsewhere<sup>6</sup>. In the above equations,  $C$  and  $q$  represent the concentration of solute in the mobile and stationary phases, respectively, and  $C_0$  represents the quantity of solute injected or, in mathematical parlance, the "strength" of the delta function input. This may be computed in the following manner:

$$C_0 = \frac{V_p}{V_0} C_p \quad (3)$$

$C_p$  is the concentration of solute in a very narrow injection pulse,  $V_p$  is the volume of that pulse, and  $V_0$  is the dead volume of the column. The adsorption/desorption rate constants,  $k_a$  and  $k_d$ , are chemical constants; that is, we are assuming that a chemical process, as opposed to a mass transfer process, is the rate-limiting sorption step.  $S_0$  is the concentration of binding sites on the adsorbent,  $\varepsilon$  is the porosity ratio, and  $t_0$  is the dead time of the column. All symbols are summarized in the symbols section.

The profile of a non-linear chromatographic peak is fully described by three dimensionless groups,  $\gamma$ ,  $k'$ , and  $KC_0$ , and dimensionless time,  $y$ . Time is rendered dimensionless in this way in order to incorporate the initial condition that the column be empty; that is, nothing may elute prior to the dead time. This time "shift" is also essential to linearizing, and hence solving, the non-linear set of equations via the Thomas transformation<sup>7,8</sup>.

The shifted time variable does, however, present a problem when solving the non-linear chromatographic equations for an impulse input. This problem arises because the solute is introduced onto the column as an infinitely high, infinitely narrow pulse at *time equal to zero*; this is in contradiction to our condition, implicit in the time "shift", that the column be initially devoid of all solute. Thus it is not surprising that while eqn. 1 accurately describes the profile of the retained peak, the delta function term (at  $y = 0$ ) does not correctly predict the split peak mass, except under linear conditions.

This is an unfortunate, but necessary, consequence of solving the non-linear system of equations with a boundary condition that is infinitely discontinuous at time equal to zero. In the derivation of eqns. 1 and 2, it was necessary to develop an expression for the boundary condition at  $y = 0$ , and because of the delta function, it was necessary to take the limit as  $y$  approached zero<sup>6</sup>. Taking the limit from the positive direction yields solutions which are trivially equal to zero, while taking the limit from the negative direction yields the solutions in eqns. 1 and 2. It can be shown, however, that when integrated over time, eqn. 1 will yield a mass which is less than or equal to unity, and the "missing mass" is, in fact, the correct split peak mass. This is the approach we have taken to compute split peak mass in our numerical calculations.

## NUMERICAL CALCULATIONS

Two sets of computer calculations were carried out. In the first, the three chromatographic parameters ( $\gamma$ ,  $k'$ , and  $KC_0$ ) were varied over a wide range, and theoretical peaks with approximately 160 points were generated. Each peak was integrated by Simpson's rule<sup>9</sup>, with the peak "beginning" being taken at  $y = 0$ , and the peak "end" being chosen as the point where the concentration fell below a threshold of  $10^{-8}$  times the peak maximum. The integrated mass was then subtracted from unity to yield the correct split peak mass. In all, 840 theoretical peaks were generated by using all possible combinations of the following chromatographic parameters:

$$k' = 1.0, 2.0, 4.0, 8.0, 12.0, 16.0, 20.0$$

$$\gamma = 0.001, 0.002, 0.005, 0.01, 0.02, 0.05, 0.10, 0.20, 0.50, 1.0$$

$$KC_0 = 0, 0.01, 0.02, 0.05, 0.10, 0.20, 0.50, 1.0, 2.0, 5.0, 10.0, 20.0$$

In the second set of computer simulations, target values of the split peak mass were selected (e.g., 10% of the solute mass), and the results of the first simulation were used to predict which chromatographic parameters would yield the desired result. The parameter space was then searched until the targeted split peak mass was bracketed, whereupon a parabolic interpolation was performed in order to find the parameters which yielded the desired target value. The resulting parameters were then checked in eqn. 1, and if the split peak mass was not within 0.2% of the target value, the above procedure was repeated until this condition was met. By this method, 41 distinct parameter sets were obtained for each of the following split peak fractions: 1%, 2%, 5%, 10%, 20%, 30%, and 40%. The peak integration procedure used in the first set of simulations was also used in this set.

All computations were carried out in double-precision Pascal on a Zenith-151 microcomputer equipped with an 8087 coprocessor.

## RESULTS AND DISCUSSION

In order to interpret the theoretical results generated by the first set of simulations, it is convenient to introduce two dimensionless groups:

$$\theta_1 = \gamma k' = k_a S_0 \varepsilon t_0 \quad (4a)$$

$$\theta_2 = \gamma KC_0 = k_a C_0 t_0 \quad (4b)$$

Of the 840 peaks generated in the first set of simulations, there were only 573 unique combinations of  $\theta_1$  and  $\theta_2$ . For those peaks which had identical values of  $\theta_1$  and  $\theta_2$ , but entirely different values of  $\gamma$ ,  $k'$ , and  $KC_0$ , the retained peak profiles differed widely in shape and breath—but the split peak mass was identical to at least fourteen significant figures. This observation validates our computational procedure, because neither  $\theta_1$  nor  $\theta_2$  are dependent upon  $k_d$ . The split peak effect must be independent of  $k_d$ , for its size depends only on the probability of a solute *adsorbing*; the probability of it *desorbing* is completely irrelevant to the size of the peak eluting at the dead volume. It therefore follows that the split peak effect can be completely described by the two

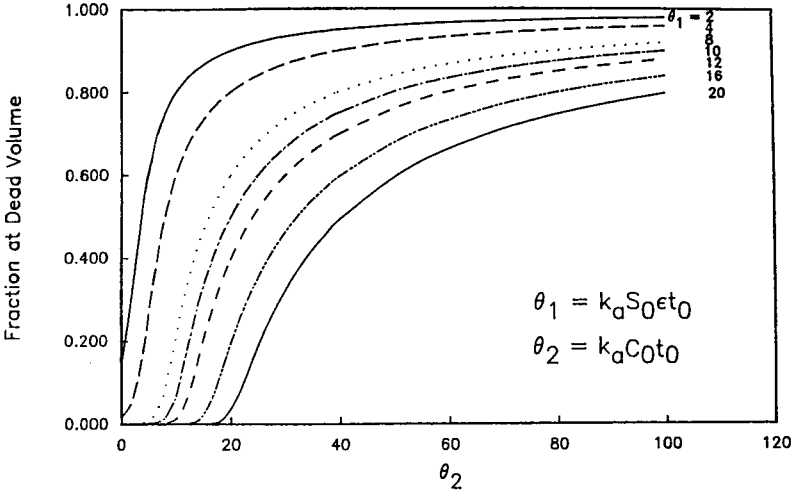


Fig. 1. Fraction of solute eluting at the dead volume as a function of both  $\theta_1$  and  $\theta_2$ .

parameters,  $\theta_1$  and  $\theta_2$ , which incorporate slow chemical adsorption (via  $k_a$ ), the concentration of binding sites ( $S_0\epsilon$ ), the flow-rate (through  $t_0$ ), and the solute load ( $C_0$ ). Some of the data that were generated in the first set of simulations are presented in Fig. 1, and in alternative form in Fig. 2. Several features of these plots are instructive. First, the data plotted in Fig. 2 yield a plot which is virtually identical to one generated by Hage and Walters<sup>5</sup> from numerical simulations. The slopes of all the lines in Fig. 2 are equal to unity at small values of  $\theta_1$ , while at large values, the lines become substantially curved. Again, these patterns in the data are identical to those found in the numerical work of Hage and Walters<sup>5</sup>.

From Figs. 1 and 2, it is evident that the split peak mass, or fraction of solute eluting at the dead volume, is a very complex, non-linear function of  $\theta_1$  and  $\theta_2$ . Herein lies the difficulty of using split peak theory to measure  $\theta_1$  and  $\theta_2$  experimentally, and

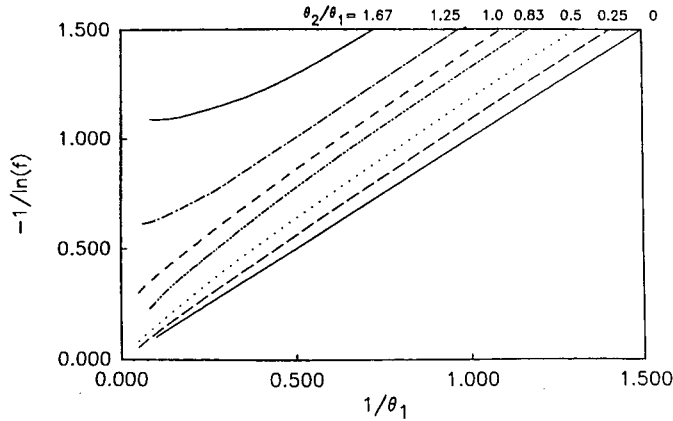


Fig. 2. Data from Fig. 1 plotted in alternative form to maintain consistency with ref. 5.

thereby obtain  $k_a$  and  $S_0$ . Simultaneous measurement of these parameters would require a series of experiments in which  $\theta_1$  and/or  $\theta_2$  were varied, and experimental plots similar to Figs. 1 or 2 constructed. Lengthy and involved computer computations would then be required to match a theoretical working curve to the experimental curve. Alternatively, the binding site concentration can be measured independently by chemical means, and then split peak behavior can be extrapolated to infinite dilution to yield  $k_a$ ; this has been the method employed by Hage and co-workers<sup>3,5</sup>.

Another way of measuring these parameters is to fit retained peaks (or breakthrough curves) to theoretical profiles<sup>6,10-13</sup>. This method has two principal advantages. First, all three parameters ( $k_a$ ,  $k_d$ , and  $S_0$ ) are accessible, as opposed to just two ( $k_a$  and  $S_0$ ); secondly, these parameters may be obtained simultaneously from *each* chromatogram. Multiple runs, while desirable for assessing the precision and accuracy of the method, are not necessary for the actual measurement of the parameters. In addition, there are practical reasons why the curve-fitting approach is to be preferred. The computations involved in the data analysis are no worse—and may even be less involved—than those required to fit working curves to experimental split peak plots. Also, the split peak method requires that a peak at the dead volume be accurately integrated; this requires that there be no unusual dead volume effects or unretained components that interfere with the split itself, and that the detector responds quickly enough.

In preparative separations, the split peak effect is obviously an undesirable artifact. In an affinity chromatographic separation, for instance, a split peak would mean that a portion of the desired product would elute in the wash along with other unretained (and undesired) components. It is therefore important to have a fundamental understanding of how the effect may be controlled, even if it is not possible—or practical—to use it in making physico-chemical measurements. For the purpose of optimizing solute throughput in a new affinity system, such as that recently reported by Hage and Walters<sup>14</sup>, it would be useful to understand how throughput is related to the fraction of unretained solute. If the throughput is taken to be the ratio  $C_0/t_0$ , then from eqns. 4a and 4b, we may define a dimensionless throughput parameter:

$$\text{TP} = \frac{\theta_2}{\theta_1^2} = \frac{C_0}{k_a(S_0\epsilon)^2 t_0} \quad (5)$$

The second set of simulations is summarized in Fig. 3. The region below each curve represents all combinations of  $\theta_1$  and  $\theta_2$  where the split peak fraction is *less than* the percentage indicated on the graph. The accuracy of these plots rests upon the assumption that chemical processes are slow relative to mass transfer, and upon prior knowledge of  $k_a$  and  $S_0$ . If these parameters have been accurately determined by alternative means, then plots such as those depicted in Fig. 3 may be used to adjust  $t_0$  (via the flow-rate) and  $C_0$  (the solute load) to achieve optimum solute throughput at a given split peak fraction.

At large values of  $\theta_1$ , all of the curves in Fig. 3 approach a straight line with a limiting slope which is greater than unity. If a small split peak fraction is specified (e.g., 1%) this slope is very close to unity, while for large split fractions (e.g., 40%), the slope is much larger (close to 2 in the latter case). It must be remembered that both  $\theta_1$  and  $\theta_2$  are proportional to  $t_0$ , the dead time of the column. This means that an

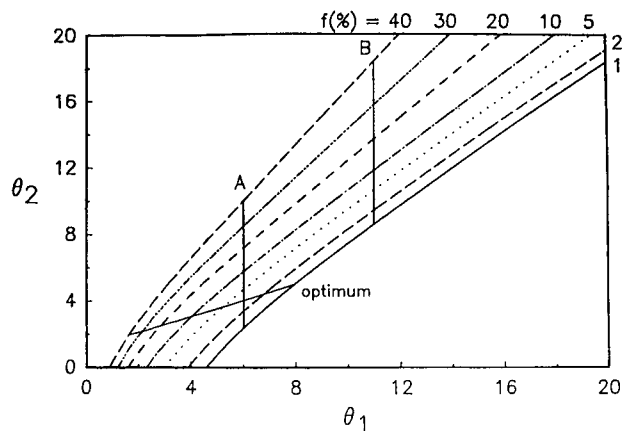


Fig. 3. Selected values of the split peak fraction, and the parameter values which give these fractions. The intersection of the optimum line with the curves represents the point of optimal solute throughput for a specified fraction. See text for details.

experimental point on any curve in Fig. 3 would move along a line with slope equal to unity as the flow-rate is changed. A point that was on, say, the 1% line would then find itself slightly above the line after a flow-rate increase; that is, the split peak fraction would be greater than the desired amount. A downward adjustment in the solute load ( $C_0$  in  $\theta_2$ ) would then be required to bring the point back onto the curve. In general, the smaller the split peak fraction that is specified, the less will  $C_0$  need downward adjustment to compensate for a flow-rate increase.

This raises the question as to how to adjust the sample load and flow-rate to achieve the maximum separation productivity. To find the optimum throughput for each of the indicated split peak fractions in Fig. 3, eqn. 5 was used to compute the dimensionless throughput for each of the 41 points on each curve. A distinct maximum was found on each curve; it was pinpointed by means of a parabolic interpolation between the three points with the highest throughput. The optimum points on each curve are given in Table I, and are connected in Fig. 3 with the solid curve labeled "optimum".

TABLE I

VALUES OF  $\theta_1$  AND  $\theta_2$  REQUIRED TO ACHIEVE THE MAXIMUM POSSIBLE SOLUTE THROUGHPUT AT VARIOUS SPLIT PEAK FRACTIONS

$f(\%)$	$\theta_1(opt)$	$\theta_2(opt)$	$TP^*$	$(1-f)TP$
1.00	7.945	4.975	0.0788	0.0780
2.00	6.762	4.383	0.0959	0.0940
5.00	5.203	3.608	0.1333	0.1266
10.0	4.025	3.038	0.1875	0.1688
20.0	2.834	2.478	0.3085	0.2468
30.0	2.126	2.153	0.4762	0.3333
40.0	1.628	1.947	0.7342	0.4405

\* TP is the dimensionless solute throughput defined in eqn. 5.

TABLE II  
NET THROUGHPUT AS A FUNCTION OF SOLUTE LOAD

Flow-rate is constant.

Line*	$f$ (%)	$TP$	$(1 - f)TP$
A	1.00	0.0657	0.0650
	10.0	0.1597	0.1438
	40.0	0.2769	0.1662
B	1.00	0.0710	0.0703
	10.0	0.0977	0.0879
	40.0	0.1518	0.0911

\* Refer to Fig. 3.

Two observations need to be made regarding the data in Table I. First, the points of optimum throughput for the chosen split peak fractions lie on an almost perfect line ( $r = 0.9997879$ ). It would therefore be possible to estimate the optimum flow-rate and sample load for *any* desired split fraction in the range 1 to 40%, provided that the physico-chemical parameters of the system were known. The last column in Table I is also interesting; it suggests that net throughput can be improved by simply tolerating more split peak mass, and adjusting the operating parameters to the optimum point. This observation is borne out by the data in Table II, which shows that increasing the sample load increases the net throughput—regardless of the concomitant increase in the split peak fraction. The improvement in net throughput, however, is much less for larger values of  $\theta_1$  (line B in Fig. 3).

## CONCLUSIONS

The theory of split peak chromatography under non-linear conditions has been discussed, and the behavior of split peaks over a wide variety of experimental conditions has been described. The computations pertain only to the case where mass transfer is fast relative to chemical sorption processes. While not ideal for making physico-chemical measurements, non-linear split peak theory may be useful in making separation design calculations—provided that the physical parameters of a chromatographic system have been accurately measured by alternative means. Universal working curves and tabular data are presented which quantitatively describe how, for a specified split fraction, solute throughput may be optimized by adjusting the flow-rate and solute load to an optimal point. In maximizing solute throughput, it is advantageous to tolerate a greater split peak fraction, while adjusting operating parameters to the computed optimum.

## LIST OF SYMBOLS

$C_0$	quantity of solute injected in a very high, narrow pulse = $C_p(V_p/V_0)$ ;
$C_p$	concentration of solute in the very narrow injection pulse;
$f$	fraction of the solute mass eluting at the dead volume;

- $I_0(x)$  zeroth order Bessel function of the first kind;  
 $I_1(x)$  first order Bessel function of the first kind;  
 $K$  equilibrium constant =  $k_a/k_d$ ;  
 $k'$  thermodynamic capacity factor =  $KS_0\varepsilon$ ;  
 $k_a$  second order rate constant for chemical adsorption;  
 $k_d$  first order rate constant for chemical desorption;  
 $q$  concentration of solute on the stationary phase;  
 $S_0$  concentration of active binding sites on the adsorbent surface. This is related to the surface coverage by<sup>6</sup>:  

$$S_0 = \frac{A_0\rho a_s}{(1 - \varepsilon_T)}$$
 where  $A_0$  is the surface coverage of sites (mol/m<sup>2</sup>),  $\rho$  is the density of the adsorbent,  $a_s$  is the specific surface area, and  $\varepsilon_T$  is the total porosity of the adsorbent<sup>6</sup>;  
 $T(u,v)$  Bessel function integral which varies between zero and unity. Evaluation of this function is discussed in ref. 6;  
 $t_0$  dead time of the column (passage time of an unretained solute which can, and does, explore the pores of the adsorbent);  
 TP dimensionless throughput (eqn. 5);  
 $V_0$  dead volume of the column;  
 $V_p$  volume of the pulse injected onto the column;  
 $y$  "shifted" time in dimensionless form =  $t/t_0 - 1$ ;  
 $\gamma$  dimensionless rate parameter =  $k_d t_0$ ;  
 $\varepsilon$  porosity ratio =  $(1 - \varepsilon_T)/\varepsilon_T$ ;  
 $\theta_1$  dimensionless capacity parameter for split peak work =  $k_a S_0 \varepsilon t_0$ ;  
 $\theta_2$  dimensionless loading parameter for split peak work =  $k_a C_0 t_0$ .

## ACKNOWLEDGEMENTS

This work was supported by a grant from the Bio-Process Technology Center of the University of Minnesota. The authors also thank David Hage for advance copies of his publications, and his helpful comments.

## REFERENCES

- 1 J. C. Giddings and H. Eyring, *J. Phys. Chem.*, 59 (1955) 416.
- 2 J. R. Sportsman and G. S. Wilson, *Anal. Chem.*, 52 (1980) 2013.
- 3 D. S. Hage, R. R. Walters and H. W. Hethcote, *Anal. Chem.*, 58 (1986) 274.
- 4 C. DeLisi, H. W. Hethcote and J. W. Brettler, *J. Chromatogr.*, 240 (1982) 283.
- 5 D. S. Hage and R. R. Walters, *J. Chromatogr.*, 436 (1988) 111.
- 6 J. L. Wade, A. F. Bergold and P. W. Carr, *Anal. Chem.*, 59 (1987) 1286.
- 7 H. C. Thomas, *J. Am. Chem. Soc.*, 66 (1944) 1664.
- 8 H. C. Thomas, *Ann. NY Acad. Sci.*, 49 (1948) 161.
- 9 R. L. Burden, J. D. Faires and A. C. Reynolds, *Numerical Analysis*, PWS Publishers, Boston, MA, 1981, p. 142.
- 10 F. H. Arnold and H. W. Blanch, *J. Chromatogr.*, 355 (1986) 13.
- 11 F. H. Arnold, H. W. Blanch and C. R. Wilke, *Chem. Eng. J.*, 30 (1985) B9.
- 12 H. A. Chase, *J. Chromatogr.*, 297 (1984) 179.
- 13 H. A. Chase, *Chem. Eng. Sci.*, 39 (1984) 1099.
- 14 D. S. Hage and R. R. Walters, *J. Chromatogr.*, 386 (1987) 37.



CHROM. 20 657

## ABSOLUTE PEAK BROADENING CALIBRATION IN SIZE-EXCLUSION CHROMATOGRAPHY USING A POLYMER-BOUND CHROMOPHORE

TUAN Q. NGUYEN\* and HENNING-H. KAUSCH

*Polymer Laboratory, Swiss Federal Institute of Technology, CH-1007 Lausanne (Switzerland)*

(Received March 21st, 1988)

---

### SUMMARY

A recently developed theory permits the determination of peak broadening in size-exclusion chromatography by combining the simultaneous signals obtained from two different detectors, one being sensitive to the mass concentration and the other to the molecular weight of the solute eluted. Based on this methodology, a new experimental technique employing polymer-bound chromophores and a standard UV detector was developed to provide information normally obtained with an absolute detector. The advantages of the method are its simplicity and the utilization of a single cell for measurements, which relieves much of the detection geometry problems inherent to other techniques. Fractions of polystyrene labelled with azobenzene groups and synthesized by radical polymerization were used. The experimental broadening parameters are critically evaluated with respect to the possible sources of error and compared with results obtained from quasi-monodisperse polymer fractions.

---

### INTRODUCTION

Since its introduction in 1964<sup>1</sup>, size-exclusion chromatography (SEC) has gained wide acceptance as a standard tool for the determination of the molecular weight (MW) distribution in polymers.

The major limitation of SEC, in common with all other chromatographic techniques, is that it is a secondary analytical tool. Precise evaluation of experimental data in terms of the molecular weight distribution depends on the availability of accurate polymer standards for the transformation of the elution volume into a scale of molecular masses. In this respect, the hydrodynamic volume approach of Benoît *et al.*<sup>2,3</sup> and the recent advent of reliable MW-sensitive detectors, like the continuous viscometer<sup>4</sup> and on-line low-angle laser light scattering photometer (LALLSP)<sup>5</sup>, reduced much of the effort and time spent on mass calibration.

One persistent problem is the lack of a simple procedure to calibrate axial dispersion in SEC. Heretofore, several methods have been proposed, but they are generally time-consuming<sup>6,7</sup>, indirect<sup>8</sup> or require sophisticated instrumentation and computation facilities<sup>9</sup> not readily available to the average polymer laboratory.

In this paper, we will describe a novel experimental technique to determine instrumental broadening, based on the application of polymer-bound chromophore. The approach is practical and the technique may be used on any standard liquid chromatograph equipped with a variable wavelength UV detector, or even better with a photodiode-array detector where signals at different wavelengths can be processed simultaneously.

The idea of using polymer molecules labelled with chromophore groups for the purpose of molecular counting is not new in itself and has been employed for over 20 years in the colorimetric end-group titration of polystyrene<sup>10</sup>. Recently, the usefulness of this class of compounds for absolute molecular weight calibration in SEC has been noted<sup>11</sup>. In any event, it does not seem that the potential of the chromophore method for axial dispersion calibration has been duly considered. Part of this neglect stems from the fact that polymer samples having the required properties for this type of application are difficult to obtain:

- the number of chromophore groups per chain must be constant, otherwise its dependency on the polymer molecular weight within the sample must be precisely known;

- the absorption spectrum of the labelled group should preferably be distinct from that of the polymer to ensure minimum peak overlap;

- an high absorption coefficient of the chromophore is needed for a good signal-to-noise ratio of the detector signal;

- absence of adsorption on the stationary phase;

- good thermal and photochemical stability of the chromophore;

- a low polydispersity of the sample is an asset although not mandatory, providing the first condition for stoichiometry is properly fulfilled.

The versatility of anionic polymerization makes it the method of choice for labelled polymer synthesis<sup>12</sup>. However, finding appropriate conditions for anionic polymerization requires time and expertise. In a first step, to evaluate the feasibility of the technique, we rely on the simpler radical polymerization system initiated with a chromophore-labelled peroxide.

## POLYMER SYNTHESIS

The monomer used was styrene. A peroxide containing azobenzene as the chromophore (Fig. 1) was selected for the radical initiation of polymerization. It was synthesized according to the protocol described by Kämmerer *et al.*<sup>13</sup>. The symmetric isomer, bis(4-phenylazo)benzoyl peroxide, although more easy to synthesize, could not be used as an homogeneous polymerization initiator due to its limited solubility in styrene and in methyl methacrylate.

The UV absorption spectrum of bound azobenzene has a maximum at 318 nm; its minimum is nearly coincident with the absorption maximum at 262 nm of the

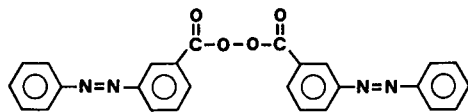


Fig. 1. Chemical structure of bis(3-phenylazo)benzoyl peroxide.

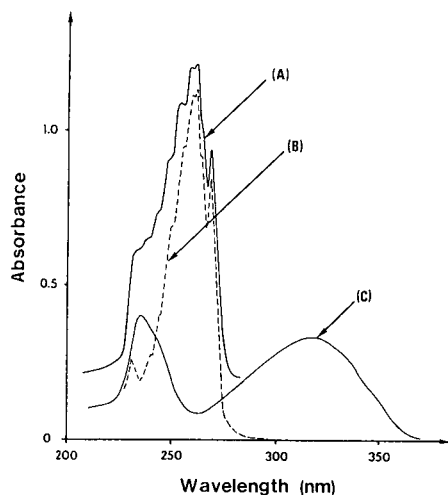


Fig. 2. UV absorption spectrum of chromophore-bound PS, deconvoluted into the azobenzene and styrene absorption bands (polymer fraction synthesized at  $4 \cdot 10^{-3} M$  peroxide, concentration = 0.500 mg/ml dichloromethane). (A) Spectrum of chromophore-bound PS; (B) spectrum of thermally initiated PS; (C) spectrum of the chromophore obtained by the difference between (A) and (B).

styrene units in polystyrene (PS) (Fig. 2). This insures a good selectivity in the detector signals obtained at these two wavelengths. Use of the azobenzene-labelled peroxide has the added advantage that its decomposition kinetics has already been investigated in styrene and in methyl methacrylate<sup>10</sup>.

In the course of polymerization, azobenzene moieties become attached to the chain backbone principally during the initiation stage but also by a chain-transfer mechanism, as revealed by detailed characterization of the synthesized polymers.

Degassed solutions of styrene, containing  $2.5 \cdot 10^{-4}$ – $10 \cdot 10^{-3} M$  peroxide, were polymerized in bulk at 70°C, in vacuum-sealed Pyrex tubes. The polymerization was stopped at conversion yields below 5% to avoid side reactions. The polymer was recovered by precipitation and repeatedly extracted with methanol to remove unreacted initiator and monomer.

#### *Characterization of labelled polymer*

The molecular weight distributions of the synthesized polymers were determined by SEC on a Waters 150C equipped with a set of Ultrastaygel columns. The variable wavelength UV detector (Perkin-Elmer LC-75) was interfaced to a Waters Data Module and a personal computer (Hewlett-Packard 9816S) for data acquisition and treatment.

The presence of a few additional azobenzene groups in the labelled polymer is unlikely to perturb significantly the hydrodynamic radius of the molecular coil as compared to homo-PS. For this reason, we used for mass calibration the same curve as established with PS standards without any further adjustment. As explained in the next section, a small correction was applied to the styrene absorbance at 262 nm to allow for band overlap with the absorbance of the chromophore group.

The decadic molar extinction coefficient of PS-bound azobenzene, measured in chloroform, is equal to  $1.67 \cdot 10^7 \text{ cm}^2 \text{ mol}^{-1}$  at the absorbance maximum of 319 nm<sup>10</sup>. Referring to this value, we determined the equivalent extinction coefficient in dichloromethane which is the eluent solvent for SEC:  $\epsilon_2(318 \text{ nm}) = 1.64 \cdot 10^7 \text{ cm}^2 \text{ mol}^{-1}$ .

The average number of chromophore groups per chain,  $\bar{n}$ , was calculated according to the Lambert–Beer law as given by the following relationship

$$\text{Absorbance (318 nm)} = \epsilon_2(318 \text{ nm}) \cdot CL\bar{n}/M_n \quad (1)$$

where  $C$  = mass concentration of the polymer in  $\text{g cm}^{-3}$ ,  $L$  = optical length of the cell in cm and  $M_n$  = number average molecular weight of the sample in  $\text{g mol}^{-1}$ .

The results, reported in Table I, showed that  $\bar{n}$  decreased with the number average molecular weight of the polymer. The sample prepared at  $2.5 \cdot 10^{-4} M$  peroxide is an exception: at this low concentration, thermal initiation competed with peroxide decomposition and the average number of azobenzenes incorporated into the polymer during this step decreased accordingly. To avoid uncontrolled uncertainty in the distribution of chromophore groups which may result from this complex kinetics, the polymer synthesized at the lowest peroxide concentration was omitted from the present studies.

Using the UV absorption spectrum of thermally initiated PS (without additive) as the reference, the absorption curve of labelled polymers was deconvoluted by difference into separate bands belonging to the styrene units and to the azobenzene group (Fig. 2). With proper normalization, all the individual bands are directly superimposable regardless of the sample, which seems to indicate that the chromophore absorption spectrum is independent of the polymer molecular weight. At 262 nm, the absorbance germane to the styrene units is given by the following relationship which was used to correct for band overlap

$$\text{Absorbance(PS)} = A(262 \text{ nm}) - 0.23 A(318 \text{ nm}) \quad (2)$$

where  $A$  = absorbance at the designated wavelength.

To determine the variation of  $n$  as a function of chain length, each polymer synthesized was fractionated into eight to ten fractions by preparative SEC, with the polydispersity ranging from 1.07 to 1.10. Each fraction was then analyzed for  $M_n$  by

TABLE I  
CHARACTERIZATION OF THE LABELLED POLYMERS

Polymerization temperature: 70°C.

Concn. of peroxide ( $M$ )	$M_w$	$M_n$	$M_w/M_n$	$\bar{n}$
0	1470 000	661 000	2.2	0
$2.5 \cdot 10^{-4}$	464 000	153 000	3.0	1.07
$1 \cdot 10^{-3}$	236 000	101 000	2.3	1.60
$4 \cdot 10^{-3}$	85 700	31 500	2.7	1.29
$10 \cdot 10^{-3}$	40 200	12 200	3.3	0.89

SEC and for the absorbances at 262 and 318 nm. The average number of chromophores for each fraction,  $n_f$ , was calculated from the ratio of absorbances originating respectively from the azobenzene groups and from the styrene units

$$n_f = (a_1/\epsilon_2) M_n A(318 \text{ nm})/[A(262 \text{ nm}) - 0.23A(318 \text{ nm})] \quad (3)$$

where  $a_1$  is the mass extinction coefficient at 262 nm of PS in dichloromethane, equal to  $2270 \text{ cm}^2 \text{ g}^{-1}$ .

The results of the characterization (Fig. 3) revealed one of the essential features of the polymerization mechanism: the number of chromophore groups per chain increases both with the chain length and the initial concentration of peroxide. The decrease of  $\bar{n}$  with the initiator concentration, as indicated in Table I, merely reflects the averaging effect over the molecular weight range present in each sample. This trend is consistent with a chain-transfer mechanism where a growing macroradical is added to the chromophore group, without modifying the UV absorption property of the azobenzene double bond<sup>10</sup>.

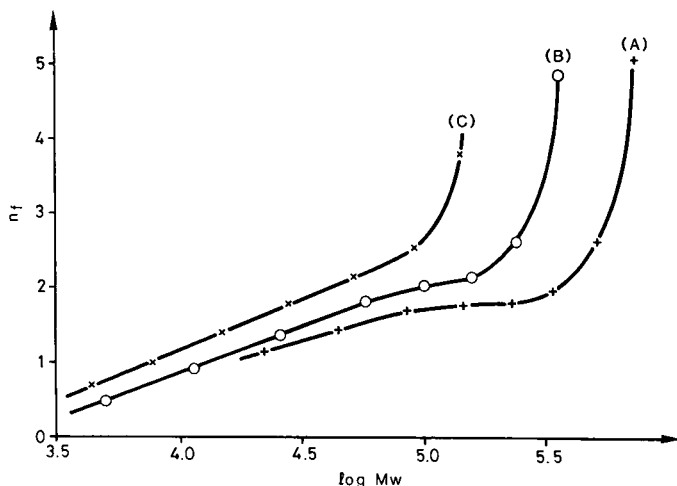


Fig. 3. Variation of chromophore stoichiometry with polymer molecular weight ( $n$  = number of azobenzene groups per polymer chain). Polymer synthesized at: (A)  $1 \cdot 10^{-3}$ ; (B)  $4 \cdot 10^{-3}$ ; (C)  $10 \cdot 10^{-3} M$  peroxide.

#### THEORETICAL BASIS FOR AXIAL DISPERSION CALIBRATION

The equations used are in essence based on the general relationships developed by Hamielec<sup>9</sup> for absolute detector systems. According to the methodology described, the axial dispersion parameters, and with certain approximations even the axial dispersion function, can be obtained by combining the signals of the same sample arising simultaneously from two different detectors. One of these detectors should be sensitive to the mass concentration and the other to the molecular weight of the eluted polymer. We will succinctly rewrite below some equations of interest for the case of a molecular detector, keeping whenever possible the same notation as in ref. 9.

Let  $F_1(V)$  be the response of the UV detector at the elution volume,  $V$ , when tuned to the maximum absorption wavelength of the polymer (262 nm for PS), and  $F_2(V)$  the detector signal at the absorption maximum of the chromophore (318 nm in dichloromethane).

For the present discussion, we will assume that  $F_1(V)$  has already been corrected for any band overlap, using eqn. 2.

The corrected absorbance  $F_1(V)$  is proportional to the mass concentration of polymer and is given by

$$F_1(V) = a_1 L \int_0^{\infty} C(V, Y) dY \quad (4)$$

where  $C(V, Y)$  is the mass concentration of polymer within the elution range  $V$  and  $V + dV$ , due to species with mean retention volumes between  $Y$  and  $Y + dY$ , and  $L$  is the optical length of the detector cell.

According to Tung<sup>14</sup>,  $F_1(V)$  can be written as a Fredholme integral of the first kind

$$F_1(V) = a_1 L \int_0^{\infty} C(Y) G(V, Y) dY \quad (5)$$

where  $G(V, Y)$  is the normalized instrumental dispersion function to be determined.

At the chromophore wavelength, the detector signal,  $F_2(V)$ , gives the concentration of azobenzene groups which is directly related to the molar concentration of the polymer

$$A(318 \text{ nm}) = F_2(V) = \varepsilon_2 L \int_0^{\infty} n(Y) C(V, Y) / M(Y) dY \quad (6)$$

where  $M(Y)$  is the calibration curve in the absence of peak broadening, and  $n(Y)$  is the number of chromophore groups per chain for species eluted between  $Y$  and  $Y + dY$  as given in Fig. 3.

By definition, the instantaneous number average molecular weight of the detector cell content at the elution volume,  $V$ , is given by:

$$M_n(V) = \frac{\int_0^{\infty} C(V, Y) dY}{\int_0^{\infty} C(V, Y) / M(Y) dY} \quad (7)$$

This quantity is proportional to the ratio of the detector signals obtained at the two wavelengths selected, 262 and 318 nm, regardless of the shape of the spreading function,  $G(V, Y)$ :

$$F_1(V)/F_2(V) = (a_1/\varepsilon_2)M_n(V)/n(V) \quad (8)$$

In order to relate  $M_n(V)$  and  $M(V)$  with an analytical expression, a common practice is to approximate  $G(V, Y)$  with a variable gaussian function of standard deviation,  $\sigma(V)$ , changing with the elution volume:

$$G(V, Y) = G(V - Y) = \frac{1}{\sigma(V) \sqrt{2\pi}} \cdot \exp \left[ -\frac{(V - Y)^2}{2\sigma(V)^2} \right] \quad (9)$$

With this simplification, a simple relationship between  $M_n(V)$  and  $M(V)$  can be obtained:

$$\frac{M_n(V)}{M(V)} = \frac{F_1(V)}{F_1[V + D_2(V) \sigma(V)^2]} \cdot \exp\{-1/2[D_2(V) \sigma(V)]^2\} \quad (10)$$

Written differently, eqn. 10 provides a means to determine the spreading parameter,  $\sigma(V)$ , from a combination of the experimental traces  $F_1(V)$  and  $F_2(V)$ :

$$F_1[V + D_2(V) \sigma(V)^2] = [a_1/n(V) \varepsilon_2]F_2(V)M(V) \cdot \exp\{-1/2[D_2(V) \sigma(V)]^2\} \quad (11)$$

In this equation, the constants  $D_1$  and  $D_2$  of the locally linearized calibration curve in the absence of peak broadening must be measured beforehand:

$$\ln M(V) = D_1(V) - D_2(V) \cdot V \quad (12)$$

For narrow MW distributions, the position at the peak apex is insensitive to the instrumental axial dispersion<sup>9</sup>. A good approximation to  $M(V)$  is actually provided by the calibration graph established with sharp PS standards.

## RESULTS AND DISCUSSION

Eqn. 11 is valid regardless of the shape of the functions  $F_1(V)$  and  $F_2(V)$ , and hence of the sample MW distribution. For practical purposes, we will distinguish however the situation where the polymer is of large polydispersity from the case of a nearly monodisperse fraction.

### *Broad MW distribution*

First,  $n(V)$  must be known precisely from separate measurements and the appropriate values substituted into eqn. 11. The ensuing steps are then exactly similar to the approach employed with an on-line mass-sensitive detector<sup>9</sup>: for any given elution volume, a single variable search permits the determination of the best value of  $\sigma(V)$  which fits the left-hand term of eqn. 12 to its right-hand counterpart.

The results of this fit are reported in Fig. 4 for one of the labelled PS fractions polymerized at  $4 \cdot 10^{-3} M$  peroxide.

The detector signals are collected at discrete sampling intervals to give a total of *ca.* 100 data points across each single chromatogram. Values situated between two data points are extrapolated by a third-order polynomial before the variable search is commenced, using in the present case the Fibonacci technique of linear optimization<sup>15</sup>. This procedure however does not work near the peak maximum where any deviation of the signal will significantly influence the value of  $\sigma$  and should be replaced by a more elaborate optimization technique. Since  $\sigma(V)$  is a monotonous function of  $V$ , the few missing points at the peak apex are more readily obtained by extrapolation from the fitted values on the ascending and descending slopes of the SEC trace (Fig. 4).

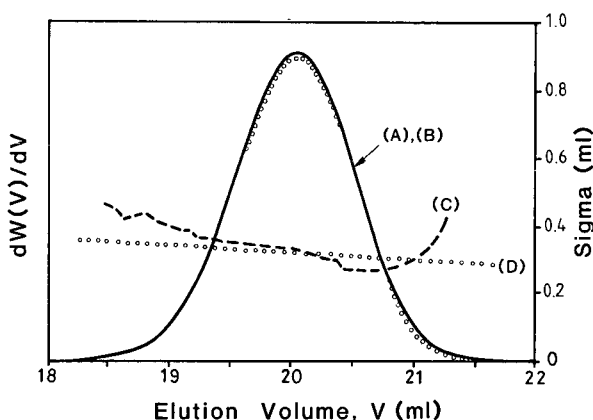


Fig. 4. Axial dispersion constant as a function of elution volume fitted with a broad MW distribution ( $4 \cdot 10^{-3} M$  peroxide,  $\mu$ Styragel columns). (A) Detector signal at 262 nm, corrected for band overlap according to eqn. 2. (B) Curve calculated from the right-hand side of eqn. 11, mostly indistinguishable from (A). (C) Results of a variable search using eqn. 11 (right ordinates). (D) Results from Fig. 6 obtained with narrow fractions of labelled polymer (right ordinates).

Theoretically, eqn. 11 should allow determination of  $\sigma(V)$  over a wide range of elution volumes with a single polymer sample. In practice, the precision of the fit is largely dependent on baseline fluctuations, on the accuracy of the MW calibration graph and in the determination of  $n(V)$ . These sources of error are cumulative, making the reliability of the results questionable. For example, the fitted  $\sigma(V)$  curve in Fig. 4 shows systematic deviation from a similar curve determined with narrow MW fractions (Fig. 5), although they have identical values when averaged over the elution range of the sample.

#### Narrow MW distribution

Samples with  $M_w/M_n \approx 1.01$ – $1.02$  are obtained from the crude polymer by multiple refractionation of the middle portion on an analytical column (Table I).

The narrow elution range which encompasses each fraction allows several levels of simplification in the determination of the axial dispersion constant. The choice of

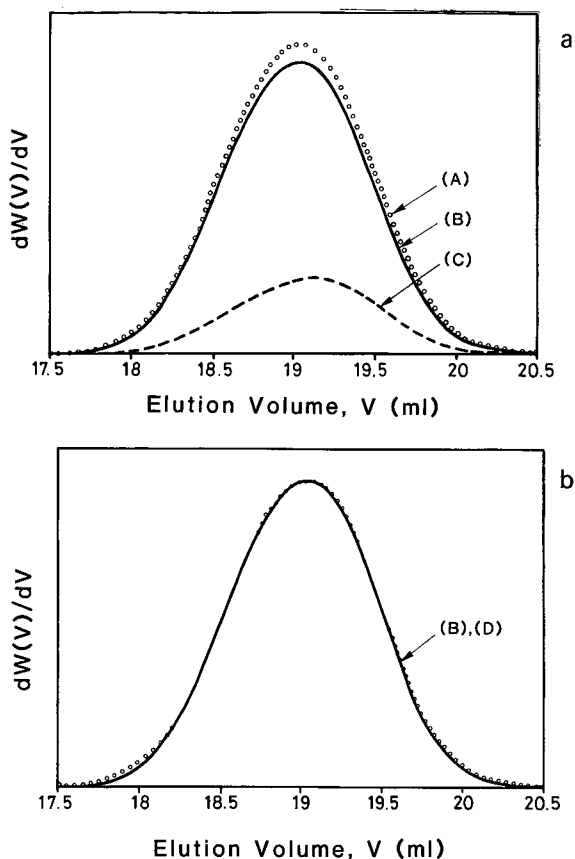


Fig. 5. Determination of  $\sigma$  by curve fitting with a narrow polymer fraction ( $4 \cdot 10^{-3} M$  peroxide,  $\mu$ Styragel columns). (a) Detector signals at 262 nm (A), at 262 nm corrected for band overlap (B) and at 318 nm (C). (b) (B) Corrected detector signal at 262 nm; (D) curve calculated from the right-hand side of eqn. 11.

the method is mainly dictated by the degree of precision and the kind of information which may be needed.

(a) Both  $n(V)$  and  $\sigma(V)$  change slowly with the elution volume. The low polydispersity of the labelled fractions permits the replacement in eqn. 11 of  $n(V)$  and  $\sigma(V)$  with average values,  $n_f$  and  $\sigma$ .

Over a limited range of the elution volume,  $D_2(V)$  can be considered constant. Let  $D_2\sigma^2 = \Delta V$ , eqn. 11 simplifies to:

$$F_1(V + \Delta V) = F_2(V) \{ M(V) \cdot \exp[-1/2(D_2\sigma)^2] (a_1/n_f\epsilon_2) \} \quad (13)$$

Since the right-hand-side expression between the round brackets is constant for a given elution volume, proper normalization of the functions  $F_1(V)$  and  $F_2(V)$  permits account to be taken of this factor without the need to know the exact value of each individual term.

A simple translation by  $\Delta V$  permits a superimposition of the two normalized curves, and hence the determination of  $\sigma$ .

(b) At the same level of approximation, *i.e.*, constant  $n_t$  and  $D_2$ , and a constant gaussian for the axial dispersion function, the spreading constant can be simply calculated from the properties of the whole polymer average molecular weights<sup>16</sup>.

At the polymer wavelength (262 nm):

$$M_n(\text{uc1}) = \frac{\int_0^\infty F_1(V) dV}{\int_0^\infty F(V)/M(V) dV} = M_n(c) \cdot \exp[-1/2(D_2\sigma)^2] \quad (14)$$

$$M_w(\text{uc1}) = \frac{\int_0^\infty F_1(V)M(V) dV}{\int_0^\infty F_2(V) dV} = M_w(c) \cdot \exp[+1/2(D_2\sigma)^2] \quad (15)$$

At the chromophore wavelength (318 nm):

$$M_n(\text{uc2}) = \frac{\int_0^\infty F_1(V)M(V) dV}{\int_0^\infty F_2(V) dV} = M_n(c) \cdot \exp[+1/2(D_2\sigma)^2] \quad (16)$$

$$M_w(\text{uc2}) = \frac{\int_0^\infty F_1(V)M(V) dV}{\int_0^\infty F_2(V)M(V) dV} = M_w(c) \cdot \exp[+3/2(D_2\sigma)^2] \quad (17)$$

The indices “uc” and “c” in the above equations mean respectively “uncorrected” and “corrected” for axial dispersion.

$D_1$  and  $D_2$  are coefficients obtained by linear regression of the calibration graph over the useful elution range of the polymer fraction.

Values obtained by combining pairs of eqns. 14–16 and 15–17 to eliminate  $M_n(c)$  and  $M_w(c)$  give a good concordance with the values obtained from whole-curve fitting using the procedure described under (d) below. This simple technique may be employed for a rapid determination of the axial dispersion constant without the use of

a computer. The extra information contained in the entire envelope of the detector signals can be used in principle for the determination of the axial dispersion function (see technique "c").

(c) If the spreading function is independent of the elution volume, it is possible to solve simultaneously the set of equations given by the detector signals at the two wavelengths and determine  $G(V, Y)^{18}$ . This method should be particularly useful in the high MW range where  $G(V, Y)$  may deviate significantly from the pure gaussian<sup>9</sup>.

(d) First,  $\sigma(V)$  is considered constant over the elution range of interest. In this case, the same curve-fitting method as described for a polymer of broad MW distribution can be used but the errors involved are much smaller due to the limited distribution of molecular masses (Fig. 5).

When several narrow samples with different MWs are available,  $\sigma(V)$  can be refitted by iteration if necessary.

We found the present procedure (d) to be the most reliable among the above-mentioned techniques for the determination of  $\sigma(V)$ .

The values of  $\sigma$  obtained by applying technique (d) for the three narrowest fractions of labelled polymers are plotted in Fig. 6. Two different sets of  $\mu$ Styragel and Ultrastayragel columns ( $10^5 \text{ \AA} + 10^4 \text{ \AA}$ ) are used. As expected,  $\mu$ Styragel columns with larger particles have dispersion constants nearly twice the values obtained with Ultrastayragel columns, particularly in the high MW range.

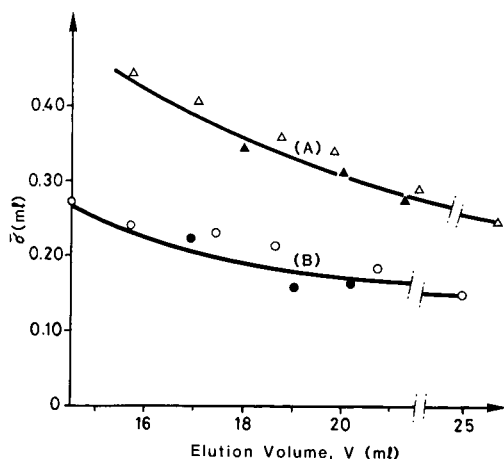


Fig. 6. Axial dispersion constant as a function of elution volume using sharp polymer fractions. (A)  $\mu$ Styragel columns ( $10^4 \text{ \AA} + 10^5 \text{ \AA}$ ):  $\blacktriangle$ , polymer-bound chromophore method;  $\Delta$ , quasi-monodisperse fraction method. (B) Ultrastayragel columns ( $10^4 \text{ \AA} + 10^5 \text{ \AA}$ ):  $\bullet$ , polymer-bound chromophore method;  $\circ$ , quasi-monodisperse fraction method.

As an independent check on the consistency of the technique, we measured  $\sigma(V)$  for nearly monodisperse PS obtained by repeated fractionation on Ultrastayragel columns ( $M_w/M_n \approx 1.01$  estimated with the recycling technique<sup>19</sup>). The influence on the peak width due to sample polydispersity is negligible at this level. The peak width at half maximum ( $= 2.35\sigma$ ) can then be used for the evaluation of the axial dispersion constant.

Visual inspection of the data points in Fig. 6 shows a good concordance between the two methods, any deviation being within the expected experimental errors involved.

#### *Precision of the technique*

In order to evaluate the reliability of the technique, we examine the influence of possible sources of errors on the accuracy of the results.

Since the signals  $F_1(V)$  and  $F_2(V)$  are obtained from two separate experiments, fluctuations of the pump flow-rate may cause additional uncertainty in the determination of  $\sigma$ . A flow-rate calibration using a low MW solute (toluene) showed that the effect is relatively small and accounted at most for 6% error on the measured values, providing the columns and the pump are both in perfect working order.

Variation of the band overlap factor in eqn. 2 from 0.1 to 0.4 resulted in the expected change in the ratio  $a_1/\epsilon_2$ , without any significant influence on the value of  $\sigma$ .

The use of constant average instead of locally linearized values for  $D_1$  and  $D_2$  (eqn. 12) tends to ab overestimation of  $\sigma$ , but the effect is small and amounts to less than 10% for a sample of broad MW distribution with  $M_w/M_n = 1.3$  even in a portion of the calibration graph where departure from linearity is appreciable.

From the SEC traces of nearly monodisperse PS samples, it was verified that the spreading function is symmetric with a gaussian shape within the elution range attainable with currently available fractions of labelled polymer (*cf.*, also Fig. 5). However, starting from molecular masses of  $\geq 10^6$  daltons, some peak skewness was observed at the same flow-rate (1.0 ml/min). For a precise determination of the MW distribution, the complete dispersion function should be used in this high MW range.

Error in the determination of chromophore stoichiometry. Taking the extreme case where any dependency of  $n$  on the chain length was neglected, we determined the spreading constant for samples of similar  $M_n$  but with different polydispersities. The

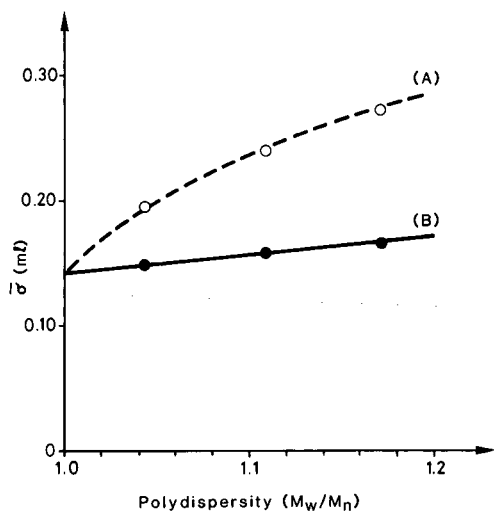


Fig. 7. Effect of chromophore stoichiometry on  $\sigma$  ( $10 \cdot 10^{-3}$  M peroxide, Ultrastyrigel columns). (A)  $n(V)$  considered constant; (B)  $n(V)$  from Fig. 3.

fraction with the largest  $M_w/M_n$  shows also the largest deviation from the correctly determined spreading constant (Fig. 7). When the chromophore stoichiometry was properly taken into account, the variation of  $\sigma$  with polydispersity was much weaker, as expected from the shape of the curve in Fig. 6. This experiment reveals in a vivid manner the importance of using the correct stoichiometry for a precise determination of  $\sigma$ .

## CONCLUSIONS

The results from the present study showed that the utilization of a chromophore-bound polymer is a direct, reliable and versatile technique for the calibration of instrumental dispersion in SEC. Unlike the LALLS photodetector, the equipment is simple and if high accuracy is not required the spreading constant can even be obtained from average molecular weights without the need for any computer data treatment.

The use of a single cell to collect complementary information on mass and molar solute concentration is a definite advantage as compared to other techniques: sampling geometry is known to give rise to non-trivial problems in LALLSP where two different detection cells are placed in series<sup>20</sup>.

As mentioned before, the whole dispersion function,  $G(V - Y)$ , is theoretically accessible with the present technique<sup>18</sup> and will be the subject of further investigation.

It is currently assumed that the spreading constant depends on the molecular mass but not on the nature of the polymer<sup>9</sup>: another application of the present technique would be to use different polymer matrices bearing the chromophore to test for the validity of this hypothesis.

The aim underlying this work was to provide SEC practitioners with polymer standards which can be used both for mass and axial dispersion calibration. At the present stage of development, the method still presents several limitations which need further improvement.

The change of the chromophore number with molecular weight, which requires careful stoichiometry analysis, can be avoided by using anionic polymerization. Except for the difficulties of chemical synthesis, the best solution would be to employ an anionic initiator bearing the chromophore group. In this case, chain termination due to impurities or side reactions cannot interfere with the chemical stoichiometry which would be exactly one chromophore group per polymer chain. The synthesis of such a compound presents probably the most challenging aspect of the problem.

Modern micro-packed columns necessitate injection volumes below 50  $\mu\text{l}$  of dilute polymer solution (typically <0.2 mg/ml for MW above  $10^6$ ). Working with such infinitesimal quantities requires a very high absorption coefficient of the chromophore group to obtain a measurable detector signal.

Even with azobenzene, which has one of the highest extinction coefficients amongst synthetic dyes, the workable range of molecular weight is still limited to <300 000. Straightforward calculations show that in order to analyze polymers in the  $10^6$  MW range, chromophore groups with extinction coefficients exceeding  $2 \cdot 10^8 \text{ cm}^2 \text{ mol}^{-1}$  are necessary. For laboratories having access to a fluorescence detector, another alternative to improve the signal-to-noise ratio would be to use polymer-bound fluorescent groups instead of absorbing chromophores.

The choice of PS as the support polymer bearing the chromophore group

facilitates MW calibration due to the wide availability of good commercial standards. The presence of PS requires however that the UV absorption spectrum of the chromophore possesses a window in the vicinity of 250–270 nm to minimize band overlap. This actually excludes compounds containing benzene rings in their structures. One exception seems to be provided by coronene which has a very high absorption coefficient at 305 nm but is virtually transparent at 262 nm. Compounds belonging to this category are worth consideration in future investigations.

#### ACKNOWLEDGEMENT

Financial support of this work from the Swiss Science Foundation is gratefully acknowledged.

#### REFERENCES

- 1 J. C. Moore, *J. Polym. Sci., Part A-2*, 335 (1964).
- 2 H. Benoît, Z. Grubisic, P. Rempp, D. Decker and J. G. Zilliox, *J. Chim. Phys. Phys. Chim. Biol.*, 63 (1966) 1507.
- 3 Z. Grubisic, P. Rempp and H. Benoît, *Polym. Lett.*, 5 (1967) 573.
- 4 A. C. Ouano, *J. Polym. Sci., Part A-1*, 10 (1972) 2169.
- 5 A. C. Ouano and W. Kay, *J. Polym. Sci., Part A-1*, 12 (1976) 1151.
- 6 L. H. Tung, J. C. Moore and G. W. Knight, *J. Appl. Polym. Sci.*, 10 (1966) 1261.
- 7 I. Tomka and G. Vancso, in *Applied Polymer Analysis and Characterization*, Hanser Publ., Munich, Vienna, New York, 1987, p. 260.
- 8 G. Glöckner, *Polymer Characterization by Liquid Chromatography*, Elsevier, Amsterdam, 1986, pp. 286–297.
- 9 A. E. Hamielec, in J. Janča (Editor), *Steric Exclusion Liquid Chromatography of Polymers*, Marcel Dekker, New York, 1984, pp. 117–160.
- 10 O. F. Olaj, J. W. Breitenbach and I. Hofreiter, *Makromol. Chem.*, 91 (1966) 264.
- 11 H. A. Andreetta, I. H. Sorokin and R. V. Figini, *Makromol. Chem. Rapid Commun.*, 6 (1985) 419.
- 12 T. Q. Nguyen and H. H. Kausch, *Makromol. Chem. Rapid Commun.*, 6 (1985) 391.
- 13 H. Kämmerer, K.-G. Steinfort and F. Rocaboy, *Makromol. Chem.*, 63 (1963) 214.
- 14 L. H. Tung, *J. Appl. Polym. Sci.*, 10 (1966) 375.
- 15 G. S. G. Beveridge and R. S. Schechter, *Optimization: Theory and Practice*, McGraw-Hill, New York, St. Louis, 1970, pp. 180–202.
- 16 A. E. Hamielec and W. H. Ray, *J. Appl. Polym. Sci.*, 13 (1969) 1319.
- 17 A. E. Hamielec, H. J. Ederer and K. H. Ebert, *J. Liq. Chromatogr.*, 4 (1981) 1697.
- 18 K. C. Berger, *Makromol. Chem.*, 16 (1978) 719.
- 19 Z. Grubisic-Gallot, L. Marais and H. Benoît, *J. Polym. Sci., Part A-2*, 14 (1976) 959.
- 20 K. Lederer, *One-Day Advanced Symposium on Size Exclusion Chromatography, Lausanne, May 13, 1987*

CHROM. 20 694

## SOLVENT SELECTIVITY IN THE RESOLUTION OF SOME REGIOISOMERIC AND DIASTEREOMERIC PROSTAGLANDIN INTERMEDIATES ON SILICA

M. LÖHMUS\*, I. KIRJANEN, M. LOPP and Ü. LILLE

*Institute of Chemistry, Estonian Academy of Sciences, Akadeemia tee 15, 200108 Tallinn (U.S.S.R.)*

(First received December 14th, 1987; revised manuscript received May 19th, 1988)

---

### SUMMARY

The possibilities of predicting the selectivity in the resolution of regioisomeric and diastereomeric prostaglandin intermediates on silica gel was investigated. A satisfactory correlation between  $\log \alpha$  and the solvent localization parameters  $m$  and  $m^0$  was obtained, confirming the importance of solvent–solute localization in determining  $\alpha$  values. The results will be useful in developing further the theory of the selectivity of resolution.

---

### INTRODUCTION

Based on the competition model<sup>1,2</sup>, Snyder and co-workers<sup>3–6</sup> pointed out three main physico-chemical factors that determine the selectivity of resolution in normal-phase (including silica gel) adsorption chromatography: (1) solvent strength selectivity; (2) solvent–solute localization (including solvent-specific solvent–solute localization) and (3) solvent–solute hydrogen bonding in stationary and mobile phases.

Nowadays, the solvent strength selectivity is almost impossible to calculate owing to the vertical adsorption of many chemical compounds<sup>7,8</sup>. It is also almost impossible to take into consideration the selectivity of resolution arising from hydrogen bonding<sup>4,6</sup>. Hence the prediction of the selectivity of resolution can be made only on the basis of solvent–solute localization, whereas maximum selectivity in the resolution of certain compounds is attainable using mobile phases with maximum or minimum values of the localization parameter<sup>3,9</sup>, which can easily be calculated from other chromatographic data.

So far it has been shown that it is mainly solvent–solute localization that is responsible for the resolution of some relatively nonpolar compounds<sup>3</sup> and many tetrasubstituted ethanes (diastereomers)<sup>7,10,11</sup>. However, it has also been reported that with more polar chromatographic systems the description of solvent selectivity by the localization terms deteriorates (the dependence of  $\log \alpha$  on the localization parameter of the pure solvent,  $m^0$ , was established)<sup>12</sup>.

This work was aimed at elucidating the possibilities of predicting the selectivity in the resolution of prostaglandin intermediates on silica gel. It is evident that the

isomers to be studied are structurally more complicated than those investigated earlier with respect to the localization theory. However, the chromatographic data reported demonstrate a relatively high importance of localization effects in determining the selectivity of resolution.

#### EXPERIMENTAL

Experiments were performed on a DuPont Model 8843 liquid chromatograph equipped with UV spectrophotometric and refractometric detectors. A Zorbax-SIL

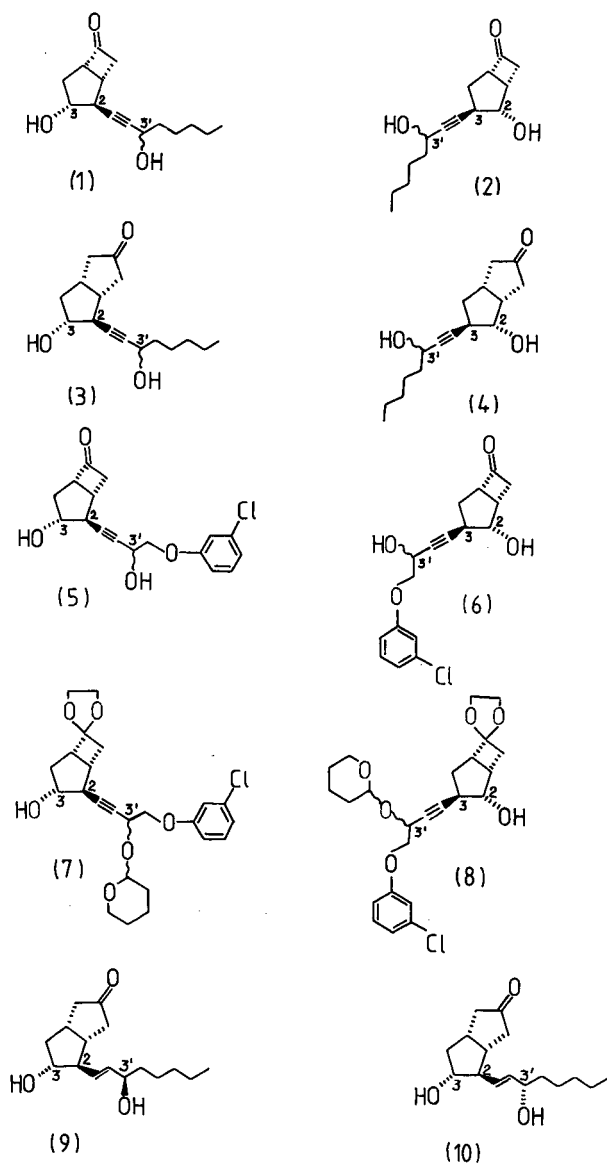


Fig. 1. Formulae of the compounds studied.

column (250 × 4.6 mm I.D.) was used and the mobile phase flow-rate was varied in the range 0.6–1.0 ml/min. The selectivity of resolution was studied in binary mobile phases A–B, where A is *n*-hexane, benzene, chloroform or dichloromethane and B is isopropanol, methanol, acetonitrile, acetone or ethyl acetate. The choice of the solvent was guided by preparative considerations. All the solvents were purchased from Reakhim, USSR. Dichloromethane was distilled before use. The other solvents were prepared as described in ref. 13.

Compounds 1–10, the formulae of which are shown in Fig. 1, were synthesized in the Laboratory of Prostanoids of the Institute of Chemistry, Academy of Sciences of the Estonian S.S.R.<sup>14</sup>. Their structures were verified by <sup>13</sup>C NMR spectroscopy.

The capacity factors ( $k'$ )<sup>15</sup> of compounds 1–10 (Table I) were calculated from the

TABLE I

CAPACITY FACTORS ( $k'$ ) OF COMPOUNDS 1–10 ON A ZORBAX-SIL COLUMN

Temperature, 35°C. Abbreviations: HX = *n*-hexane; BE = benzene; CH = chloroform; IP = isopropanol; ME = methanol; AN = acetonitrile; AC = acetone; EA = ethyl acetate; DCM = dichloromethane.

Mobile phase (v/v)	Mobile phase No.	Compound									
		1	2	3	4	5	6	7	8	9	10
HX-IP:											
80:20	1	—	—	—	—	1.09	1.54	—	—	—	—
85:15	2	1.33	1.84	2.52	1.90	1.75	2.46	—	—	5.32	4.36
90:10	3	2.90	1.99	2.61	4.01	3.48	2.63	2.07	1.75	—	—
93:7	4	—	3.84	5.69	4.16	—	4.73	2.20	—	—	—
95:5	5	—	4.14	5.99	—	—	5.08	3.04	2.67	—	—
			—	—	—	—	—	3.24	—	—	—
			—	—	—	—	—	4.32	4.06	—	—
								4.64			
BE-IP:											
95:5	6	—	—	—	—	1.46	1.79	—	—	—	—
96:4	7	2.46	3.07	5.17	3.71	—	—	—	—	—	—
			3.15								
97:3	8	4.23	5.23	9.23	6.63	3.71	4.57	0.79	1.18	—	—
			5.34					0.85	1.29		
98:2	9	—	—	—	—	7.88	9.90	1.52	2.52	—	—
								1.75	2.71		
99:1	10	—	—	—	—	—	—	3.51	7.47	—	—
								4.68	7.67		
									8.96		
									8.96		
CH-IP:											
95:5	11	—	—	—	—	1.39	1.60	—	—	—	—
96:4	12	1.68	1.88	2.61	2.14	—	—	—	—	3.87	3.87
97:3	13	2.39	2.66	3.32	2.77	4.90	5.64	0.70	1.52	—	—
					2.95			0.80	1.53		
97.5:2.5	14	—	—	—	—	6.78	7.84	0.95	2.16	—	—
								1.10	2.45		

(Continued on p. 80)

TABLE I (continued)

Mobile phase (v/v)	Mobile phase No.	Compound									
		1	2	3	4	5	6	7	8	9	10
98:2	15	—	—	—	—	—	—	1.43 1.68	3.44 3.53 4.05 4.05	—	—
98.5:1.5	16	—	—	—	—	—	—	2.14 2.40	5.30 5.41 6.33 6.33	—	—
<i>BE-ME:</i>											
95:5	17	—	—	—	—	1.09	1.03	—	—	2.68	2.68
97:3	18	4.30	4.39	7.13	5.38	2.27	2.27	—	—	—	—
98:2	19	—	—	—	—	4.31	4.48	0.74 0.82	0.91	—	—
99:1	20	—	—	—	—	—	—	1.92 2.21	3.35 3.56	—	—
99.5:0.5	21	—	—	—	—	—	—	3.05 3.94	6.76 7.00 8.19 8.19	—	—
<i>CH-ME:</i>											
96:4	22	—	—	—	—	0.92	0.86	—	—	—	—
97:3	23	1.97	1.97	2.55	2.10	1.66	1.60	—	—	—	—
98:2	24	3.43	3.75	5.09	4.11	3.58	3.58	0.54	0.78 0.81	—	—
98.3:1.7	25	—	—	—	—	4.82	4.95	—	—	—	—
98.5:1.5	26	—	—	—	—	—	—	0.76 0.86	1.61 1.80	—	—
98.8:1.2	27	—	—	—	—	—	—	1.26 1.48	2.90 2.95 3.34 3.34	—	—
99:1	28	—	—	—	—	—	—	1.41 1.67	3.16 3.26 3.66 3.66	—	—
99.2:0.8	29	—	—	—	—	—	—	1.73 2.07	4.18 4.28 4.99 4.99	—	—
<i>BE-AN:</i>											
0:40	30	—	—	—	—	—	—	—	—	3.18	5.57
70:30	31	—	—	—	—	0.78	1.02	—	—	—	—
75:25	32	—	—	—	—	1.14	1.54	—	—	—	—
80:20	33	2.33	3.31	6.02	4.17	1.69	2.37	—	—	—	—
85:15	34	—	—	—	—	3.17	4.42	1.00 1.26	1.62 1.83	—	—
90:10	35	—	—	—	—	—	—	1.99 2.56	3.66 3.66 4.81 4.93	—	—

TABLE I (continued)

Mobile phase (v/v)	Mobile phase No.	Compound									
		1	2	3	4	5	6	7	8	9	10
CH-AN:											
60:40	36	—	—	—	—	—	—	—	—	2.03	3.36
70:30	37	—	—	—	—	0.78	0.98	—	—	3.40	5.96
80:20	38	2.26	3.19	—	—	1.97	2.60	—	—	—	—
85:15	39	3.56	5.03	—	—	3.51	4.64	—	—	—	—
90:10	40	—	—	—	—	8.46	11.3	1.63	4.12	—	—
									2.05	4.12	
									5.41		
									5.54		
93:7	41	—	—	—	—	—	—	2.87	8.32	—	—
								3.86	8.32		
									11.4		
									11.6		
BE-AC:											
80:20	42	0.91	1.33	1.84	1.32	0.89	1.21	—	—	3.13	4.61
90:10	43	3.27	4.76	7.37	5.53	3.30	4.73	0.78	1.11	—	—
								0.85	1.31		
95:5	44	—	—	—	—	—	—	2.24	4.17	—	—
								2.61	5.01		
CH-AC:											
85:15	45	2.25	3.60	—	—	2.07	3.05	—	—	—	—
88:12	46	3.87	6.17	—	—	3.66	5.26	0.75	1.57	—	—
								0.89	1.93	—	—
94:6	47	—	—	—	—	—	—	2.11	5.41	—	—
								2.50	6.97		
96:4	48	—	—	—	—	—	—	3.52	10.4	—	—
								4.43	14.0		
HX-EA:											
20:80	49	—	—	—	—	—	—	—	—	1.14	1.63
30:70	50	—	—	—	—	0.52	1.01	—	—	1.78	2.50
							1.07				
40:60	51	—	—	—	—	0.85	1.73	—	—	2.87	3.88
							1.79				
50:50	52	1.29	2.71	3.17	2.05	1.61	3.17	—	—	—	—
			2.79				3.27				
55:45	53	1.61	3.34	4.40	2.74	—	—	—	—	—	—
			3.48								
60:40	54	2.19	4.60	—	—	3.11	6.29	—	—	—	—
			4.75				6.49				
65:35	55	3.11	6.49	—	—	4.53	9.08	2.36	2.36	—	—
			6.73				9.42	2.69	2.43		
									2.89		
									2.89		
70:30	56	—	—	—	—	—	—	3.35	3.51	—	—
								3.35	3.62		
								3.82	4.31		
								3.86	4.35		

(Continued on p. 82)

TABLE I (continued)

Mobile phase (v/v)	Mobile phase No.	Compound									
		1	2	3	4	5	6	7	8	9	10
75:25	57	—	—	—	—	—	—	4.96 4.96 5.67 5.78	5.44 5.67 6.71 6.80	—	—
<i>BE-EA:</i>											
40:60	58	—	—	—	—	—	—	—	—	2.00	2.97
50:50	59	—	—	—	—	—	—	—	—	3.18	5.12
60:40	60	—	—	—	—	0.91	1.92	—	—	5.72	9.56
70:30	61	1.78	3.72 3.84	—	—	1.71	3.48	—	—	—	—
80:20	62	4.03	8.10 8.27	—	—	4.00	7.76	1.72 2.04	2.41 2.51 3.13 3.13	—	—
90:10	63	—	—	—	—	—	—	5.03 6.43	9.30 9.54 12.5 12.5	—	—
<i>CH-EA:</i>											
50:50	64	—	—	—	—	0.85	1.75 1.80	—	—	2.79	4.48
60:40	65	—	—	—	—	1.39	2.81 2.88	—	—	—	—
65:35	66	1.97	4.15 4.26	3.19	4.30	—	—	—	—	—	—
70:30	67	2.71	5.49 5.65	—	—	2.69 2.73	5.29 5.38	—	—	—	—
75:25	68	—	—	—	—	4.06 4.17	7.77	1.40 1.64	2.61 2.70 3.42 3.42	—	—
80:20	69	—	—	—	—	6.72 6.89	12.4	2.01 2.45	4.37 4.52 5.83 5.83	—	—
85:15	70	—	—	—	—	—	—	2.94 3.79	7.39 7.62 10.2 10.2	—	—
<i>DCM-EA:</i>											
60:40	71	—	—	—	—	0.83	1.52	—	—	—	—
70:10	72	1.87	3.28	—	—	1.44	2.53	—	—	—	—
80:20	73	3.66	6.02	—	—	3.12 3.21	4.97	1.37 1.65	2.56 3.39	—	—

chromatograms plotted on a recorder. To improve the precision of measurements, the chart speed was chosen so that the values of the measured distances exceeded 5 cm. Reproducibility measurements of the given  $k'$  values were shown to have a relative standard deviation of less than 1%. The column void volume ( $V_0$ ) determined as the elution volume of toluene using *n*-hexane-isopropanol (75:25) as the mobile phase, was 3.41 ml.

For regioisomeric pairs 1-2, 3-4, 5-6 and 7-8, the selectivity ( $\alpha$ )<sup>15</sup> (Table II) was

TABLE II

$\alpha$  VALUES FOR RESOLUTION OF ISOMER PAIRS 1-10, THE SOLVENT STRENGTH,  $\epsilon_{AB}$ , OF THE MOBILE PHASES USED, THE MOLAR FRACTION OF SOLVENT B IN THE ADSORBED MONOLAYER,  $\theta_B$ , AND THE LOCALIZATION PARAMETER OF MOBILE PHASES,  $m$

Column, Zorbax-SIL.

Mobile phase No.*	Compound pair					$\epsilon_{AB}$	$\theta_B$	$m$
	1-2	3-4	5-6	7-8	9-10			
1	—	—	1.45	—	—	0.421	0.93	0.84
2	1.44	0.74	1.45	—	0.82	0.401	0.92	0.83
3	1.38	0.70	1.41	0.82	—	0.383	0.91	0.83
4	—	—	—	0.85	—	0.368	0.89	0.82
5	—	—	—	0.91	—	0.356	0.88	0.82
6	—	—	1.22	—	—	0.383	0.56	0.50
7	1.26	0.72	—	—	—	0.367	0.51	0.43
8	1.25	0.72	1.23	1.51	—	0.345	0.44	0.32
9	—	—	1.26	1.60	—	0.321	0.35	0.22
10	—	—	—	2.02	—	0.291	0.22	0.11
11	—	—	1.14	—	—	0.364	0.47	0.43
12	1.12	0.82	—	1.0	0.350	0.42	0.36	—
13	1.11	0.86	1.15	2.03	—	0.331	0.35	0.29
14	—	—	1.16	2.25	—	0.322	0.31	0.26
15	—	—	—	2.42	—	0.312	0.26	0.22
16	—	—	—	2.57	—	0.301	0.21	0.19
17	—	—	0.95	—	1.0	—	—	—
18	1.02	0.76	1.0	—	—	—	—	—
19	—	—	1.04	1.17	—	—	—	—
20	—	—	—	1.67	—	—	—	—
21	—	—	—	2.16	—	—	—	—
22	—	—	0.94	—	—	—	—	—
23	1.0	0.82	0.96	—	—	—	—	—
24	1.09	0.81	1.0	1.47	—	—	—	—
25	—	—	1.03	—	—	—	—	—
26	—	—	—	2.10	—	—	—	—
27	—	—	—	2.29	—	—	—	—
28	—	—	—	2.23	—	—	—	—
29	—	—	—	2.42	—	—	—	—

(Continued on p. 84)

TABLE II (continued)

Mobile phase No.*	Compound pair					$\epsilon_{AB}$	$\theta_B$	$m$
	1-2	3-4	5-6	7-8	9-10			
30	—	—	—	—	1.75	0.455	0.80	0.97
31	—	—	1.31	—	—	0.436	0.73	0.90
32	—	—	1.31	—	—	0.422	0.68	0.85
33	1.42	0.69	1.35	—	—	0.404	0.63	0.76
34	—	—	1.40	1.53	—	0.380	0.55	0.61
35	—	—	—	1.87	—	0.348	0.44	0.39
36	—	—	—	—	1.66	0.448	0.77	0.96
37	—	—	1.26	—	1.75	0.426	0.69	0.88
38	1.41	—	1.32	—	—	0.392	0.58	0.71
39	1.41	—	1.32	—	—	0.369	0.50	0.53
40	—	—	1.34	2.61	—	0.336	0.39	0.39
41	—	—	—	2.95	—	0.314	0.30	0.29
42	1.42	0.72	1.37	—	1.47	0.428	0.71	0.80
43	1.47	0.75	1.43	1.48	—	0.379	0.57	0.57
44	—	—	—	1.89	—	0.331	0.40	0.30
45	1.60	—	1.47	—	—	0.400	0.61	0.70
46	1.59	—	1.44	2.13	—	0.383	0.56	0.60
47	—	—	—	2.9	—	0.336	0.38	0.36
48	—	—	—	3.03	—	0.314	0.29	0.26
49	—	—	—	—	1.43	0.460	0.99	0.60
50	—	—	2.00	—	1.40	0.447	0.99	0.60
51	—	—	2.07	—	1.35	0.429	0.98	0.60
52	2.13	0.65	2.00	—	—	0.406	0.97	0.60
53	2.12	0.62	—	—	—	0.394	0.97	0.60
54	2.13	—	2.05	—	—	0.381	0.96	0.59
55	2.13	—	2.04	1.05	—	0.365	0.95	0.59
56	—	—	—	1.10	—	0.347	0.94	0.59
57	—	—	—	1.15	—	0.332	0.93	0.59
58	—	—	—	—	1.49	0.428	0.87	0.58
59	—	—	—	—	1.61	0.414	0.83	0.56
60	—	—	2.12	—	1.67	0.400	0.78	0.55
61	2.12	—	2.04	—	—	0.380	0.70	0.50
62	2.03	—	1.94	1.49	—	0.352	0.59	0.40
63	—	—	—	1.91	—	0.311	0.40	0.19
64	—	—	2.09	—	1.61	0.411	0.80	0.56
65	—	—	2.05	—	—	0.395	0.74	0.54
66	2.13	0.74	—	—	—	0.385	0.70	0.52
67	2.06	—	1.97	—	—	0.375	0.65	0.48
68	—	—	1.88	2.00	—	0.362	0.59	0.43
69	—	—	1.82	2.30	—	0.347	0.53	0.37
70	—	—	—	2.63	—	0.330	0.44	0.29
71	—	—	1.83	—	—	0.380	0.60	0.44
72	1.75	—	1.76	—	—	0.362	0.49	0.33
73	1.64	—	1.57	1.97	—	0.343	0.36	0.23

\* See Table I.

calculated as the ratio of the  $k'$  value of 3-alkynyl-substituted isomers to that of 2-alkynyl-substituted isomers. In some instances the resolution of diastereomers at C-3' took place. With compounds 7 and 8, diastereomers at a carbon atom in the masking tetrahydropyranyl group were also resolved (see Table I). Therefore, the values were calculated using the mean values of the capacity factors given in Table I (it is evident that regioisomers are more easily resolvable than the respective diastereomers).

For diastereomers 9 and 10,  $\alpha$  was calculated as the ratio of  $k'$  of isomer 10 to that of isomer 9 (Table II).

#### CALCULATIONS

The solvent strength ( $\varepsilon_{AB}$ ) of the mobile phases (Table II) was determined using the equation<sup>4,6</sup>

$$\varepsilon_{AB} = \varepsilon_A + \frac{\log(N_B \cdot K + 1 - N_B)}{\alpha' n_B} \quad (1)$$

where

$$K = 10^{\alpha' n_B (\varepsilon_B - \varepsilon_A)} \quad (2)$$

$N_B$  = molar fraction of solvent B in the mobile phase;  $\alpha'$  = adsorbent activity function ( $\alpha' = 0.57$ )<sup>10,12</sup>;  $n_B$  = molecular area of solvent B (isopropanol, 4.4; acetonitrile, 3.1; acetone, 4.2; ethyl acetate, 5.2)<sup>6,16</sup>;  $\varepsilon_A$  and  $\varepsilon_B$  = solvent strengths for pure solvents A and B, respectively (for solvents A, the following  $\varepsilon_A$  values were used: *n*-hexane, 0.0; benzene, 0.25; chloroform, 0.26; dichloromethane, 0.30)<sup>6,17</sup>.

As the solvent strength of the localizing solvent B is different for the localized ( $\varepsilon'_B$ ) and delocalized ( $\varepsilon''_B$ ) molecules, then  $\varepsilon_B$  depends also on the localization function  $\%_{lc}$ <sup>4,6,16,18</sup>:

$$\varepsilon_B = \%_{lc} (\varepsilon'_B - \varepsilon''_B) + \varepsilon''_B \quad (3)$$

The localization function depends on the molar fraction of solvent B in the adsorbed monolayer  $\theta_B$ <sup>4,6,16,18</sup>:

$$\%_{lc} = (1 - \theta_B) [1/(1 - 0.94\theta_B) - 14.5\theta_B^2] \quad (4)$$

The value of  $\theta_B$  depends on  $K$  and  $N_B$ <sup>12,18</sup>:

$$\theta_B = \frac{KN_B}{N_A + KN_B} \quad (5)$$

where  $N_A$  is the molar fraction of solvent A in the mobile phase.

The  $\varepsilon_B$  values were calculated from eqns. 2–5 using the iterative method. From these equations the  $\theta_B$  values were also found (Table II).  $\varepsilon'_B$  and  $\varepsilon''_B$  were taken from refs. 6 and 16 or calculated using eqn. 15 and Table I in ref. 6. For methanol-containing

TABLE III  
VALUES OF  $\epsilon'_B$  AND  $\epsilon''_B$  FOR THE SOLVENT SYSTEMS STUDIED

Solvent system*	$\epsilon'_B$	$\epsilon''_B$
HX-IP	1.83	0.60
BE-IP	0.80	0.60
CH-IP	0.76	0.60
BE-AN	0.60	0.52
CH-AN	0.58	0.52
BE-AC	0.68	0.53
CH-AC	0.66	0.53
HX-EA	0.94	0.48
BE-EA	0.53	0.48
CH-EA	0.52	0.48
DCM-EA	0.48	0.48

\* Abbreviations as in Table I.

mobile phases it was impossible to calculate  $\epsilon_B$ . For clarity these values are given in Table III.

The localization parameters ( $m$ ) of the mobile phases (Table II) were calculated using the equation<sup>3</sup>

$$m = m^0 f(\theta_B) + m_A^0 f(\theta_A + \theta_B) - f(\theta_B) \quad (6)$$

where  $f(\theta_A)$  = solvent-localization function, which varies with  $\theta_B$  [the  $f(\theta_B)$  values were found by means of the  $\theta_B$  values by interpolating the data in Table 3 in ref. 3];  $f(\theta_A + \theta_B) = 1$ ;  $m_A^0$  = solvent-localization parameter for pure solvent A (for chloroform and dichloromethane,  $m_A^0 = 0.10$ ; for benzene and *n*-hexane,  $m_A^0 = 0.0$ )<sup>6</sup>;  $m^0$  = solvent-localization parameter for pure solvent B.

The  $m^0$  values were taken from ref. 12 (isopropanol, 0.85; acetonitrile, 1.05; acetone, 0.96; ethyl acetate, 0.60). For methanol  $m^0$  was not available in the literature.

## RESULTS AND DISCUSSION

The dependence of the  $\log \alpha$  values on the localization parameters  $m$  and  $m^0$  using eleven solvent systems was studied as an example on compound pairs 1–2, 5–6 and 7–8, for which a significant amount of experimental data was obtained. The methanol-containing mobile phases were not studied in this respect owing to the lack of  $m^0$  and  $\epsilon'$  values for methanol in the literature.

Solutes with hydroxyl, carbonyl and ether functionalities compete with polar solvent molecules for active silanol OH groups on the silica surface, and this solvent–solute localization to some extent influences the selectivity of separation. However, Fig. 2 demonstrates the absence of a linear  $\log \alpha$ – $m$  correlation for the resolution of the regioisomeric pairs of ketonediols 1–2 and 5–6 (the correlation coefficient  $r = 0.06$ ). This is not surprising because polar solvents with proton acceptor and donor properties (see Table I in ref. 19) participate in solvent–solute interactions,

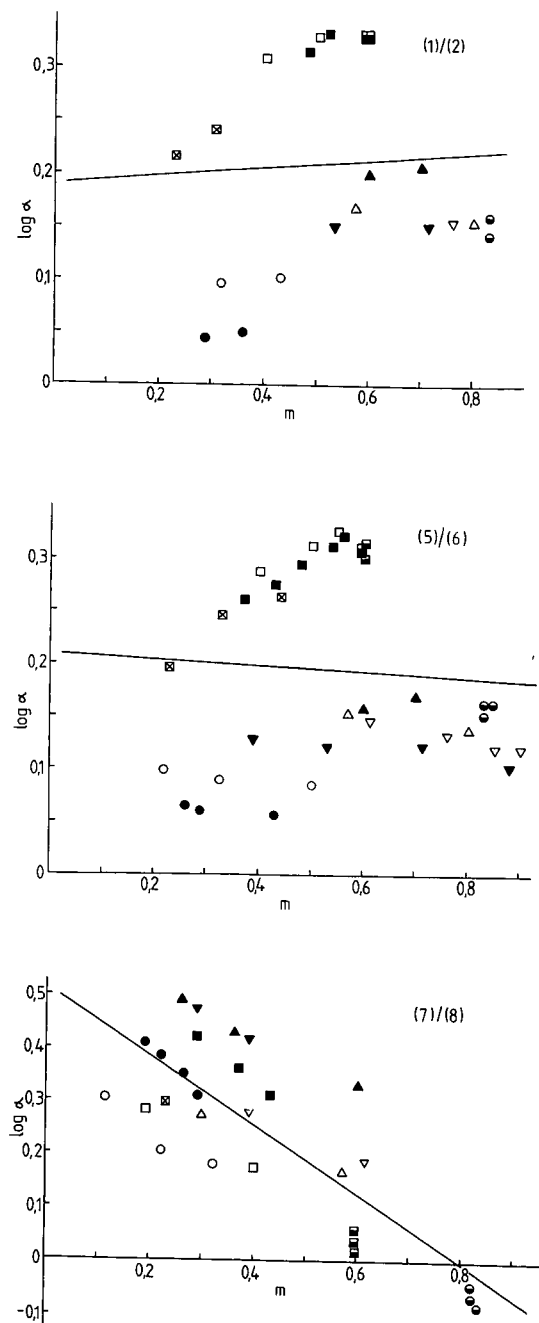


Fig. 2. Dependence of  $\log \alpha$  on the mobile phase localization parameter  $m$  for the resolution of compounds 1-2, 5-6 and 7-8 ( $r = 0.06, 0.06$  and  $0.79$ , respectively). Solvent systems: ●,  $n$ -hexane-isopropanol; ○, benzene-isopropanol; ●, chloroform-isopropanol; ▽, benzene-acetonitrile; ▼, chloroform-acetonitrile; △, benzene-acetone; ▲, chloroform-acetone; ◻,  $n$ -hexane-ethyl acetate; ◻, benzene-ethyl acetate; ■, chloroform-ethyl acetate; ⊠, dichloromethane-ethyl acetate.

particularly hydrogen bonds, which effect the selectivity in a different way to the localization effects. As a result, the log  $\alpha$ - $m$  correlation is absent.

The protection of one hydroxyl and carbonyl function in two ketonediacols, 5  $\rightarrow$  7 and 6  $\rightarrow$  8, results in a much better log  $\alpha$ - $m$  correlation ( $r = 0.79$ ). It is evident that the hydrogen bonds with the hydroxyl groups in the 2/3-position and ether oxygen (including ketal oxygen) influence the selectivity of separation in a similar manner to the localization effects.

It is also worth mentioning the intramolecular hydrogen bond between the C-3 hydroxyl group and the ketal oxygen atom of the carbonyl-protecting group at C-6 for compound 7 demonstrated in ref. 20. In compound 8 such a hydrogen bond is absent.

An increase in the proportion of the more polar solvent in the solvent systems probably results in stronger hydrogen bonding between the mobile phase and compound 8, which leads to a decreased retention and, therefore, to lower  $\alpha$  values in all the solvent systems studied. It is likely that a similar interaction with compound 7 is precluded owing to the intramolecular hydrogen bond. The latter can also contribute to the less extensive localization in compound 7 compared with 8 (see below).

Further, an attempt was made to determine quantitatively the contribution of hydrogen bonding to the separation selectivity of the less polar compounds 7 and 8. In *n*-hexane-isopropanol and *n*-hexane-ethyl acetate systems (correspondingly mobile phases 5 and 57 in Table II), the monolayer on the silica surface is complete ( $\theta_B > 0.88$ ) and solvent-solute localization has reached its steady level. Further increases in the proportions of isopropanol and ethyl acetate in the mobile phase, accompanied by certain changes in the solvent strength,  $\Delta\epsilon_{AB}$  (systems 3-4 and 55-56), may influence the separation selectivity only due to the hydrogen bonds and solvent strength. The influence of the latter on the separation of isomers is negligible<sup>4,6,8</sup>. As the absolute values of selectivity changes are determined by the arbitrarily chosen mobile phases,

TABLE IV

VALUES OF THE  $\theta_B$  INTERVAL, SELECTIVITY CHANGE ( $\Delta\log \alpha$ ), MOBILE PHASE STRENGTH CHANGE ( $\Delta\epsilon_{AB}$ ) AND  $\Delta\log \alpha/\Delta\epsilon_{AB}$  RELATIONSHIP IN THE SOLVENT SYSTEMS USED FOR SEPARATION OF REGIOISOMERS 7 AND 8

Solvent system*	$\theta_B$ interval	$\Delta\log \alpha$	$\Delta\epsilon_{AB}$	$\Delta\log \alpha/\Delta\epsilon_{AB}$
HX-IP	0.88-0.91	0.045	0.027	1.67
HX-EA	0.93-0.95	0.040	0.033	1.21
				Mean: 1.44
BE-IP	0.22-0.44	0.126	0.054	2.33
CH-IP	0.21-0.35	0.103	0.030	3.43
BE-AN	0.35-0.38	0.087	0.032	2.72
CH-AN	0.31-0.34	0.053	0.022	2.41
BE-AC	0.33-0.38	0.106	0.048	2.21
CH-AC	0.31-0.38	0.153	0.069	2.22
BE-EA	0.40-0.59	0.108	0.041	2.63
CH-EA	0.44-0.59	0.119	0.032	3.73
				Mean: 2.72

\* Abbreviations as in Table I.

then in order to compare the selectivity changes in various mobile phases in this instance it is reasonable to relate the values of  $\Delta \log \alpha$  to  $\Delta \epsilon_{AB}$ . The  $\Delta \log \alpha / \Delta \epsilon_{AB}$  values form the absolute scale for selectivity changes.

As can be seen in Table IV, the mean  $\Delta \log \alpha / \Delta \epsilon_{AB}$  value for the systems with a complete monolayer afford about 50% of this value for eight systems with an incomplete monolayer. Therefore, the hydrogen bond and solvent-solute localization contribute to the separation selectivity of compounds 7 and 8 almost equally.

However, it should be borne in mind that a certain part of the hydrogen bonds in the mobile phase can be cancelled out by the corresponding bonds in the completed monolayer (see below).

It appears that in the resolution of compounds 7 and 8 the variation of the nonpolar or weakly polar solvent in the mobile phase in the sequence *n*-hexane-benzene-chloroform results in a greater increase in selectivity than with polar solvents (see Fig. 2). For example, the transition from *n*-hexane to benzene and from benzene to chloroform in the isopropanol-containing binary systems ( $\Delta m = 0.6$ ) results in an approximately 0.5 unit increase in  $\log \alpha$  for the partially blocked ketonediols 7 and 8 (in

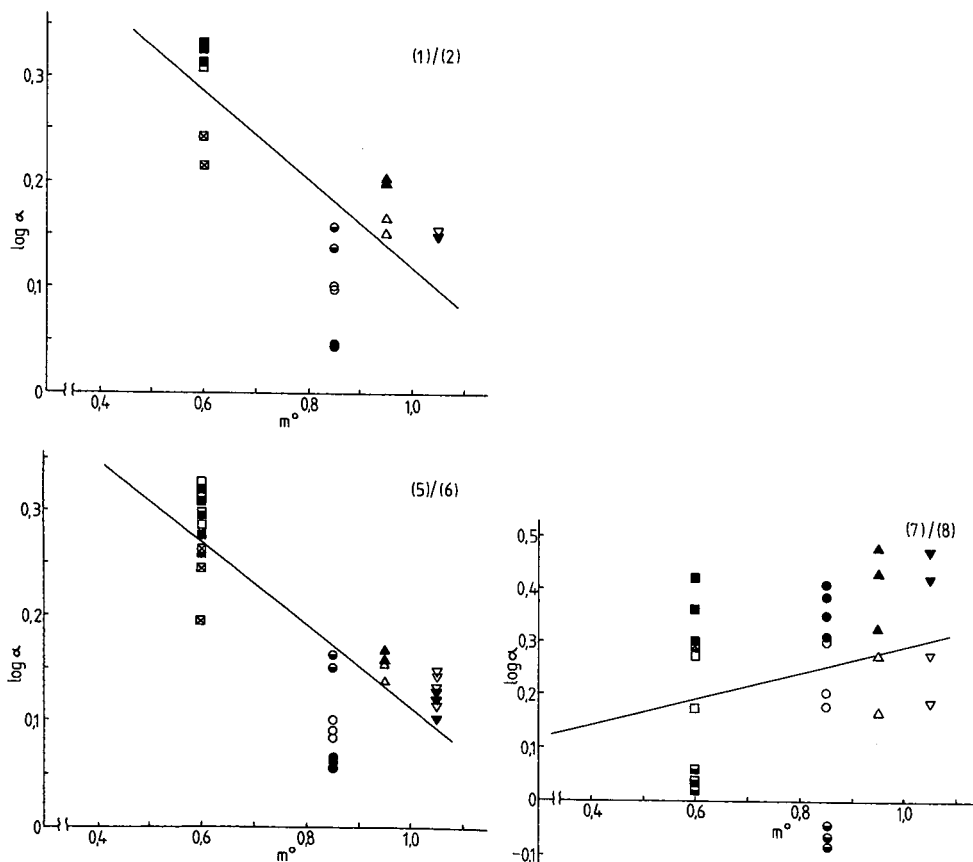
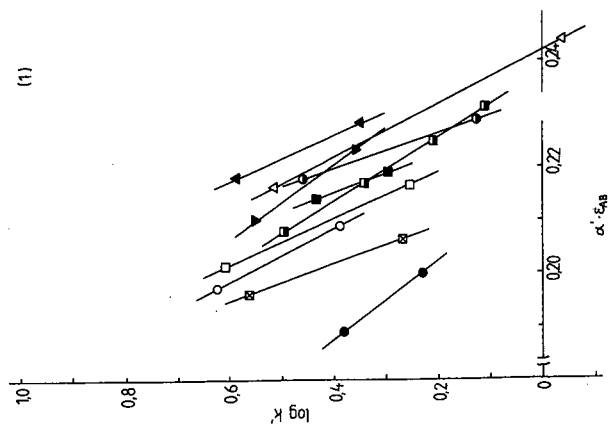
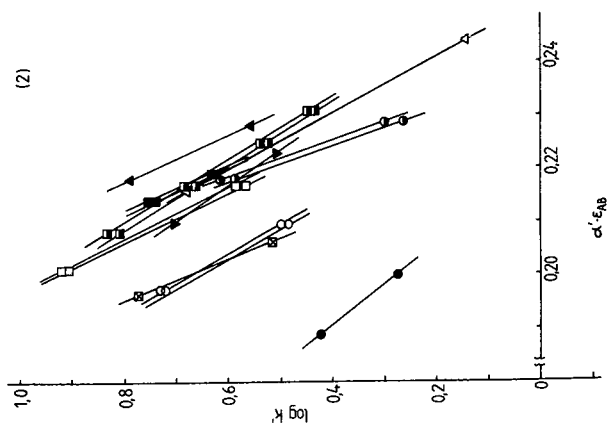
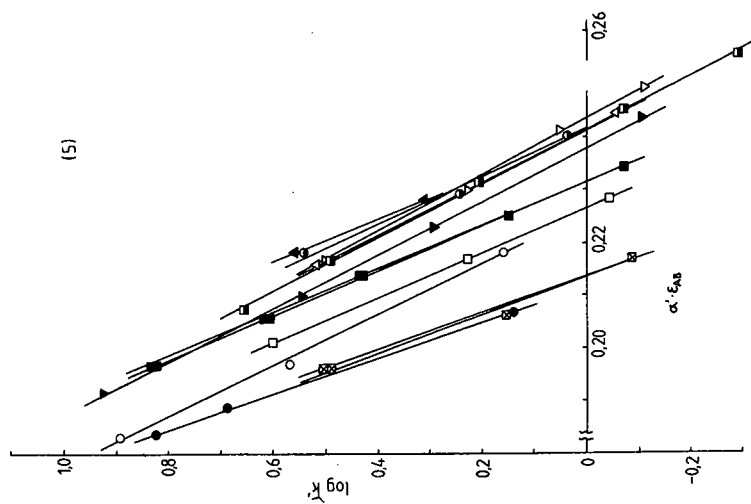


Fig. 3. Dependence of  $\log \alpha$  on the localization parameter of solvent B ( $m^0$ ) for the resolution of compounds 1-2, 5-6 and 7-8 ( $r = 0.76, 0.83$  and  $0.25$ , respectively). Solvent systems as in Fig. 2.



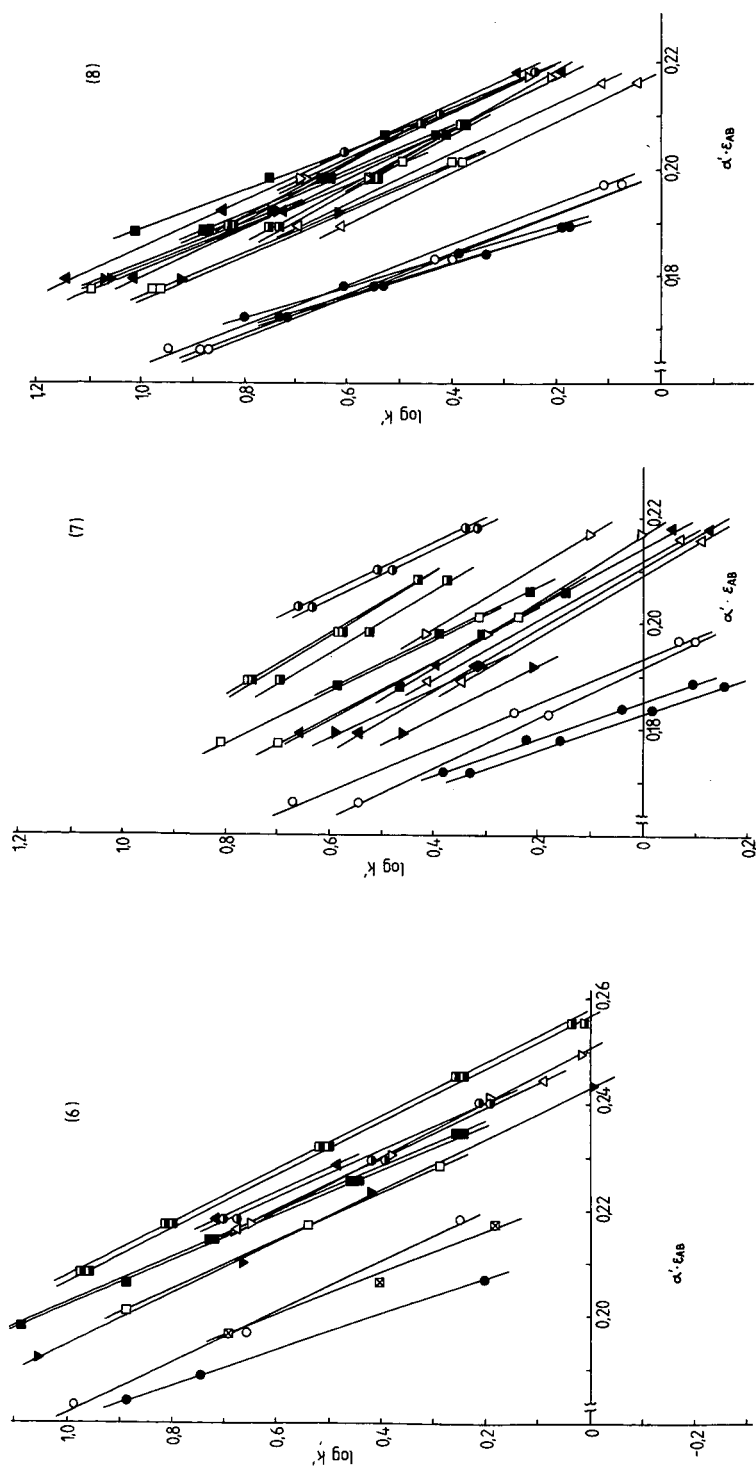


Fig. 4. Dependence of  $\log k'$  on  $\alpha' \epsilon_{AB}$  for compounds 1, 2 and 5-8. Solvent systems as in Fig. 2.

the case of the first transition the elution order is reversed). With a change in the benzene-containing mobile phases isopropanol–ethyl acetate–acetone–acetonitrile ( $\Delta m = 0.5$ ),  $\log \alpha$  increases only by about 0.1 unit. A similar change in the chloroform-containing systems ( $\Delta m = 0.4$ ) gives about a 0.2-unit increase in  $\log \alpha$ . Therefore, for compounds 7 and 8, the best way to vary  $m$  and control the localization effects is to vary the less polar component in the mobile phase. In this case solvent–solute interactions remain almost unchanged.

Naturally this is not so in the chloroform-containing mobile phase in which, owing to the strong proton-donor properties of chloroform, an additional source of selectivity appears. This is clearly seen on comparing the separation selectivity of compounds 7 and 8 in the systems benzene–acetone ( $N_B = 0.118$ ) and chloroform–acetone ( $N_B = 0.131$ ) (mobile phases 45 and 48 in Table II). The change from benzene to chloroform is accompanied by a selectivity increase from 1.48 to 2.13.

As mentioned above, with the ketonediol pairs 1–2 and 5–6 strong hydrogen bonding results in the disappearance of the dependence of  $\log \alpha$  on  $m$ . This is also confirmed by the fact (as seen in Fig. 2) that in some solvent systems the selectivity of resolution increases with increasing concentration of more polar components in the mobile phase (corresponding to an increase in  $m$ ), whereas in other systems it decreases.

Snyder *et al.*<sup>12</sup> concluded that in mixtures of weakly polar and strongly polar solvents the selectivity of resolution is determined by the strongly polar solvent and that in resolving the diastereomers of the substituted 2,3-diphenylglutaric acids a linear dependence of  $\log \alpha$  on the localization parameter of pure solvent B,  $m^\circ$ , results. Therefore we examined the data on the resolution of compounds 1–2, 5–6 and 7–8 in the coordinates  $\log \alpha - m^\circ$  (Fig. 3). As can be seen, the selectivity of the resolution of the partially masked ketonediols 7 and 8 does not depend on  $m^\circ$ . On resolution of 1–2 and 5–6, a linear dependence of  $\log \alpha$  on  $m^\circ$  ( $r = 0.76$  and  $0.83$ , respectively) can clearly be seen.

However, it is also seen from Fig. 3 that for the experimental points obtained by resolution with the mobile phases benzene–isopropanol and chloroform–isopropanol, a deviation from a straight line takes place. This phenomenon can be explained by Fig. 4, in which the dependence of  $\log k'$  of compounds 1–2 and 5–8 on the product of  $\alpha'$  and the solvent strength  $\varepsilon_{AB}(\alpha', \varepsilon_{AB})$  of all the mobile phases used is shown. For all the compounds studied, the positions of the lines for the solvent systems benzene–isopropanol, chloroform–isopropanol and also dichloromethane–ethyl acetate are clearly different to those of the eight other systems. In other words, if these solvent systems are used to achieve the given retention, mobile phases with a significantly lower solvent strength are required. This phenomenon in the systems benzene–isopropanol and chloroform–isopropanol consist in the formation of hydrogen bonding associates between the solute and solvent molecules in the mobile phase. It is likely that in *n*-hexane–isopropanol the presence of such associates in the monolayer ( $\theta_B \approx 1.0$ ) will cancel out the mobile phase influence and the  $\varepsilon_{AB}$  value in this system does not seem anomalously low. It seems difficult to us to explain why the retention is anomalous in dichloromethane–ethyl acetate.

If we consider the resolution in the solvent systems benzene–isopropanol, chloroform–isopropanol and dichloromethane–ethyl acetate as exceptional and reject the experimental points corresponding to these solvent systems in Fig. 3 for

compounds 1–2 and 5–6, then an increase in  $r$  to 0.94 and 0.97, respectively, results.

We consider that the 3-alkynyl-substituted isomers 2, 6 and 8 localize to a greater extent than the 2-alkynyl-substituted isomers. This is evident from Figs. 2 and 3 and the definition of selectivity (see Experimental). It means that 3-alkynyl-substituted isomers are structurally more suitable for interactive with the silanol OH groups on the silica surface.

## CONCLUSIONS

The possibility of predicting the selectivity of the resolution of some regioisomeric bicyclic ketonediol (intermediates of prostaglandins) by means of the mobile phase localization parameters  $m$  and  $m^0$  has been demonstrated. The resolution of partially blocked regioisomers can be described by solvent–solute localization; for their resolution it is necessary to proceed from the required retention ( $k' = 2$ –5). By using known techniques mobile phase compositions can be found, and these permit the calculation of  $m$ . The mobile phases for which the  $m$  values are lower afford the highest selectivity of resolution of compounds such as 7 and 8.

The resolution of regioisomers having free hydroxyl and carbonyl groups can be described by the localization parameter of pure strong solvents,  $m^0$ . To achieve maximum resolution of regioisomers, the use of mobile phases containing polar solvents with lower  $m^0$  values is required.

It has also been shown that the resolution of the given compounds depends strongly on the hydrogen bonding between solutes and solvents whose prediction of  $\alpha$  values is complicated using mathematical relationships. Therefore, the use of the localization parameters  $m$  and  $m^0$  is suitable only for a preliminary and approximate choice of the mobile phase. To achieve maximum resolution and to elucidate the role of solute-solvent interactions, further study is required.

## REFERENCES

- 1 L. R. Snyder, *Anal. Chem.*, 46 (1974) 1384.
- 2 L. R. Snyder and H. Poppe, *J. Chromatogr.*, 184 (1980) 363.
- 3 L. R. Snyder, J. L. Glajch and J. J. Kirkland, *J. Chromatogr.*, 218 (1981) 299.
- 4 L. R. Snyder, *J. Chromatogr.*, 255 (1983) 3.
- 5 L. R. Snyder, *LC, Liq. Chromatogr. HPLC Mag.*, 1 (1983) 478.
- 6 L. R. Snyder, in Cs. Horvath (Editor), *High-Performance Liquid Chromatography*, Vol. 3, Academic Press, New York, 1983, p. 157.
- 7 L. R. Snyder, *Principles of Adsorption Chromatography*, Marcel Dekker, New York, 1968.
- 8 S. C. Ruckmick and J. R. Hurtubise, *J. Chromatogr.*, 360 (1986) 343.
- 9 M. D. Palamareva and L. R. Snyder, *Chromatographia*, 19 (1984) 352.
- 10 M. D. Palamareva, B. J. Kurtev, M. P. Mladenova and B. M. Blagoev, *J. Chromatogr.*, 235 (1982) 299.
- 11 L. R. Snyder, *J. Chromatogr.*, 245 (1982) 165.
- 12 L. R. Snyder, M. D. Palamareva, B. J. Kurtev, L. Z. Viteva and J. N. Stefanowski, *J. Chromatogr.*, 354 (1986) 107.
- 13 M. Lõhmus, A. Paju, N. Samel, M. Lopp and U. Lille, *Eesti NSV Tead. Akad. Toim. Keem.*, 35 (1986) 142.
- 14 M. Lopp, *Eesti NSV Tead. Akad. Toim. Keem.*, 36 (1987) 165.
- 15 L. R. Snyder and J. J. Kirkland, *Introduction to Modern Liquid Chromatography*, Wiley-Interscience, New York, 2nd ed., 1979.
- 16 L. R. Snyder and J. L. Glajch, *J. Chromatogr.*, 248 (1982) 165.

- 17 J. L. Glajch and L. R. Snyder, *J. Chromatogr.*, 214 (1981) 21.
- 18 L. R. Snyder and J. L. Glajch, *J. Chromatogr.*, 214 (1981) 1.
- 19 L. R. Snyder, *J. Chromatogr.*, 92 (1974) 223.
- 20 R. J. Cave, C. C. Howard, G. Klinkert, R. F. Newton, D. P. Reynolds, A. H. Wadsworth and S. M. Roberts, *J. Chem. Soc., Perkin Trans.*, 1 (1979) 2954.

CHROM. 20 687

## GROUP CONTRIBUTIONS TO HYDROPHOBICITY AND ELUTION BEHAVIOUR OF PYRIDINE DERIVATIVES IN REVERSED-PHASE HIGH-PERFORMANCE LIQUID CHROMATOGRAPHY

FEDERICO GAGO

*Department of Pharmacology, University of Alcalá de Henares, Madrid (Spain)*

JULIO ALVAREZ-BUILLA\*

*Department of Organic Chemistry, University of Alcalá de Henares, Madrid (Spain)*  
and

JOSÉ ELGUERO

*Instituto de Química Médica, C.S.I.C., Madrid (Spain)*

(First received March 7th, 1988; revised manuscript received May 23rd, 1988)

---

### SUMMARY

The mean hydrophobic contributions,  $\pi_m^*$ , of substituents in a sample of 34 monosubstituted pyridines has been determined by using reversed-phase high-performance liquid chromatography. The values are compared with those obtained for benzene.

---

### INTRODUCTION

The logarithm of the octanol–water partition coefficient of a compound,  $\log P_{o/w}$ , is a parameter frequently used as a measure of hydrophobicity in the study of quantitative structure–activity relationships (QSARs) in drug design and pharmacology. It has been classically determined by the “shake-flask” method<sup>1</sup>, but lately many attempts have been made to simplify this determination, especially by means of chromatographic techniques<sup>2,3</sup>. Although some novel methods such as droplet counter-current chromatography<sup>4</sup> and micellar chromatography<sup>5</sup> have been reported, reversed-phase high-performance liquid chromatography (RP-HPLC) with hydro-organic mobile phases continues to be the most widely used and the best studied alternative so far.

Two different methods exist for the calculation of approximate  $\log P_{o/w}$  values, namely the  $\pi$  approach and the fragment approach.  $\pi$  was initially proposed<sup>6</sup> as a substituent parameter for the replacement of an hydrogen on an aromatic carbon atom and was later extended to aliphatic carbon systems. The summation of these hydrophobic contributions from each constitutive group will afford estimates of  $\log P_{o/w}$ , but deviations are often observed that need be accounted for by interaction terms<sup>7,8</sup>. *De novo* calculation of these  $\log P_{o/w}$  values may be attempted by making use of the fragment method of Rekker<sup>9</sup> and Hansch and Leo<sup>10</sup>.

Work directed to the determination of hydrophobicity by indirect means has focused on the benzene ring, taking into account its relative simplicity. Heteroaromatics, on the other hand, have received comparatively much less attention due in part to their greater complexity but also to the fact that many of their  $\log P_{o/w}$  values are lacking. For these reasons, few papers have dealt with the problem in detail<sup>11,12</sup>.

Before the determination of the hydrophobic contributions from substituents in this sort of structures is undertaken, it should be borne in mind that a monosubstituted ring system possessing one or several heteroatoms behaves as a di- or polysubstituted benzene, since the heteroatoms exert  $\pi$ -donor or  $\pi$ -acceptor effects<sup>13</sup>. Therefore, the substituent electronic and/or steric effects on each position of the ring are different and, as has already been discussed for benzenoid compounds<sup>7,8</sup>, hydrophobic contributions are also expected to vary. This question has also been raised for heterocycles, but to date information is scarce<sup>11</sup>. These discrepancies may generate errors capable of vitiating any attempt at QSAR analysis in which  $\pi$  values obtained from the benzene ring are incautiously used to study substituent effects on heterocyclic systems.

In this paper we present a simple and rapid RP-HPLC method of interest for the estimation of  $\log P_{o/w}$  values of pyridine derivatives. By means of multiple regression analysis (MRA) it has been possible to derive  $\pi_m^*$  values for several substituents chosen for their frequent use in QSAR studies: F, Cl, Br,  $\text{CH}_3\text{O}$ ,  $\text{CHO}$ ,  $\text{COCH}_3$ ,  $\text{CONH}_2$ ,  $\text{CO}_2\text{CH}_3$ ,  $\text{CN}$ ,  $\text{CH}_3$ ,  $\text{NH}_2$ , phenyl and *tert.*-butyl, in a similar fashion to that described for substituents on the benzene ring<sup>14</sup>.

## EXPERIMENTAL

### Materials

The chemicals were of analytical grade (Merck and Aldrich) and were collected from laboratory stock and from colleagues. Methyl carboxylates were synthesized from the corresponding acids, and amides (commercial nicotinamide excepted) were obtained from the respective carbonitriles by standard procedures. 4-Methoxypyridine was synthesized by treating the corresponding commercial N-oxide with phosphorus tribromide<sup>15</sup>. The identity of these compounds was verified by IR and NMR spectroscopy, and the purity by HPLC.

### Apparatus

All experiments were performed on a Series 10 Perkin-Elmer liquid chromatograph equipped with a fixed-wavelength detector at 254 nm. A 10- $\mu\text{m}$  C<sub>18</sub> Perkin-Elmer and a 5- $\mu\text{m}$  LC-18 Supelco column, both 25 cm  $\times$  4.6 mm I.D., were used throughout. Retention times were computed by an Hewlett-Packard 3390A integrator. Isocratic elution with three different mixtures of HPLC-grade methanol and 0.015 M triethylamine, *i.e.*, 65:35, 55:45 and 45:55 was maintained at a constant flow-rate of 1.0 ml min<sup>-1</sup> at room temperature.

### Methods

**General procedures.** Samples were dissolved in methanol at a concentration that permitted their UV detection with injections of up to 10  $\mu\text{l}$  (typically 5  $\mu\text{l}$ ) and yielded similar peak areas. The column dead time,  $t_0$ , was determined by injection of 10  $\mu\text{l}$  of

pure methanol. From the solute retention time,  $t_R$ , the logarithm of the capacity factor,  $k'$ , was calculated:

$$\log k' = \log [(t_R - t_0)/t_0]$$

All measurements were made at least in triplicate. The average reproducibility of each run was better than 3%.

*Evaluation of the chromatographic system.* In RP-HPLC, addition to the eluent of amines that "mask" the unmodified surface silanols present on the stationary phase can serve to "deactivate" the column. One of the favourite amines used for this purpose is triethylamine (TEA), of relatively small size and soluble enough in the usual mobile phases<sup>16,17</sup>. It has been shown to compete for silanols with solutes having a basic nitrogen in their molecule<sup>17</sup>.

Pyridine ( $pK_a = 5.20$ ) is particularly sensitive to free silanols, and for this reason it has been used as solute to test the capacity of various modifiers to reduce peak tailing<sup>18</sup>. The presence of TEA ( $pK_a = 11.01$ ) produces more rapid elution and improves peak shape at relatively low concentrations. Because of these properties, TEA was chosen as the base modifier in this work, at a concentration of 0.015 *M* in water, mixed in different proportions with methanol. In spite of the high pH of the resulting solutions, no column deterioration was detected for as long as the experiment lasted.

A preliminary study using the conventional C<sub>18</sub> Perkin-Elmer column showed that the quality of the correlations between the reported  $\log P_{o/w}$  values<sup>10,11</sup> and the retention times (expressed as  $\log k'$ ) was very good (Table I). The compound that deviated most was 4-aminopyridine (32) which showed an irregular behaviour, and for that reason was excluded from the regression analysis. This deviation was dependent upon the concentration of organic modifier in the eluent and was least for an eluent composition of methanol-0.015 *M* TEA in water (45:55).

The latter mobile phase composition was chosen to investigate the elution behaviour of the whole set of 28 derivatives for which  $\log P_{o/w}$  was reported, including pyridine itself (Table II), in a persilylated column packed with a C<sub>18</sub> alkylated adsorbent of smaller particle size (5  $\mu\text{m}$ ). Under these new conditions (Fig. 1), 4-aminopyridine deviated even less, and the quality of the regression line for  $\log P_{o/w}$  vs.  $\log k'$  was very good indeed (Fig. 1), as is shown by the squared correlation

TABLE I

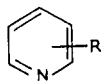
CORRELATION BETWEEN  $\log P_{o/w}$  AND  $\log k'$  FOR PYRIDINE DERIVATIVES IN THREE MOBILE PHASES OF DIFFERENT COMPOSITIONS

$$\log P_{o/w} = a + b \log k'$$

	<i>a</i>	<i>b</i>	<i>r</i>	<i>n</i>	<i>s</i>	<i>F</i>
65:35	1.751	2.407	0.970	16	0.0102	444
55:45	1.371	2.083	0.982	22	0.085	1069
45:55	1.005	1.754	0.982	22	0.085	1079

TABLE II

## PHYSICO-CHEMICAL DATA FOR THE PYRIDINE DERIVATIVES



Hydrophobicity values ( $\log P$ ) described in the literature<sup>10,11</sup>; retention data ( $\log k'$ ) on a Supelco LC-18 column with methanol-0.015 *M* TEA (45:55); experimentally determined  $\log P^*$  values; difference between literature  $\log P$  and  $\log P^*$  values ( $\Delta \log P$ ) and  $pK_a$  values<sup>19</sup>.

No.	R	$\log P$	$\log k'$	$\log P^*$	$\Delta \log P$	$pK_a$
1	H	0.65	-0.167	0.80	-0.150	5.20
2	2-F	—	-0.153	0.82	—	-0.44
3	3-F	—	-0.079	0.92	—	2.97
4	2-Cl	1.27	0.067	1.12	0.152	0.72
5	3-Cl	1.33	0.248	1.37	-0.036	2.81
6	4-Cl	1.28	0.255	1.37	-0.096	3.83
7	2-Br	1.38	0.151	1.23	0.147	0.79
8	3-Br	1.58	0.343	1.50	0.084	2.84
9	4-Br	1.54	0.342	1.49	0.045	3.78
10	2-OCH <sub>3</sub>	1.34	0.228	1.34	0.002	3.28
11	4-OCH <sub>3</sub>	1.00	0.014	1.04	-0.040	6.62
12	2-CHO	—	-0.373	0.51	—	3.80
13	3-CHO	—	-0.538	0.29	—	3.80
14	4-CHO	—	-0.578	0.23	—	4.77
15	2-COCH <sub>3</sub>	0.83	-0.081	0.91	-0.086	—
16	3-COCH <sub>3</sub>	0.43	-0.369	0.52	-0.091	—
17	4-COCH <sub>3</sub>	0.54	-0.320	0.59	-0.048	—
18	2-CONH	0.29	-0.554	0.27	0.022	—
19	3-CONH	-0.37	-1.061	-0.43	0.056	—
20	4-CONH	-0.28	-1.061	-0.43	0.146	—
21	2-COOCH <sub>3</sub>	0.27	-0.549	0.27	-0.005	—
22	3-COOCH <sub>3</sub>	0.81	-0.043	0.97	-0.160	—
23	4-COOCH <sub>3</sub>	0.87	0.002	1.03	-0.159	—
24	2-CN	0.50	-0.376	0.51	-0.012	—
25	3-CN	0.36	-0.437	0.43	-0.068	—
26	4-CN	0.46	-0.412	0.46	-0.002	—
27	2-CH <sub>3</sub>	1.11	0.064	1.11	-0.004	5.97
28	3-CH <sub>3</sub>	1.20	0.150	1.23	-0.032	5.60
29	4-CH <sub>3</sub>	1.22	0.151	1.23	-0.013	6.03
30	2-NH	0.49	-0.369	0.52	-0.031	6.86
31	3-NH	0.11	-0.709	0.05	-0.054	5.98
32	4-NH	0.26	-0.317	0.59	-0.330	0.17
33	4-Phenyl	2.45	0.986	2.37	0.074	5.55
34	4- <i>tert</i> .-Butyl	—	1.016	2.42	—	5.99
35	2,4,6-(CH <sub>3</sub> ) <sub>3</sub>	2.01	0.690	1.97	0.039	—

coefficient ( $r^2 = 0.983$ ), standard error ( $s = 0.087$ ) and  $F$  test ( $F = 1466$ ), for 28 examples (compound 32 was excluded). The resulting equation was:

$$\log P_{o/w} = 1.019 (\pm 0.017) + (1.367 \pm 0.036) \log k' \quad (1)$$

This points to the fact that hydrophobicity is the major factor affecting the retention of pyridine in RP-HPLC under these conditions. This chromatographic

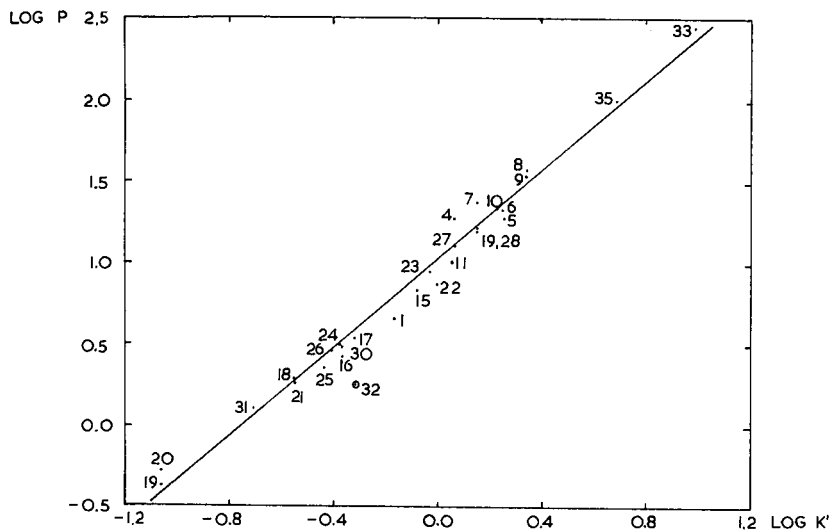


Fig. 1. Correlation, as expressed in eqn. 1, between  $\log P_{o/w}$  for 28 pyridines (Table II) and their  $\log k'$  values in methanol-0.015 *M* TEA (45:55).

system provides a longer lifetime of the stationary phase and a more stable baseline during experiments than when octanol-coated silica is used<sup>11,12</sup>. In addition, its greater simplicity and the fact that no special techniques are required to prepare the column make this method a useful alternative for obtaining hydrophobicity data for pyridines.

## RESULTS

### *Group contributions to hydrophobicity*

By interpolating the experimentally obtained  $\log k'$  value for each compound in eqn. 1, a new series of 35  $\log P$  values were calculated and termed  $\log P^*$  (Table II). The difference, if any, between the experimental  $\log P^*$  and the reported  $\log P_{o/w}$  was indicated as  $\log P$ . Furthermore, Scherrer and Howard<sup>19</sup> proposed to correct the  $\log P$  values by taking into account the  $pK_a$  of the substrate. In order to check whether the goodness of fit of eqn. 1 was improved by adding a second term in  $pK_a$ , we carried out a multiple regression<sup>20</sup> with the sixteen pyridines of Table II whose  $pK_a$  values were known<sup>21</sup>. The resulting equation (eqn. 2) is very similar to eqn. 1:

$$\log P_{o/w} = 1.179 (\pm 0.029) + (1.398 \pm 0.033) \log k' - (0.035 \pm 0.005) pK_a \quad (2)$$

$$r^2 = 0.979$$

The coefficient of the basicity term is small but its sign shows that when the basicity increases this somewhat corrects the retention term. However, 4-amino-pyridine (32) is still the compound that deviates most (from eqn. 1,  $\log P_{o/w} = 0.59$ ; from eqn. 2,  $\log P_{o/w} = 0.41$ ; experimental value from Table II, 0.26).

The retarding effect of basic compounds, and especially 32, is presumably due to their binding to the unmasked residual silanol sites at the surface of the C<sub>18</sub> stationary phase<sup>16</sup>.

An examination of the log  $P^*$  values of Table II shows that, excluding 4-aminopyridine (32), these values are quite similar for positions 3 and 4 (mean difference, 0.03; maximum difference, 0.07 log  $P^*$  units, for COCH<sub>3</sub>) but quite different for *ortho*-substituted pyridines (mean difference, 0.33; maximum difference, 0.73 log  $P^*$  units, for COOCH<sub>3</sub>).

Thus, it is justifiable to consider the log  $P^*$  value for a substituent at a position 3 or 4 (or the average value when both are available) as representative of the contribution of this group to the hydrophobicity of substituted pyridines: F (0.92), Cl (1.37), Br (1.50), OCH<sub>3</sub> (1.04), CHO (0.26), COCH<sub>3</sub> (0.55), CONH<sub>2</sub> (−0.43), COOCH<sub>3</sub> (1.00), CN (0.44), CH<sub>3</sub> (1.23), NH<sub>2</sub> (0.05), phenyl (2.37) and *tert*.-butyl (2.42).

In Table III are reported the  $\pi_m^*$  values for pyridines corresponding to

$$\log P_{3(4)}^* - \log P_H^* = \log P_{3(4)}^* - 0.80$$

together with  $\pi_m^*$  values for benzenes taken from one of our earlier studies<sup>14</sup>, and to Hansch's  $\pi$  values<sup>10</sup>.

The substituent contributions from halogen and methoxy groups to pyridine hydrophobicity in 3- and 4-positions were quantitatively similar to those obtained from the benzene system by RP-HPLC<sup>14</sup>. In the case of formyl, acetyl, carboxamide, methyl carboxylate and cyano, however, they were significantly higher, *i.e.*, their character was less hydrophilic. The methyl, phenyl and *tert*.-butyl groups were the only ones to show lower hydrophobicity, although this result might be partly due to the

TABLE III

MEAN HYDROPHOBIC CONTRIBUTIONS OF SUBSTITUENTS ON THE PYRIDINE RING,  $\pi_m^*$

Calculated from subset of 3- and 4-isomers, compared with the corresponding  $\pi_m^*$ <sup>14</sup> and  $\pi$ <sup>10</sup> values found for benzene ring derivatives.

Substituent	$\pi_m^*$ Pyridine	$\pi_m^*$ Benzene	$\pi$ Benzene
F	0.12	0.08	0.14
Cl	0.57	0.58	0.71
Br	0.70	0.67	0.86
OCH <sub>3</sub>	0.24	0.21	−0.02
CHO	−0.54	−0.64	−0.65
COCH <sub>3</sub>	−0.25	−0.43	−0.55
CONH <sub>2</sub>	−1.23	(−1.71)	−1.49
CO <sub>2</sub> CH <sub>3</sub>	0.20	0.12	−0.01
CN	−0.36	−0.60	−0.57
CH <sub>3</sub>	0.43	0.54	0.56
NH <sub>2</sub>	−0.75	—	−1.23
Phenyl	1.57	—	1.96
<i>tert</i> .-Butyl	1.62	—	1.98

excessive relative retention of pyridine ( $\pi = -0.150$ ), which would lead to an underestimate of the effect of the substituent on the pyridine ring.

We failed to explain the deviation of the group contribution at the 2-position from this mean value in terms of electronic or steric parameters, but it is suggested that the substituent at this position might affect the hydration state of the annular nitrogen, resulting in a variation both in its partitioning between *n*-octanol and water and in its retention in the chromatographic system. A similar hypothesis has been advanced to explain the effect of *ortho* substitution in disubstituted benzenes<sup>8</sup>.

#### ACKNOWLEDGEMENTS

We thank CAICYT (Comisión Asesora de Investigación Científica y Técnica) for financial support.

#### REFERENCES

- 1 T. Fujita, I. Iwasa and C. Hansch, *J. Am. Chem. Soc.*, 86 (1964) 5175.
- 2 R. Kaliszan, *J. Chromatogr. Sci.*, 22 (1984) 362.
- 3 H. Terada, *Quant. Struct. Act. Relat.*, 5 (1986) 81.
- 4 F. Gago, J. Alvarez-Builla and J. Elguero, *J. Chromatogr.*, 360 (1986) 247.
- 5 F. Gago, J. Alvarez-Builla, J. Elguero and J. C. Diez-Masa, *Anal. Chem.*, 59 (1987) 921.
- 6 C. Hansch and T. Fujita, *J. Am. Chem. Soc.*, 86 (1964) 1616.
- 7 A. Leo, *J. Chem. Soc., Perkin Trans. 2*, (1983) 825.
- 8 N. El Tayar, H. Van de Waterbeemd and B. Testa, *Quant. Struct. Act. Relat.*, 4 (1985) 69.
- 9 R. F. Rekker, *The Hydrophobic Fragmental Constant*, Elsevier, Amsterdam, 1977.
- 10 C. Hansch and A. Leo, *Substituent Constants for Correlation Analysis in Chemistry and Biology*, Wiley, New York, 1979.
- 11 S. J. Lewis, M. S. Mirrlees and P. J. Taylor, *Quant. Struct. Act. Relat.*, 2 (1983) 100.
- 12 S. J. Lewis, M. S. Mirrlees and P. J. Taylor, *Quant. Struct. Act. Relat.*, 2 (1983) 1.
- 13 A. Albert, *Heterocyclic Chemistry*, Athlone, London, 1959, p. 31.
- 14 F. Gago, J. Alvarez-Builla and J. Elguero, *J. Liq. Chromatogr.*, 6 (1987) 1031.
- 15 A. R. Katritzky and J. M. Lagowsky, *Chemistry of the Heterocyclic N-Oxides*, Academic Press, London, 1971, p. 200.
- 16 Cs. Horváth, in C. F. Simpson (Editor), *Techniques in Liquid Chromatography*, Wiley, New York, 1982.
- 17 K. E. Bij, Cs. Horváth, W. R. Melander and A. Nahum, *J. Chromatogr.*, 203 (1981) 65.
- 18 J. E. Garst and W. C. Wilson, *J. Pharm. Sci.*, 73 (1984) 1616.
- 19 R. A. Scherrer and S. M. Howard, *J. Med. Chem.*, 20 (1977) 53.
- 20 UNISTAT; *Statistical Package for Sinclair ZX Spectrum*, Unisoft Ltd., London, 1984.
- 21 E. F. V. Scriven, in A. J. Boulton and A. Mc Killop (Editors), *Comprehensive Heterocyclic Chemistry*, Vol. 2, Pergamon, London, 1984, part 2A, p. 171.



CHROM. 20 679

## ROLE OF THE ALKYL CHAIN LENGTH OF THE ION INTERACTION REAGENT, FLOW-RATE, COLUMN PACKING AND DETECTION IN ION INTERACTION REVERSED-PHASE HIGH-PERFORMANCE LIQUID CHROMATOGRAPHY IN SEPARATIONS OF ANIONS USING AMINE SALICYLATES

M. C. GENNARO

*Department of Analytical Chemistry, University of Torino, Via P. Giuria, 5-10125 Torino (Italy)*

(First received April 21st, 1988; revised manuscript received May 24th, 1988)

---

### SUMMARY

The effect of different factors on retention in ion interaction reversed-phase high-performance liquid chromatography was investigated. In particular, the factors considered were the alkyl chain length of the lipophilic cation of the ion interaction reagent, the flow-rate, the size of the stationary phase packing and the choice of detector. The reagents used and compared were hexylamine, octylamine and decylamine salicylates, and the stationary phases were C<sub>18</sub> reversed phase with packing sizes of 5 (spherical) and 10  $\mu$ m (irregular). A comparison was made between UV spectrophotometric (direct and indirect) and conductometric detections. Mixtures of inorganic and organic anions were separated and also some real samples. The system studied was shown to be suitable for analysis of nitrates in drinking waters and for the evaluation of the contents of some organic acids (acetic, succinic, malic and tartaric) in vinegars.

---

### INTRODUCTION

Previous work performed in this laboratory<sup>1,2</sup> dealt with separations of anions: the use of different ion interaction reagents was compared and the mechanism which governs retention discussed. The results obtained correspond well with proposed mechanisms<sup>3–5</sup>, which postulate for lipophilic ions the formation of an electrical double layer on the surface. In this way the adsorption process is associated with a step involving electrostatic forces. This hypothesis is also able to explain<sup>2</sup> the formation of the so-called system peaks, namely “injection” and “system” peaks, whose presence characterizes this chromatographic technique.

Literature reports concerning ion interaction chromatography<sup>6–10</sup> all agree as to its versatility, due to the possibility of changing different parameters, such as the alkyl chain length of the lipophilic cation of the ion interaction reagent, the flow-rate, the stationary phase packing, and the method of detection.

In the present paper the use of octylamine salicylate is considered, due to its

ability to retain both organic and inorganic anions and its good general properties. As salicylate ions are characterized by an high molar absorptivity ( $\epsilon = 308 \pm 2 \text{ mol}^{-1} \text{ cm}^{-1}$  at  $\lambda = 254 \text{ nm}$ ) and a relatively low ionic conductivity, the use of octylamine salicylate allows spectrophotometric (both direct and indirect) and conductometric detections.

For comparison, some experiments were also performed by using hexylamine salicylate and decylamine salicylate as ion interaction reagents, at different flow-rates.

Mixtures of typical anions and examples of the analysis of anions in real samples were considered.

## EXPERIMENTAL

### *Apparatus*

Analyses were carried out using a Varian LC 5000 chromatograph, equipped with a Vista 401 data system and an UV-100 spectrophotometric detector. Alternatively, a Wescan 213 A conductometric detector was employed; a 1 V exit was used in order to interface it to the Vista 401 data system. Merck Lichrospher RP-18,  $5 \mu\text{m}$ , and LiChrosorb RP-18,  $10 \mu\text{m}$ , columns were used. For pH measurement, an Orion 811 pH-meter equipped with a combined glass-calomel electrode was employed.

### *Chemicals*

Ultra-pure water from a Millipore Milli-Q was used for preparation of solutions. Hexylamine, octylamine and decylamine were Fluka analytical grade reagents. Salicylic acid and all other reagents were Carlo Erba analytical grade chemicals. The solutions to be used as eluents were prepared by dissolving weighed amount of the corresponding amines in ultra-pure water and bringing the solutions to a  $\text{pH } 6.2 \pm 0.4$  by additions of salicylic acid. Taking into account the acidic formation constants of the amines, the eluent compositions so prepared are not exactly stoichiometric. Nevertheless, for simplicity, they will be mentioned henceforth as amine salicylates.

In order to condition the chromatographic system, eluent was allowed to flow through the column until a stable baseline was obtained. Generally, times not less than 1 h were necessary. Eluent solutions were prepared each second day.

The reproducibility of retention times was very good for sequential measurements, but it was a little poorer for different eluent preparations and column conditionings. This effect has been observed by other authors and can be ascribed to a very low residual irreversible functionalization (*i.e.*, the alteration induced on the stationary phase by the interactions with the alkyl chain of the amines of the eluent) of the stationary phase. Retention data listed in the tables refer to the reproducibility obtained for different preparations.

Between uses, the column was regenerated by passage of water-methanol (1:1). No particular deterioration of the column was observed with respect to its use in other chromatographic techniques.

The samples of vinegars were prepared only for filtering up to  $0.45 \mu\text{m}$  and diluting 1:10 (v/v) in ultra-pure water.

## RESULTS AND DISCUSSION

Table I shows retention times for some typical inorganic anions, obtained by using octylamine salicylate as the eluent (flow-rate  $2.0 \text{ ml/min}$ ) and Lichrospher

TABLE I

RETENTION TIMES,  $t_R$ , FOR SOME INORGANIC ANIONS

Ion interaction reagent: 0.0050 *M* octylamine salicylate; flow-rate 2.0 ml/min. Column: Merck Lichrospher RP-18, 5  $\mu$ m.

Anion	$t_R$ (min)
Carbonate, chloride, sulphide, bromide	$2.0 \pm 0.3$
Nitrite, fluoride	$2.3 \pm 0.3$
Iodide, nitrate, chlorate, bromate, iodate, perchlorate	$2.5 \pm 0.3$
Thiocyanate	$3.8 \pm 0.3$
Arsenate	$5.4 \pm 0.4$
Orthophosphate	$5.6 \pm 0.5$
Pyrophosphate	$9.7 \pm 0.4$
Chromate	$11.8 \pm 0.5$
Sulphide, sulphate	$20.0 \pm 0.8$

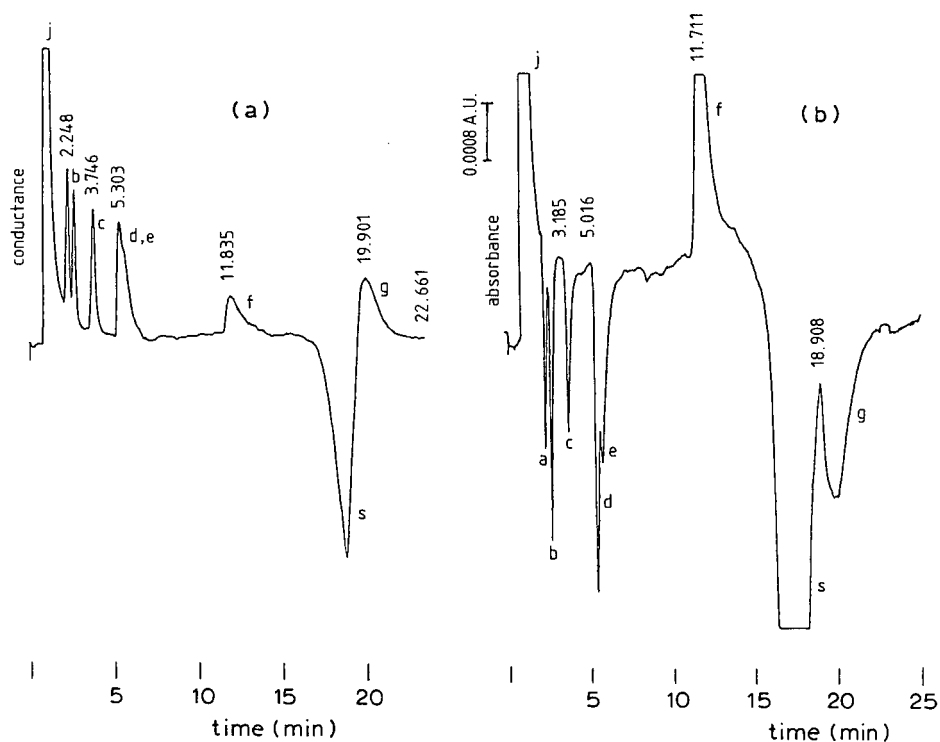


Fig. 1. Comparison between conductometric (a) and spectrophotometric ( $\lambda = 254$  nm) (b) detection in the separation of a typical mixture. Ion interaction reagent: 0.0050 *M* octylamine salicylate. Flow-rate: 2.0 ml/min. Column: Merck Lichrospher RP-18, 5  $\mu$ m. Peaks: j = injection peak; a = nitrites (30.0 ppm); b = nitrates (30.0 ppm); c = thiocyanates (50.0 ppm); d = arsenates (100.0 ppm); e = orthophosphates (60.0 ppm); f = chromates (100.0 ppm); g = sulphates (50.0 ppm); s = system peak.

RP-18, 5  $\mu\text{m}$ , as the stationary phase. The chromatograms of Fig. 1, recorded under these conditions for a mixture of nitrites, nitrates, thiocyanates, arsenates, orthophosphates, chromates and sulphates, compare the use of two different detectors: conductometric and spectrophotometric. It is seen that spectrophotometric detection (Fig. 1b) permits a general enhanced sensitivity. This applies both to anions which being transparent at  $\lambda = 254 \text{ nm}$  are detected indirectly as peaks of negative sign and to chromates which, due to their molar absorptivity at this wavelength, appear as positive peaks. Spectrophotometric detection offers as well a general enhanced resolution and, in particular, allows separation between arsenates and orthophosphates.

Fig. 2 shows, for a mixture of nitrites, nitrates, thiocyanates, arsenates and orthophosphates, the effect on the retention of a variation of the flow-rate from 2.0 (a) to 1.0 ml/min (b), all other conditions being constant. The retention times increase as the flow-rate decreases, consequently, even if the baseline noise increases, a good separation between arsenates and orthophosphates is obtained.

The effect of flow-rate was the same for all the cases investigated, as evidenced by the retention data in Table II recorded at flow-rate ranging between 0.8 and 3.5 ml/min for both octylamine salicylate and decylamine salicylate eluents. The increase in retention times with decreasing flow-rate also applies to the system peaks.

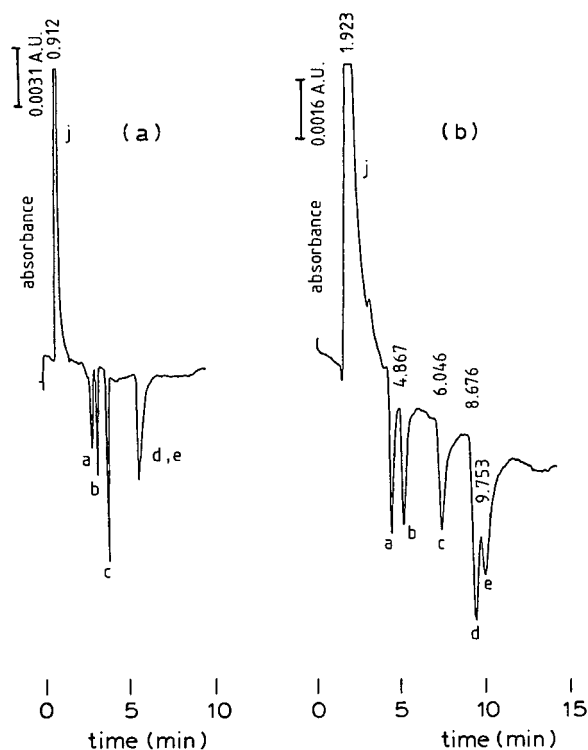


Fig. 2. The effect of the flow-rate on the separation of a typical mixture. Injection: 100  $\mu\text{l}$ . UV detection ( $\lambda = 254 \text{ nm}$ ). Ion interaction reagent: 0.0050 *M* octylamine salicylate. Column: Merck Lichrospher RP-18, 5  $\mu\text{m}$ . Peaks: j = injection peak; a = nitrites (15.0 ppm); b = nitrates (15.0 ppm); c = thiocyanates (25.0 ppm); d = arsenates (60.0 ppm); e = orthophosphates (60.0 ppm). Flow-rates: 2.0 (a); 1.0 ml/min (b).

TABLE II

## EFFECT OF FLOW-RATE ON THE RETENTION TIMES OF SOME TYPICAL ANIONS

Average times are reported. Column: Merck Lichrospher RP-18, 5  $\mu$ m.

	<i>Flow-rate (ml/min)</i>							
	3.5	3.0	2.5	2.0	1.5	1.2	1.0	0.8
<i>Ion interaction reagent: 0.0050 M octylamine salicylate</i>								
System peak	14.0	16.0	18.5	23.0	31.0	38.0	56.0	
Carbonate				2.0				4.9
Nitrite				2.2			4.9	5.5
Iodide				2.5				6.5
Nitrate	1.7	1.7	2.4	2.5	3.6	4.5	5.5	6.6
Perchlorate				2.6				8.5
Thiocyanate	2.2	2.4	3.2	3.8	4.8	6.0	6.7	9.2
Arsenate				5.8			9.2	11.9
Phosphate				6.0			9.8	12.6
Sulphate		12.9	15.4	20.0	25.4			
<i>Flow-rate (ml/min)</i>								
	3.3	3.0	2.5	2.0	1.5			
<i>Ion interaction reagent: 0.0050 M decylamine salicylate</i>								
System peak	17.2	19.0	21.5	26.5	35.0			
Chloride	4.3	4.4	5.4	6.5	8.7			
Bromide			5.9	7.0				
Fluoride			6.2	7.3				
Iodide			6.5	8.0				

Fig. 3 shows the chromatogram recorded, under the same experimental conditions as in Fig. 1b, for a mixture of carbonates (50.0 ppm), nitrites (5.0 ppm), iodides (10.0 ppm), nitrates (5.0 ppm), perchlorates (15.0 ppm), thiocyanates (15.0 ppm), arsenates (50.0 ppm) and orthophosphates (50.0 ppm). A good separation for the eight anions is obtained in as little as 8 min. Thus interference from the system peak is avoided as its retention time is about 23 min under these conditions.

For comparison, similar mixtures were analyzed after equilibration of the flow-rate at 0.8 ml/min (Fig. 4). As expected, increased retention times are obtained, but no particular advantage is achieved on this occasion, nor in the separation of arsenates and orthophosphates. As above, spectrophotometric detection generally allows a better resolution than conductometric detection. In particular, the separation between iodides and nitrates, whose retention times are very similar to each other, is of special interest. The molar absorptivity of iodides at this wavelength results in the formation of a positive peak which can easily be identified and separated from the near negative one due to the transparent nitrates.

The effect on retention of the alkyl chain length of the lipophilic cation of the interaction is shown in Table III, in which retention times for some anions and hexylamine, octylamine and decylamine salicylate as interaction reagents (flow-rate

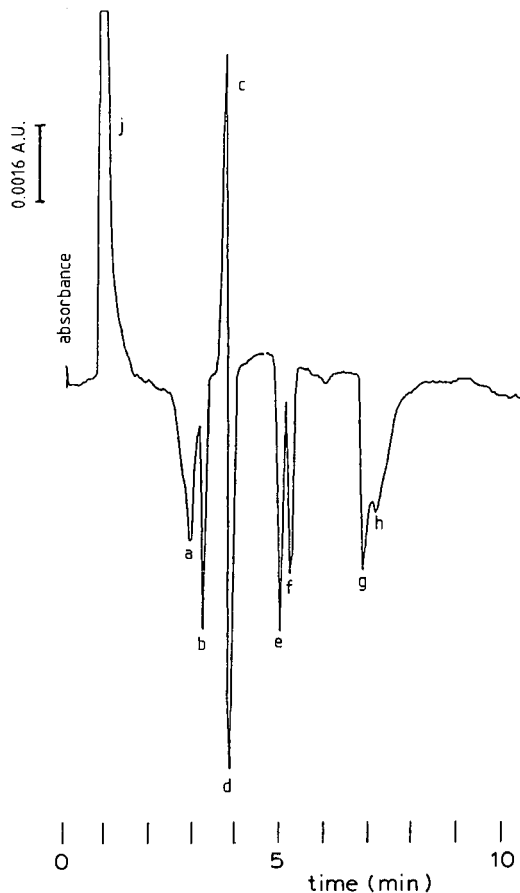


Fig. 3. Separation of a typical mixture. Volume injected:  $100\ \mu\text{l}$ .  $\lambda = 254\ \text{nm}$ . Ion interaction reagent:  $0.0050\ M$  octylamine salicylate. Flow-rate:  $2.0\ \text{ml/min}$ . Column: Merck Lichrospher RP-18,  $5\ \mu\text{m}$ . Peaks: j = injection peak; a = carbonates ( $50.0\ \text{ppm}$ ); b = nitrites ( $5.0\ \text{ppm}$ ); c = iodides ( $10.0\ \text{ppm}$ ); d = nitrates ( $5.0\ \text{ppm}$ ); e = perchlorates ( $15.0\ \text{ppm}$ ); f = thiocyanates ( $15.0\ \text{ppm}$ ); g = arsenates ( $50.0\ \text{ppm}$ ); h = orthophosphates ( $50.0\ \text{ppm}$ ).

$2.0\ \text{ml/min}$ ) are listed. The longer the alkyl chain, the longer are the retention times, *cf.*, the chromatograms in Fig. 5. The same mixture of eight anions, previously separated with octylamine salicylate (Fig. 3), shows practically null retention for all its components when the interaction reagent is hexylamine salicylate (Fig. 5a). On the other hand, the use of decylamine salicylate permits (Fig. 5b) an acceptable separation between chlorides, bromides, fluorides and iodides.

Table IV lists retention times obtained for some organic acids for different stationary phase packings and octylamine salicylate concentrations ( $0.0050$  and  $0.100\ M$ ).

For all the anions investigated, increased concentration leads to increased retention. This can be explained through a greater functionalization of the stationary phase induced by a more concentrated eluent.

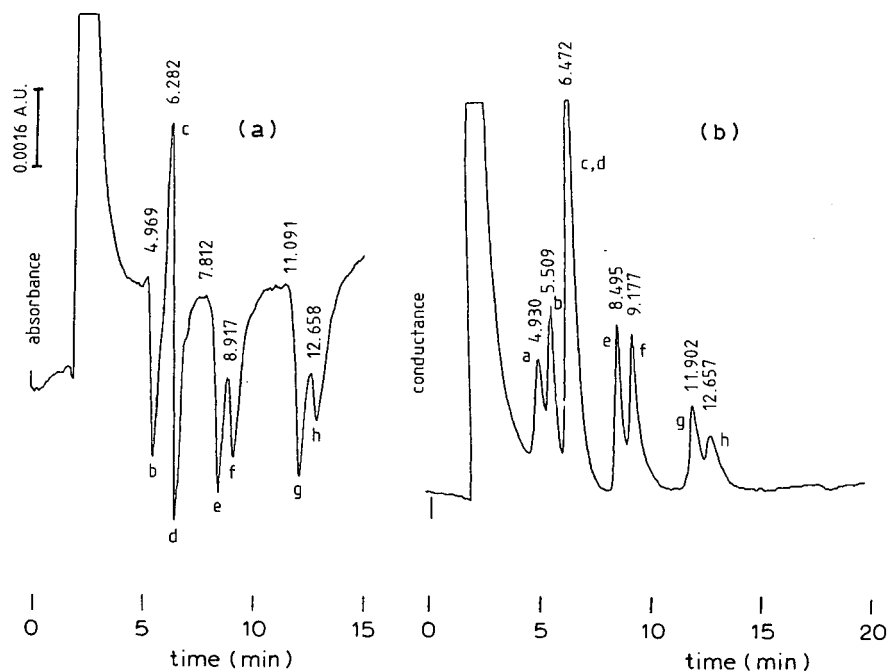


Fig. 4. Effects of the flow-rate (*cf.*, fig. 3) and detection. Ion interaction reagent: 0.0050 *M* octylamine salicylate. Flow-rate: 0.8 ml/min. Column: Merck Lichrospher RP-18, 5  $\mu$ m. (a) UV detection ( $\lambda = 254$  nm): separation of the mixture as in Fig. 3, without carbonates. (b) Conductometric detection: separation of the mixture as in Fig. 3.

As far as the column packings are concerned, retentions on the RP-18, 10  $\mu$ m, packing are less than those obtained on the RP-18, spherical 5  $\mu$ m. This difference can reasonably be ascribed to the greater total surface area available for functionalization by the 5- $\mu$ m particles, even when the extent of endcapping and the percentage binding in the two columns are taken into account.

TABLE III

EFFECT OF THE ALKYL CHAIN LENGTH OF THE ION INTERACTION REAGENT ON THE RETENTION TIMES OF SOME TYPICAL ANIONS

Column: Merck Lichrospher RP-18, 5  $\mu$ m. Flow-rate: 2.0 ml/min. n.r. = Not retained.

	$t_R$ (min)		
	Hexylamine salicylate	Octylamine salicylate	Decylamine salicylate
System peak	$16.0 \pm 0.8$	$23.0 \pm 0.8$	$27.0 \pm 0.8$
Chloride	n.r.	$2.0 \pm 0.3$	$6.5 \pm 0.3$
Bromide	n.r.	$2.0 \pm 0.3$	$7.0 \pm 0.3$
Fluoride	n.r.	$2.3 \pm 0.3$	$7.3 \pm 0.4$
Iodide	n.r.	$2.5 \pm 0.3$	$8.0 \pm 0.4$
Nitrate	n.r.	$2.5 \pm 0.3$	$8.3 \pm 0.4$

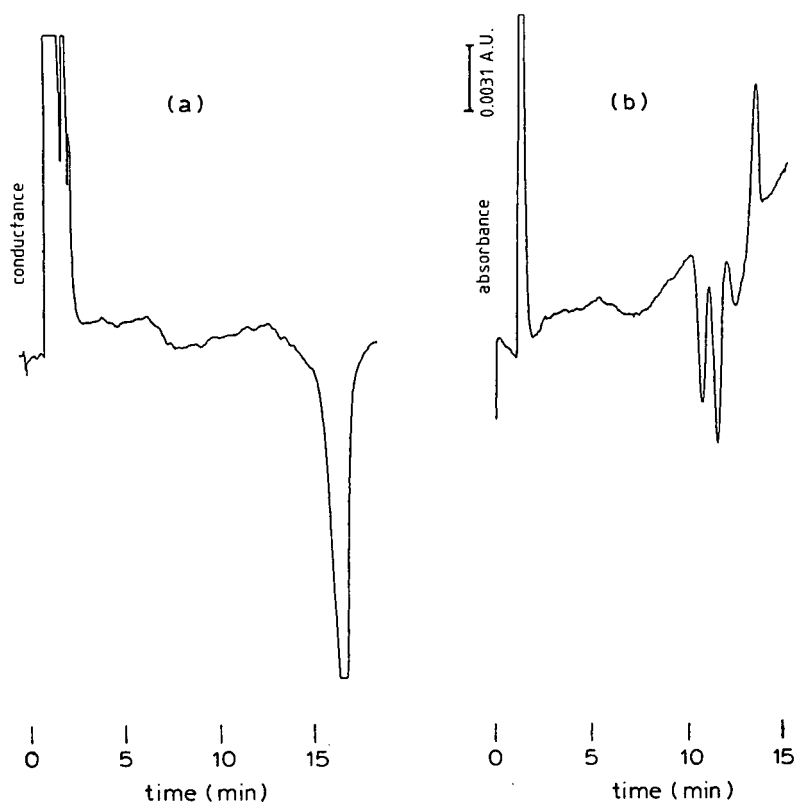


Fig. 5. (a) Ion interaction reagent: 0.0050 *M* hexylamine salicylate. All other conditions as in Fig. 3. (b) Ion interaction reagent: 0.0050 *M* decylamine salicylate. Flow-rate: 1.5 ml/min. UV detection ( $\lambda = 254$  nm). Separation of a mixture containing chlorides, bromides, fluorides, iodides (each 30.0 ppm). Volume injected 100  $\mu$ l.

TABLE IV

EFFECT OF THE ION INTERACTION REAGENT CONCENTRATION,  $C_{IIR}$ , AND COLUMN PACKING SIZE ON THE RETENTION TIMES OF SOME ORGANIC ANIONS

Ion interaction reagent: octylamine salicylate.

Acid	$C_{IIR} = 0.0050$ M LiChrosorb RP-18 10 $\mu$ m	$C_{IIR} = 0.0100$ M LiChrosorb RP-18 10 $\mu$ m	$C_{IIR} = 0.0050$ M Lichrospher RP-18 5 $\mu$ m
Acetic	$2.4 \pm 0.2$	$2.5 \pm 0.2$	$2.7 \pm 0.2$
Lactic	$2.7 \pm 0.2$	$2.7 \pm 0.2$	$3.1 \pm 0.3$
Butyric	$4.4 \pm 0.4$	$4.5 \pm 0.2$	$4.6 \pm 0.3$
Succinic	$6.0 \pm 0.4$	$7.2 \pm 0.2$	$10.6 \pm 0.2$
DL-Malic	$7.5 \pm 0.5$	$8.8 \pm 0.3$	$14.8 \pm 0.2$
Tartaric	$8.5 \pm 0.5$	$10.5 \pm 0.3$	$20.3 \pm 0.5$

*Applications to real samples*

**Water supply.** Fig. 6 shows an example of the quantitation of nitrates and chlorides in a water from a rural pipeline in the Italian Piedmont region, suspected of an anomalous content of nitrates. The chromatographic conditions are as follows: 0.0050 *M* octylamine salicylate as ion interaction reagent; flow-rate 1.5 ml/min; RP-18, spherical 5  $\mu\text{m}$  column; UV (254 nm) detection. The figure shows some typical chromatograms recorded after injection of 100  $\mu\text{l}$  pipeline water (Fig. 6a), standard solution of nitrates (50.0 ppm) (Fig. 6b), standard solution of chlorides (10.0 ppm) (Fig. 6c), pipeline water after standard addition of 40.0 ppm nitrates (Fig. 6d) and pipeline water after standard addition of 15.00 ppm of chlorides (Fig. 6e).

The quantitation was performed by use of a standard calibration graph of peak area and confirmed by the method of internal standard additions. The good agreement of the two series of measurements yielded the content of chlorides as  $4.7 \pm 0.5$  ppm. The content of nitrates is  $58 \pm 1$  ppm and exceeds the amount permitted for drinking water.

**Vinegars.** Data in Table IV permitted the best conditions to be chosen for the analysis of some vinegars for the content of organic acids. By using 0.0050

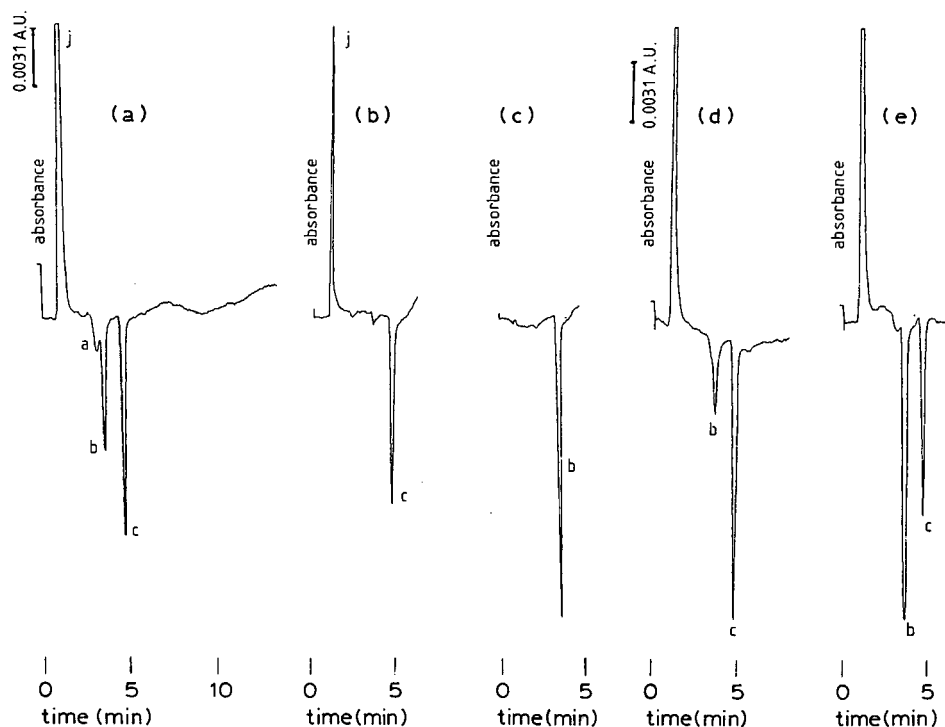


Fig. 6. Chromatograms of water from a rural pipeline. Ion interaction reagent: 0.0050 *M* octylamine salicylate. UV detection ( $\lambda = 254$  nm). Column: Merck Lichrospher RP-18, 5  $\mu\text{m}$ . Peaks: j = injection peak; a = carbonates; b = chlorides; c = nitrates. Volume injected: 100  $\mu\text{l}$ . (a) Pipeline water; (b) standard nitrates (50.0 ppm); (c) standard chlorides (10.0 ppm); (d) pipeline water after standard addition of 40.00 ppm of nitrates; (e) pipeline water after standard addition of 15.0 ppm of chlorides.

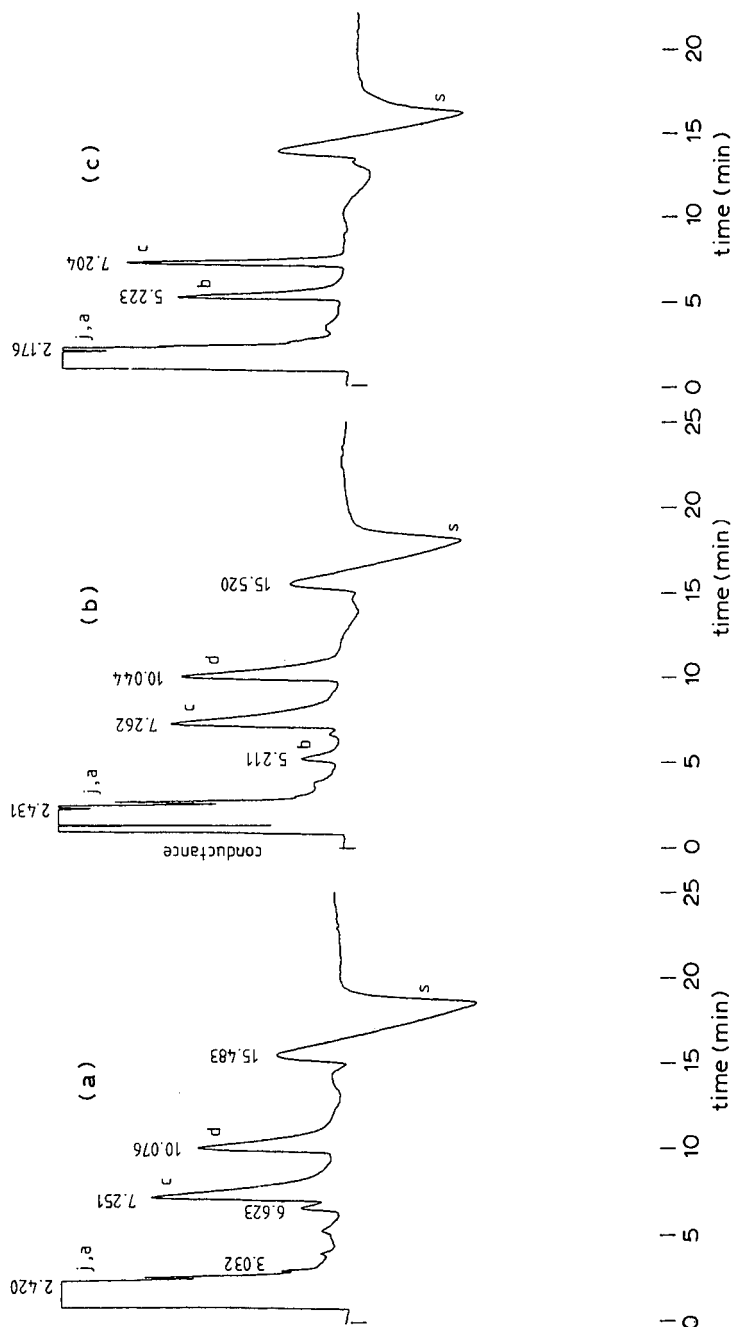


Fig. 7. Chromatograms of samples of vinegars diluted 1:100 (v/v). Volume injected: 100  $\mu$ l. Ion interaction reagent: 0.0050 *M* octylamine salicylate. Flow-rate: 2.0 ml/min. Column: Merck LiChrosorb RP-18, 10  $\mu$ m. Conductometric detector. Peaks: j = injection peak; a = acetic; b = succinic; c = malic; d = tartaric acid; s = system peak. (a) Laboratory vinegar; (b) and (c) commercial vinegars.

*N*-Octylamine salicylate, conductometric detection and an LiChrosorb RP-18, 10  $\mu\text{m}$ , column, a laboratory-made vinegar and two commercial products were compared. From the chromatograms in Fig. 7 it is seen that succinic acid is practically absent from the laboratory-made vinegar, whilst the two commercial vinegars show substantial differences as regards the contents of succinic and tartaric acids.

In conclusion, this chromatographic technique can be applied to different real samples. Liquid samples require no pretreatment other than filtration. The biggest advantage offered by the technique is its versatility because it is possible to change so many different parameters that are able to affect retention. Moreover the sensitivity is satisfactory, taking into account that no derivatization reaction is employed. Nevertheless, the sensitivity for the particular species of interest can be enhanced or optimized through suitable choice of the conditions.

#### REFERENCES

- 1 M. C. Gennaro, M. Sbuttoni, E. Mentasti, C. Sarzanini and V. Porta, *Ann. Chim. (Rome)*, 78 (1988) 137.
- 2 M. C. Gennaro, *J. Liq. Chromatogr.*, 10 (1987) 3347.
- 3 B. A. Bidlingmeyer, *J. Chromatogr. Sci.*, 18 (1980) 525.
- 4 W. E. Hammers, C. N. M. Aussems and M. Janssen, *J. Chromatogr.*, 360 (1986) 1.
- 5 J. Ståhlberg, *J. Chromatogr.*, 356 (1986) 231.
- 6 B. B. Wheals, *J. Chromatogr.*, 262 (1983) 61.
- 7 W. E. Barber and P. W. Carr, *J. Chromatogr.*, 316 (1984) 211.
- 8 M. Dreux, M. Lafosse, P. Agbo-Hazoumé, B. Chaabane-Doumandji, M. Gibert and Y. Léui, *J. Chromatogr.*, 354 (1986) 119.
- 9 B. A. Bidlingmeyer, C. T. Santasania and F. V. Warren, Jr., *Anal. Chem.*, 59 (1987) 1843.
- 10 M. Lookabaugh, I. S. Krull and W. R. LaCourse, *J. Chromatogr.*, 387 (1987) 301.



CHROM. 20 711

## INFLUENCE OF BONDING CHEMISTRY ON THE REORDERING/RESOLUTION OF SILICA IMMOBILIZED ALKYL CHAINS

S. S. YANG and R. K. GILPIN\*

*Department of Chemistry, Kent State University, Kent, OH 44242 (U.S.A.)*

(First received March 24th, 1988; revised manuscript received June 9th, 1988)

---

### SUMMARY

The reordering/resolution of silica modified with mono-, di-, and trireactive alkylsilanes has been studied. Under totally aqueous conditions, the onset for reordering has been found to begin at approximately the same temperature irrespective of the attachment chemistry. These results support the idea that bonding occurs heterogeneously in patches and that within a patch spacing is controlled by silanol concentration.

---

### INTRODUCTION

The most popular means of preparing liquid chromatographic phases is by covalently binding organosilanes to porous silica. Chloro and alkoxy reagents are used most often. The bonding chemistry and resulting surface can be classified by the number of reactive groups in the silylating reagent.

Monoreactive silanes such as octyldimethylchlorosilane generate singularly attached structures. The degree and homogeneity of coverage are dependent on various parameters including surface silanol concentration, pore size and geometry, ligand size, shape and polarity, etc.

Surfaces prepared from polyreactive silanes such as octylmethyldichlorosilane and octyltrichlorosilane are even more complicated and less easily defined. Generally only one group in a polyreactive silane monomer will react with the surface. Depending on the existence of moisture, the remaining reactive groups can either cross-link or can be hydrolyzed and undergo further reactions with excess reagent. In the latter case, polymers are formed which are only loosely attached to the surface. Although polymeric bonded phases have greater hydrolytic stability than equivalent monomeric phases, they are more difficult to control and are less reproducible. If the surface silanization is performed under anhydrous conditions, the reactions are limited to the surface<sup>1–4</sup>.

On a molecular level basis, the conformation and motional dynamics of bonded phases are dependent on chain length<sup>5,6</sup>, solvent composition and polarity<sup>7</sup>, temperature<sup>5</sup>, etc. Under totally aqueous conditions, the immobilized chains undergo thermally induced reordering/resolution. This process has been studied for both

non-polar<sup>8</sup> and polar<sup>9</sup> phases. In the former case, reordering/resolution has been explained in terms of chain-chain (cohesive), chain-solvent (hydrophobic), and solvent-surface (specific) interactions. However, in the latter case additional specific interactions arising from the functional group also must be considered<sup>9</sup>. The onset temperature ( $T_0$ ) for reordering can be obtained from nonlinearity in a plot of  $\ln k'$  vs.  $1/T$ . The experimental details have been discussed<sup>5,8,9</sup>.  $T_0$  has been determined for a number of polar and nonpolar phases. For a particular homologous series of anchored groups, a linear correlation exists between the reordering/resolution temperature and the boiling point of the corresponding nonimmobilized compounds<sup>8</sup>.

Although the effect of chain length, surface coverage, and functionality on surface reorientation has been studied<sup>5,8,9</sup>, the role of bonding chemistry (*e.g.*, the type of attachment between stationary phase and silica surface) has not been examined. In the current work, the reordering/resolution of silica modified with mono-, di-, and trireactive alkylsilanes has been investigated. For comparative purpose, all silanization reactions were carried out under anhydrous conditions.

## EXPERIMENTAL

### *Chemicals*

*n*-Octyldimethylchlorosilane, *n*-decyldimethylchlorosilane, *n*-octyl-methyldichlorosilane, and *n*-decylmethyldichlorosilane were obtained from Petrarch (Levittown, PA, U.S.A.) and were used as received. LiChrosorb Si 60 ( $d_p \approx 10 \mu\text{m}$  and surface area  $550 \text{ m}^2/\text{g}$ ) was purchased from Merck (Darmstadt, F.R.G.). Mobile phases were prepared (v/v basis) from HPLC-grade acetonitrile (Aldrich; Milwaukee, WI, U.S.A.) and deionized water which was purified using a Milli-Q reagent water system (Millipore; El Paso, TX, U.S.A.).

### *Preparation of bonded phases and columns*

Each of the above organosilanes was used to chemically modify LiChrosorb Si 60 as previously described<sup>5</sup>. Toluene was used as the refluxing solvent. All reactions were carried out under dry nitrogen. The modified materials were thoroughly rinsed and then packed into  $250 \text{ mm} \times 2.3 \text{ mm}$  I.D. stainless-steel columns using a dynamic procedure<sup>10</sup>. A sample was removed from each reaction bath, dried and analyzed by combustion. The data obtained are summarized in Table I.

### *Chromatographic studies*

All chromatographic studies were performed using a Laboratory Data Control (Riviera Beach, FL, U.S.A.) Model Constametric IIG liquid chromatographic pump with a UV detector. Column temperature was controlled in a water bath with a Tempunit (Techne; Princeton, NJ, U.S.A.) model TU-14 zero cross-over proportional controller and a Neslab (Neslab instruments; Portsmouth, NH, U.S.A.) Model EN-350 flowthrough liquid cooler. The flow-rate was monitored with a liquid flow meter (Model F1080A, Phase Separations; Queensferry, U.K.). A more detailed description of the hardware has been described elsewhere<sup>5</sup>.

The temperature studies were carried out as described previously using phenol and resorcinol as test solutes<sup>8</sup>. Prior to data collection, each column was conditioned with 100 ml of acetonitrile followed by 100 ml of the mobile phase, water. Acetonitrile was chosen as the organic conditioning solvent to minimize entrapment problems<sup>11</sup>.

A complete evaluation consisted of three sequential steps: (i) initially, solute retention was measured every 5°C from 10°C to 80°C, (ii) the column was then cooled to the starting temperature and step i repeated, and (iii) the column cooled to the initial temperature and step i repeated a third time but retention measurements were made at 10°C increments. In all cases, the complete evaluation cycle was carried out twice for each column. Column void volume was measured with  $^2\text{H}_2\text{O}$ .

## RESULTS AND DISCUSSION

Summarized in Table I are the experimentally determined reordering/resolution temperatures for equivalent bonded phases prepared using mono-, di- and trireactive reagents.  $T_0$  was respectively 40.6°C, 41.6°C, and 40.7°C for the  $\text{C}_8$  phases and 60.9°C, 61.5°C, and 60.1°C for the  $\text{C}_{10}$  phases. Also included in Table I are the standard deviations in the data. These values are based on multiple column preparations and at least four replicate measurements made on each batch. The data for trichlorosilane surfaces are from previously published work<sup>5</sup>.

TABLE I  
ONSET TEMPERATURE FOR SURFACE REORDERING/RESOLUTION

Silylating agents	Reactive* groups	%Carbon**	Temperature (°C)
<i>n</i> -Octyldimethylchlorosilane	1	10.6	40.6 ± 0.49
<i>n</i> -Octylmethyldichlorosilane	2	10.5	41.6 ± 1.02
<i>n</i> -Octyltrichlorosilane	3	9.5	40.7 ± 0.71
<i>n</i> -Nonyltrichlorosilane	3	9.7	51.8 ± 2.10
<i>n</i> -Decyldimethylchlorosilane	1	12.0	60.9 ± 0.35
<i>n</i> -Decylmethyldichlorosilane	2	12.4	61.5 ± 0.48
<i>n</i> -Decyltrichlorosilane	3	12.3	60.1 ± 1.00

\* Number of reactive chlorines in the silylating agent.

\*\* Average values for preparations. All normalized carbon was within a range where  $T_0$  has found not to vary with coverage (ref. 5).

The reordering began at approximately the same temperature for a given chain length (*i.e.*, within the experimental standard deviation of the current measurements) and a similar incremental change in  $T_0$  was noted for each additional methylene group in the chain irrespective of the attachment chemistry.

The data in Table I suggest that within the range of coverages studied the controlling factor for group spacing is the silanol distribution not the bonding chemistry. This idea is consistent with previous studies<sup>2</sup> where the maximum surface concentrations of three silylating agents, octyltrichlorosilane, octylmethyldichlorosilane and octyldimethylchlorosilane, were identical within experimental error (2.35, 2.40, 2.35  $\mu\text{mol}/\text{m}^2$  respectively). The results from this latter investigation were explained on the basis of similarity in cross-sectional area of the silylating molecules irrespective of the number of reactive groups.

The current data along with data obtained in related studies, where  $T_0$  also has

been found to be independent of coverage once a certain minimum level is reached<sup>5</sup>, are consistent with the idea that bonding occurs heterogeneously in patches or clusters of chains. Although surface coverage is dependent upon the number or size of patches, within a patch the closest spacing is controlled by silanol concentration. Likewise, the spacing of adjacent chains is similar from patch to patch. Therefore, for bonded phases with the same chain length, a similar degree of overlap is obtained regardless of differences in bonding chemistry. This thus gives rise to the same onset temperature.

A patch model for bonded groups immobilized on silica is also supported by various spectrometric measurements. For example, luminescence<sup>12</sup> and infrared<sup>13</sup> methods have been used to examine nonuniformity of bonding and spacing for [3-(3-pyrenyl)propyl]dimethylchlorosilane and cyanoalkyl groups respectively. In both cases, the bonded groups were found to be heterogeneously distributed in organically rich patches. Similar results were observed chromatographically<sup>6</sup> where longer bonded alkyl chains were found to form aggregates which exhibited liquid-like behavior.

The above results imply that the bonding chemistry has little if any effect on the onset temperature for reordering/resolution at least when bonding is carried out under reaction conditions which limit attachment to the surface. For this condition to hold there must be a similar degree of chain-chain interaction irrespective of attachment chemistry. Thus the extent of overlap between two immobilized groups is determined by the distance between their points of attachment not the number of reactive groups in the silylating agent.

#### ACKNOWLEDGEMENT

Support from DARPA-ONR Contract N0014-86-K-0772 is acknowledged.

#### REFERENCES

- 1 R. K. Gilpin and M. F. Burke, *Anal. Chem.*, 45 (1973) 1383.
- 2 P. Roumeliotis and K. K. Unger, *J. Chromatogr.*, 149 (1978) 211.
- 3 D. W. Sindorf and G. E. Maciel, *J. Am. Chem. Soc.*, 105 (1983) 3767.
- 4 R. K. Gilpin and M. E. Gangoda, *J. Chromatogr. Sci.*, 21 (1983) 352.
- 5 R. K. Gilpin and J. A. Squire, *J. Chromatogr. Sci.*, 19 (1981) 195.
- 6 C. H. Lochmuller and D. R. Wilder, *J. Chromatogr. Sci.*, 17 (1979) 574.
- 7 R. P. W. Scott and C. F. Simpson, *J. Chromatogr.*, 197 (1980) 11.
- 8 S. S. Yang and R. K. Gilpin, *J. Chromatogr.*, 394 (1987) 295.
- 9 S. S. Yang and R. K. Gilpin, *J. Chromatogr.*, 408 (1987) 93.
- 10 R. K. Gilpin and W. R. Sisco, *J. Chromatogr.*, 194 (1980) 285.
- 11 R. K. Gilpin, M. E. Gangoda and A. E. Krishen, *J. Chromatogr. Sci.*, 20 (1982) 345.
- 12 C. H. Lochmuller, A. S. Colborn, M. L. Hunnicutt and J. M. Harris, *Anal. Chem.*, 55 (1983) 1344.
- 13 B. R. Suffolk and R. K. Gilpin, *Anal. Chem.*, 57 (1985) 596.

CHROM. 20 632

## SEPARATION OF CAROTENOL FATTY ACID ESTERS BY HIGH-PERFORMANCE LIQUID CHROMATOGRAPHY

FREDERICK KHACHIK\* and GARY R. BEECHER

*U.S. Department of Agriculture, Agricultural Research Service, Beltsville Human Nutrition Research Center, Nutrient Composition Laboratory, Building 161, BARC-East, Beltsville, MD 20705 (U.S.A.)*

(First received March 22nd, 1988; revised manuscript received May 4th, 1988)

---

### SUMMARY

Employing isocratic and gradient-elution high-performance liquid chromatography (HPLC) a number of straight-chain fatty acid esters (decanoate, laurate, myristate, palmitate) of violaxanthin, auroxanthin, lutein, zeaxanthin, isozeaxanthin, and  $\beta$ -cryptoxanthin, prepared by partial synthesis, have been separated on a  $C_{18}$  reversed-phase column. Several chromatographic conditions were developed that separated a mixture of di-fatty acid esters (dimyristate, myristate palmitate mixed ester, dipalmitate) of violaxanthin, auroxanthin, lutein, and zeaxanthin in a single chromatographic run. Hydroxycarotenoids such as lutein, zeaxanthin, and isozeaxanthin that are not easily separated by HPLC on  $C_{18}$  reversed-phase columns, can be readily separated after derivatization with fatty acids and chromatography of their esters. Chromatographic conditions for optimum separation of carotenoids from various classes are discussed.

---

### INTRODUCTION

The importance of generating accurate qualitative and quantitative data on carotenoids, which are among the largest naturally occurring groups of compounds found in plants, foods, and animals, has resulted in development of rugged analytical techniques that can separate, identify, and quantify these compounds<sup>1–4</sup>. This is primarily owing to the recent epidemiological evidence that have suggested an inverse relationship between consumption of fruits and vegetables and the risk of incidence of several types of human cancers<sup>5</sup>. These studies have associated carotenoids as one of the possible active ingredients in foods that their high consumption, has been correlated with reduction in cancer rates. Improvements in analytical techniques, particularly high-performance liquid chromatography (HPLC), have been important in the development of separation conditions for various classes of carotenoids isolated from food extracts. There are numerous reports on the separation of various classes of carotenoids by HPLC; however, the separation of carotenol fatty acid esters, one of the classes of carotenoids often isolated from natural products, has not received much attention. The extracts from certain fruits and vegetable (*i.e.* oranges, apricots,

peaches, prunes, red bell peppers, squash), in which carotenoids are usually esterified with straight-chain fatty acids, are customarily saponified to remove the fatty acids and regenerate the hydroxycarotenoids<sup>6</sup>. Therefore, the development of a rapid HPLC method that can separate carotenol fatty acid esters within a reasonable time is required in order to assess the various carotenoids species predominant in foods as they are consumed by human beings. Among a few literature reports on HPLC of carotenol fatty acid esters is the work by Gregory *et al.*<sup>7</sup> and Philip and Chen<sup>8</sup>, who recently separated the carotenol fatty acid esters in red bell peppers and Naval orange peel by HPLC. Similarly, Fisher and Kocis<sup>9</sup> have separated carotenol fatty acid esters of paprika pigments by HPLC. The separation of carotenoids and carotenol fatty acid esters isolated from the petals of marigold (*Tagetes erecta* L.) and primrose (*Primula vulgaris* L.) flowers have also been reported<sup>10,11</sup>. Recently, we reported the separation, identification, and quantification of the predominant carotenoids and carotenol fatty acid esters in extracts from several varieties of squash by HPLC<sup>12-14</sup>. Chromatographic conditions were developed that separated as many as 25 carotenoids as well as several of their stereoisomers, which were assigned to four classes of compounds: xanthophylls, carotenol mono-fatty acid esters, hydrocarbon carotenoids, and carotenol di-fatty acid esters.

In this report we have extended our studies on separation of carotenol fatty acid esters to a number of other carotenoids and have developed several chromatographic eluents that can be employed to separate straight-chain di-fatty acid esters (didecanoate, dilaurate, dimyristate, myristate palmitate mixed ester, dipalmitate) of some of the synthetic and common naturally occurring carotenoids (violaxanthin, auroxanthin, lutein, zeaxanthin, isozeaxanthin) by HPLC on a C<sub>18</sub> reversed-phase column. The various chromatographic conditions (isocratic and gradient) described in this report readily accomplish the simultaneous separation of mixtures of carotenol fatty acid esters containing various fatty acid side chains. Finally, these conditions have been employed to separate mixtures of fatty acid esters of lutein, zeaxanthin, and isozeaxanthin, whose parent hydroxycarotenoids are not readily separated by HPLC on C<sub>18</sub> reversed-phase columns.

## EXPERIMENTAL\*

### Apparatus

A Beckman Model 114M ternary solvent delivery system equipped with a Beckman Model 421 controller was interfaced into a Hewlett-Packard 1040A rapid-scanning UV-VIS photodiode array detector. The data were stored and processed by means of a Hewlett-Packard 9000/series 300 (ChemStation) computing system which was operated with a Hewlett-Packard Model-9153B disc drive, color display monitor Model-35741, and a Model 7470A plotter. The chromatographic runs for  $\alpha$ - and  $\beta$ -carotene and fatty acid esters of lutein, zeaxanthin, isozeaxanthin, and  $\beta$ -cryptoxanthin were monitored at 450 nm, while violaxanthin and auroxanthin fatty acid esters were monitored at 442 and 400 nm, respectively. In some cases where the

---

\* Mention of a trademark or proprietary product does not constitute a guarantee or warranty of the product by the U.S. Department of Agriculture, and does not imply its approval to the exclusion of other products that may also be suitable.

separation of mixtures of carotenol fatty acid esters were of particular interest, the chromatographic runs were simultaneously monitored at all the above three wavelengths. The absorption spectra of the carotenoids were recorded between 200 and 600 nm as frequent as 1 scan/5 s (maximum scanning capability = 1 scan/100 ms). The HPLC detection limit for carotenol fatty acid esters was approximately 1  $\mu\text{g/ml}$ .

#### *Column*

Separations were performed on a stainless-steel (25 cm  $\times$  4.6 mm I.D.) Spheri-5 RP-18 (5- $\mu\text{m}$  spherical particles) column (Applied Biosystem, Analytical Division of Kratos, Ramsey, NJ, U.S.A.) which was protected with a Brownlee guard cartridge (3 cm  $\times$  4.6 mm I.D.) packed with Spheri-5 C<sub>18</sub> (5- $\mu\text{m}$  particle size).

#### *Chromatographic procedures*

The separations of carotenoids and carotenol fatty acid esters were carried out under three sets of HPLC conditions employing eluents A, B, and C. These eluents are described below. The retention times of various carotenol fatty acid esters (see Table I) with eluents A, B, and C were obtained by duplicate injection of each individual compound as well as injection of several mixtures of these components. These retention times which were obtained on a Spheri-5 RP-18 column were slightly different from the retention times of some of the carotenol fatty acid esters separated on a Rainin Microsorb C<sub>18</sub> reversed-phase column<sup>13</sup>. Carotenoids and carotenol fatty acid esters were injected in the appropriate HPLC solvents (eluents A, B and C) to prevent chromatographic artifacts and HPLC peak distortion of these compounds<sup>15</sup>. Carotenol fatty acid esters prepared by partial synthesis were purified by thin-layer chromatography (TLC) employing eluent D. The  $R_F$  values of several of these carotenol fatty acid esters with this eluent are shown in Table II.

#### *Eluent A (isocratic/gradient)*

This eluent consisted of an isocratic mixture of methanol (10%, pump A), acetonitrile (85%, pump C), and methylene chloride-hexane (1:1) (5%, pump B) at time 0, which was followed by a gradient beginning at time 10 and completed at time 40 (min). The final composition of the gradient mixture at time 40 was: methanol (10%), acetonitrile (45%), and methylene chloride-hexane (1:1) (45%). The column flow-rate was 0.7 ml/min. At the end of the gradient the column was re-equilibrated under the initial isocratic conditions for 20 min at a flow-rate of 1.5 ml/min and finally for 5 min at 0.7 ml/min.

#### *Eluent B (isocratic/gradient)*

This eluent consisted of an isocratic mixture of methanol (15%), acetonitrile (65%), and methylene chloride-hexane (1:1) (20%) at time 0, which was followed by a gradient beginning at time 23 min and completed at time 33. The final composition of the gradient mixture was: methanol (15%), acetonitrile (40%), methylene chloride-hexane (1:1) (45%). The column flow-rate was 0.7 ml/min. At the end of the gradient the column was re-equilibrated under the initial isocratic conditions for 20 min.

#### *Eluent C (isocratic)*

This eluent consisted of an isocratic mixture of methanol (20%), acetonitrile

TABLE I

HPLC RETENTION TIMES OF CAROTENOL FATTY ACID ESTERS SEPARATED UNDER VARIOUS CHROMATOGRAPHIC CONDITIONS EMPLOYING ELUENTS A, B OR C

Conditions are as described in the text. The chemical structures of carotenoids and carotenol fatty acid esters are shown in Fig. 1.

Fatty acid side chains	Retention time (min)								
	Violaxanthin (I)			Auroxanthin (II)			Lutein (III)		
	A	B	C	A	B	C	A	B	C
(A) Decanoyl ( $C_{10}$ ) $R_1 = R_2 = CH_3(CH_2)_nCO$ , $n = 8$	31.7	28.7	5.4	32.7	29.6	5.9	38.1	32.3	8.0
(B) Lauroyl ( $C_{12}$ ) $R_1 = R_2 = CH_3(CH_2)_nCO$ , $n = 10$	36.5	32.5	7.0	37.5	33.6	7.6	42.5	36.8	10.5
(C) Myristoyl ( $C_{14}$ ) $R_1 = R_2 = CH_3(CH_2)_nCO$ , $n = 12$	40.3	35.1	8.5	41.3	36.2	9.2	45.6	40.1	13.6
(D) Myristoyl/palmitoyl $R_1 = CH_3(CH_2)_{12}CO$ $R_2 = CH_3(CH_2)_{14}CO$	42.1	36.6	9.8	43.1	37.6	10.6	47.4	42.0	15.9
(E) Palmitoyl ( $C_{16}$ ) $R_1 = R_2 = CH_3(CH_2)_nCO$ , $n = 14$	43.8	38.0	11.2	44.7	39.0	12.2	49.5	44.0	19.0

\* For  $\beta$ -cryptoxanthin, a monohydroxy carotenoid, mixed carotenol fatty acid ester is not applicable.

(40%), methylene chloride-hexane (1:1) (40%). The column flow-rate with this eluent was 0.7 ml/min.

#### Eluent D (isocratic)

Carotenol fatty acid esters were purified on  $C_{18}$ -reversed-phase thin-layer plates (20 × 20 cm, layer thickness 200  $\mu$ m; Whatman) employing methanol (15%), acetonitrile (35%), methylene chloride (25%), and hexane (25%) as eluent.

#### Reagents and materials

The reference samples of (3*R*,3'*R*)-zeaxanthin, (3*R*)- $\beta$ -cryptoxanthin and 15,15'-*cis*- $\beta$ -carotene were provided by Hoffman-La Roche, Basel, Switzerland. Lutein was isolated from kale (*Brassica oleracea*, variety acephala) according to published procedures<sup>2</sup>. Isozeaxanthin was prepared from the reduction of canthaxanthin (Fluka, New York, U.S.A.) with lithium aluminium hydride<sup>16</sup>. The straight-chain fatty acid ( $C_{10}$ ,  $C_{12}$ ,  $C_{14}$ ,  $C_{16}$ , and mixed  $C_{14}/C_{16}$ ) esters of hydroxycarotenoids were prepared by partial synthesis from the parent hydroxycarotenoids and the corresponding fatty acid chlorides in the presence of triethylamine according to the general procedure described in text. Violaxanthin fatty acid esters were prepared by epoxidation of the corresponding zeaxanthin fatty acid esters with *m*-chloroperbenzoic acid (MCPBA) according to the general procedure described in text. Violaxanthin myristate palmitate mixed ester was similarly prepared from

<i>Zeaxanthin (IV)</i>			<i>Isozeaxanthin (V)</i>			<i>β-Cryptoxanthin (VI)</i>		
<i>A</i>	<i>B</i>	<i>C</i>	<i>A</i>	<i>B</i>	<i>C</i>	<i>A</i>	<i>B</i>	<i>C</i>
39.3	33.9	8.3	37.6	31.8	7.7	36.5	29.2	8.2
43.2	37.6	11.0	41.8	36.7	10.1	39.1	33.8	9.4
46.3	40.9	14.9	45.3	39.7	13.5	41.5	36.3	10.9
48.2	42.6	17.5	47.1	41.5	15.8			
50.4	44.9	20.6	49.2	43.5	18.6	43.7	38.1	12.7

epoxidation of zeaxanthin myristate palmitate mixed ester. Auroxanthin and auroxanthin fatty acid esters were prepared from violaxanthin and violaxanthin fatty acid esters upon treatment with catalytic amount of methanolic hydrogen chloride reagent<sup>17,18</sup>. Free violaxanthin was obtained from saponification of violaxanthin fatty

TABLE II

$R_F$  VALUES OF CAROTENOL FATTY ACID ESTERS SEPARATED BY THIN-LAYER CHROMATOGRAPHY EMPLOYING ELUENT D

Conditions as described in the text. The chemical structures of carotenoids are shown in Fig. 1.

<i>Fatty acid side chains</i>	$R_F$			
	<i>Violaxanthin (I)</i>	<i>Lutein (II)</i>	<i>Zeaxanthin (IV)</i>	<i>Isozeaxanthin (V)</i>
(C) Myristoyl ( $C_{14}$ ) $R_1 = R_2 = CH_3(CH_2)_nCO$ , $n = 12$	0.47	0.33	0.35	0.32
(D) Myristoyl/palmitoyl $R_1 = CH_3(CH_2)_{12}CO$ $R_2 = CH_3(CH_2)_{14}CO$	0.45	0.30	0.32	0.29
(E) Palmitoyl ( $C_{16}$ ) $R_1 = R_2 = CH_3(CH_2)_nCO$ , $n = 14$	0.43	0.27	0.29	0.26

acid esters and it was also isolated and characterized from extracts of acorn squash according to published procedures<sup>13,14</sup>. The reference samples of all-*trans*- $\alpha$ - and all-*trans*- $\beta$ -carotene (Sigma, St. Louis, MO, U.S.A.) were further purified by recrystallization from methylene chloride-methanol. HPLC-grade solvents, methanol, acetonitrile, methylene chloride, and hexane (Fisher Scientific, Pittsburgh, PA, U.S.A.) were used without further purification.

*General procedures for preparation of carotenol fatty acid esters by partial synthesis*

*Lutein fatty acid esters*

A solution of an appropriate fatty acid chloride (0.0040 mmol) in dry benzene (1 ml) was added to a solution of lutein (0.0018 mmol) and triethylamine (0.054 mmol) in benzene (5 ml) and the reaction mixture was stirred under an atmosphere of nitrogen at 40°C for 20 min. The product was washed with water and 10% methanol in water and it was dried over sodium sulfate. The excess of solvent was evaporated under reduced pressure and the residue was chromatographed (eluent D). The main yellow zones ( $R_F$  = 0.22–0.33, Table II) of lutein difatty acid esters were removed and identified from their UV–VIS absorption and mass spectra. The spectroscopic evidence for structural determination of carotenol fatty acid esters have been described elsewhere<sup>14</sup>.

*Lutein myristate palmitate mixed esters.* A solution of lutein in benzene was added to a mixture of myristoyl chloride and palmitoyl chloride (1:1) in benzene in the presence of triethylamine and the reaction mixture was allowed to proceed as above. The examination of the isolated product after chromatography (same as above) by HPLC revealed the presence of lutein dimyristate, lutein dipalmitate, and lutein myristate palmitate mixed esters. Under the various chromatographic conditions employed (eluent A, B and C), the two possible regio-isomers of lutein myristate palmitate mixed esters,  $\beta,\epsilon$ -carotene-3-monol monomyristate-3'-monol mono-palmitate and  $\beta,\epsilon$ -carotene-3-monol monopalmitate-3'-monol monomyristate, were not resolved.

*Zeaxanthin, isozeaxanthin and  $\beta$ -cryptoxanthin fatty acid esters*

The various fatty acid esters of zeaxanthin, isozeaxanthin, and  $\beta$ -cryptoxanthin were similarly prepared by partial synthesis from their parent compounds and purified by chromatography (eluent D) according to the procedure described above for the preparation of lutein di-fatty acid esters.

Zeaxanthin and isozeaxanthin myristate palmitate mixed esters were prepared similar to the procedure described for lutein mixed esters.

*Violaxanthin fatty acid esters*

A solution of each of the zeaxanthin fatty acid esters (0.0018 mmol) in hexane was allowed to react with *m*-chloroperbenzoic acid (0.0040 mmol) under an atmosphere of nitrogen at room temperature for 4 h and the course of the reaction was followed by TLC. (eluent D). After work-up, violaxanthin fatty acid esters were purified by chromatography (eluent D). Violaxanthin myristate palmitate mixed ester was similarly prepared from zeaxanthin myristate palmitate mixed ester. The HPLC retention times and absorption spectra of synthetic violaxanthin fatty acid esters under

various chromatographic conditions were identical to those of authentic samples of violaxanthin fatty acid esters isolated from a variety of acorn squash (*Cucurbita Pepo*) grown in New Jersey, U.S.A.<sup>13,14</sup>. The violaxanthin fatty acid esters prepared by partial synthesis according to this procedure were presumably a mixture of configurational isomers of violaxanthin in which the fatty acid side chains may have a *cis*- or *trans*-relationship with respect to the epoxide ring. Under the chromatographic conditions employed (eluents A, B and C) these stereoisomeric violaxanthin fatty acid esters were not resolved.

The conversion of violaxanthin fatty acid esters [ $\lambda_{max.} = 442$  nm in HPLC solvents (eluents A, B and C)] to auroxanthin fatty acid esters [ $\lambda_{max.} = 402$  nm in HPLC solvents (eluents A, B and C)] was effected with catalytic amount of methanolic hydrogen chloride and resulted in a 40-nm hypsochromic shift in the absorption maximum of the former<sup>17,18</sup>.

## RESULTS AND DISCUSSION

The chemical structures of the carotenol fatty acid esters separated by HPLC are shown in Fig. 1. The absolute configuration of some of the carotenol fatty acid esters that were prepared by partial synthesis for the present study are not known with certainty. Since the reference samples of various configurational isomers of carotenoids and carotenol fatty acid esters were not available, it was not possible to evaluate the efficiency of the chromatographic systems (eluents A, B and C) that were developed in the present study for separation of optical isomers of carotenoids. The separation of configurational isomers of carotenoids has been reported by Ruttimann *et al.*<sup>19</sup>, who elegantly developed a method for qualitative and quantitative determination of (3*R*,3'*R*)-, (3*R*,3'*S*; *meso*)- and (3*S*,3'*S*)-zeaxanthin and (3*R*,3'*R*,6'*R*)-, (3*R*,3'*S*,6'*S*)-, and (3*S*,3'*S*,6'*S*)-lutein. This method was based on the reaction of zeaxanthin and lutein isomers with (*S*)-(+)- $\alpha$ -(1-naphthyl)ethyl isocyanate to afford diastereomeric dicarbamates, which were separated by HPLC. However, derivatization of crotenol fatty acid esters by this method is not possible as the hydroxyl groups have already been substituted with fatty acid side chains. Alternatively, carotenol fatty acid esters may be saponified and then derivatized according to this procedure. Although the various chromatographic conditions developed in the present study may not resolve the configurational isomers of carotenol fatty acid esters, they allow the convenient separation of various naturally occurring carotenol fatty acid esters that are commonly found in fruits and vegetables. The HPLC retention times of several carotenol fatty acid esters separated by HPLC are shown in Table I. These retention times were obtained for each of the individual carotenol fatty acid esters prepared by partial synthesis as well as mixtures of C<sub>10</sub>, C<sub>12</sub>, C<sub>14</sub>, C<sub>14</sub>/C<sub>16</sub>, C<sub>16</sub> fatty acid esters of each carotenoid under various chromatographic conditions (eluents A, B and C). From the retention times in Table I, it is quite clear that not only the C<sub>10</sub>-C<sub>16</sub> carotenol fatty acid esters of each of the hydroxycarotenoids are well separated from each other, but certain mixtures of these carotenol fatty acid esters may also be separated simultaneously. This is clearly demonstrated in the HPLC profiles of a mixture of dimyristate, dipalmitate, and myristatè palmitate mixed esters of violaxanthin, auroxanthin, lutein, and zeaxanthin with eluents A and C in Fig. 2. Under various chromatographic conditions employed (eluents A, B and C) on a C<sub>18</sub> reversed-phase

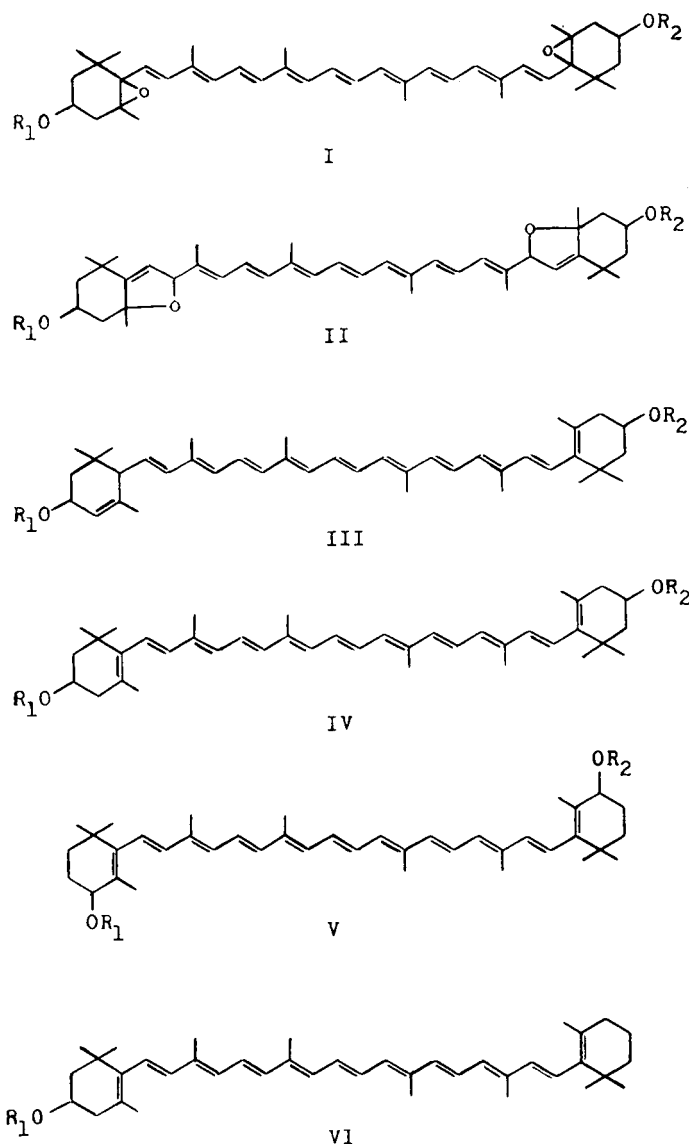


Fig. 1. The chemical structures of carotenol fatty acid esters. Where  $R_1 = R_2 = H$ , I = violaxanthin, II = auroxanthin, III = lutein, IV = zeaxanthin, V = isozeaxanthin, VI =  $\beta$ -cryptoxanthin. The absolute configuration of these carotenoids are not shown. Where  $R_1$  and  $R_2$  are fatty acid esters see Table I for identification of each carotenol fatty acid ester.

HPLC column, the violaxanthin fatty acid esters are eluted first and each of the esters are then followed by auroxanthin fatty acid esters. This order of elution on  $C_{18}$  also holds for the non-esterified violaxanthin and auroxanthin<sup>2</sup>. The detection of violaxanthin and auroxanthin fatty acid esters in various eluents is best accomplished by monitoring the chromatographic runs at 442 and 400 nm simultaneously, as indicated in Fig. 2 by the light solid line (HPLC trace monitored at 442 nm) and the

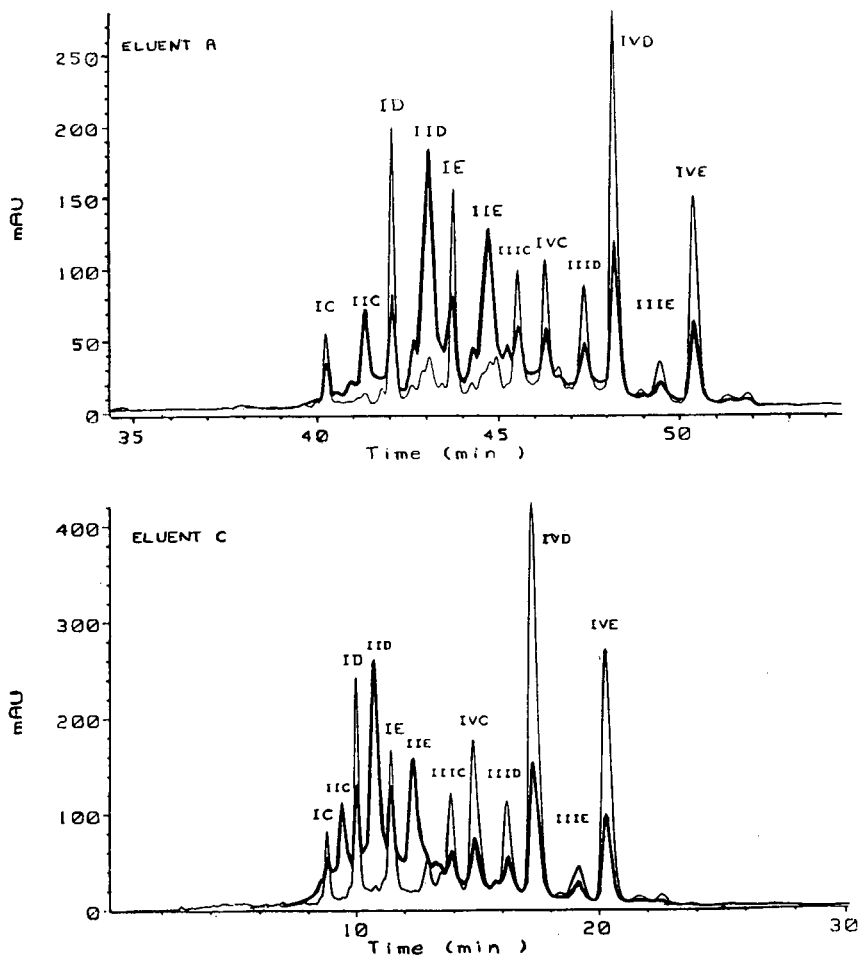


Fig. 2. HPLC profiles of a mixture of violaxanthin, auroxanthin, lutein, and zeaxanthin dimyristate, myristate palmitate mixed esters, and dipalmitate. Upper trace, eluent A; lower trace, eluent C. Chromatographic conditions and peak identification (Table I) as described in the text. Light solid lines are the HPLC traces monitored at 442 nm and dark solid lines are the HPLC traces monitored at 400 nm.

dark solid line (HPLC trace monitored at 400 nm). The rearrangement of violaxanthin fatty acid esters ( $\lambda_{\max.} = 442$  nm in the HPLC solvents) induced by light, heat, or traces of acids results in the formation of auroxanthin fatty acid esters ( $\lambda_{\max.} = 402$  nm in the HPLC solvents). This rearrangement is accompanied by a 40-nm hypsochromic shift in the absorption maximum of violaxanthin fatty acid esters as shown in Fig. 3 in the absorption spectra of violaxanthin and auroxanthin myristate palmitate mixed esters in the HPLC solvents.

In the order of elution on a  $C_{18}$  reversed-phase HPLC column, following violaxanthin and auroxanthin fatty acid esters, lutein and zeaxanthin fatty acid esters are eluted, respectively, with virtually no HPLC peak interference (see Fig. 2). Although the separation of the mixture of carotenol fatty acid esters described above

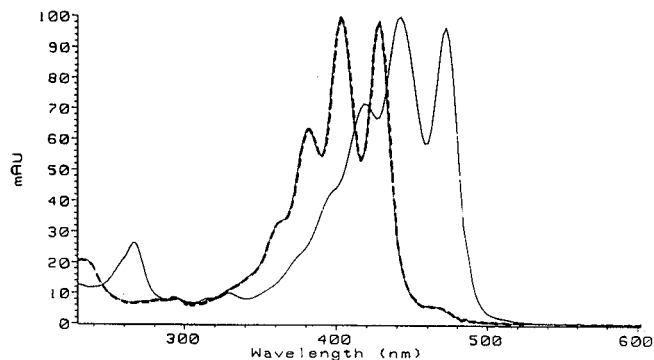


Fig. 3. Absorption spectra of violaxanthin myristate palmitate (—,  $\lambda_{max}$  = 442 nm) and auroxanthin myristate palmitate (----,  $\lambda_{max}$  = 402 nm) in the HPLC solvents (eluent A or B or C). Conditions as described in the text.

may not be typical of the chromatographic profile of carotenoid extracts from natural sources, it focuses on the separation of some of the most common hydroxycarotenoids that may be esterified with common straight chain fatty acids (myristic and palmitic acid). There is no doubt that if the fatty acid esters of these carotenoids were all present in an extract from a biological source, under the chromatographic conditions employed, some HPLC peak interference between some of these esters will be inevitable. However, in most fruits and vegetables (*i.e.* oranges, apricots, peaches, prunes, and squash), where naturally occurring carotenoids are usually esterified, only fatty acid esters of selected carotenoids from each group are found to be present at one time<sup>12</sup>.

From the retention times of carotenol fatty acid esters (Table I) within each group it seems clear that as the number of carbon atoms on the fatty acid side chains of the carotenol esters are increased the retention times of these compounds with various eluents are also increased. There seems to be no correlation between these increments and the number of the carbon atoms in the fatty acid side chains of carotenol esters. This finding is not in agreement with the observation made by Philip and Chen<sup>8</sup>, who reported that under their chromatographic conditions, a steady increase in retention times of a number of carotenol fatty acid esters (*i.e.*  $\beta$ -cryptoxanthin, lutein, violaxanthin) resulted as the number of carbon atoms in the fatty acid side chains of these carotenoids were increased. At first the lack of such correlation was contributed to the lack of reproducibility of gradient chromatography, however after prolonged re-equilibration of the HPLC column and repeated injection of the several synthetic and naturally occurring carotenol esters under various isocratic and gradient chromatographic conditions, such correlations could not be established. A possible explanation for the absence of such correlation has been provided in our earlier report on separation of carotenol fatty acid esters<sup>13</sup>.

The chromatographic conditions developed for the separation of esterified carotenoids can also be employed to resolve selected carotenol fatty acid esters, whose parent hydroxycarotenoids are less readily separated by HPLC. The separation of a mixture of some of these carotenoids is discussed below.

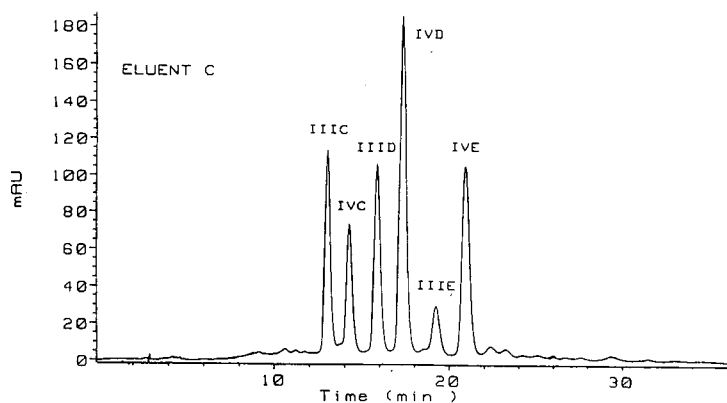


Fig. 4. HPLC profile of a mixture of lutein and zeaxanthin dimyristate, myristate palmitate mixed esters, and dipalmitate. Chromatographic conditions (eluent C) and peak identification (Table I) as described in the text.

#### *Separation of lutein and zeaxanthin fatty acid esters*

Although the non-esterified lutein and zeaxanthin can only be separated by HPLC employing eluent A, the fatty acid esters of these carotenoids are readily separated by HPLC with eluents A, B and C. A typical chromatographic profile (eluent C) of a mixture of dimyristate, myristate palmitate mixed esters, and dipalmitate esters of lutein and zeaxanthin is shown in Fig. 4. Each of the lutein fatty acid esters are eluted prior to their corresponding zeaxanthin fatty acid esters. This order of elution on  $C_{18}$  reversed-phase column also holds for the non-esterified lutein and zeaxanthin, as it will be demonstrated in the HPLC profile of a mixture of these compounds later in this text. The HPLC peak identification of a mixture such as this can be simply accomplished by comparison of the retention times of each peak in the mixture with those of the individually synthesized reference samples of these compounds. Such HPLC peak assignments can be further complemented by monitoring absorption spectra of these compounds by a rapid scanning photodiode array detector. For example, the

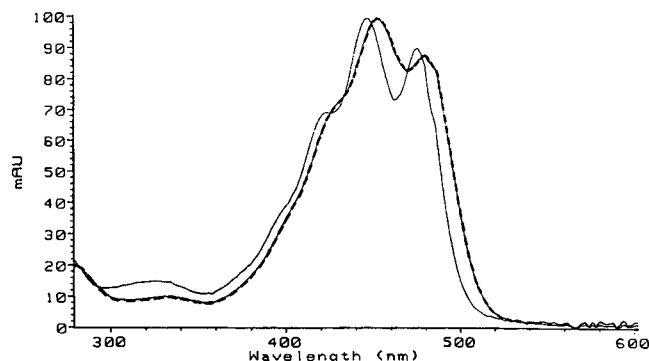


Fig. 5. Absorption spectra of lutein myristate palmitate (—,  $\lambda_{max.} = 446$  nm) and zeaxanthin myristate palmitate (---,  $\lambda_{max.} = 454$  nm) mixed esters in the HPLC solvents (eluents A or B or C); conditions as described in the text.

absorption spectra of lutein fatty acid esters with a maximum at 446 nm, can be readily distinguished from the absorption spectra of zeaxanthin fatty acid esters, which have a maximum at 454 nm in the HPLC solvents. This is clearly demonstrated in the absorption spectra of lutein myristate palmitate and zeaxanthin myristate palmitate mixed esters in Fig. 5. However, in the case of carotenol fatty acid esters isolated from the extracts of natural products, additional spectroscopic evidence (*i.e.* nuclear magnetic resonance, mass spectrometry) is often necessary to establish the structure of these compounds without ambiguity. As pointed out earlier (see the experimental section) the major disadvantage of these HPLC conditions is their inability to separate the two possible regio-isomers of mixed lutein myristate palmitate. In case of the other hydroxycarotenoids studied in the present report this does not present a problem since owing to the molecular symmetry of these compounds only one mixed carotenol fatty acid ester of myristate and palmitate can be formed naturally and/or synthetically. Since the predominant carotenol fatty acid esters from natural sources are normally esterified with myristic and palmitic acid, no attempt was made in the present study to investigate the chromatographic properties of the other mixed carotenol fatty acid esters that may be prepared by random esterification of the dihydroxycarotenoids with fatty acids.

### Separation of isozeaxanthin and zeaxanthin fatty acid esters

The separation of isozeaxanthin and zeaxanthin by HPLC, under chromatographic conditions employed (eluent A), only resulted in partial separation of these compounds and the HPLC peak of isozeaxanthin appeared as a trailing shoulder on that of zeaxanthin. However, the di-fatty acid esters of these hydroxycarotenoids were readily separated under various chromatographic conditions. The chromatographic profile of a mixture of isozeaxanthin and zeaxanthin didecanoate, dilaurate, dimyristate, myristate palmitate mixed esters, and dipalmitate is shown in Fig. 6. It is interesting to note that although isozeaxanthin is eluted (eluent A) after zeaxanthin on a C<sub>18</sub> reversed-phase HPLC column, this order of elution is reversed for the di-fatty

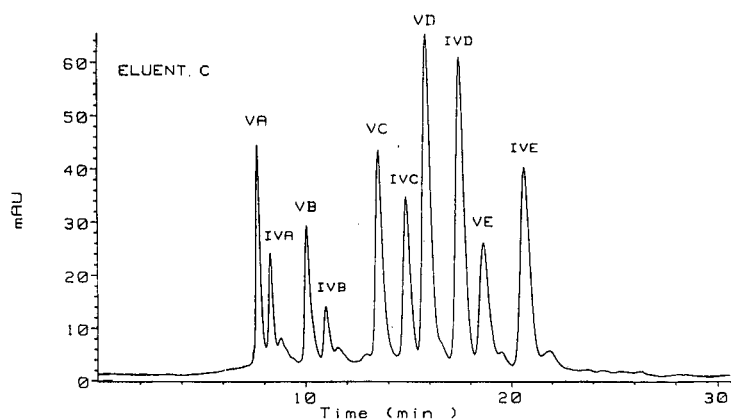


Fig. 6. HPLC profile of a mixture of isozeaxanthin and zeaxanthin didecanoate, dilaurate, dimyristate, myristate palmitate mixed esters, and dipalmitate. Chromatographic conditions (eluent C) and peak identification (Table I) as described in the text.

acid esters of these compounds under various chromatographic conditions (eluent A, B and C). The ease with which the esters of zeaxanthin (IV) and isozeaxanthin (V) are separated in comparison with their parent compounds is probably due to the fatty acid side chains in these hydrocarotenoids that induce a more pronounced effect by these non-allylic and allylic substituents. This pronounced effect influences the parameters that affect intermolecular interactions (*i.e.* dispersion, dipole, and hydrogen bonding) between these carotenol esters and solvent molecules sufficiently different to allow the separation of these compounds.

#### *Separation of $\beta$ -cryptoxanthin fatty acid esters*

Chromatographic profile of a mixture of  $\beta$ -cryptoxanthin decanoate, laurate, myristate, and palmitate is shown in Fig. 7. Each of the synthetic all-*trans*- $\beta$ -cryptoxanthin fatty acid esters was shown to contain small amount of a mono-*cis* isomer which appeared as a shoulder following their all-*trans* isomers. These mono-*cis* isomers ( $\lambda_{\max.} = 450$  nm) were tentatively identified from their UV-VIS absorption spectra, monitored by a photodiode array detector in the HPLC solvents (eluent A, B and C), which exhibited a hypsochromic shift of 4 nm from the absorption maximum of all-*trans*- $\beta$ -cryptoxanthin fatty acid esters ( $\lambda_{\max.} = 454$  nm). Under various chromatographic conditions employed, the HPLC peaks of the fatty acid esters of  $\beta$ -cryptoxanthin in most cases do not interfere with the HPLC peaks of other carotenol esters such as lutein and zeaxanthin. This is particularly important in the chromatographic evaluation of some natural extracts in which selected fatty acid esters of  $\beta$ -cryptoxanthin, lutein, and zeaxanthin are all present.

#### *Optimum separation conditions for carotenoids and carotenol fatty acid esters*

In the study presented in this report we described various chromatographic conditions such as eluents A, B and C that separate the fatty acid esters of several common naturally occurring carotenoids. These eluents each have a unique application in the separation of carotenoids and their related esters depending on the presence or absence of various classes of carotenoids in a given extract from natural products. In

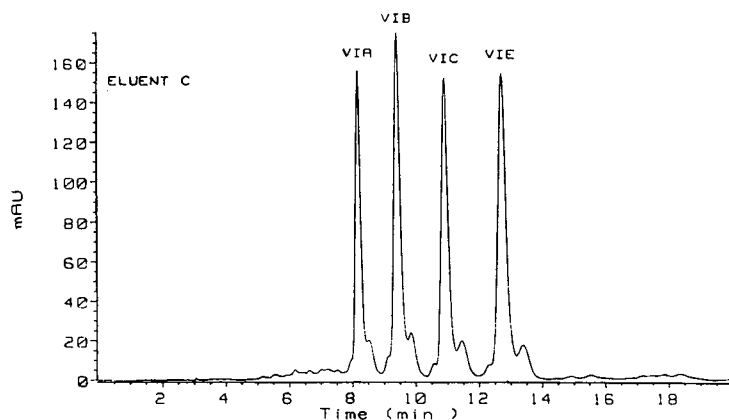


Fig. 7. HPLC profile of  $\beta$ -cryptoxanthin decanoate, laurate, myristate, and palmitate. Chromatographic conditions (eluent C) and peak identification (Table I) as described in the text.

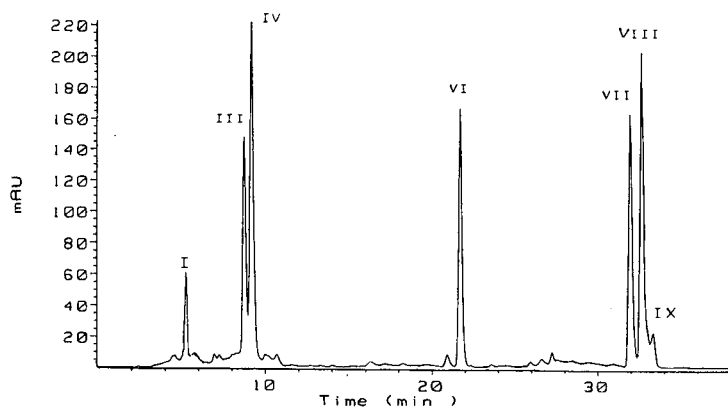


Fig. 8. HPLC profile of a mixture of violaxanthin (I), lutein (III), zeaxanthin (IV),  $\beta$ -cryptoxanthin (VI), all-*trans*- $\alpha$ -carotene (VII), all-*trans*- $\beta$ -carotene (VIII), and 15,15'-*cis*- $\beta$ -carotene (IX). Chromatographic conditions (eluent A) as described in the text.

an attempt to provide an insight into the application of these chromatographic conditions for an optimum separation of some of the naturally occurring carotenoids and their esters, each of these eluents are discussed below.

**Eluent A.** This eluent can be employed almost universally to separate a wide range of carotenoids and carotenol fatty acid esters. The chromatographic profile of a mixture of violaxanthin (I), lutein (III), zeaxanthin (IV),  $\beta$ -cryptoxanthin (VI),  $\alpha$ -carotene (VII),  $\beta$ -carotene (VIII) and its 15,15'-*cis*-isomer (IX) is shown in Fig. 8. Under these chromatographic conditions some of the most common naturally occurring carotenoids that belong to the four classes of xanthophylls, carotenol mono-fatty acid esters, hydrocarbon carotenoids, and carotenol difatty acid esters can be separated simultaneously<sup>13</sup>. This eluent is particularly useful in separations in which carotenol fatty acid esters and their non-esterified parent compounds are all present in the mixture.

**Eluent B.** Although HPLC with this eluent has been shown to accomplish the separation of carotenol mono-fatty acid esters, hydrocarbon carotenoids, and carotenol di-fatty acid esters as efficiently as eluent A<sup>13</sup>, it fails to separate xanthophylls such as violaxanthin, lutein, and zeaxanthin. The major advantage with this eluent is its shorter HPLC analysis time in comparison to eluent A (see Table I).

**Eluent C.** This eluent provides a convenient isocratic separation for carotenol di-fatty acid esters and does not separate the other classes of carotenoids. This isocratic HPLC condition is particularly important for separation and isolation of carotenol fatty acid esters on both analytical and preparative scales. The reasonably short analysis time with this eluent provides a convenient method for the HPLC analysis of extracts from natural sources in which, carotenoids are only present in the esterified forms.

### Nomenclature

For convenience the trivial names of several naturally occurring carotenoids have been used throughout this text. The trivial and systematic names as well as chemical structures of these carotenoids with  $\epsilon$ - and  $\beta$ -type end groups have been tabulated by Straub<sup>20</sup>.

## ACKNOWLEDGEMENTS

We would like to thank Hoffmann-La Roche & Co. (Basel, Switzerland) for their generous gift of carotenoid reference samples. Partial support by the National Cancer Institute through reimbursable agreement Y01-CN-30609 is acknowledged.

## REFERENCES

- 1 G. R. Beecher and F. Khachik, *J. Natl. Cancer Inst.*, 73 (1984) 1397-1404.
- 2 F. Khachik, G. R. Beecher and N. F. Whittaker, *J. Agric. Food Chem.*, 34 (1986) 603-616.
- 3 F. Khachik and G. R. Beecher, *J. Agric. Food Chem.*, 35 (1987) 732-738.
- 4 G. R. Beecher and F. Khachik, in T. Moon and M. Micozzi (Editors), *Nutrition and Cancer Prevention: The Role of Micronutrients*, Marcel Dekker, New York, 1988, Ch. 5, in press.
- 5 M. Micozzi, in T. Moon and M. Micozzi (Editors), *Nutrition and Cancer Prevention: The Role of Micronutrients*, Marcel Dekker, New York, 1988, Ch. 3, in press.
- 6 G. Noga and F. Lenz, *Chromatographia*, 17 (1983) 139-142.
- 7 G. K. Gregory, T. S. Chen and T. Philip, *J. Food Sci.*, 52(4) (1987) 1071-1073.
- 8 T. Philip and T.-S. Chen, *J. Chromatogr.*, 435 (1988) 113-126.
- 9 C. Fisher and J. A. Kocis, *J. Agric. Food Chem.*, 35 (1987) 55-57.
- 10 W. Gau, H.-J. Ploschke and C. Wünsche, *J. Chromatogr.*, 262 (1983) 277-284.
- 11 F. Zonta, B. Stancher and G. P. Marletta, *J. Chromatogr.*, 403 (1987) 207-215.
- 12 F. Khachik, G. R. Beecher and W. R. Lusby, presented at the 8th International Symposium on Carotenoids, Boston, MA, July 27-31, 1987.
- 13 F. Khachik and G. R. Beecher, *J. Agric. Food Chem.*, 36 (1988) in press.
- 14 F. Khachik, G. R. Beecher and W. R. Lusby, *J. Agric. Food Chem.*, 36 (1988) in press.
- 15 F. Khachik, G. R. Beecher, J. Vanderslice and G. Furrow, *Anal. Chem.*, 60 (1988) 807-811.
- 16 F. J. Petrcek and L. Zechmeister, *J. Am. Chem. Soc.*, 78 (1956) 1427-1434.
- 17 C. H. Eugster and P. Karrer, *Helv. Chim. Acta*, 40 (1957) 69-79.
- 18 K. Tsukida and L. Zechmeister, *Arch. Biochem. Biophys.*, 74 (1958) 408-426.
- 19 A. Ruttimann, K. Schiedt and M. Vecchi, *J. High Resolut. Chromatogr. Chromatogr. Commun.*, 6 (1983) 612-616.
- 20 O. Straub, in H. Pfander (Editor), in collaboration with M. Gerspacher, M. Rychener and R. Schwabe, *Key to Carotenoids*, Birkhauser, Basel, 2nd ed., 1987.



CHROM. 20 669

## CROSS-AXIS SYNCHRONOUS FLOW-THROUGH COIL PLANET CENTRIFUGE FOR LARGE-SCALE PREPARATIVE COUNTER-CURRENT CHROMATOGRAPHY

### I. APPARATUS AND STUDIES ON STATIONARY PHASE RETENTION IN SHORT COILS

YOICHIRO ITO\* and TIAN-YOU ZHANG\*

*Laboratory of Technical Development, National Heart, Lung, and Blood Institute, Bethesda, MD 20892 (U.S.A.)*

(First received March 14th, 1988; revised manuscript received May 26th, 1988)

---

#### SUMMARY

Using a new cross-axis synchronous flow-through coil planet centrifuge with a 20-cm revolutionary radius, the retention of the stationary phase for nine solvent systems was studied with short coils mounted at two different locations on three holders with 5-, 15- and 25-cm hub diameters. Coils mounted 10 cm to the left of the center of a holder produced a much improved retention of most of the solvent systems compared with the same coils mounted at the center of the holder. In the lateral coil position the retention was found to be affected by the direction of the planetary motion and the head–tail elution mode. This phenomenon may be attributed to the effect of the lateral force field acting asymmetrically between the upper and lower halves of the coil.

---

#### INTRODUCTION

Recently, a cross-axis synchronous flow-through coil planet centrifuge (X-axis CPC) has been developed in our laboratory for performing preparative counter-current chromatography (CCC). The system utilizes a novel mode of planetary motion to achieve highly efficient chromatographic separations of solutes on the preparative scale<sup>1,2</sup>. The centrifugal force field generated by this planetary motion provides efficient three-dimensional mixing of two solvent phases in a coiled column to nearly double the partition efficiency obtained by existing high-speed CCC systems<sup>3</sup>. The capability of the X-axis CPC has been demonstrated by preparative-scale separations of dinitrophenyl (DNP) amino acids and dipeptides by a prototype apparatus with a 10-cm revolutionary radius<sup>2</sup>. More recent studies have indicated that the system can be applied efficiently to form separations with a long multilayer coil<sup>4</sup>.

---

\* Permanent address: Beijing Institute of New Technology Application, Beijing, China.

In this paper we describe a further development of the X-axis CPC obtained by increasing both the revolutionary radius and column holder dimensions. A new large prototype with a 20-cm revolutionary radius has been tested with respect to stationary phase retention and partition efficiency using standard sets of two-phase solvent systems to compare the performance with those of existing high-speed CCC systems. The use of a large revolutionary radius and a proper choice of column orientation on the holder have considerably improved the retention of the stationary phase, especially for hydrophilic solvent systems, which are extremely useful for separating peptides and other polar compounds. Studies on the partition efficiency and preparative capability of the apparatus are described in Part II.

#### APPARATUS

The principle and basic design of the X-axis CPC have been described previously<sup>1</sup>. The synchronous planetary motion of the apparatus is illustrated schematically in Fig. 1, where the coil holder disc with the bundle of flow tubes is drawn in successive positions as it revolves around the central axis of the centrifuge. The disc revolves around the central axis of the centrifuge and simultaneously rotates about its own axis at the same angular velocity in the indicated directions. In doing so, the holder disc constantly maintains its axis in a tangential orientation to a path formed by revolution with a fixed distance,  $R$ , from the centrifuge axis. Consequently, the axes of revolution and rotation in the planetary motion form a cross to each other, hence the name of the instrument.

The above synchronous planetary motion bears two important functions for performing CCC. First, the synchronous rotation of the holder disc steadily unwinds the twist of the tubing caused by the revolution, thus permitting continuous elution of the mobile phase through the rotating column without the use of a rotary seal device, which would cause various complications such as leakage, contamination, etc. The

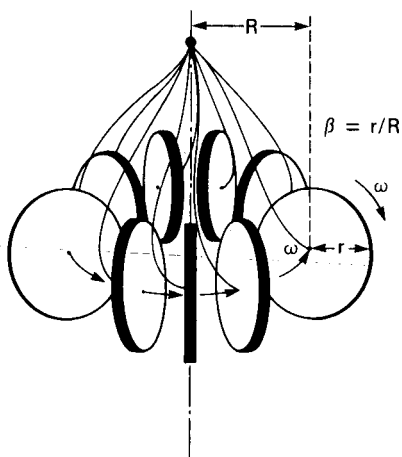


Fig. 1. Successive positions of coil holder in cross-axis synchronous flow-through coil planet centrifuge. Because of the synchronous planetary motion of the holder, the bundle of flow tubes becomes free of twisting.

planetary motion further generates a unique pattern of the centrifugal force field which permits more efficient chromatographic separations of solutes in a multilayer coil at a high flow-rate, as previously described<sup>1,2</sup>.

Fig. 2A is a photograph of the second prototype X-axis CPC with a 20-cm revolutionary radius used in these studies. The rotary frame of the apparatus consists of a pair of butterfly-shaped aluminium side-plates rigidly bridged together with upper and lower aluminium plates and several additional links to hold a column holder and a counterweight holder horizontally in symmetrical positions at a distance of 20 cm from the central axis of the centrifuge. The rotary frame is driven by a motor (Electro-Craft, Hopkins, MN, U.S.A.) via a pair of toothed pulleys, one mounted on

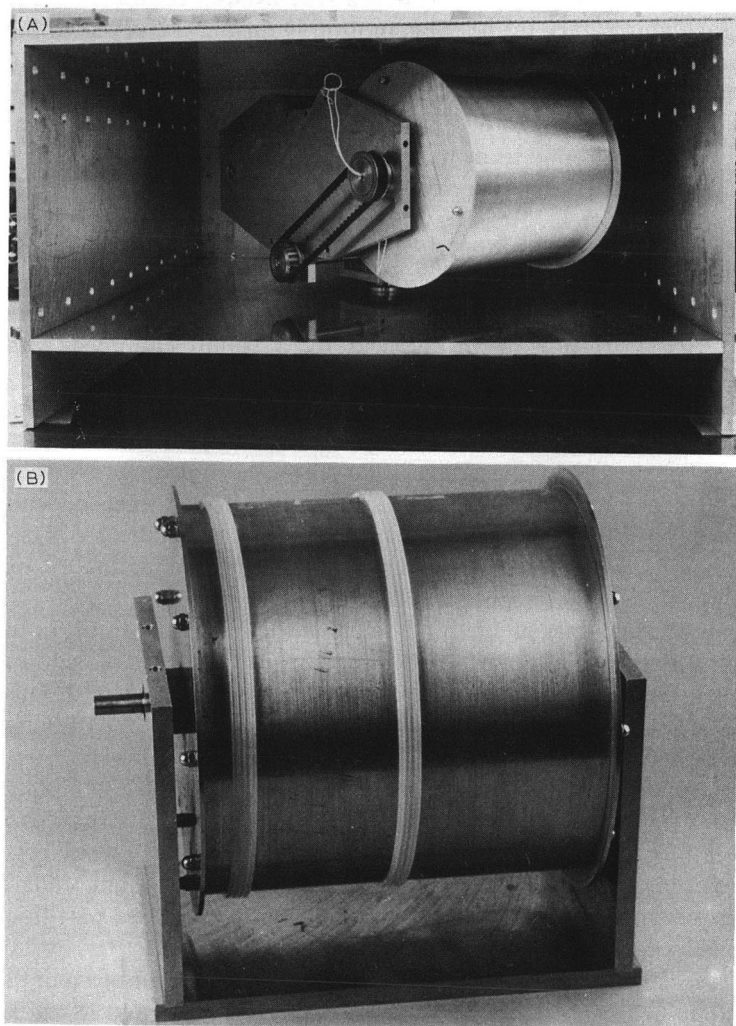


Fig. 2. (A) The cross-axis synchronous flow-through coil planet centrifuge with a 20-cm revolutionary radius. The apparatus holds a 25-cm diameter coil holder. (B) Central ( $l = 0$  cm) and lateral ( $l = -10$  cm) coil positions on the 25-cm diameter holder which is held on the stand.

the motor shaft and the other on the central shaft of the rotary frame, through a toothed belt at the bottom of the centrifuge. In order to support the heavy weight of the rotary frame (*ca.* 32 kg), a thrust bearing (not shown in the photograph) is embedded at the bottom plate of the centrifuge around the central shaft.

Synchronous planetary motion of the holders is introduced by means of coupling a set of three miter gears ( $45^\circ$ ), all identical in shape. One miter gear, called the stationary sun gear (plastic), is mounted rigidly on the bottom plate coaxially around the central shaft of the rotary frame, while other two planetary miter gears (steel) are positioned symmetrically over the sun gear. Each planetary gear is equipped with a countershaft which extends radially toward the periphery through a ball-bearing, embedded in the lower portion of the side-plate, to hold a toothed pulley securely on the distal end. The above gear arrangement produces a synchronous rotation of each countershaft on the revolving rotary frame. This motion is further conveyed to the respective holder by coupling the toothed pulley on the countershaft to the identical pulley mounted at one end of the holder shaft with a toothed belt. Consequently, both the column holder and counterweight holder undergo the desired synchronous planetary motion, *i.e.*, rotation around its own axis and revolution around the central axis of the centrifuge at the same angular velocity, as illustrated schematically in Fig. 1.

Flow tubes from the holder are first led through the center hole of the holder shaft and then, making a loop, passed through a guide ring attached to the side-plate to enter the side hole of the central shaft of the rotary frame where they exit the centrifuge through a stationary guide pipe projecting down from the top plate of the centrifuge. Near the exit hole, each flow tube is firmly held by a clamp equipped with a silicone-rubber pad. These flow tubes are lubricated with grease and protected by a piece of Tygon tubing to prevent direct contact with metal parts. With proper care, the flow tubes can maintain their function for many months of operation.

The revolutionary speed of the apparatus can be regulated in a range between 0 and 500 rpm in either direction at high stability by a speed control unit (Electro-Craft). A plastic baffle placed close to the rotary frame around the periphery of the centrifuge case (not shown) reduced windage, resulting in a reduction of the torque by over 30% at the maximum speed of 500 rpm.

In order to apply various types of column holders in the same apparatus, both the column holder and counterweight holder are designed to be easily removable from the rotary frame simply by loosening a pair of screws on each bearing block. This design also facilitates mounting the coiled column on the holder and determining a proper counterweight mass to be applied for balancing the centrifuge system.

Two sets of column holders were fabricated. The first set consists of long spool-shaped holders (measuring 25 cm between the flanges) with different hub diameters ranging from 5 to 25 cm (the largest holder is shown in Fig. 2). Each holder is paired with a proper counterweight mass to be mounted on the counterweight holder. These column holders were used to measure stationary phase retention and partition efficiency in short coils mounted at two different locations on the holder, *i.e.*, at the center and at 10 cm to the left of the center (Fig. 2B). The second set consists of a pair of identical spool-shaped holders each measuring 5 cm between the flanges and 15 cm in hub diameter. These holders are used exclusively for mounting long multilayer coils suitable for large-scale preparative separations. They are mounted symmetrically on both sides of the rotary frame to effect perfect balancing of the centrifuge system

without the use of a counterweight. Two columns can be connected in series with a transfer tube or each can be used separately in tandem. Further details for the column design and preparation of the multilayer coils are described in Part II.

## EXPERIMENTAL

### *Reagents*

Two-phase solvent systems were prepared from *n*-hexane, ethyl acetate, chloroform, *n*-butanol, *sec*-butanol and methanol (glass-distilled chromatographic grade, Burdick and Jackson Labs., Muskegon, MI, U.S.A.), acetic acid (reagent grade, J. T. Baker, Phillipsburg, NJ, U.S.A.) and distilled water.

### *Preparation of two-phase solvent systems*

The following nine volatile two-phase solvent systems were prepared: *n*-hexane–water, *n*-hexane–methanol, ethyl acetate–water, ethyl acetate–acetic acid–water (4:1:4 by volume), chloroform–water, chloroform–acetic acid–water (2:2:1), *n*-butanol–water, *n*-butanol–acetic acid–water (4:1:5) and *sec*-butanol–water. Each solvent mixture was thoroughly equilibrated in a separatory funnel at room temperature by repeated shaking and degassing (by opening the stopcock), and separated before use.

### *Preparation of coiled columns*

These studies were performed with short coils of 2–3 m  $\times$  2.6 mm I.D. PTFE tubing (Zeus Industrial Products, Raritan, NJ, U.S.A.) wound coaxially around the holders of 5-, 15- and 25-cm hub diameters. For each holder, the coil was mounted at two different locations, either at the center of the holder ( $l = 0$  cm) or 10 cm to the left of the center of the holder ( $l = -10$  cm) (Fig. 2B). Although right-handed coils were mainly used, the left-handed coil was also tested at  $l = -10$  cm on the 25-cm diameter holder. These columns were firmly held on the holder with several pieces of fiber-glass reinforced adhesive tape.

Each end of the coil was directly connected to a 1 m  $\times$  0.85 mm I.D. flow tube without the use of a bulky commercial flanged connector, which would distort the helical configuration near the junction. The connection was made by inserting a series of smaller diameter tubing into one another, resembling concentric circles from the end, until the smallest I.D. of 0.85 mm emerges from the center. This tubing was PTFE with sizes 2.1 mm I.D. and 2.8 mm O.D. and also 1.3 mm I.D. and 2.1 mm O.D.

### *Measurement of stationary phase retention*

Experiments were performed according to a previously described procedure<sup>2</sup>. For each coil, retention was measured for the nine two-phase solvent systems. For each measurement, the coil was first entirely filled with the stationary phase. Then the apparatus was run at a desired revolutionary speed while the mobile phase was pumped through the coil at 120 ml/h with a Chromatronix Cheminert pump (Chromatronix, Sunnyvale, CA, U.S.A.). The effluent from the outlet of the coil was collected into a 25-ml graduated cylinder to measure the volume of the stationary phase eluted from the coil and the total volume of the mobile phase eluted. During the run, the temperature inside the centrifuge was controlled at  $22 \pm 1^\circ\text{C}$  by placing an ice-bag

directly over the top plate of the centrifuge. The run was continued for 10 min or slightly longer so that the effluent volume exceeded the total capacity of the coil. Then, the apparatus was stopped and the coil was emptied by connecting the inlet of the coil to a nitrogen gas line at a pressure of *ca.* 80 p.s.i. The coil was then flushed with several milliliters of methanol miscible with both phases. Finally, the coil was again flushed with several milliliters of the stationary phase to be used in the next experiment. During emptying and flushing of the coil with nitrogen, the apparatus was rotated at a moderate speed of 100–200 rpm in a direction making the coil outlet the head to promote the drainage of the column contents.



For the coils mounted at the center of the coil holder, the measurements were mainly performed in two elution modes as shown in Table I, each at four different revolutionary speeds of 200, 300, 400, and 500 rpm using both upper and lower phases as the mobile phase in each solvent system. It has been observed that the coils mounted at 10-cm left from the center of the holder, where the laterally acting centrifugal force field becomes asymmetric, yield different levels of stationary phase retention according to the direction of the planetary motion and handedness of the coil as well as the head-tail elution mode, thus totaling eight combinations of experimental conditions as summarized in Table II. All these combinations were tested with the 25-cm diameter holder at 500 rpm by the use of both right-handed and left-handed coils each mounted at 10 cm left from the center of the holder. In the rest of the cases, the measurements were limited to four combinations with right-handed coils at 500 rpm. Any experimental condition which produced significant degree of retention at 500 rpm was further examined under reduced revolutionary speeds of 400, 300 and 200 rpm to obtain phase distribution diagrams described below.

### Phase distribution diagrams

From each experiment, retention of the stationary phase was expressed as a percentage relative to the total column capacity according to the expression,  $100 (V_c + V_f - V_s)/V_c$ , where  $V_c$  denotes the total capacity of the coil;  $V_f$ , free space in the flow tubes; and  $V_s$ , the volume of the stationary phase eluted from the coil.

TABLE I

TWO ELUTION MODES AT CENTRAL COIL POSITION ( $l = 0$  cm)

Planetary motion	Head-tail elution mode (handedness of coil)*	Combined elution modes**	Design in PDD***
$P_I$ 	Head-to-tail (R)	$P_I$ -H	———
$P_{II}$ 	Tail-to-head (R)	$P_{II}$ -T	-----



\* R = Right-handed.

\*\* H = Head-to-tail; T = tail-to-head.

\*\*\* PDD = Phase distribution diagram.

TABLE II

EIGHT DIFFERENT ELUTION MODES AT LATERAL COIL POSITION ( $l = -10$  cm)

Planetary motion		Head-tail elution mode	Inward-outward elution mode (handedness of coil*)	Combined elution mode**	Symbols in PDD***
$P_I$		Head-to-tail	Inward (R)	$P_I$ -H-I	○—○
		Head-to-tail	Outward (L)	$P_I$ -H-O	○—○
		Tail-to-head	Inward (L)	$P_I$ -T-I	●---●
		Tail-to-head	Outward (R)	$P_I$ -T-O	●---●
$P_{II}$		Head-to-tail	Inward (L)	$P_{II}$ -H-I	△—△
		Head-to-tail	Outward (R)	$P_{II}$ -H-O	△—△
		Tail-to-head	Inward (R)	$P_{II}$ -T-I	▲---▲
		Tail-to-head	Outward (L)	$P_{II}$ -T-O	▲---▲

\* R = right-handed; L = left-handed.

\*\* H = head-to-tail; T = tail-to-head; I = inward; O = outward.

\*\*\* PDD = phase distribution diagram.

Using the retention data thus obtained, the hydrodynamic distribution of the two solvent phases in the coil was summarized in a phase distribution diagram which was constructed by plotting percentage retention of the stationary phase as a function of rotational speed for each mobile phase. A group of retention curves produced by different elution modes but otherwise identical experimental conditions can be illustrated in the same diagram. In order to distinguish each elution mode in the phase distribution diagram, a set of symbolic designs was used to draw phase distribution curves as illustrated in Tables I and II.

## RESULTS AND DISCUSSION

A series of experiments was performed with nine two-phase solvent systems to study the distribution of two solvent phases in the coil mounted on a set of holders located at the center of the holder ( $l = 0$  cm) and 10 cm to the left of the center ( $l = -10$  cm). The results obtained revealed the important findings that the degree of stationary phase retention was different at the two locations on the same holder and that in the lateral coil position retention of the stationary phase was significantly affected by the direction of the planetary motion and the head-tail elution modes. Therefore, the results obtained from these two coil locations are described separately.

### Phase distribution diagrams obtained from central coil position ( $l = 0$ cm)

The results of phase retention studies obtained with the central coil position are summarized in Fig. 3, where a set of phase distribution diagrams is arranged according to the format used in the previous studies<sup>2</sup>. In this figure, each column consists of phase distribution diagrams obtained from the solvent system labelled and arranged from left to right in the order of the hydrophobicity of the major organic component. As indicated in the left-hand margin, the top three rows show the retention of the lower phase obtained by elution with the upper phase, and the bottom three rows the

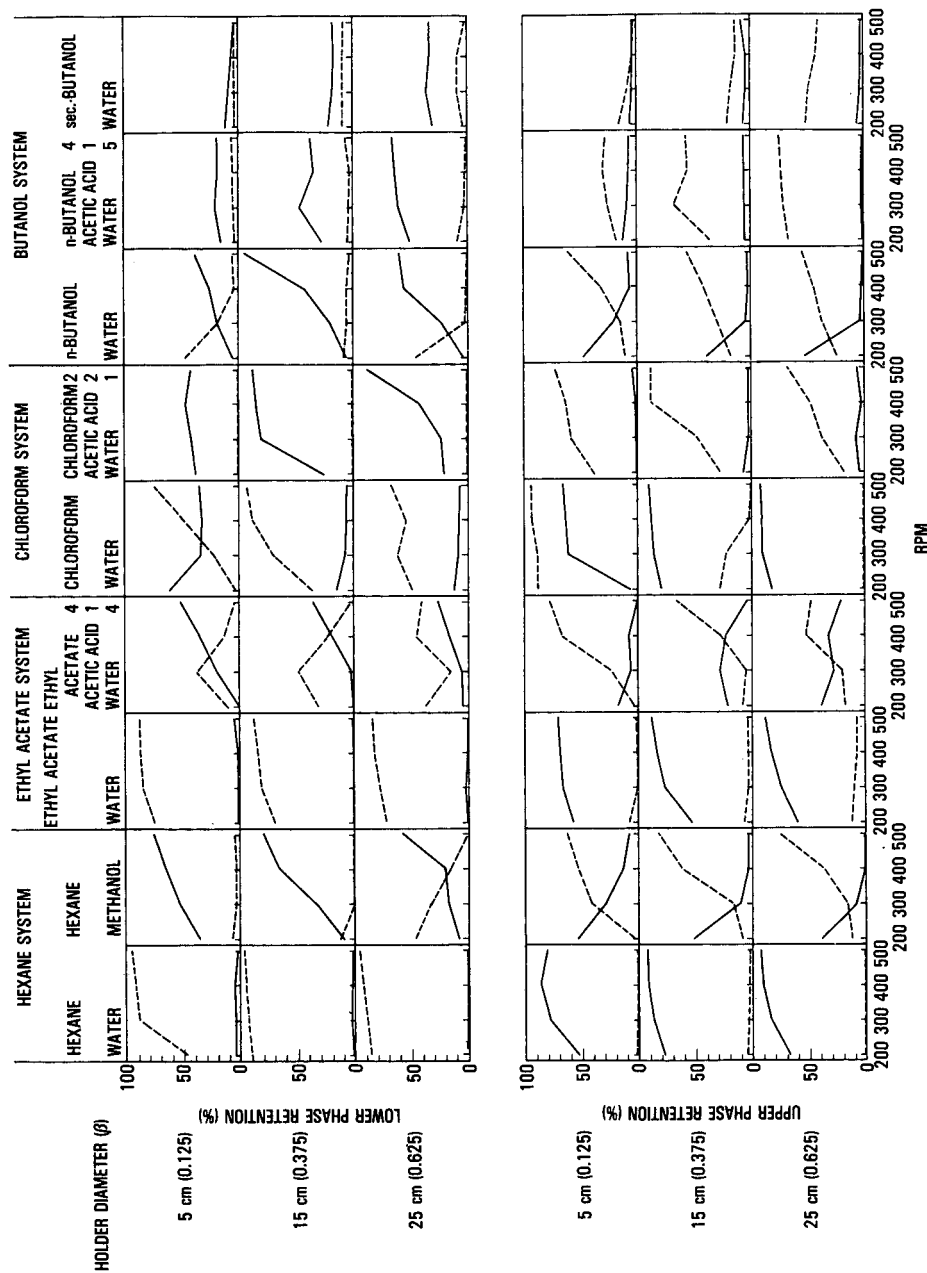


Fig. 3. A set of phase distribution diagrams for nine volatile solvent systems obtained from the central coil position ( $l = 0$  cm). See Table I for designs for phase distribution curves. (—) Head  $\rightarrow$  tail; (---) tail  $\rightarrow$  head.

retention of the upper phase by elution with the lower phase, and within each mobile phase group the first row was obtained with the 5-cm diameter coil or at  $\beta = 0.125$ , the second row with the 15-cm diameter coil or at  $\beta = 0.375$  and the third row with the 25-cm diameter coil or at  $\beta = 0.625$ . As defined previously<sup>1</sup> and shown in Fig. 1,  $\beta$  is the ratio between the radius of rotation (distance from the central axis of the holder to the coil) and the radius of revolution (distance from the central axis of the centrifuge to the axis of the holder). This determines both the magnitude and direction of the centrifugal force field acting on the various locations of the holder. Two retention curves in each diagram were obtained from each elution mode: the solid curve indicates the head-to-tail elution and the broken curve the tail-to-head elution.

Phase distribution diagrams obtained from the central coil position in this study share common features with those from the original X-axis CPC with a 10-cm revolutionary radius and may be similarly divided into three categories according to hydrophobicity or polarity of the solvent system.

Hydrophobic binary solvent systems characterized by high interfacial tension between the two phases, including hexane–water, ethyl acetate–water and chloroform–water, show high retention when the upper phase is eluted from the tail toward the head (broken curves in the upper column) or the lower phase from the head toward the tail (solid curves in the lower column). On the other hand, hydrophilic solvent systems associated with low interfacial tension, such as *n*-butanol–acetic acid–water (4:1:5) and *sec.*-butanol–water, display an opposite hydrodynamic trend, giving better retention by eluting either the upper phase from the head toward the tail (solid curves in the upper column) or the lower phase from the tail toward the head (broken curves in the lower column). The rest of the solvent systems with intermediate degrees of hydrophobicity generally show a hydrodynamic trend similar to that of the hydrophilic solvent systems but mostly yield a much higher retention level. In both hydrophilic and intermediate solvent systems, the retention is sensitively affected by the  $\beta$  values. In the hydrophilic solvent group the retention is substantially improved at greater  $\beta$  values whereas retention of the intermediate solvent systems changes with the  $\beta$  values in various ways. Hexane–methanol is more highly retained at small  $\beta$  values whereas chloroform–acetic acid–water (2:2:1) shows the highest retention at the moderate  $\beta$  value of 0.375.

The overall results obtained with the central coil position indicate that, compared with the original X-axis CPC operated at 200–800 rpm, the present system yields a lower retention for intermediate solvent systems but a substantially improved retention of hydrophilic solvent systems at large  $\beta$  values.

#### *Phase distribution diagrams obtained from lateral coil position ( $l = -10$ cm)*

A set of phase distribution diagrams obtained from the coil mounted 10 cm to the left of the center of the holder is illustrated in Fig. 4 with the same format as used in Fig. 3.

As mentioned earlier, the coil mounted at a lateral location is subjected to an asymmetric lateral force field between the upper and lower halves of the rotating holder, thus causing different levels of retention according to the combination of direction of the planetary motion and elution modes of the mobile phase. The possible combinations are summarized in Table II. As defined in the table, planetary motion  $P_I$  is identical with the motion of the disc shown in Fig. 1, and  $P_{II}$  is the reversed motion

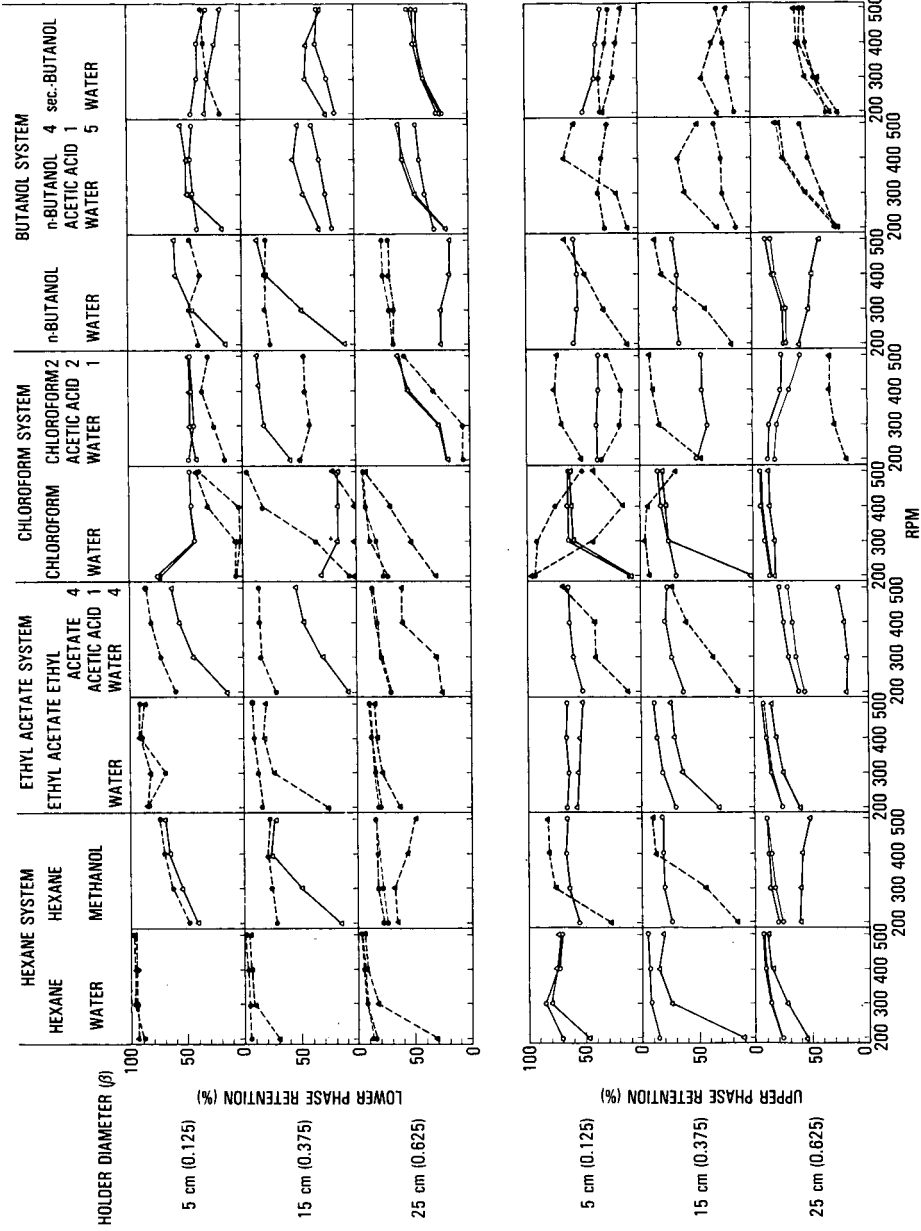


Fig. 4. A set of phase distribution diagrams for nine volatile solvent systems obtained for the lateral coil position ( $l = 10$  cm). See Table II for symbols of phase distribution curves.

resulting in both rotation and revolution of the holder being reversed. In each planetary motion, the mobile phase can be eluted in either the head-to-tail or the tail-to-head mode, thus yielding four different combinations. For each of these four combinations, there is a choice of elution in either the inward or outward direction, which requires the use of both right-handed and left-handed coils. Consequently, a total of eight experimental conditions are possible for each solvent system. Table II shows a set of symbolic designs which were used to distinguish phase distribution curves obtained from different experimental conditions.

All these combinations were first examined with the 25-cm diameter holder ( $\beta = 0.625$ ) at 500 rpm (Table III) and among those the three combinations with the best retention were further tested at various revolutional speeds to draw phase distribution curves as shown in Fig. 4 (bottom row in each mobile phase group). These data clearly indicated that the choice of inward-outward elution modes has little effect on the retention. This is seen by the small difference in the heavy and light lines connecting the same symbols. Therefore, the remainder of the studies on the 15- and 5-cm diameter holders were performed exclusively with the right-handed coils to investigate the effects of the two other parameters, *i.e.*, the planetary motion and the head-tail elution mode. All four combinations possible with the right-handed coils were tested at 500 rpm and two or more combinations which produced significant retention values were further studied at lower rpm to obtain the remaining phase distribution curves (Fig. 4).

The overall results of the retention studies on the lateral coil position revealed a considerable improvement in retention over those obtained with the central coil position for almost all solvent systems. Intermediate solvent systems such as hexane-methanol, ethyl acetate-acetic acid-water (4:1:4) and *n*-butanol-water produced excellent retention for all  $\beta$  values with the proper elution mode. A great improvement in retention was also observed in hydrophilic solvent systems which are extremely useful for separations of polar compounds. The retention of *n*-butanol-acetic acid-water (4:1:5) exceeded the 50% level for all  $\beta$  values while that of *sec.*-butanol-water reached 50% at  $\beta = 0.625$ . Although chloroform-containing solvent systems failed to show substantial improvements in retention, they gave satisfactory retention between  $\beta$  values of 0.375 and 0.625, with the highest retention at  $\beta \approx 0.375$ . The foregoing results clearly indicate that the lateral coil position permits satisfactory retention of the stationary phase in all the solvent systems examined, provided that the proper combination of planetary motion and head-tail elution mode is chosen.

Retention data obtained with the two coil positions on each holder can be more conveniently compared in each mobile phase if expressed in a single diagram as shown in Fig. 5A-C. In each diagram, the abscissa indicates the retention values obtained at the central coil position at 500 rpm and the ordinate, those obtained at the lateral coil position under otherwise identical experimental conditions. Each data point is marked with a specific symbol assigned for the applied experimental condition (planetary motion and head-tail elution mode) as indicated in Table II (see also the caption to Fig. 5). In order to specify the applied solvent systems, these points are individually labelled 1-9, each number corresponding to a particular two-phase solvent system as specified in the figure caption.

A diagonal drawn in each diagram divides the whole area into two equal parts;

TABLE III

RETENTION (%) OF STATIONARY PHASE IN A COIL POSITIONED Laterally ON THE 25-cm DIAMETER HOLDER AT 500 rpm

Mobile phase	Solvent system*							
	Hexane-water		Hexane-methanol		EtOAc-water		EtOAc-AcOH-water (4:1:4)	
	Condition**	%	Condition	%	Condition	%	Condition	%
Upper	$P_I$ -T-O	97.2	$P_I$ -T-I	85.0	$P_I$ -T-O	91.0	$P_I$ -T-I	87.0
	$P_I$ -T-I	96.9	$P_I$ -T-O	83.1	$P_I$ -T-I	89.8	$P_I$ -T-O	86.4
	$P_{II}$ -T-O	94.4	$P_{II}$ -T-I	74.3	$P_{II}$ -T-I	85.9	$P_{II}$ -T-I	74.6
	$P_{II}$ -T-I	94.4	$P_{II}$ -T-O	49.2	$P_{II}$ -T-O	85.3	$P_{II}$ -T-O	61.6
	$P_I$ -H-O	1.7	$P_{II}$ -H-I	27.1	$P_I$ -H-O	2.3	$P_{II}$ -H-I	20.9
	$P_I$ -H-I	1.7	$P_{II}$ -H-O	20.9	$P_I$ -H-I	1.7	$P_{II}$ -H-O	18.4
	$P_{II}$ -H-O	1.7	$P_I$ -H-O	6.2	$P_{II}$ -H-I	1.7	$P_I$ -H-O	7.9
	$P_{II}$ -H-I	0.6	$P_I$ -H-I	0.8	$P_{II}$ -H-O	0.6	$P_I$ -H-I	5.1
Lower	$P_I$ -H-O	94.4	$P_I$ -H-I	89.8	$P_I$ -H-I	93.5	$P_I$ -H-I	78.5
	$P_I$ -H-I	93.5	$P_I$ -H-O	89.3	$P_I$ -H-O	92.1	$P_I$ -H-O	70.6
	$P_{II}$ -H-I	90.1	$P_{II}$ -H-O	56.5	$P_{II}$ -H-O	87.3	$P_{II}$ -H-O	45.2
	$P_{II}$ -H-O	89.8	$P_{II}$ -H-I	51.4	$P_{II}$ -H-I	85.3	$P_{II}$ -H-I	27.1
	$P_{II}$ -T-O	2.8	$P_{II}$ -T-O	17.5	$P_{II}$ -T-I	9.3	$P_{II}$ -T-O	14.7
	$P_I$ -T-I	2.3	$P_I$ -T-I	16.9	$P_{II}$ -T-O	8.5	$P_{II}$ -T-I	11.0
	$P_{II}$ -T-I	2.0	$P_{II}$ -T-I	13.3	$P_I$ -T-O	6.8	$P_I$ -T-O	7.9
	$P_I$ -T-O	2.0	$P_I$ -T-O	9.0	$P_I$ -T-I	5.6	$P_I$ -T-I	5.6

\* EtOAc = ethyl acetate; AcOH = acetic acid; CHCl<sub>3</sub> = chloroform; BuOH = butanol.

\*\* Elution mode as described in Table II.

the area above the line indicates the improved retention for the lateral position and that below the line lowered retention. The longer the distance of a point from the diagonal, the greater is the effect on retention. The diagram is also divided evenly into four small squares by thin lines, each square having a specific implication: the upper left and lower right squares represent satisfactory retention of over 50% in the lateral coil ( $l = -10$  cm) and in the centered coil ( $l = 0$  cm), respectively, while the upper right square provides satisfactory retention for both coils and the lower left square unsatisfactory retention for either coil. Further, if the upper right square contains two different symbols with the same shading and the same number, satisfactory retention is provided in the coil mounted throughout the width of the holder ( $-10$  cm  $< l < 10$  cm), whereas if the same is observed in the upper left square, satisfactory retention is limited to both left and right lateral positions excluding the central part of the holder ( $l = -10$  cm and 10 cm).

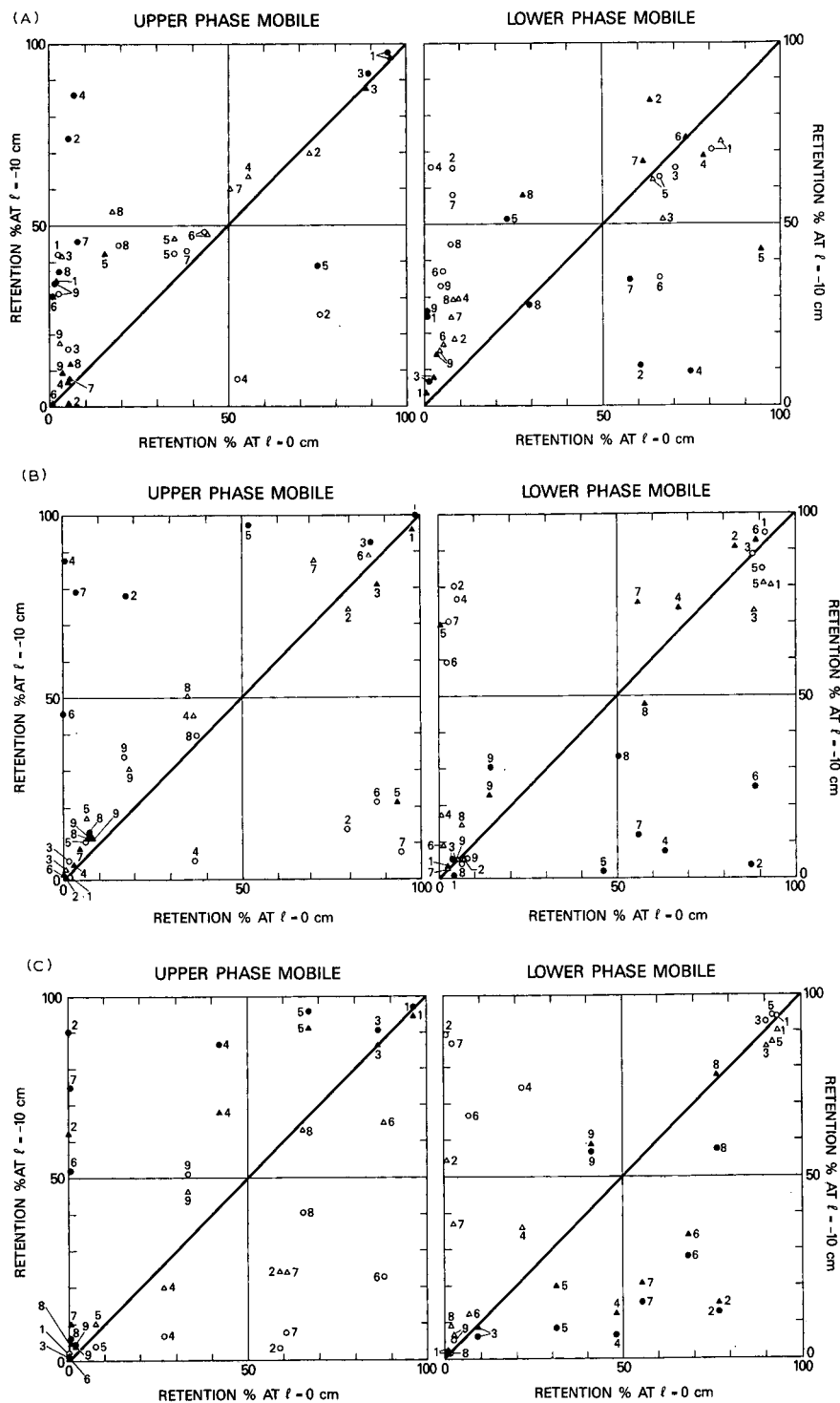
While the above indication for applicability of the coil positions can also be extracted from Figs. 3 and 4 and Table III without much difficulty, these diagrams further furnish invaluable information by disclosing a peculiar hydrodynamic effect associated with the lateral coil position. For example, in Fig. 5B ( $\beta = 0.375$ ) solid circles (tail-to-head elution under planetary motion,  $P_I$ ) and open triangles (head-to-tail elution under planetary motion  $P_{II}$ ) dominate above the diagonal if the upper phase is mobile (left), whereas open circles (head-to-tail elution under planetary

<i>CHCl<sub>3</sub>-water</i>		<i>CHCl<sub>3</sub>-AcOH-water (2:2:1)</i>		<i>n-BuOH-water</i>		<i>n-BuOH-AcOH-water (4:1:5)</i>		<i>sec.-BuOH-water</i>	
Condition	%	Condition	%	Condition	%	Condition	%	Condition	%
<i>P<sub>I</sub></i> -T-I	96.0	<i>P<sub>II</sub></i> -H-I	65.0	<i>P<sub>I</sub></i> -T-I	77.4	<i>P<sub>II</sub></i> -H-I	64.1	<i>P<sub>I</sub></i> -H-O	52.5
<i>P<sub>I</sub></i> -T-O	95.5	<i>P<sub>II</sub></i> -H-O	64.4	<i>P<sub>I</sub></i> -T-O	71.5	<i>P<sub>II</sub></i> -H-O	62.1	<i>P<sub>I</sub></i> -H-I	49.2
<i>P<sub>II</sub></i> -T-O	94.4	<i>P<sub>I</sub></i> -T-I	57.3	<i>P<sub>II</sub></i> -H-O	30.2	<i>P<sub>I</sub></i> -H-O	46.9	<i>P<sub>II</sub></i> -H-O	47.5
<i>P<sub>II</sub></i> -T-I	87.6	<i>P<sub>I</sub></i> -T-O	46.6	<i>P<sub>II</sub></i> -H-I	17.8	<i>P<sub>I</sub></i> -H-I	33.7	<i>P<sub>II</sub></i> -H-I	45.8
<i>P<sub>II</sub></i> -H-O	10.2	<i>P<sub>I</sub></i> -H-O	24.3	<i>P<sub>II</sub></i> -T-I	10.2	<i>P<sub>II</sub></i> -T-I	7.6	<i>P<sub>I</sub></i> -T-O	8.2
<i>P<sub>II</sub></i> -H-I	9.6	<i>P<sub>I</sub></i> -H-I	21.5	<i>P<sub>II</sub></i> -T-O	9.0	<i>P<sub>I</sub></i> -T-I	7.3	<i>P<sub>II</sub></i> -T-O	6.2
<i>P<sub>I</sub></i> -H-O	3.9	<i>P<sub>II</sub></i> -T-I	0	<i>P<sub>I</sub></i> -H-O	8.0	<i>P<sub>I</sub></i> -T-O	4.5	<i>P<sub>II</sub></i> -T-I	0.8
<i>P<sub>I</sub></i> -H-I	3.4	<i>P<sub>II</sub></i> -T-O	0	<i>P<sub>I</sub></i> -H-I	7.3	<i>P<sub>II</sub></i> -T-O	1.1	<i>P<sub>I</sub></i> -T-I	0.6
<i>P<sub>I</sub></i> -H-O	94.9	<i>P<sub>I</sub></i> -H-I	74.9	<i>P<sub>I</sub></i> -H-I	88.7	<i>P<sub>II</sub></i> -T-O	78.5	<i>P<sub>II</sub></i> -T-I	61.6
<i>P<sub>I</sub></i> -H-I	93.8	<i>P<sub>I</sub></i> -H-O	58.2	<i>P<sub>I</sub></i> -H-O	84.7	<i>P<sub>II</sub></i> -T-I	75.7	<i>P<sub>I</sub></i> -T-O	58.2
<i>P<sub>II</sub></i> -H-O	87.0	<i>P<sub>II</sub></i> -T-I	35.0	<i>P<sub>II</sub></i> -H-I	40.7	<i>P<sub>I</sub></i> -T-I	58.2	<i>P<sub>II</sub></i> -T-O	56.5
<i>P<sub>II</sub></i> -H-I	87.0	<i>P<sub>II</sub></i> -T-O	33.1	<i>P<sub>II</sub></i> -H-O	33.3	<i>P<sub>I</sub></i> -T-O	57.1	<i>P<sub>I</sub></i> -T-I	55.9
<i>P<sub>II</sub></i> -T-I	22.6	<i>P<sub>I</sub></i> -T-O	32.2	<i>P<sub>II</sub></i> -T-I	25.4	<i>P<sub>II</sub></i> -H-I	10.7	<i>P<sub>II</sub></i> -H-I	8.5
<i>P<sub>II</sub></i> -T-O	17.7	<i>P<sub>I</sub></i> -T-I	24.3	<i>P<sub>II</sub></i> -T-O	16.9	<i>P<sub>II</sub></i> -H-O	7.3	<i>P<sub>I</sub></i> -H-I	6.8
<i>P<sub>I</sub></i> -T-I	10.2	<i>P<sub>II</sub></i> -H-I	14.7	<i>P<sub>I</sub></i> -T-O	16.1	<i>P<sub>I</sub></i> -H-I	2.0	<i>P<sub>II</sub></i> -H-O	5.1
<i>P<sub>I</sub></i> -T-O	6.8	<i>P<sub>II</sub></i> -H-O	10.1	<i>P<sub>I</sub></i> -T-I	15.3	<i>P<sub>I</sub></i> -H-O	1.7	<i>P<sub>I</sub></i> -H-O	3.9

motion  $P_I$ ) and solid triangles (tail-to-head elution under planetary motion  $P_{II}$ ) dominate above the diagonal if the lower phase is mobile (right). These findings strongly suggest that the direction of the planetary motion is in some way closely related to the head-tail elution mode to govern the hydrodynamics in the lateral coil position, thus providing an important clue for speculation on the hydrodynamic mechanism associated with the X-axis CPC as discussed below.

#### *Hydrodynamic effect of the lateral coil shift: a hypothesis*

As described earlier, lateral shift or replacement of the coil results in a considerable improvement in retention of the stationary phase in almost all of the solvent systems examined. In order to explain this phenomenon, we must first consider the centrifugal force field generated by the planetary motion of the holder previously analysed<sup>1</sup>. Fig. 6 shows the distribution of the centrifugal force vectors acting on the rotating holder at various  $\beta$  values in both central ( $l = 0$  cm) (right) and lateral ( $l = -10$  cm) (left) coil positions. In each diagram,  $O_b$  is on the central axis of the holder and the axis of the centrifuge is shown as a vertical line tangent to the outermost circle labelled  $\beta = 1.0$  on the left side of each diagram. The centrifugal force acting on various points of the holder is divided into two components, *i.e.*, arrows for the main force vectors acting in the  $X_b$ - $Y_b$  plane and the thick columns for the secondary force vectors acting perpendicularly to the  $X_b$ - $Y_b$  plane, where the ascending columns



indicate the force vectors directed above the plane and the descending columns the force vectors acting below the plane. As clearly shown in these diagrams, the lateral shift of the point along the axis of the holder develops an asymmetric lateral force field (columns) between the upper and the lower halves of the holder, while the main centrifugal force field acting across the axis of the holder remains unaltered.

Both the enhanced retention of the stationary phase in the lateral coil position and the close correlation between the planetary motion and the head-tail elution mode observed in Fig. 5 may be explained on the basis of this asymmetry of the laterally acting force field.

Fig. 7 illustrates coils at the lateral position on the holder undergoing planetary motion  $P_I$  (left) and planetary motion  $P_{II}$  (right). Because rotation and revolution are simultaneously reversed, these two planetary motions produce the identical force field while reversed rotation of the holder causes reversal of the head-tail orientation of the coil. Under the main centrifugal force field directed radially toward the right as indicated by a large arrow, the upper (lighter) phase is driven toward the left and the lower (heavier) phase toward the right in major portions of the coil.

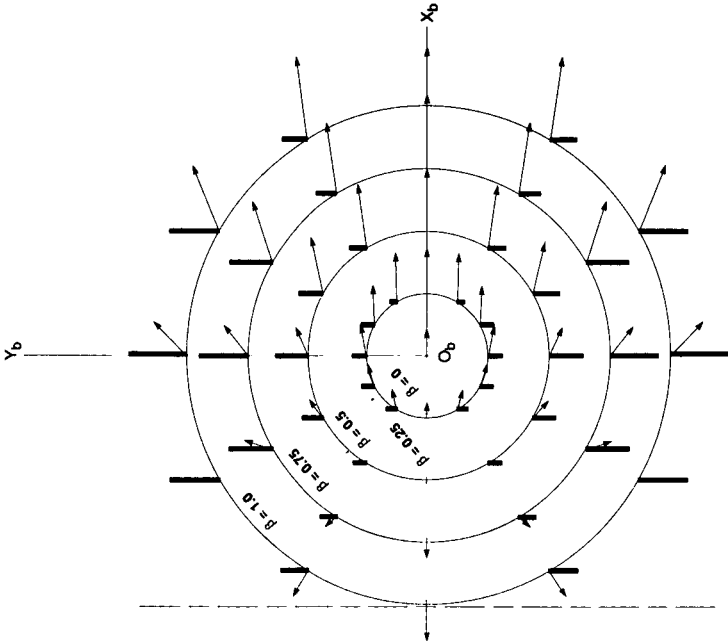
In Fig. 7 (left), planetary motion  $P_I$  determines the coil rotation, hence the head-tail orientation of the coil as indicated by a pair of curved arrows at the top and the bottom of the diagram. Owing to the asymmetric lateral force field between the upper and lower halves of the coil, the countercurrent movement of the two solvent phases is accelerated in the upper portion of the coil owing to suppressed emulsification while the movement is decelerated in the lower portion of the coil owing to enhanced emulsification. Consequently, in this situation the tail-to-head elution of the upper phase (solid circles in Fig. 5B, left) and the head-to-tail elution of the lower phase (open circles in Fig. 5B, right) result in enhanced retention of the stationary phase.

In Fig. 7 (right), planetary motion  $P_{II}$  reverses both the rotation and the head-tail orientation of the coil as illustrated. Owing to the asymmetric lateral force field left unaltered, the countercurrent movement of the two solvent phases is similarly accelerated on the upper portion of the coil and decelerated in the lower portion of the coil. Therefore, in this case the head-to-tail elution of the upper phase (open triangles in Fig. 5B, left) and the tail-to-head elution of the lower phase (solid triangles in Fig. 5B, right) result in enhanced retention of the stationary phase.

In the 25-cm diameter holder ( $\beta = 0.625$ ), the hydrodynamic effects on the lateral coil position are substantially modified, as observed in Fig. 5C, where solid symbols dominate above the diagonal in the left diagram (enhanced tail-to-head movement of the upper phase) and open symbols dominate above the diagonal in the right diagram (enhanced head-to-tail movement of the lower phase). This may be caused by the lateral force field acting on the proximal and distal portions of the coil to alter hydrodynamic trends of the two solvent phases to promote tail-to-head movement of the upper phase and head-to-tail movement of the lower phase, as briefly

Fig. 5. Comparison of retention between the central and lateral coil positions. (A) 5-cm hub diameter; (B) 15-cm hub diameter; (C) 25-cm hub diameter. Symbols:  $\circ$ , planetary motion  $P_I$ , head-to-tail elution mode;  $\bullet$ , planetary motion  $P_I$ , tail-to-head elution mode;  $\triangle$ , planetary motion  $P_{II}$ , head-to-tail elution mode;  $\blacktriangle$ , planetary motion  $P_{II}$ , tail-to-head elution mode. Solvent systems: 1 = hexane-water; 2 = hexane-methanol; 3 = ethyl acetate-water; 4 = ethyl acetate-acetic acid-water (4:1:4); 5 = chloroform-water; 6 = chloroform-acetic acid-water (2:2:1); 7 = *n*-butanol-water; 8 = *n*-butanol-acetic acid-water (4:1:5); 9 = *sec.*-butanol-water.

FORCE DISTRIBUTION AT CENTRAL COIL POSITION  
( $l = 0$  cm)



FORCE DISTRIBUTION AT LATERAL COIL POSITION  
( $l = -10$  cm)

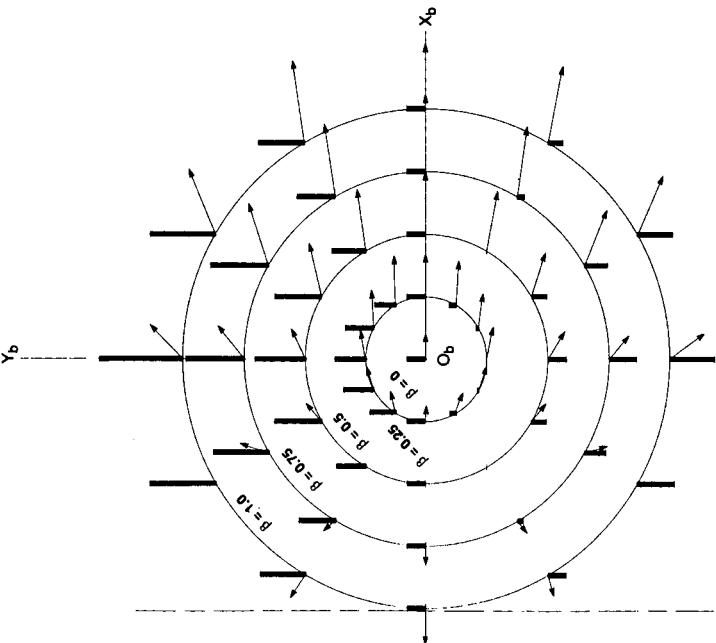


Fig. 6. Force distribution diagrams at two locations of the coil on the holder in the cross-axis synchronous flow-through coil planet centrifuge. Right, central position ( $l = 0$  cm); left, lateral position ( $l = -10$  cm).

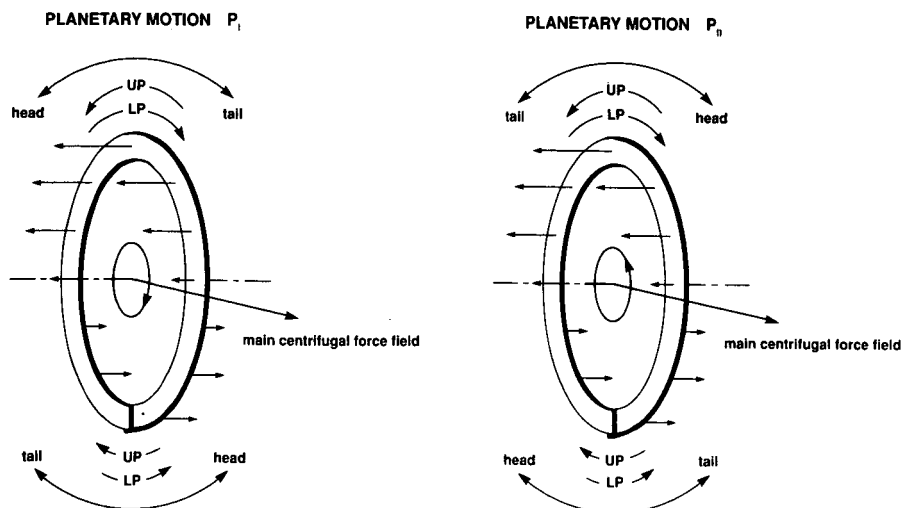


Fig. 7. Hydrodynamic effects of the asymmetric lateral force field formed at the lateral coil position ( $l = -10$  cm). Left, planetary motion  $P_I$ ; right, planetary motion  $P_{II}$ . UP, upper (lighter) phase; LP, lower (heavier) phase.

suggested elsewhere<sup>5</sup>. On a large diameter holder, this effect may overcome that of the asymmetric lateral force field acting on the upper and lower sides of the coil. The latter effects, however, are still evident within each elution mode, *i.e.*, a solid circle always locates above the solid triangle in Fig. 5C (left) and an open triangle above the open circle in Fig. 5C (right) for each solvent system.

#### ACKNOWLEDGEMENT

The authors are deeply indebted to Mr. Jimmie L. Slemph, Division of Research Services, Biomedical Engineering and Instrumental Branch, National Institutes of Health, for fabrication of the apparatus.

#### REFERENCES

- 1 Y. Ito, *Sep. Sci. Technol.*, 22 (1987) 1971.
- 2 Y. Ito, *Sep. Sci. Technol.*, 22 (1987) 1989.
- 3 Y. Ito, J. Sandlin and W. G. Bowers, *J. Chromatogr.*, 244 (1982) 247.
- 4 Y. Ito, *J. Chromatogr.*, 403 (1987) 77.
- 5 Y. Ito, *J. Liq. Chromatogr.*, 11 (1988) 1.



CHROM. 20 670

## CROSS-AXIS SYNCHRONOUS FLOW-THROUGH COIL PLANET CENTRIFUGE FOR LARGE-SCALE PREPARATIVE COUNTER-CURRENT CHROMATOGRAPHY

### II\*. STUDIES ON PARTITION EFFICIENCY IN SHORT COILS AND PREPARATIVE SEPARATIONS WITH MULTILAYER COILS

YOICHIRO ITO\* and TIAN-YOU ZHANG\*\*

*Laboratory of Technical Development, National Heart, Lung, and Blood Institute, Bethesda, MD 20892 (U.S.A.)*

(First received March 14th, 1988; revised manuscript received May 26th, 1988)

---

#### SUMMARY

A series of experiments was conducted to evaluate the partition efficiency of the cross-axis synchronous flow-through coil planet centrifuge. The preliminary studies indicated that short coils (5 m) mounted on 15- and 25-cm diameter holders in either a central or a lateral location produce a high partition efficiency of over 100 theoretical plates. Under the optimum operating conditions, the preparative capability of the countercurrent chromatograph was demonstrated on gram-scale separations of DNP-amino acids and dipeptides in a pair of multilayer coils connected in series with a total capacity of 1600 ml.

---

#### INTRODUCTION

Successful separation in counter-current chromatography (CCC) mainly depends on two parameters, retention of the stationary phase in the separation column and partition efficiency<sup>1</sup>. Studies on stationary phase retention described in Part I have shown that the present CCC scheme yields satisfactory levels of retention for various two-phase solvent systems and that the retention can be improved by choosing lateral coil positions on the holder. This second series of experiments was performed to investigate the partition efficiency of the coiled column using the operating conditions which have produced significant levels of stationary phase retention.

This paper describes the results of partition efficiency studies using two sets of standard test samples and two-phase solvent systems: DNP (dinitrophenyl) amino acid separation in chloroform–acetic acid–0.1 *M* hydrochloric acid (2:2:1) and dipeptide separation in *n*-butanol–acetic acid–water (4:1:5). Preliminary studies were performed

---

\* For Part I, see *J. Chromatogr.*, 449 (1988) 135.

\*\* Permanent address: Beijing Institute of New Technology Application, Beijing, China.

with single-layer coils (5 m) mounted on a set of holders with various hub diameters each at central and lateral positions as in the previous studies on retention of the stationary phase (Part I). The preparative capability of the method was demonstrated by the separation of gram amounts of samples in a pair of long multilayer coils connected in series (total volume of 1600 ml) and mounted symmetrically on both sides of the rotary frame of the centrifuge.

## EXPERIMENTAL

### *Apparatus*

The design of the apparatus was described in detail in Part I. This second prototype cross-axis synchronous flow-through coil planet centrifuge has a 20-cm revolutionary radius and can be rotated at up to 500 rpm, which produces about 56 *g* on the axis of the holder.

### *Separation columns*

Two different types of coiled columns were used for partition efficiency studies: single-layer short coils for preliminary or model studies and long multilayer coils for preparative separations.

Short coils were each prepared from 5 m of 2.6 mm I.D. PTFE tubing of approximately 28-ml capacity by winding it onto the holder hub (5-, 15- or 25-cm diameter), making a single layer coil. The number of helical turns varied according to the hub diameters: 6 turns for 25-cm hub diameter, 10 turns for 15-cm hub diameter and 30 turns for 5-cm hub diameter. As in Part I, the coil was mounted at two different locations on each holder, at the center ( $l = 0$  cm) and 10 cm to the left of the center ( $l = -10$  cm). At the side of the 5-cm diameter holder there was not enough space, so 5 m of tubing was wound in a double layer. Each coil was securely fixed on the holder hub with several pieces of fiber-glass reinforced adhesive tape. Each end of the coil was connected to a 1-m long flow tube of 0.85 mm I.D., using short pieces of intermediate-size PTFE tubing. These flow tubes were led to the outside of the centrifuge as described in Part I.

The multilayer coil was prepared from a long piece of 2.6 mm I.D. PTFE tubing by winding it onto a spool-shaped holder (15-cm hub diameter), making multiple coiled layers between a pair of flanges spaced 5 cm apart. The column consisted of 14 layers of coil with a total capacity of about 800 ml. The  $\beta$  value varied from 0.375 at the internal terminal to 0.625 at the external terminal. A pair of similar multilayer coils was symmetrically mounted, one on each side of the rotary frame, in either the central or lateral location on the holder shafts. These two columns were connected in series with a flow tube in such a way that the external terminal of the first column joins the internal terminal of the second column. In this way perfect balancing of the centrifuge system is ensured and the two columns are always subjected to an ideal elution mode. Fig. 1 shows the apparatus equipped with a pair of multilayer coils in the central position of the holder shafts. The columns can be shifted along the holder shaft to optimize the hydrodynamic conditions.

### *Reagents*

Solvents such as chloroform and *n*-butanol were of glass-distilled chromato-

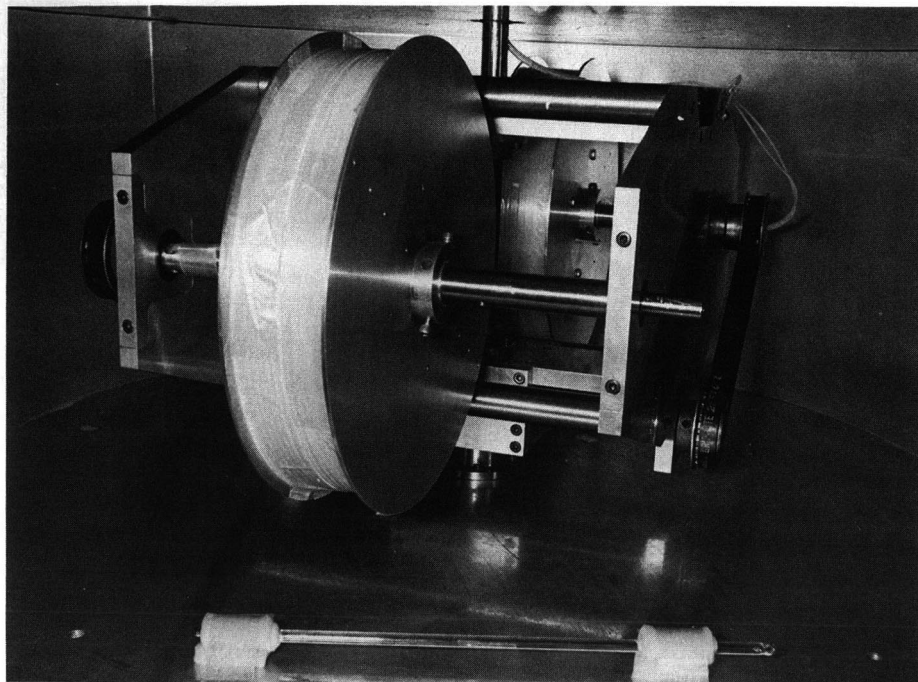


Fig. 1. The cross-axis synchronous flow-through coil planet centrifuge with 20-cm revolutionary radius equipped with a pair of large multilayer coil separation columns.

graphic grade (Burdick & Jackson Labs., Muskegon, MI, U.S.A.) and others, acetic acid and *n*-butanol for preparative separations, were of analytical-reagent grade (J. T. Baker, Phillipsburg, NJ, U.S.A.). Hydrochloric acid (1 *M*) and all test samples including L-valyl-L-tyrosine (Val-Tyr), L-tryptophyl-L-tyrosine (Trp-Tyr), N-2,4-dinitrophenyl-DL-glutamic acid (DNP-Glu) and N-2,4-dinitrophenyl-L-alanine (DNP-Ala) were obtained from Sigma (St. Louis, MO, U.S.A.).

#### *Preparation of two-phase solvent systems and sample solutions*

Two types of solvent systems were prepared: chloroform-acetic acid-0.1 *M* hydrochloric acid (2:2:1) for DNP-amino acid separations and *n*-butanol-acetic acid-water (4:1:5) for dipeptide separations. Each solvent system was thoroughly equilibrated in a separatory funnel at room temperature by repeated vigorous shaking and degassing several times. The samples were also dissolved in these solutions.

Sample solutions for DNP-amino acid separations were prepared as follows. For the preliminary studies with short coils, equal amounts of DNP-Glu and DNP-Ala were dissolved in the upper aqueous phase to make the concentration of each component 0.5% (w/v), and 0.2 ml of the sample solution was loaded in each experiment. For large-scale preparative chromatography in the multilayer coils, 2 or 5 g of the DNP-amino acids were dissolved in equal volumes of the upper and the lower phases to bring the total volume to 50 or 100 ml, respectively.

For the preliminary separations in short coils, the peptides were dissolved in the

lower aqueous phase to make concentrations of Val-Tyr and Trp-Tyr 1 and 0.3% (w/v), respectively, and 0.2 ml of this solution was used for each run. For the preparative separations in the multilayer coils, 1 g of Val-Tyr and 0.3 g of Trp-Tyr were dissolved in 100 ml of the solvent system.

For concentrated sample solutions used in preparative separations, the settling times of the two solvent phases were measured to ensure satisfactory retention of the stationary phase in the column<sup>2,3</sup>. A 2-ml volume of each phase of a sample solution was delivered into a 5-ml capacity graduated glass cylinder which was then sealed with a glass stopper. For each test, the cylinder was gently inverted five times to mix the contents and then placed in the upright position to measure the time required for the solvent mixture to form two distinct layers. The test was repeated several times to obtain the mean value.

#### *Preliminary separations with short coils*

As described in Part I, preliminary studies were performed with short coils mounted at the center ( $l = 0$ ) or to one side ( $l = -10$  cm) on three different holders (5-, 15- and 25-cm hub diameters).

For each separation, the coil was first entirely filled with the stationary phase followed by injection of the sample solution (0.2 ml) through the sample port. Then, the apparatus was run at a uniform revolutionary speed while the mobile phase was eluted through the coil at a flow-rate of 120 ml/h. The effluent from the outlet of the coil was monitored continuously with an LKB Uvicord S instrument at 278 nm and fractionated into test-tubes with an LKB fraction collector. Each fraction containing 1 ml was diluted with 2 ml of methanol and the absorbance was determined at 430 nm (DNP-amino acids) or 280 nm (dipeptides) in a Zeiss PM6 spectrophotometer. The absorbance is plotted in Figs. 2, 3, 5, 6, etc. The experiments were performed by applying revolutionary speeds of 200, 300, 400 and 500 rpm using both the upper and the lower phases as the mobile phase. After each separation, the volume of the stationary phase retained in the coil was measured by collecting the column contents in a 50-ml graduated cylinder after connecting the coil inlet to a pressurized nitrogen line under slow rotation of the coil in the tail-to-head elution mode.

At the central coil position ( $l = 0$  cm), the above separations were performed for each mobile phase in a single elution mode of either head-to-tail or tail-to-head elution, whichever yielded the higher retention of the stationary phase as determined in the studies of Part I. With the lateral coil position ( $l = -10$  cm), where the retention of the stationary phase is affected by both the planetary motion and head-tail elution mode, separations were performed by selecting the suitable elution mode for each planetary motion ( $P_I$  and  $P_{II}$ ) for each choice of the mobile phase.

---

#### *Preparative separations with multilayer coils*

Using the optimal experimental conditions determined by preliminary separations, preparative-scale CCC separations were performed with a pair of multilayer coils symmetrically mounted one on each side of the centrifuge rotor at either the central or the lateral location on the holder shafts.

The preparative separations were carried out as follows. The entire column (a pair of multilayer coils connected in series) was first filled with the stationary phase. This was followed by injection of the sample solution through the sample port. Then,

the centrifuge was run at 400 or 450 rpm in the desired direction ( $P_I$  or  $P_{II}$ ) while the mobile phase was eluted through the column at a uniform flow-rate of 120 ml/h in the appropriate head-tail elution mode. The effluent from the outlet of the column was monitored continuously with an LKB Uvicord S instrument at 278 nm and collected in 15-ml fractions (7.5 min) in an LKB fraction collector. An aliquot of each fraction (20–50  $\mu$ l) was mixed with 3 ml of methanol and the absorbance was determined at 430 nm for the DNP-amino acids and 280 nm for the dipeptides in a Zeiss PM6 spectrophotometer.

After each separation was completed, the retention of the stationary phase was measured by collecting the column contents by pushing with pressurized nitrogen as described above.

#### *Determination of partition efficiency*

In both preliminary and preparative separations, the partition efficiency was measured in terms of theoretical plates from the elution profile of the sample peaks using the conventional gas chromatographic equation

$$N = (4R/w)^2 \quad (1)$$

where  $N$  is the partition efficiency expressed as the number of theoretical plates (T.P.),  $R$  the retention volume or time of the peak maximum, and  $w$  the peak width measured in the same unit as  $R$ .

The partition efficiency was also evaluated by the degree of resolution between the two peaks using the equation

$$R_\sigma = 2(R_2 - R_1)/(w_2 + w_1) \quad (2)$$

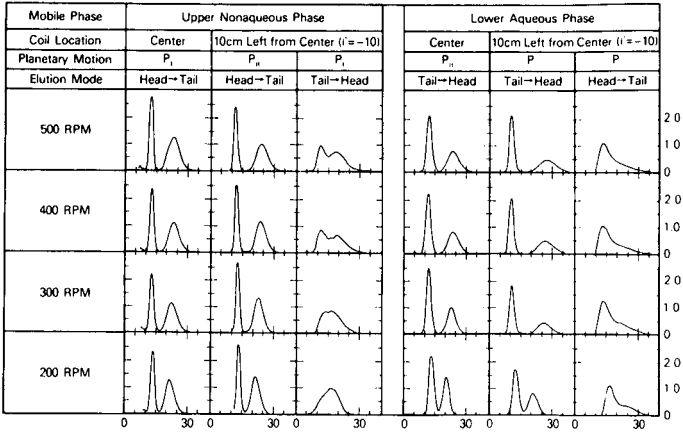
where  $R_\sigma$  is the peak resolution expressed in  $4\sigma$  units ( $\sigma$  is the standard deviation in a normal distribution),  $R_1$  and  $R_2$  the retention volumes or times of the first and second peaks, respectively, and  $w_1$  and  $w_2$  the peak widths for the first and second peaks, respectively, expressed in the same unit as retention  $R^4$ .

## RESULTS AND DISCUSSION

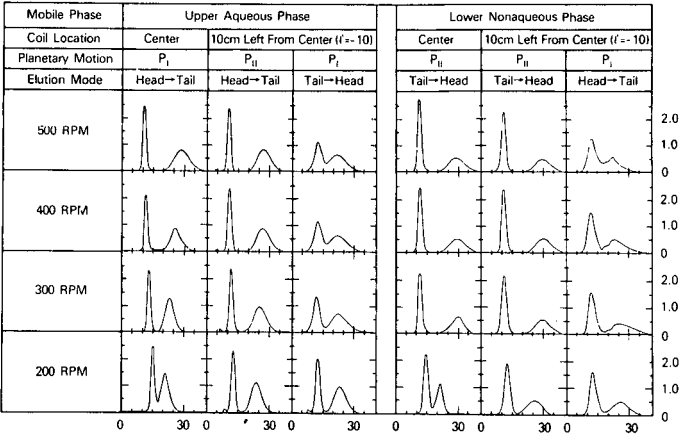
#### *Partition efficiency studies with short coils*

Fig. 2 shows three sets of chromatograms of DNP-amino acids (DNP-Glu and DNP-Ala) obtained with short coils mounted on the holders with hub diameters of 5 cm (top), 15 cm (middle) and 25 cm (bottom), each in the central and lateral positions on the holder. These separations were obtained under the optimal operating conditions, which were determined by preliminary studies on stationary phase retention as described in Part I. In each set of diagrams, the chromatographic charts are arranged according to the applied revolutionary speeds (rows) and elution mode (columns). The three left-hand columns were obtained with the upper aqueous phase mobile and the three right-hand columns with the lower non-aqueous phase mobile. For each mobile phase group, the results shown in the left column were obtained with the central coil position ( $l = 0$  cm) and those in the middle and right columns were

5 cm  
Diameter Holder  
( $\beta = 0.125$ )

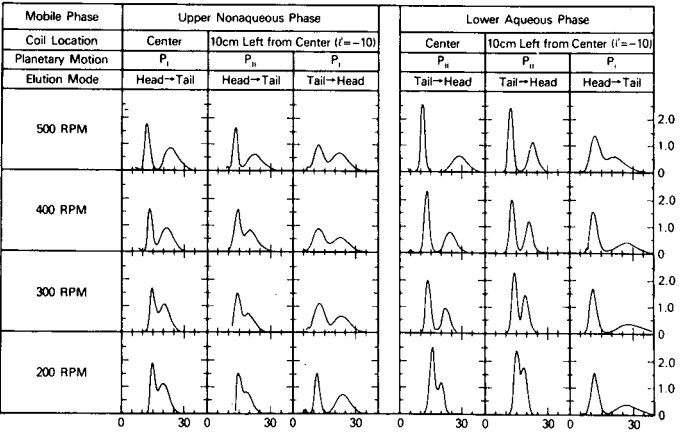


15 cm  
Diameter Holder  
( $\beta = 0.375$ )



Absorbance (430 nm)

25 cm  
Diameter Holder  
( $\beta = 0.625$ )



TIME (min)

Fig. 2. Results of DNP-amino acid separations with short coils. Solvent system, chloroform-acetic acid-0.1 M hydrochloric acid (2:2:1); sample size, 2 mg; flow-rate, 120 ml/h.

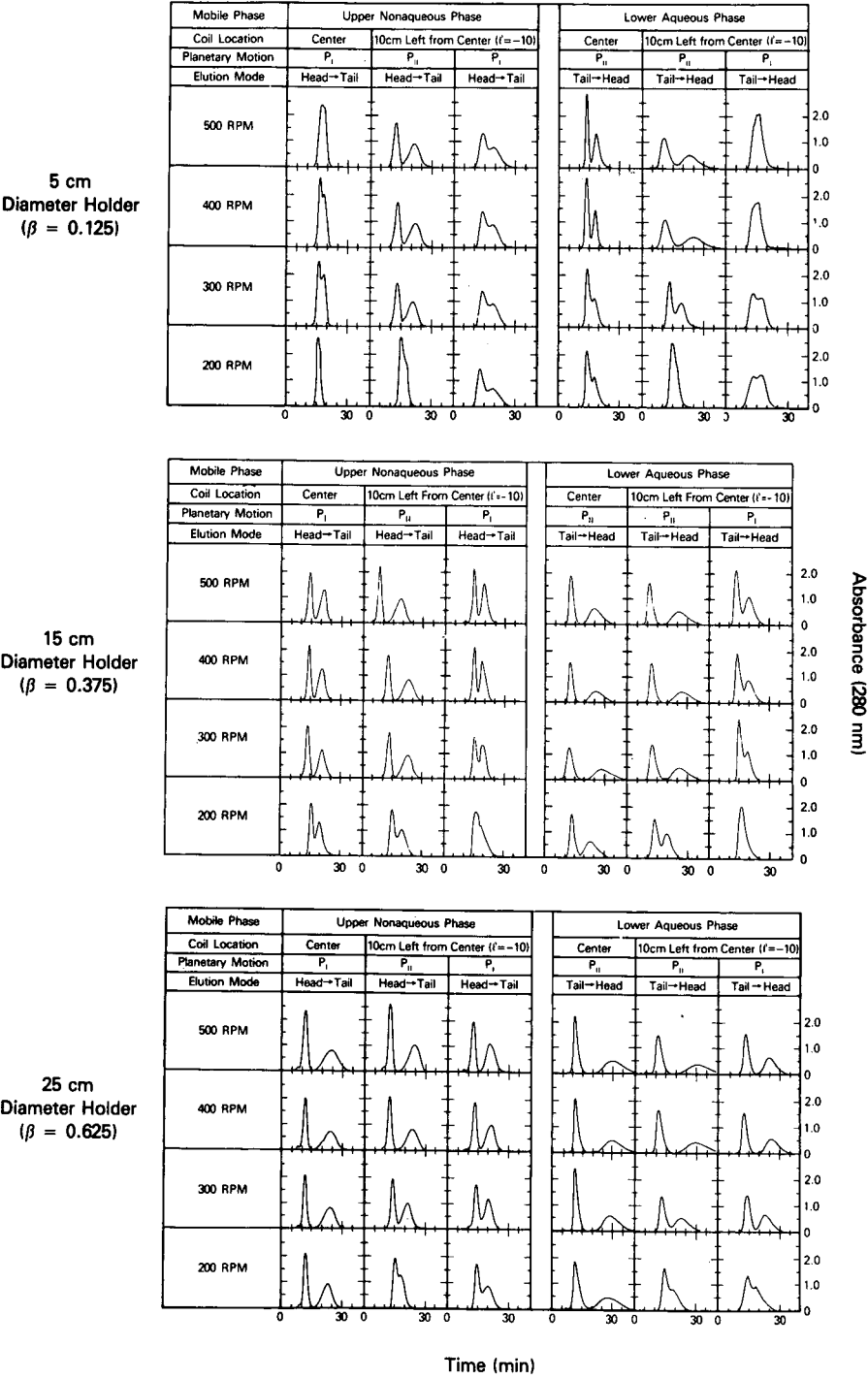


Fig. 3. Results of dipeptide separations with short coils. Solvent system, *n*-butanol–acetic acid–water (4:1:5); sample size, 2.6 mg; flow-rate, 120 ml/h.

obtained with the laterally positioned coil ( $l = -10$  cm), each using the indicated planetary motion and head-tail elution mode.

In Fig. 2 (top) (5-cm hub diameter,  $\beta = 0.125$ ) a good peak resolution is observed in both the central and lateral positions with head-to-tail elution of the upper phase or tail-to-head elution of the lower phase. Chromatograms obtained with the reversed elution mode in the lateral coil position ( $P_I$  planetary motion) show poor peak resolution despite the fair degree of stationary phase retention of over 40%. With one exception (right column, lower phase mobile), separations are substantially improved with an increased revolutionary speed of up to 400–500 rpm where, with both mobile phase groups, the lateral coil position gives a slightly higher peak resolution than the central coil position.

All the separations shown in the middle panel of Fig. 2 are considerably improved with the coil mounted on the 15-cm hub diameter ( $\beta = 0.375$ ), which coincides with a higher retention of the stationary phase [see the phase distribution diagrams for chloroform-acetic acid-water (2:2:1) in Figs. 3 and 4 in Part I]. In both central and lateral positions with the head-to-tail elution of the upper phase or the tail-to-head elution of the lower phase, two peaks were completely resolved at revolutionary speeds of 300 rpm or greater. Chromatograms obtained with the lateral coil position using the reversed elution mode ( $P_I$  planetary motion), which gives poor peak resolution at  $\beta = 0.125$ , yield fair degrees of peak resolution at the higher  $\beta$  value, especially at lower rpm. With the larger hub diameter of 25 cm ( $\beta = 0.625$ ), the peak resolutions of most chromatograms obtained with the head-to-tail elution mode (the left and the middle columns in each mobile phase group) are again decreased, apparently owing to depletion of the stationary phase retained in the coil.

Fig. 3 similarly shows separations of dipeptides (Val-Tyr and Trp-Tyr) using *n*-butanol-acetic acid-water (4:1:5) with short coils mounted on a set of holders with 5-cm (top), 15-cm (middle) and 25-cm (bottom) hub diameters at the central and lateral positions, with the same format as in Fig. 2. Because of the unique hydrodynamic distribution characteristic of this hydrophilic (or polar) solvent system, head-to-tail elution of the upper phase and tail-to-head elution of the lower phase were applied throughout the experiment. In the central coil position, the small  $\beta$  value of 0.125 (5-cm hub diameter) gives a poor peak resolution, apparently owing to the lower retention of the stationary phase, whereas the large  $\beta$  value of 0.625 (25-cm hub diameter) yields excellent peak resolution at revolutionary speeds ranging from 300 to 500 rpm. In the lateral coil position, the two modes of planetary motion ( $P_I$  and  $P_{II}$ ) produced different results. Chromatograms obtained under planetary motion  $P_{II}$  (middle column in each mobile phase group) show an excellent peak resolution, which substantially exceeds that obtained at the central coil position, whereas chromatograms obtained under planetary motion  $P_I$  (right column in each mobile phase group) show much lower peak resolution. These results are closely correlated with the retention level of the stationary phase (see Figs. 3 and 4 in Part I): the greater the retention of the stationary phase, the higher is the peak resolution. This finding strongly suggests that various other two-phase solvent systems, including the hydrophobic hexane and ethyl acetate systems and the hydrophilic *sec*-butanol system, will produce much more efficient separations in the lateral coil position than in the central position (compare Fig. 3 with Fig. 4 in Part I).

Fig. 4 illustrates the relationship between the percentage retention of the

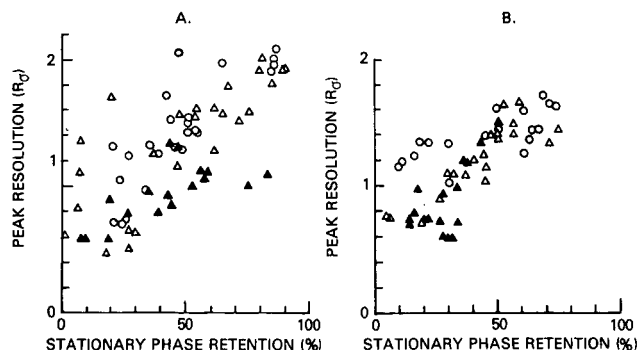


Fig. 4. Correlation between peak resolution and stationary phase retention. (A) DNP-amino acid separation; (B) dipeptide separation.  $\circ$ , Central coil position;  $\Delta$ , lateral coil position ( $P_{II}$ );  $\blacktriangle$ , lateral coil position ( $P_I$ ).

stationary phase and peak resolution  $R_D$  for (A) DNP-amino acid separations and (B) dipeptide separations. In both diagrams, circles indicate the data obtained with the central coil position (left columns in each mobile phase group in Fig. 2) and open and solid triangles the data obtained with the lateral coil position under the planetary motions  $P_{II}$  and  $P_I$ , respectively (middle and right columns in each mobile phase group in Fig. 2). All these groups show a significant positive correlation ( $r = 0.70$ – $0.86$ ) between the stationary phase retention and the resulting peak resolution. These figures may be an underestimation as unresolved peaks due to extensive loss of the stationary phase are all eliminated from the data.

Similar studies on the relationship between the stationary phase retention and partition efficiency (theoretical plates) revealed various degrees of negative correlation ranging from  $-0.7$  to  $-0.22$ . The above results clearly indicate that increased stationary phase retention in CCC will improve the peak resolution, while the number of theoretical plates may be a useful parameter for evaluating the performance of the preparative CCC systems only if the retention of the stationary phase remains in a normal range (over 50% of the total column capacity).

Partition efficiencies (mean T.P. values of two peaks) of DNP-amino acid separations obtained from the short coils under the optimal experimental conditions of over 50% stationary phase retention are about 100 T.P. or 5 cm/T.P. (one T.P. is produced by a 5-cm length of coil), which is comparable to the performance of the first prototype X-axis CPC with a 10-cm revolutionary radius as reported previously<sup>5</sup>. The above partition efficiency doubles those produced by the existing high-speed CCC apparatus<sup>6</sup> while the time required for the separation in the present method is also proportionally increased owing to the slower flow-rate necessary for the elution of the mobile phase to achieve a satisfactory level of stationary phase retention.

#### *Preparative separations with multilayer coils*

In order to demonstrate the preparative capability of the present system, gram-scale separations were performed on each set of test samples in a pair of multilayer coils connected in series (1600 ml capacity) using the optimal operational conditions determined in the preliminary studies with the short coils.

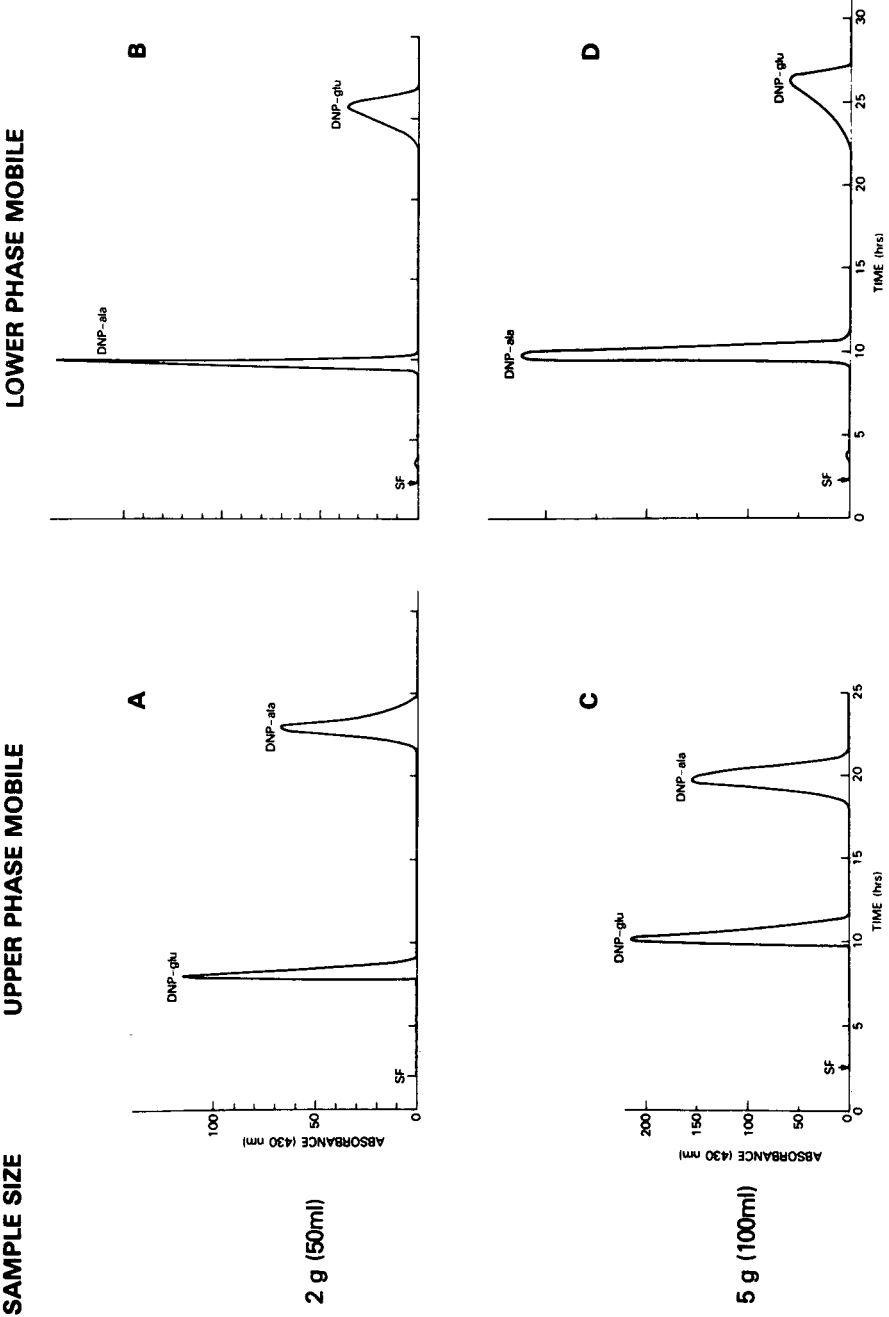


Fig. 5. Preparative chromatograms for DNP-amino acids. Coil position, center ( $l = 0$  cm); solvent system, chloroform-acetic acid-0.1 *M* hydrochloric acid (2:2:1); sample size, 2 and 5 g; flow-rate, 120 ml/h; revolution speed, 450 rpm. SF = Solvent front.

Fig. 5 shows preparative separations of the DNP-amino acid mixture in the central column position. Four chromatograms are arranged according to the sample size and the choice of the mobile phase as indicated. Samples of 2 and 5 g were separated at a flow-rate of 2 ml/min at 450 rpm using either the upper or lower phase as the mobile phase. In all chromatograms, DNP-Glu and DNP-Ala peaks are well resolved and eluted in 22–27 h. Owing to the non-linear isotherm produced by high sample concentrations, all peaks display various degrees of skewness, which is enhanced with the 5-g sample size especially for DNP-Glu with the lower phase mobile (Fig. 5, bottom right). The partition efficiency measured from the DNP-Ala peaks ranges from 2000–2700 T.P. for the 2-g sample to 1000–1250 T.P. for the 5-g sample. The above T.P.s are substantially lower than the estimated value of 5000 T.P. calculated from the results obtained on the short coils, apparently owing to the increased sample size. Separations of DNP-amino acids obtained with the lateral column position produced similar chromatograms.

Preparative separations of the dipeptide mixture (containing 1 g of Val-Tyr and 0.3 g of Trp-Tyr) were difficult, mainly for the following reasons. The high concentration of the dipeptide sample in the *n*-butanol solvent system raised the phase viscosity, as manifested by an increase in the settling time from 39 to 58 s, which in turn reduced the retention of the stationary phase. Further, a high sample concentration increased the non-linear isotherm, particularly for Trp-Tyr, which produced markedly skewed peaks with a considerable shift of the peak maximum. Under these circumstances, multilayer coils in the central column position failed to resolve two peaks when the upper phase was used as the mobile phase. However, chromatography in the lateral column position produced complete separation of the two peaks regardless of the choice of the mobile phase.

Fig. 6 shows chromatograms of the dipeptides obtained with the lateral column position by eluting with (A) the upper and (B) the lower phase mobile. The non-linear isotherm of Trp-Tyr produced skewed peaks deviating toward the Val-Tyr peaks. Compared with the DNP-amino acid separations shown in Fig. 5, these dipeptide

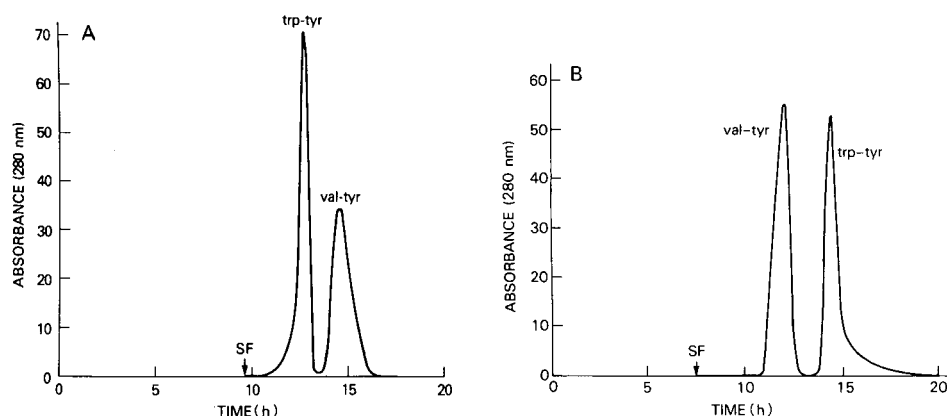


Fig. 6. Preparative chromatograms of dipeptides. Coil position, lateral ( $l = -10$  cm); solvent system, *n*-butanol-acetic acid-water (4:1:5); sample size, 1.3 g; flow-rate, 120 ml/h; revolution speed, 400 rpm. (A) Upper phase mobile; (B) lower phase mobile. SF = Solvent front.

separations show a much lower peak resolution, which resulted from extensive loss of the stationary phase from the column. The retention of the stationary phase in these dipeptide separations was 17% for the upper phase mobile and 26% for the lower phase mobile. Various problems associated with the use of hydrophilic solvent systems with low interfacial tension and high viscosity may be further alleviated by optimizing the location of the separation column. The results of these studies indicate that the retention of the hydrophilic butanol systems can be improved by increasing the  $\beta$  value and/or the distance of lateral deviation ( $\pm l$ ) of the multilayer coil.

#### REFERENCES

- 1 Y. Ito, *J. Biochem. Biophys. Methods*, 5 (1981) 105.
- 2 Y. Ito and W. D. Conway, *J. Chromatogr.*, 301 (1984) 405.
- 3 Y. Ito, *CRC Crit. Rev. Anal. Chem.*, 17 (1986) 65.
- 4 W. D. Conway and Y. Ito, *J. Liq. Chromatogr.*, 8 (1985) 2195.
- 5 Y. Ito, *Sep. Sci. Technol.*, 22 (1987) 1989.
- 6 Y. Ito, J. Sandlin and W. G. Bowers, *J. Chromatogr.*, 244 (1982) 247.

CHROM. 20 681

## SOLVENT EXTRACTION CLEAN-UP FOR PRE-TREATMENT IN AMINO ACID ANALYSIS BY GAS CHROMATOGRAPHY

### APPLICATION TO AGE ESTIMATION FROM THE D/L RATIO OF ASPARTIC ACID IN HUMAN DENTINE

IWAO ABE\*, HIDEAKI TSUJIOKA and TAMOTSU WASA

*College of Engineering, University of Osaka Prefecture, 4-804 Mozu-Umemachi, Sakai, Osaka (Japan)*

(Received May 19th, 1988)

---

#### SUMMARY

Solvent extraction, a clean-up method for samples for the determination of amino acids by gas chromatography, was investigated and compared with a conventional ion-exchange purification. Amino acids were esterified with isopropanol and extracted with various organic solvents. The solubilities of the amino acid isopropyl esters increased with increasing solvent polarity and the size of the amino acids. The optimum pH was found to be 10.5. The method was applied to the estimation of ages by measurement of the D/L ratio of aspartic acid in human dentine. The D/L ratios so determined were slightly lower than from the ion-exchange method with respect to all dentines examined. However, there were little or no significant differences in the ages estimated by both methods, and the correlation coefficient of this method was 0.982. The method is suitable for the enantiomeric analysis of amino acids, and has several advantages in the technique and time.

---

#### INTRODUCTION

Analysis of amino acids by gas chromatography (GC) is an universally accepted method for the determination of mixtures of biochemical, clinical, geological and other interest. The method complies with the demands for more precise, sensitive, automatic and inexpensive techniques.

In 1966, Gil-Av *et al.*<sup>1</sup> discovered an enantioselectivity in N-trifluoroacetyl (TFA)-L-isoleucine lauryl ester which when coated on a glass capillary enabled the resolution of enantiomeric alanine derivatives. After continuous development of this type of stationary phase for improvement of the enantioselectivity and thermal stability<sup>2-8</sup>, Frank *et al.*<sup>9</sup> reported that a well known Chirasil-Val enables the resolution of all protein amino acids in the form of their N-pentafluoropropionyl-isopropyl esters within 28 min.

GC enantiomeric analysis of amino acids has been applied in various fields of research for the determination of the D/L ratio in synthetic<sup>10</sup> and naturally occurring<sup>11</sup>

mixtures. The age-dating from the D/L ratio of amino acids is of interest. Helfman and Bada<sup>12</sup> reported that human age could be estimated from the extent of aspartic acid racemization in dentinal collagen. This has been recognized as a convenient technique for deducing human age, especially in forensic medicine<sup>13</sup>.

With regard to the practical GC analysis of amino acids, the sample clean-up process is indispensable prior to derivatization. This process is required not only for desalting the sample, but also for the removal of various kinds of materials which sometimes interfere with the amino acid peaks as they are or in the form of decomposition products. Conventionally, the ion-exchange method is used with a strong cation- and (or) anion-exchange resin in a short glass column of 5–10 ml in volume. However, the limitations and disadvantages of this method have been reported by several authors<sup>14,15</sup>. The method requires the passage of hydrochloric acid and sodium hydroxide for the activation of the resins. This activation is laborious and lengthy in the case when numerous samples have to be analyzed.

Enantiomeric analysis of amino acids has been applied essentially to the determination of D/L ratios, or the percentages of the D-enantiomers, of individual amino acids, not to the quantitation of the total amounts. Therefore, slight losses of constituents during the formation of derivatives are not taken into account. In consideration of these practical requirements, we investigated a solvent extraction purification of samples and applied it to the age estimation from the D/L ratio of aspartic acid contained in human dentine ranging in ages from 18 to 60 years.

## EXPERIMENTAL

### *Reagents*

All amino acids and hydroxyapatite were obtained from Sigma (St. Louis, MO, U.S.A.). Isopropanol and dichloromethane were obtained from Wako (Osaka, Japan), and once distilled from analytical grade. Biphenyl was from Tokyo Kasei, Japan. Dowex 50W-X8 (50–100 mesh) was from Muromachi Kagaku (Tokyo, Japan). All other reagents were of analytical grade (Wako). The 6 M hydrochloric acid was prepared by distilling twice diluted concentrated hydrochloric acid in an all-glass apparatus and finally adjusting the concentration by addition of doubly distilled water. The normality was verified by withdrawing a 1.00-ml aliquot, mixing with 20 ml of water and titrating with standardized sodium hydroxide solution. The buffer solution was prepared by the gentle addition of 0.2 M ammonium hydroxide to 0.2 M ammonium chloride and adjusting the pH to 9.0, 9.5, 10, 10.5 and 11, respectively. The measurement of pH was carried out by means of a Corning Digital 112 pH meter.

### *Amino acid stock solution*

A standard amino acid stock solution was prepared by the dissolution of nine amino acids (L-Ala, L-Val, Gly, L-Leu, L-Pro, L-Hyp, L-Asp, L-Phe, L-Glu) in 0.1 M hydrochloric acid to a concentration of 10  $\mu$ mol/ml of each. The solution was stable for at least 2 months upon storage in a refrigerator.

### *Ion-exchange column*

The cation-exchange column was prepared by adding 5 ml of Dowex 50W-X8 (50–100 mesh) to a glass column fitted with a quartz-wool plug. The column was

activated by thorough washing with 6 *M* hydrochloric acid (30 ml), water (50 ml), 2 *M* sodium hydroxide (30 ml), water (50 ml), at least twice. Subsequently, 6 *M* hydrochloric acid (30 ml) was passed through the column, followed by washing washed with water to neutrality.

Biphenyl was used as an internal standard for the determination of the distribution ratio of amino acid esters. A standard solution was prepared by dissolving it in dichloromethane to a concentration of 4  $\mu\text{mol/ml}$ . The solution was stored in a refrigerator.

### *Apparatus*

Gas chromatography (GC) was performed using a Shimadzu GC-7AG instrument equipped with dual flame ionization detectors. A digital integrator, Shimadzu C-R1A was used for the determination of peak areas. Both packed and capillary columns were employed. In the case of the packed column, 0.5% EGA on Chromosorb W AW, 100–120 mesh (Gasukuro Kogyo, Tokyo, Japan) in a 2 m  $\times$  2.6 mm I.D. coiled glass column was used. The laboratory-made silylated glass capillary column (25 m  $\times$  0.3 mm I.D.) was statistically coated with 0.3% chirally modified silicone GE-XE-60<sup>16</sup>.

### *Determination of the distribution ratio and extraction efficiencies of amino acid esters*

A 100- $\mu\text{l}$  volume of the amino acid standard solution was pipetted into a PTFE-lined screw cap Pyrex tube (100 mm  $\times$  13 mm). The solvent was removed by use of a nitrogen flow and the contents were esterified with 2.00 ml of acetyl chloride-isopropanol (2:8, v/v)<sup>17</sup>. After the solution had been evaporated to dryness, 1.00 ml of the buffer and 1.00 ml of solvent were added successively by a Pipetman (Gilson, France). The tube was tightly capped and shaken vigorously for 3 min. The tube was centrifuged at 2300 *g* for about 3 min, and the mixture was cleanly separated into two layers. For the determination of the distribution ratio of amino acid esters between the aqueous and organic layers, 50  $\mu\text{l}$  of each fraction were sampled by a microlitre syringe, 10  $\mu\text{l}$  of TFA were added to both fractions, which were vacuum dried suspended in 1 ml of dichloromethane and acylated with 200  $\mu\text{l}$  of trifluoroacetic anhydride (TFAA). The solution was heated at 100°C for 10 min, and the excess of reagents was carefully evaporated. The dried residue was dissolved in 50  $\mu\text{l}$  of the biphenyl internal standard solution. Finally, 2–3  $\mu\text{l}$  aliquots were injected into the 0.5% EGA packed column.

### *Treatment of dentine*

The treatment of dentine was carried out according to a previous method<sup>12,18</sup> with slight modification. Fig. 1 shows the treatment process using the solvent extraction method(I) and the ion-exchange method(II), respectively. The dentine isolated was washed successively with 0.1 *M* hydrochloric acid, water and acetone with ultrasonication, and dried in a vacuum desiccator. About 5 mg of the dried dentine were weighed into a PTFE-lined screw cap Pyrex tube (100 mm  $\times$  13 mm) and 2 ml of distilled 6 *M* hydrochloric acid were added. The tube was tightly capped and heated in a laboratory-made block heater at  $100 \pm 0.5^\circ\text{C}$  for 6 h to hydrolyse the dentinal collagen. After cooling to room temperature, the excess of hydrochloric acid was removed by rotary evaporation below 40°C. The dried residue was treated as follows.

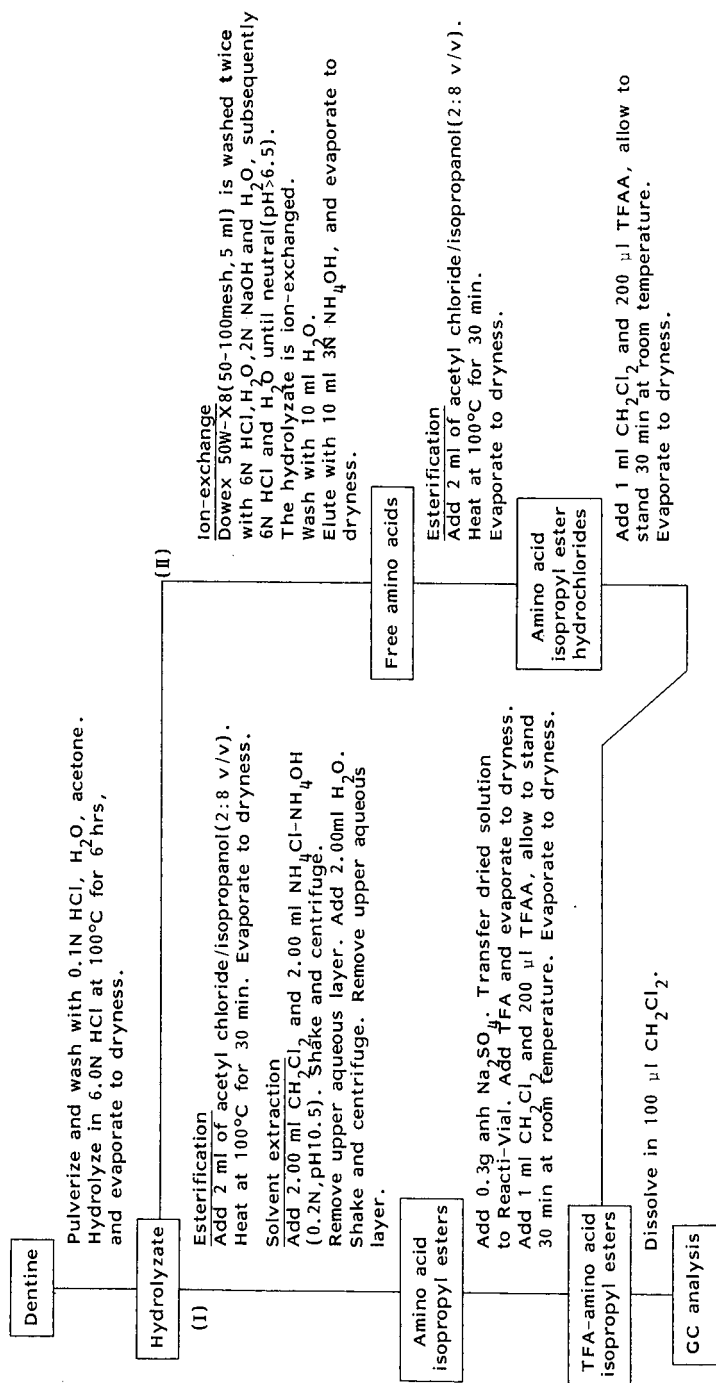


Fig. 1. Procedure for the treatment of dentine; (I) solvent extraction method; (II) ion-exchange method.

*Solvent extraction method (SEM).* The dried residue was subjected to direct esterification without any pre-treatment in 2.00 ml of esterification reagents at 100°C for 30 min. The excess of reagents was removed by evaporation under a stream of nitrogen. Following the addition of 2.00 ml of dichloromethane, and an equivalent volume of the buffer (pH 10.5), the tube was tightly capped and shaken vigorously for 3 min. After centrifugation at 2300 g for 3 min, the upper aqueous layer was discarded. The extraction was repeated with the addition of a 2.00 ml of water. A 0.3-g amount of anhydrous sodium sulphate was added to the residual solvent for the dehydration. The solution was transferred to a Reacti-Vial by a Pasteur pipette taking care not suck up the sodium sulphate. A 10- $\mu$ l portion of TFA was applied to the solution to convert amino acid isopropyl esters into non-volatile TFA salts. After the excess of reagents had been removed under a stream of nitrogen, the dry residue was dissolved in 1 ml of dichloromethane, ultrasonicated and acylated with 200  $\mu$ l of TFAA at room temperature for 30 min. The excess of reagents and solvent were removed under a gentle stream of nitrogen at 40°C. A 100- $\mu$ l volume of dichloromethane was added to dissolve the final derivatives and 1–3  $\mu$ l aliquots were injected into glass capillary column.

*Ion-exchange method (IEM).* The dry residue was dissolved in 10 ml of 0.1 M hydrochloric acid, passed through the column of Dowex 50W-X8, washed with 10 ml of water and the amino acids were eluted with 10 ml of 3 M ammonium hydroxide. The solvent was evaporated to dryness in a rotary evaporator at below 40°C. A 2.00-ml volume of esterification reagent was added to the dry residue and the mixture was heated to 100°C for 30 min. The vial was opened and the excess of reagents was removed under a stream of nitrogen with heating at 100°C. A 1-ml portion of dichloromethane and 200  $\mu$ l of TFAA were added to the dry amino acid ester hydrochlorides and the mixture was left at room temperature for 30 min. The excess of reagents was evaporated to dryness under a gentle stream of nitrogen and the residue was dissolved in 100  $\mu$ l of dichloromethane.

#### *Operational conditions for GC*

Typical operating conditions for GC using the EGA packed column are as follows: injector temperature, 250°C; carrier gas, helium; inlet pressure, 2.5 kg/cm<sup>2</sup>; oven temperature, 80°C, programmed to 190°C at 7.5°C/min.

In a case of the capillary column the conditions were as follows: injector temperature, 250°C; carrier gas (helium) flow-rate, 45 ml/min; splitting ratio, 1:40; oven temperature, 80°C, held for 4 min and then programmed to 190°C at 4°C/min.

#### RESULTS AND DISCUSSION

##### *Distribution ratio and pH*

Since the amino group is a water-miscible function, the distribution ratios of amino acid esters depend largely on the pH of the buffer added. The relationship between the distribution ratio,  $D$ , and the pH of the buffer can be approximated as<sup>19</sup>

$$\log D = \log K_2 - \log K_1 + \text{pH} \quad (1)$$

where  $K_1$  is the equilibrium constant associated with the protonation of the amino acid

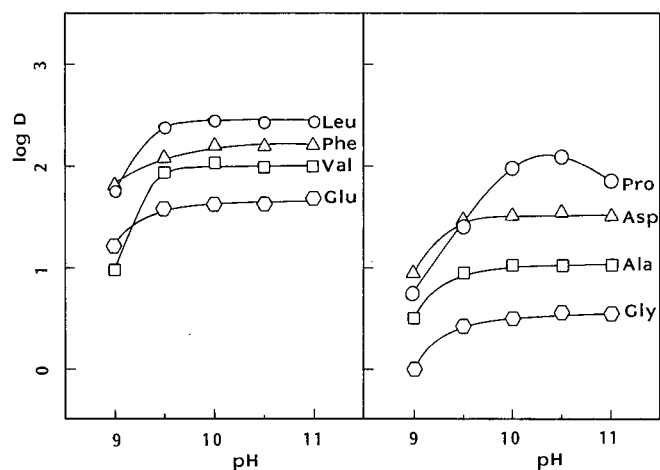


Fig. 2. Influence of pH on the distribution ratio of amino acid isopropyl esters.

isopropyl ester in the aqueous layer, and  $K_2$  is that related to the distribution of the amino acid isopropyl ester between the organic and aqueous layers. Fig. 2 illustrates this relationship. The distribution ratio,  $D$ , becomes constant at  $\text{pH} > 10$ , except for Pro which shows a maximum in  $D$  at  $\text{pH} 10.5$ . The optimum pH for the buffer extraction was 10.5. Table I shows the extraction efficiencies (EE) for the amino acid isopropyl esters in diethyl ether, chloroform, carbon tetrachloride and dichloromethane as the extraction solvents. EE was calculated from

$$\text{EE (\%)} = 100 \cdot \frac{C_{A,S}V_S}{C_{A,S}V_S + C_{A,B}V_B} = 100 \cdot \frac{D}{D + V_S/V_B} \quad (2)$$

where  $C_{A,S}$  and  $C_{A,B}$  are the concentrations of amino acid isopropyl ester in the solvent and buffer, respectively,  $V_S$  and  $V_B$  are the volumes of solvent and buffer, respectively. The values of EE increased with increasing solvent polarity. Therefore, chloroform or dichloromethane, the high polarity solvents, enabled efficient extraction of Val, Leu, Pro, Asp, Phe and Glu, a little lower with Ala and Gly. Carbon tetrachloride was the next most effective, except for Ala, Gly and Hyp. Diethyl ether was least effective among the solvents tested. From these data, dichloromethane is the most suitable solvent for extraction, considering also its low boiling point.

TABLE I

EXTRACTION EFFICIENCIES (%) FOR AMINO ACID ISOPROPYL ESTERS

NM = Not measurable.

Solvent	Ala	Val	Gly	Leu	Pro	Hyp	Asp	Phe	Glu
Diethyl ether	27	87	12	70	56	5	87	94	96
Chloroform	85	99	50	99	99	33	99	97	99
Carbon tetrachloride	67	96	42	99	98	NM	92	99	96
Dichloromethane	91	97	80	98	99	24	98	98	99

TABLE II  
RECOVERIES (%) OF AMINO ACIDS

Procedure as shown in Fig. 1.

<i>Treatment method</i>	<i>Ala</i>	<i>Val</i>	<i>Gly</i>	<i>Leu</i>	<i>Pro</i>	<i>Hyp</i>	<i>Asp</i>	<i>Phe</i>	<i>Glu</i>
Solvent extraction	39	79	11	90	90	7	95	92	96
Ion exchange	81	80	77	80	82	96	93	77	90

#### *Recovery of amino acids*

Table II shows the recoveries (%) of amino acids by SEM and IEM. The recoveries were obtained by dividing each datum by the quantitative value obtained directly from a derivatized standard amino acid mixture. The recoveries of Ala, Gly and Hyp were low in SEM, but the other amino acids were recovered comparably or even more effectively than with IEM. The recoveries in IEM were not constant for all amino acids. Although the recoveries in SEM were not quantitative, with respect to Leu, Pro, Asp, Phe and Glu, this method is considered to be better in this respect than IEM. For the quantitative analysis of these amino acids or for enantiometric analysis of all amino acids except Hyp, SEM is preferred.

#### *Esterification of amino acids in the presence of salt*

Since amino acids are functionalized with amino (imino) and carboxyl groups, their simultaneous extraction into an organic solvent without any pre-treatment is impossible. In this study, amino acids were esterified to give lipophilic properties before extraction. We investigated the influence of salt on the esterification of amino acids with isopropanol. Hydroxyapatite was used as a salt which constitutes human teeth. Table III shows the esterification yield of amino acids with isopropanol in the presence of various amounts of hydroxyapatite. The procedure is as follows.

A 2 M hydrochloric acid solution of a hydroxyapatite was mixed with a 100- $\mu$ l volume of amino acid stock solution in a Reacti-Vial in an appropriate ratio and dried under a stream of nitrogen with heating at 100°C. The mixture was esterified with isopropanol and acylated with TFAA as described. Finally, the derivatives were dissolved in a 100  $\mu$ l of biphenyl internal standard solution and 2–3  $\mu$ l aliquots were injected for GC. The esterification yields decreased gradually with increasing amount of hydroxyapatite. This is particularly masked for Val. Other amino acids show

TABLE III  
ESTERIFICATION YIELDS (%) OF AMINO ACIDS IN THE PRESENCE OF HYDROXYAPATITE

<i>Hydroxyapatite/amino acid (M/M)</i>	<i>Ala</i>	<i>Val</i>	<i>Gly</i>	<i>Leu</i>	<i>Pro</i>	<i>Asp</i>	<i>Phe</i>	<i>Glu</i>
0	100	100	100	100	100	100	100	100
10	80	85	89	99	93	92	98	99
50	73	78	82	88	90	92	102	99
100	85	82	88	98	85	83	101	95
200	76	69	96	85	82	87	91	88

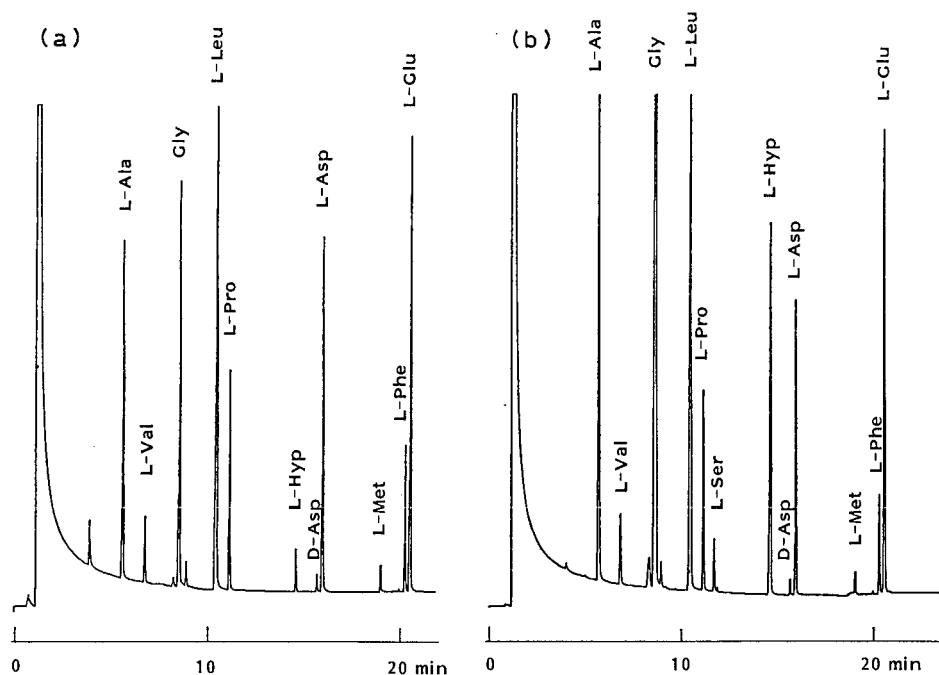


Fig. 3. Chromatogram of amino acids in dentine (41 years old, masculine): (a) solvent extraction method; (b) ion-exchange method. For other conditions see text.

76–96% of the yields in the case of a 200-fold (*M/M*) addition of hydroxyapatite per each amino acid.

#### *Age estimation from the D/L ratio of Asp in human dentine*

Fig. 3a shows a typical chromatogram of amino acids in dentine treated with SEM and Fig. 3b that with IEM. Comparing (a) with (b), the peak areas of Ala, Gly and Hyp obtained by SEM were smaller than those by IEM. However, the areas of Leu, Pro, Asp, Phe and Glu obtained by SEM were almost the same as those by IEM. The D-amino acid was observed only for Asp in (a) and (b). Table IV presents the D/L ratio of Asp and the coefficient of variation (C.V.) determined from seven types of teeth ranging in ages from 18 to 60 years. The D/L ratios obtained from SEM were slightly lower than those from IEM. The reason for this is not yet fully understood, but it might be due to a low degree of racemization when Asp is adsorbed on or desorbed from the ion-exchange resin and when evaporated from the ammonium hydroxide after elution from the ion-exchange column. Since the average C.V. obtained by SEM is somewhat smaller than that obtained by IEM, SEM is believed to be superior in reproducibility to IEM.

Fig. 4 shows a plot of

$$\ln \frac{1 + D/L}{1 - D/L} = 2kt + C \quad (3)$$

TABLE IV  
RACEMIZATION OF ASP IN HUMAN DENTINE

Age (years)	Number of samples	Solvent extraction		Ion exchange	
		D/L	C.V. (%)	D/L	C.V. (%)
18	6	0.034	7.84	0.037	9.67
27	6	0.043	4.81	0.044	7.18
36	6	0.046	8.85	0.048	4.63
41	7	0.050	1.86	0.051	2.99
49	6	0.051	2.86	0.052	3.39
54	5	0.059	2.73	0.060	5.01
60	6	0.061	3.57	0.063	3.13

based on the data given in Table IV where  $t$  is the age of the dentine in years and  $k$  is the racemization rate constant of Asp. A least squares fit of the data yields for

$$\ln \frac{1 + D/L}{1 - D/L} = 2 \cdot 6.2 \cdot 10^{-4}t + 0.048 \quad (4)$$

$$\ln \frac{1 + D/L}{1 - D/L} = 2 \cdot 6.05 \cdot 10^{-4}t + 0.052 \quad (5)$$

for SEM and IEM respectively. The correlation coefficient,  $r$ , was 0.982 for SEM and 0.984 for IEM. It is thought that  $r$  needs to be improved in order to specify the kind of the tooth and the sampling site of the dentine in the tooth.

## CONCLUSIONS

Solvent extraction clean-up, a purification method of samples for GC analysis, showed excellent recoveries of amino acids except Ala, Gly and hydroxy amino acids compared with the conventional ion-exchange clean-up. This method is of special interest for enantiomeric analysis. D/L ratios determined by SEM were smaller slightly

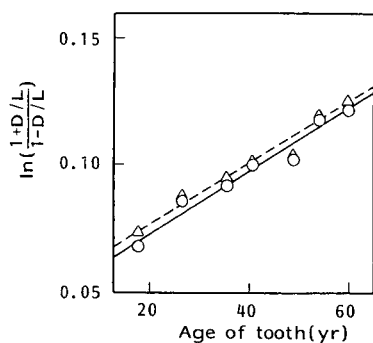


Fig. 4. Plot of  $\ln[(1 + D/L)/(1 - D/L)]$  for Asp against the age of dentine: —, solvent extraction method; ---, ion-exchange method.

than those by IEM. The method is thought to be suitable for the treatment of apatite or calcareous materials. On the contrary, organic matter causes difficulties (interference with amino acid peaks).

#### REFERENCES

- 1 E. Gil-Av, B. Feibush and R. Charles-Sigler, *Tetrahedron Lett.*, 10 (1966) 1009.
- 2 E. Gil-Av and B. Feibush, *Tetrahedron Lett.*, 35 (197) 3345.
- 3 E. Gil-Av, B. Feibush and R. Charles-Sigler, in A. B. Littlewood (Editor), *Gas Chromatography 1966*, Institute of Petroleum, London, 1967, p. 227.
- 4 W. A. König, W. Parr, H. A. Lichtenstein, E. Bayer and J. Oro, *J. Chromatogr. Sci.*, 8 (1970) 183.
- 5 W. A. König and G. J. Nicholson, *Anal. Chem.*, 47 (1975) 951.
- 6 B. Feibush, *J. Chem. Soc., Chem. Commun.*, (1971) 544.
- 7 R. Charles, U. Beitler, B. Feibush and E. Gil-Av, *J. Chromatogr.*, 112 (1975) 121.
- 8 I. Abe, T. Kohno and S. Musha, *Chromatographia*, 11 (1978) 393.
- 9 H. Frank, G. J. Nicholson and E. Bayer, *J. Chromatogr. Sci.*, 15 (1977) 174.
- 10 H. Frank, G. J. Nicholson and E. Bayer, *J. Chromatogr.*, 146 (1978) 197.
- 11 M. H. Engel and B. Nagy, *Nature (London)*, 296 (1982) 837.
- 12 P. M. Helfman and J. L. Bada, *Nature (London)*, 262 (1976) 279.
- 13 S. Ohtani and K. Yamamoto, *Bull. Forensic Med. Jpn.*, 41 (1987) 181.
- 14 P. Hušek, G. Herzogová and V. Felt, *J. Chromatogr.*, 236 (1982) 493.
- 15 D. Labadarios, G. S. Shephard, E. Botha, L. Jackson, I. M. Moodie and J. A. Burger, *J. Chromatogr.*, 383 (1986) 281.
- 16 I. Abe, S. Kuramoto and S. Musha, *J. Chromatogr.*, 258 (1983) 35.
- 17 H. Frank, D. Bimboes and G. J. Nicholson, *Chromatographia*, 12 (1979) 168.
- 18 P. M. Helfman and J. L. Bada, *Proc. Natl. Acad. Sci. U.S.A.*, 72 (1975) 2891.
- 19 M. Tanaka, *Chemistry in Solvent Extraction*, Kyoritsu, Shuppan, Tokyo, 1977, p. 84 (in Japanese).

CHROM: 20 676

## MODIFIED METHOD FOR ANALYSIS OF C<sub>2</sub>–C<sub>5</sub> HYDROCARBONS IN AN AROMATIC-ALKANE MATRIX USING AN AUTOMATED THERMAL DESORBER

ALEXANDER BIANCHI\* and HAROLD A. COOK

*Industrial Hygiene and Environmental Affairs Laboratory, Room 22, Health Centre, Industrial Hygiene and Environmental Affairs Department, Exxon Chemical Co., Fawley Oil Refinery, Southampton (U.K.)*

(First received January 22nd, 1988; revised manuscript received May 11th, 1988)

---

### SUMMARY

An automated thermal desorber, Model ATD-50 (manufactured by Perkin-Elmer), packed with a Tenax-TA cold trap was used in conjunction with a 50 m × 0.22 mm I.D. fused-silica BP-1 capillary column to separate light hydrocarbons entrained in an aromatic-alkane mixture. Injection of samples was achieved using the standard injection port fitted to the ATD-50. Collection of the material at –30°C on the cold trap preceded volatilisation and desorption of the trapped volatiles across 1 m of a heated fused-silica transfer line and onto the head of the column. The column oven is held at –35°C, where refocussing of the desorbed materials takes place. The oven is held isothermally for 8.5 min at –35°C before commencing a dual ramp temperature programme to fully separate the mixture. Sharp, near symmetrical component peaks are obtained across a 235°C span. Cooling is achieved using bottled liquid carbon dioxide pumped into the rear of the gas chromatograph oven.

The method overcomes the need for multiple column systems, heartcutting steps or sample splitting for the analysis of light hydrocarbons and liquid mixtures. An added advantage is that users of ATD-50 systems can use the equipment for both adsorbent tube desorption and conventional hypodermic syringe liquid analysis. The method separates some 32 simple components varying in volatility from methane to 1,2,3-trimethylbenzene in less than 30 min.

---

### INTRODUCTION

Chemical, environmental and industrial hygiene analysts in the petroleum and chemical industries have often experienced difficulties when attempting to analyse samples containing components whose boiling points are significantly different, *i.e.* ethane to trimethylbenzenes. Typically, the sample(s) can only be analysed for a particular range of components determined by their boiling points and method of sample injection at the expense of the remaining components. Further attempts at full range analysis by gas chromatography (GC) have included splitting the sample under conditions of reduced or increased temperature and pressure, *e.g.* partial distillation

and subsequent analysis of the separated fractions by different chromatographic methods.

Amongst the disadvantages encountered using these techniques are the loss or chemical alteration of key components and the error involved in renormalisation steps when attempting to recalculate the total individual component concentrations for the whole sample. Particular difficulties can be encountered when attempting to analyse for ethane (boiling point  $-89^{\circ}\text{C}$ ) and 1,3,5-trimethylbenzene (boiling point  $165^{\circ}\text{C}$ ) in the same sample.

Previous approaches to this problem have involved GC techniques designed to elute all  $\text{C}_2$ – $\text{C}_4$  components as a single sharp peak and optimise on separation of  $\text{C}_{5+}$  components<sup>1,2</sup>. Assumption-based calculations are then used to quantify the various  $\text{C}_2$ – $\text{C}_4$  contributions to the single peak area based on supplementary analytical data on related process streams<sup>3</sup>. Alternatively, some analysts have attempted pressure filling gas syringes and injecting an aliquot of this material into a separate GC set up to optimise on separation of the lighter components. Comparison of data from both techniques is then performed to calculate the ratio of  $\text{C}_1$ ,  $\text{C}_2$ ,  $\text{C}_3$  and  $\text{C}_4$  summed components to  $\text{C}_{5+}$  summed components<sup>4,5</sup>. These methods have never yielded consistent satisfactory performance in the laboratory.

Recent GC methods for the total analysis of organic materials increasingly employ cryogenic or "cold-trapping" techniques to focus analytes on the GC column<sup>6</sup>. These methods have included (a) standard injections onto GC columns operated at ambient temperature where the column is cool relative to the injector temperature<sup>7</sup>; (b) direct column cold trapping of analytes in gaseous samples<sup>8,9</sup>; (c) refocussing analytes undergoing thermal desorption, either from (i) Tenax-TA adsorption tubes used in direct air sampling<sup>10–13</sup>, headspace water sampling<sup>14</sup>, purge and trap water sampling<sup>15–18</sup>, and direct water sampling<sup>19</sup> or (ii) activated charcoal carbon tubes, utilised in the closed loop stripping of aqueous samples<sup>20</sup>, and direct air sampling<sup>21</sup>.

A variety of cold trapping techniques have been investigated. The most commonly used involve (a) Monitoring the GC column at temperatures significantly below the boiling point of the desired components of interest utilising liquid carbon dioxide or liquid nitrogen, (b) maintaining the front section of the column at cryogenic temperatures, (c) cryotrapping in a section of unpacked or uncoated tubing at the inlet connection to the column, (d) cryotrapping on an uncoated, coiled loop of presilylated capillary glass tubing, of which 25 cm is immersed in liquid nitrogen<sup>20</sup>. This latter technique was not reported as totally successful since breakthrough losses of compounds (boiling points  $<70^{\circ}\text{C}$ ) occurred, and concluded that such volatile organics could not be quantitatively recondensed by simple capillary cold trapping. GC cryogenic techniques are typically compromised by problems involving the collection of large quantities of water vapour, presenting major difficulties for subsequent GC analysis<sup>11</sup>. Such problems include sample losses, absorption effects, side reactions and the cross-contamination of samples.

A straightforward, one-step method was therefore developed utilising existing GC equipment to trap, refocus and separate simple, petroleum-related components of varying volatilities for subsequent complete GC analysis, affording total analysis of volatile materials within the sample.

## EXPERIMENTAL

### *Chemicals*

Standards were freshly prepared using analytical-grade purity materials. Gas mixtures and pure gases were blended (Air Products, Bracknell, U.K.) using both gravimetric and volumetric methods, and injected into sealed all-glass vessels (Hampshire Glassware Scientific, Southampton, U.K.). The gas blends were injected into glass vessels filled to achieve zero headspace with individually prepared liquid organic mixtures. (Sigma, Poole, U.K.). Concentration ratios were adjusted in subsequent standards to cover the typical ranges encountered in "plant process" samples. Immediately prior to injection, fresh standards were stored in polystyrene "picnic" boxes lined with dry ice. Individual hypodermic syringes (Scientific Glass Engineering, Milton Keynes, U.K.) were dedicated to each standard in order to minimise cross-contamination effects. Each syringe was previously solvent cleaned and dried in a stream of ultra-pure nitrogen.

Tenax-TA (20 mg), was packed into the ATD-50 cold-trap (Perkin-Elmer, Beaconsfield, U.K.) and sealed with silanised glass wool. The Tenax was then pre-conditioned at 250°C, at 20 ml/min carrier gas flow-rate before use.

### *Instrumentation*

The ATD-50 is a multi-functional instrument the principal role of which is for the analysis of organic vapours at very low concentrations (sub-part per million)<sup>22</sup>. Depending upon the adsorbent material selected for the cold-trapping packing, the trap itself can act as a primary trap over a temperature range spanning from -30°C to 250°C for liquid samples directly injected into the injection port. This is a facility in addition to its' role as a secondary trap for adsorbent tubes desorbed via the normal tube desorption sequence. Cooling of the trap is achieved electronically negating the need or dependance on heat exchange or refrigerant fluids. Retention of the sample when the trap is cooled therefore depends on chromatographic factors rather than condensation. Volatile compounds can now be injected using the "single-stage desorption" as they are quickly released or "fired" from the trap when it is heated up to 250°C. The trap is heated at a rate exceeding 1000°C per min to a defined upper limit of 300°C, sending a narrow band of concentrated sample through the fused-silica transfer line to the gas chromatograph.

Deactivated 1 m × 0.22 mm I.D. fused-silica (Chrompack, London, U.K.) was connected and run from the exit point of the cold trap through the heated transfer line jacket and into the rear of the GC oven, a Perkin-Elmer Model 8320. The silica line was then coiled in the oven and connected via a graphite ferrule into a lined stainless-steel union. The exit point of the union is attached in turn to a cradle mounted 50 m × 0.22 mm I.D. BP-1 wall-coated open-tubular fused-silica capillary column, 0.5 µm film thickness (SGE). The end of the column was then inserted into the outer edge of the flame ionisation detector, at 275°C. Both the ATD-50 and the Model 8320 gas chromatograph were linked to a programmable Perkin-Elmer Model LCI-100 computing integrator to yield chromatographic plotting and retention data.

Subambient cooling of the GC oven was achieved by piping copper tubing directly via a pumping valve accessory directly into the rear of the oven from the carbon dioxide cylinder.

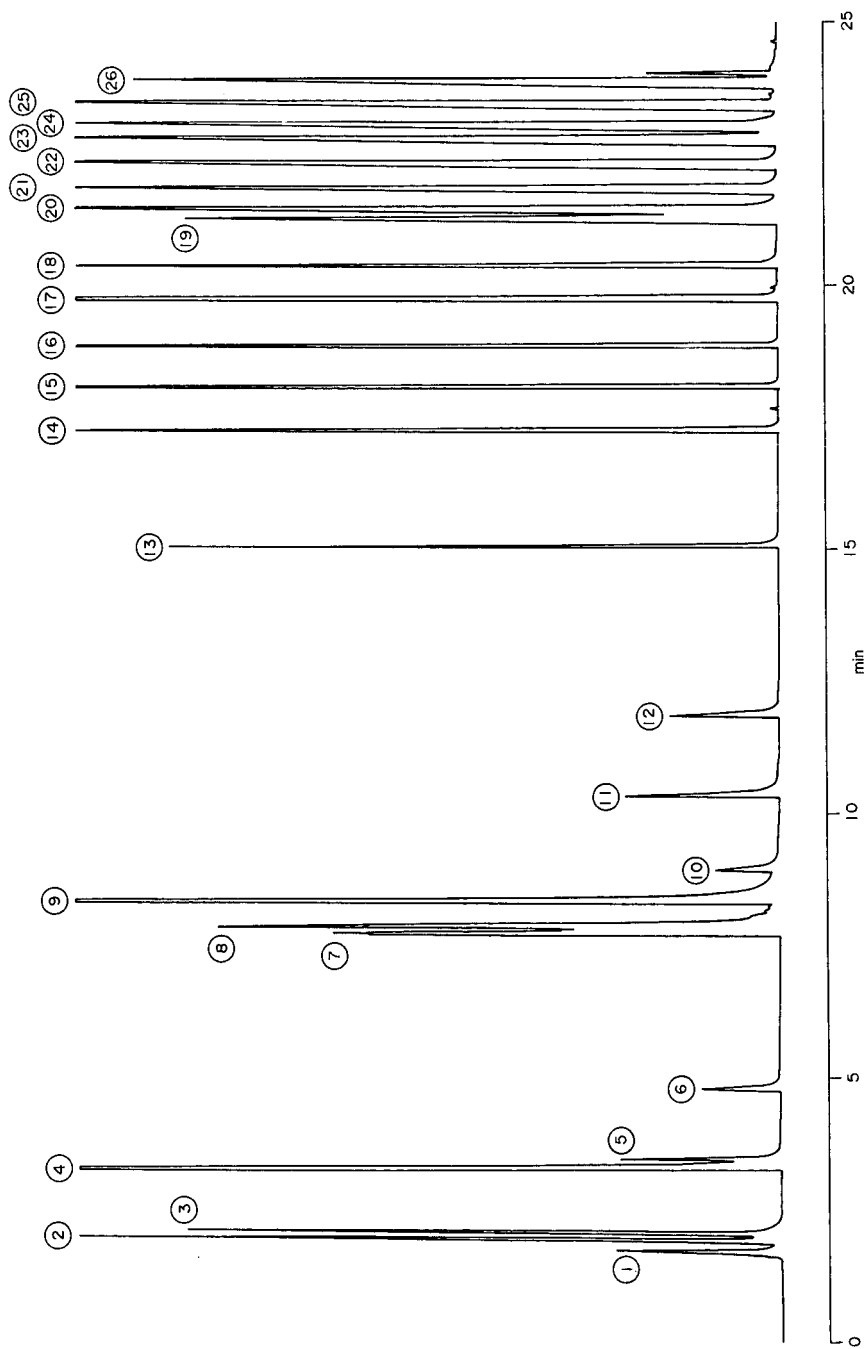


Fig. 1. Chromatogram of calibration standard illustrating the separation of 26 components using the method described in the text. For peak identification see Table I.

*System operating parameters.* The final selected GC system conditions instituted were as follows. Carrier gas: ultra-pure helium 5.5 grade (Air Products). ATD-50: cold trap packing, 20 mg Tenax-TA; cold trap low temperature, -30°C; cold trap high temperature, 250°C; split ratio (combined), 200:1.

*Gas chromatograph.* Detector temperature, 275°C; carrier gas flow-rate, 1 ml/min. Temperature conditions. Oven temperature: -35°C; isothermal time 1, 8.5 min; ramp rate 1, 20°C/min; oven temperature 2, 60°C; isothermal time 2, 1.0 min; ramp rate 2, 10°C/min; oven temperature 2, 200°C; final hold time, 1.0 min.

### *Analytical procedure*

Liquid carbon dioxide was pumped into the GC oven until pre-selected cooling temperatures were held and stabilised for a minimum of 3 min. Selected low temperatures were set from -10°C, then decreasing by 5°C steps for each successive GC run down to a minimum start temperature of -50°C. This temperature was determined by experimental observation of the separation performance of the column. Aliquots of the calibration standards varying from 0.4 µl to 0.8 µl were then injected directly into the ATD-50 injection port. Samples were allowed to collect on the cold trap for 15 ± 3 s at -30°C and immediately "fired" into the transfer line.

Upon entering the head of the chilled column, the sample eluates are partially refocussed prior to movement of the chromatographic band down the column. Column flow-rate was measured at 1.0 ml/min. Experiments were then conducted to investigate the low temperature separation of the hydrocarbon components before the column temperature was increased, *i.e.* ramped, in order to separate out the higher boiling materials within a reasonable time profile. Temperature control parameters were recorded and compared with retention and peak area data.

## RESULTS AND DISCUSSION

A specimen chromatogram obtained utilising the procedure described in the text is presented in Fig. 1. The peaks are uniformly sharp and exhibit peak widths of less than 6 s at the base. Complete baseline separation was not achieved for all components under the finally selected operating conditions as a balance was sought between optimum separation *versus* GC analysis runtime.

Marginal peak tailing effects were found to be a function of the multiple connections inherent in the chromatographic system design. These could be reduced by looping 1 m from the front end of the column up the heated transfer line jacket and connecting it directly to the cold trap exit, so removing the deactivated transfer line completely<sup>23</sup>. Cryofocussing was found to result in enhanced sensitivity and improved resolution of all components<sup>24</sup>. Overall system stability was found to be nearly constant. Retention data values for 26 key components typical of those found in petroleum-related "process" activities are presented in Table I. Relative response factor constancy *versus* concentration was observed for all components over a six month time period for calibration components of similar polarity<sup>25</sup>.

At temperatures lower than -35°C, all components with boiling points between methane and *cis*-butene-2 exhibited excessive band spreading and comparatively small relative peak areas. This was attributed to condensation effects on the column and breakdown in the internal flow dynamics and therefore separating characteristics of

TABLE I

RETENTION TIME DATA FOR 26 COMPONENTS SELECTED AS KEY REPRESENTATIVE MATERIALS FOUND IN TYPICAL PETROLEUM RELATED SAMPLES

Standard deviation data based on 10 runs.

Peak No. (Fig. 1)	Component	Retention time (min) $\pm$ S.D.	Peak No. (Fig. 1)	Component	Retention time (min) $\pm$ S.D.
1	Methane	1.72 $\pm$ 0.02	14	<i>n</i> -Hexane	17.24 $\pm$ 0.02
2	Ethylene	1.93 $\pm$ 0.01	15	Benzene	18.17 $\pm$ 0.03
3	Ethane	2.16 $\pm$ 0.02	16	<i>n</i> -Heptane	18.86 $\pm$ 0.02
4	Propylene	3.30 $\pm$ 0.02	17	Toluene	19.75 $\pm$ 0.03
5	Propane	3.51 $\pm$ 0.02	18	<i>n</i> -Octane	20.39 $\pm$ 0.02
6	Isobutane	4.86 $\pm$ 0.03	19	Ethylbenzene	21.29 $\pm$ 0.04
7	Isobutylene	7.82 $\pm$ 0.02	20	<i>m</i> -Xylene	21.38 $\pm$ 0.03
8	<i>n</i> -Butene	7.93 $\pm$ 0.02	21	<i>o</i> -Xylene	21.81 $\pm$ 0.02
9	1,3-Butadiene	8.46 $\pm$ 0.03	22	Isopropylbenzene	22.32 $\pm$ 0.04
10	<i>n</i> -Butane	8.98 $\pm$ 0.02	23	<i>n</i> -Propylbenzene	22.74 $\pm$ 0.02
11	<i>trans</i> -Butene-2	10.36 $\pm$ 0.02	24	1,3,5-Trimethylbenzene	23.01 $\pm$ 0.02
12	<i>cis</i> -Butene-2	11.89 $\pm$ 0.02	25	1,2,4-Trimethylbenzene	23.47 $\pm$ 0.03
13	<i>n</i> -Pentane	15.16 $\pm$ 0.03	26	1,2,3-Trimethylbenzene	23.91 $\pm$ 0.03

the column at  $-40^{\circ}\text{C}$ . SGE do not, however, state a minimum operating temperature for the BP-1 column.

Utilising the finally selected GC conditions it was also possible to achieve complete separation of homologous  $\text{C}_5$ ,  $\text{C}_6$  and  $\text{C}_7$  branched isomers spiked into the basic calibration mixture within the 25-min analysis time. It was also possible to run the column up to  $300^{\circ}\text{C}$  to separate *n*-alkanes up to  $\text{C}_{14}$ . Separation of homologous alkenes (olefins) is also feasible by reducing ramp rate 2 to  $5^{\circ}\text{C}$  per min.

Perkin-Elmer claim the ATD-50 can process samples whose boiling points range from  $-90^{\circ}\text{C}$  to  $+300^{\circ}\text{C}$  (ref. 22), the extremely narrow concentrated band of sample eluting from the cold trap exit port being wholly compatible with most types of GC analysis. With the exception of methane (boiling point  $-180^{\circ}\text{C}$ ), the ATD-50 was found to be at least capable of coping with samples whose boiling points are as low as  $-110^{\circ}\text{C}$  (i.e. ethylene,  $-109.3^{\circ}\text{C}$ ).

This method is now used routinely in the laboratory and has proved exceptionally reliable, having been used to analyse over 200 liquefied petroleum gas samples either as adsorbent trapped airborne vapours or as liquid "process" samples.

## CONCLUSION

The comparatively high analytical system efficiency achieved by combining a thermal desorption system, cryogenic methods and high-resolution capillary GC has much to commend to the petroleum environmental chemist. The simultaneous analysis of complex mixtures containing materials ranging from ethylene to substituted benzenes pose complex analytical challenges. Although the laboratory already equipped with an automated thermal desorber should have little difficulty in adopting this system, the method is easily transposable to an ordinary gas chromatograph with

cryogenic facilities at minimum cost. In effect, the method offers (1) a simple one-step technique, (2) significant analytical flexibility, (3) excellent relative retention time reproducibility and (4) quick turnaround on analysis time.

## REFERENCES

- 1 E. F. Smith and K. E. Paulsen, in R. L. Grob (Editor), *Modern Practice of Gas Chromatography*, Wiley, New York, 2nd ed., 1986, p. 658.
- 2 IP Oil Pollution Analysis Committee, *Marine Pollution by Oil*, Applied Science Publishers, Barking, 1974, p. 142.
- 3 ASTM Standards Committee, *Determination of C<sub>2</sub> through C<sub>5</sub> Hydrocarbons in Gasolines by Gas Chromatography*, ASTM No. D2427-82, *Annual Book of ASTM Standards, Section 5, Volume 05.02*, American Society for Testing and Materials, Philadelphia, PA, 1987, p. 242.
- 4 ASTM Standards Committee, *Analysis of Natural Gas Liquids by Gas Chromatography*, ASTM No. D2597-83, *Annual Book of ASTM Standards, Section 5, Volume 05.02*, American Society for Testing and Materials, Philadelphia, PA, 1987, p. 384.
- 5 David Storer, Chrompack Packard (UK) Ltd., Reading, personal communication.
- 6 J. F. Pankow, *J. High Resolut. Chromatogr. Chromatogr. Commun.*, 6 (1983) 292.
- 7 K. Grob and G. Grob, *J. Chromatogr. Sci.*, 7 (1969) 587.
- 8 D. E. Harsh, D. R. Cronn and W. R. Slater, *J. Air Pollut. Control Assoc.*, 29 (1979) 975.
- 9 J. F. Pankow and M. E. Rosen, *J. High Resolut. Chromatogr. Chromatogr. Commun.*, 7 (1984) 504.
- 10 K. J. Krost, E. D. Pellizzari, S. G. Walburn and S. A. Hubbard, *Anal. Chem.*, 54 (1982) 810.
- 11 R. H. Brown and C. J. Purnell, *J. Chromatogr.*, 178 (1979) 79.
- 12 W. Bertsch, R. C. Chang and A. Zlatkis, *J. Chromatogr. Sci.*, 12 (1974) 175.
- 13 A. Zlatkis, H. A. Lichtenstein and A. Tishbee, *Chromatographia*, 6 (1973) 67.
- 14 M. Novotny and M. L. Lee, *Experientia*, 29 (1973) 1038.
- 15 W. Bertsch, E. Anderson and G. Holzer, *J. Chromatogr.*, 112 (1975) 701.
- 16 D. Kalman, R. Dills, C. Perera and F. DeWalle, *Anal. Chem.*, 52 (1980) 1993.
- 17 T. C. Sauer Jr., *Org. Geochem.*, 3 (1981) 91.
- 18 J. F. Pankow, L. M. Isabelle and T. J. Kristensen, *Anal. Chem.*, 54 (1982) 1815.
- 19 P. P. Kuo, E. S. K. Chian, F. B. DeWalle and J. H. Kim, *Anal. Chem.*, 49 (1977) 1023.
- 20 J. W. Graydon and K. Grob, *J. Chromatogr.*, 254 (1983) 265.
- 21 J. O. Levin and L. Carleborg, *Ann. Occup. Hyg.*, 31 (1987) 31.
- 22 R. A. Hurrell, *Int. Environm. Saf.*, June (1981) 18.
- 23 E. Woolfendon, Perkin-Elmer Co., Beaconsfield, personal communication.
- 24 P. L. Wylie, *Chromatographia*, 21 (1986) 251.
- 25 K. Grob, Jr., G. Grob and K. Grob, in R. R. Freeman (Editor), *High Resolution Gas Chromatography*, Hewlett Packard, Avondale, PA, 1981, 2nd ed., Ch. 6, p. 115.



CHROM. 20 671

## GAS CHROMATOGRAPHIC SEPARATION AND CHEMOMETRIC ANALYSIS OF MANDARIN ESSENTIAL OILS\*

A. COTRONEO and GIOVANNI DUGO

*Dipartimento Farmaco-Chimico, Università di Messina, I-98100 Messina (Italy)*  
and

L. FAVRETTO\* and L. GABRIELLI FAVRETTO

*Dipartimento di Economia e Merceologia delle Risorse Naturali e della Produzione, Università di Trieste, I-34100 Trieste (Italy)*

(Received May 23rd, 1988)

---

### SUMMARY

Capillary gas chromatography with flame ionization detection was applied to the separation of components of mandarin essential oils. Fifty-nine genuine samples were considered over the period October 1982–January 1983. Essential oils were obtained from unripened green fruits and ripened red fruits, as well as from fruits at intermediate ripening. Thirty-four pure components were systematically identified, but only 13 were used as variables for the further characterization by a chemometric procedure. Principal component analysis was applied to the differentiation of samples with different maturation and obtained with different technologies.

---

### INTRODUCTION

Capillary gas chromatography is a frequently used method for the fractionation of components of essential oils, but few reports of the fractionation of Italian mandarin essential oils have appeared<sup>1–3</sup>. In this study a systematic approach was adopted in order to characterize mandarin essential oils from Sicily. Two extreme types of fruits were considered for the extraction of the essential oils, green and red fruit, the former corresponding to the unripened and the latter to the completely ripened fruit. The first can be collected during October and a part of November, the second from December to January; in November, from 20 to 30 generally mixed samples can be collected. As essential oils extracted from green fruits seem to be different from those extracted from red fruits, their use is also different; therefore there is the problem of their identification, two traditional technological procedures (pressing or peeling) being commonly applied in Sicily<sup>1</sup>. Chemometric analysis<sup>4</sup> was applied as a tentative method to differentiate mandarin essential oils obtained from green and red fruits as well as the technologies involved in the extraction.

---

\* 23rd paper of the series "On the Genuineness of Citrus Essential Oils".

## EXPERIMENTAL

### *Sampling*

Fifty-nine samples were first classified according to the technological procedure involved in the extraction of the essence, *i.e.*, pressing (marked in all figures by triangles) or peeling (circles). Each sample was representative of 50 kg of industrial essence and was further labelled according to the maturation stage of the fruit. Green fruits were therefore considered in the early period of maturation (October 21th to November 17th, 1982, in Sicily), red fruits later (December 1st, 1982 to January 31st, 1983). Green fruits were marked by open, red fruits by darkened circles or triangles. Stages of intermediate ripening (November 17th to 30th, 1982) were indicated by a horizontal dash.

### *Gas chromatographic analysis*

The percentage composition based on the peak areas was determined by gas chromatography (GC) using a Carlo Erba gas chromatograph series Mega Model 5160 and a Shimadzu data processor C-R3A under the following experimental conditions: column, SE-52 glass or fused-silica capillary (25 m  $\times$  0.32 and 0.45 mm I.D. respectively); column temperature, 60 (8 min) to 100°C at 3°C/min to 130°C at 2.5°C/min, to 180°C at 3°C/min; injector and detector temperatures, 280°C; carrier gas, hydrogen, 0.40 kg/cm<sup>2</sup>; injection mode, split; detection, flame ionization.

A certain number of essential oil samples were also fractionated by chromatography on neutral alumina columns, under the following conditions: column, glass, 1.6 cm I.D.; adsorbent, neutral alumina, grade II activity, 20 g; sample 100  $\mu$ l essential oil. Eluents: fraction 1 (hydrocarbons), light petroleum (b.p. 30–50°C; fraction 2 (esters) light petroleum–diethyl ether (97:3); fraction 3 (carbonyl compounds) light petroleum–diethyl ether (80:20, v:v) (20°C); fraction 4 (alcohols), diethyl ether.

### *Chemometric procedures*

An  $n \times q$  data matrix, consisting of  $j = 1, 2 \dots q$  variables and  $i = 1, 2 \dots n$  analyzed essential oils, was the starting point for further chemometric investigations. The selection of variables is discussed in detail in the next section. Standardization of the data vector for each variable produced an autoscaled  $Z$  matrix, from which the correlation matrix,  $R$ , was calculated and used as a starting matrix in principal component analysis (PCA)<sup>5,6</sup>.

Principal components (PCs) were determined by considering eigenvalues,  $\lambda_j$ , and associated eigenvectors,  $v_j$ , calculated from the characteristic equation  $(R - \lambda_j I)v_j = 0$  ( $I$  is the identity matrix). In order to choose the number,  $p$  of PCs ( $p < q$ ) which is adequate to represent the  $q$  original variables, the criterion of explained variance was adopted. Correlations,  $s_{jk}$ , between the  $j$ -th variable and the  $k$ -th PC were calculated and represented vectorially. The  $Y$  matrix ( $n \times p$ ) of PC scores was estimated from the eigenvector matrix,  $V$ . An orthogonal rotation (Normal Varimax) was also tentatively applied in order to ameliorate the separation among groups of scores. All calculations were performed by means of a SPSS-version 9 program<sup>7</sup> run on a CDC Cyber 170-730 D computer.

## RESULTS AND DISCUSSION

*Gas chromatographic analysis*

In Fig. 1 is reported a typical chromatogram of a mandarin essential oil. Nearly all the thirty-four compounds identified can be baseline resolved on the phase and

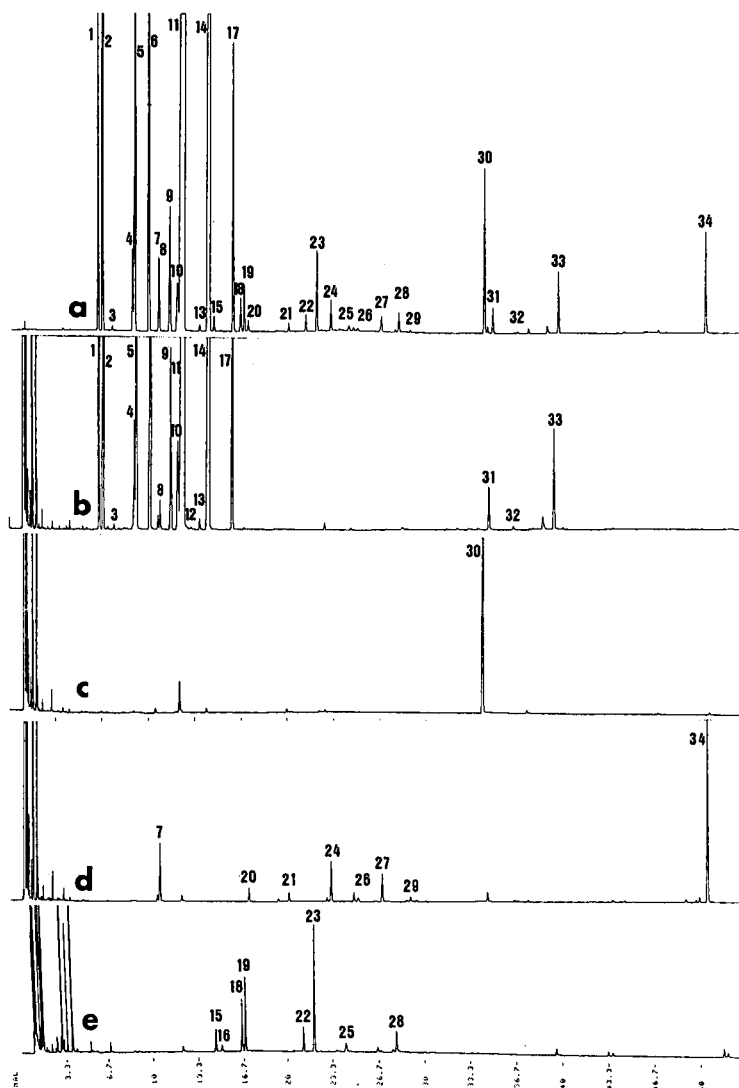


Fig. 1. Chromatogram of a mandarin essential oil and the fractions obtained from its separation on a neutral alumina column. (a) Mandarin essential oil; (b) terpene fraction; (c) esters; (d) carbonyl compounds; (e) alcohols. Peaks: 1 =  $\alpha$ -thujene; 2 =  $\alpha$ -pinene; 3 = camphene; 4 = sabinene; 5 =  $\beta$ -pinene; 6 = myrcene; 7 = octanal; 8 =  $\alpha$ -phellandrene; 9 =  $\alpha$ -terpinene; 10 = *p*-cymene; 11 = limonene; 12 = *cis*- $\beta$ -ocimene; 13 = *trans*- $\beta$ -ocimene; 14 =  $\gamma$ -terpinene; 15 = *cis*-thujenol; 16 = octanal; 17 = terpinolene; 18 = *trans*-thujenol; 19 = linalool; 20 = nonanal; 21 = citronellal; 22 = terpinen-4-ol; 23 = decanal; 24 =  $\alpha$ -terpineol; 25 = nerol; 26 = neral; 27 = geranial; 28 = thymol; 29 = undecanal; 30 = methyl N-methylantranilate; 31 = caryophyllene; 32 = humulene; 33 = farnesene; 34 = sinensal.



chromatographic conditions adopted. The values of the concentration (peak area) derived from this type of chromatogram were used for the determination of the relative amount of each compound. Other traces (Fig. 1b–e) corresponding to terpene fraction, esters, carbonyl compounds and alcohols were also used for the further identification of each component.

From the chromatogram of Fig. 1a, limonene appears to be the predominant component of mandarin essential oil, followed by  $\gamma$ -terpinene,  $\alpha$ -pinene, myrcene,  $\beta$ -pinene and other minor components.

The selection of the variables to be considered in the further chemometric data processing depends on (i) the mean abundance in the set of samples considered, (ii) the intra-laboratory repeatability and (iii) the classificatory power of each variable.

Only components having a mean concentration higher than 0.2% were first tentatively considered as variables. Under this condition, twelve variables were taken into consideration, but *p*-cymene was excluded, it is unstable and its concentration strongly depends on the time interval between preparation and analysis. However, two other variables with averages in the range 0.1–0.2% were considered. So the following variables were considered: (1)  $\alpha$ -thujene; (2)  $\alpha$ -pinene; (3) sabinene; (4)  $\beta$ -pinene; (5) myrcene; (6)  $\alpha$ -terpinene; (7) limonene; (8)  $\gamma$ -terpinene; (9) terpinolene; (10) linalool; (11)  $\alpha$ -terpineol; (12) methyl N-methylantranilate; (13) sinensal.

The intra-laboratory reproducibility was evaluated from six repeated analyses of a sample of essential oil. As far as the considered variables are concerned, the following mean values,  $\bar{x}$  (and coefficients of variation, C.V.) were obtained for each component: (1) 0.80 (0.87); (2) 2.18 (0.73); (3) 0.25 (1.21); (4) 1.50 (0.47); (5) 1.76 (0.63); (6) 0.40 (0.74); (7) 72.50 (0.13); (8) 17.53 (0.31); (9) 0.80 (0.62); (10) 0.10 (2.97); (11) 0.12 (1.74); (12) 0.36 (2.79); (13) 0.26 (5.68%). This list clearly shows that the predominant compounds (limonene,  $\gamma$ -terpinene) are characterized by a low C.V. (<0.5%), and the C.V. is also low (<1%) for some minor constituents ( $\alpha$ -,  $\beta$ -pinene, myrcene). In the evaluation of the experimental variability, some compounds in the range  $1.0 \geq \bar{x} \geq 0.1$  show a C.V. comparable with the previous ones ( $\alpha$ -thujene,  $\alpha$ -terpinene, terpinolene). Sabinene, linalool,  $\alpha$ -terpineol, methyl N-methylantranilate and sinensal are characterized by a C.V.  $\leq 6\%$  and this fact indicates the good analytical response obtained with the stationary phase SE-52, as well as with other experimental conditions, which allow an intra-laboratory repeatability adequate for further chemometric processing.

#### *Differentiation of essential oils*

In order to differentiate the essential oils from green and red fruits, a data matrix of  $n = 38$  samples,  $p = 13$  variables was first considered and analyzed by PCA. In Table I is reported as an example the corresponding *R* matrix from which the following sequence of positive eigenvalues are calculated: 8.71, 1.50, 1.20, 0.94, 0.35, 0.11, 0.09, 0.06, 0.02 and four values less than 0.01.

The number of PCs was estimated from the sequence of the eigenvalues. Only eigenvalues greater than 1, were considered, and so about 88% of the total variance is explained by this rule. In this way, thirteen variables were reduced to three PCs.

The PC scores were considered in projection (Fig. 2). The scores for green and red mandarin fruits appear to be completely separated in this projection. Moreover, the two technological extraction procedures are also differentiated.

The association of variable vectors is indicated in the first quadrant of the

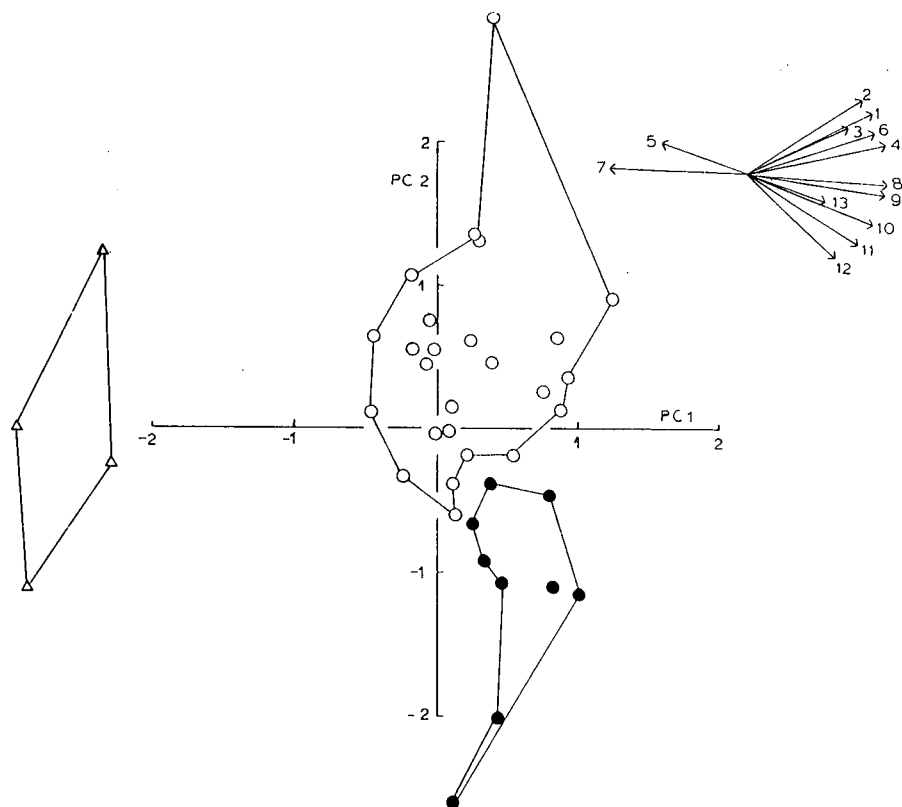


Fig. 2. Scores of the principal components (PC 1, PC 2) of 38 mandarin essential oils, obtained from green fruits by pressing (○) or peeling (●), and from red fruits by pressing (△). The association between the PCs and variable vectors is indicated.

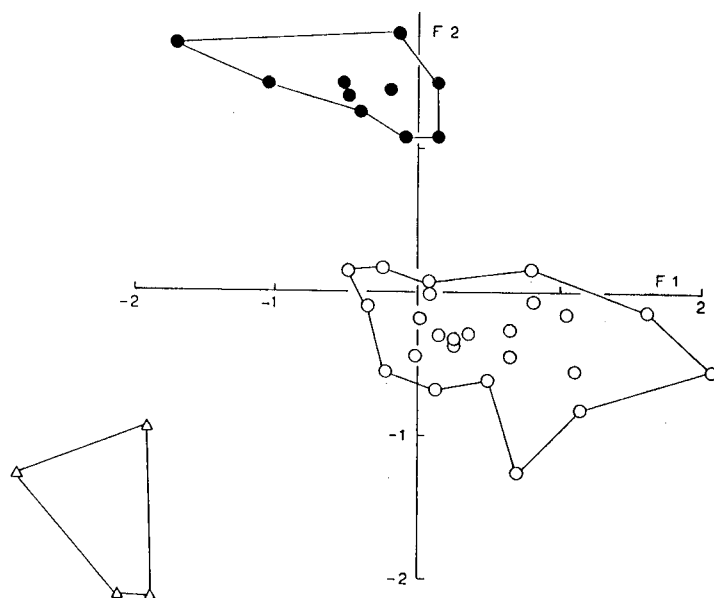


Fig. 3. Projection of scores on the two principal factors (F1, F2) of 38 mandarin essential oils, obtained after an orthogonal rotation. Symbols as in Fig. 2.

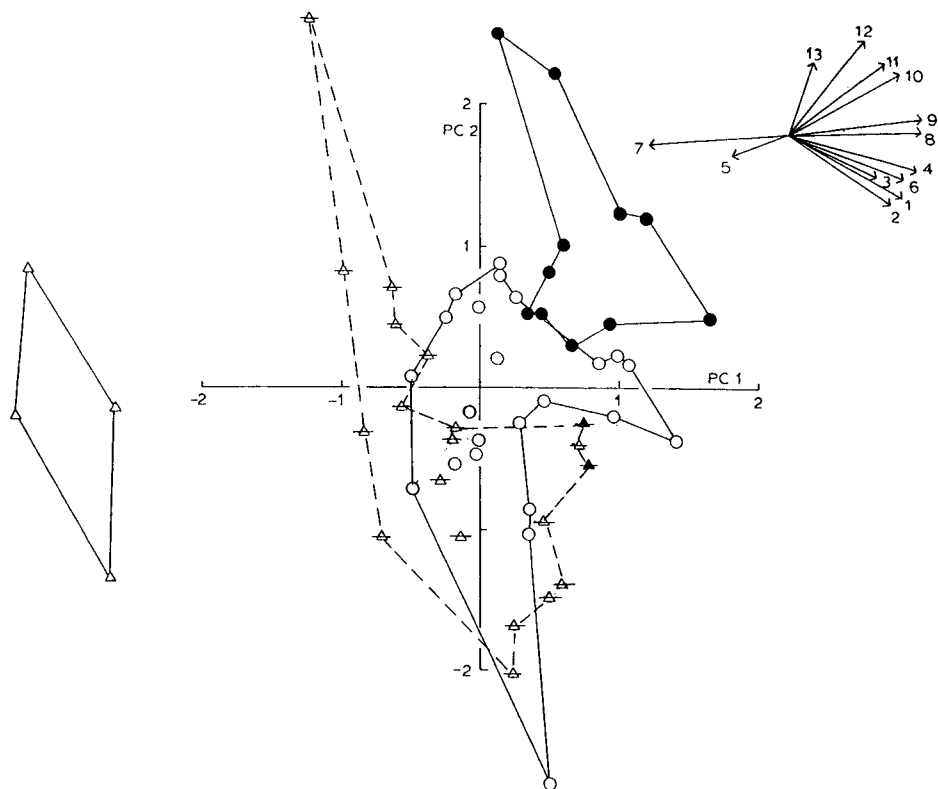


Fig. 4. Scores of the two principal components (PC 1, PC 2) of 59 mandarin essential oils, obtained from green fruits by pressing ( $\circ$ ) or peeling ( $\bullet$ ), and from red fruits by pressing ( $\triangle$ ). Twenty-one oils having an intermediate degree of ripening are marked by an horizontal dash ( $\triangle$ , essential oils obtained by pressing;  $\blacktriangle$ , essential oils obtained by peeling). Associations between PCs and variable vectors are indicated.

projection. Nearly all variables appear to be positively or negatively correlated to the first PC, except for variable 13, which is strongly associated to the third PC. An orthogonal rotation further improves the separation between the factor scores, as is seen in Fig. 3.

In order to investigate the effect of the presence of essential oils of mandarin fruits having an intermediate maturation, a  $13 \times 59$  data matrix was considered. From the corresponding  $R$  matrix (not reported), four eigenvalues greater than 1 were extracted, explaining about 93% of the total variance.

The PC scores are displayed in Fig. 4. In this projection a clear separation is again observed between the few points pertaining to pressed red fruits and other points. Moreover a tendency to separation is seen between points for pressed and peeled green fruits, but the points for the samples at intermediate ripening appear to be superposed upon those for green pressed fruits. In the same plot the variable association is also reported. The vector fan is essentially the same as in that in Fig. 2, with some minor variations. An orthogonal rotation improves the separation among

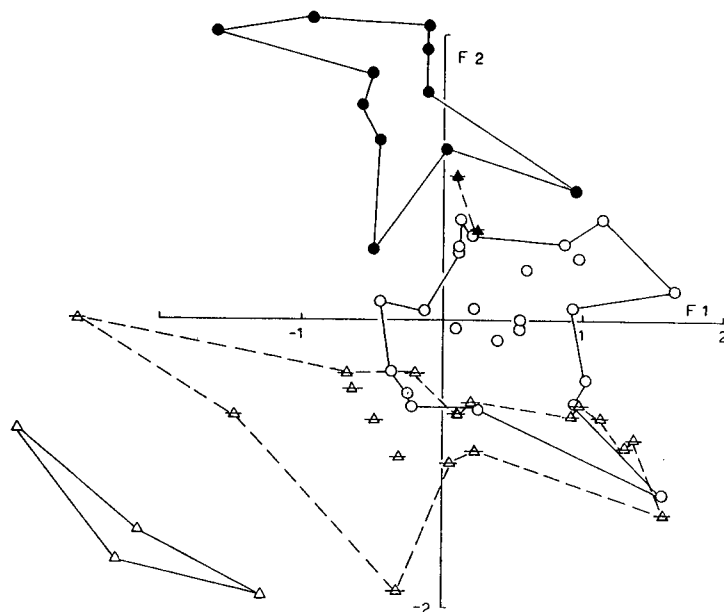


Fig. 5. Projection of scores on the two principal factors (F1, F2) of 59 mandarin essential oils, obtained after an orthogonal rotation. Symbols as in fig. 4.

different clusters of points (Fig. 5), although a small degree of overlapping is observed for the pressed green fruits and those of intermediate ripening.

From an analytical point of view, gas chromatographic procedures, in combination with chemometric methods of data handling, seem to be a fruitful approach to resolving problems of product differentiation in the essential oils industry.

#### ACKNOWLEDGEMENT

We gratefully acknowledge the assistance of Mrs. Rossana Levi.

#### REFERENCES

- 1 G. Dugo, A. Cotroneo, G. Licandro and A. Verzera, *Essenze Derivati Agrumari*, 54 (1984) 62.
- 2 G. Dugo and A. Cotroneo, *Proc. Int. IFEAT Conf., Taormina, November 3-4, 1987*.
- 3 G. Dugo, M. Rouzer, A. Verzera, A. Cotroneo and I. Merenda, *Parfums, Cosmet., Aromes*, in press.
- 4 H. Martens and H. Jr. Russwurm, *Food Research and Data Analysis*, Applied Science, London, 1982.
- 5 R. Gnanadesikan, *Methods for Statistical Data Analysis of Multivariate Observations*, Wiley, New York, 1977.
- 6 L. Lebart, A. Monnéau and K. M. Warwick, *Multivariate Descriptive Statistical Analysis. Correspondence Analysis and Related Techniques for Large Matrices*, Wiley, New York, 1984.
- 7 H. H. Nie, C. H. Hull, J. G. Jenkins, K. Steinbrenner and D. H. Bent, *Statistical Package for the Social Sciences*, McGraw-Hill, New York, 2nd ed., 1975.

CHROM. 20 667

## PERFLUORINATED ACIDS AS ION-PAIRING AGENTS IN THE DETERMINATION OF MONOAMINE TRANSMITTERS AND SOME PROMINENT METABOLITES IN RAT BRAIN BY HIGH-PERFORMANCE LIQUID CHROMATOGRAPHY WITH AMPEROMETRIC DETECTION

MIKLÓS PATTHY\* and RÓZSA GYENGE

*Institute for Drug Research, Szabadságarcosok útja 47–49, 1045 Budapest (Hungary)*

(First received March 14th, 1988; revised manuscript received May 24th, 1988)

---

### SUMMARY

The behaviour of trifluoroacetate and heptafluorobutyrate as pairing ions for the reversed-phase ion-pair separation of monoamine transmitters and related metabolites was studied. The performance of systems with the perfluorinated acids was compared with that of systems containing sodium octyl sulphonate and was found to be better in terms of peak resolution combined with total analysis time, day-to-day reproducibility and the time required for attaining initial chromatographic equilibrium. Rat brain samples were deproteinized in the acidified mobile phase, injected directly on to a high-performance liquid chromatographic column and quantitated using an amperometric detector. Sample run times were 6–8 min, at a relatively low flow-rate. The detection limits achieved are fairly uncommon with conventional bore columns. The two perfluorinated acids studied differ in the dominant mechanisms of ion-pair formation and show selectivity differences as a result.

---

### INTRODUCTION

High-performance liquid chromatography (HPLC) with amperometric detection is now a method of choice for the determination of catecholamines, indoleamines and related metabolites in the central nervous system. Reversed-phase ion-pair HPLC has frequently been used for the separation of these compounds<sup>1–8</sup>. Much work has been carried out in order to study the effects of the variables that control the separations, using systematic sequential methods<sup>9–14</sup> and computer-aided optimization strategies<sup>15</sup>. Optimal conditions can be selected in terms of peak resolution combined with total analysis time by a systematic study of the influence of some mobile phase variables (pH, nature and concentration of the ion-pairing agent, percentage of the organic modifier) and by examining a variety of reversed-phase packing materials and column dimensions.

Several ion-pairing agents have been described that give satisfactory results in the analysis of monoamine transmitters and related metabolites. Although some workers have used trichloroacetate as a pairing ion with remarkable success<sup>10,16</sup>, ion-pairing agents belonging to the alkanesulphonate (or sulphate) class have been in

common use since the late 1970s<sup>9,17</sup>. However, most of the methods using these pairing ions [of which sodium octyl sulphonate (SOS) has been the most popular] require fairly long sample run times if both catecholamines and indoles are to be resolved in the same chromatographic run. Also, as equilibrium is attained in 12–16 h, the “start-up” time for an assay procedure may be unacceptably long with the larger alkylsulphonates in the eluent<sup>10,14</sup>.

The excellent resolving power of perfluorinated acids in the ion-pair separation of proteins and peptides<sup>18</sup> and aminoglycoside antibiotics<sup>19</sup> and the isolation of peptide hormones<sup>20</sup> has been well documented. In this work, we investigated the behaviour of some perfluorinated carboxylic acids [trifluoroacetic acid (TFA) and heptafluorobutyric acid (HFBA)] as providers of pairing ions for the separation of biogenic amines [noradrenaline (NA), adrenaline (A), dopamine (DA) and serotonin (5-hydroxytryptamine, 5-HT)] and some of their metabolites [3,4-dihydroxyphenylacetic acid (DOPAC), homovanillic acid (HVA) and 5-hydroxyindoleacetic acid (5-HIAA)] using reversed-phase HPLC systems combined with amperometric detection.

Mobile phase conditions for systems containing TFA, HFBA or SOS (for comparison) as ion-pairing agents were optimized in a known, systematic way. Three types of reversed-phase packing material and columns of three lengths were examined. Comparing the peak resolutions combined with total analysis times obtained in optimized systems with TFA, HFBA or SOS in the eluent and the same chromatographic column we found that the performance of the TFA and HFBA systems compares favourably with that of the SOS systems. Using TFA or HFBA as the pairing ion, baseline resolution of all analytes of interest was achieved within 6–8 min, even at a relatively low flow-rate. Low background noise and  $k'$  values together resulted in sensitivities that are fairly uncommon with conventional bore columns. Optimized TFA and HFBA systems were used for the determination of monoamine transmitters and their metabolites in rat brain striatum and hypothalamus.

## EXPERIMENTAL

### *Chromatography*

The HPLC system included a Varian 8500 pulse-free pump (Varian, Palo Alto, CA, U.S.A.), a Rheodyne 7125 injection valve (Rheodyne, Berkeley, CA, U.S.A.) fitted with a 200- $\mu$ l loop, a Model LC-4A thin-layer amperometric detector (Bioanalytical Systems, West Lafayette, IN, U.S.A.) with graphite paste (CP-S) as the working electrode operated at 0.75 V vs. an Ag–AgCl reference electrode and a Type OH-814/1 strip-chart recorder (Radelkis, Budapest, Hungary).

Chromatographic supports were packed in stainless-steel columns (Bio-Separation Technologies, Budapest, Hungary). The chromatographic columns and the compositions of the mobile phases are specified in the figure legends. The mobile phase was sonicated and degassed under vacuum for 1 min before use. All separations were carried out at ambient temperature.

### *Chemicals*

Materials and their sources were as follows. NA bitartrate, A hydrochloride, DA hydrochloride, isoproterenol hydrochloride and DOPAC were obtained from Sigma

(St. Louis, MO, U.S.A.) and  $\alpha$ -methyldopamine ( $\alpha$ -MDA) hydrobromide from Merck, Sharp and Dohme (West Point, PA, U.S.A.). HVA and the Servachrom packing material [Polyol, RP-18 (5  $\mu$ m)] were purchased from Serva (Heidelberg, F.R.G.), the Vydac 218 TPB C<sub>18</sub> (10  $\mu$ m) packing material from The Separations Group (Hesperia, CA, U.S.A.) and the Nucleosil 5 C<sub>18</sub> (5  $\mu$ m) and Nucleosil 3 C<sub>18</sub> (3  $\mu$ m) packing materials from Macherey, Nagel & Co. (Düren, F.R.G.). The 5-HT creatinine sulphate complex, 5-HIAA, dipotassium hydrogen orthophosphate (K<sub>2</sub>HPO<sub>4</sub>), the disodium salt of ethylenediaminetetraacetic acid (EDTA) and trichloroacetic acid (TCA) were obtained from Reanal (Budapest, Hungary). Sodium hydrogensulphite (NaHSO<sub>3</sub>) and methanesulphonic acid (MSA), which we purified on a charcoal column, were supplied by Fluka (Buchs, Switzerland), acetonitrile (LiChrosolv) and sodium perchlorate by Merck (Darmstadt, F.R.G.) and SOS by Supelco (Bellefonte, PA, U.S.A.). The perfluorinated acids (Sequanal quality), TFA and HFBA, were obtained from Pierce (Rockford, IL, U.S.A.). All other chemicals used were of analytical-reagent grade.

All solutions were prepared with deionized, glass-distilled water. Stock solutions of the analytes of interest were prepared at a concentration of 0.1 mg/ml in the respective mobile phase containing  $4 \cdot 10^{-4}$  M NaHSO<sub>3</sub> as antioxidant. Standard solutions were prepared every 2 weeks from a portion of the stock solutions after appropriate dilution in the same solvent. All solutions were stored at  $-20^{\circ}\text{C}$ .

#### *Sample preparation*

Adult male OFA rats weighing 200–250 g were killed by decapitation. The brain was removed within 30 s and dissected on ice. The regions of interest were immediately cooled with dry-ice and stored at  $-20^{\circ}\text{C}$  until analysed. For analysis, pieces of tissue (4–50 mg) were weighed in conical 1.5-ml test-tubes and a solution (200–500  $\mu$ l) consisting of the respective mobile phase (the pH of which was previously adjusted to 3 with 42.5% orthophosphoric acid),  $4 \cdot 10^{-4}$  M NaHSO<sub>3</sub> and the internal standard ( $\alpha$ -MDA  $\cdot$  HBr) (1.0 and 0.2  $\mu$ g/ml for examination of the striatum and hypothalamus, respectively) was pipetted into the tubes. The mixture was sonicated at 200 W for about 5 s while kept on ice, and the homogenate was centrifuged for 10 min at 15 000 g and  $4^{\circ}\text{C}$ . An aliquot of the supernatant was injected on to the chromatographic column.

Quantitations were performed from calibration graphs of peak-height ratio relative to the internal standard against concentration.

## RESULTS AND DISCUSSION

#### *Choice of the reversed-phase column packing material*

Reversed-phase supports from different suppliers can show large differences in chromatographic behaviour<sup>11,15</sup>. In order to find a suitable packing material for our studies, three different supports were tested. NA, 5-HT and HVA were chosen as test compounds. As shown in Table I, both Nucleosil C<sub>18</sub> (5  $\mu$ m) and Servachrom RP-18 (5  $\mu$ m) packings gave good retention for NA. The capacity factor ( $k'$ ) was calculated using the equation  $k' = (t_R - t_0)/t_0$ , where  $t_0$  and  $t_R$  are the retention times of an unretained solute and the solute in question, respectively. All three packing materials exhibited remarkable chromatographic efficiency ( $N$ ) for the acid metabolite, HVA;  $N$  was calculated using the equation  $N = 5.54(t_R/w_{1/2})^2$ , where  $t_R$  is the retention time

TABLE I

## CHROMATOGRAPHIC DATA FOR SOME COMMERCIAL COLUMN PACKING MATERIALS

Column (and main eluent variables*)	Test com- pound	$k'$		$N/m$		Peak asymmetry**	
		SOS	HFBA	SOS	HFBA	SOS	HFBA
<i>Servachrom RP-18 (5 <math>\mu</math>m) (170 (4.0 mm I.D.))</i>	NA	0.87	1.27	6129	17 600	1.83	1.28
(A) 0.2 mM SOS, 6% acetonitrile, pH 4.68	5-HT	8.56	12.90	4879	10 794	2.33	1.48
(B) 15 mM HFBA, 6% acetonitrile, pH 4.15	HVA	4.97	8.08	19 100	18 867	1.16	1.18
0.83 ml/min (both)							
<i>Vydac 218TPB C<sub>18</sub> (10 <math>\mu</math>m) (220 <math>\times</math> 4.0 mm I.D.)</i>	NA	0.49	0.60	14 073	22 950	1.50	1.08
(A) 0.4 mM SOS, 6% acetonitrile, pH 4.15	5-HT	3.79	4.40	12 568	19 527	1.59	1.12
(B) 15 mM HFBA, 6% acetonitrile, pH 4.05	HVA	2.79	3.07	16 564	20 018	1.25	1.06
0.83 ml/min (both)							
<i>Nucleosil 5 C-18 (5 <math>\mu</math>m) (120 <math>\times</math> 4.0 mm I.D.)</i>	NA	1.79	1.29	47 408	60 210	1.08	1.03
(A) 0.75 mM SOS, 6% acetonitrile, pH 4.32	5-HT	18.0	13.10	47 958	54 760	1.03	1.05
(B) 15 mM HFBA, 6% acetonitrile, pH 4.20	HVA	7.92	7.19	52 533	70 420	1.02	1.02
0.83 ml/min (both)							

\* The eluent was a mixture of a 0.05 *M* phosphate buffer and acetonitrile containing the pairing ion.

\*\* Peak asymmetry was measured at 10% of the peak height and a chart speed of 2.5 cm/min.

of the solute in question and  $w_{1/2}$  is the width of the peak at half-height. Based on the excellent peak symmetry values and overall chromatographic performance, the Nucleosil support was chosen for further optimization studies. For some separations the Vydac column was also used.

#### *Dependence of $k'$ on the nature and concentration of the pairing ion*

Both TFA and HFBA are fully dissociated and available for ion pairing at pH higher than 2.0 (their  $pK_a$  values are 0.23 and 0.17, respectively). The capacity factors of the analytes of interest are plotted as a function of the concentration of TFA and HFBA in Figs. 1 and 2, respectively. Apart from the nature of the pairing ion, other chromatographic variables were identical in both systems. As shown in Fig. 1, there was a 2-fold increase in the retention of the amines when the TFA concentration was raised from 0 to 50 mM. The same increase in HFBA concentration resulted in an average 8-fold increase in the retention of the amines (Fig. 2). The amine curve shapes are similar to those obtained for  $C_4$ – $C_8$  alkyl sulphates<sup>17</sup> and TCA<sup>10</sup>. Whereas the capacity factors for the acids (DOPAC, HVA and 5-HIAA) are unaffected by the presence of TFA in the eluent (Fig. 1), there is a sharp concave downward turn in the  $k'$  vs. [HFBA] plots for these acids when the HFBA concentration is raised from 0 to 2 mM (Fig. 2), indicating a higher retention for acids in eluents containing TFA and a marked difference in the ion-interaction mechanisms of TFA and HFBA in reversed-phase systems in general.

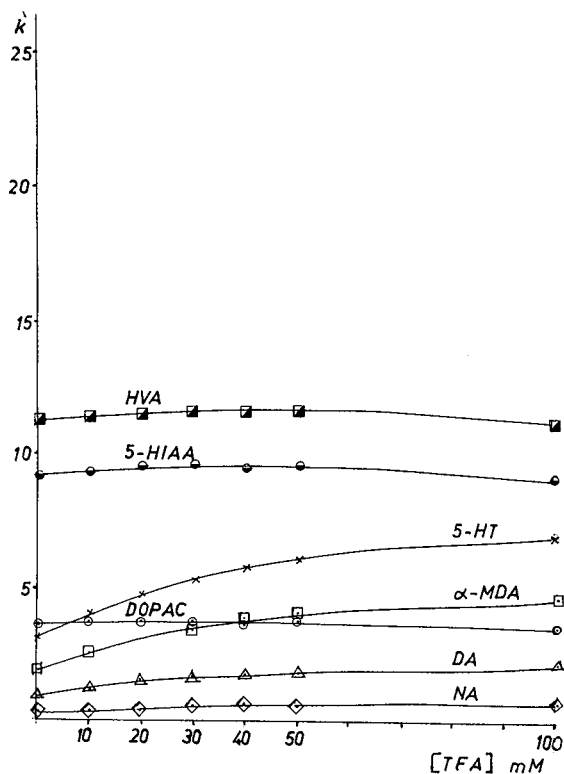


Fig. 1. Dependence of  $k'$  on the concentration of TFA in the eluent. Column: Nucleosil  $C_{18}$  (5  $\mu$ m), 100  $\times$  4.0 mm I.D. Eluent: aqueous buffer (pH: 4.15)–acetonitrile (94:6); the aqueous buffer consisted of 0.05  $M$   $K_2HPO_4$ , 0.1  $mM$  EDTA and 0–100  $mM$  TFA (TFA concentrations: 0, 10, 20, 30, 40, 50 or 100  $mM$ ). The pH of the aqueous buffer was adjusted to 4.15 using 42.5% (w/v) orthophosphoric acid or 5  $M$  potassium hydroxide solution. Flow-rate: 0.83 ml/min.

#### *Dependence of $k'$ on mobile phase pH and acetonitrile admixture*

The mobile phase pH greatly affects the  $k'$  values for the acidic metabolites. The decrease in  $k'$  for the acids with increasing pH is dramatic in both TFA and HFBA systems and the  $k'$  values are indirectly related to the degree of ionization of the metabolite of interest at a given pH (see Figs. 3 and 4). The retention of the acidic metabolites is most sensitive to a change in mobile phase pH between pH 3 and 5.5, as expected for acids with  $pK_a \approx 4.7$ . In accordance with the difference between the two pairing ions observed in Figs. 1 and 2, the retention of an acid of interest is lower (at each pH) in an HFBA system than in systems containing TFA.

As their  $pK_a$  values are higher than 6.0, the amines carry the same charge over the pH range examined and their retention is relatively unaffected by changes in the mobile phase pH.

The addition of acetonitrile produced a decrease in  $k'$  for all compounds examined without major changes in the relative retentions either in TFA systems (Fig. 5) or in those prepared with HFBA. For acetonitrile concentrations between 0 and 6% the log  $k'$  values fall on straight lines in both systems.

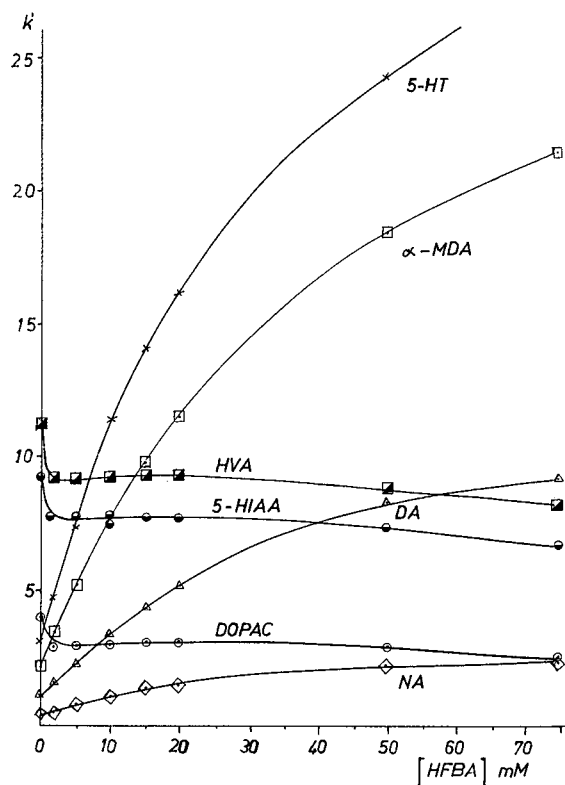


Fig. 2. Dependence of  $k'$  on the concentration of HFBA in the eluent. HFBA concentrations in the aqueous buffer: 0, 2, 5, 10, 15, 20, 50 or 75 mM. Other details as in Fig. 1.

#### *Comparison of TFA and HFBA with pairing ions of different nature*

In order to position TFA and HFBA in the group of anionic ion-pairing agents, their influence on the retentions of some monoamines and acidic metabolites was compared with those of some pairing ions of different nature. The pairing ions studied were used in equimolar concentrations (except SOS) and without salt control, but under otherwise identical chromatographic conditions. As shown in Table II, TFA behaves much like perchlorate, an inorganic pairing ion, whereas HFBA is very similar in character to TCA and SOS. The difference between the two groups lies in the fact that, under the conditions of the study, perchlorate and trifluoroacetate ions cannot bind to the hydrophobic surface of the support (they cannot form a primary ion layer on the surface) and, as a result, they exercise no electrostatic repulsion toward molecules of identical charge (DOPAC, 5-HIAA, HVA) binding to the stationary phase. Hence, increasing the concentration of TFA in the eluent causes no decrease in the retention of the acidic metabolites, as was shown in Fig. 1. On the other hand, the negative retention shifts ( $k'_p - k'_0$ ) of DOPAC, 5-HIAA and HVA caused by TCA, HFBA or SOS in the eluent (see Table II) indicate a fairly strong binding of these pairing ions to the lipophilic stationary phase. These pairing ions do form, on the support surface, a negatively charged primary ion layer, expelling the acidic

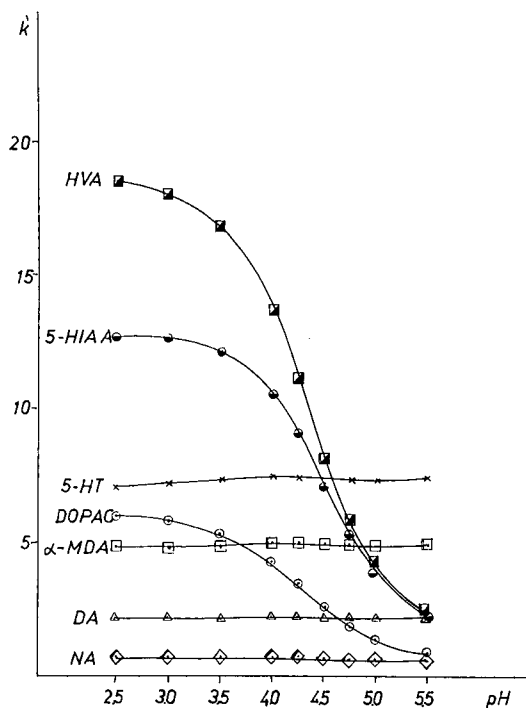


Fig. 3. Dependence of  $k'$  on eluent pH in a TFA system. TFA concentration in the aqueous buffer: 100 mM. The pH of the aqueous buffer varied between 2.0 and 6.0. Capacity factors were measured at pH 2.5, 3.0, 3.5, 4.0, 4.25, 4.5, 4.75, 5.0 and 5.5. Other details as in Fig. 1.

metabolites from the layer on the support even at concentrations below 2 mM (see Fig. 2).

### Selectivity

Inspection of the above data shows that, under the conditions of the study, there is a marked difference in the chromatographic behaviour of TFA and HFBA in ion-pair reversed-phase systems. Whereas TFA can bind to the hydrophobic surface of the support in the form of a neutral ion pair only (in association with a sufficiently hydrophobic cationic counter ion), HFBA can bind to the surface as a solvated anion and also as a neutral ion pair. Consequently, the dominant mechanism of the chromatographic process with TFA is ion-pair formation in the mobile phase and binding of the neutral complex to the non-polar stationary phase. Hence the so-called dynamic ion-exchange model<sup>21</sup> and the ion-interaction model<sup>22</sup> cannot be the underlying mechanisms in ion-pair chromatography with TFA. With HFBA, however, all three of the proposed models can more or less explain the chromatographic process.

At a mobile phase pH of 4.20, which appears to be the optimal pH in both TFA and HFBA systems (see Figs. 3 and 4), the elution orders with TFA and HFBA are NA, DA, DOPAC,  $\alpha$ -MDA, 5-HT, 5-HIAA, HVA and NA, DOPAC, DA, 5-HIAA, HVA,  $\alpha$ -MDA, 5-HT, respectively. The remarkable difference in these elution orders

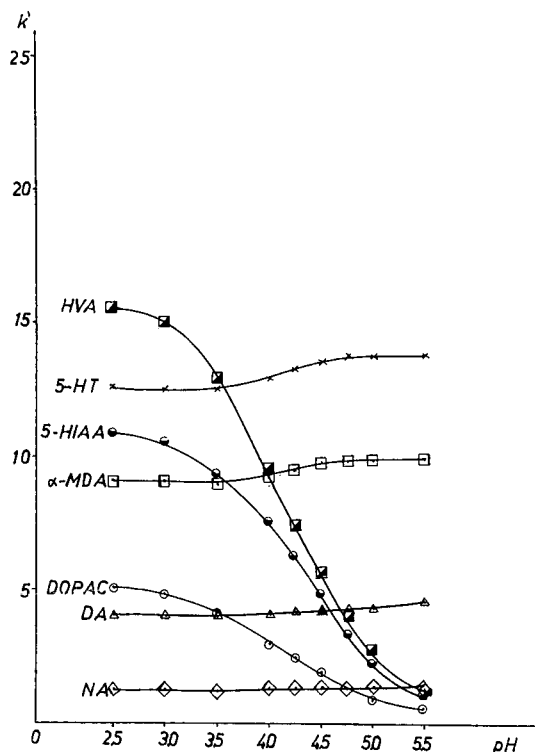


Fig. 4. Dependence of  $k'$  on eluent pH in an HFBA system. HFBA concentration in the aqueous buffer: 15 mM. Other details as in Figs. 1 and 3.

clearly shows that TFA systems are more retentive for the acids, and HFBA systems (like SOS systems) are more retentive for the amines. Our results demonstrate that in the perfluorinated carboxylic acids series special selectivity effects are obtained as a function of the chain length. This is in agreement with the conclusion of a recent study on the ion-pair separation of aminoglycoside antibiotics<sup>19</sup>. On the other hand, the retention shift data with MSA and SOS in Table II seem to support earlier suggestions that no special selectivity effects can be expected on changing the chain length of alkylsulphonate pairing ions<sup>23</sup>. We have no simple explanation of the difference in chromatographic behaviour between MSA and TFA.

#### *Optimization of the TFA and HFBA chromatographic systems*

Our aim was to separate the compounds under study in the minimal time with maximal resolution, and also to achieve as low detection limits as possible with conventional bore columns. Maximum sensitivity (combined with low residual current and background noise) can be expected from carbon paste working electrodes<sup>24,25</sup>. With careful handling, the long-term stability of pre-tested carbon-paste electrodes is much better than that of glassy carbon electrodes (which may need frequent repolishing) if the aqueous eluent contains not more than 8% of acetonitrile. Eluents containing more than 8% of acetonitrile are not practical anyway, as the resolution of

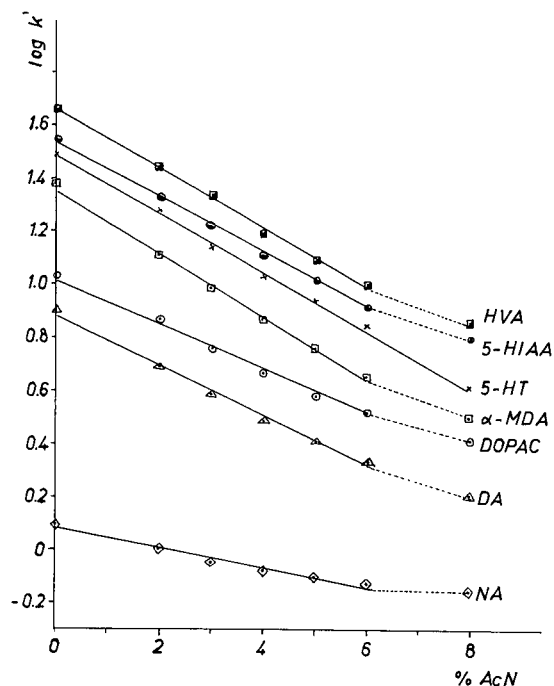


Fig. 5. Dependence of  $k'$  on acetonitrile (ACN) content in a TFA system. TFA concentration in the aqueous buffer: 100 mM. pH of aqueous buffer: 4.15. The acetonitrile concentration in the eluent was varied between 0 and 10% (v/v). Capacity factors were measured at acetonitrile concentrations of 0, 2, 3, 4, 5, 6 and 8%. Other details as in Fig. 1.

TABLE II

INFLUENCE OF VARIOUS PAIRING IONS ON THE RETENTION OF MONOAMINES AND ACIDIC METABOLITES

$k'_o$  =  $k'$  value for an analyte of interest obtained in a system without pairing ion (eluent buffer only);  $k'_p$  =  $k'$  value for an analyte of interest obtained in the eluent buffer for  $k'_o$  containing 20 mM of the specified pairing ion in addition.

Compound examined	$k'_o$ (buffer*)	$k'_p - k'_o$					
		MSA**	HClO <sub>4</sub> **	TFA**	TCA**	HFBA**	SOS***
NA	0.31	0.02	0.14	0.17	0.45	1.15	2.14
DA	0.81	0.05	0.33	0.49	1.33	4.05	6.79
α-MDA	1.57	0.10	0.69	1.05	2.95	9.38	15.65
5-HT	2.43	0.14	1.19	1.57	4.22	12.05	20.45
DOPAC	2.85	-0.01	0.05	0.02	-0.23	-0.61	-0.40
5-HIAA	6.93	-0.03	0.06	0.05	-0.28	-1.31	-1.17
HVA	8.56	-0.13	0.16	0.06	-0.68	-1.80	-1.97

\* The eluent buffer was a mixture of 0.05 M phosphate (pH: 4.25) and 6% acetonitrile. The column was Nucleosil 5 C<sub>18</sub> (100 × 4.0 mm I.D.).

\*\* Pairing ion, 20 mM.

\*\*\* 2.0 mM (instead of 20 mM) sodium octylsulphate in the buffer.

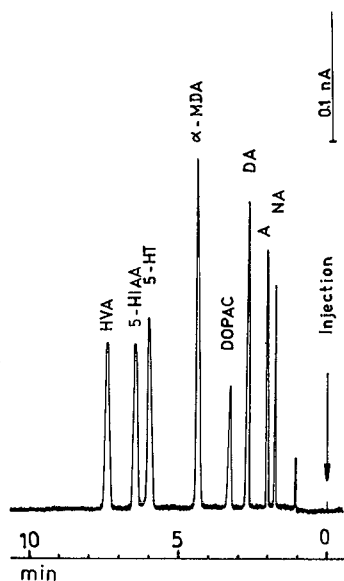


Fig. 6. Separation of standards in an optimized TFA system. Column: Nucleosil  $C_{18}$  ( $5\ \mu\text{m}$ ),  $100 \times 4.0\ \text{mm}$  I.D. Eluent: aqueous buffer (pH 4.20)–acetonitrile (92:8); TFA concentration in the aqueous buffer: 100 mM; other components in the aqueous buffer as in Fig. 1. Flow-rate: 0.83 ml/min.

the analytes of interest deteriorates quickly with higher concentrations of the organic modifier (see Fig. 5).

The optimal concentration of acetonitrile in both the TFA and HFBA systems is between 5.5 and 8%. The optimal pH range for the separation of the compounds studied is 4.05–4.35 in both systems (see Figs. 3 and 4), and the most advantageous pairing ion concentrations appear to be 100 mM for TFA and 12–16 mM for HFBA (see Figs. 1 and 2), the concentrations being determined in part by the requirement that a  $k'$  value of 0.65–0.70 is necessary in our methods for NA to be well resolved from early eluting unknown compounds in a sample. Fig. 6 shows a chromatogram of standards obtained with a Nucleosil 5  $C_{18}$  column ( $100 \times 4.0\ \text{mm}$  I.D., without a pre-column) in a highly optimized TFA system. In this system plate counts ( $N$  per metre) of over 100 000 were generated, allowing a separation to take place in less than 8 min even at a relatively low flow-rate (0.83 ml/min).

Some further improvement in speed can be achieved with a shorter column and a packing material of smaller particle size (in order to maintain a stable baseline and high sensitivity, we did not increase the flow-rate). Fig. 7 shows a chromatogram of standards obtained on a Nucleosil 3  $C_{18}$  column ( $30 \times 4.0\ \text{mm}$  I.D. with a  $20 \times 4.0\ \text{mm}$  I.D. pre-column) in an optimized TFA system. A representative chromatogram of a sample of rat striatum in the same system is shown in Fig. 8. Fig. 9 shows a chromatogram of standards obtained in an optimized HFBA system and Fig. 10 presents a representative chromatogram of a sample of rat hypothalamus in the same system. In both instances the column was the same as in Fig. 7. The average plate counts in Figs. 7–10 are lower than expected ( $N \approx 93\ 000/\text{m}$ ), presumably owing to the

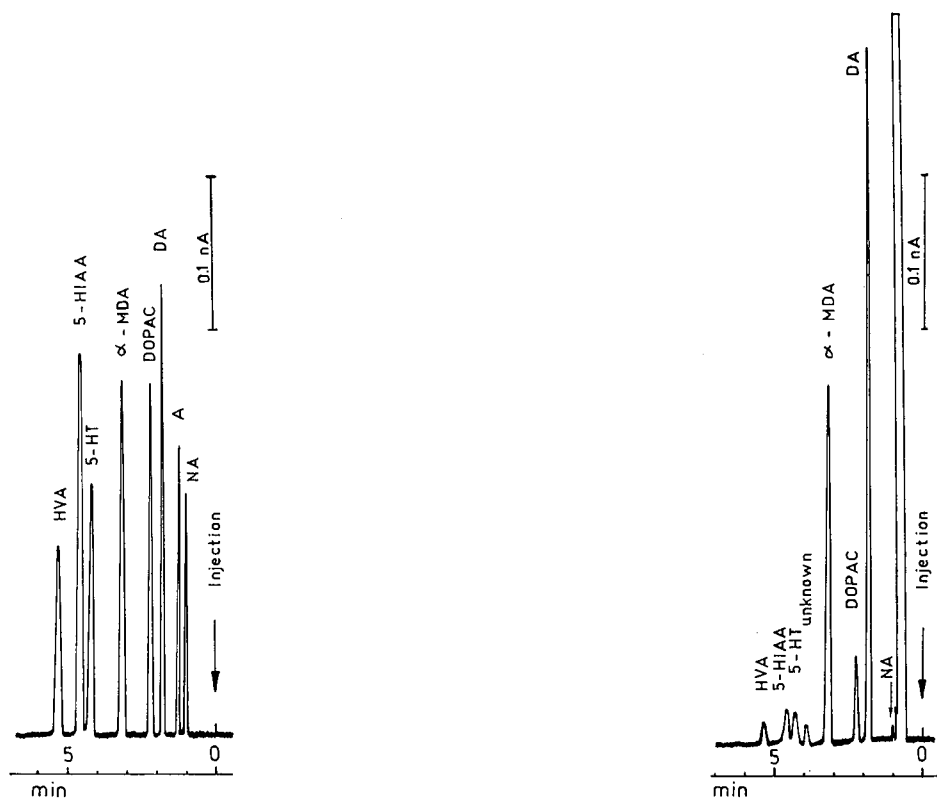


Fig. 7. Separation of standards in an optimized TFA system. Column: Nucleosil  $C_{18}$  ( $3\ \mu\text{m}$ ),  $30 \times 4.0\ \text{mm}$  I.D., with a  $20 \times 4.0\ \text{mm}$  I.D. pre-column. Eluent: aqueous buffer (pH 4.30)–acetonitrile (94:6). Amounts injected: 25 pg (Na, A); 50 pg (DA, DOPAC, 5-HT), 75 pg (5-HIAA) and 200 pg (HVA). Other details as in Fig. 6.

Fig. 8. Representative chromatogram of striatal tissue (untreated rat) after direct injection of centrifuged homogenate. Column and eluent as in Fig. 7.

pre-column, but the resolutions are still good. No chromatographic interference was found.

For fast analyses and high sensitivity it is essential that the  $k'$  values are as low as possible, which in turn also means that the solvent fronts should be as "clean" as possible. If homogenization is carried out with the acidified mobile phase, even direct injection of the extracts causes a narrow solvent front eluting earlier than  $k' = 0.6$ , indicating that the broad solvent fronts in earlier papers were the consequence of a chromatographic imbalance after the injection of perchloric acid-containing homogenates rather than of an excessive amount of impurities in the sample. At proper homogenization buffer-to-tissue ratios the mobile phase is at least as effective as 0.1 *M* perchloric acid in extraction efficiency and in precipitating tissue proteins<sup>13,14</sup>.

The sensitivity of this assay is more than sufficient to determine each of the amines and the metabolites studied in an extract derived from about 0.5 mg of tissue.

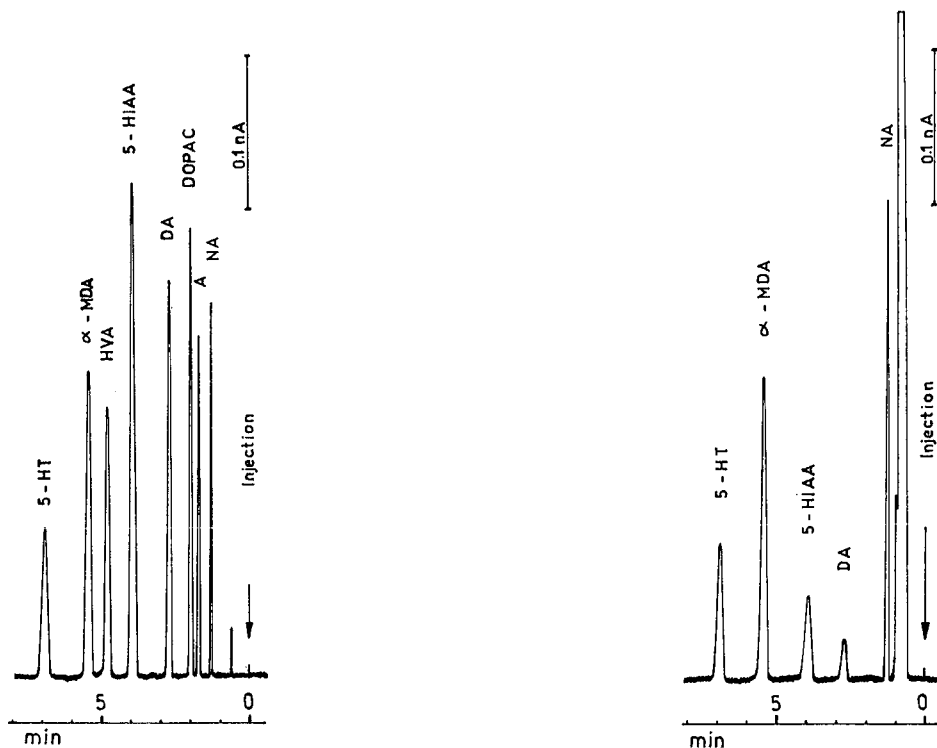


Fig. 9. Separation of standards in an optimized HFBA system. Column as in Fig. 7. Eluent: aqueous buffer (pH 4.35)-acetonitrile (94:6). HFBA concentration in the aqueous buffer: 12 mM. Other details as in Fig. 1.

Fig. 10. Representative chromatogram of hypothalamic tissue (untreated rat) after direct injection of centrifuged homogenate. Column and eluent were as in Fig. 9.

The detection limits for these compounds (amount injected, twice the noise) in the system shown in Fig. 7 were as follows: 1.25 pg for NA, 1.05 pg for A, 1.30 pg for DA, 1.70 pg for DOPAC, 2.35 pg for 5-HT, 2.35 pg for 5-HIAA and 12.5 pg for HVA. Table III shows the control levels of the amines and metabolites studied in rat striatum and hypothalamus, as measured under the conditions in Fig. 9. Although A is essentially missing in most regions of the vertebrate brain, the HPLC systems presented here also resolve this compound. The resolution with the short column used under the conditions in Figs. 7 and 9 was not impaired provided that the sample volume injected was kept below 30  $\mu$ l. For larger loads the Vydac column was used. A typical chromatogram of standards obtained from this conventional column (220  $\times$  4.0 mm I.D., 10  $\mu$ m particle size) in an HFBA system is shown in Fig. 11. The often used internal standards isoproterenol and  $\alpha$ -MDA are very similar in their chromatographic properties, but in our systems the use of the latter was slightly more advantageous.

#### *Comparison of optimized systems*

For comparison, we also optimized SOS-containing systems with all three

TABLE III

## CONTROL LEVELS OF AMINES AND METABOLITES IN RAT STRIATUM AND HYPOTHALAMUS

Results are expressed in ng/g wet tissue  $\pm$  S.E.M. ( $n = 5$ ).

Brain area	NA	A	DA	DOPAC	HVA	5-HT	5-HIAA
Striatum	55 $\pm$ 11	ND*	9123 $\pm$ 381	1520 $\pm$ 145	878 $\pm$ 129	418 $\pm$ 42	717 $\pm$ 35
Hypothalamus	1570 $\pm$ 118	ND*	140 $\pm$ 35	ND*	ND*	1210 $\pm$ 210	705 $\pm$ 30

\* ND, not detectable.

columns indicated in Figs. 6, 7 and 11, and compared the separation speeds (the reciprocal of the time needed for a complete chromatographic run) obtained in optimized SOS systems with those shown in Figs. 6, 7, 9 and 11. Other criteria of the comparisons were  $k'_{NA} \geq 0.6$  and  $R_{s\ i,j} \geq 1.3$ , where  $R_{s\ i,j}$  is the resolution of adjacent peaks of compounds  $i$  and  $j$ . Resolution was calculated using the equation  $R_s = 2(t_{R_2} - t_{R_1})/(w_1 + w_2)$ , where  $t_{R_1}$  is the retention time of compound  $i$ ,  $t_{R_2}$  is the retention time of compound  $j$ ,  $w_1$  is the peak width (at the base) of compound  $i$  and  $w_2$  is the peak width of compound  $j$ , both expressed in time units. We found that at identical  $k'_{NA}$  values and sufficient resolution the separation speed of optimized SOS systems was, on average, 20% lower than that of TFA systems and 5–10% lower than that of HFBA systems. Selectivity differences and the lower plate counts achieved with

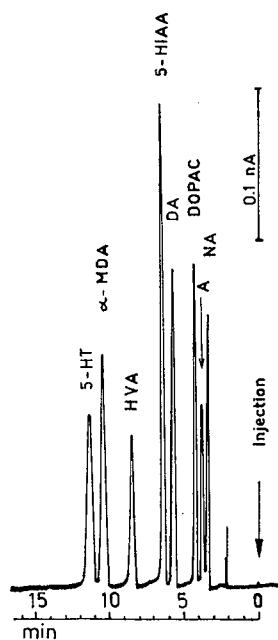


Fig. 11. Separation of standards on a conventional column in an optimized HFBA system. Column: Vydac 218 TPB  $C_{18}$  (10  $\mu$ m), 200  $\times$  4.0 mm I.D., with a 20  $\times$  4.0 mm I.D. pre-column. Eluent: aqueous buffer (pH 4.05)–acetonitrile (94:6). HFBA concentration in the aqueous buffer: 15 mM. Other details as in Fig. 1.

SOS systems (see Table I) may explain the difference in the separation speeds attainable.

Other areas of comparison were the time needed to achieve equilibration and the day-to-day reproducibility of the separations. As was shown in an earlier paper, the equilibration time is directly related to the size of the pairing ion employed<sup>26</sup>. In the equilibration studies we measured the retention times of HVA and 5-HT. By definition, initial equilibrium conditions were reached when the changes in the retention times of HVA and 5-HT in optimized TFA, HFBA or SOS systems were within  $\pm 1$  s (the injections considered were 30 min apart and the temperature and flow-rate were constant). Equilibrium in SOS, HFBA and TFA systems was reached in 13, 2.5 and 2.0 h, respectively.

The day-to-day reproducibility of the separations was poorer with SOS systems than with HFBA or TFA systems. With SOS systems the concentration of the pairing ion must be held constant within narrow limits (the optimal concentration is around 0.5 mM). As a consequence, a slight change in ambient temperature or in the conditions of eluent degassing may induce unwanted changes in the separation patterns. With HFBA and TFA systems these concentration limits are 25 and 200 times wider, respectively, allowing better day-to-day reproducibility.

## CONCLUSIONS

The results show that short-chain perfluorinated carboxylic acids are a very attractive alternative to alkylsulphonates in the reversed-phase ion-pair separation of monoamine transmitters and related metabolites. TFA and HFBA are fully compatible with amperometric detection.

The sample analysis time of 6–8 min is a significant improvement over most published procedures (higher separation speeds were achieved at much higher flow-rates and column back-pressures<sup>27</sup>). The short, conventional bore Nucleosil columns used provide an excellent compromise for maintaining a high sample throughput, low back-pressures and detection limits approaching those achieved in microbore systems<sup>28,29</sup>.

Selectivity differences between TFA and HFBA systems have been explained by the suggestion that TFA and HFBA differ in the dominant mechanisms of ion-pair formation.

## ACKNOWLEDGEMENTS

The authors thank Mrs. E. Blazsek for excellent technical assistance and Mrs. P. Fazekas for typing the manuscript. Special thanks are due to S. Juhász of B.S.T. (Budapest) for packing the chromatographic columns.

## REFERENCES

- 1 J. Wagner, P. Vitali, M. G. Palfreyman, M. Zraika and S. Huot, *J. Neurochem.*, 38 (1982) 1241–1254.
- 2 G. S. Mayer and R. E. Shoup, *J. Chromatogr.*, 255 (1983) 533–544.
- 3 S. M. Lasley, I. A. Michaelson, R. D. Greenland and P. M. McGinnis, *J. Chromatogr.*, 305 (1984) 27–42.
- 4 M. G. Hadfield, C. Milio and N. Narasimhachari, *J. Chromatogr.*, 369 (1986) 449–453.

- 5 I. C. Kilpatrick, M. W. Jones and O. T. Phillipson, *J. Neurochem.*, 46 (1986) 1865–1876.
- 6 R. F. Seegal, K. O. Brosch and B. Bush, *J. Chromatogr.*, 377 (1986) 131–144.
- 7 C. Kim, M. B. Speisky and S. N. Kharouba, *J. Chromatogr.*, 386 (1987) 25–35.
- 8 P. Herregodts, Y. Michotte and G. Ebinger, *J. Chromatogr.*, 421 (1987) 51–60.
- 9 T. P. Moyer and N.-S. Jiang, *J. Chromatogr.*, 153 (1978) 365–372.
- 10 P. A. Asmus and C. R. Freed, *J. Chromatogr.*, 169 (1979) 303–311.
- 11 O. Magnusson, L. B. Nilsson and D. Westerlund, *J. Chromatogr.*, 221 (1980) 237–247.
- 12 R. L. Michaud, M. J. Bannon and R. H. Roth, *J. Chromatogr.*, 225 (1981) 335–345.
- 13 C. D. Kilts, G. R. Breese and R. B. Mailman, *J. Chromatogr.*, 225 (1981) 347–357.
- 14 C. F. Saller and A. I. Salama, *J. Chromatogr.*, 309 (1984) 287–298.
- 15 P. Wester, J. Gottfries, K. Johansson, F. Klintebäck and B. Winblad, *J. Chromatogr.*, 415 (1987) 261–274.
- 16 B. H. C. Westerink, *J. Liq. Chromatogr.*, 6 (1983) 2337–2351.
- 17 C. Horváth, W. Melander, I. Molnár and P. Molnár, *Anal. Chem.*, 49 (1977) 2295–2305.
- 18 W. C. Mahoney, *Biochim. Biophys. Acta*, 704 (1982) 284–289.
- 19 G. Inchauspe, P. Delrieu, P. Dupin, M. Laurent and D. Samain, *J. Chromatogr.*, 404 (1987) 53–66.
- 20 M. Patthy, D. H. Schlesinger, J. Horváth, M. Mason-Garcia, B. Szoke and A. V. Schally, *Proc. Natl. Acad. Sci. U.S.A.*, 83 (1986) 2969–2973.
- 21 J. C. Kraak, K. M. Jonker and J. F. K. Huber, *J. Chromatogr.*, 142 (1977) 671–688.
- 22 B. A. Bidlingmeyer, *J. Chromatogr. Sci.*, 18 (1980) 525–539.
- 23 Á. Bartha, Gy. Vigh, H. A. H. Billiet and L. de Galan, *J. Chromatogr.*, 303 (1984) 29–38.
- 24 C. A. Marsden, *Methodol. Surv. Biochem. Anal.*, 14 (1984) 319–330.
- 25 M. Patthy, R. Gyenge and J. Salát, *J. Chromatogr.*, 241 (1982) 131–139.
- 26 R. Gloor and E. L. Johnson, *J. Chromatogr. Sci.*, 15 (1977) 413–423.
- 27 P. Y. T. Lin, M. C. Bulawa, P. Wong, L. Lin, J. Scott and C. L. Blank, *J. Liq. Chromatogr.*, 7 (1984) 509–538.
- 28 T. A. Durkin, E. J. Caliguri, I. N. Mefford, D. M. Lake, I. A. Macdonald, E. Sundstrom and G. Jonsson, *Life Sci.*, 37 (1985) 1803–1810.
- 29 A. Carlsson, T. Sharp, T. Zetterström and U. Ungerstedt, *J. Chromatogr.*, 368 (1986) 299–308.



CHROM. 20 663

## OPTIMIZING COPPER-BICINCHONINATE CARBOHYDRATE DETECTION FOR USE WITH WATER-ELUTION HIGH-PERFORMANCE LIQUID CHROMATOGRAPHY: A TECHNIQUE TO MEASURE THE MAJOR MONO- AND OLIGOSACCHARIDES IN SMALL PIECES OF WHEAT ENDOSPERM

T. DAVID UGALDE\*, J. PIETER M. FABER and COLIN F. JENNER

*Department of Plant Physiology, Waite Agricultural Research Institute, University of Adelaide, Glen Osmond, S.A. 5064 (Australia)*

(First received February 17th, 1988; revised manuscript received May 16th, 1988)

---

### SUMMARY

Modifications are described to the copper–bicinchoninate detection of reducing sugars to increase sensitivity when used in conjunction with water-elution high-performance liquid chromatography and post-column catalytic hydrolysis of some oligosaccharides to a reducing form. The lowest limit of detection, taken to be the amount of substance that produces a peak height twice the noise level, was about 1 ng for a number of reducing and non-reducing sugars. Colour formation was linear (< 5% deviation) and reproducible (S.D. < 10% at extremes) for detection response equivalent to between 10 ng and 2.5 µg glucose. Use of this technique to measure the major monosaccharides and oligosaccharides in very small pieces of wheat endosperm is described.

---

### INTRODUCTION

Detection of reducing sugars using post-column chemical reactions is simple, highly sensitive and uses reagents that are not highly corrosive. The copper–bicinchoninate technique is based on the reduction of Cu(II) by reducing sugars and the subsequent formation of a deep lavender complex between Cu(I) and 2,2'-bicinchoninate. It was designed originally to detect sugars eluted with 89% ethanol<sup>1</sup>, then was developed further for use with borate buffer<sup>2,3</sup>.

The copper–bicinchoninate technique is well-suited to sugar analysis by high-performance liquid chromatography (HPLC) using the new generations of columns that use water only as the mobile phase<sup>4</sup> and with strongly acidic cation exchangers that hydrolyse some oligosaccharides to reducing form<sup>5</sup>. Without further development, however, the copper–bicinchoninate technique is not as sensitive as a similar detection technique based on 4-aminobenzoic acid hydrazide<sup>6</sup>. Nevertheless,

---

\* Present address: Institute for Irrigation and Salinity Research, Department of Agriculture and Rural Affairs, Tatura, Victoria 3616, Australia.

the copper–bicinchoninate technique is attractive on a number of accounts. For instance, the chemical solutions a and b are more stable than the corresponding solutions of the 4-aminobenzoic acid hydrazide technique, indeed may be kept for months at room temperature if kept in the dark<sup>7,8</sup>, and the mixture of solutions a and b, in contrast, does not require refrigeration before use<sup>8</sup>.

This paper reports modifications to the copper–bicinchoninate detection system to improve sensitivity when used in conjunction with water-elution separation of sugars and on-column hydrolytic conversion of some oligosaccharides to reducing form. The use of this modified technique to measure the major monosaccharides and oligosaccharides in very small pieces of wheat endosperm is described.

## EXPERIMENTAL

The HPLC system comprised two pumps (Waters 510 for mobile phase and Milton-Roy 396-31 for detection reagent, both fitted with high sensitivity pulse dampeners), autoinjector (Waters Wisp 710B), two column heater blocks (controlled by the Waters temperature control module), variable-wavelength spectrophotometer (Waters 481, set at 562 nm), refractive index detector (Varian RI-3) and the Waters 840 control station.

Sugars were separated by Waters SugarPak column (30 cm × 6.5 mm I.D., polystyrene cation-exchange resin in calcium form, 10 µm particle size) or Waters DextroPak column (radial compression cartridge, 10 cm × 8 mm I.D., C<sub>18</sub>, 10 µm particle size) using water only as the mobile phase (0.5 ml/min). A hydrolytic column (12 cm × 4.6 mm I.D.) consisting of Dowex 50W, 16% cross-linked, 200–400 mesh (regenerated periodically with 2 ml 1 M nitric acid) was placed either before or after the analytical column depending on experimental requirements. This resin material is rigid and open which gave long column life and allowed the regeneration solution to be introduced by syringe. Also it is cheap and readily available.

The copper–bicinchoninate solution was essentially as described by Churms<sup>7</sup>. The surfactant Brij 35 was added to solution b, however, to prevent possible deposition of calcium carbonate in the reaction coil which may result from the slow release of calcium from the SugarPak column<sup>4</sup>. Composition of the copper–bicinchoninate solution: Solution a was CuSO<sub>4</sub> · 5H<sub>2</sub>O (1.0 g) and aspartic acid (3.7 g) dissolved in 1 l of high-purity water. Solution b was 2,2'-bicinchoninic acid (Sigma, 4,4'-dicarboxy 2,2'-biquinoline, 2.0 g), Na<sub>2</sub>CO<sub>3</sub> · 10H<sub>2</sub>O (38.0 g) and Brij 35 [Pierce, 30% (w/w), 3 ml] dissolved in 1 l of high-purity water. Colour reagent was a mixture (1:1) of a and b, degassed before use, protected from light.

The rate of calcium release from the SugarPak column is a function of temperature, hence the column was held at the minimum temperature that still provided sufficient isomerization of sugars within the column to prevent anomer separation (*i.e.* 75°C, as determined with glucose, results not shown in detail). The DextroPak column was operated at laboratory temperature.

On-column hydrolysis of sucrose, induced by calcium loss from the SugarPak column, developed to 1% after 6 h of continual use at 75°C (results not shown in detail). Accordingly, this column was regenerated frequently [calcium-EDTA (Sigma, disodium calcium salt), 500 mg/l, 90°C, 2 h, *e.g.* after 6 h use].

The reaction coil consisted of 3, 6, 9 or 12 m × 0.5 mm I.D. stainless-steel tubing

located in a separate heater block. Boiling and outgassing in the hydrolytic column and reaction coil was prevented by inserting a restrictor and cooling coil (1.5 m  $\times$  0.23 mm I.D. stainless-steel tubing) before the spectrophotometer and a backpressure valve (50 p.s.i.) after it.

Grains of wheat (*Triticum turgidum* var. durum cv. Fransawi), grown under controlled environment conditions (21°C/16°C, 14 h light, photon flux density 560  $\mu\text{mol}/\text{m}^2/\text{s}$  at 400–700 nm), were harvested after 7 h of the day cycle twenty days after anthesis. All other tissues were peeled away from the endosperm, and the endosperm cavity was flushed with water (1 ml over 15 s). As soon as each endosperm was prepared (always within 1 min of harvest), it was plunged into hot (75°C) 90% ethanol, blended and extracted. Pooled supernatants (from six grains) were dried under vacuum and redissolved in pentachlorophenol solution (300  $\mu\text{g}/\text{l}$ ).

## RESULTS AND DISCUSSION

### *Flow-rate of the copper-bicinchoninate solution*

The volume ratio of copper-bicinchoninate solution to column mobile phase ranges between 0.7:1<sup>9</sup> and 4.0:1<sup>3</sup>. With water-elution HPLC, the volume ratio can be reduced substantially (Fig. 1). A ratio of 0.3:1 was chosen for all subsequent work.

### *Interaction of temperature and reaction time on the formation of colour*

Colour yield for glucose and fructose, as related to temperature and reaction time is shown in Fig. 2. Reaction time was varied by using different lengths of reaction coil. The optimum balance between colour formation and decay occurred at 110°C with a reaction time of 1.8 min (6 m reaction coil). These conditions produced maximum signal-to-noise ratio and near-minimum band spreading (not shown).

### *Performance of the hydrolytic column*

Equal amounts of sucrose, glucose and fructose were injected with the hydrolytic column placed between the analytical column and the copper-bicinchoninate

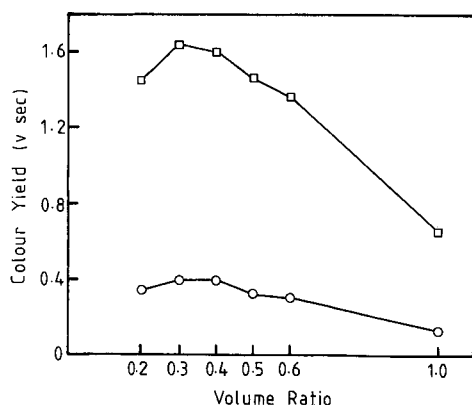


Fig. 1. Colour yield as a function of the volume ratio of copper-bicinchoninate reagent to mobile phase for 500 ng of glucose (○) and fructose (□). Flow-rate of mobile phase = 0.5 ml/min, length of reaction coil = 6 m, reaction temperature = 90°C.

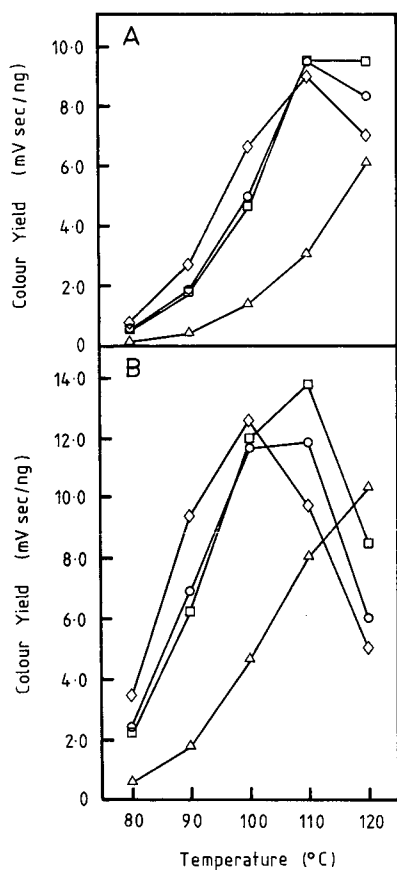


Fig. 2. Colour yield as a function of temperature and reaction time for glucose (A) and fructose (B); ◇ = 3.6 min, ○ = 2.7 min, □ = 1.8 min and △ = 0.9 min.

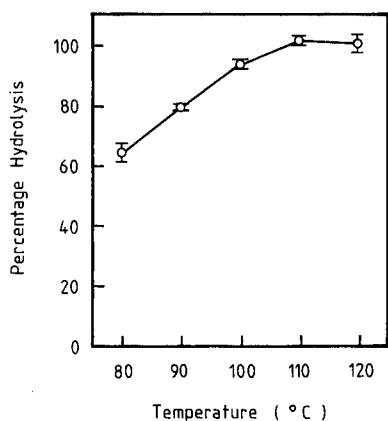


Fig. 3. Hydrolysis of sucrose (100 ng on-column) as a function of temperature; mean  $\pm$  1 S.D. of three replicates.

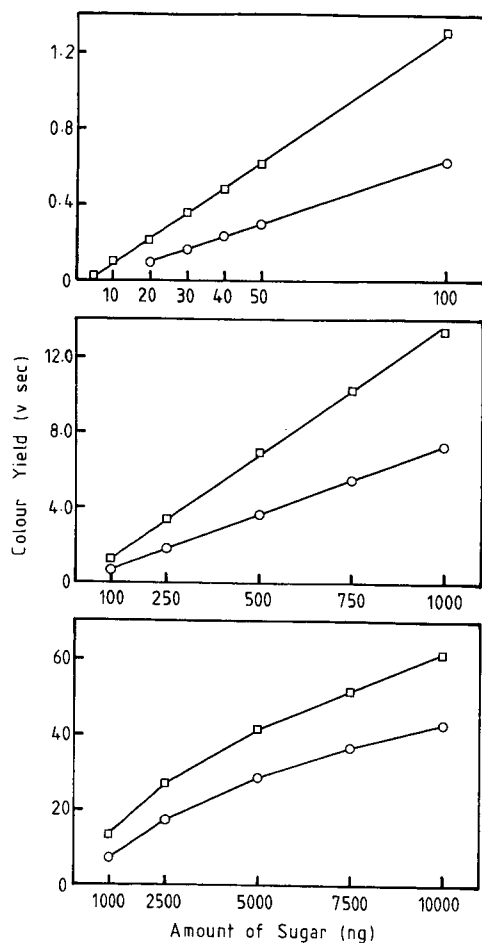


Fig. 4. Colour yield of glucose (○) and fructose (□) as a function of amount on column. (Mean of two replicates shown).

TABLE I

LOWEST LIMIT OF DETECTION AND MINIMUM ANALYSABLE AMOUNT OF A NUMBER OF SUGARS

See text for definitions. Mobile phase, water at 0.5 ml/min; copper-bicinchoninate solution, 0.15 ml/min; reaction time, 1.8 min; temperature of hydrolytic column and reaction coil, 110°C.

Sugar	Lowest limit of detection (ng)	Minimum analysable amount (ng)
Glucose	1.0	10
Fructose	0.5	5
Sucrose	1.0	7
Maltose	2.0	20
Raffinose	3.0	25
Stachyose	5.0	50

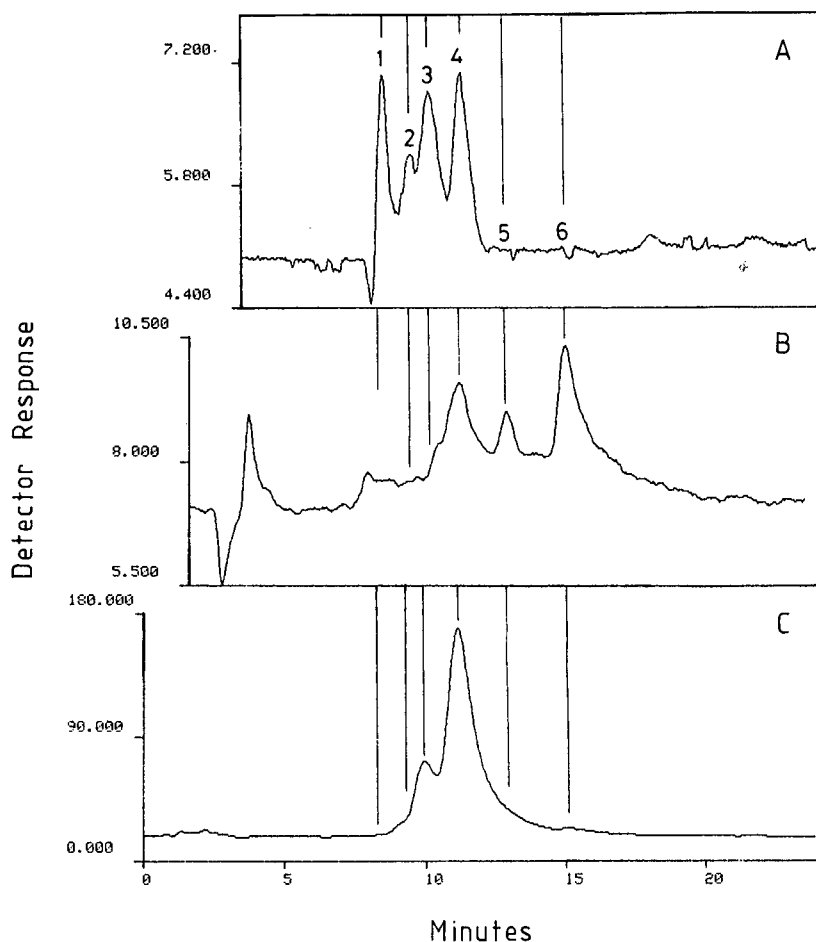


Fig. 5. Analysis of the ethanolic extract of wheat endosperm using the SugarPak column and three methods of detection: differential refractometry (A), the copper-bicinchoninate system (B), and the copper-bicinchoninate system with the hydrolytic column (C). Peaks: 1 = position of amino acids, salts; 2 and 3 = oligosaccharides with DP > 2; 4 = sucrose, maltose; 5 = glucose; 6 = fructose.

detection system. The degree of sucrose hydrolysis was determined by colour yield at the retention time of sucrose relative to the mean colour yield of glucose and fructose. Hydrolysis was complete at 110°C (Fig. 3) and independent of amount on column between 20 ng and 5 µg (not shown).

In a second test, the hydrolytic column was placed in front of the analytical column and differential refractometry was used for detection. In this way, the appearance of the products of hydrolysis was measured concurrent with the decrease in the original compound. At 110°C, sucrose was hydrolyzed completely, producing equal amounts of glucose and fructose. Raffinose was hydrolyzed to fructose and melibiose, and stachyose to fructose and manninotriose. Maltose was unaffected. Evidently, under the conditions described  $\alpha$ -D-(1-2) linkages were hydrolyzed while  $\alpha$ -D-(1-4) and  $\alpha$ -D-(1-6) linkages remained essentially intact.

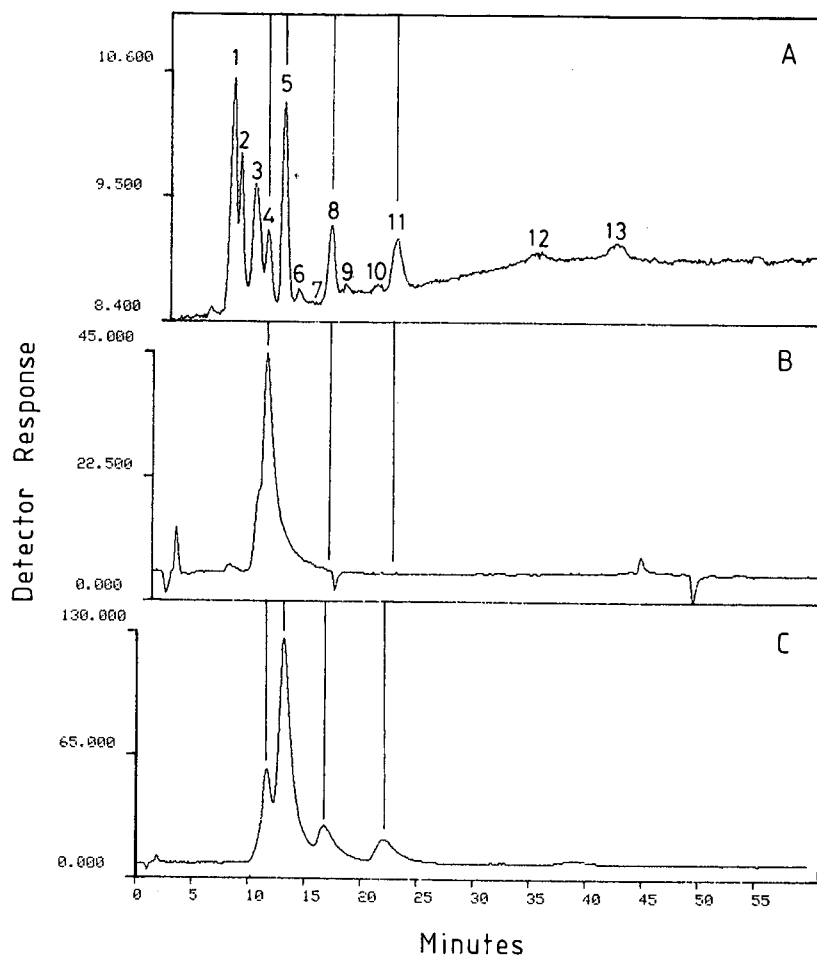


Fig. 6. As Fig. 5. Analysis using DextroPak column. Peaks: 1 and 2 = position of salts, amino acids, organic acids; 3 = hexoses, amino acids; 4 = maltose; 5 = sucrose; 6, 10 = unknown; 7 = stachyose; 8, 11, 13 = fructans; 9, 12 = artifacts with differential refractometry.

#### *Linearity and range*

Colour yield was linear ( $<5\%$  deviation) for glucose between 10 ng and  $2.5\ \mu\text{g}$  and for fructose between 5 ng and  $1.5\ \mu\text{g}$  (Fig. 4). Table I shows the lowest limit of detection (defined as the amount of substance injected onto the column that produces a peak height twice the noise level<sup>10</sup> and the minimum analysable amount (S.D.  $<10\%$  from six injections) for a number of carbohydrates.

#### *Routine use*

Our experimental programme called for a technique to measure the major soluble carbohydrates in very small pieces of wheat endosperm (100–150 ng dry weight). While it is difficult to compare sensitivities of different techniques without a direct side-by-side test and possibly further development, the copper-bicinchoninate

TABLE II

RETENTION TIMES AND RELATIVE RESPONSE FACTORS OF SOME STANDARD SUGARS AND SOME SUGARS EXTRACTED FROM WHEAT ENDOSPERM AFTER SEPARATION ON THE DEXTROPAK COLUMN

Peak numbers refer to peaks described in Fig. 6. Values for standard sugars are the mean of two replicates and the values for extracted sugars are the mean of four replicates. Mobile phase, water at 0.5 ml/min; copper–bicinchoninate solution, 0.15 ml/min; reaction time, 1.8 min; temperature of hydrolytic column and reaction coil, 110°C. ND = not detected.

	<i>Standard sugars</i>			<i>Extracted sugars</i>				
	<i>Maltose</i>	<i>Sucrose</i>	<i>Raffinose</i>	<i>Peak 4</i>	<i>Peak 5</i>	<i>Peak 6</i>	<i>Peak 11</i>	<i>Peak 13</i>
Detection by differential refractometry								
Retention time (min)	8.7	10.1	14.4	8.7	10.1	14.5	20.2	42.0
Detection using copper bicinchoninate system								
Retention time (min)	10.2			10.1				41.5
Relative response factor*	464	NIL	NIL	547	ND	ND	ND	13
Detection using hydrolytic column plus copper bicinchoninate system								
Retention time (min)	11.8	13.2	16.7	11.7	13.1	16.8	22.1	39.0
Relative response factor*	507	1205	190	569	1357	777	492	149

\* Relative response factor = the ratio of the response factor value for detection using the described method to the response factor value for differential refractometry. In effect, it is a measure of the colour yield per unit of refractive index.

technique, as described, seemed at least as sensitive as the similar detection system based on 4-aminobenzoic acid hydrazide (Table I<sup>6,8</sup>).

The copper–bicinchoninate technique, with the hydrolytic column and the reaction coil placed in the one heater block at 110°C, has been used routinely for several years now, although this high temperature does accelerate performance decline of the hydrolytic column and the packing must be changed periodically.

Extracts from whole wheat endosperms were analyzed using the SugarPak and DextroPak columns with three methods of detection: differential refractometry, the copper–bicinchoninate system, and the copper–bicinchoninate system with the hydrolytic column (Figs. 5 and 6). Detection response was used as the first step in solute identification. For instance the retention time of peak number 8 after separation using the DextroPak column (see Fig. 6) suggested raffinose, but its detection response did not (Table II). Component analysis of the oligosaccharide(s) of peak number 8 showed later that no galactose was present, only glucose and fructose.

For routine determinations, the extracts of the small pieces of wheat endosperm were analyzed using the copper–bicinchoninate system in two ways: the SugarPak column without the hydrolytic column (Fig. 5b) and the DextroPak with the hydrolytic column (Fig. 6c). This allowed analysis of all the major monosaccharides and oligosaccharides in wheat endosperm with a high degree of sensitivity and precision.

A more detailed account of the component analysis of the oligosaccharides and of the distribution of soluble sugars within the wheat grain is to be published elsewhere.

#### ACKNOWLEDGEMENTS

We are grateful to B. Walker and M. Dowling of Waters Chromatography Division, Australia, who coached us in the art of HPLC usage. The work was assisted by grants to C.F.J. from Wheat Research Council.

#### REFERENCES

- 1 K. Mopper and E. M. Grindler, *Anal. Biochem.*, 56 (1973) 440.
- 2 K. Mopper, *Anal. Biochem.*, 87 (1978) 162.
- 3 M. Sinner and J. Puls, *J. Chromatogr.*, 156 (1978) 197.
- 4 A. W. Wolkoff, M. E. M. Dicks, J. B. McCabe and W. R. Day, *Proceedings of the Pittsburgh Conference, Atlantic City, NJ*, 1983, paper 472.
- 5 P. Vrátný, R. W. Frei, U. A. Th. Brinkman and M. W. F. Nielen, *J. Chromatogr.*, 295 (1984) 355.
- 6 P. Vrátný, U. A. Th. Brinkman and R. W. Frei, *Anal. Chem.*, 57 (1984) 224.
- 7 S. C. Churms, in G. Zweig and J. Sherma (Editors), *CRC Handbook of Chromatography, Vol. 1, Carbohydrates*, CRC Press, Boca Raton, FL, 1982, p. 175.
- 8 R. A. Femia and R. Weinberger, *J. Chromatogr.*, 402 (1987) 127.
- 9 J. Barr and P. Nordin, *Anal. Biochem.*, 108 (1980) 313.
- 10 K. P. Hupe, G. Rozing and H. Schrenker, in A. Henschen, K. P. Hupe, F. Lottspeich and W. Voelter (Editors), *High-Performance Liquid Chromatography in Biochemistry*, VCH publishers, 1985, p. 79.



CHROM. 20 644

## HIGH-PERFORMANCE LIQUID CHROMATOGRAPHIC DETERMINATION OF GLUCOSIDES (GLUCOSE CONJUGATES) WITH POST-COLUMN REACTION DETECTION COMBINING IMMOBILIZED ENZYME REACTORS AND LUMINOL CHEMILUMINESCENCE

PHILIP J. KOERNER, Jr.\* and TIMOTHY A. NIEMAN\*

*Department of Chemistry, University of Illinois, 1209 W. California St., Urbana, IL 61801 (U.S.A.)*

(Received April 11th, 1988)

---

### SUMMARY

This detection method makes use of sequential immobilized enzyme reactors (IMER) to first hydrolyze  $\beta$ -D-glucosides to  $\beta$ -D-glucose (using  $\beta$ -glucosidase) and then to produce hydrogen peroxide from the  $\beta$ -D-glucose (using glucose oxidase); the hydrogen peroxide is then detected with luminol chemiluminescence. This method has been used for the determination of individual  $\beta$ -D-glucosides (phenyl, *p*-nitrophenyl, and salicin) via flow-injection analysis and has been extended to the determination of a mixture of glucosides following their separation via reversed-phase high-performance liquid chromatography. The use of up to 30% acetonitrile in the buffered mobile phase had very little effect on the efficiency of the  $\beta$ -glucosidase and glucose oxidase enzyme reactors; overall the use of acetonitrile did not affect the linear working range or detection limits for the glucosides. Chromatographic detection limits are approximately  $0.1 \mu\text{M}$  (2 pmol) with a linear working range of more than three decades.

---

### INTRODUCTION

In recent years chemiluminescence (CL) has become an attractive detection method for analytical determinations due to the very low detection limits and wide linear working ranges which can be obtained while using relatively simple instrumentation<sup>1–3</sup>. However, analytical applications of CL based detection have been limited due to the lack of selectivity inherent to the CL reaction. This problem can be overcome by coupling the sensitivity of CL detection with a highly selective chemical or physical step, such as enzymatic reactions<sup>4–7</sup>, immunoassay<sup>3,8–10</sup>, or liquid chromatography<sup>11–23</sup>.

The CL reaction of interest in this study is the luminol (3-aminophthalhydrazide) reaction. This reaction has been used in conjunction with enzyme reactions

---

\* Present address: E.I. DuPont Co., Chemicals and Pigments Dept., Jackson Laboratory/Building 1155(U), Wilmington, DE 19898, U.S.A.

for the determination of a variety of species. Analytes which can be converted in one or more enzymatic reactions to hydrogen peroxide have been quantitated by luminol CL. The luminol CL reaction has also been applied to the detection of organic species separated by high-performance liquid chromatography (HPLC)<sup>13-17</sup> and for the detection of metal ions separated as their chloro complexes on a strong anion-exchange column<sup>22,23</sup>.

There have been two reports in the literature on the combined use of HPLC with enzyme reactions followed by CL detection; however, neither utilized the luminol CL reaction. The first involved the enzymatic hydrolysis of  $\beta$ -D-glucuronides to glucuronic acid which was then detected with the lucigenin CL reaction after potential interferants (other organic reductants) were removed by anion-exchange chromatography<sup>12</sup>. The second involved the reversed-phase separation of a mixture containing acetylcholine and choline followed by enzymatic conversion to hydrogen peroxide and peroxyoxalate CL detection<sup>21</sup>. We report here the first example of the coupling of HPLC with enzyme reactions and luminol CL detection.

The use of the luminol CL reaction has been investigated in this study for the analytical determination of  $\beta$ -D-glucosides.  $\beta$ -D-Glucosides are conjugates of  $\beta$ -D-glucose and "foreign" molecules (such as herbicides and other potentially toxic organic species). These conjugates are produced primarily in plants (and to a lesser extent in mammals) as a means of metabolizing and eliminating these foreign molecules. The formation of glucosides in plants is analogous to the formation of glucuronides (conjugates of glucuronic acid) in mammals. Glucuronides are formed in the liver and serve to eliminate otherwise insoluble and potentially toxic organic species, thus permitting their elimination from the body.

The enzyme  $\beta$ -glucosidase specifically catalyzes the hydrolysis of  $\beta$ -D-glucosides to produce  $\beta$ -D-glucose and the corresponding organic compound (aglycon). The enzyme glucose oxidase catalyzes the oxidation of  $\beta$ -D-glucose to produce hydrogen peroxide which will then react with an alkaline solution of luminol to generate CL. An example of this scheme is shown for a  $\beta$ -D-glucoside in Fig. 1. In this study the  $\beta$ -glucosidase and glucose oxidase have been immobilized by covalent attachment to controlled pore glass (CPG) and packed into small columns, or immobilized enzyme reactors (IMER). The sample, in a buffered stream, first passed through the  $\beta$ -glucosidase IMER where the glucoside bond is hydrolyzed to produce glucose, and then passes through the glucose oxidase IMER where the glucose reacts to produce hydrogen peroxide. The enzymatically generated hydrogen peroxide is then quantitated by the luminol CL reaction.

In this paper a method for the determination of glucosides using immobilized enzymes and CL detection is reported. This enzyme coupled CL detection method is then extended to the determination of a mixture of glucosides after separation on a reversed-phase column.

## EXPERIMENTAL

### Reagents

The glucosides used in this study were: salicin (2-(hydroxymethyl)phenyl- $\beta$ -D-glucoside), phenyl- $\beta$ -D-glucoside, and *p*-nitrophenyl- $\beta$ -D-glucoside (all from Sigma). The structures of these glucosides are shown in Fig. 2. The corresponding aglycons

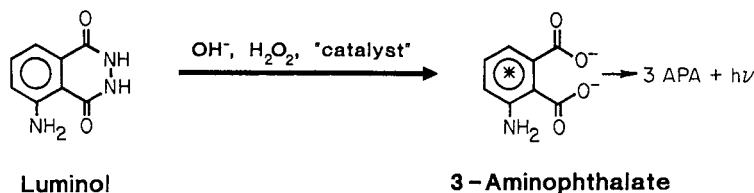
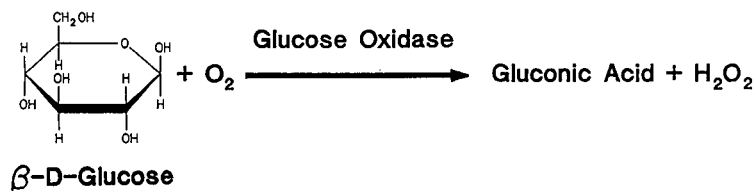
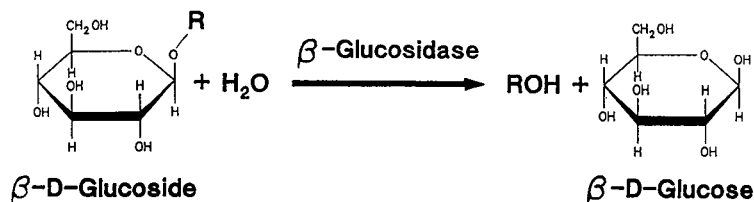


Fig. 1. Reaction scheme for the determination of  $\beta$ -D-glucosides via luminol chemiluminescence.

used to study their effects on CL detection were: phenol (Mallinckrodt), and *p*-nitrophenol (Aldrich).

The enzymes used in this study were  $\beta$ -glucosidase and glucose oxidase.  $\beta$ -Glucosidase (E.C. 3.2.1.21) was obtained from Fluka (from almonds) with an activity of  $\sim 6$  units/mg with salicin as the substrate at pH 5.0 at 37°C. Glucose oxidase (E.C. 1.1.3.4) was obtained from Amano Enzymes (from *Aspergillus* sp.) with an activity of 109 units/mg with glucose as the substrate at pH 5.1 at 35°C.

The reagents used for enzyme immobilization include 3-aminopropyltriethoxysilane obtained from Petrarch Systems and glutaraldehyde (25% in water) obtained from Eastman Kodak. Enzymes were immobilized onto controlled pore glass (CPG) obtained from Electro Nucleonics with 125–180  $\mu\text{m}$  diameter (80–120 mesh) and 250 Å average pore size, and onto CPG with 37–74  $\mu\text{m}$  diameter (200–400 mesh) and 547 Å average pore size.

Luminol was obtained from Aldrich. Horseradish peroxidase (E.C. 1.11.17) was obtained from Sigma as Type I with an activity of 95 units/mg. Hemin was obtained from Sigma as Type I. All other chemicals were analytical reagent grade. All chemicals were used as purchased without further purification. All solutions were prepared with water purified by a Millipore/Continental Milli-Q water purification system.

Stock solutions (10 mM) of all glucosides were prepared fresh daily by weighing accurately and dissolving with water. Serial dilutions of the stock solutions with water yielded the required working solutions which were prepared immediately prior to use.

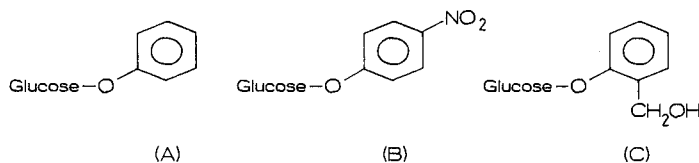


Fig. 2. Structures of glucosides studied: (A) phenyl glucoside, (B) *p*-nitrophenyl glucoside and (C) salicin.

A stock solution (10 mM) of glucose was prepared in a similar fashion and could be stored refrigerated for 3–4 days before significant decomposition occurred. Working solutions were prepared from this stock solution prior to use. Working solutions of hydrogen peroxide were prepared fresh daily by serial dilution from 30% (10 M) hydrogen peroxide.

The chemiluminescence reagent solution used contained 0.4 mM luminol, 8 mg/l horseradish peroxidase (HRP), 2  $\mu$ M hemin, and 0.1 M sodium phosphate dibasic buffered at pH 11.6. This solution was prepared from a stock solution of 2 mM luminol in 0.5 M sodium phosphate dibasic (pH 11.4) and a stock solution of 2 mM hemin by the appropriate dilution in water. The HRP was added as a solid and the solution diluted to volume.

The HPLC mobile phase were prepared fresh daily and filtered through a 0.2- $\mu$ m Nylon 66 membrane filter (Rainin) and then degassed prior to use.

#### Enzyme immobilization

Glutaraldehyde-bound CPG was prepared as described previously<sup>24,25</sup>. To 0.5 g of glutaraldehyde-bound CPG was added 10 ml of 0.05 M sodium pyrophosphate (pH 7.5) containing either 100 mg of glucose oxidase (10 900 units) or 100 mg of  $\beta$ -glucosidase (ca. 600 units). The enzyme immobilization proceeded as described previously<sup>25</sup>. The immobilized glucose oxidase and  $\beta$ -glucosidase were stored in 0.05 M sodium pyrophosphate buffer (pH 7.5) at ca. 5°C.

For the flow injection analysis studies the immobilized enzymes were slurry packed into plexiglas columns 2.25 in.  $\times$  0.125 in. I.D. The column was capped with nylon end fittings containing 20  $\mu$ m stainless-steel frits and designed to accept 1/4–28 fittings for easy insertion into the flow system.

For the HPLC studies the immobilized enzymes were slurry packed under vacuum into 70 mm  $\times$  2.0 mm I.D. stainless-steel HPLC guard columns (Whatman). The columns were equipped with zero-dead-volume end fittings containing 2  $\mu$ m stainless-steel frits and designed to accept 1/16 in. Swagelok (female) fittings for incorporation into the HPLC flow system.

#### Instrumentation

The glucoside analyses were carried out with the flow injection system shown in Fig. 3. A Rainin Rabbit peristaltic pump was used to pump each of two channels, one containing buffer and the other containing the CL reagent solution, at a flow-rate of 1.5 ml/min. Samples of the glucoside of interest (77  $\mu$ l) were injected with a Rheodyne Model 5250 sample injection valve into the buffer stream, which contained 1 mM phosphate buffered at pH 6.5 and 0–30% acetonitrile (v/v). The sample was then carried through an IMER containing immobilized  $\beta$ -glucosidase and an IMER

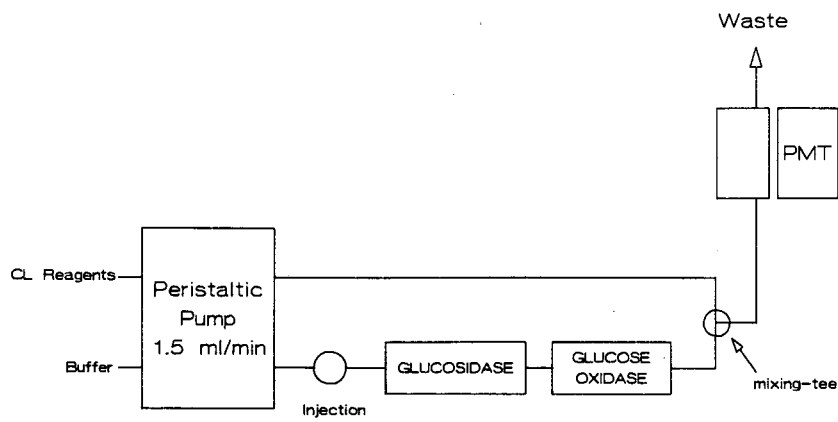


Fig. 3. Flow system used for flow injection determinations.

containing immobilized glucose oxidase. The sample in the buffer stream then combined at a mixing-tee with the CL reagent solution and passed through a short segment (80 mm  $\times$  1.0 mm I.D.) of microporous PTFE tubing (Anspec) to remove any air bubbles present and on to the flow cell.

For the analysis of mixtures of glucosides the HPLC flow system shown in Fig. 4 was used. Isocratic HPLC separations were carried out using a modular HPLC system consisting of an Altex Model 110A HPLC pump, a silica pre-column, an Altex Model 210 injection valve equipped with a 20- $\mu$ l sample loop, a Partisil ODS-2 guard column (70 mm  $\times$  2.0 mm I.D.), a high-pressure in-line filter (Scientific Systems) with replaceable 0.5- $\mu$ m frits, and an HPLC column. Chromatographic separations were obtained using a DuPont Zorbax ODS column (5  $\mu$ m, 250 mm  $\times$  4.6 mm I.D.). In this system the buffer, 1 mM phosphate (pH 6.5) with 0–30% acetonitrile (v/v), was delivered at a flow-rate of 1.0 ml/min. After passing through the HPLC system the column effluent passed through the  $\beta$ -glucosidase and glucose IMERs, then was combined at a mixing-tee with the CL reagent solution which was delivered with

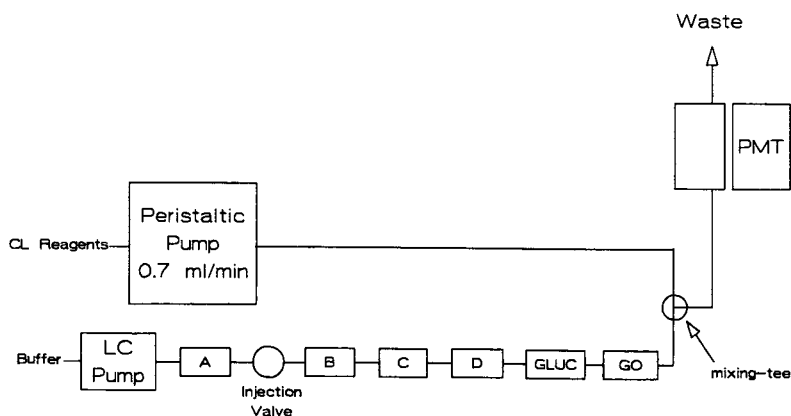


Fig. 4. HPLC flow system. A = Silica pre-column; B = guard column; C = column prefilter; D = analytical column; GLUC = glucosidase IMER; GO = glucose oxidase IMER.

a peristaltic pump at a flow-rate of 0.7 ml/min. The combined solution then passed through the flow cell.

In both the flow injection and HPLC systems described above, the flow cell (with a volume of 50  $\mu$ l) was placed directly adjacent to the photomultiplier tube (Hamamatsu 1P28 biased at  $-960$  V) where the CL emission was detected. The signal was then amplified by a Pacific Precision Instruments Model 126 photometer and output to a strip chart recorder.

Optimization of separation conditions, and determination of the retention times of the various glucosides, was initially carried out with the HPLC system shown in Fig. 4 using an Altex Model 153 UV-VIS detector to monitor the column effluent.

#### *Determination of IMER activities*

The efficiency of the glucose oxidase IMERs were determined by measuring the quantity of hydrogen peroxide produced from the oxidation of  $\beta$ -D-glucose in a single pass through the enzyme reactor. A 77- $\mu$ l sample of 10  $\mu$ M D-glucose was carried through the IMER in a buffered flowing stream and the hydrogen peroxide produced quantitated by luminol CL. The signal obtained was corrected for the fact that a solution of D-glucose at equilibrium contains only 64% of the  $\beta$ -anomer, and then compared with the signal obtained for a similar injection of 10  $\mu$ M hydrogen peroxide.

In a similar fashion the efficiency of the  $\beta$ -glucosidase IMERs were determined. A 77- $\mu$ l sample of 10  $\mu$ M *p*-nitrophenyl- $\beta$ -D-glucoside was carried through the  $\beta$ -glucosidase and glucose oxidase IMERs and the hydrogen peroxide produced quantitated by luminol CL. The signal obtained was corrected for the efficiency of the glucose oxidase column and then compared with the signal obtained for a similar injection of 10  $\mu$ M hydrogen peroxide. The efficiency of the  $\beta$ -glucosidase IMERs were also determined by measuring the quantity of glucoside which was hydrolyzed in a single pass through the enzyme reactor. A 77- $\mu$ l sample of 1.0 mM *p*-nitrophenyl- $\beta$ -D-glucoside was carried through the IMER in a buffered flowing stream, the hydrolyzed glucoside was collected in a volumetric flask, and the amount of *p*-nitrophenol in this solution was quantitated by measuring the absorbance of the solution at 400 nm.

## RESULTS AND DISCUSSION

#### *Flow injection detection of $\beta$ -D-glucosides*

The flow injection system used in this study is essentially the same as that used for the determination of glucose and other sugars using immobilized enzymes and luminol CL detection<sup>25</sup>. Of these sugars only glucose has a corresponding oxidase enzyme which will produce hydrogen peroxide as a product of an enzymatic reaction. Therefore, in order to quantitate the other sugars by CL they must first be converted to glucose via other enzymatic reactions. Similarly,  $\beta$ -D-glucosides cannot react directly with an enzyme to produce hydrogen peroxide but must first be hydrolyzed by  $\beta$ -glucosidase to produce  $\beta$ -D-glucose which can then be quantitated by CL after reaction with glucose oxidase to produce hydrogen peroxide. Since the hydrolysis of  $\beta$ -D-glucosides produces only  $\beta$ -D-glucose, there is no need for the presence of the enzyme mutarotase, which catalyzes the interconversion of the  $\alpha$  and  $\beta$  anomers of D-glucose.

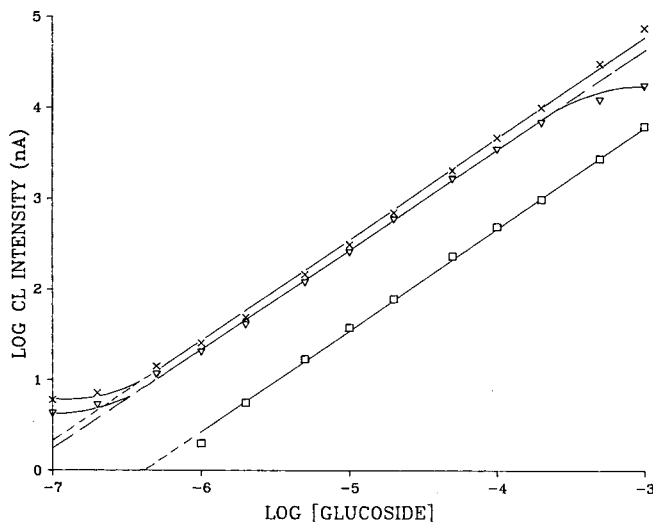


Fig. 5. Flow injection working curves for  $\beta$ -D-glucosides.  $\nabla$  = Salicin,  $\square$  = phenyl glucoside and  $\times$  = *p*-nitrophenyl glucoside.

Using the flow injection system shown in Fig. 3 with an aqueous carrier stream that contained 1 mM phosphate (pH 6.5), working curves for the three glucosides were obtained and are shown in Fig. 5. The log-log working curves for the three "model" glucosides (salicin, phenyl glucoside, and *p*-nitrophenyl glucoside) are linear and cover over three orders of magnitude. Detection limits for these glucosides are on the order of  $\sim 0.5 \mu\text{M}$  ( $\sim 40$  pmol). These glucoside detection limits are comparable to those obtained for the flow injection analysis of sugars using immobilized enzymes and luminol CL detection<sup>25</sup>.

The lower CL intensities observed for equal concentrations of phenyl glucoside relative to those observed for salicin and *p*-nitrophenyl glucoside may have resulted from the inhibition of either enzyme by the aglycon produced after hydrolysis of the glucoside by  $\beta$ -glucosidase. To check this possibility, solutions containing equimolar amounts of  $\beta$ -D-glucose and the aglycons of interest (phenol and *p*-nitrophenol) were prepared. The CL signal obtained after a sample of each solution was carried through the glucose oxidase IMER was compared with the signal obtained for a solution containing only an equimolar amount of  $\beta$ -D-glucose. The CL signals were all of equal intensity. Repeating the same series of injections through the  $\beta$ -glucosidase and glucose oxidase IMERs yielded similar results. Therefore, the lower intensity CL signal observed for phenyl glucoside does not appear to be the result of any inhibition of the enzymes by the aglycon produced upon hydrolysis. The difference in signal intensity observed for a given glucoside concentration is probably caused by the difference in reaction rates and efficiency of the enzyme  $\beta$ -glucosidase for each glucoside. The rate of reaction, as well as the efficiency, of  $\beta$ -glucosidase has been shown to vary with the identity of the substrate<sup>26,27</sup>.

### Mobile phase considerations

To convert the flow injection system to an HPLC system required insertion of a chromatographic column between the injector and the first enzyme column. It was therefore necessary that the mobile phase requirements of the separation be compatible with those of the enzyme reactions and CL detection.

It was expected that in order to obtain a separation of a mixture of these glucosides via reversed-phase HPLC, a significant amount of an organic solvent as modifier would be required in the buffered mobile phase. Therefore, it was necessary to first investigate the effects such an organic solvent would have on the enzyme reactions and the luminol CL reaction. Acetonitrile and methanol are commonly used as organic modifiers in reversed-phase HPLC; however, methanol is known to cause the denaturing of enzymes, thereby making them inactive. In addition, Van Zoonen *et al.*<sup>28</sup> have recently shown that a glucose oxidase IMER retained 25% of its original efficiency when a buffered carrier stream containing 80% (v/v) acetonitrile was used. Therefore, the use of acetonitrile in the buffered carrier stream, and its effect on the enzyme reactions and the luminol CL reaction, was investigated.

Increasing the acetonitrile from 0–30% (v/v) in the 1 mM phosphate carrier stream (buffered at pH 6.5) led to an increase in the observed CL signals for hydrogen peroxide, glucose, and *p*-nitrophenyl glucoside. This is demonstrated in Fig. 6, which shows a plot of CL intensity *versus* percentage acetonitrile for 10  $\mu$ M hydrogen peroxide, 10  $\mu$ M glucose, and 10  $\mu$ M *p*-nitrophenyl glucoside. Using a 1-mM phosphate carrier stream (pH 6.5) containing 0–30% acetonitrile, the efficiencies of the  $\beta$ -glucosidase and glucose oxidase IMERs used in the flow injection studies were determined by CL. The efficiency of the glucose oxidase IMER varies between 80 and 100% while the efficiency of the  $\beta$ -glucosidase IMER varies between 85 and 100%. There is no apparent correlation between the efficiencies of the IMERs and the

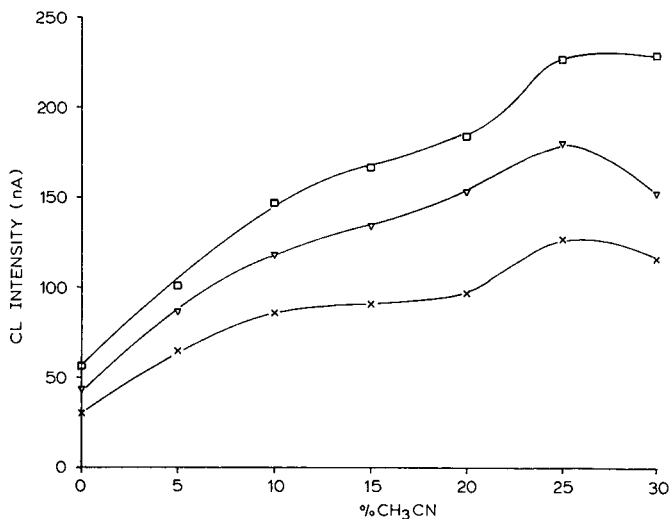


Fig. 6. Plot of CL intensity *vs.* percentage acetonitrile in 1 mM phosphate (pH 6.5) carrier stream. □ = 10  $\mu$ M Hydrogen peroxide, × = 10  $\mu$ M glucose and ▽ = 10  $\mu$ M *p*-nitrophenyl glucoside. The solid lines are drawn merely to connect the data points and not to indicate a particular model for the data relationship.

percentage acetonitrile in the carrier stream. The efficiency of the  $\beta$ -glucosidase IMER was also determined by the absorbance method using *p*-nitrophenyl glucoside as the substrate. For a carrier stream containing 0% acetonitrile, the efficiency determined by absorbance was in agreement with the value obtained by CL.

The efficiency of the IMERs was found to be reversibly affected by the presence of acetonitrile in the carrier stream. The efficiency of the IMERs could be restored by flushing the IMERs with 10 mM phosphate buffer (pH 6.5) for 20 min after it had been exposed to a carrier stream containing acetonitrile.

The higher CL intensities observed in the presence of acetonitrile were somewhat puzzling. Profiles of the CL intensity *versus* time for 0 and 20% acetonitrile were obtained via stopped-flow analysis and were found not to differ significantly in shape. Both profiles show that peak CL intensity is reached after a short induction period, remains at the peak level for several seconds, and then decreases exponentially back to the background over a period of 2 min. In the system containing 20% acetonitrile the peak CL intensity is *ca.* 3.5 times greater than in the system containing no acetonitrile. The background CL emission (*i.e.*, in the absence of hydrogen peroxide) is also increased in the presence of acetonitrile. The presence of acetonitrile may be affecting the quantum efficiencies of the CL process; however, further experiments are required before the effect of acetonitrile on the luminol CL reaction can be more fully understood.

The presence of 0–30% acetonitrile in the buffered carrier stream does not significantly affect the working curves for the model glucosides. The working curves remain linear over greater than three orders of magnitude and the slope changes only slightly, increasing from 1.1 to 1.2 as the percentage acetonitrile increases. The detection limits also remain approximately equal to those obtained in the absence of acetonitrile.

Since the mobile phase pH is a parameter that might be adjusted in optimizing a chromatographic separation, the effect of mobile phase pH on the detection of glucosides was investigated. The work was centered around pH 6.5 because the optimum pH for the use of immobilized glucose oxidase has been reported to be 6.5 (ref. 25). The data obtained are tabulated in Table I. Although pH 6.5 gave the best results, any pH between 6 and 7 would give satisfactory results. For a separation to be carried out at a pH much lower than 6, a pH change between the analytical column and the IMERs would be required since enzymes typically suffer from a loss of activity at very acidic pHs. The buffering capacity of the mobile phase carrying the analyte through the analytical column and the IMERs was kept low (1 mM) so that when this

TABLE I  
EFFECT OF pH ON CL SIGNALS FOR MODEL GLUCOSIDES

	CL intensities (nA)		
	pH 6.0	pH 6.5	pH 7.0
50 $\mu$ M Salicin	16	32	31
200 $\mu$ M Phenyl glucoside	5	12	11
50 $\mu$ M <i>p</i> -Nitrophenyl glucoside	211	230	204

stream mixed with the CL reagent solution (buffered at pH 11.6 with 100 mM phosphate) the resulting solution would remain close to pH 11.6, which is optimal for the luminol CL reaction.

### *Chromatographic separations*

Separations of the glucosides were obtained with a Zorbax ODS (5  $\mu$ m) column using a mobile phase containing 25% acetonitrile in 1 mM phosphate buffered at pH 6.5.

The HPLC system was configured for use with the IMERs and CL detection as diagrammed in Fig. 4. To minimize resolution degradation within the enzyme reactors and associated tubing several changes were made in going from the flow injection system to the HPLC system. The enzymes were immobilized on smaller size CPG (37–74  $\mu$ m) and packed into stainless-steel guard columns, and smaller tubing (0.012 in. I.D.) was used to connect the IMERs to the CL flow cell. With these changes to the flow system the resolution of the glucoside separation obtained with CL detection was 1.2 while with UV detection the resolution was 1.9. The difference in resolution is attributable to dispersion of the analyte bands in the IMERs and to some dilution of the analyte bands caused by the post-column addition of the CL reagent solution.

While the enzymes immobilized on the larger size CPG were useful in the flow injection determination of glucosides, the use of the smaller size CPG was necessary to maintain the resolution of the glucoside separation. Due to the excessive back pressure generated, the use of the smaller CPG as a support for immobilized enzymes is not amenable for use in a flow injection system unless a HPLC pump is used to deliver the buffered carrier stream through the IMERs. A peristaltic pump cannot maintain a constant flow-rate against the higher back pressures created by the use of the 37–74  $\mu$ m CPG. The efficiencies of the  $\beta$ -glucosidase and glucose oxidase IMERs used in the HPLC studies were determined using the chromatographic mobile phase and found to be 72% for glucose oxidase (using the CL method) and 62% for  $\beta$ -glucosidase (using *p*-nitrophenyl- $\beta$ -D-glucoside as the substrate and the absorbance method).

Another factor which could affect the resolution of the separation, as well as the peak CL intensities observed, is the flow-rate of the CL reagents added to the mobile phase downstream of the IMERs. A post-column reagent flow-rate which is too fast could lead to significant dilution of the analyte bands and result in broader and less intense peaks. The flow-rate used to deliver the CL reagents which gave the best results was 0.7 ml/min. Faster flow-rates led to a slight decrease in resolution and less intense peaks, while slower flow-rates gave somewhat lower CL intensities.

Using the conditions which were found to give the best results, a chromatogram demonstrating the separation and CL detection of a mixture containing salicin, phenyl glucoside, and *p*-nitrophenyl glucoside was obtained and is shown in Fig. 7. The chromatographic detection limit for *p*-nitrophenyl glucoside was determined to be *ca.* 0.1  $\mu$ M (*ca.* 2 pmol).

A somewhat better detection limit, in terms of number of moles injected, was observed under the chromatographic conditions compared with the flow injection conditions. This is probably due to the difference in the overall solution flow-rate through the flow cell. Since the efficiencies of the  $\beta$ -glucosidase and glucose oxidase IMERs are approximately equal in the flow injection and HPLC systems, the amount of hydrogen peroxide being produced from a given glucoside concentration is about

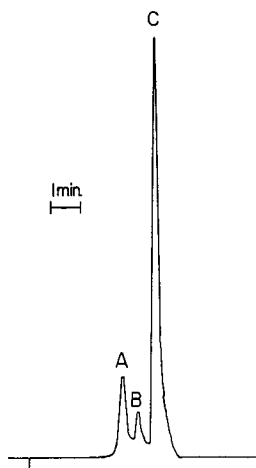


Fig. 7. Isocratic separation of glucoside mixture on Zorbax ODS column (5  $\mu\text{m}$ ) with a mobile phase containing 25% acetonitrile in 1 mM phosphate (pH 6.5). Flow-rate = 1.0 ml/min. A = 50  $\mu\text{M}$  Salicin, B = 200  $\mu\text{M}$  phenyl glucoside and C = 50  $\mu\text{M}$  *p*-nitrophenyl glucoside.

the same. Thus, a faster total flow-rate for the solution passing through the flow cell will lead to the observation of somewhat lower peak CL intensities.

## CONCLUSIONS

Determinations of glucosides typically found as metabolic products of herbicides and pesticides in plants have been reported using a variety of methods<sup>29–31</sup>. Typically the determination of glucosides involves hydrolysis, followed by a chromatographic separation, and detection of the aglycon by UV absorbance or photoconductivity<sup>30,31</sup>. The aglycon 5-hydroxychlorsulfuron, formed by hydrolysis of the glucoside of chlorsulfuron, has been detected at 1.5  $\mu\text{g/ml}$  (*ca.* 30 pmol) using absorbance detection at 254 nm and at 0.10  $\mu\text{g/ml}$  (*ca.* 2 pmol) using photoconductivity detection<sup>31</sup>.

The detection method for glucosides described here using enzymatic reactions and CL detection is simple, fast, yields wide working ranges, and detection limits which are comparable to those reported using other methods. This method offers several advantages over the alternate methods described above. First, it is easier and faster since it utilizes HPLC followed by on-line enzymatic hydrolysis of the glucosides. The use of on-line enzymatic reactions avoids the long reaction times (up to 6 h) and elevated temperatures (37°C) required for the complete enzymatic hydrolysis of glucosides in solution. Second, this method can be extended to the determination of any  $\beta$ -D-glucosides. The photoconductivity detector, while sensitive to the detection of molecules containing sulfur, nitrogen, phosphorous, and halogen atoms, is not suitable for the detection of simpler glucosides. Absorbance methods are limited to the detection of glucosides containing a native chromophore. The detection limits achieved for the glucosides in this investigation are better than those achieved with UV absorbance detection and are comparable to those reported using photoconductivity

detection. Finally, although not done here, the method could be easily adapted to detection of  $\alpha$ -glucosides by using an IMER containing  $\alpha$ -glucosidase instead of, or in addition to, the  $\beta$ -glucosidase column used here.

#### ACKNOWLEDGEMENTS

This work was funded, in part, by DuPont. The authors thank Richard K. Trubey (Agricultural Products Department, DuPont) for supplying the Zorbax ODS column and for several helpful discussions.

#### REFERENCES

- 1 W. R. Seitz, *CRC Crit. Rev. Anal. Chem.*, 13 (1981) 1–58.
- 2 T. J. N. Carter and L. J. Kricka, in L. J. Kricka and T. J. N. Carter (Editors), *Clinical and Biochemical Luminescence*, Marcel Dekker, New York, 1982, Ch. 7, pp. 135–151.
- 3 M. L. Grayeski, in J. G. Burr (Editor), *Chemi- and Bioluminescence*, Marcel Dekker, New York, 1985, Ch. 12, pp. 469–493.
- 4 W. R. Seitz, *Methods Enzymol.*, 57 (1978) 445–462.
- 5 D. T. Bostick and D. M. Hercules, *Anal. Chem.*, 47 (1975) 447–452.
- 6 D. Pilosof and T. A. Nieman, *Anal. Chem.*, 54 (1982) 1698–1701.
- 7 C. A. Koerner and T. A. Nieman, *Anal. Chem.*, 58 (1986) 116–119.
- 8 L. J. Kricka and T. J. N. Carter, in L. J. Kricka and T. J. N. Carter (Editors), *Clinical and Biochemical Luminescence*, Marcel Dekker, New York, 1982, Ch. 8, pp. 153–178.
- 9 W. Klingler, C. J. Strasburger and W. G. Wood, *Trends Anal. Chem.*, 2 (1983) 132–13.
- 10 H. R. Schroeder, *Trends Anal. Chem.*, 1 (1982) 352–354.
- 11 R. L. Veazey and T. A. Nieman, *J. Chromatogr.*, 200 (1980) 153–162.
- 12 L. L. Klopff and T. A. Nieman, *Anal. Chem.*, 57 (1985) 46–51.
- 13 A. MacDonald and T. A. Nieman, *Anal. Chem.*, 57 (1985) 936–940.
- 14 T. Hara, M. Toriyama and T. Ebuchi, *Bull. Chem. Soc. Jpn.*, 58 (1985) 109–114.
- 15 T. Kawasaki, M. Maeda and A. Tsuji, *J. Chromatogr.*, 328 (1985) 121–126.
- 16 S. R. Spurlin and M. M. Cooper, *Anal. Lett.*, 19 (1986) 2277–22.
- 17 P. J. Koerner, Jr. and T. A. Nieman, *Mikrochim. Acta*, II (1987) 79–90.
- 18 S. Kobayashi and K. Imai, *Anal. Chem.*, 52 (1980) 424–427.
- 19 S. Kobayashi, J. Sekino and K. Imai, *Anal. Biochem.*, 112 (1981) 99–104.
- 20 K. W. Sigvardson and J. W. Birks, *Anal. Chem.*, 55 (1983) 432–435.
- 21 K. Honda, K. Miyaguchi, H. Nishino, H. Tanaka, T. Yao and K. Imai, *Anal. Biochem.*, 153 (1986) 50–53.
- 22 W. R. Seitz and D. M. Hercules, in M. J. Cormier, D. M. Hercules and J. Lee (Editors), *Chemiluminescence and Bioluminescence*, Plenum Press, New York, 1973, pp. 427–449.
- 23 M. P. Neary, W. R. Seitz and D. M. Hercules, *Anal. Lett.*, 7 (1974) 583–590.
- 24 K. Hool and T. A. Nieman, *Anal. Chem.*, 59 (1987) 869–872.
- 25 C. A. K. Swindlehurst and T. A. Nieman, *Anal. Chim. Acta*, 205 (1988) 195–205.
- 26 S. Veibel, in J. B. Sumner and K. Myrback (Editors), *The Enzymes: Chemistry and Mechanism of Action*, Vol. 1, Academic Press, New York, 1950, Ch. 6, pp. 583–620.
- 27 R. L. Nath and H. N. Rydon, *Biochem. J.*, 57 (1954) 1–10.
- 28 P. van Zoonen, I. de Herder, C. Gooijer, N. H. Velthorst and R. W. Frei, *Anal. Lett.*, 19 (1986) 1949–1961.
- 29 V. T. Edwards, A. L. McMinn and A. N. Wright, in D. H. Hutson and T. R. Roberts (Editors), *Progress in Pesticide Biochemistry*, Vol. 2, Wiley New York, 1982, Ch. 3, pp. 71–125.
- 30 P. B. Sweetser, G. S. Schow and J. M. Hutchinson, *Pest. Biochem. Physiol.*, 17 (1982) 18–23.
- 31 E. W. Zahnow, *LC, GC, Mag. Liq. Gas Chromatogr.*, 4 (1986) 644–651.

CHROM. 20 675

## PREPARATIVE CHROMATOGRAPHY OF OLIGOGALACTURONIC ACIDS

LANDIS W. DONER\*, PETER L. IRWIN and MICHAEL J. KURANTZ

*U.S. Department of Agriculture, ARS, Eastern Regional Research Center, Philadelphia, PA 19118 (U.S.A.)*

(First received February 4th, 1988; revised manuscript received May 11th, 1988)

---

### SUMMARY

A mixture of oligogalacturonic acids was prepared by partial enzymatic hydrolysis of citrus pectin-derived  $\alpha$ -D-polygalacturonic acid. Both a commercial fungal "pectinase" preparation and a purified *endo*-polygalacturonase isolated from this source by chromatography on carboxymethyl Sephadex C-50 were used to catalyze the hydrolysis. Different product distributions resulted, but even when using pectinase there was no evidence for the formation of unsaturated products from activity of polygalacturonic acid lyase. Individual oligogalacturonic acids were isolated by step-gradient elution (sodium formate, pH 4.7) from the macroporous strong base anion-exchange resin AG MP-1 in the formate form. Pure oligomers to heptagalacturonic acid were isolated in a single run, including gram quantities of tri-, tetra-, and pentagalacturonic acid. The individual oligogalacturonic acids were characterized by fast-atom bombardment mass spectrometry in positive and negative modes.

---

### INTRODUCTION

The dominant structural feature of pectin in the cell walls of higher plants is a linear 1  $\rightarrow$  4- $\alpha$ -linked D-galactopyranuronic acid chain (Fig. 1). In pectin, the carboxyl groups are esterified to various degrees with methoxyl groups. Fundamental studies in both plant biochemistry and pathology have required procedures for the production and isolation of pure oligogalacturonic acids from pectin. The availability of sufficient quantities of such standards with known degrees of polymerization (DP) allows examination of substrate specificities and kinetics of *exo*- and *endo*-polygalacturonases<sup>1</sup>, and polygalacturonic acid lyases from various sources<sup>2,3</sup>. Also, it is known that oligogalacturonic acids which result from the action of such enzymes on plant cell walls elicit defense responses by the host plant against certain microorganisms<sup>4–6</sup>. Often the response is elicited by fragments with discrete DP values, so preparative methods for these compounds to use in bioassays are required.

Both polystyrene and Sephadex based strong anion-exchange packings have been used for the separation of oligogalacturonic acids. The polystyrene based resins have higher loading capacity and are especially useful for separation of lower DP oligomers. Dowex 1-X8 in the formate form was applied to the separation of DP-1

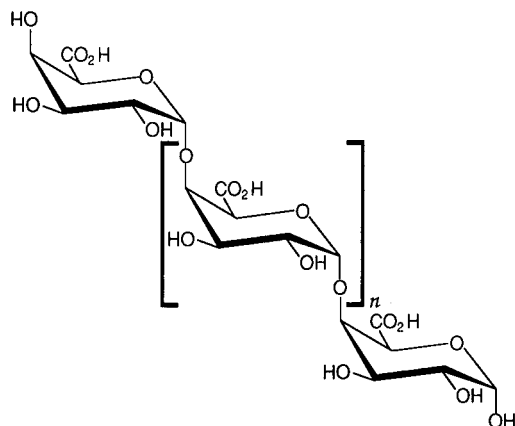


Fig. 1. Polygalactopyranuronic acid structure.

through DP-8, but re-chromatography of pooled fractions was required to obtain pure compounds<sup>7</sup>. Similar results were achieved using AG 1-X8, a refined form of Dowex 1-X8 (ref. 8). Separation on both resins utilized step gradient elutions with sodium formate (pH 4.7). Large elution volumes were used, and the gravity flow-rates were quite slow, so separations required several days. For baseline resolution of small quantities of oligogalacturonic acids to about DP 10, and some resolution of even higher oligomers, chromatography on DEAE-Sephadex A-25 is effective<sup>5</sup>, but also very time-consuming. QAE-Sephadex has also been used to isolate milligram quantities of higher oligomers<sup>9</sup>.

In this report, we describe the first application of the macroporous strong base anion-exchange resin AG MP-1 in the formate form to the isolation of oligogalacturonic acids to DP-7. To our knowledge, this resin has not previously applied to carbohydrate separations, but its versatility has been exemplified in separations of nucleotides<sup>10</sup> and proteins<sup>11,12</sup>. Preparative-scale separations of oligogalacturonic acids on AG MP-1 are more rapid, selective, and efficient than on other resins.

## EXPERIMENTAL

### *Resin conversion*

AG MP-1 anion-exchange resin ( $\text{Cl}^-$ , 200–400 mesh) was purchased from Bio-Rad Labs. (Richmond, CA, U.S.A.) and converted to the formate form as follows. The hydroxide form was generated by stirring the resin (500 ml) in 1.0 *M* sodium hydroxide (12 l) for 3 h. After settling the resin and decanting the alkali, it was rinsed with water (3 l) in a column mode, until the pH of the eluent was about 9. Then 1.0 *M* formic acid (2 l) was passed through the column, followed by water (2.4 l). The resin was removed to a beaker and twice stirred and decanted from water (2.0 l), under which it was stored. These last washings removed excess formic acid and resin fines, which affect chromatographic performance of the resin.

### Monitoring column fractions

Oligogalacturonic acids were qualitatively determined by high-performance thin-layer chromatography (HPTLC)<sup>13</sup> on silica gel (4.5  $\mu$ m particle size, 200  $\mu$ m layer) HPTLC plates (10  $\times$  10 cm), type HP-K (Whatman, Clifton, NJ, U.S.A.). Elution of the plates at 35°C with ethanol–25 mM acetic acid (42:58) allowed effective resolution of products to DP-9. Spots were detected by spraying plates with a solution<sup>14</sup> of aniline (4 ml), diphenylamine hydrochloride (4.0 g), *tert*.-butyl alcohol (120 ml), and ethanol (80 ml), and placing them on a hot plate for a few seconds. For quantitation of oligogalacturonic acids in column fractions, the colorimetric method based on reaction with *m*-hydroxybiphenyl<sup>15</sup> was used.

### Isolation of *endo*-polygalacturonase from “pectinase”

The crude pectinase (50 ml, *Aspergillus niger* source, solution in 40% aqueous glycerol, Sigma, St. Louis, MO, U.S.A.) was dialyzed for 2 h against water, changing to new dialysis tubing each 20 min due to cellulase breakdown of the tubing. The pectinase was then dialyzed against 20 mM sodium acetate buffer (pH 4.4) for 2 h at 4°C, again with frequent changes of the dialysis tubing. The retentate (about 400 ml) was passed through a column of 300 ml carboxymethyl Sephadex C-50 (sodium exchanged), and eluted with 1 l acetate buffer (20 mM, pH 4.4). Proteins were fractionated by eluting with a linear gradient (1.2 l) of 0 to 0.3 M sodium chloride in 20 mM acetate buffer (pH 4.4), monitoring for protein at 280 nm. Three activities were separated, an *exo*-polygalacturonase followed by two *endo*-polygalacturonases. The final peak (*endo*-2, elution volume from 600 to 850 ml) possessed a specific activity of 1219 units/mg protein, while pectinase possessed an activity of just 9.1 units/mg protein. One unit liberates 1.0  $\mu$ M reducing carbohydrate from polygalacturonic acid per min at pH 4.0 at 25°C. A total of  $5320 \pm 150$  units *endo*-2 was isolated and was used for subsequent polygalacturonic acid (PGA) hydrolyses. Enzyme activity was determined by the 2-cyanoacetamide spectrophotometric assay for monitoring formation of reducing end groups from PGA<sup>16</sup>.

### Partial hydrolysis of PGA with *endo*-polygalacturonase

A solution of PGA (21.0 g, citrus origin, Sigma) in water (2.0 l) was adjusted to pH 4.4 with sodium hydroxide. Sodium chloride (11.7 g) was added to a concentration of 0.1 M. Some precipitated PGA was re-dissolved by heating to 30°C and readjusting the pH to 4.4. Purified *endo*-2 (300 units) was added, and the solution was maintained at 30°C and shaken at 150 rpm for 4 h. After adjusting to pH 7.0 with sodium hydroxide, barium acetate (13.8 g) was stirred into the solution, which was then cooled to 10°C. The insoluble precipitate which formed was removed by vacuum filtration through Celite. The oligogalacturonic acid mixture was then precipitated by stirring an equal volume of acetone into the filtrate. The precipitate was collected by centrifugation at 4000 g, and stirred into water (400 ml). Barium salts of the oligogalacturonic acids were converted to the free acid form by stirring for 3 h with 75 ml of Amberlite IR-120 (H<sup>+</sup>) ion-exchange resin (Aldrich, Milwaukee, WI, U.S.A.). The resin was removed by filtration and washed with an additional 150 ml water. Combined filtrates were lyophilized to yield the oligogalacturonic acid mixture (16.6 g, 79% yield).

*Chromatographic separation of endo-polygalacturonase (endo-2) generated oligogalacturonic acids on AG MP-1 ( $\text{HCOO}^-$ )*

AG MP-1 ( $\text{HCOO}^-$ ) resin (520 ml) was slurried with water and packed into a glass column ( $60.0 \times 3.8$  cm I.D.) after inserting a glass wool plug into the column end. An aqueous solution of the oligogalacturonic acid mixture (7.0 g/350 ml), produced by hydrolysis of PGA by endo-2, was passed through the column. The resin was eluted with water (350 ml), followed by a step-gradient of sodium formate, pH 4.7, consisting of the following: 0.33 M, 200 ml; 0.36 M, 400 ml; 0.39 M, 1 l; 0.42 M, 1 l; 0.45 M, 800 ml; 0.55 M, 1 l; 0.65 M, 800 ml; and 0.75 M, 500 ml. The gravity flow-rate was 2.4 ml/min and fractions of 19 ml were collected. Each third tube was monitored both by HPTLC<sup>13</sup> (described above) and colorimetry<sup>15</sup>, but either procedure allowed the pooling of tubes containing pure oligomers of like DP. Tubes were pooled as follows: DP-2 (51–71), DP-3 (75–84), DP-4 (96–198), DP-5 (213–270), and DP-6 (283–288). Galacturonic acid-containing tubes (28–36) were discarded.

The quantity of product in each fraction was determined from the colorimetric assay or estimated by HPTLC. A 50% molar excess of barium acetate was stirred into each pooled fraction, and the individual oligogalacturonic acids were precipitated as their barium salts by addition of acetone (3 volumes to DP-2 fraction, 2 volumes to DP-3 and DP-4, and 1 volume to DP-5 and DP-6). The precipitates were collected by centrifugation at 4000 g, and stirred into water (100 ml). Amberlite IR-120 ( $\text{H}^+$ ) was then added, from 10 to 40 ml, in proportion to the quantity of barium acetate that had been added to each fraction. After stirring for 1 h, the resin was removed by filtration and washed with another 50 ml water. Filtrates were combined and lyophilized, yielding the oligogalacturonic acids.

*Partial hydrolysis of PGA with pectinase*

PGA (20.0 g) was stirred into 0.1 M sodium bicarbonate (800 ml) over the course of 1 h, during which time the pH of the solution dropped from 8.21 to 4.28. Pectinase (3.2 ml, 370 units) was added, and after stirring for 3 min, the reaction was quenched by heating to 80°C in a water bath. After cooling to about 50°C, the solution was clarified by filtration through celite. Oligogalacturonic acids were precipitated by addition of 95% aqueous ethanol (2 volumes), and collected by centrifugation at 4000 g. The centrifugate was twice washed with absolute ethanol, re-centrifuged, and dried *in vacuo* at 40°C to yield the oligogalacturonic acid mixture (17.1 g, 85.5%).

*Chromatographic separation of pectinase generated oligogalacturonic acids on AG MP-1 ( $\text{HCOO}^-$ )*

AG MP-1 ( $\text{HCOO}^-$ ) resin (133 ml) was packed as a slurry with water into a glass column ( $40 \times 2.2$  cm). A water (100 ml) solution of the oligogalacturonic acid mixture (2.0 g) produced by partial pectinase hydrolysis of PGA was passed through the column. The resin was eluted with water (100 ml), followed by a step-gradient of sodium formate (pH 4.7), consisting of the following: 0.30 M, 100 ml; 0.37 M, 100 ml; 0.44 M, 150 ml; 0.50 M, 200 ml; 0.55 M, 200 ml; 0.60 M, 250 ml; and 0.65 M, 250 ml. The eluent was delivered with a high-performance liquid chromatography pump (Perkin-Elmer Series 3, Norwalk, CT, U.S.A.) at a flow-rate of 2.4 ml/min, and fractions of 6 ml were collected. Each tube was monitored by colorimetry<sup>15</sup> and each fourth tube by HPTLC<sup>13</sup>. Either procedure allows appropriate pooling of fractions.

Tubes were pooled as follows: DP-2 (37–50); DP-3 (64–72); DP-4 (84–100); DP-5 (112–136); DP-6 (140–166); and DP-7 (188–202). Galacturonic acid-containing tubes (16–31) were discarded. Pure oligomers were isolated after precipitation of their barium salts from acetone and converted to the acid forms as described above for separation of *endo*-polygalacturonase generated oligogalacturonic acids.

#### *Separation of sugar acids on AG MP-1 (HCOO<sup>-</sup>)*

Galactonic acid, galacturonic acid, and glucuronic acid (40 mg each) in 2.0 ml water were applied to a column of 20 ml AG MP-1 (HCOO<sup>-</sup>), packed as a slurry with water. The column was eluted at 2.9 ml/min with a formic acid step-gradient consisting of the following: 0.02 M, 50 ml; 0.05 M, 50 ml; 0.07, 100 ml; and 0.10 M, 50 ml. Column fractions (5.0 ml) were monitored for composition by HPTLC at 35°C as described above, except that ethanol–25 mM acetic acid (65:35) was used as irrigant. Galactonic acid, galacturonic acid, and glucuronic acid resided in fractions 21–23, 27–31, and 37–45, respectively.

#### *Mass spectrometric analysis of oligogalacturonic acids*

Fast-atom bombardment mass spectra were recorded at the Center for Advanced Food Technology, Rutgers University, New Brunswick, NJ, U.S.A. using a VG-Analytical 7070E mass spectrometer in the negative ([M – H]<sup>-</sup>) and positive ([M + Na]<sup>+</sup>) ionization modes. For analysis in the negative mode, samples were slurried in a small amount of aqueous methanol, then dissolved in dithiothreitol–dithioerythritol (3:1). Signals observed in the positive mode result from sodium attachment, possibly from ppm sodium contamination in the sample.

## RESULTS AND DISCUSSION

Oligogalacturonic acid mixtures to be resolved by chromatography on AG MP-1 (HCOO<sup>-</sup>) were generated by incubation of polygalacturonic acid (PGA) with commercial fungal pectinase and with *endo*-polygalacturonase (*endo*-PGA<sub>ase</sub>) isolated from this crude preparation. The PGA substrate was earlier determined to have a number-average degree of polymerization ( $\overline{DP}_n$ ) of about 35 (ref. 17). The plot of incubation time *versus*  $\overline{DP}_n$  is shown in Fig. 2, which is based upon results of kinetic studies with PGA and purified oligogalacturonic acids of DP-3 through DP-7. The pectinase enzyme is useful for the rapid preparation of pure oligogalacturonic acids (DP 2–7) in lower yields.

Isolation from pectinase of two fractions with *endo*-PGA<sub>ase</sub> activity on carboxymethyl Sephadex C-50 is shown in Fig. 3. The final *endo*-2 peak possessed a specific activity of 1219 units/mg protein, representing a 134-fold purification over *endo*-activity in the crude pectinase. The earlier eluting *endo*-1 peak possessed a much lower specific activity (Fig. 2). The HPTLC profiles with time of the *endo*-2 catalyzed hydrolysis of PGA are shown in Fig. 4 (lanes a–e), along with the final profile of the 3-min pectinase reaction (lane f) and standards of DP-1 through DP-7 (lanes g–m). Note the presence of high DP oligomers at the origin in lane f for the pectinase-catalyzed hydrolysis (oligomers of DP greater than 9 have no mobility in this HPTLC system), along with a significant level of DP-1 due to the presence of *exo*-PGA<sub>ase</sub>.

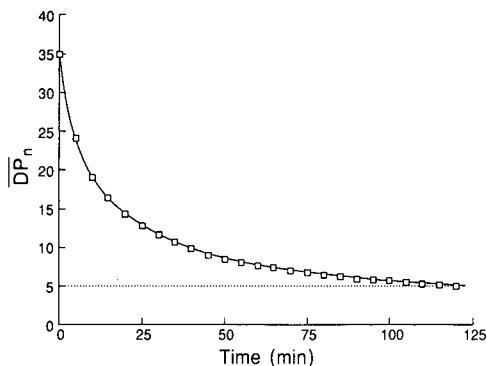


Fig. 2. Plot of the estimated number-average degree of polymerization ( $\overline{DP}_n$ ) of polygalacturonic acid hydrolysis products *versus* incubation time with an *endo*-polygalacturonase ( $14 \mu\text{mole min}^{-1}$  per g of polygalacturonic acid). This estimation is based upon the observation that there is a 2% decrease in relative enzyme activity,  $\frac{\partial R}{\partial t}$ , for each unit decrease in substrate DP. The calculation was performed as follows:

$$\overline{DP}_n)_i = \frac{M}{\left[ (R)_{i-2} + \int_{t_{i-2}}^{t_{i-1}} \left( \frac{\partial R}{\partial t} \right)_{i-1} dt \right] N}$$

where  $M$  is the mass of the starting polymer solute,  $N$  is the molecular weight of the galacturonic acid monomer and  $(R)_i$  is the number of moles of reducing end groups at various times,  $t_i$ .

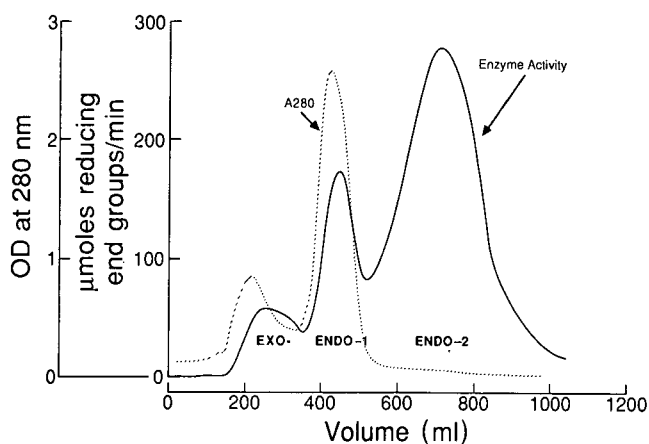


Fig. 3. Chromatographic profile of enzymes in crude pectinase on a carboxymethyl Sephadex C-50 column. Mobile phase: linear gradient of 0–0.3  $M$  sodium chloride in 20  $mM$  sodium acetate buffer, pH 4.4.



Fig. 4. HPTLC on silica gel. Lanes a–e, time course of oligogalacturonic acid formation resulting from partial hydrolysis of polygalacturonic acid by purified *endo*-polygalacturonase (0.5, 1, 2, 3 and 4 h, respectively); lane f, oligogalacturonic acid profile resulting from partial hydrolysis of polygalacturonic acid by pectinase; lanes g–m, galacturonic acid, and pure oligogalacturonic acids DP-2 through DP-7, respectively.

Incubation of PGA with *endo*-2 resulted in increasing proportions of oligomers from DP-3 through DP-5 with time (lanes a–e), no high DP oligomers after 1 h, and minimal DP-1. Since oligogalacturonic acid profiles in mixtures generated by pectinase and *endo*-2 catalyzed hydrolysis of PGA were quite different, optimal step-gradient programs for separation of oligomers on AG MP-1 ( $\text{HCOO}^-$ ) resin also varied.

The resolution of DP-1 through DP-6 oligomers, produced by action of *endo*-2 on PGA, is shown in Fig. 5. From the 7.0 g applied to the column, a total of 5.672 g (81.0% total yield of oligogalacturonic acids DP-2 through DP-6) was obtained. Gram quantities of pure DP-3 through DP-5 were obtained, more rapidly than previously described<sup>7,8</sup>, and without the need for re-chromatography in order to obtain pure oligomers. The only column fractions that contained more than one oligomer were tubes 85–95, apparent from HPTLC analysis. These tubes were discarded and appropriate tubes of like DP were combined and processed to yield the pure oligogalacturonic acids.

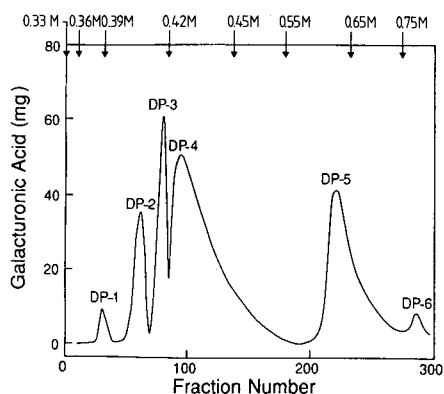


Fig. 5. Separation on AG MP-1 ( $\text{HCOO}^-$ ) of oligogalacturonic acids (7.0 g, DP-1 through DP-6) resulting from partial hydrolysis by purified *endo*-polygalacturonase (*endo*-2) of polygalacturonic acid. Chromatographic conditions: mobile phase, sodium formate (pH 4.7); flow-rate, 2.4 ml/min; fraction volume, 19 ml; detection, *m*-hydroxybiphenyl assay<sup>15</sup>.

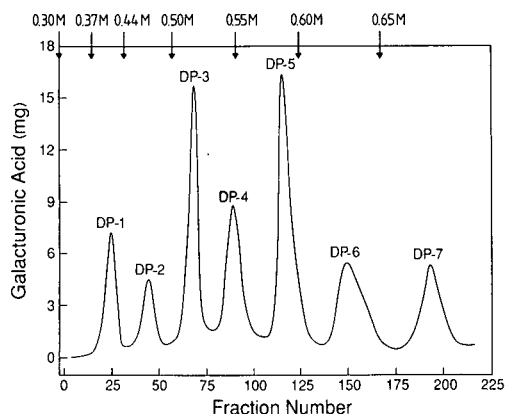


Fig. 6. Separation on AG MP-1 ( $\text{HCOO}^-$ ) of oligogalacturonic acids (2.0 g, DP-1 through DP-7) resulting from partial hydrolysis by pectinase of polygalacturonic acid. Chromatographic conditions: mobile phase, sodium formate (pH 4.7); flow-rate, 2.4 ml/min; fraction volume, 6 ml; detection, *m*-hydroxybiphenyl assay<sup>15</sup>.

Chromatography of the oligogalacturonic acid mixture (2.0 g) produced by pectinase catalyzed hydrolysis is shown in Fig. 6. The sodium formate (pH 4.7) step-gradient used above for the *endo*-2 produced mixture was modified, since the product profile (Fig. 4) as well as the sample and column size had changed. Pure oligomers through DP-7 were obtained, and the separation required less than 9 h. A total of 0.839 g (42% total yield of oligogalacturonic acids DP-2 through DP-7) was obtained. So nearly double the yield of useful products was obtained using purified *endo*-2. This was because significant levels of both galacturonic acid (DP-1) from *exo*-PGA<sub>ase</sub> activity and higher-DP oligomers result from partial hydrolysis of PGA with pectinase. Yields are summarized in Table I.

TABLE I

OLIGOGALACTURONIC ACIDS ISOLATED AFTER PARTIAL HYDROLYSIS OF POLY-GALACTURONIC ACID WITH *endo*-POLYGALACTURONASE AND PECTINASE

Product	<i>endo</i> -Polygalacturonase*		Pectinase**	
	Yield (g)	Yield (%)	Yield (g)	Yield (%)
Digalacturonic acid	0.480	6.8	0.031	1.5
Trigalacturonic acid	1.500	21.4	0.114	5.7
Tetragalacturonic acid	2.561	36.6	0.155	7.7
Pentagalacturonic acid	1.080	15.4	0.237	11.8
Hexagalacturonic acid	0.051	0.7	0.200	10.0
Heptagalacturonic acid	—	—	0.102	5.1
Total	5.672	81.0	0.839	41.9

\* 7.0 g polygalacturonic acid substrate.

\*\* 2.0 g polygalacturonic acid substrate.

Separations as efficient as those above can be achieved at flow-rates higher than 2.4 ml/min, provided that proportions of column input sample to column bed volume are reduced to 1 g/100 ml. For example, by applying a column head pressure of 2.5 p.s.i. nitrogen, flow-rates were increased to 4.0 ml/min, and a 1.0-g sample (produced by pectinase) yielded pure oligogalacturonic acids in less than 5 h. Yields from DP-2 through DP-7 were 10, 60, 80, 130, 90 and 100 mg, respectively. Product mixtures contained high levels of galacturonic acid (resulting from *exo*-PGA<sub>asc</sub> activity), much of which remained in the supernatant when desired mixtures were precipitated by addition of 2 volumes of ethanol.

For separations of oligogalacturonic acids on strong base anion-exchange resins such as AG MP-1, formate would appear to be the most suitable resin counter ion and column eluent. In an earlier attempt to separate oligogalacturonic acids on Dowex 1-X8, the acetate form rather than formate form of the resin was used along with acetate as eluent<sup>18</sup>. The resin displayed a lower relative selectivity for acetate than for formate and higher oligogalacturonic acids were strongly retained on the column. Also, organic acid counter ions and eluents are preferable to inorganic anions such as orthophosphate because their barium salts are highly soluble in acetone-water

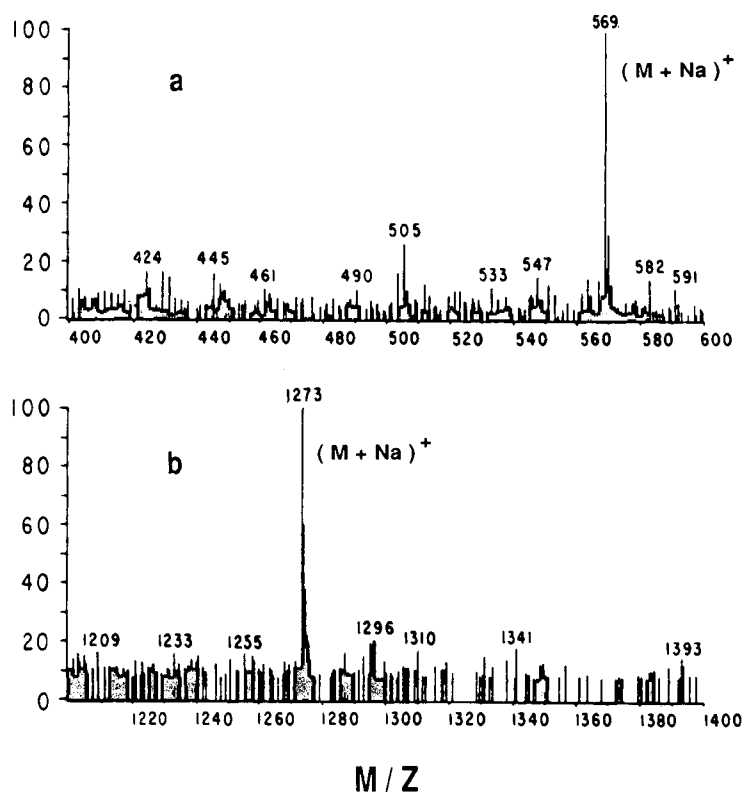


Fig. 7. Fast-atom bombardment mass spectrum in positive mode ( $[M + Na]^+$ ) of DP-3 and DP-7.

solutions, which facilitates the precipitation of individual oligogalacturonic acids in pooled column fraction as their barium salts.

Characterization of the isolated products as pure oligogalacturonic acids was accomplished by UV spectroscopy and mass spectrometry. The absence of UV absorption at 235 nm confirmed the absence of terminal 4,5-unsaturated galacturonic acid residues, which would have resulted from polygalacturonic acid lyase-catalyzed hydrolysis of PGA. Such products, differing by a single carbon-carbon double bond from the desired oligomers, potentially could have co-chromatographed with the desired oligogalacturonic acids. Fast-atom bombardment mass spectral analysis, in the negative ( $[M-H]^-$ ) and positive ( $[M+Na]^+$ ) ionization modes confirmed both the structures and purity of the products. Expected molecular ions ( $m/z = 176DP + 18 + 23$ ) resulted in the positive mode for oligomers from DP-2 to DP-7, as shown in Fig. 7 for DP-3 and DP-7. In the negative mode, spectra revealed the expected molecular ions ( $m/z = 176DP + 18 - 1$ ) and ions resulting from loss of successive galacturonic acid residues. For example, DP-7 gave the  $[M-H]^-$  ion at  $m/z$  1249 as well as peaks at  $m/z$  1073 (DP-6), 897 (DP-5) and 721 (DP-4).

The separation of individual sugar acids on AG MP-1 ( $HCOO^-$ ) was tested, using a step-gradient eluent of formic acid (0.02–0.10 *M*). Effectively resolved in 1.5 h on a column of 20 ml resin were 40 mg each of galactonic acid ( $pK_a$  3.60), galacturonic acid ( $pK_a$  3.42), and glucuronic acid ( $pK_a$  3.20). As expected on an anion-exchange column, these acids were eluted in order of decreasing  $pK_a$ . The separation of these compounds was more efficient than previously achieved by gravity flow chromatography. It is likely that this procedure can be adapted to the simple preparative separations of other sugar acids.

## CONCLUSION

A commercial fungal pectinase preparation and an *endo*-polygalacturonase with high specificity isolated from pectinase have been used to catalyze the partial hydrolysis of citrus pectin-derived polygalacturonic acid. Column chromatography on the macroporous anion-exchange resin AG MP-1 (formate), using step-gradient elution with sodium formate (pH 4.7) allowed the isolation of pure oligogalacturonic acids, from DP-2 through DP-7. Column fractions were monitored by HPTLC and by colorimetric reaction with *m*-hydroxybiphenyl. Yields of desired oligomers were doubled by using purified *endo*-polygalacturonase rather than pectinase to catalyze PGA hydrolysis. Separations were superior in terms of speed and efficiency compared to those previously reported on the gel-type AG 1-X8 and Dowex 1-X8 anion-exchange resins. The identity and purity of isolated oligogalacturonic acids was confirmed by fast-atom bombardment mass spectrometry. By employing more limited hydrolysis with the *endo*-enzyme, and extending the gradient beyond 0.75 *M* sodium formate, it should be possible to isolate oligogalacturonic acids beyond DP-7. Preliminary experiments demonstrated that closely related acidic monosaccharides can also be efficiently resolved on AG MP-1.

## ACKNOWLEDGEMENT

We are grateful to Lorraine L. Sivieri for providing technical assistance.

## REFERENCES

- 1 R. Pressey, in M. L. Fishman and J. J. Jen (Editors), *Chemistry and Function of Pectins* (ACS Symposium Series 310), American Chemical Society, Washington, DC, 1986, p. 157.
- 2 P. Albersheim, H. Neukom and H. Deuel, *Helv. Chim. Acta*, 43 (1960) 1422.
- 3 C. W. Nagel and R. H. Vaughn, *Arch. Biochem. Biophys.*, 94 (1961) 328.
- 4 E. A. Nothnagel, M. McNeil, A. Dell and P. Albersheim, *Plant Physiol.*, 71 (1983) 916.
- 5 D. F. Jin and C. A. West, *Plant Physiol.*, 74 (1984) 989.
- 6 P. D. Bishop and C. A. Ryan, *Methods Enzymol.*, 138 (1987) 715.
- 7 C. W. Nagel and T. M. Wilson, *J. Chromatogr.*, 41 (1969) 410.
- 8 B. A. Dave, R. H. Vaughn and I. B. Patel, *J. Chromatogr.*, 116 (1976) 395.
- 9 K. R. Davis, A. G. Darvill, P. Albersheim and A. Dell, *Plant Physiol.*, 80 (1986) 568.
- 10 J. T. Axelson, J. W. Bodley and T. F. Walseth, *Anal. Biochem.*, 116 (1981) 357.
- 11 L. G. Morin and E. G. Barton, *Clin. Chem.*, 29 (1983) 1741.
- 12 J. T. Axelson, J. W. Bodley, J. Chen, P. C. Dunlop, L. P. Rosenthal, R. W. Viskup and T. F. Walseth, *Anal. Biochem.*, 142 (1984) 373.
- 13 L. W. Doner, P. L. Irwin and M. J. Kurantz, *Carbohydr. Res.*, 172 (1988) 292.
- 14 R. W. Bailey and E. J. Bourne, *J. Chromatogr.*, 4 (1960) 206.
- 15 N. Blumenkrantz and G. Asboe-Hansen, *Anal. Biochem.*, 54 (1973) 484.
- 16 K. C. Gross, *HortScience*, 17 (1982) 933.
- 17 M. L. Fishman, P. E. Pfeffer, R. A. Barford and L. W. Doner, *J. Agric. Food Chem.*, 32 (1984) 372.
- 18 C. W. Nagel and M. M. Anderson, *Arch. Biochem. Biophys.*, 112 (1965) 322.



CHROM. 20 642

## COMPARISON OF HIGH-PERFORMANCE LIQUID CHROMATOGRAPHIC AND ATOMIC SPECTROMETRIC METHODS FOR THE DETERMINATION OF Fe(III) AND Al(III) IN SOIL AND CLAY SAMPLES

MARY MEANEY, MICHELLE CONNOR, CHRISTOPHER BREEN\* and MALCOLM R. SMYTH\*  
*School of Chemical Sciences, NIHE Dublin, Glasnevin, Dublin 9 (Ireland)*

(First received February 10th, 1988; revised manuscript received May 17th, 1988)

---

### SUMMARY

A comparison has been made of high-performance liquid chromatographic and atomic absorption spectrometric methods for the determination of Fe(III) and Al(III) in soil and clay samples, following five different digestion/extraction schemes. Good correlations were obtained in the case of Fe(III) determinations in both matrices, but correlation was only achieved for Al(III) determinations following an hydrochloric acid digestion and a dithionite–citrate–bicarbonate extraction of the clay sample. Attempts have been made to explain the differences in results between the two methods in terms of the Al(III) species which are likely to be present following extraction. Confirmatory evidence to support some of the conclusions made with respect to the speciation of these metal ions in these matrices has been obtained using X-ray diffraction studies.

---

### INTRODUCTION

The identification and quantitation of bioavailable metal species in soil and clay samples proves to be of continuing interest<sup>1,2</sup>. Consequently, the development of methodology for the “speciation” and quantitation of metal ions held in amorphous or semi-crystalline forms outside the formal, structural packets in soil and clay samples (*i.e.* “extra-framework” forms) is of considerable importance for bioavailability studies. To this end, a variety of different extraction procedures have been developed, principally to investigate the nature of iron oxides in soil and clay matrices. Mehra and Jackson<sup>3</sup> introduced the dithionite–citrate–bicarbonate (DCB) method for the extraction of iron oxides of different crystallinities, encompassing water-soluble, exchangeable and organic-bound iron species. McKeague and Day<sup>4</sup>, however, pioneered the use of oxalate to extract amorphous, non-crystalline or poorly ordered iron oxides. In addition, various strong acid extractions have been reported which are

---

\* Present address: Department of Chemistry, Sheffield City Polytechnic, Pond Street, Sheffield S1 1WB, U.K.

supposed to approximate to "total" iron content<sup>5,6</sup>, whereas the use of pyrophosphate is supposed to extract only organic-bound Fe(III) complexes<sup>7</sup>.

Bloom *et al.*<sup>8</sup> developed a spectrophotometric method for the determination of "available" aluminium, which involved the use of 8-hydroxyquinoline (oxine) as extractant, at a wavelength of 395 nm. However, a 15-min extraction period was necessary to surmount the interference from Fe(III), and probably resulted in a change in the speciation of Al(III) during the extraction process. In an attempt to overcome this, James *et al.*<sup>9</sup> used a 15-s extraction period combined with an estimate of the Fe(III) interference from the absorbance at 600 nm. This type of background correction is, however, laborious and prone to large error.

The extraction method employed in the analysis of metal ions in soils and clays is therefore of obvious importance in the development of any "speciation" scheme. The detection of metal ions following these extraction procedures may be carried out using a variety of techniques; the most commonly employed methods being based on colorimetry or atomic absorption spectrometry (AAS). In recent years, however, much interest has been shown in the application of high-performance liquid chromatography (HPLC) for trace metal analysis. A variety of ligands have been investigated in this regard, including the dithiocarbamates<sup>10,11</sup>, dithizone<sup>12</sup>, 1,10-phenanthrolines<sup>13</sup> and oxine<sup>14</sup>. We have recently reported on the use of oxine as a ligand in an HPLC method for the determination of Cu(II) and Fe(III) in anaerobic adhesive formulations<sup>15</sup>. In this paper, we report on the use of this particular ligand for the determination of Fe(III) and Al(III) in soil and clay samples. A major potential advantage of using this ligand for this application is that it may also be used as the extractant of the metal ions from the original soil or clay sample.

## EXPERIMENTAL

### Materials

All chemicals used were of analytical grade. Soil samples were taken from a fixed locality on the NIHE campus, sieved to obtain a particle size of 2 mm or less, and dried in an oven at 110°C. The clay sample used was an untreated Wyoming montmorillonite described by Breen *et al.*<sup>16</sup>. All aqueous solutions were prepared in distilled water, further purified by passage through a Milli-Q water purification system. All organic solvents used were of HPLC-grade. Sample preparation cartridges (Sep-Pak) were obtained from Waters. The C<sub>18</sub> column used in this study was obtained from Supelchem, and was a 25 cm × 4.6 mm steel column containing LC-18-DB (5 µm particle size) packing material. A Guard-PAK (Waters) guard column containing 10-µm µBondapak C<sub>18</sub> packing material (end capped) was used to protect the analytical column.

### Apparatus

The HPLC system used in this study consisted of an Applied Chromatography Systems (ACS) Model 352 ternary gradient pump connected to a Rheodyne 7125 injection valve and a Shimadzu Model SPD-6A variable-wavelength spectrophotometric detector. AAS was carried out using an Instrumentation Laboratory (IL) Model 357 AA/AE spectrophotometer.

### Methods

#### *Digestion/extraction procedures*

(1) *Hydrofluoric acid digestion*. Dried soil or clay (0.1 g) was shaken with 5.0 ml 40% hydrofluoric acid in a PTFE vessel for 24 h, and the extract diluted to 1 part in 300 parts water, prior to analysis.

(2) *Hydrochloric acid digestion*. Dried soil or clay (0.1 g) was shaken with 100.0 ml 36% hydrochloric acid for 24 h. Analysis was carried out on 1:100 and 1:25 dilutions in water for soil and clay samples, respectively.

(3) *Dithionite-citrate-bicarbonate extraction*. This was carried out according to the method of Mehra and Jackson<sup>3</sup>.

(4) *Oxalate extraction*. This was carried out according to the method of McKeague and Day<sup>4</sup>.

(5a) *Oxine extraction for Fe(III)*. Dried soil or clay (0.5 g) was extracted for 4 h with 40.0 ml of (0.5%) oxine dissolved in 0.02 M acetate buffer, pH 4.0. A 2.0-ml aliquot of each extract was then passed through a silica Sep-Pak. The metal ion-oxine complex was then eluted with 4 ml methanol before analysis.

(5b) *Oxine extraction for Al(III)*. This was carried out according to the method of James *et al.*<sup>9</sup>, with the following modifications: (i) the oxine concentration was reduced to 0.5%, (ii) the reaction was stopped by centrifugation instead of extraction with butyl acetate, which interfered with subsequent HPLC analysis.

#### *HPLC analysis*

The conditions used for the HPLC analysis of Fe(III) and Al(III) were the same as those reported previously<sup>15</sup>. The mobile phase contained acetonitrile (containing  $1 \cdot 10^{-2}$  M oxine)-0.02 M acetate buffer pH 6.0 (containing 0.2 M potassium nitrate) (50:50). Standard solutions of metal ions or extracts from soil or clay samples were injected directly onto the column through the injection port without any external formation of the complex.

#### *Atomic absorption spectrometry*

The conditions used for AAS measurements for Fe(III) are: light source, hollow cathode; lamp current, 8 mA; wavelength, 248.3 nm; slit width, 80  $\mu$ m; burner head, single slot; band pass, 0.3 nm; flame description, air-acetylene, oxidising, fuel lean, blue. For Al(III) they are: light source, hollow cathode; lamp current, 8 mA; wavelength, 309.3 nm; slit width, 320  $\mu$ m; burner head, nitrous oxide; band-pass, 1.0 nm; flame description, nitrous oxide-acetylene, reducing, fuel rich, red.

#### *X-ray diffraction*

Oriented samples for X-ray diffraction (XRD) analysis were prepared by evaporating an aqueous slurry of soil or clay onto a microscope slide (15  $\times$  10 mm). The slide was then placed in the goniometer of a Phillips Model PW1050 diffractometer operating at 40 kV and 20 mA using CuK $\alpha$  radiation ( $\lambda$  = 1.5418 Å). The XRD profiles were recorded at 2°(2 $\theta$ ) min<sup>-1</sup> from 0–60°(2 $\theta$ ). In the case of the hydrofluoric acid digestion, the extract contained almost no solid matter, and a small portion of the extract was poured onto the glass slide, where some crystals formed.

## RESULTS AND DISCUSSION

*X-ray diffraction studies*

The XRD profile of the untreated soil sample is shown in Fig. 1, and illustrates that the major, indexable, crystalline component of this soil sample is  $\alpha$ -quartz (Q). In contrast, the XRD profile of the untreated clay (C) sample (Fig. 1b) indicates the presence of several impurities including mica (M), kaolin (K), quartz (Q) and Feldspar (F), but exhibits no peaks commensurate with crystalline Fe- or Al-containing species such as goethite, lepidocrocite or gibbsite, respectively.

The effect of increasing severity of three of the extraction/digestion procedures reported in this paper on the XRD traces obtained for the clay sample is illustrated in Fig. 1c–e. The DCB extract was not washed prior to collecting the XRD data, and this accounts for the three characteristic sodium chloride (N) peaks shown in Fig. 1c. The XRD trace obtained for the hydrochloric acid digest is shown in Fig. 1d, and shows that treatment with this 36% hydrochloric acid causes no noticeable degradation of the structural clay lattice, and reflects the greater resistance of aluminous silicates to

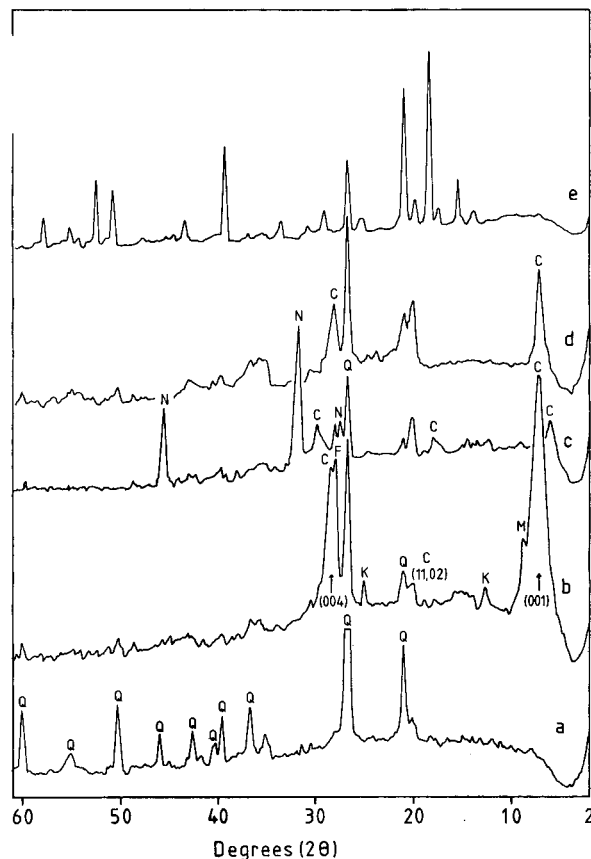


Fig. 1. XRD profiles for (a) untreated soil, (b) untreated clay, (c) DCB-extracted clay, (d) hydrochloric acid digested clay, and (e) hydrofluoric acid digested clay.

acid attack compared to the magnesium rich analogues. The reduced intensity of the Q and F peaks in the DCB extract most probably reflects the physical loss of sample rather than preferential extraction, whilst the Feldspar peak for the hydrochloric acid digested clay (Fig. 1d) lies below the 005 reflection marked C at around  $28^\circ(2\theta)$ . The XRD trace obtained for the hydrofluoric acid digest of the clay (Fig. 1e) illustrates emphatically that treatment with hydrofluoric acid has a devastating effect on the clay, leaving few identifiable reflections. In a similar manner, only the hydrofluoric acid digestion procedure had any marked effect on the diffraction profile of the soil sample.

#### *Digestion/extraction methods*

The results obtained using both HPLC and AAS for the percentages of Fe(III) and Al(III) in the soil and clay samples following the various digestion/extraction procedures detailed under Experimental are given in Table I. A typical trace obtained for the separation of Fe(III) and Al(III) using HPLC is shown in Fig. 2. A detection wavelength of 400 nm was employed, which lies between the  $\lambda_{\max}$  values for the oxine complexes of Fe(III) and Al(III) at 450 and 375 nm, respectively. Limits of detection of the order of 1–2 ppm for Fe(III) and Al(III) were typically achieved using both methods.

#### *Hydrofluoric acid digestion*

The values obtained for the percentage Fe(III) in the soil and the clay represent the “total” metal content, because the hydrofluoric acid completely digests the samples, as shown from the XRD trace in Fig. 1e. The results obtained using both

TABLE I

CONCENTRATIONS OF Fe(III) AND Al(III) OBTAINED USING HPLC AND AAS FOLLOWING DIGESTION/EXTRACTION PROCEDURES

n.d. = not detected.

<i>Extractant</i>	<i>Sample</i>	<i>HPLC</i>		<i>AAS</i>	
		<i>Fe(III)</i> (%)	<i>Al(III)</i> (%)	<i>Fe(III)</i> (%)	<i>Al(III)</i> (%)
HF	Soil	$2.38 \pm 0.18$	$0.09 \pm 0.002$	$2.36 \pm 0.12$	$2.64 \pm 0.09$
	Clay	$1.60 \pm 0.05$	$0.25 \pm 0.005$	$1.64 \pm 0.12$	$7.51 \pm 0.44$
HCl	Soil	$1.69 \pm 0.04$	$0.20 \pm 0.01$	$1.71 \pm 0.02$	$0.42 \pm 0.01$
	Clay	$0.75 \pm 0.01$	$0.14 \pm 0.01$	$0.75 \pm 0.01$	$0.15 \pm 0.01$
DCB	Soil	$1.39 \pm 0.06$	$1.33 \pm 0.04$	$1.46 \pm 0.03$	$1.70 \pm 0.04$
	Clay	$0.18 \pm 0.01$	$0.004 \pm 1 \cdot 10^{-4}$	$0.16 \pm 0.01$	$0.003 \pm 1 \cdot 10^{-4}$
Oxalate	Soil	$0.08 \pm 0.01$	$0.04 \pm 0.005$	$0.08 \pm 0.005$	$0.07 \pm 0.005$
	Clay	$0.04 \pm 0.005$	$0.04 \pm 0.001$	$0.04 \pm 0.001$	$0.08 \pm 0.001$
Oxine	Soil	$0.05 \pm 0.005$	n.d.	$0.05 \pm 0.005$	n.d.
	Clay	$0.02 \pm 0.001$	n.d.	$0.02 \pm 0.001$	n.d.

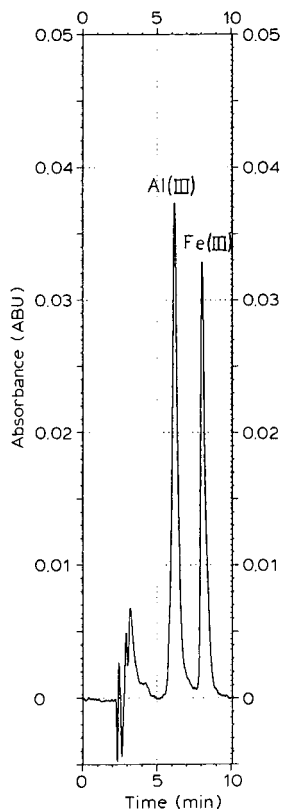


Fig. 2. HPLC separation of a 10 ppm mixture of Fe(III) and Al(III) with spectrophotometric detection. Conditions: flow-rate 1 ml/min; detection wavelength 400 nm.

HPLC and AAS are in good agreement, and show that the Fe(III) content of the soil sample exceeds that of the clay.

The values obtained for the percentage Al(III) in the soil and clay using HPLC were consistently lower than those obtained using AAS. This is probably due to the fact that Al(III) forms a much stronger complex with fluoride ions than with oxine, and hence prevents any *in situ* formation of the Al(III)–oxine complex on the column. With the high temperatures used in the rich nitrous oxide–acetylene flame, the Al(III)–fluoride complexes will be atomised, hence giving rise to a more accurate value of the Al(III) content in the soil or clay. Consequently, greater cognisance should be afforded the AAS results, particularly since the value of 7.51% Al(III) in the clay sample is close to that reported previously<sup>16</sup>.

#### *Hydrochloric acid digestion*

The values obtained for the percentage Fe(III) in the soil and clay were shown to be in good agreement using both instrumental methods of analysis. In the case of Al(III), the results for the clay were in good agreement, but the percentage Al(III) in the soil was found to be nearly double using AAS when compared to HPLC. The

reason for this discrepancy is not clear, but may be due to the nature of the "extra-framework" Al(III) in the respective matrices. From the results of the XRD studies, it is clear that the 36% hydrochloric acid digestion is not as effective as hydrofluoric acid at breaking down the structural units of the soil and clay matrices, and thus this digestion procedure can only yield results that approximate to "total" metal ion content.

#### *Dithionite-citrate-bicarbonate extraction*

This extraction technique, which is based on the strong reducing properties of dithionite, was developed to extract oxides of different crystallinity, including water-soluble, exchangeable and organic-bound metal<sup>3</sup>. The optimum pH for this extraction is 7–8, and this is maintained by the buffering capacity of the bicarbonate anion. Citrate is employed to complex the reduced metal ion.

The values obtained for the percentages of Fe(III) and Al(III) (Table I) show that whilst the HPLC and AAS results for percentage Fe(III) are in good agreement, the HPLC results for percentage Al(III) in the soil sample are somewhat lower than those obtained by AAS. This probably reflects competition between citrate and oxine for Al(III), which is a problem in the HPLC assay, but not in AAS where the citrate complex would be broken down. Consequently, since the HPLC method relies on complexation of free metal ion with oxine, the difference between the two results may relate to the amount of Al(III)–citrate complex present following extraction. One further interpretation, which cannot be ruled out, is that the DCB method extracts organic-bound Al(III) which would be determined by AAS but not by HPLC. The higher values for the percentage Al(III) in the soil compared to those obtained following hydrochloric acid digestion may be explained by the possible presence of semi-crystalline iron oxides containing a substantial amount of Al(III). It is difficult to obtain evidence for the presence of these phases, because as Schulze and Schwertmann<sup>17</sup> have found in both naturally occurring and synthetic goethites, the substitution of Fe(III) by Al(III) substantially reduces the intensity of peaks in the diffraction profile.

#### *Oxalate extraction*

The oxalate extraction was introduced by McKeague and Day<sup>4</sup> to extract the "active" fraction of metal ions from soils. This includes amorphous, non-crystalline or poorly ordered metal oxides and also includes organic-bound metal. The technique is based on complexation of metal ions by oxalate at pH 2–3. In this study, extractions were carried out at pH 2 and 3, but little difference was noticed in the percentage metal ion concentrations obtained. The results obtained for the percentage Fe(III) and Al(III) in soil and clay samples following this extraction procedure at pH 3 are given in Table I. Once again there is good agreement between the HPLC and AAS values for the percentage Fe(III), but not for the percentage Al(III). However, it is unlikely that the source of this discrepancy is due to the competitive chelation observed in the DCB method because there is a digestion step using nitric acid–sulphuric acid prior to analysis, which should break down any Al(III)–oxalate complex and/or organic-bound Al(III). Unfortunately, this acid digestion step lowers the pH of the extract prior to the analysis stage, and studies with comparable standard solutions indicate that these low pH values suppress absorbance readings in AAS and affects the

complexation of Al(III) with oxine, resulting in lower values than anticipated for the HPLC method. The reason that the values obtained for the percentage Al(III) using HPLC are higher in the soil and lower in the clay following the oxalate extraction compared with the dithionite–citrate–bicarbonate extraction may be due to the fact that oxalate is a better extractant of amorphous Al(III) species<sup>4</sup> which are suggested to be more prevalent in the soil than the clay from the XRD studies.

#### *Oxine extraction*

Methods employing oxine as an extractant for “available” Al(III) in soils have been reported in the literature<sup>8,9</sup>, but this extractant has not been widely used for determinations of Fe(III) in soil and clay samples. We have therefore investigated the use of oxine for Fe(III) determinations in these matrices based on the method of James *et al.*<sup>9</sup> reported for Al(III).

The extraction method involving oxine was optimised with respect to time of extraction, pH and isolation of the complex using Sep-Pak cartridges. The extraction time was varied between 2 and 72 h, but periods in excess of 4 h gave comparable results. Previous studies<sup>14,15</sup> have shown that the formation of the oxine–Fe(III) complex is optimal in the pH range 4–6, although analysis of the soil extracts indicated that slightly higher values were obtained at pH 4 than at pH 6. Furthermore, the use of a silica Sep-Pak was found to be an effective means for isolation of the complex formed, in addition to acting as a means of sample “clean-up”, as observed previously<sup>15</sup>. It was found that 4 ml of methanol was required to quantitatively remove 20- $\mu$ g of oxine–Fe(III) complex from the Sep-Pak.

The results in Table I show that there is good agreement between the HPLC and AAS results for the percentage Fe(III) in soil and clay samples using this extraction method. No detectable concentrations of Al(III) were found in any of the oxine extracts by either HPLC or AAS, although spiking a soil sample with 5 ppm Al(III) resulted in HPLC and AAS values of 5.03 and 5.30 ppm Al(III), respectively. This suggests that oxine will only extract extremely labile Al(III) from these matrices.

#### CONCLUSIONS

A comparison of the results in Table I show a good agreement in the percentage Fe(III) values obtained from both soil and clay using both HPLC and AAS. The percentage Fe(III) extracted using the various methods decreased in the order HF > HCl > DCB > oxalate > oxine. This is to be expected considering the different mechanisms by which these extractions/digestions operate. It is interpreted from the results that the hydrofluoric acid extraction yields a value relating to the “total” Fe(III) content. Because of the specific nature of the DCB and oxalate extraction procedures for crystalline and non-crystalline oxides, respectively, the different values for the percentage Fe(III) arising from these procedures can be explained. The difference between the hydrofluoric acid results and those obtained using the DCB extraction can be attributed to the amount of Fe(III) which forms an integral part of the lattice structure of the clay, and perhaps also that of the soil. The difference between the DCB and oxalate extractions for Fe(III) can be attributed to the amount of crystalline iron oxides present in these matrices, even though they were too small in particle size to be observed using XRD analysis. The difference between the oxalate

results and those obtained using the oxine extraction is most probably due to "exchangeable" Fe(III) species.

The results obtained with the 36% hydrochloric acid digestion suggest a small ingress of acid into the octahedral layer, thus leaching out a small amount of Fe(III) associated with the lattice structure. In the case of Al(III), the percentage values obtained in both soil and clay were found to be in good agreement for the hydrochloric acid digestion and the DCB extraction for the clay using both HPLC and AAS. The results obtained using the other extraction procedures, however, were found to be much lower using HPLC compared to AAS, especially for the soil. This is mainly due to the competition between oxine and the various extractants employed for Al(III).

Although this paper has necessarily limited itself to the analysis of a single soil and a single clay sample, it has, however, highlighted the possibility of employing HPLC (i) as a multi-element approach to the determination of metal ions in soils and clays, and (ii) to provide information on the speciation of metal ions, provided that experiments have been carried out taking into consideration the matrix involved as well as the sample preparation. If lower limits of detection were required than are possible using the approaches described in this paper, then these could be achieved for the HPLC method by employing the technique of "external formation" of the oxine-Fe(III) or oxine-Al(III) complex prior to injection onto the column, and for the AAS method by employing a flameless approach to atomisation.

#### REFERENCES

- 1 A. S. Campbell and U. Schwertmann, *Clay Miner.*, 20 (1985) 515.
- 2 A. A. Jones and A. M. Saleh, *Clay Miner.*, 21 (1986) 85.
- 3 O. P. Mehra and M. L. Jackson, *Proceedings of 7th National Conference on Clays and Clay Minerals, Washington, DC, 1960*, pp. 317-327.
- 4 J. A. McKeague and J. H. Day, *Can. J. Soil Sci.*, 46 (1966) 13.
- 5 E. Byrne, *Chemical Analysis of Agricultural Materials*, An Foras Taluntais, Johnstown Castle, 1979, p. 116.
- 6 S. P. McGrath and C. H. Cunliffe, *J. Sci. Food Agric.*, 36 (1985) 794.
- 7 P. J. Loveland and P. Digby, *J. Soil Sci.*, 25 (1984) 243.
- 8 P. R. Bloom, R. M. Weaver and M. B. McBride, *Soil Sci. Soc. Am. J.*, 42 (1978) 713.
- 9 B. R. James, C. J. Clark and S. J. Riha, *Soil Sci. Soc. Am. J.*, 47 (1983) 893.
- 10 A. M. Bond and G. G. Wallace, *Anal. Chem.*, 56 (1984) 2055.
- 11 R. M. Smith, *Anal. Proc.*, 21 (1984) 73.
- 12 E. Inatimi, *J. Chromatogr.*, 256 (1983) 253.
- 13 J. W. O'Laughlin and R. S. Hanson, *Anal. Chem.*, 52 (1980) 2263.
- 14 A. M. Bond and Y. Nagaosa, *Anal. Chim. Acta*, 178 (1985) 197.
- 15 J. Mooney, M. Meaney, R. G. Leonard, G. G. Wallace and M. R. Smyth, *Analyst (London)*, 112 (1987) 1555.
- 16 C. Breen, A. T. Deane and J. J. Flynn, *Clay Miner.*, 22 (1987) 169.
- 17 D. G. Schulze and U. Schwertmann, *Clay Miner.*, 22 (1987) 83.



CHROM. 20 664

## DETERMINATION OF POLYCYCLIC AROMATIC COMPOUNDS IN FISH TISSUE

DETLEF A. BIRKHOLZ\*

*Enviro-Test Laboratories, 9936 - 67th Ave., Edmonton, Alberta T6E 0P5 (Canada)*

RONALD T. COUTTS

*Faculty of Pharmacy and Pharmaceutical Sciences, University of Alberta, Edmonton, Alberta T6G 2N8 (Canada)*

and

STEVE E. HRUDEY

*Department of Civil Engineering, University of Alberta, Edmonton, Alberta T6G 2N8 (Canada)*

(First received December 7th, 1987; revised manuscript received May 20th, 1988)

---

### SUMMARY

A method is presented for the analysis of polycyclic aromatic hydrocarbons (PAHs), polycyclic aromatic sulfur heterocycles (PASHs), and basic polycyclic aromatic nitrogen heterocycles (PANHs) in fish. The analytical procedure includes Soxhlet extraction of prepared fish tissue with methylene chloride followed by gel permeation chromatography (GPC) using Bio-beads SX-3. For PAHs/PASHs, further cleanup is performed using adsorption chromatography on Florisil (5% water deactivated) and elution with hexane. For basic PANHs further cleanup of the fish extracts after GPC is achieved using liquid-liquid partitioning with 6 *M* hydrochloric acid and chloroform and then basifying the aqueous phase and extracting it with chloroform. Analysis of fortified fish samples was performed using capillary gas chromatography with flame ionization detection and capillary gas chromatography-mass spectrometry. Good agreement was observed for both methods of analysis when applied to fish samples fortified with PAHs, PASHs and basic PANHs at 0.1 to 1  $\mu\text{g/g}$ , suggesting that the method is effective at removing interfering biogenic compounds prior to analysis. Average recovery of PAHs/PASHs from fortified fish tissue was 87% and 70% for fish tissue fortified at 0.24–1.1 and 0.024–0.11  $\mu\text{g/g}$ , respectively. Average recovery for basic PANHs was 97% for fish fortified at 1.2–1.4  $\mu\text{g/g}$ .

---

### INTRODUCTION

Current emphasis on the development of alternate energy sources has stimulated production of synthetic fuels derived from oil shale, tar sands and coal. Although technology for producing liquid and solid fuels from these feed stocks has been available since the early 1900's (Rubin *et al.*<sup>1</sup>), the chemical characterization of these products has recently received increased attention. It is now clearly necessary to

identify and eliminate specific toxic and carcinogenic compounds in order to reduce environmental and occupational health hazards associated with the production and the combustion of these materials.

As part of a study of the uptake and elimination of toxic components isolated from thermally cracked heavy oil (coker distillate fractions) by fish, the need arose to develop a method to determine the presence of polycyclic aromatic compounds in fish tissue. Of particular interest were the polycyclic aromatic hydrocarbons (PAHs), polycyclic aromatic sulfur heterocycles (PASHs), and the basic polycyclic aromatic nitrogen heterocycles (PANHs). The accumulation and metabolism of toxic PAH by fish is well documented (Varanasi and Malins<sup>2</sup>, Vandermuelen<sup>3</sup>, Sinkkonen<sup>4</sup>, and Krahn and Malins<sup>5</sup>, and the accumulation of PASHs from petroleum sources by fish has also been well studied (Ogata *et al.*<sup>6</sup>, Ogata and Miyake<sup>7</sup>, and Paasivirta *et al.*<sup>8</sup>). High levels of PAHs and PASHs have been reported in the tissue of brown bullhead catfish taken from the contaminated Black River in Ohio (Lee *et al.*<sup>9</sup> and Vassilaros *et al.*<sup>10</sup>). Upon examination, this fish was found to have several cholangiomas (bile duct tumors) (Vassilaros *et al.*<sup>10</sup>). A number of pathological conditions have been observed in fish from polluted coastal waters and estuaries. Hepatic neoplasia have been linked to the presence of aromatic hydrocarbons in bottom sediments (Malins *et al.*<sup>11,12</sup>).

Recently, interest has focused on the study of PANHs in environmental samples. Of particular interest are the basic PANHs (which are primarily azaarenes and primary aromatic amines); these compounds are highly mutagenic as determined by the Ames test (Pelroy and Petersen<sup>13</sup>, Guerin *et al.*<sup>14</sup>, Wilson *et al.*<sup>15</sup> and Hsie *et al.*<sup>16</sup>). Because many carcinogenic chemicals are also mutagenic (McCann *et al.*<sup>17</sup>), the Ames test has been used to predict risks to human health. The presence of basic PANHs in the environment is of concern because many of these compounds are known mutagens and/or carcinogens (Dipple<sup>18</sup>). For example, quinoline and all of its monomethyl isomers were found to be mutagens in the Ames salmonella/microsomal assay (Dong *et al.*<sup>19</sup>). Recently, it has been shown that basic PANHs such as acridine and quinoline are readily taken up by fish (Southworth *et al.*<sup>20</sup> and Bean *et al.*<sup>21</sup>), and hepatic neoplasms and other hepatic lesions in English sole may be correlated to the presence of basic PANHs in sediment (Malins *et al.*<sup>11</sup>). There is ample reason then to analyze fish, taken from the environment for PAHs, PASHs and PANHs in order to ascertain their bioconcentration and the effects these chemicals are having on the environment.

Although many methods exist for the determination of PAHs in fish, relatively few procedures exist for the determination of PAHs, PASHs and basic PANHs in fish. Vassilaros *et al.*<sup>10</sup> presented such a method which involved alkaline hydrolysis, liquid-liquid extraction followed by alumina and gel permeation cleanup. We tried this method and found the alkaline hydrolysis method to be messy and time consuming, especially for fish with high lipid content. Furthermore, interference from biogenic compounds was observed upon analysis using capillary gas chromatography-flame ionization detection (GC-FID) suggesting that GC was not a suitable procedure for the screening of fish samples prepared by the method of Vassilaros *et al.*<sup>10</sup>.

The purpose of this paper is to describe an analytical method for the extraction, cleanup and high-resolution gas chromatographic analysis of PAHs, PASHs and basic PANHs in fish tissues.

## MATERIALS AND METHODS

*Chemicals*

6,7-Dimethylquinoline (6,7-DMQ) and 6,8-dimethylquinoline (6,8-DMQ) were synthesized in the University of Alberta Chemistry Department using the procedure of Manske *et al.*<sup>22</sup>. Purity was determined to be greater than 98% using GC-FID and GC-mass spectrometry (GC-MS). Naphthalene, benzothiophene, 1-methylnaphthalene, 2,6-dimethylnaphthalene, 2,3,5-trimethylnaphthalene, and dibenzothiophene were obtained from Aldrich and reported to be greater than 97% pure. Acenaphthene-d<sub>10</sub> was obtained from Merck, Sharpe and Dome. Anhydrous sodium sulfate, celite, concentrated hydrochloric acid, glacial acetic acid, and distilled in glass dichloromethane and hexane were obtained from Fisher Scientific. Florisil (PR grade, 60–80 mesh) was purchased from Floridin. 6 M Hydrochloric acid was prepared from concentrated acid and purified by extraction with methylene chloride prior to use. Anhydrous sodium sulfate and celite were purified by continuous Soxhlet extraction with methylene chloride for 16 h. Following extraction the solvent was evaporated in a vacuum oven (maintained at 50°C) and the material stored in a convection oven maintained at 130°C until required. BioBeads SX-3 (Bio-Rad) were swollen with elution solvent (methylene chloride-hexane; 1:1, v/v) overnight and wet packed into a chromatographic column (19 mm I.D.) to a bed height of 50 cm. Prior to use the column was washed with several bed volumes of elution solvent. All glassware used in the analytical procedure was soaked overnight in a detergent solution (RSB-35, Pierce), rinsed with hot water followed by pesticide-grade acetone and methylene chloride, and dried in an oven maintained at 250°C for 4 h.

*Preparation and extraction of fish tissue*

Fish tissue samples (muscle) were prepared according to the method of Benville and Tindle<sup>23</sup>. This involved grinding frozen tissue with dry ice in a Waring blender until a fine flour was obtained. Ground samples were then transferred to 250 ml wide-mouth jars, covered with aluminum foil and placed in a freezer maintained at -80°C overnight in order to allow the CO<sub>2</sub> to sublime. Thawed subsamples (20 g) were mixed with 80 g of purified anhydrous sodium sulfate, gently packed into a glass Soxhlet extraction thimble (with extra coarse glass frit) containing approximately 1 in. of purified celite and extracted with approximately 300 ml of methylene chloride for 6 h in a Soxhlet extractor equipped with a Freidrich condenser. Following extraction, the extract was concentrated to approximately 5 ml with the aid of a rotary evaporator operated under reduced pressure and with the water bath temperature maintained at 35°C.

*Cleanup of fish tissue extracts*

Cleanup of tissue samples was performed using gel permeation chromatography (GPC). This involved diluting the extract to 10 ml with methylene chloride-hexane (1:1, v/v) and applying it to a 750 mm × 19 mm I.D. chromatographic column containing 500 mm of BioBeads SX-3 swollen with elution solvent (methylene chloride-hexane, 1:1). The column was drained to the head of the gel. The extract container was rinsed with a further 10-ml of elution solvent which was transferred to the column. Again the column was drained to the head of the gel. A 250-ml addition

funnel was then filled with 230 ml of elution solvent and attached to the chromatographic column for elution. The first 75 ml of eluate (which contains primarily lipid material) were discarded and the next 75 ml (which contains primarily xenobiotics) collected. The eluate was then concentrated to approximately 5 ml with the aid of a rotary evaporator.

For the analysis of PAHs/PASHs, hexane (20 ml) was added to the final 5 ml of the GPC eluate and the mixture was concentrated on a rotary evaporator to a volume of approximately 2 ml. This extract was applied to a chromatographic column which was prepared by wet packing 10 g of 5% water deactivated Florisil (w/v) into a 10 mm I.D. chromatography column. The PAHs/PASHs were eluted with 50 ml of hexane, which was concentrated to 1.0 ml using a rotary evaporator followed by nitrogen blowdown.

For basic PANHs such as dimethylquinolines, the 5-ml GPC eluate was quantitatively transferred to a 250-ml separatory by extracting three times with 2 ml chloroform. An acid-base partition was performed by adding an additional 19 ml of chloroform to the separatory funnel, thoroughly mixing the contents and extracting three times with 25 ml 6 *M* hydrochloric acid. The combined aqueous layer was cooled in an ice bath, and basified using 6 *M* sodium hydroxide to pH > 11. Following extraction of the basified solution with 3 × 25 ml of chloroform, the extract was dried by passage through a column containing sodium sulfate (20 g), concentrated on a rotary evaporator to approximately 2 ml and quantitatively transferred to a calibrated 5-ml centrifuge tube with two 1-ml washings of chloroform. The ensuing extract was then concentrated to 1.0 ml with the aid of a nitrogen evaporator.

#### *GC and GC-MS*

GC was performed on a Hewlett-Packard (HP) Model 5880, or a Varian Model 3500 gas chromatograph. The HP instrument was equipped with a split/splitless injector (operated in the splitless mode), autosampler, flame ionization detector, level four data processing capability and a 30 m × 0.32 mm I.D. fused-silica, wall-coated DB-1301 capillary column (J&W Scientific). The carrier gas was helium (linear velocity was 31 cm/s at 280°C), and the temperature was increased from 40 to 280°C at 10°C/min beginning 1 min after injection. The oven temperature was maintained at 280°C for 20 min and the injector and detector temperatures were maintained at 270 and 300°C respectively. The injector was purged with helium 30 s after the injection of 2 µl of sample.

The Varian GC instrument was equipped with a split/splitless injector (operated in the splitless mode), flame ionization detector Model 600 data system and a 30 m × 0.32 mm I.D. fused-silica wall-coated DB-5 capillary column (J&W Scientific). Conditions of analysis were the same as those employed with the HP instrument except that the linear velocity was 28 cm/s at 300°C.

GC-MS was performed by interfacing a HP Model 5980 gas chromatograph to a HP Model 5970 quadrupole mass spectrometer. The GC instrument was equipped with a split/splitless injector (operated in the splitless mode), and a 12.5 m × 0.2 mm I.D. fused-silica wall-coated HP-1 capillary column (Hewlett-Packard). The carrier gas was helium (linear velocity was 36 cm/s at 300°C), and the temperature was increased from 40 to 300°C at 10°C/min beginning 1 min after injection. The oven temperature was maintained at 300°C for 8 min, and the injector, transfer line and ion source were maintained at 250, 300, and 220°C, respectively. Data was acquired 2 min

after injection using a HP Model 59970C data system. MS scans (from 35 to 350 a.m.u.) were obtained every 1.36 s.

### Recovery study

Aliquots of prepared fish muscle (Rainbow trout; 20 g) were fortified with the following PAHs/PASHs: naphthalene, benzothiophene, 1-methylnaphthalene, 2,6-dimethylnaphthalene, 2,3,5-trimethylnaphthalene, and dibenzothiophene. Fish muscle was also fortified with the following basic PANHs: 6,7-dimethylquinoline and 6,8-dimethylquinoline. Concentrations of these chemicals ranged from 24 ng/g to 1.39  $\mu\text{g/g}$  (Tables I–IV).

## RESULTS

The results summarized in Table I were obtained from fish fortified with PAHs/PASHs. Analysis was performed using the Varian gas chromatograph and quantitation was performed using external standards (ESTD) and an internal standard, namely acenaphthene- $\text{d}_{10}$  (ISTD). From Table I it is apparent that recovery better than 80% was obtained for the PAHs/PASHs at concentration levels of 0.24–1.1  $\mu\text{g/g}$ . Precision of the method (as expressed by the relative standard deviation, R.S.D.) was satisfactory and ranged from 4 to 10% of the mean. Little gain in precision was observed by using an internal standard during quantitation in place of external standards.

Since GC analysis using FID is a non-specific method of analysis, a more specific method, namely, GC/MS was used to analyze one of the fortified fish samples for PAHs/PASHs and the results were compared to those obtained by GC-FID. GC-MS quantitation was performed using the general principals outlined by the United States Environmental Protection Agency<sup>24</sup>. Results are summarized in Table II.

It is apparent from Table II that there is close agreement between the analysis of

TABLE I  
RECOVERY OF PAHs/PASHs FROM FORTIFIED FISH MUSCLE

Analyte	Concentration ( $\mu\text{g/g}$ )	n	Mean recovery (%)	R.S.D. (%)	Quantitation method (ESTD/ISTD)
Naphthalene	0.97	4	86	5.1	ESTD
	0.97	4	85	4.8	ISTD
Benzothiophene	1.1	4	85	4.5	ESTD
	1.1	4	81	5.7	ISTD
1-Methylnaphthalene	1.0	4	88	4.3	ESTD
	1.0	4	85	5.4	ISTD
2,6-Dimethylnaphthalene	1.0	4	88	6.1	ESTD
	1.0	4	87	6.6	ISTD
2,3,5-Trimethylnaphthalene	0.24	4	93	10.1	ESTD
	0.24	4	85	9.0	ISTD
Dibenzothiophene	1.0	4	92	9.2	ESTD
	1.0	4	84	6.4	ISTD

TABLE II

ANALYSIS OF FORTIFIED FISH MUSCLE BY GC-FID AND GC-MS

Analyte	Concentration ( $\mu\text{g/g}$ )	Recovery (%) by	
		GC-FID	GC-MS
Naphthalene	0.97	84	89
Benzothiophene	1.1	81	93
1-Methylnaphthalene	1.1	88	91
2,6-Dimethylnaphthalene	1.0	90	100
2,3,5-Trimethylnaphthalene	0.24	92	95
Dibenzothiophene	1.0	88	96

fortified fish muscle using GC/FID and GC-MS analysis. The slightly higher recovery observed for the GC/MS analysis may be due to slight concentration of the extract during storage prior to the GC/MS analysis. The close agreement between the two methods of analysis is indicative of the excellent cleanup obtained using the GPC/Florisil combination. A chromatogram obtained from fish tissue fortified with PAHs/PASHs is depicted (Fig. 1). The peaks appearing before naphthalene were determined, by GC/MS, to be alkylated benzenes and were observed to be present in control fish samples. The source of these alkylated benzenes was determined to be the hexane, which was used in both the GPC and Florisil cleanup steps. The only biogenic materials found to be present in this chromatogram eluted as two significant peaks after dibenzothiophene (Fig. 1). However, these peaks were found to be present in only

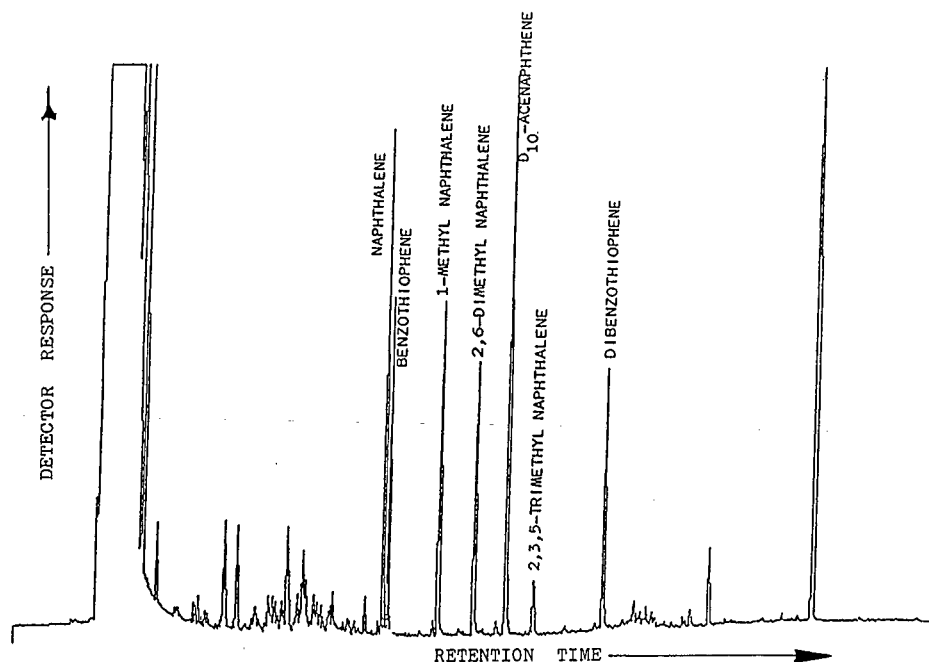


Fig. 1. Fish muscle fortified with PAH/PASHs.

TABLE III  
GC-FID AND GC-MS ANALYSIS OF FISH TISSUE FORTIFIED AT 0.1  $\mu\text{g/g}$

Analyte	Concentration (ng/g)	Recovery (%)			
		Spike 1		Spike 2	
		GC-FID	GC-MS	GC-FID	GC-MS
Naphthalene	96.9	114	93	256	138
Benzo(b)thiophene	104	107	68	153	65
1-Methylnaphthalene	106	93	79	86	53
2,6-Dimethylnaphthalene	100	81	77	65	68
2,3,5-Trimethylnaphthalene	24		74	155	65
Dibenzothiophene	104	88	77	82	78

two samples out of 12 processed, and are of unknown origin, but were probably introduced during GPC and/or Florisil cleanup. Rigorous calibration of the GPC and Florisil chromatography would likely eliminate these compounds.

In order to test the range of concentrations which could be detected using this method, two samples of fish tissue were fortified at low levels and subjected to GC/FID and GC-MS analysis. Table III is a summary of these findings.

From Table III it can be seen that there is reasonable agreement between the GC/FID and GC/MS analysis of fish tissue samples fortified at 24 to 100 ppb\*. The generally higher results obtained by GC/FID are likely due to the non-specificity of the method. Therefore, for quantitation of low levels of PAHs/PASHs in fish, GC-MS is the recommended method of choice. It is worth noting that even at 20 ppb acceptable levels of recovery were observed using GC-MS analysis. GC-MS data was obtained via scanning and extracted ion current profiles were generated for the analytes of interest and internal standard prior to integration and calculation. It is anticipated that larger signal-to-noise ratios could be obtained using selected-ion monitoring techniques and hence lower levels of detection could be realized. However, decreasing the analyte concentration could result in losses of material by adsorption onto glass surfaces etc., therefore a realistic detection limit of 10–20 ppb based on 20 g of fish and using our method is considered valid.

Table IV is a summary of the results obtained for the GC-FID analysis of basic PANHs in fortified fish muscle. Table IV reveals excellent recoveries of dimethylquinolines from fortified fish tissue using Soxhlet extraction followed by GPC and acid-base partition cleanup. Precision (defined as R.S.D.) is also acceptable and similar to that observed for the PAH/PASH analyses. Furthermore, GC-MS analysis of one fortified fish sample for 6,7-DMQ produced recoveries similar to those observed using GC-FID analysis, and indicative of effective cleanup. Reference to Fig. 2 reveals a GC-FID chromatogram obtained from fortified fish muscle and virtually free of any biogenic interfering material.

We have developed an analytical method capable of detecting accurate and precise levels of PAHs/PASHs and basic PANHs in samples of fish muscle. Good

\* Throughout the article the American billion ( $10^9$ ) is meant.

TABLE IV

## ANALYSIS OF DIMETHYLQUINOLINES IN FORTIFIED FISH MUSCLE

Analyte	Concentration ( $\mu\text{g/g}$ )	n	Mean recovery (%)	R.S.D. (%)
6,8-Dimethylquinoline	1.39	4	96	8.2
6,7-Dimethylquinoline	1.15	4	98	7.0

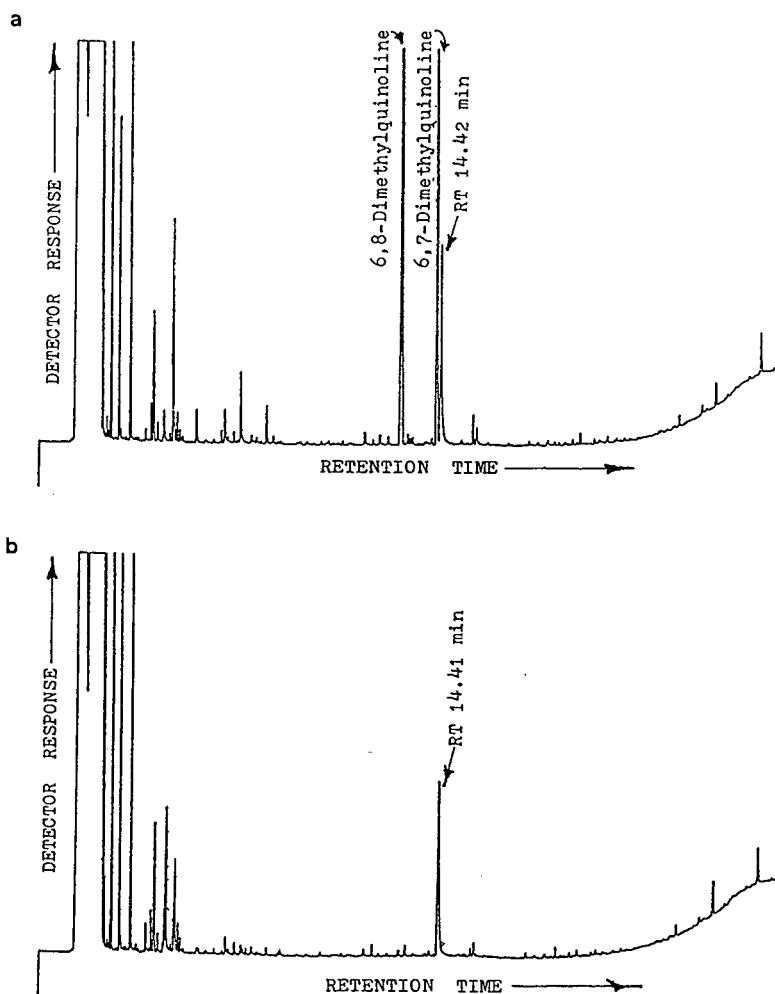


Fig. 2. (a) Fish muscle fortified with 6,7- and 6,8-dimethyl quinoline; (b) control fish muscle.

TABLE V  
MUSCLE CONCENTRATION OBSERVED IN FISH EXPOSED TO PANHs AND PASHs

Analyte	Mean exposure concentration (mg/l)	Exposure time (h)	Mean muscle concentration (µg/g)	Number of exposures
6,7-Dimethylquinoline*	1.0	7.5	6.1	3
6,8-Dimethylquinoline*	1.1	8.0	14	3
Benzothiophene**	0.67	8.0	19	3

\* Data taken from Birkholz *et al.*<sup>25</sup>.

\*\* Data obtained from Dromey<sup>26</sup>.

agreement was observed between GC-FID and GC-MS analysis which indicates substantial removal of biogenic material during cleanup. The use of GC-FID as a screening method is desirable because of accessibility by most laboratories and low cost relative to GC-MS. This method was applied to the analysis of muscle obtained from fish exposed to 6,7-DMQ, 6,8-DMQ and benzothiophene. Muscle concentrations were determined immediately after exposure and after depuration. A summary of muscle concentrations observed in fish after exposure to the three chemicals is shown in Table V. From this table it is apparent that PANHs and PASHs are bioconcentrated by fish from water.

A summary of muscle concentrations observed in fish following depuration of the three chemicals is given in Table VI. From Tables V and VI it is apparent that PANHs and PASHs have different rates of uptake and elimination. The uptake, elimination, and biotransformation of PANHs by fish is more fully described by Birkholz *et al.*<sup>25</sup> The uptake, elimination and biotransformation of PASHs is described by Dromey<sup>26</sup>.

In conclusion we have developed a precise and accurate method for the determination of PAHs, PASHs and PANHs in fish muscle. The sensitivity of the method was found to be more than adequate when applied to study of the uptake and elimination of PASHs and PANHs by exposed fish.

TABLE VI  
CONCENTRATION OF PANHs AND PASHs IN FISH MUSCLE FOLLOWING EXPOSURE AND DEPURATION

Analyte	Number of exposures	Mean exposure concentration (µg/l)	Exposure time (h)	Depuration time (h)	Muscle concentration (µg/g)
6,7-Dimethylquinoline*	3	0.97	9.5	69	0.56
6,8-Dimethylquinoline*	3	1.1	7.0	63	0.49
Benzothiophene**	3	0.67	8.0	65	2.2

\* Data obtained from Birkholz *et al.*<sup>25</sup>.

\*\* Data obtained from Dromey<sup>26</sup>.

## ACKNOWLEDGEMENTS

The authors wish to acknowledge the technical assistance of Mrs. Joyce Hudson and the helpful suggestions of Dr. F. M. Pasutto (University of Alberta, Faculty of Pharmacy and Pharmaceutical Science). Special thanks are also extended to Dr. W. Ayer (University of Alberta, Department of Chemistry) for providing the dimethyl-quinolines used in this study.

## REFERENCES

- 1 I. B. Rubin, M. R. Guerin, A. A. Hardigree and J. L. Epler, *Environ. Res.*, 12 (1976) 358-365.
- 2 U. Varanasi and D. C. Malins, in D. C. Malins (Editor), *Effects of Petroleum on Arctic and Subarctic Marine Environments and Organisms*, Vol. 2, Academic Press, New York, 1977, pp. 175-270.
- 3 J. H. Vandermeulen in J. H. Vandermeulen and S. E. Hrudehy (Editors), *Oil in Freshwater: Chemistry, Biology and Countermeasure Technology*, Pergamon Press, New York, 1987, pp. 267-303.
- 4 S. Sinkkonen, *Toxicol. Environ. Chem.*, 5 (1982) 217-225.
- 5 M. M. Krahn and D. C. Malins, *J. Chromatogr.*, 248 (1982) 99-107.
- 6 M. Ogata, Y. Miyake and Y. Yamasaki, *Water Res.*, 13 (1979) 613-618.
- 7 M. Ogata and Y. Miyake, *J. Chromatogr. Sci.*, 18 (1980) 594-605.
- 8 J. Paasivirta, R. Herzsuh, M. Lahtipera, J. Pellinen and S. Sinkkonen, *Chemosphere*, 10 (1981) 919-928.
- 9 M. L. Lee, D. L. Vassilaros and D. W. Later, *Int. J. Environ. Anal. Chem.*, 11 (1982) 251-262.
- 10 D. L. Vassilaros, P. W. Stoker, G. M. Booth and M. L. Lee, *Anal. Chem.*, 54 (1982) 106-112.
- 11 D. C. Malins, M. M. Krahn, M. S. Myers, L. D. Rhodes, D. W. Brown, C. A. Krone, B. B. McCain and S. L. Chan, *Carcinogenesis*, 6 (1985) 1463-1469.
- 12 D. C. Malins, B. B. McCain, D. W. Brown, S.-L. Chan, M. S. Myers, J. T. Landahl, P. G. Prohaska, A. J. Friedman, L. D. Rhodes, D. G. Burrows, W. D. Gronlund and H. O. Hodgins, *Environ. Sci. Technol.*, 18 (1984) 705-713.
- 13 R. A. Pelroy and M. R. Petersen, *Environ. Health Perspect.*, 30 (1979) 191-203.
- 14 N. R. Guerin, C.-H. Ho, T. K. Rao, B. R. Clark and J. L. Epler, *Environ. Res.*, 23 (1980) 42-53.
- 15 B. W. Wilson, R. A. Pelroy and J. T. Cresto, *Mutat. Res.*, 79 (1980) 193-202.
- 16 A. W. Hsie, P. A. Brimer, J. P. O'Neill, J. L. Epler, M. R. Guerin and H. H. Mayphoon, *Mutat. Res.*, 78 (1980) 79-84.
- 17 J. McCann, E. Choi, E. Yamasaki and B. N. Ames, *Proc. Natl. Acad. Sci. U.S.A.*, 72 (1975) 5135-5139.
- 18 A. Dipple, in C. E. Searle (Editor), *Chemical Carcinogens (ACS Monograph, Vol. 173)*, American Chemical Society, Washington, DC, 1976, pp. 245-313.
- 19 M. Dong, I. Schmeltz, E. La Voie and D. Hoffmann, in P. W. Jones and R. I. Freudenthal (Editors), *Carcinogenesis, Vol. 3*, Raven Press, New York, 1978, pp. 97-108.
- 20 G. R. Southworth, B. R. Parkhurst and J. J. Beauchamp, *Water Air Soil Pollut.*, 12 (1979) 331-341.
- 21 R. M. Bean, D. D. Dauble, B. L. Thomas, R. W. Hanf, Jr. and E. K. Chess, *Aquatic Toxicol.*, 7 (1985) 221-239.
- 22 R. H. F. Manske, L. Marrion and F. Leger, *Can. J. Research*, 20(B) (1942) 133-145.
- 23 P. E. Benville, Jr. and R. C. Tindle, *J. Agric. Food Chem.*, 18 (1970) 948-949.
- 24 United States Environmental Protection Agency, *United States Federal Register*, 49 (1984) 153-174.
- 25 D. A. Birkholz, R. T. Coutts and S. E. Hrudehy, *Xenobiotica*, (1988) submitted for publication.
- 26 E. M. Dromey, *Uptake, Elimination and Tainting with Polycyclic Aromatic Sulfur Heterocycles*, M.Sc. dissertation, University of Alberta, Dept. of Civil Engineering, Alberta, 1988.

CHROM. 20 686

## DETECTION OF TRACE LEVELS OF THIODIGLYCOL IN BLOOD, PLASMA AND URINE USING GAS CHROMATOGRAPHY-ELECTRON-CAPTURE NEGATIVE-ION CHEMICAL IONISATION MASS SPECTROMETRY

ROBIN M. BLACK\* and ROBERT W. READ

*Chemical Defence Establishment, Porton Down, Salisbury, Wiltshire SP4 0JQ (U.K.)*

(First received March 14th, 1988; revised manuscript received May 23rd, 1988)

---

### SUMMARY

A sensitive method has been developed for the detection and quantitative determination of thiodiglycol in blood, plasma and urine. Samples were extracted from Clin Elut columns and cleaned up on C<sub>18</sub> Sep-Pak cartridges (blood, plasma) or Florisil Sep-Pak cartridges (urine). Tetradeuterothiodiglycol was added to the sample prior to extraction as internal standard. Thiodiglycol was converted to its bis-(pentafluorobenzoate) derivative and analysed by capillary gas chromatography-electron-capture negative-ion chemical ionisation mass spectrometry using selected ion monitoring. Levels of thiodiglycol down to 1 ng/ml (1 ppb) could be detected in 1-ml spiked blood and urine samples; calibration curves were linear over the range 5– or 10–100 ng/ml. Blood and urine samples from a number of control subjects were analysed for background levels of thiodiglycol. Concentrations up to 16 ng/ml were found in blood, but urine levels were below 1 ng/ml.

---

### INTRODUCTION

The use of mustard gas, bis(2-chloroethyl) sulphide, in the Iran–Iraq conflict has stimulated renewed interest in the verification of mustard poisoning in victims of chemical warfare attacks. Although the isolation and detection of sulphur mustard immediately after spiking into blood or urine is relatively straightforward<sup>1–3</sup>, the detection of free sulphur mustard in the body fluids of hospitalised casualties is unlikely, due to its chemical reactivity and extensive metabolism. A more fruitful compound for detection may be thiodiglycol, the hydrolysis product of sulphur mustard, which was shown by metabolism studies in rats to be excreted, either free or conjugated, as a minor metabolite in urine<sup>4,5</sup>. A method for the detection of thiodiglycol in urine was reported by Wils *et al.*<sup>6</sup>, and a similar method has more recently been employed by Vycudilik<sup>7</sup> to analyse urine samples from casualties of chemical attacks. Since thiodiglycol is not easily isolated from aqueous media, both methods employed treatment of urine with concentrated hydrochloric acid to convert any thiodiglycol present to sulphur mustard. The latter was then recovered by adsorption from the headspace<sup>6</sup>, or by steam distillation and extraction<sup>7</sup>, and readily

detected by gas chromatography-mass spectrometry (GC-MS). These methods enabled the detection of levels down to the equivalent of 10–20 ng of thiodiglycol in 10–20 ml aliquots of urine. They did not however discriminate between thiodiglycol, its conjugates, or indeed any other moiety which may convert to sulphur mustard on treatment with hydrochloric acid. An important finding reported by Wils *et al.*<sup>6</sup> was the detection of thiodiglycol, or other compound converting to mustard using the acid conversion procedure, in the urine of control subjects at levels up to 55 ng/ml. The identity of the endogenous compound present in urine was not determined, but the results indicated that the detection of thiodiglycol in urine using this method was ambiguous with regard to verification of exposure to sulphur mustard. In this present paper we report an alternative and very sensitive method of detecting thiodiglycol, which isolates the latter directly from biological fluids using a simple procedure. By appropriate pretreatment of the samples the method can discriminate between free thiodiglycol, conjugates sensitive to enzymatic hydrolysis, and other compounds hydrolysing to thiodiglycol under acidic conditions. The screening of ten control subjects for thiodiglycol is also reported.

## EXPERIMENTAL

### Materials

Thiodiglycol was purchased from Aldrich (Gillingham, U.K.) and redistilled before use. Standard solutions of thiodiglycol were made up in acetone at concentrations of 0.1–100 µg/ml. Fisons (Loughborough, U.K.) Distol-grade ethyl acetate and methanol, and Aldrich HPLC-grade toluene were used. For derivatisation pentafluorobenzoyl chloride (puriss) was purchased from Fluka Chemicals (Glossop, U.K.) and pyridine (Regis derivatisation grade) from Pierce and Warriner (Chester, U.K.). Florisil Sep-Pak and C<sub>18</sub> Sep-Pak cartridges were purchased from Waters Assoc. (Northwich, U.K.) and were conditioned with methanol (5 ml) and ethyl acetate (5 ml) before use. Clin Elut columns (1003) were made by Analytichem International (Harbor City, CA, U.S.A.); they were washed with methanol (3 × 5 ml) and dried in a vacuum oven at 60°C prior to use. All glassware was pretreated with Aquasil siliconising fluid (Pierce and Warriner).

1,1,1',1'-Tetradeuterothiodiglycol was prepared by reacting sodium sulphide with ethyl bromoacetate to give diethyl 2,2'-thiodiglycolate, followed by reduction with lithium aluminium deuteride. Purity was judged by MS to be >97%, containing < 0.1% of non-deuterated thiodiglycol. Samples of fresh urine and blood were collected from healthy male volunteers. Rat urine was collected over a 24-h period from two male Porton strain rats dosed intraperitoneally with sulphur mustard (1.58 mg/kg). Hydrolysis of conjugates was performed with  $\beta$ -glucuronidase type H-2 (Sigma, Poole, U.K.) (a crude solution of *Helix Pomatia*, possessing both  $\beta$ -glucuronidase and sulphatase activity), or with concentrated hydrochloric acid (BDH, Analar, Poole, U.K.).

### Extraction and clean-up

Blood or plasma (1 ml), to which tetradeuterothiodiglycol (10 ng) in acetone (10 µl) was added, was absorbed onto a 3-ml Clin Elut tube, connected directly to a C<sub>18</sub> Sep-Pak cartridge. The tube and cartridge were eluted with ethyl acetate (5 × 5 ml),

collecting the eluate in a 50-ml round bottomed flask. The extract was concentrated to *ca.* 1 ml on a rotary evaporator at 30°C, and then transferred to a 1-ml vial, rinsing the flask with methanol (0.5 ml). The combined extract and washings were concentrated to dryness under a stream of nitrogen at 40°C. If required this concentrate could be stored at -20°C.

Urine was treated similarly except that a normal-phase Florisil Sep-Pak cartridge was used in place of the C<sub>18</sub> cartridge. For the enzymatic hydrolysis of conjugates, urine (1 ml) was buffered at pH 5 with 0.1 M sodium acetate-acetic acid (0.4 ml) and incubated with  $\beta$ -glucuronidase solution (0.1 ml) at 37°C for 24 h. Acid hydrolysis was performed by incubating urine (1 ml) with concentrated hydrochloric acid (0.1 ml) at 37°C for 48 h; the acid was then neutralised with 5 M sodium hydroxide. Extraction and clean-up were performed as above.

#### *Derivatisation*

To the dried residue from the clean-up was added pyridine (50  $\mu$ l) and pentafluorobenzoyl chloride (10  $\mu$ l). The mixture was vortexed and then stood at ambient temperature for 5 min. The solution was made up to 500  $\mu$ l with toluene (440  $\mu$ l), vortexed and centrifuged; aliquots (2  $\mu$ l) of the supernatant were injected. This derivatised solution was stable for 4 weeks when stored at -20°C, but was usually analysed immediately.

#### *GC-MS analysis*

Analyses were performed using a Finnigan 4600 gas chromatograph-mass spectrometer. The gas chromatograph was fitted with a 25 m  $\times$  0.22 mm I.D. bonded-phase column coated with OV-1701, film thickness 0.25  $\mu$ m (Thames Chromatography, Maidenhead, U.K.), inserted directly into the mass spectrometer source [additional analyses were performed using 12 m  $\times$  0.22 mm BP-5, BP-10 and BP-20 columns (SGE, U.K.)]. Helium at 15 p.s.i. was used as carrier gas. The oven was held at 90°C for 0.5 min, programmed from 90 to 230°C at 25°C/min, from 230 to 260°C at 4°C/min, and finally held at 260°C for 2 min. Splitless injections (2  $\mu$ l) were made using a split delay of 0.5 min, septum purge 2 ml/min, split flow 50 ml/min; injector temperature, 265°C; transfer line temperature, 260°C.

The mass spectrometer was operated in the selected ion monitoring mode using negative ion chemical ionisation with methane as reagent gas; ion source pressure 0.8 Torr; source temperature 100°C; electron energy 150 eV; emission current 0.3 mA. M<sup>-</sup> ions were monitored for thidiglycol bis(pentafluorobenzoate), *m/z* 510, and its tetradeuterated analogue, *m/z* 514; dwell time 0.157 s; total scan time 0.5 s. The retention time for thiodiglycol bis(pentafluorobenzoate) was *ca.* 10 min with the tetradeuterated analogue eluting 1.5 s earlier.

Quantitation was performed by comparing the computer integrated peak area for *m/z* 510 at the appropriate retention time with that for the internal standard monitoring *m/z* 514. Calibration curves were established in samples of blood and urine, previously shown to contain < 1 ng/ml of thiodiglycol, spiked at concentrations of 1, 5, 10, 25, 50, 75 and 100 ng/ml. These calibration curves were shown to be superimposable, within the limits of experimental error, on calibration curves constructed from standard solutions of thiodiglycol and internal standard. A calibration was also established in a pooled plasma sample, found to contain 6 ng/ml of

endogenous thiodiglycol, and the calibration curve shown to be parallel to that constructed from standard solutions but with a positive offset corresponding to the background level. Because of the difficulty in obtaining truly blank samples, subsequent quantitation of unknowns was performed against a calibration curve constructed from standard solutions on the same day as the analysis. For similar reasons, recoveries were estimated using tetradeuterothiodiglycol by comparing the appropriate peak areas for 10 ng/ml spiked into blood and urine with those of standard solutions containing 10 ng. Glassware/reagent blanks were run as negative controls before the analysis of each unknown sample.

## RESULTS AND DISCUSSION

The recovery and purification of low-molecular-weight water-soluble compounds from aqueous media presents a difficult problem. Generally a compromise between recovery and clean-up has to be accepted. In previous studies of water-soluble trichothecene mycotoxins we employed Clin Elut extraction columns to recover polar compounds from urine, followed by a chromatographic clean-up<sup>9</sup>. A similar though modified procedure was found suitable for thiodiglycol. Because of the moderate volatility of thiodiglycol, and the possibility of oxidation reactions or adsorption onto glassware, efforts were made to keep manipulations to a minimum. For blood and plasma, a sufficiently clean extract was obtained simply by passing the eluate from the extraction column directly through a reversed-phase silica C<sub>18</sub> cartridge. For urine, which contains a high percentage of more polar materials, a normal-phase clean-up was preferred, a Florisil cartridge retaining the most polar components. Recoveries of tetradeuterothiodiglycol spiked at levels of 10 ng/ml were determined as 50–70% in

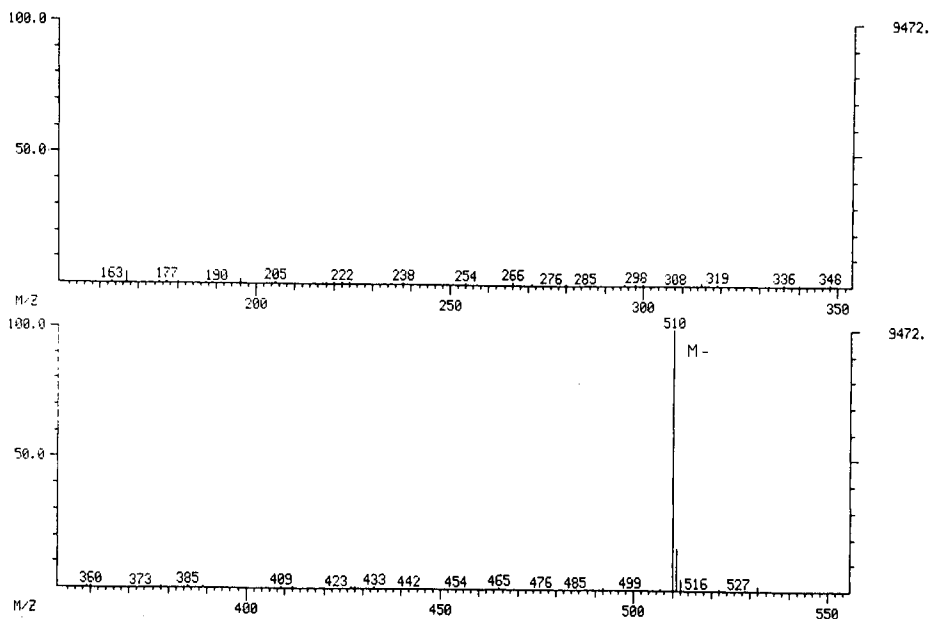


Fig. 1. NCI mass spectrum of thiodiglycol bis(pentafluorobenzoate).

blood, and 60–80% in urine (six determinations), the major losses being incurred at the extraction stage.

In our previous work<sup>9</sup> on the trace analysis of trichothecene mycotoxins, electron-capture negative-ion chemical ionisation (NICI) was found to give optimum sensitivity and selectivity for trace analysis in body fluids. We explored several possible derivatives of thiodiglycol which might be suitable for detection using NICI. The flophemesyl and heptafluorobutryl derivatives gave very weak  $M^-$  ions. In contrast the bis(pentafluorobenzoyl) derivative was found to concentrate almost all of its ion current in the molecular ion, enabling great sensitivity to be obtained in the selected ion mode. Fig. 1 shows the NICI mass spectrum of thiodiglycol bis(pentafluorobenzoate). In contrast the electron-impact positive ion spectrum showed no molecular ion, the parent ion being  $m/z$  239 ( $C_6F_5COOCH_2CH_2^+$ ) with the non-informative ion  $m/z$  195 ( $C_6F_5CO^+$ ) also accounting for a large proportion of the ion current. Fig. 2 shows a selected ion current profile using NICI for 400 fg injected into the gas chromatograph. Although very weak additional ions are observable in the NICI spectrum, the concentration of the ion current into a single ion (plus isotopic ions) does present problems of confirmation of identification at trace levels. Raising the source temperature and pressure failed to induce fragmentation of the molecular ion. In this present work, to be confident that a compound we detected in control blood samples at the retention time of thiodiglycol was in reality thiodiglycol, we repeated the analysis using three additional GC columns of varying selectivity (BP-5, BP-10 and BP-20). In each case the compound eluted at the retention time for thiodiglycol bis(pentafluorobenzoate). Additional support for the identification was obtained from selected ion monitoring of  $m/z$  510 at 5000 mass resolution using a VG 7070EQ magnetic sector instrument. The selected ion current profile at 5000 resolution, for a blood sample found to contain 13 ng/ml of thiodiglycol, is shown in Fig. 3.

The linearity of the method for quantitation was good over the range 5–100 ng/ml in plasma and urine, and 10–100 ng/ml in blood (linearity at higher levels was not assessed). The non-linear lower parts of the curve were consistent and quantitation at very low levels was performed using calibration points at 0, 1, 5 and 10 ng/ml. The calibration curve obtained for thiodiglycol spiked into urine is shown in Fig. 4. Regression analysis of the linear portion of the curve gave the equation  $y =$

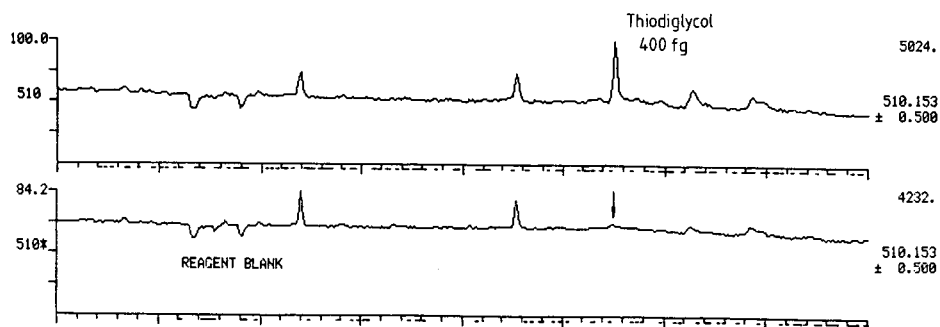


Fig. 2. Selected ion current profile monitoring  $m/z$  510 for thiodiglycol bis(pentafluorobenzoate), equivalent to 400 fg thiodiglycol injected.

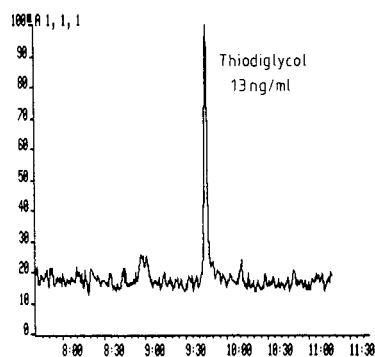


Fig. 3. Selected ion current profile monitoring  $m/z$  510 at 5000 resolution, showing the detection of thiodiglycol (13 ng/ml) in a control blood sample.

$0.101x - 0.142$  ( $r = 0.999$ ), compared to a calibration from standards,  $y = 0.100x - 0.247$  ( $r = 0.999$ ). The calibration curve for blood (obtained several weeks earlier) gave the equation  $y = 0.149x - 0.694$  ( $r = 0.999$ ), compared to a calibration from standards,  $y = 0.150x - 0.555$  ( $r = 0.998$ ). Moderate to good precision was obtained. Six replicate determinations on a sample of blood, found to contain a natural background of thiodiglycol determined as 12 ng/ml, gave a coefficient of variation of 5.3%. Four replicate determinations for samples of blood, previously shown to contain natural levels of thiodiglycol determined as 6 ng/ml and spiked with additional thiodiglycol at 50 ng/ml, gave a coefficient of variation of 4.6% (mean 53 ng/ml). Six replicate determinations for urine spiked at 20 ng/ml gave a coefficient of variation of

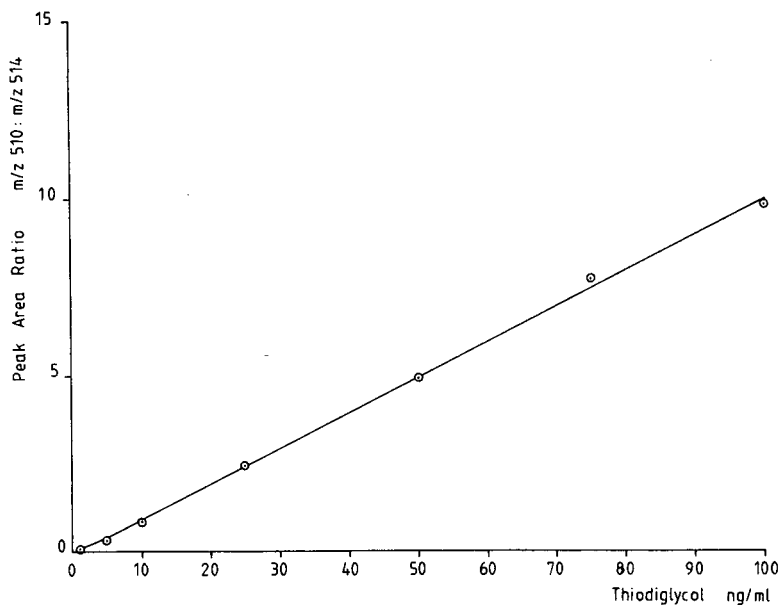


Fig. 4. Calibration curve for thiodiglycol in urine (slope = 0.101, correlation = 0.999).

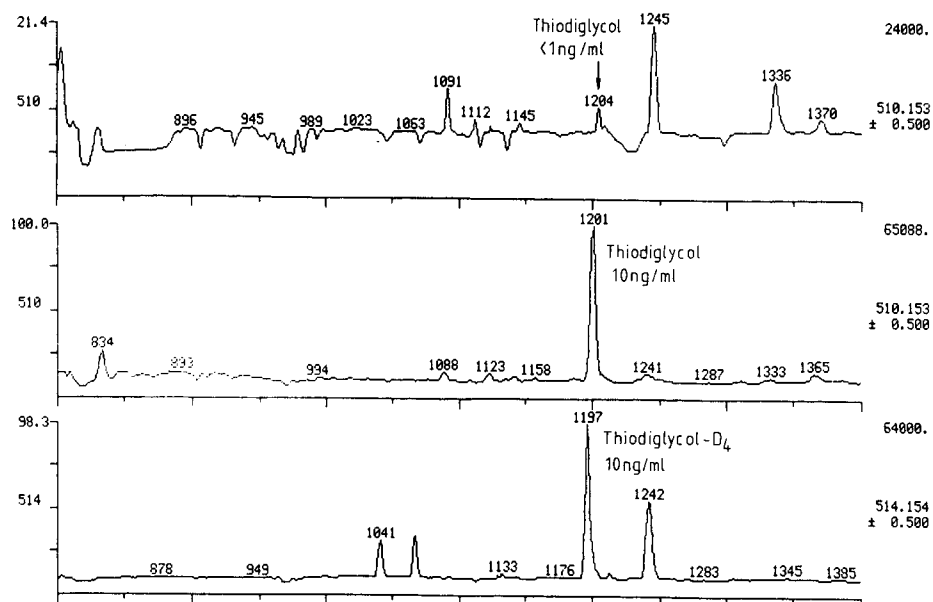


Fig. 5. Selected ion current profiles showing the detection of trace levels ( $<1$  ng/ml) of thiodiglycol in a control blood sample (upper), the same sample spiked with 10 ng/ml (middle), and the trace for the internal standard (10 ng/ml) (lower).

4.1% (mean 19.3 ng/ml). Based on a signal-to-noise ratio of at least 3:1 the method readily detected levels of 1 ng/ml spiked into 1-ml samples of blood and urine previously shown to contain  $<1$  ng/ml. Fig. 5 shows the selected ion current profiles for a sample of blood found to contain  $<1$  ng/ml of thiodiglycol and after spiking with an additional 10 ng/ml. The ion current for thiodiglycol is seen against a clean background (the data system has normalised the background for the unspiked sample to the highest peak). Plasma behaved similarly to whole blood. Fig. 6 shows selected ion current profiles for a sample of urine which contained no detectable thiodiglycol above the noise level (*i.e.*  $<1$  ng/ml), and the same sample spiked with 10 ng/ml of thiodiglycol. The background monitoring of the molecular ion of thiodiglycol was again relatively clean, but some background was observed in human urine monitoring the molecular ion for the deuterated internal standard; it did not however interfere with quantitation.

During subsequent work we attempted to extend the method to the pentafluorobenzoates of the sulfoxide and sulphone analogues of thiodiglycol. Under similar derivatising conditions the sulfoxide was found to convert in high yield to thiodiglycol bis(pentafluorobenzoate), a reaction which presumably involves a variation of the Pummerer rearrangement of sulfoxides; this reaction is being investigated. The method therefore does not distinguish between thiodiglycol and its sulfoxide, a possible metabolite. It can be extended to the sulphone whose bis(pentafluorobenzoyl) derivative also concentrates nearly all of its ion current in the  $M^+$  ion,  $m/z$  542 using NICI. However peak shape was poor using similar GC conditions and sensitivity and detection limits were about an order worse.

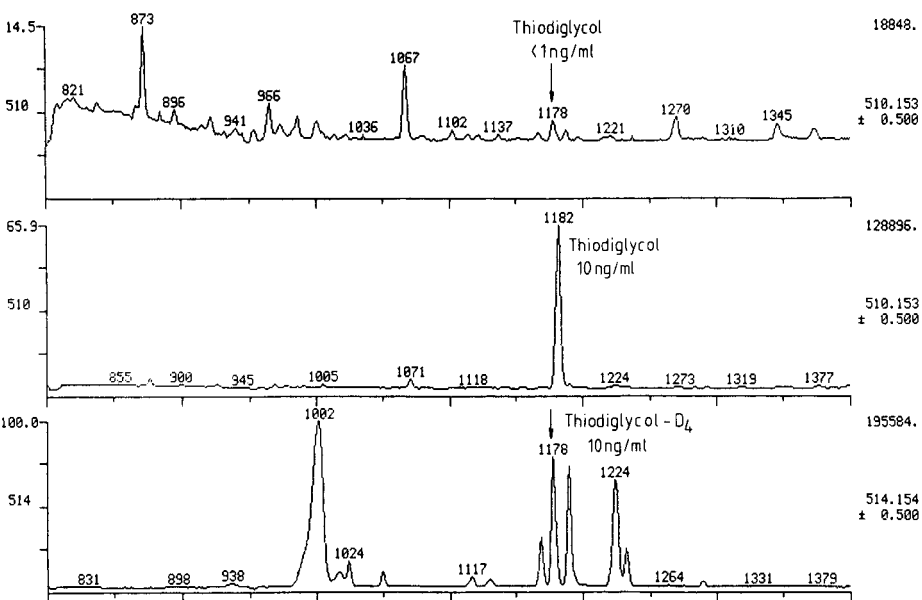


Fig. 6. Selected ion current profiles from a control urine sample (upper), the same sample spiked with thiodiglycol (10 ng/ml) (middle), and the trace for the internal standard (lower).

Samples of blood and urine from ten male volunteers were analysed for thiodiglycol. The results are summarised in Table I. Only two of the blood samples contained levels below 1 ng/ml, though both of these showed detectable peaks at the retention time for thiodiglycol (*e.g.* Fig. 5). Levels up to 16 ng/ml were detected, most being around the 10 ng/ml level. In contrast none of the urine samples, taken from the

TABLE I  
ANALYSIS OF BLOOD AND URINE SAMPLES FROM CONTROL SUBJECTS

— = No sample.

Subject No.	Thiodiglycol (ng/ml)	
	Blood	Urine
1	13	<1*
2	11	<1
7	12	<1*
8	9	<1
9	16	<1*
10	10	<1
11	10	<1
12	6	<1
59	<1	—
60	<1	—

\* Also <1 ng/ml after treatment with  $\beta$ -glucuronidase and conc. hydrochloric acid.

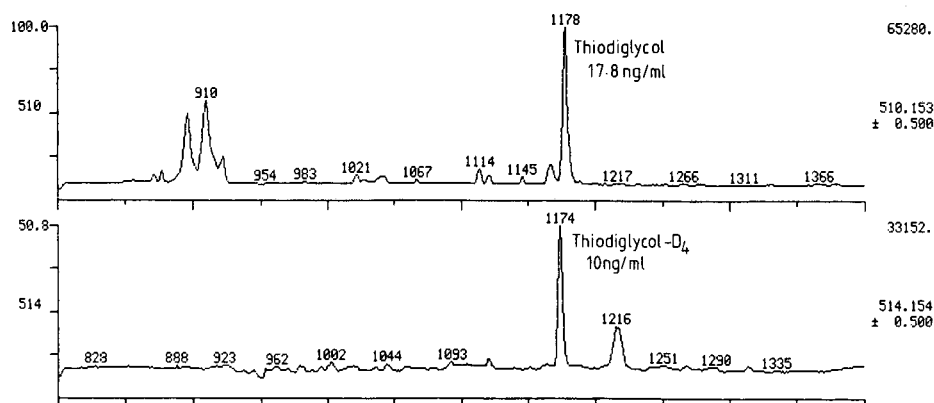


Fig. 7. Selected ion current profile showing the detection of thiodiglycol (18 ng/ml) in rat urine.

same volunteers at the same time as the blood samples, contained free thiodiglycol at levels above 1 ng/ml. Urine from subjects with the highest levels in blood was also analysed after treatment with  $\beta$ -glucuronidase (which also possesses some sulphatase activity), and after treatment with hydrochloric acid. Again levels of thiodiglycol present remained below 1 ng/ml. These differences between blood and urine levels may simply reflect dilution in urine though metabolism is an additional possibility. The analyses of urine samples from control subjects contrast with those reported by Wils *et al.*<sup>6</sup>, who found levels up to the equivalent of 55 ng/ml. These differences may reflect variations in diet, or possibly result from the differing hydrolysis conditions used although treatment of our samples with hydrochloric acid at 95–100°C for 1 h gave results no different from those obtained when incubated at 37°C. Clearly a much larger number of control subjects will need to be analysed for thiodiglycol before any firm conclusions can be drawn about endogenous levels.

To demonstrate that the method could detect thiodiglycol in biological fluids after exposure to sulphur mustard, analyses were performed on samples of urine from two rats dosed intraperitoneally with sulphur mustard (1.59 mg/kg). No thiodiglycol was detected in the rat urine prior to dosing. Relatively small amounts of free thiodiglycol (18 ng/ml, both rats) were observed in the 24-h urine (Fig. 7). Much less background was observed in rat urine monitoring  $m/z$  514 of the internal standard. Treatment of the rat urine with  $\beta$ -glucuronidase increased levels of thiodiglycol more than five fold (91 and 148 ng/ml), and treatment with concentrated hydrochloric acid more than 10 fold (256 and 388 ng/ml). Elimination profiles for thiodiglycol and its conjugates, and the identification of these conjugates and other metabolites present, are currently under investigation.

#### ACKNOWLEDGEMENTS

Tetradethiothiodiglycol was prepared by Dr. J. M. Harrison. Rat urine was supplied by Dr. D. J. Howells and Miss J. Hambrook.

## REFERENCES

- 1 G. Machata and W. Vycudilik, in A. Heyndrickx (Editor), *Proceedings of the First World Congress: New Compounds in Biological and Chemical Warfare, Ghent, May 21-23, 1984*, Koninklijke Bibliotheek Albert I, pp. 53-55.
- 2 A. Heyndrickx, J. Cordonnier and A. De Bock, in A. Heyndrickx (Editor), *Proceedings of the First World Congress: New Compounds in Biological and Chemical Warfare, Ghent, May 21-23, 1984*, Koninklijke Bibliotheek Albert I, pp. 102-109.
- 3 W. Vycudilik, *Forensic Sci. Int.*, 28 (1985) 131.
- 4 C. Davison, R. S. Rozman and P. K. Smith, *Biochem. Pharmacol.*, 7 (1961) 65.
- 5 J. J. Roberts and G. P. Warwick, *Biochem. Pharmacol.*, 12 (1963) 1329.
- 6 E. J. Wils, A. G. Hulst, A. L. de Jong, A. Verweij and H. L. Boter, *J. Anal. Toxicol.*, 9 (1985) 254.
- 7 W. Vycudilik, *Forensic Sci. Int.*, 35 (1987) 67.
- 8 R. M. Black, R. J. Clarke and R. W. Read, *J. Chromatogr.*, 367 (1986) 103.
- 9 P. Begley, B. E. Foulger, P. D. Jeffery, R. M. Black and R. W. Read, *J. Chromatogr.*, 367 (1986) 87.

CHROM. 20 658

## DETERMINATION OF NATIVE FOLATES IN MILK AND OTHER DAIRY PRODUCTS BY HIGH-PERFORMANCE LIQUID CHROMATOGRAPHY

DOUGLAS L. HOLT\*, RANDY L. WEHLING\* and MICHAEL G. ZEECE

*Department of Food Science and Technology, 134 Filley Hall, University of Nebraska, Lincoln, NE 68583-0919 (U.S.A.)*

(Received May 16th, 1988)

---

### SUMMARY

Folates were measured in dairy products by high-performance liquid chromatography without prior sample clean-up. Detection limits for individual folates range from 0.3 to 7.3 ng/g. The folates were extracted from the sample matrix by adjusting the pH to 4.5 with acetic acid, centrifuging to remove precipitated proteins, and treating with conjugase to remove multiple polyglutamate residues. Folates were separated from other sample components using a reversed-phase column with a methanol-phosphate buffer (pH 6.8), and ion-pairing with tetrabutylammonium ion. Fluorescence was found to be the most useful detection technique. Fluorescence detection of reduced forms of the vitamin was achieved by post-column pH adjustment of the eluent with phosphoric acid, while the parent folic acid molecule required chemical oxidation with hypochlorite in order to obtain a fluorescent response.

---

### INTRODUCTION

Folic acid and several related compounds are important cofactors in human nutrition, where they play a role in one carbon transfers in the biosynthesis and degradation of proteins and nucleic acids<sup>1–4</sup>. Their activity in nucleic acid synthesis has led to the use of folate antagonists in anti-cancer therapy<sup>5</sup>. Folates are extremely labile when subjected to oxidation and heat, and it is thought that many food processing operations result in a significant destruction of the vitamers<sup>6–10</sup>, although recent evidence has indicated that folates may be protected by other food components<sup>8</sup>. On the other hand, the instability of the vitamers may lead to underestimation of the levels naturally occurring in foodstuffs, due to the destruction of significant amounts during analysis<sup>3,11</sup>. The loss of folates during analysis is one of the major impediments to the measurement of these compounds by the nutritional chemist.

An additional complication in the analysis of folates is the extremely low levels

---

\* Present address: Dole Packaged Foods, Technical Center, 2102 Commerce Drive, San Jose, CA 95131, U.S.A.

present in most foods. Except for a few cases such as liver and yeast extract, the folate levels in most foods are less than 100 ng/g<sup>3,5</sup>. Thus, destruction of even limited amounts of folates during sample preparation may reduce the total folate level below detection limits.

Folates are usually measured by microbiological assay. This method, while highly sensitive (detection limits approach 10 ppt), is very tedious and can provide only limited information on the actual forms of folate present in a sample<sup>12</sup>. Additionally, microbiological assays are often subject to multiple interferences from the sample matrix. Several researchers have attempted to circumvent these problems by using a chromatographic separation prior to microbiological assay. The microbiological assay then serves as a sensitive detector for the chromatographic separation<sup>13</sup>.

In recent years, high-performance liquid chromatography (HPLC) has been used to determine the levels of folates in several matrices including liver, blood, infant formula, and milk<sup>14,15</sup>. Gregory *et al.*<sup>15</sup> have described a procedure that uses sample clean-up on an open ion-exchange column, followed by HPLC separation and fluorescence detection. Certain folates required a post-column oxidation to form fluorescent derivatives. Other researchers have measured folates in plasma and serum by using a thin-layer electrochemical detector<sup>16,17</sup>. In this paper, we describe the application of these two detection techniques to the determination of folates at biological levels in dairy products, in combination with a reversed-phase column and ion-pairing to separate folates from interferences in the sample matrix. A method has been developed that eliminates the need for extensive sample clean-up prior to injection onto the HPLC column.

## EXPERIMENTAL

### *Standards and samples*

Individual folate standards were obtained from Sigma (St. Louis, MO, U.S.A.) or Dr. B. Schirks laboratory (Switzerland), and used without further purification. Purity of the standards was assessed by chromatographic separation with ultraviolet detection at 280 nm. Standard solutions (usually 1000 ng/ml) were prepared in 0.01 *M* sodium phosphate buffer (pH 4.5), containing 0.1% ascorbate and 0.01 *M* 2-mercaptoethanol (MCE). A 10 000 ng/ml solution (in 0.01 *M* phosphate buffer, pH 6.8, containing 0.1% ascorbate and 0.01 *M* MCE) was used to prepare spiked samples, which were allowed to stand for 1.0 h prior to extraction.

Raw milk was obtained from a mixed milking of approximately 50 cows at a local dairy and was analyzed on the day collected. Pasteurized milk and other processed dairy products were obtained from local retail outlets.

### *Extraction of folates from dairy products*

Milk and other fluid dairy products were adjusted to pH 4.5 with glacial acetic acid, and then stirred for 1.0 h with a low speed magnetic stirrer. Samples of cottage cheese or yogurt were homogenized for 1 min in a Waring blender, then adjusted to pH 4.5. All samples were then centrifuged for 10 min at a minimum of 1000 *g*. The supernatant was decanted, and a solution of sodium phosphate buffer (pH 4.5) containing 10% ascorbate and 1 *M* MCE added, so that the final concentrations of ascorbate and MCE were 0.1% and 0.01 *M* respectively. The supernatant was then

treated with 0.1 ml of a conjugase preparation, previously isolated from hog kidneys<sup>15</sup>, and incubated at 37°C in sealed tubes for 2 h. This conjugase treatment was determined to be sufficient to convert 10 µg/ml folic acid pentaglutamate to the monoglutamate within 30 min. After incubation, the samples were centrifuged at 10 000 *g* for 10 min, filtered through 0.45-µm filters, and stored on ice in the dark prior to injection. Standard solutions and spiked samples used for determining recoveries were treated in an identical manner.

### Chromatography

Water for the liquid chromatographic mobile phase was distilled and deionized. HPLC grade methanol was used without further purification. Tetrabutylammonium dihydrogenphosphate was purchased as a 1.0 *M* solution (Aldrich, Milwaukee, WI, U.S.A.) and added to the mobile phase at 50 ml/l. The mobile phase was prepared by dissolving 0.560 g dipotassium hydrogenphosphate and 0.480 g potassium dihydrogenphosphate in a small amount of water in a 1-l flask. The pH of this aqueous buffer was carefully adjusted to 6.8 with phosphoric acid or potassium hydroxide, prior to dilution to 1.0 l with water or methanol. A phosphate buffer-methanol (50:50) solution, and a 100% aqueous phosphate buffer were maintained separately and mixed to form the mobile phase using the high pressure mixing system of the chromatographic hardware. All solvents were filtered through 0.45-µm filters prior to use.

The analytical column used was a Rainin (Woburn, MA, U.S.A.) C<sub>18</sub> Microsorb Short-One™ (10 cm × 4.6 mm I.D., 3 µm spherical packing). A Brownlee (Santa Clara, CA, U.S.A.) cartridge system, equipped with a 1.5 cm × 3.2 mm I.D. guard column packed with a 7-µm widepore C<sub>18</sub> packing material, was installed ahead of the analytical column. Flow-rate through the analytical column was 1.0 ml/min. The column was flushed with distilled water, followed by methanol, after each working day.

The chromatographic system consisted of two Beckman 110B solvent delivery pumps, a Beckman 420 system controller, and a Beckman Model 210A sample injection valve equipped with a 100-µl loop. Detection was either with a Bioanalytical Systems (West Lafayette, IN, U.S.A.) LC-4B amperometric detector fitted with a glassy carbon electrode, and operated at 900 mV *versus* an Ag/AgCl reference electrode, or with a Kratos (Ramsey, NJ, U.S.A.) 980 variable-wavelength fluorescence detector (excitation 238 nm, emission > 340 nm). Sensitivity was generally set at 10 nA f.s. for the amperometric detector. High voltage on the fluorescence detector photomultiplier tube was set at 10% over the autocalibration value (approximately 800 V), and the range setting was generally 0.01 µA. The time constant was set at 5 s. The entire chromatographic system was operated at ambient temperature. Chromatograms were recorded with a Spectra-Physics 4270A (San Jose, CA, U.S.A.) recording integrator.

Preceding the fluorescence detector, post-column pH adjustment of the eluent stream was achieved by pumping 0.25 ml/min of a 4.25% (v/v) aqueous phosphoric acid solution through a reaction tee, using a Milton Roy Mini-pump (Riviera Beach, FL, U.S.A.). The reaction tee has been previously described by Mauro *et al.*<sup>18</sup>. When required, a post-column chemical oxidant was substituted for the phosphoric acid solution. The oxidizing solution consisted of 0.005% sodium hypochlorite, 0.1

M sodium dihydrogenphosphate and 0.2 M sodium chloride in water (pH 3.0), and was added to the eluent stream at 0.25 ml/min, as suggested by Gregory *et al.*<sup>15</sup>.

## RESULTS AND DISCUSSION

### Chromatography

The chromatographic system was a modification of that developed by Duch *et al.*<sup>19</sup>. Conditions were modified in order to optimize the separation of folates from sample interferences. Reversed-phase columns from several manufacturers were evaluated with respect to their suitability for this particular separation. A high efficiency column packed with a 3  $\mu$ m C<sub>18</sub> packing material (Rainin Short One) provided excellent separation of the various folate forms (Fig. 1), and a relatively long life (over 500 injections) with the mobile phase conditions used.

The separation of folate standards was only slightly affected by varying the pH of the mobile phase between 6.0 and 7.0. However, retention times of several components in milk were significantly changed by variations in mobile phase pH. The optimum separation of 5-methyltetrahydrofolate, the predominant form of folate in milk, from the sample matrix was obtained at pH 6.8 (Fig. 2). On the other hand, methanol concentration strongly influenced the retention of folates on the analytical column. Mobile phase methanol contents between 12 and 25% gave no change in the elution order of folates, but the retention times of 5-methyltetrahydrofolate, the most strongly retained vitamer, varied from 8 to 45 min depending on methanol concentration. The retention times and calculated efficiency factors ( $k'$ ) for various folates under selected isocratic conditions are presented in Table I. Gradient elution, where the methanol content was varied from 0 to 20% over 15 min, was successfully employed to separate

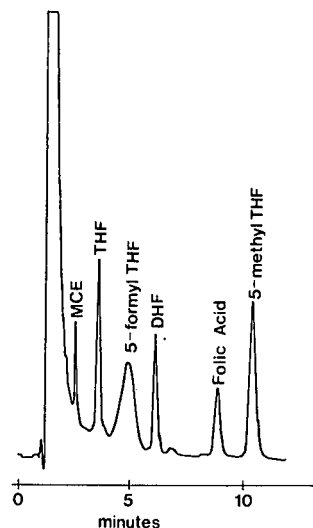


Fig. 1. Separation of several folates including tetrahydrofolate (THF), 5-formyltetrahydrofolate (5-formyl THF), dihydrofolate (DHF), folic acid, and 5-methyltetrahydrofolate (5-methyl THF) under isocratic conditions using 20% methanol. Folates were detected by ultraviolet absorption at 280 nm.

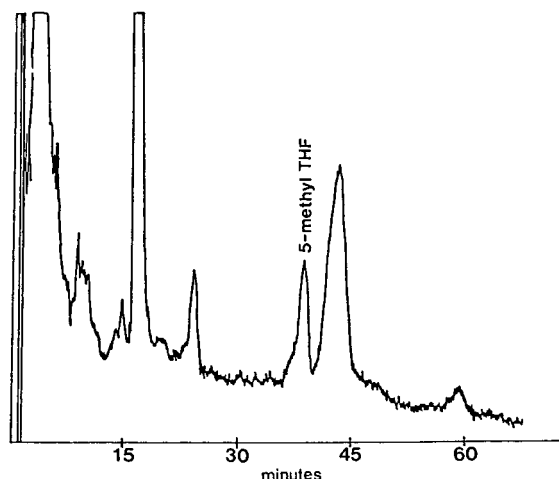


Fig. 2. Chromatogram of milk showing the naturally occurring 5-methyltetrahydrofolate (5-methyl THF). Fluorescence detection following post-column pH adjustment was used to quantitate the 5-methyl THF.

up to six different folates from interferences in the milk matrix. However, since only 5-methyltetrahydrofolate was found to occur naturally at significant levels in dairy products, isocratic conditions at 16% methanol can routinely be employed to quantitate this form.

### Detection

As ultraviolet absorption detection was found to lack sufficient sensitivity to detect the low levels of folates naturally present in dairy foods, more sensitive detection techniques were investigated. Recent advances in electronics and detector cell design have led to an increased use of electrochemical detection (ED) with HPLC separations<sup>20</sup>. ED can be both highly selective and sensitive under ideal conditions. Examination of cyclic voltammograms of folates (Fig. 3) indicated that an oxidative cell potential of 900 mV would provide detection, and was compatible with the mobile

TABLE I

RETENTION TIMES ( $t_R$ ) AND CAPACITY FACTORS ( $k'$ ) FOR VARIOUS FOLATES SEPARATED UNDER ISOCRATIC CONDITIONS USING DIFFERENT METHANOL CONCENTRATIONS

Folate	14% Methanol		18% Methanol		20% Methanol	
	$t_R$ (min)	$k'$	$t_R$ (min)	$k'$	$t_R$ (min)	$k'$
Tetrahydrofolate	4.32	2.76	3.60	2.13	3.40	1.96
5-Formyltetrahydrofolate	16.87	13.67	10.80	8.39	7.90	5.87
Dihydrofolate	22.57	18.63	13.98	11.16	9.73	7.46
10-Formyltetrahydrofolate	30.75	25.74	16.05	12.96	11.20	8.74
Folic acid	32.36	27.14	16.32	13.19	11.32	8.84
5-Methyltetrahydrofolate	50.17	42.63	25.84	21.47	12.08	9.50

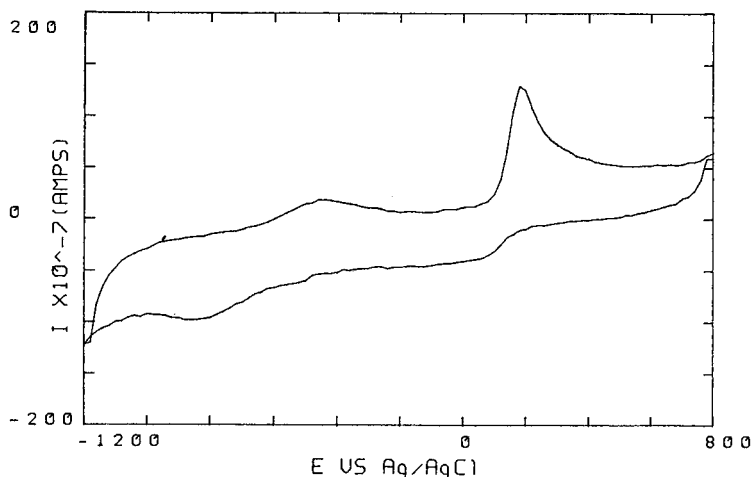


Fig. 3. Cyclic voltammogram of 2 mM 5-methyltetrahydrofolate dissolved in the methanol-phosphate buffer HPLC mobile phase. Potentials shown are measured vs. an Ag/AgCl reference electrode. The voltage was swept from +800 mV to -1200 mV and back at a scan rate of 250 mV/s.

phase used in this separation. Hydrodynamic voltammograms of several folates also indicated that ED would be a viable technique (Fig. 4). However, the instability of folates due to oxidation required that high levels of reducing agents, such as ascorbate and/or MCE, be included during the extraction steps<sup>5,9,21</sup>. These high levels (0.1% and 0.01 M, respectively) created significant interferences in the oxidative electrochemical detection of folates. Several attempts to remove these reducing agents with solid phase extraction techniques prior to injection were unsuccessful. No protocol could be devised that would eliminate ascorbate and MCE without loss of some early eluting folates. In addition, complete recovery of highly retained folates required the use of solvents that were detrimental to the stability of the vitamins, and to the

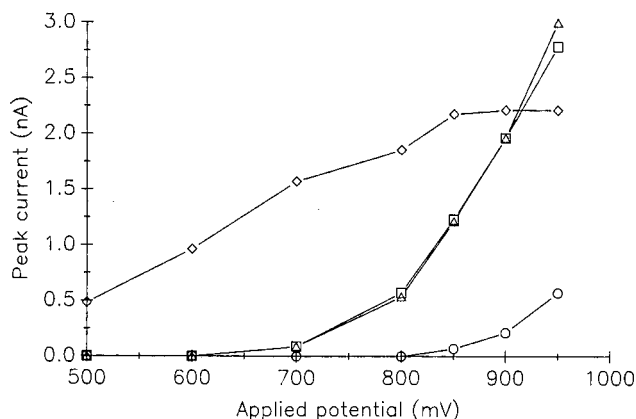


Fig. 4. Hydrodynamic voltammograms for 5-formyltetrahydrofolate ( $\Delta$ ), dihydrofolate ( $\square$ ), 5-methyltetrahydrofolate ( $\diamond$ ), and folic acid ( $\circ$ ). Potentials shown are measured vs. an Ag/AgCl reference electrode.

resolution of the HPLC separation. Attempts to use column switching techniques similar to those reported by Wegner *et al.*<sup>17</sup> were also unsuccessful. The slight changes in pressure and/or temperature induced during column switching resulted in severe baseline disturbances at the high detector sensitivity settings required to measure low levels of folates.

Gregory *et al.*<sup>15</sup> have reported the use of native fluorescence to detect extremely low levels of folates. Initial attempts to use this technique met with failure. However, it was discovered that the fluorescence of many folates is strongly dependent on pH. With a post-column adjustment of the mobile phase pH to < 3, and use of an optimized excitation wavelength (238 nm), very satisfactory detection levels for the folates were achieved (Table II). The pH reduction also quenched the fluorescence of several interfering compounds from milk.

The parent folic acid molecule did not fluoresce after a simple pH adjustment. However, post-column chemical oxidation of folic acid with hypochlorite, as suggested by Gregory *et al.*<sup>15</sup>, did produce a fluorescent compound that could be measured at slightly different wavelengths (365 nm excitation, > 410 nm emission). Post-column oxidation destroyed the fluorescence of the other folates examined, resulting in the need for two injections of each sample in order to detect all possible folate forms. Folic acid was not expected to be present in biological samples<sup>5,9</sup>, and was not found in any of the dairy products tested.

#### *Sample preparation*

In order to minimize potential losses of folates due to oxidation during extraction, every attempt was made to simplify sample preparation. Treatment with conjugase was necessary to remove interferences from polyglutamate forms of the individual vitamins. The polyglutamate forms of some folates can be separated under chromatographic conditions similar to those employed here, but resolution and detection of folylpolyglutamates is difficult<sup>22</sup>.

Levels of ascorbate and MCE were optimized so that folate stability during extraction was maximized. It was discovered that high levels of ascorbate (>0.5%)

TABLE II

DETECTION LIMITS, REPRODUCIBILITY OF INJECTION AND RECOVERY DATA FOR SEVERAL FOLATES

<i>Folate</i>	<i>Detection limit (ng/g)*</i>	<i>Reproducibility, R.S.D. (%)</i>	<i>Recovery (%)</i>
Tetrahydrofolate	5.7	13.20**	73.4
5-Formyltetrahydrofolate	5.1	4.10***	99.4
Dihydrofolate	4.6	2.73§	79.6
10-Formyltetrahydrofolate	7.3	1.69§	82.3
Folic acid	1.7	6.43**	100.1
5-Methyltetrahydrofolate	0.3	3.46**	97.4

\* Using 100 µl injection.

\*\* Determined at 10 ng/ml.

\*\*\* Determined at 50 ng/ml.

§ Determined at 100 ng/ml.

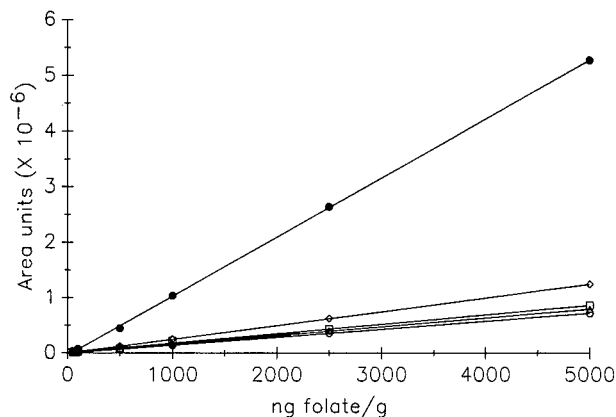


Fig. 5. Linearity of the fluorescence response for several folates including 5-methyltetrahydrofolate (●), tetrahydrofolate (◇), dihydrofolate (□), 10-formyltetrahydrofolate (△), and 5-formyltetrahydrofolate (○).

caused folic acid to precipitate in phosphate buffer. By reducing the ascorbate concentration to 0.1%, with the addition of 0.01 *M* MCE to the sample, most folates were adequately stabilized (Table II). Recoveries were determined by addition of standards to seven samples of pasteurized milk at levels of 100 ng/g sample. The low recovery of tetrahydrofolate (73.4%) is probably due to the extreme instability of this form of the vitamin. It is unlikely that the highly unstable tetrahydrofolate is present in dairy products at significant levels, and none was found in any of the samples analyzed.

The combination of ion-pairing separation and fluorescence detection provided selectivity sufficient to resolve the folates of interest from other sample components, making prior sample cleanup unnecessary. The elimination of all clean-up steps minimizes the chances for oxidation of the folates.

#### *Statistical considerations*

The reproduction of the chromatography, detection, and integration was evaluated by making a series of seven injections of a mixed folate standard (Table II). Relative standard deviations ranged from a low of 1.69% for 10-formyltetrahydrofolate to a high of 13.2% for tetrahydrofolate. The linearities of the fluorescence responses for several folates were determined by addition of a mixed standard to milk at levels equivalent to 50, 100, 500, 1000, 2500, and 5000 ng of individual folate/g sample, with each level in duplicate. Standards of 5-methyltetrahydrofolate were also included at levels of 1 and 10 ng/g. Correlation coefficients were greater than 0.98 in all cases (Fig. 5).

#### CONCLUSIONS

The method described above has been applied to the determination of folates in both raw and pasteurized bovine milk. In both cases, the only form of folate found in significant levels was 5-methyltetrahydrofolate. The average folate content of three samples of raw milk was  $66.7 \pm 3.3$  ng/g, while seven samples of pasteurized milk

resulted in an average value of  $49.6 \pm 1.7$  ng/g. These results agree well with literature values<sup>3</sup> obtained by microbiological assay using *Lactobacillus casei* as the test organism (55 ng/g and 50 ng/g for raw and pasteurized milk, respectively). The HPLC procedure has also been successfully applied to the determination of folates in other dairy products including cottage cheese, cultured buttermilk, and yogurt.

In summary, a reversed-phase separation with ion-pairing is coupled with fluorescence detection to measure six different folates at native levels in milk and dairy products. The response for each of the folates is linear over the range of interest. The method has an advantage over previous procedures, in that sample clean-up and pre-concentration steps on open columns are not required, thereby minimizing the potential for loss of the vitamers during sample preparation, and significantly reducing the analysis time.

#### ACKNOWLEDGEMENTS

This work was funded in part by the National Dairy Promotion and Research Board (U.S.A.), administered in cooperation with the National Dairy Council. This is Paper No. 8623, Journal Series, Nebraska Agricultural Station, Lincoln, NE 68583-0704, U.S.A.

#### REFERENCES

- 1 R. Deacon, I. Chanarin, M. Lumb and J. Perry, *J. Clin. Pathol.*, 38 (1985) 1349.
- 2 M. A. Moore, F. Ahmed and R. B. Dunlap, *J. Biol. Chem.*, 261 (1986) 12745.
- 3 B. A. Rolls, in M. Rechcigal (Editors), *Handbook of Nutritive Value of Processed Food*, CRC Press, Boca Raton, FL, 1982, p. 383.
- 4 H. Weissbach and R. T. Taylor, *Vitam. Horm.*, 28 (1970) 415.
- 5 R. L. Blakley and S. J. Benkovic, *Folates and Pterins, Vol. 1, Chemistry and Biochemistry of Folates*, Wiley, New York, 1984.
- 6 B. P. F. Day and J. F. Gregory, *J. Food Sci.*, 48 (1983) 581.
- 7 S. C. deSousa and R. R. Eitenmiller, *J. Food Sci.*, 51 (1986) 626.
- 8 J. F. Gregory, K. A. Ristow, D. S. Sartain and B. L. Damron, *J. Agric. Food Chem.*, 32 (1984) 1337.
- 9 J. F. Gregory, *J. Assoc. Off. Anal. Chem.*, 67 (1984) 1015.
- 10 J. D. O'Brein, I. J. Temperley, J. P. Brawn and J. M. Scott, *Am. J. Clin. Nutr.*, 28 (1975) 438.
- 11 J. E. Ford, *Challenges to Contemporary Dairy Analytical Techniques*, Royal Society of Chemistry, London, 1984, p. 179.
- 12 D. S. Wilson, C. K. Clifford and A. J. Clifford, *J. Micronutr. Anal.*, 3 (1987) 55.
- 13 S. D. Wilson and D. W. Horne, *Anal. Biochem.*, 142 (1984) 529.
- 14 B. P. Day and J. F. Gregory, *J. Agric. Food Chem.*, 29 (1981) 374.
- 15 J. F. Gregory, D. B. Sartain and B. P. Day, *J. Nutr.*, 114 (1984) 341.
- 16 M. Kohashi, K. Inoue, H. Sotoyoshi and K. Iwai, *J. Chromatogr.*, 382 (1986) 303.
- 17 C. Wegner, M. Trotz and H. Nau, *J. Chromatogr.*, 378 (1986) 55.
- 18 D. J. Mauro and D. L. Wetzel, *J. Chromatogr.*, 299 (1984) 281.
- 19 D. S. Duch, S. W. Bowers and C. A. Nichol, *Anal. Biochem.*, 130 (1983) 385.
- 20 J. C. Hoogvliet, *Pharm. Weekblad Sci. Ed.*, 8 (1986) 198.
- 21 S. D. Wilson and D. W. Horne, *Proc. Natl. Acad. Sci. U.S.A.*, 80 (1983) 6500.
- 22 R. N. Reingold and M. F. Picciano, *J. Chromatogr.*, 234 (1982) 171.



CHROM. 20 646

## DETECTION AND DETERMINATION OF COMMON BENZODIAZEPINES AND THEIR METABOLITES IN BLOOD SAMPLES OF FORENSIC SCIENCE INTEREST

### MICROCOLUMN CLEANUP AND HIGH-PERFORMANCE LIQUID CHROMATOGRAPHY WITH REDUCTIVE ELECTROCHEMICAL DETECTION AT A PENDENT MERCURY DROP ELECTRODE

J. B. F. LLOYD\* and D. A. PARRY

*Home Office Forensic Science Laboratory, Gooch Street North, Birmingham B5 6QQ (U.K.)*

(First received April 11th, 1988; revised manuscript received May 16th, 1988)

---

#### SUMMARY

Benzodiazepines in the blood samples typical of forensic science work are recovered from 100–250  $\mu$ l amounts of blood (diluted with aqueous sodium octyl sulphate to suppress protein binding) onto microcolumns of Porapak-T, and finally eluted into 60- $\mu$ l volumes of aqueous acetonitrile. The eluates may be taken directly for analysis by high-performance liquid chromatography (HPLC) with reductive amperometric detection at a pendent mercury drop electrode held at potentials down to  $-1.2$  V vs. Ag/AgCl. For high sensitivity work the electrode is preceded by a coulometric detector fitted with porous carbon electrodes held at 0 V (proprietary reference electrode). The technique detects all of the commonly encountered benzodiazepines and others except clobazam, which contains no azomethine group. The detection limits generally are in the range 1–5 ng/ml (40–200 pg HPLC-injected) in haemolyzed human blood, with recovery values of 84–95%, depending on the actual benzodiazepine, over the range examined ( $\leq 2.14$   $\mu$ g/ml). The respective values for the metabolites of nitrazepam are 8–12 ng/ml and 75–84%. The technique is very much less susceptible to the interferences afflicting other commonly applied techniques, and facilitates considerably the analysis of degraded samples.

---

#### INTRODUCTION

Although many techniques have become available for the analysis of benzodiazepines and their metabolites in body fluids<sup>1–4</sup>, difficulties remain in the detection and quantitation of these compounds in the blood samples routinely encountered in forensic science casework. Such samples are varyingly and usually extensively haemolyzed and are often putrified. Large amounts of solidified and coagulated materials may be present, and there may be serious contamination by plasticizers and by components of the elastomers, e.g. in rubber septa, that the samples may contact

during their collection and storage. The quantities of blood available for examination may be small, and further restricted by the requirements of other analyses.

Usually the samples are examined first by radioimmunoassay techniques that are broadly-specific to this group of compounds<sup>5</sup>. Any cross-reactivity is then subject to identification by other techniques, which commonly depend on chromatography in some form, and in turn depend considerably for their effectiveness on an efficient sample-preparation procedure. Until recently, as in clinical practice, liquid-liquid extraction procedures have predominated<sup>6-9</sup>, but there are obvious possibilities in the use of the solid-phase extraction techniques that are well established in the analysis of the more tractable samples encountered clinically<sup>10-15</sup>.

In forensic science work, as elsewhere, the application of solid-phase extraction has been promoted by the commercial availability of prepacked column and cartridge extraction assemblies. We are aware of no published applications, forensically, to the benzodiazepines, but applications have been reported in the detection of morphine<sup>16</sup>, morphine and codeine<sup>17</sup>, and several anti-inflammatory drugs<sup>18</sup>. Given a sufficient amount of undegraded sample these applications are of undoubted value, but problems emerge with small and degraded samples. In our experience the assemblies tend to become blocked (although a recently developed technique apparently prevents this<sup>19</sup>), and the relatively large amount of adsorbent often present necessitates a final elution either with a large volume of a weak eluent and consequent excessive dilution, or with a strong eluent and consequent poor selectivity.

The small-scale transfer of the benzodiazepines into microlitre volumes can be made by solid-phase extraction onto a loose adsorbent, after liquid-liquid extraction and evaporation steps<sup>20</sup>; and triazolam has been extracted from *post mortem* samples by the direct addition of loose adsorbent<sup>21</sup>. Both techniques give the non-aqueous solutions required for the subsequent gas chromatography. However, if reversed-phase liquid chromatography can be used there is no need for transfer to non-aqueous solvents, and advantage can be taken of the superior stability of the benzodiazepines under liquid chromatography conditions. For the satisfactory gas chromatography of some benzodiazepines derivatization may be required<sup>20</sup>.

Recently, for use in conjunction with reversed-phase liquid chromatography, microcolumn cleanup techniques have been applied in the examination of small and highly complex samples for traces of explosives and firearms residues. A summary of most of this work is available<sup>22</sup>. As described here these techniques have now been adapted to the examination of blood samples for benzodiazepines. The manipulation is straightforward, and with a throughput time limited by the chromatographic run-time, which is within 10 min for all of the commonly encountered benzodiazepines.

Most of the published work on the liquid chromatography of the benzodiazepines has employed ultraviolet absorbance detection; but nearly all of these compounds are electrochemically reducible at practicable electrode potentials<sup>1,23,24</sup>, and high-performance liquid chromatographic (HPLC) techniques employing the effect have been described<sup>25-27</sup>. Despite this, for only those compounds carrying very readily reduced substituents has electrochemical detection given sensitivities competitive with those from ultraviolet absorbance, mainly because of the interference caused by the reduction of traces of oxygen dissolved in the eluents. To a lesser extent, difficulties have arisen due to contamination and irreproducibility of some working electrodes, and to the noise levels generated by dropping mercury electrodes. However,

following from the work on explosives traces none of these problems remains of significance<sup>28</sup>, and reductive mode detection employing a pendent mercury drop electrode is now a routinely applied technique in this laboratory. The electrode response characteristics are highly reproducible (from one year to the next), and the technique is as easily used as any other offering parts-per-billion sensitivity. The application to the common benzodiazepines and their metabolites at these sensitivity levels is described in the following.

## EXPERIMENTAL

### *Materials*

Solvents are HPLC grade (Rathburn); disodium hydrogenphosphate and potassium dihydrogenphosphate are Aristar grade (BDH). Sodium octyl sulphate is HPLC grade (Eastman Kodak).

The Porapak-T (Millipore-Waters), 75–100  $\mu\text{m}$ , is Soxhlet-extracted with acetonitrile for 8 h and dried, finally, under vacuum at room temperature. At monthly intervals the adsorbent is washed with acetonitrile at a filter pump and vacuum-dried.

The benzodiazepines are reference compounds provided by the Central Research Establishment, Home Office Forensic Science Service, U.K. The 6-nitro-quinoline (98%, Aldrich) gives a single chromatography peak at usual sensitivity levels.

Blood samples are equine blood stabilized with oxalate (Gibco); and human blood, stabilized with citrate, from rejected transfusion bags (National Blood Transfusion Service, U.K.). Other samples, variously stabilized, are from routine casework. To haemolyze them, samples are frozen and thawed.

### *HPLC equipment and conditions*

The essential details are as in the work on the electrochemical detection of explosives, recently summarized<sup>28</sup>. Briefly, the detector (EG&G Brookdeal, Model 310, with the 174A control unit) is a modified hanging mercury drop electrode maintained usually at  $-1.2\text{ V}$  vs.  $\text{Ag}/\text{AgCl}$  (0.5  $M$  aq. lithium chloride); the electrode drop size is 6 mg, given by the "L" setting on the control unit; and the separation between the eluent jet and the tip of the mercury capillary is 0.7 mm. The only routine maintenance of the electrode unit is the occasional reinstallation of a freshly silanized glass capillary. The silanization procedure given in the manufacturer's manual is followed with one important modification. After the glass surface has been cleaned by washes in turn with aqueous hydrofluoric acid and water, the treatment is repeated with 0.2% (w/v) aqueous sodium hydroxide and water before the capillary is dried and silanized. Such capillaries give *ca.* six months use before instability of the mercury drop necessitates their replacement.

On occasions, either or both an ultraviolet (240 nm) absorbance detector (Pye Unicam, LC-UV detector) and a coulometric detector (Environmental Sciences Associates, Model 5100A Coulochem with a 5010 analytical cell) have been inserted upstream of the mercury electrode. The coulometric detector, with both of its porous carbon working electrodes set at 0 V (proprietary reference electrode), enables the background current at the mercury electrode to be appreciably reduced in work at high sensitivities.

The separations of the common benzodiazepines are made on  $150 \times 4.5$  mm columns of ODS-Hypersil (Shandon),  $3 \mu\text{m}$ , at  $40^\circ\text{C}$ . The eluent, 1 ml/min, is methanol–1-propanol–aqueous phosphate (100:7.5:80, v/v/v), where the aqueous phosphate (pH 6.0) is 0.0174 M in potassium dihydrogenphosphate and 0.0026 M in disodium hydrogenphosphate. The injection volume of the deoxygenated samples<sup>29</sup> is  $10 \mu\text{l}$ . Some less common and more strongly retained benzodiazepines can be separated rapidly on a  $100 \times 4.5$  mm column of CPS-Hypersil (Shandon) under otherwise unaltered conditions. Along with the other straightforward precautions necessary to exclude oxygen<sup>28</sup> the eluent reservoir is kept under a gentle reflux when the chromatograph is in use. The often recommended vigorous purging of the eluent with an inert gas is quite unnecessary, although the introduction of a low gas flow (*ca.* 5 ml/min) through a porous frit in the eluent is essential to the establishment of a smooth reflux.

#### *Extraction and cleanup equipment and reagents*

The sodium octyl sulphate is made up to 0.2% (w/v) in aqueous 0.1 M disodium hydrogenphosphate. The microcolumn eluents are acetonitrile–water [7:4 and 1:8 (v/v), subject to the retentivity of the batch of Porapak-T used].

Centrifugal filters are made from 1.5-ml polypropylene centrifuge tubes. A hole, *ca.* 1 mm, is pierced in the apex of a tube, and 10–20 mg of Soxhlet-extracted (methanol, 8 h) cotton wool is pushed firmly down into the apex. An unmodified tube is used as a receiver. Disposable microcolumns of 5 mg of the Porapak-T in  $60 \text{ mm} \times 1 \text{ mm}$  I.D. PTFE tubing (Alltech) are prepared as otherwise previously described<sup>30</sup>. At this stage only about one third of the column tube is filled. The columns may be stored indefinitely, but immediately before use 50–100  $\mu\text{l}$  of acetonitrile and then a similar volume of water is drawn through them at a filter pump. Membrane microfilters, 0.45- $\mu\text{m}$  pore size PTFE (Gelman, Acro LC3S), and 250- $\mu\text{l}$  polypropylene microcentrifuge tubes (Alpha Laboratories) are Soxhlet-extracted (methanol, 8 h) and dried  $\leq 80^\circ\text{C}$ .

The elution equipment is a chromatography injection valve (Rheodyne, Model 7125) fitted with a 1-ml sample loop that serves as a reservoir for one of the eluents. The valve is connected to a conventional HPLC pump, the inlet flow lines of which have been replaced with 1 mm I.D. stainless-steel tubing to minimize the internal volume of the equipment. The pump is charged with the other of the eluents and set to a flow of 1  $\mu\text{l/s}$ . A timing unit controls the pump. For 60- $\mu\text{l}$  fractions the system gives a coefficient of variation of 4%. At this low flow-rate bubble formation in the pump chambers can be troublesome, but is readily avoided if the eluents are sonicated before use. (The back pressure of the columns is negligible: any type of pump could be used, or the columns could be eluted manually from a syringe.)

#### *Sample cleanup and processing procedures*

A flowchart summarizing these procedures is shown in Fig. 1.

The sample is spun through one of the centrifugal filters. This removes coarse particulates and coagulated material; cellular material passes through. The filtrate is mixed and a portion,  $\leq 250 \mu\text{l}$ , is transferred to a 1.5-ml polypropylene centrifuge tube. A sample size of  $100 \mu\text{l}$  is sufficient in most cases. If the volume of unfilterable material can be disregarded, the actual quantity of blood required for analysis may be pipetted

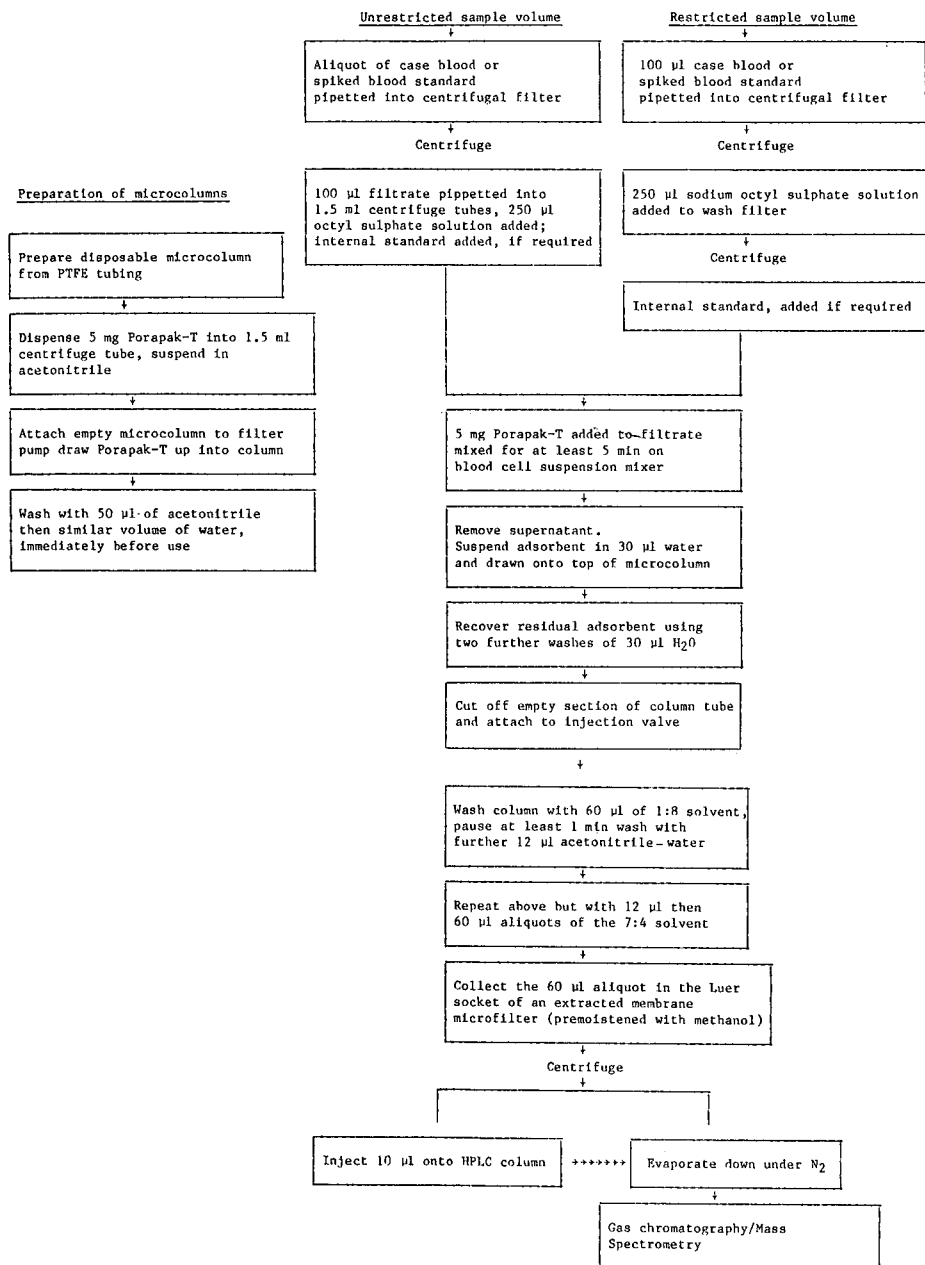


Fig. 1. Sample preparation and processing: schematic flowchart representation of the details given in Experimental.

directly onto the filter and washed through at the centrifuge with the next added reagent. This minimizes sample wastage on the filter.

Into the sample is dispensed 250 µl of the octyl sulphate solution and 5 mg of the Porapak-T. The mixture is kept in suspension for not less than 5 min on a blood cell

suspension mixer, the adsorbent is allowed to settle out for a similar time, and the supernatant is removed. The adsorbent is drawn onto the top of a microcolumn (attached at its outlet to a filter pump) with three 30- $\mu$ l volumes of water, the section of the column tube remaining empty is cut off, and the column is attached to the injection valve. Elution is conducted first with 60  $\mu$ l of the 1:8 solvent. After a pause of not less than 1 min, when a slowly desorbing blood pigment is released, the elution is continued in turn with 12  $\mu$ l of the same solvent (12  $\mu$ l is the approximate column void), and with 12  $\mu$ l and 60  $\mu$ l increments of the 7:4 solvent. The benzodiazepines appear in the last increment. This is collected in the Luer socket of an extracted membrane microfilter (premoistened with methanol), and centrifuged through the membrane into a micro-centrifuge tube. The centrifugate is taken for chromatography directly. If necessary, part of it may be evaporated down in a stream of nitrogen and transferred to any solvent appropriate, *e.g.*, to gas chromatography or mass spectrometry.

Quantitative determinations are standardized against spiked blood samples. Internal standards, in aqueous methanol, may be added directly to the samples or to the octyl sulphate solution. For general-purpose work the 6-nitroquinoline added at 2–20 ng per sample is convenient. If a benzodiazepine is used the addition is made directly into the sample: the alternative mode can result in losses due to precipitation and adsorption of the less polar benzodiazepines.

TABLE I

HYDRODYNAMIC VOLTAMMETRIC RESPONSE DATA OF SOME BENZODIAZEPINES, THEIR METABOLITES, AND 6-NITROQUINOLINE UNDER HPLC CONDITIONS

The data are from peak area measurements.

Compound	Response*		
	Relative to equimolar 6-nitroquinoline, at $-1.2$ V	Relative to the individual compounds' responses at $-1.2$ V	
		$-1.1$ V	$-1.0$ V
7-Acetamidonitrazepam**	0.34	0.13	<0.05
7-Aminonitrazepam**	0.30	0.05	<0.05
Chlordiazepoxide	0.68	1.00	0.70
Demoxepam**	0.72	0.67	0.49
Desmethylchlordiazepoxide**	0.52***	0.90	0.81
Desmethyldiazepam**	0.27	0.33	<0.05
Diazepam	0.34	0.36	<0.05
Loprazolam	1.23	0.82	0.48
Lorazepam	0.30	0.45	<0.05
Lormetazepam	0.27	0.20	<0.05
Nitrazepam	0.97	0.74	0.69
6-Nitroquinoline	(1.00)	0.79	0.75
Oxazepam	0.35	0.23	<0.05
Temazepam	0.32	0.10	<0.05
Triazolam	0.38	0.98	0.44

\* Means of duplicated determinations. The maximum difference within a pair of duplicates was 0.08 (desmethyldiazepam at  $-1.1$  V).

\*\* Metabolites.

\*\*\* Impurity peaks present.

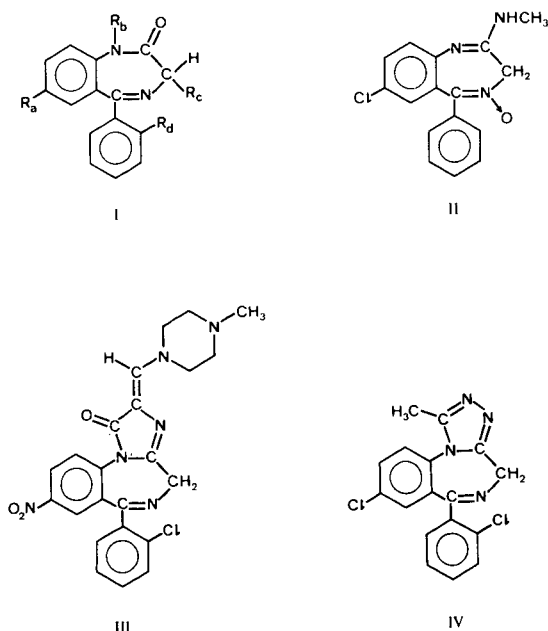


Fig. 2. Structural formulae of common benzodiazepines and their metabolites: 7-acetamidonitrazepam (I,  $R_a = \text{CH}_3\text{CONH}$ ,  $R_b = R_c = R_d = \text{H}$ ); 7-aminonitrazepam (I,  $R_a = \text{NH}_2$ ,  $R_b = R_c = R_d = \text{H}$ ); chlordi-azepoxide (II); demoxepam (II, the desmethylamino lactam); desmethylchlordi-azepoxide (II, the desmethyl analogue); desmethyldiazepam (I,  $R_a = \text{Cl}$ ,  $R_b = R_c = R_d = \text{H}$ ); diazepam (I,  $R_a = \text{Cl}$ ,  $R_b = \text{CH}_3$ ,  $R_c = R_d = \text{H}$ ); lorazepam (I,  $R_a = \text{Cl}$ ,  $R_b = \text{H}$ ,  $R_c = \text{OH}$ ,  $R_d = \text{Cl}$ ); lormetazepam (I,  $R_a = \text{Cl}$ ,  $R_b = \text{CH}_3$ ,  $R_c = \text{OH}$ ,  $R_d = \text{Cl}$ ); nitrazepam (I,  $R_a = \text{NO}_2$ ,  $R_b = R_c = R_d = \text{H}$ ); oxazepam (I,  $R_a = \text{Cl}$ ,  $R_b = \text{H}$ ,  $R_c = \text{OH}$ ,  $R_d = \text{H}$ ); temazepam (I,  $R_a = \text{Cl}$ ,  $R_b = \text{CH}_3$ ,  $R_c = \text{OH}$ ,  $R_d = \text{H}$ ); triazolam (IV).

## RESULTS AND DISCUSSION

The work has been concerned primarily with the benzodiazepines approved for supply on a British National Health Service prescription—the “limited list”. Those examined in detail, together with some metabolites of them, are listed in Table I; structural formulae are given in Fig. 2 (comprehensive listings are available in the cited literature<sup>2,3</sup>). Except for clonazepam all of the benzodiazepines encountered during the period of development and application of the described techniques (14 months; 87 cases, 64 positive) are included in the table. Clonazepam (1 case) and the benzodiazepines available on private prescription have been less closely examined, but with the result that the described work is equally applicable to them without significant modification. The only exception is clobazam, which is not amenable to reductive detection and has not been involved in any submitted casework.

### *Electrochemical characteristics*

Except for that of clobazam, the characteristic diazepine ring of the compounds contains an azomethine bond (Fig. 2) reducible at accessible potentials on a mercury electrode<sup>23</sup>. More readily reduced nitro, amine oxide and heterocyclic functions occasionally are present, which confers detectability at carbon electrodes<sup>25,31</sup>. However, the mercury electrode is applicable generally.

Some reponse characteristics under the HPLC conditions of the compounds of interest are given in Table I. At  $-1.2$  V, *vs.* Ag/AgCl, the data are expressed relative to 6-nitroquinoline. To a first approximation, they may be interpreted on the assumption that azomethine, amine oxide and nitro groups are undergoing, respectively, their 2-, 2- and 4-electron reductions to the secondary amine and to the incompletely reduced derivatives of the last two groups<sup>32,33</sup>. There is no evidence of the reductive dehydroxylation undergone by the hydroxybenzodiazepines under some conditions<sup>34</sup>. In loprazolam the response is probably augmented by reduction processes within this nitrocompound's more complex heterocyclic structure. There seems to be a similar participation in the case of triazolam where, as Table I shows, at  $-1.0$  V a substantial response persists relative to this compound's response at  $-1.2$  V, in contrast to the solely azomethine reductions (relative responses  $<0.05$ ). Presumably, reduction within the ring structure of the nitroquinoline, along with reduction of the nitro group, is responsible for the coincidence between the nitroquinoline and nitrazepam at  $-1.2$  V.

For work with nanogram amounts the potential limit, because of baseline drift, is in the region of  $-1.4$  V. At this potential a substantially increased response is obtained from the amine oxide- and nitro-substituted benzodiazepines, but not from the others. The result is expected on the above assumption that at  $-1.2$  V only the azomethine reductions are complete.

### *Background currents*

It has often been suggested that reductive detection techniques are difficult to use because of the requirement for a deoxygenated eluent if a low background current and, hence, a stable baseline and a satisfactory sensitivity are to be obtained. However, there should be no difficulty if the eluent reservoir is maintained under a slow reflux whilst the system is in use, if all of the eluent flow lines are of stainless steel, and if the eluent flow is stopped completely when the system is not in use<sup>28</sup>. Some years ago it was demonstrated on the basis of ultraviolet absorbance results that for practical HPLC use the reflux technique is much more effective than the commonly employed sparging technique<sup>35</sup>; and in view of our own results and those available from a variety of other techniques, which have been reviewed recently<sup>36</sup>, this remains the position.

For the detection of the benzodiazepines down to the 50 ng/ml level the reflux technique is all that is necessary, and results in background currents of 5–20 nA, cathodic (chromatographic peak heights are in the range 0.25–2.5 nA per ng of benzodiazepine injected). Aerated eluents give background currents of *ca.* 20  $\mu$ A.

The installation of the upstream coulometric detector with both of the porous carbon working electrodes at 0 V (proprietary reference electrode) lowers the background current at the mercury electrode to 2–6 nA, cathodic; and with a regularly used system a stable baseline is obtained after a short running time, *e.g.*, 10 min. Without this installation an hour's running time may be needed. Potentials at the carbon electrodes more cathodic than 0 V effect little further depression of the background current. The substances undergoing reduction at the carbon electrodes are unknown, but traces of oxygen may not be involved: at 0 V oxygen is not significantly reduced on this type of electrode<sup>37</sup>, and the electrodes proved ineffective in attempts to depress the response of the mercury electrode to oxygenated eluents. The carbon electrodes operated at negative potentials, *e.g.*  $-0.7$  V, to some extent respond to the

readily reduced benzodiazepines, but the response is inefficient and noisy, and of little use for nanogram amounts relative to the mercury electrode.

### HPLC conditions

The general order of elution of the benzodiazepines under the present conditions agrees with the relevant published data from octadecylsilyl columns in aqueous methanolic eluents<sup>38</sup>. However, to display distinguishable peaks from all of the benzodiazepines of interest and to separate them from occasionally seen contaminants on a single chromatogram, the addition of 1-propanol to the eluent is necessary. The chromatogram of a standard mixture is shown in Fig. 3. If 1-propanol is not present, triazolam, lorazepam and oxazepam are unresolved from one another. So too are chlordiazepoxide and lormetazepam. Under the conditions of Fig. 3 desmethyl-chlordiazepoxide (not included in the mixture) is unresolved from lorazepam, but readily distinguished by the voltammetric response ratios (Table I); and clonazepam overlaps nitrazepam, although the individual retention times are distinguishable with

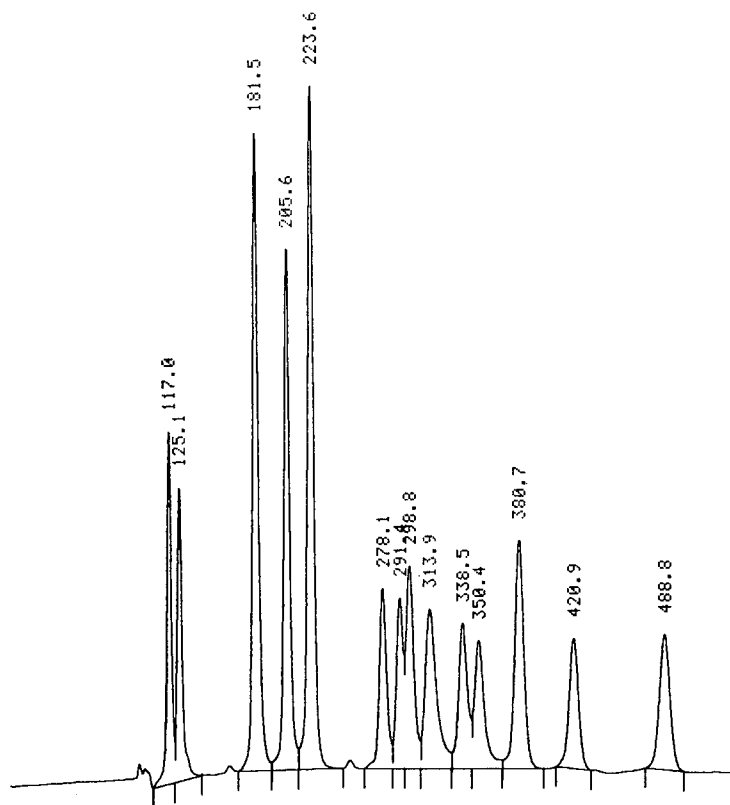


Fig. 3. Reductively detected liquid chromatogram of a mixture of standard compounds (5–10 ng) under the conditions given in Experimental. The retention times (s) are superscripted on the peaks. Identities in order of elution are: 7-aminonitrazepam (117.0 s), 7-acetamidonitrazepam (125.1 s), 6-nitroquinoline (181.5 s), demoxepam (205.6 s), nitrazepam (223.6 s), triazolam (278.1 s), lorazepam (291.4 s), oxazepam (298.8 s), loprazolam (313.9 s), temazepam (338.5 s), lormetazepam (350.4 s), chlordiazepoxide (380.7 s), desmethyl-diazepam (420.9 s), diazepam (488.8 s). The maximum peak amplitude is 20 nA.

clonazepam running slightly ahead. The pair may be resolved if the propanol is omitted from the eluent. As the column ages loprazolam is increasingly retained relative to the other benzodiazepines, probably because of the interaction of this comparatively basic compound with developing active sites. The effect may be countered by increases in the propanol content of the eluent, *e.g.*, by increments of 10% in the propanol present. Probably greater modification would be necessary to adapt the eluent to different batches of the column packing. Except for the switching to the cyanopropyl-bonded column, unmodified conditions may be used for the more strongly retained compounds such as medazepam and flurazepam.

#### *Cleanup procedure*

The various adsorbents and ion exchange resins investigated include the Porapak -Q, -R, -S and -T (Millipore-Waters), Chromosorb-104 (Johns-Manville), Amberlite XAD-4 and Amberlyst-15 (Rohm and Haas), and Partisil-SCX (Whatman). The last two are ion exchange materials that, in the hydrogen form, gave excellent recoveries from blood of all of the benzodiazepines except triazolam, most of which apparently decomposed. Of the other adsorbents, Porapak-T proved to be the most satisfactory in terms of the cleanliness and efficiency of the extractions, and of the convenience of its use. The relatively high density of this adsorbent promotes clean sedimentation from its mixtures with diluted blood.

From aqueous solutions the values of the distribution ratios for the adsorption of benzodiazepines on Porapak-T are in the range 1000–2000 ml/g. In blood samples, however, the extent of adsorption sometimes is substantially less than these values require. The effect occurs most strongly in transfusion bloods, and negligibly in degraded samples and in samples of equine blood, and can be suppressed by the addition of fatty acids, and by sodium octyl and dodecyl sulphates. Diazepam and temazepam are the most strongly affected. Presumably adsorption on the Porapak is in competition with binding to serum albumin; diazepam and temazepam are known to be relatively strongly bound<sup>39</sup>; fatty acids compete with benzodiazepines for binding sites on serum albumin<sup>40</sup>; the binding varies widely between samples<sup>41</sup>; and the structure of serum albumin is disrupted by alkyl sulphates<sup>42</sup>. Sodium octyl sulphate is used to suppress the binding in preference to the dodecyl sulphate particularly because the dodecyl sulphate tends to retain temazepam specifically in solution, probably within micelles. Evidently, in many published extraction techniques the binding may be ignored. The need to suppress it here arises from the use of a small proportion of the extractant to the sample.

The transfer of the loose adsorbent from the sample to the top of a prepacked microcolumn minimizes loss of the less strongly retained compounds (triazolam and the nitrazepam metabolites) during the transfer and subsequent washing. Relatively low concentrations of acetonitrile effect the desorption, which provides, therefore, a small volume of substantially aqueous extract that may be used for HPLC directly. The optimal concentration of acetonitrile may vary between batches of Porapak-T, however. Of three batches examined, the two with which the work described has been conducted were indistinguishable, but the other was appreciably more retentive.

#### *Detection limits and recoveries*

In Table II are given detection limits obtained from spiked, haemolyzed

TABLE II

DETECTION LIMITS AND REPEATABILITY OF RECOVERIES OF SOME BENZODIAZEPINES AND THEIR METABOLITES FROM HAEMOLYZED HUMAN BLOOD

Compound	Detection limit* (ng/ml)	Mean recovered concentration** (ng/ml)	
		Spiked at 66.9 ng/ml	Spiked at 2140 ng/ml
7-Acetamidonitrazepam	7.8	56.8 (2.96)	2324 (45.3)
7-Aminonitrazepam	12.4	55.9 (1.85)	1638 (25.1)
Chlordiazepoxide HCl	1.5	59.5 (1.43)	1973 (41.1)
Demoxepam	1.1	59.5 (1.73)	2074 (38.3)
Desmethyldiazepam	2.1	57.2 (2.28)	1889 (48.8)
Diazepam	1.8	56.4 (0.68)	1827 (65.7)
Loprazolam	2.1	63.2 (1.28)	2021 (47.9)
Lorazepam	1.1	57.7 (1.98)	1916 (45.2)
Lormetazepam	3.1	56.5 (1.72)	1901 (50.0)
Nitrazepam	0.32	30.5 (0.60)***	1066 (25.3)***
Oxazepam	1.8	57.0 (1.91)	1905 (44.8)
Temazepam	3.7	56.6 (1.51)	1865 (44.0)
Triazolam	2.0	64.0 (1.55)	2128 (50.3)

\* Taken as three standard deviations of determinations ( $n = 7$ ) in the range 1–5 ng/ml.\*\*  $n = 6$ ; values in parentheses are standard deviations.

\*\*\* Half the indicated spike.

transfusion blood (in many techniques the plastics additives contaminating this material interfere). The detection limits are calculated as three standard deviations of the benzodiazepines recovered (expressed as concentrations in the blood) from 250- $\mu$ l samples spiked in the range 1–5 ng/ml. Evidently, most of the detection limits lie in this range, corresponding to HPLC injections of 40–200 pg. For the majority of the benzodiazepines this is well below the therapeutic level although approached by some low dosage forms. Triazolam is an example, for which a chromatogram from the blood spiked at 5 ng/ml is given in Fig. 4A. The unspiked blood is shown in Fig. 4B, and exhibits no peaks beyond 150 s where most of the benzodiazepines occur. The electrode potential used here ( $-1.2$  V) is considerably more cathodic than necessary. Triazolam may be detected readily at less negative potentials (Table I) with an approximate halving of the background current (at  $-1.0$  V) and a corresponding improvement in the detection limit.

Included in Table II are repeatability data at concentrations well above the detection limits. The results are distributed with standard deviations corresponding to coefficients of variation in the range 1.2–5.2%. The upper limit is due to the acetamidonitrazepam, which is eluted in the early, congested region of the chromatograms.

Table III gives results from recovery experiments made on blood samples spiked with twofold increasing concentrations of up to 2.14  $\mu$ g/ml. The nitroquinoline is included here because of its use in some of the work as an internal standard. Because of the extended concentration range taken, a variance-weighted least squares regression<sup>43</sup> was applied, with variance estimates derived from the data in Table II on the assumption that the standard deviations vary linearly with the magnitude of the recovered concentrations, and decrease to the limiting values used in the estimates of

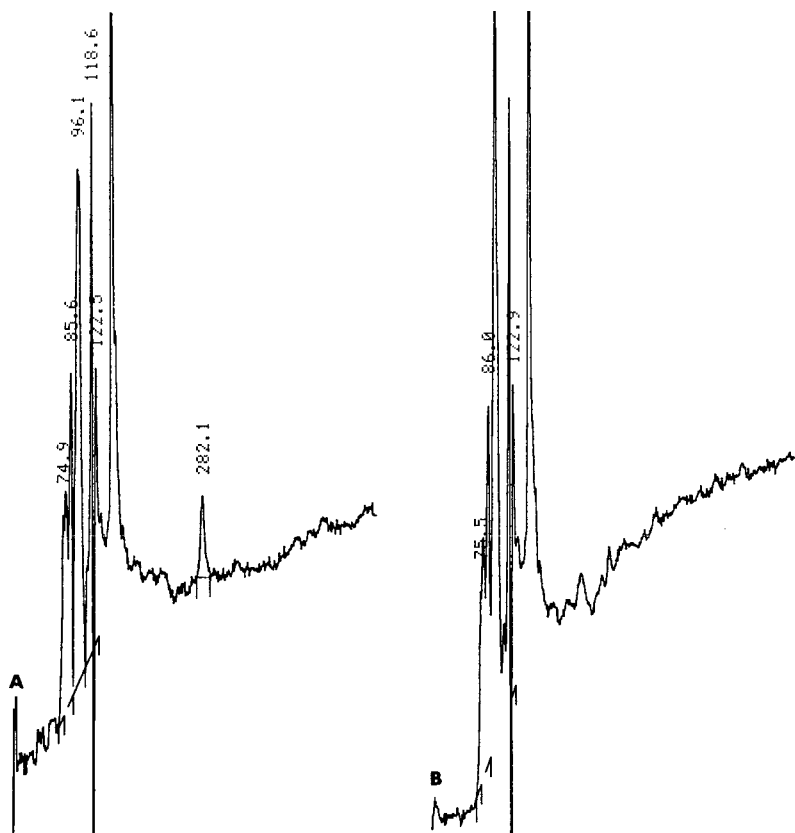


Fig. 4. Chromatograms of extracts from haemolyzed human blood: spiked with 5 ng/ml triazolam (A), and unspiked (B). The triazolam peak is at 282.1 s, with an amplitude of 80 pA (reductive detection).

the detection limits. Apart from the aminonitrazepam result, the data in Table III correspond to recoveries overall of 83.9% (oxazepam, acetamidonitrazepam) to 95.3% (loprazolam).

#### *Results with reference to ultraviolet absorbance detection and other techniques*

The generally lower recoveries (83.9%, 75.4%), and their greater variation, of the nitrazepam metabolites (Table III) might be improved under modified conditions, particularly by the use of more aqueous eluents, but at a cost of increased running times and poorer detection limits for the other benzodiazepines. Even so, the technique yields results previously obtained with considerable difficulty or not at all. In Fig. 5B is shown an example of a degraded blood sample submitted in a nitrazepam overdose case. Typically, no nitrazepam remained in the blood, but the chromatogram is dominated by an intense peak formed by 7-aminonitrazepam (121.9 s) at an estimated concentration of 600 ng/ml. The sometimes-detected acetamido metabolite is absent here. The only other strong peak is due to the internal standard (6-nitroquinoline). The immunoassay technique<sup>5</sup> is insensitive to nitrazepam metabolites even at this concentration. Also present in the sample were small amounts of desmethyldiazepam

TABLE III

RECOVERY EXPERIMENTS: LEAST SQUARES LINEAR REGRESSION (VARIANCE-WEIGHTED) OF CONCENTRATIONS FOUND ON CONCENTRATIONS ADDED TO HAE-MOLYZED HUMAN BLOOD OF SOME BENZODIAZEPINES, THEIR METABOLITES, AND 6-NITROQUINOLINE

The regressions were parameterized with data included in Table II. None of the sets of recovery data varied significantly from linearity (runs test), or exhibited an intercept differing significantly from zero.

<i>Compound</i>	<i>Range (ng/ml)</i>	<i>n</i>	<i>Correlation coefficient</i>	<i>Slope (recovery ratio)</i>	<i>Standard error of slope</i>
7-Acetamidonitrazepam	16.7–2140	7	0.9988	0.839	0.018
7-Aminonitrazepam	16.7–2140	7	0.9966	0.754	0.028
Chlordiazepoxide	8.4–2140	9	0.9991	0.912	0.014
Demoxepam	8.4–2140	9	0.9993	0.948	0.014
Desmethyldiazepam	8.4–2140	9	0.9991	0.879	0.014
Diazepam	8.4–2140	9	0.9989	0.864	0.015
Loprazolam	8.4–2140	9	0.9990	0.953	0.016
Lorazepam	8.4–2140	9	0.9990	0.881	0.016
Lormetazepam	8.4–2140	9	0.9991	0.890	0.014
Nitrazepam	4.2–1070	9	0.9996	0.940	0.011
6-Nitroquinoline	2.1–535	9	0.9993	0.985	0.014
Oxazepam	8.4–2140	9	0.9986	0.839	0.017
Temazepam	8.4–2140	9	0.9989	0.873	0.015
Triazolam	8.4–2140	9	0.9993	0.872	0.014

and diazepam (60 and 20 ng/ml, respectively), as the chromatogram in Fig. 5B shows. The desmethyldiazepam could be detected, in line, by ultraviolet absorbance at 240 nm (Fig. 5A). This peak (431.3 s) has been used to scale the chromatogram to give a peak height equal to the same component in the electrochemically detected chromatogram. The comparison between the two demonstrates immediately the inferior selectivity of the ultraviolet detection. The aminonitrazepam peak, which should be similar in height to the peak in Fig. 5B (from experiments with the pure compounds), is entirely swamped by irrelevant material. Several such peaks are present, diazepam is undetectable, and the desmethyl compound is only a minor component of the chromatogram.

The result illustrated in Fig. 5 is representative of a number of comparisons that have been made. Out of 14 examples from casework, ultraviolet detection gave readily interpreted chromatograms in 6 cases. Of the remainder, 4 were too complex to be of any value, and 4 could be interpreted with reference to the electrochemically detected chromatograms. Evidently a commonly held view, formed without apparent reference to selectivity, that ultraviolet detection gives at least comparable if not superior sensitivity to reductive detection of the benzodiazepines carrying no readily reducible substituents, is not applicable to the type of samples involved here—the improved electrochemical sensitivity notwithstanding. It may be argued that the cleanup procedure is more suitable for the electrochemical technique. However, from our earlier use of liquid-liquid extractions and of solid phase extractions employing the commercially available cartridges, in conjunction with ultraviolet detection, far more complex extracts were obtained than now. Also the present extracts are found to

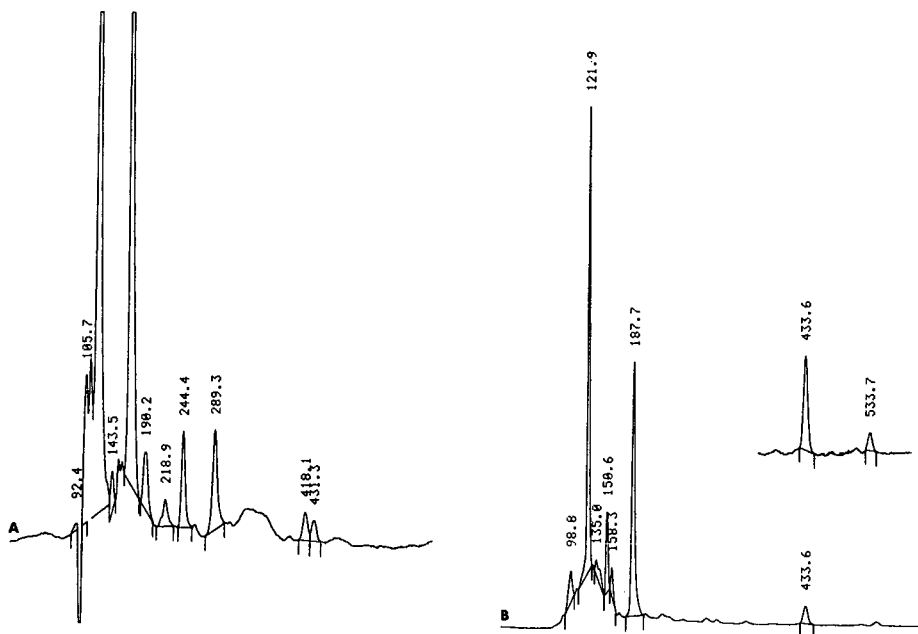


Fig. 5. Chromatogram of an extract of *post mortem* blood with ultraviolet absorbance detection at 240 nm (A) and reductive detection (B). The peak assignments (chromatogram B) are 7-aminonitrazepam (121.9 s), internal standard (187.7 s), desmethyldiazepam (433.6 s) and diazepam (533.7 s). The chromatograms are scaled to give similar peak heights for desmethyldiazepam (at 431.3 s in A), for which the approximate amplitudes are 0.0016 absorbance units (A), and 0.95 nA (B).

be far cleaner by gas chromatography with electron capture and mass spectrometric detection.

Oxidative detection at the porous carbon electrodes was briefly investigated. In agreement with the published results<sup>44</sup> a number of the benzodiazepines could be detected, but many interfering peaks were present in the chromatograms of casework samples.

#### Examples of "difficult" samples

Shown in Fig. 6 are chromatograms of three *post mortem* blood samples (A–C) from cases not involving benzodiazepines, and a chromatogram from a sample submitted in connection with a road traffic offence (D). All the chromatograms are scaled to the same sensitivity. Sample C was undegraded; A and B are examples of partly putrified material, and illustrate the insensitivity of the technique to the interferences due to decomposition products.

Sample D was obtained in a glass vial crimp-sealed with a rubber septum. The chromatogram includes peaks due to the internal standard (180.6 s), oxazepam (297.5 s) and temazepam (337.1 s). The respective concentrations of the benzodiazepines are 60 and 570 ng/ml. The other major peak (394.1 s) is characteristic of this particular make of septum, and is an extreme example of an occasionally encountered contamination. Possibly a sulphur-containing compound is responsible. No interference occurs with any of the benzodiazepines, all of which are well separated from

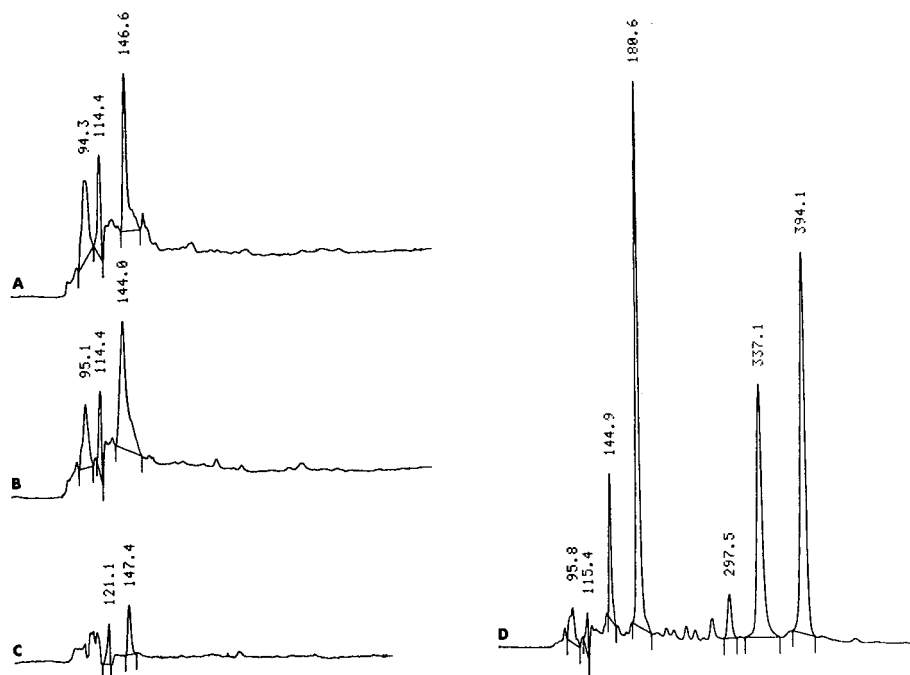


Fig. 6. Chromatograms (reductive detection) of "difficult" samples: *post mortem* bloods from non-benzodiazepine cases, putrefied (A, B) and undegraded (C); and a sample from a road traffic offence case that shows a strong peak (394.1 s) due to the particular brand of specimen container. Other peaks in D are internal standard (180.6 s), oxazepam (297.5 s) and temazepam (337.1 s). All the chromatograms are scaled to the same sensitivity. The peak amplitude of the internal standard peak (D) is 10.2 nA.

this position. The problems caused to some other analytical techniques by this type of interference are notorious<sup>4,5</sup>.

#### *Analytical considerations and results*

For usual reasons it is desirable that in internally standardized determinations the standard should be a benzodiazepine closely matched to the adsorption characteristics of the analyte on both Porapak-T and octadecylsilyl silica, and to the analyte's electrochemical characteristics. In a drugs-abuse case, however, several benzodiazepines may be present. When a number of such samples are collectively in process, the choice of a benzodiazepine to occupy a position vacant in all of the chromatograms may not be possible. The 6-nitroquinoline used in the present work has proved to be a useful compromise, found after a considerable search, when no benzodiazepine is available, although some sacrifice in accuracy for some analytes is involved. A number of relevant characteristics of the compound are given in Tables I and III.

The results, standardized with the nitroquinoline, from a blind trial are given in Table IV. The person preparing the trial was asked to make up five representative samples with any of the benzodiazepines on the limited list, and their metabolites. There was no specification of how many compounds were to be used of the complete

TABLE IV

## BLIND TRIAL ON SPIKED, HAEMOLYZED HUMAN BLOOD SAMPLES

 $n = 3$ .

Sample No.	Compound	Spike (ng/ml)	Found	
			Range (ng/ml)	Mean error (%)
1	7-Aminonitrazepam	199	206–252	+13.1
	Nitrazepam	99.6	101–103	+1.84
	Lorazepam	60.0	57.6–61.5	–0.89
2	Temazepam	99.0	87.6–89.4	–10.8
	Desmethyldiazepam	297	274–277	–7.42
	Diazepam	594	56.9–576	–3.49
3	Triazolam	99.6	93.2–98.2	–3.41
	Oxazepam	199	182–190	–6.51
	Temazepam	99.6	95.9–96.0	–3.68
4	Demoxepam	199	181–193	–5.35
	Chlordiazepoxide	99.6	89.9–95.0	–6.62
	Desmethyldiazepam	59.8	57.1–60.4	–1.39
5	Loprazolam	59.3	56.8–58.7	–3.04
	Lormetazepam	59.3	57.0–59.0	–1.91

set made available. As the table shows, all the compounds were correctly identified, with no false positives; and the quantitative results are within reasonable agreement, on the basis of the data already given, with the quantities added to the blood.

## CONCLUSION

The described techniques have considerably increased the facility with which the benzodiazepines can be detected and determined in degraded samples, and have made possible a variety of novel observations that will be reported elsewhere. During the course of this work it has become apparent that the cleanup procedure might provide the basis of a more comprehensive scheme, and that a variety of other compounds of casework interest are amenable to reductive detection. We look forward to pursuing these points.

## REFERENCES

- 1 J. M. Clifford and W. F. Smyth, *Analyst (London)*, 99 (1974) 241.
- 2 J. A. F. de Silva, in E. Usdin, P. Skolnick, J. F. Tallman Jr., D. Greenblatt and S. M. Paul (Editors), *Pharmacology of Benzodiazepines*, MacMillan, London, 1982, p. 239.
- 3 H. Schutz, *Benzodiazepines*, Springer-Verlag, Berlin, 1982.
- 4 A. C. Mehta, *Talanta*, 31 (1984) 1.
- 5 C. P. Goddard, A. H. Stead, P. A. Mason, B. Law, A. C. Moffat, M. McBrien and S. Cosby, *Analyst (London)*, 111 (1986) 525.

- 6 A. S. Curry, *Poison Detection in Human Organs*, Thomas Books, Illinois, 3rd ed., 1976, p. 214.
- 7 M. A. Peat and L. Kopjak, *J. Forensic Sci.*, 24 (1979) 46.
- 8 H. W. Peel and B. J. Perrigo, *J. Anal. Toxicol.*, 4 (1980) 105.
- 9 H. M. Stevens, *J. Forensic Sci. Soc.*, 25 (1985) 67.
- 10 A. W. Missen, *Clin. Chem.*, 22 (1976) 927.
- 11 H. Sawada, A. Hara, S. Asano and Y. Matsumoto, *Clin. Chem.*, 22 (1976) 1596.
- 12 T. J. Good and J. S. Andrews, *J. Chromatogr. Sci.*, 19 (1981) 562.
- 13 M. J. Koenigbauer, S. P. Assenza, R. C. Willoughby and M. A. Curtis, *J. Chromatogr.*, 413 (1987) 161.
- 14 G. de Groot and A. M. L. J. Grotenhuis-Mullenders, in R. A. A. Maes (Editor), *Topics in Forensic and Analytical Toxicology*, Elsevier, Amsterdam, 1987, p. 95.
- 15 P. Mura, A. Piriou, P. Fraillon, Y. Papet and D. Reiss, *J. Chromatogr.*, 416 (1987) 303.
- 16 R. W. Abbott, A. Townshend and R. Gill, *Analyst (London)*, 112 (1987) 397.
- 17 I. R. Tebbett, *Chromatographia*, 23 (1987) 377.
- 18 C. M. Moore and I. R. Tebbett, *Forensic Sci. Int.*, 34 (1987) 155.
- 19 I. R. Tebbett, unpublished results.
- 20 J. M. F. Douse, *J. Chromatogr.*, 301 (1984) 137.
- 21 G. Koves and J. Wells, *J. Anal. Toxicol.*, 10 (1986) 241.
- 22 J. B. F. Lloyd, *J. Energ. Mater.*, 4 (1986) 239.
- 23 W. F. Smyth, M. R. Smyth, J. A. Groves and S. B. Tan, *Analyst (London)*, 103 (1978) 497.
- 24 M. A. Brooks and J. A. F. de Silva, *Talanta*, 22 (1975) 849.
- 25 W. Lund, M. Hannisdal and T. Greibrokk, *J. Chromatogr.*, 173 (1979) 249.
- 26 M. R. Hackman and M. A. Brooks, *J. Chromatogr.*, 222 (1981) 179.
- 27 H. B. Hanekamp, W. H. Voogt, R. W. Frei and P. Bos, *Anal. Chem.*, 53 (1981) 1362.
- 28 J. B. F. Lloyd, *Anal. Proc.*, 24 (1987) 239.
- 29 J. B. F. Lloyd, *J. Chromatogr.*, 256 (1983) 323.
- 30 J. B. F. Lloyd, *J. Chromatogr.*, 330 (1985) 121.
- 31 E. Ruiz, M. H. Blanco, E. L. Abad and L. Hernandez, *Analyst (London)*, 112 (1987) 697.
- 32 J. M. Clifford and W. F. Smyth, *Z. Anal. Chem.*, 264 (1973) 149.
- 33 M. A. Brooks, J. J. B. Bruno, J. A. F. de Silva and M. R. Hackman, *Anal. Chim. Acta*, 74 (1975) 367.
- 34 H. Oelschlager, J. Volke, G. T. Lim and U. Bremer, *Arch. Pharm.*, 303 (1970) 364.
- 35 J. N. Brown, M. Hewins, J. H. M. Van Der Linden and R. J. Lynch, *J. Chromatogr.*, 204 (1981) 115.
- 36 M. E. Rollic, G. Patonay and I. M. Warner, *Ind. Eng. Chem. Rsch.*, 26 (1987) 1.
- 37 J. B. F. Lloyd, *Anal. Chim. Acta*, 199 (1987) 161.
- 38 R. Gill, B. Law and J. P. Gibbs, *J. Chromatogr.*, 356 (1986) 37.
- 39 E. M. Sellers, C. A. Naranjo, V. Khouw and D. J. Greenblatt, in E. Usdin, P. Skolnick, J. F. Tallmann Jr., D. Greenblatt and S. M. Paul (Editors), *Pharmacology of Benzodiazepines*, MacMillan, London, 1982, p. 271.
- 40 P. V. Desmond, R. K. Roberts, A. J. J. Wood, G. D. Dunn, G. R. Wilkinson and S. Schenker, *Br. J. Clin. Pharm.*, 9 (1980) 171.
- 41 R. F. Johnson, S. Schenker, R. K. Roberts, P. V. Desmond and G. R. Wilkinson, *J. Pharm. Sci.*, 68 (1979) 1320.
- 42 J. Steinhartdt and J. A. Reynolds, *Multiple Equilibria in Proteins*, Academic Press, New York, 1969, p. 234.
- 43 J. S. Garden, D. G. Mitchell and W. N. Mills, *Anal. Chem.*, 52 (1980) 2310.
- 44 W. F. Smyth, J. S. Burmicz and A. Ivaska, *Analyst (London)*, 107 (1983) 1019.
- 45 M. W. White, *J. Forensic Sci. Soc.*, 22 (1984) 404.



CHROM. 20 648

## ISOTACHOPHORESIS OF QUATERNARY 4,4'-BIPYRIDILIUM SALTS

### ANALYTICAL CONTROL OF SYNTHESIS AND PURIFICATION PROCEDURES

PETER STEHLE\* and PETER FÜRST

*Institute for Biological Chemistry and Nutrition, University of Hohenheim, Stuttgart (F.R.G.)*  
and

RICHARD RATZ and HERMANN RAU

*Institute for Chemistry, University of Hohenheim, Stuttgart (F.R.G.)*

(First received April 27th, 1988; revised manuscript received May 19th, 1988)

---

#### SUMMARY

Analytical capillary isotachopheresis (ITP) was employed to monitor the synthesis and subsequent purification of the quaternary bipyridylium salt 1-methyl-1'-[(3*S*)(-)-methylpinanyl]-4,4'-bipyridinium dichloride. The main synthetic product, intermediate and overreaction products as well as the starting material were analyzed in amounts of less than 1 µg in a single experiment. In addition to the qualitative approach, ITP allows an easy quantitative evaluation, thereby facilitating direct consideration of the reaction conditions used as well as enabling the optimization of purification steps.

---

#### INTRODUCTION

Quaternary 4,4'-bipyridylium salts are widely used as reversible redox systems, especially in agriculture as herbicides<sup>1</sup> and in laboratory systems as electron relays designed for solar energy conversion<sup>2</sup>. Starting from the simplest molecule of this class, 1,1'-dimethyl-4,4'-bipyridinium dichloride (methylviologen MV, Paraquat®), many chemically modified compounds have been tested in this respect, *e.g.*, viologen surfactants, substituted viologens and unsymmetrically substituted viologens<sup>2,3</sup>.

The details of the transfer of an electron from a donor to an acceptor molecule in solution have been investigated<sup>4</sup>, thereby utilizing the principle of diastereomerism in order to examine the relative importance of solvent and solute participation in modelling the transition state<sup>5</sup>. Such studies require the synthesis of optically active viologens in high purity. Owing to the complexity of the synthesis and the subsequent purification process, a proper analytical control of these procedures is a prerequisite to obtaining pure products in high yields.

In the present study, analytical isotachopheresis (ITP) was, for the first time, employed to monitor the synthesis and purification of 1-methyl-1'-[(3*S*)(-)-methylpinanyl]-4,4'-bipyridinium dichloride (PMV-Cl<sub>2</sub>).

## MATERIALS AND METHODS

The starting materials for the synthesis were 4,4'-bipyridine (purified by sublimation), freshly distilled methyl iodide and (3*S*)(-)-iodo- or bromo-methylpinane. The latter compound was prepared from (3*S*)(-)-formylpinane by reduction with NaBH<sub>4</sub> and substitution of the hydroxy group by tetrabromomethane or by tosylation and substitution by iodide ion.

Butanol as a solvent was distilled before use. Nitromethane was dried over phosphorus pentoxide and distilled at about 100 mbar. Tetrahydrofuran was dried over potassium hydroxide, purified using alumina, (desiccated for 12 h at 450°C; 70 cm × 4.5 cm column), subsequently boiled with LiAlH<sub>4</sub> and distilled. Toluene was dried over LiAlH<sub>4</sub>.

Following conventional techniques<sup>6</sup>, the synthesis of PMV salts was carried out by two different routes.

*Synthesis I*

In the first step, 4,4'-bipyridine was quaternized with methyl iodide (concentration ratio 1.6:1.0) in benzene as a solvent at room temperature to yield MV iodide. Unreacted 4,4'-bipyridine and the side product 1,1'-dimethyl-4,4'-bipyridinium diiodide (M<sub>2</sub>V diiodide) was extracted stepwise with dried toluene and acetonitrile, respectively.

In the second step, MV iodide was treated with (3*S*)(-)-methylpinanyl bromide in boiling *n*-butanol. The reaction product was converted into a dichloride by ion-exchange chromatography and subsequently freeze dried to give a light yellow flaky product which was moderately hygroscopic.

*Synthesis II*

Using dried nitromethane as a solvent, 4,4'-bipyridine was treated (48 h under reflux) with methylpinanyl iodide. The resulting extremely hygroscopic product 1-[(3*S*)(-)-methylpinanyl]-4-(4'-pyridyl)pyridinium bromide (PV bromide) was purified by gel chromatography on a glass column (45 cm × 3 cm) packed with Bio-Gel P-2 (200–400 mesh; Bio-Rad, Richmond, CA, U.S.A.) and using distilled water as the eluent. PV bromide was then converted into a tetrafluoroborate salt (PV-BF<sub>4</sub>) by adding a 12.5% solution of ammonium tetrafluoroborate. Subsequently, a solution of PV-BF<sub>4</sub> in acetonitrile was stirred for 4 days at room temperature in the presence of an 1.5-fold excess of methyl iodide. The dark red crystalline product was converted into a tetrafluoroborate salt by ion-exchange chromatography (Dowex 50W 1-X8, 200–400 mesh, 30 cm × 1.5 cm, loaded with BF<sub>4</sub>) and then freeze dried to give a pure white non-hygroscopic product.

The structures of all the target products synthesized were confirmed by mass spectrometry and nuclear magnetic resonance spectrometry<sup>4</sup>. Intermediate and end-products were analyzed isotachophoretically in the concentrations and amounts given in the figures.

*Analytical isotachophoresis*

Cationic isotachophoretic analysis were performed by using a 2127 LKB Tachophor (LKB, Bromma, Sweden) with an automatic driving control unit<sup>7,8</sup>.

Separations were carried out in a PTFE capillary (230 mm  $\times$  0.55 mm I.D.). Conductivity and UV (254 nm) signals were monitored by employing a two-channel recorder (Kipp & Zonen, Delft, The Netherlands) with a chart speed of 6 cm/min. The separations required about 15 min and the current upon detection was 60  $\mu$ A.

As the leading electrolyte, a 10 mM solution of potassium acetate containing 0.4% hydroxypropylmethylcellulose (HPMC; Dow Chemical, Midland, MI, U.S.A.) was used, titrated to pH 5.0 with concentrated acetic acid. The terminating electrolyte buffer contained 20 mM hydrochloric acid. These electrolyte solutions were prepared from analytical grade chemicals (E. Merck, Darmstadt, F.R.G.) using ultrapure water ( $> 15 \text{ M}\Omega/\text{cm}$ )<sup>9</sup>.

## RESULTS

### *Analysis of intermediate and end-products of synthesis I*

Compared with the isotachopheretic pattern of the electrolyte system, the isotachopherogram of the intermediate product derived after the first synthesis step is illustrated in Fig. 1. Only one non-UV-adsorbing impurity from the chemicals used was present in the electrolyte system (Fig. 1A). For the intermediate product, one major UV-adsorbing zone corresponding to the main synthetic product  $\text{MV}^+$  and two minor UV-absorbing zones, one of them not fully separated from the electrolyte impurity, were detected (Fig. 1B). These two minor zones were identified in doping experiments (Fig. 2). Addition of the starting material 4,4'-bipyridine resulted in a lengthening of zone 3 (Fig. 2A), whereas zone 1 corresponded to the overreaction product  $\text{M}_2\text{V}^{2+}$  (Fig. 2B).

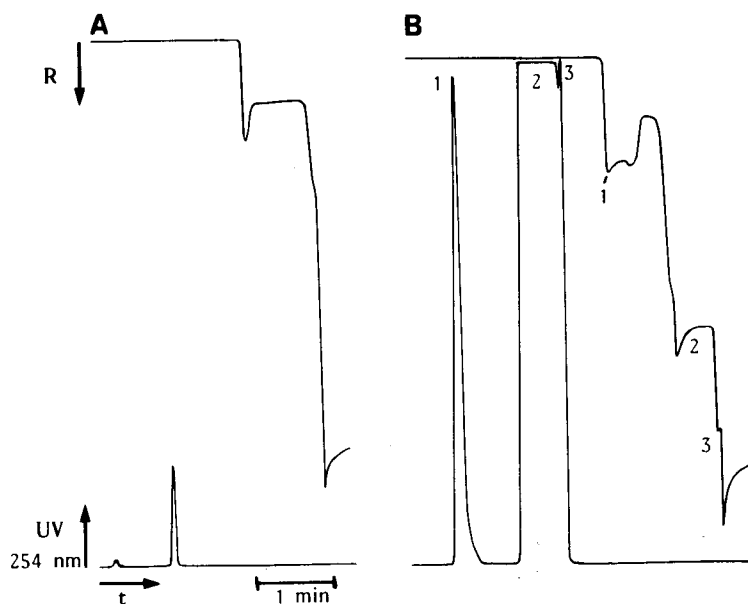


Fig. 1. Isotachopheretic analysis of the intermediate product (synthesis route I): (A) electrolyte system; (B) crude product (2.5  $\mu$ l injected, corresponding to 1.25  $\mu$ g material). Key: 1 =  $\text{M}_2\text{V}^{2+}$ ; 2 =  $\text{MV}^+$ ; 3 = 4,4'-bipyridine.

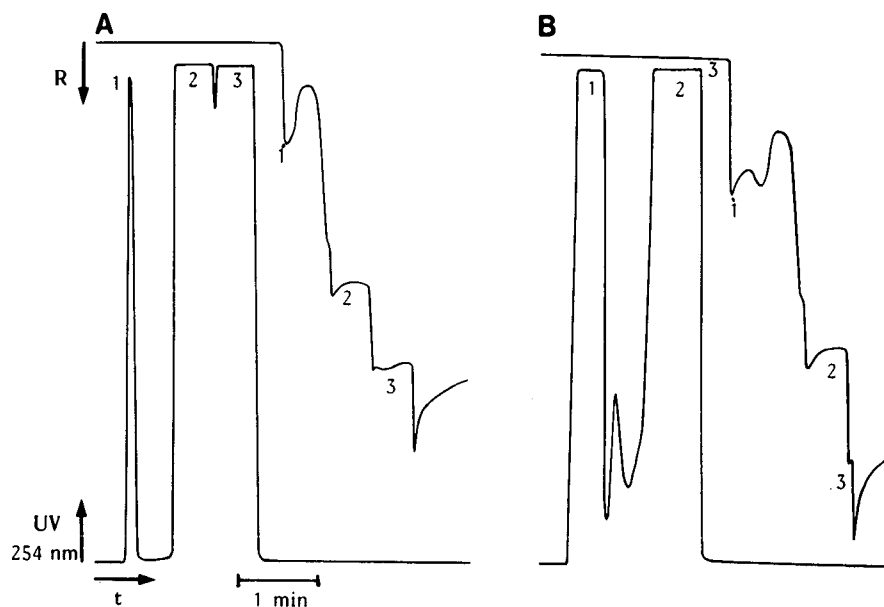


Fig. 2. Isotachopheric analysis of the intermediate product (synthesis route I) with addition of 4,4'-bipyridine (A) and  $M_2V^{2+}$  (B), respectively. For the separations, 2.5  $\mu$ l were injected, corresponding to 1.25  $\mu$ g of each solute. Key as in Fig. 1.

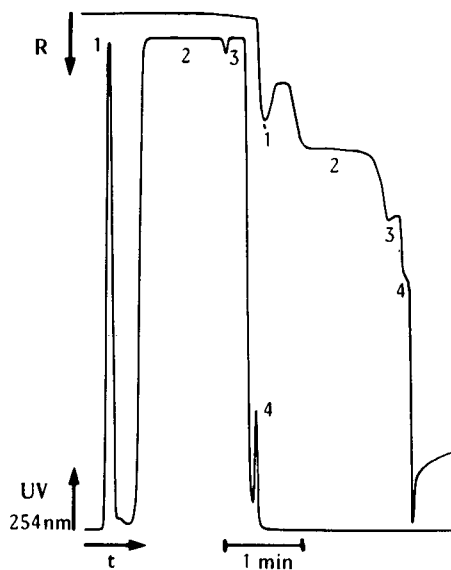


Fig. 3. Isotachopheric analysis of the crude product derived after the second synthesis step (route I) (5  $\mu$ l injected, corresponding to 2.5  $\mu$ g material). Key: 1 =  $M_2V^{2+}$ ; 2 = unknown; 3 =  $PMV^{2+}$ ; 4 =  $MV^{+}$ .

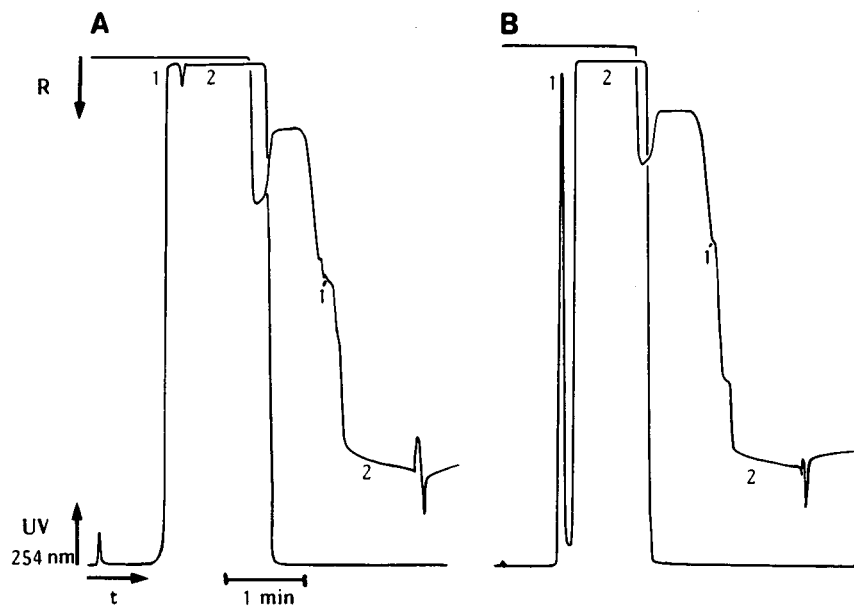


Fig. 4. Isotachopheric analysis of the intermediate product (synthesis route II) before (A) and after (B) gel chromatographic purification. For each separation, 5  $\mu$ l were injected, corresponding to 2.5  $\mu$ g material. Key: 1 =  $P_2V^{2+}$ ; 2 =  $PV^+$ .

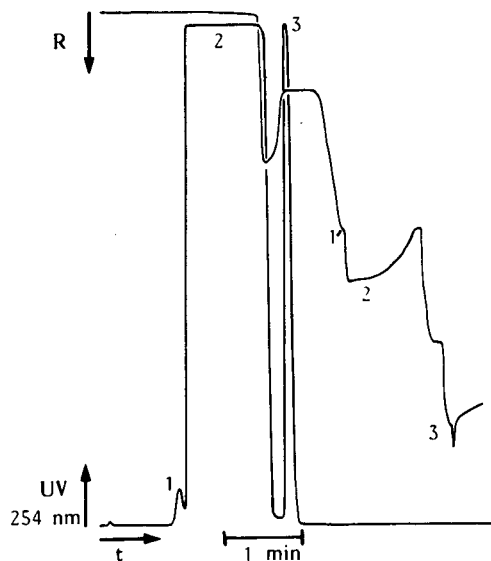


Fig. 5. Isotachopheric analysis of the crude product derived after the second synthesis step (route II) (5  $\mu$ l injected, corresponding to 2.5  $\mu$ g material). Key: 1 =  $P_2V^{2+}$ ; 2 =  $PMV^{2+}$ ; 3 =  $PV^+$ .

Analysis of the final product after the second synthesis step revealed four UV-absorbing zones (Fig. 3). Evidently, two of the minor zones corresponded to the intermediate product  $MV^+$  and the overreaction product  $M_2V^{2+}$ , respectively. Surprisingly, only small amounts of the desired product  $PMV^{2+}$  were detected. Owing to the lack of a suitable reference substance, the main synthetic compound could not be identified.

#### *Analysis of intermediate and end-products of synthesis II*

The isotachopherogram of the crude material derived after the first synthesis step as well as the isotachophoretic pattern of the purified product are illustrated in Fig. 4. Analysis of the crude material (Fig. 4A) revealed two UV-absorbing zones corresponding to the main synthetic product  $PV^+$  and the overreaction product 1,1'-bis[(3*S*)(-)-methylpinanyl]-4,4'-bipyridinium dication ( $P_2V^{2+}$ ). Repeated gel chromatographic purification of the crude material resulted in a significant decrease in the concentration of  $P_2V^{2+}$  (Fig. 4B).

At least three distinct UV-absorbing zones were detected after methylation of  $PV^+$  (Fig. 5). In addition to the main synthetic product  $PMV^{2+}$ , small amounts of the starting compound  $PV^+$  were detectable, indicating an incomplete reaction to  $PMV^{2+}$ . The third zone corresponded to the overreaction product  $P_2V^{2+}$  which could not be completely removed after the first synthesis step (Fig. 4).

#### DISCUSSION

The synthesis of unsymmetrical quaternary 4,4'-bipyridilium salts requires a two-step procedure in which the starting compound 4,4'-bipyridine is quaternized twice with two different alkyl halogenides. Owing to the strong influence of various factors, *e.g.*, solvent polarity and stereochemistry of the alkyl halogenides used, on the course and the yield of the reaction, a proper control of both the synthesis and subsequent purification procedures is necessary in order to obtain pure products in high amounts. Usually mass spectrometry, NMR and IR spectroscopy as well as elemental analysis are used for the identification and purity control of bipyridinium salts. Mass spectrometric analysis of salts, however, is extremely difficult due to the low volatility of such compounds. Furthermore, an adequate use of NMR spectroscopy requires the availability of pure products.

In the present study, ITP was used to monitor the synthesis and subsequent isolation of  $PMV^{2+}$ . Apparently, by applying a cationic electrolyte system at pH 5, it is feasible simultaneously to analyze the starting compound 4,4'-bipyridine, the end-product  $PMV^{2+}$  as well as intermediate and overreaction products (Figs. 1–5). In addition to this qualitative approach, ITP affords information about the composition of the samples analyzed without the necessity to analyze reference substances. Since the conductivity zone length is not influenced by substance-specific properties, *e.g.*, absorption coefficients, a relative quantification of sample ions with similar molecular weights and net charge is appropriate by simply measuring the corresponding zone length<sup>7,10</sup>. This combined qualitative and quantitative approach enables a direct evaluation of the course of the reaction and, when necessary, further optimization and/or change of the reaction conditions.

Obviously, only small amounts of the product  $PMV^{2+}$  are formed in synthesis

route I (Fig. 3). Since during the first synthesis step an almost complete reaction was observed (Fig. 1), the low yield of  $\text{PMV}^{2+}$  must be due to the formation of an undesired product during the second step (Fig. 3). Based on these results, a modified synthesis procedure (route II) with a reversed order of the quaternization steps was employed, enabling the synthesis of  $\text{PMV}^{2+}$  in high purity and acceptable yield (Figs. 4 and 5). In this connection it is of note that these differences in the purity of  $\text{PMV}^{2+}$ , derived from syntheses I and II, respectively, could not be revealed by mass spectrometry and NMR spectroscopy<sup>4</sup>.

As illustrated in Fig. 4, it was feasible to analyze directly the reaction mixture after the first synthesis step (A) as well as to monitor the enrichment of the intermediate product  $\text{PV}^+$  during gel chromatographic purification (B). This easy possibility to determine rapidly the degree of purity of an intermediate product is an obvious advantage for the performance of the subsequent synthesis step.

In the present investigation, capillary ITP has been proven to be a sensitive, reliable and rapid method to monitor the synthesis and subsequent purification of  $\text{PMV}^{2+}$ . Thus, this electrophoretic technique may represent a valuable alternative to commonly used analytical methods in this field, enabling greater control of the synthesis of quaternary 4,4'-bipyridylium salts.

#### ACKNOWLEDGEMENT

The support of the Fonds der Chemischen Industrie, Frankfurt, is gratefully acknowledged.

#### REFERENCES

- 1 L. A. Summers, *The Bipyridinium Herbicides*, Academic Press, London, 1980.
- 2 M. Grätzel, in J. S. Connolly (Editor), *Photochemical Conversion and Storage of Solar Energy*, Academic Press, New York, 1981, Ch. 5.
- 3 A. Harriman and M. A. West, *Photogeneration of Hydrogen*, Academic Press, London, 1982.
- 4 R. Ratz, *Thesis*, University of Hohenheim, Stuttgart, 1986.
- 5 H. Rau, *Chem. Rev.*, 83 (1983) 535.
- 6 Houben-Weyl, *Methoden der organischen Chemie*, Band XI/2, Georg Thieme, Stuttgart, 1962, p. 565.
- 7 P. Stehle and P. Fürst, *J. Chromatogr.*, 346 (1985) 271.
- 8 P. Stehle, H.-P. Bahsitta and P. Fürst, *J. Chromatogr.*, 370 (1986) 131.
- 9 P. Stehle, B. Kühne, P. Pfaender and P. Fürst, *J. Chromatogr.*, 249 (1982) 408.
- 10 F. M. Everaerts, J. L. Beckers and Th. P. E. M. Verheggen (Editors), *Isotachophoresis: Theory, Instrumentation and Applications*, Elsevier, Amsterdam, Oxford, New York, 1976.

CHROM. 20 680

## Note

### Extraction chromatography of alkanethiols

ZBIGNIEW H. KUDZIN\*

*Institute of Chemistry, University of Łódź, Narutowicza 68, 90-136 Łódź (Poland)*  
and

WŁODZIMIERZ KOPYCKI

*Institute of Organic Chemistry, Technical University of Łódź, Żwirki 36, 90-924 Łódź (Poland)*  
(First received November 24th, 1987; revised manuscript received May 24th, 1988)

Thiols are formed as by-products in many petrochemical and carbochemical processes. Low-molecular-weight alkanethiols also occur as odours, flavours or metabolites. For this reason, their isolation and determination have been the subject of numerous investigations<sup>1</sup>, and still constitute an important analytical and technological problem<sup>2–4</sup>.

Due to the high volatilities of simple alkanethiols, their quantitation is mainly based on gas-liquid chromatography, especially since the introduction of sulphur-sensitive detections<sup>3–8</sup>. This high volatility, and the sensitivity to oxidation, has meant that the liquid chromatography of free alkanethiols has so far been the subject of few chromatographic reports. Thus, free alkanethiols have been separated by reversed-phase thin-layer chromatography (RP-TLC)<sup>9</sup>, by TLC ligand chromatography<sup>10</sup> and also by high-performance liquid chromatography (HPLC)<sup>8,11,12</sup>. Möckel undertook an extensive study of the HPLC partition chromatography of alkanethiols and other sulphur compounds, together with theoretical considerations.

Some procedures used for the liquid chromatography of alkanethiols were based on their prederivatization as 2,4-dinitrophenyl thioethers<sup>4</sup>, 2,5-dinitrobenzoyl thioesters<sup>4</sup>, mixed disulphides with 2,4-dinitrothiophenol<sup>13</sup> and 5-mercapto-2-nitrobenzoic acid<sup>14</sup>, 4-alkanethialdehydes<sup>4</sup> and S-alkylthioglycolic amides<sup>4</sup>.

The possibility of separation of alkanethiols by counter-current distribution and distribution chromatography, in which the extraction equilibria of thiols in hydrocarbon-alkaline phase systems were taken into consideration, was also been described by us<sup>15–17</sup>. As a continuation of this research program<sup>15,17</sup>, we present here an attempt to correlate the pH-dependent extraction equilibria of thiols (between an alkaline mobile phase and hexadecane stationary phase systems) and their mobilities in partition chromatography. The results enable the separation of low-molecular-weight ( $R \leq C_6$ ) alkanethiol mixtures on the millimol scale.

### EXPERIMENTAL

All chemicals and supports were commercially available (Merck). The aqueous alkaline buffer solutions were prepared by mixing standardized solutions of 0.1 M glycine and 0.1 M sodium hydroxide. The stock solutions of thiols (1 and 0.2 M)

were prepared by dilution of thiols in methanol. Determinations of thiols were performed by thiomercurometric titration according to the Wroński procedure<sup>18</sup>.

The elution isotherms of thiols were determined by reversed-phase partition chromatography, using the apparatus illustrated in Fig. 1. The column was made of glass, double stopped with screw-threaded joints SQ-18 tubes (250 × 15 mm I.D.)<sup>19</sup>. The packing, 43.5% hexadecane on a polyamide support, gave reproducible results for in the range of 10–1000  $\mu\text{mol}$  thiols, with average recoveries of about 80–90%. Packing of hexadecane on inorganic supports (silica gels, Chromosorbs) was stable only at low concentrations (up to 5%) of hexadecane and exhibited low extraction abilities.

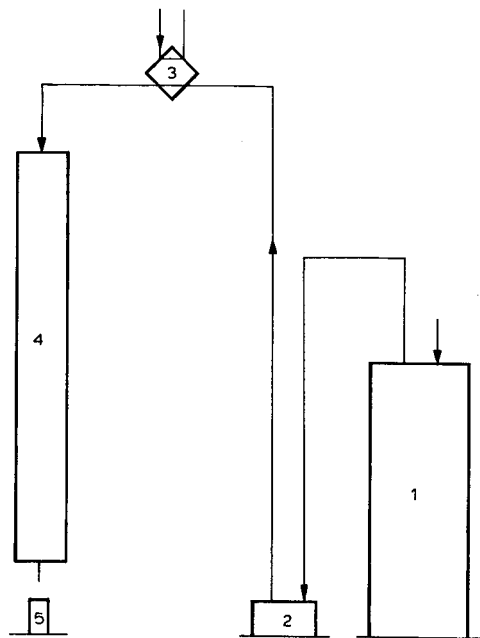


Fig. 1. The chromatographic system applied. 1 = Reservoir of mobile phase; 2 = peristaltic pump; 3 = sample-loop system; 4 = column; 5 = fraction collector.

The thiols were introduced on the column by means of a sample-loop system (100  $\mu\text{l}$ ). The flow of mobile phase through the column (5 ml min<sup>-1</sup>) was exerted by means of a peristaltic pump Model Unipan 394 M.

## RESULTS AND DISCUSSION

The acidity of the sulphydryl group results in a characteristic, strongly pH-dependent distribution of thiols in aqueous–hydrocarbon biphasic systems<sup>15,17</sup>. The total extraction equilibrium in such a system is determined both by the partition equilibrium and by the dissociation equilibrium of the thiols, and characterized by the value of the extraction coefficient,  $D$ .

$$D = \frac{[\text{RSH}]_n}{[\text{RSH}]_a + [\text{RS}^-]_a} = k_0 \cdot \frac{1}{1 - \frac{K}{[\text{H}^+]}} \quad (1)$$

where  $[\text{RSH}]_i$  and  $[\text{RS}^-]_i$  represents the concentrations of thiol and thiolate anion in the non-polar ( $i=n$ ) and aqueous ( $i=a$ ) phase respectively,  $k_0$  = partition coefficient of thiol,  $K$  = dissociation constant of thiol and  $[\text{H}^+]$  = concentration of hydrogen ion.

Earlier<sup>15</sup> it was established that the low-molecular-weight thiols ( $R \leq \text{C}_6\text{H}_{13}$ ) when extracted in non-polar-polar phase systems undergo characteristic distribution, and when  $K \gg [\text{H}^+]$  there is a linear dependence between the concentration of hydrogen ion and coefficient  $D$ :

$$D = k_0 \cdot \frac{[\text{H}^+]}{K} \quad \text{and} \quad \log D = \log \frac{k_0}{K} - \text{pH} \quad (2)$$

On the other hand, when  $K \ll [\text{H}^+]$  the extraction coefficients of the thiols are equal to their partition coefficients ( $D = k_0$ ), which are dependent on the interaction of thiols with both phases of the extraction (partition) system. The  $D$  factors determine also the mobilities in partition chromatography, characterized in thin-layer chromatography by the coefficients  $R_F$  and  $R_M$ , and in column chromatography by the retention volumes  $V'_R$  or  $V_R$ <sup>20,21</sup>

$$R_M = \log \frac{1 - R_F}{R_F} = \log D + \log \frac{V_{\text{st}}}{V_M} \quad (3)$$

$$V_R - V_M = V'_R = \frac{1}{1 - \frac{K}{[\text{H}^+]}} \cdot \frac{V_{\text{st}}}{V_M} \quad (4)$$

where  $V_{\text{st}}$  = volume of the stationary (non-polar) phase and  $V_M$  = column volume of the mobile phase.

Eqn. 4 was experimentally verified for the chromatographic system with hexadecane as the stationary phase and aqueous alkaline buffer solutions as the mobile phase. The column volume of the mobile phase was determined on the basis of the elution isotherm of sodium sulphide at pH 12.9. The corresponding isotherms of thiols as a function of the mobile phase pH are presented in Fig. 2.

As a consequence of eqns. 4 and 2, the relationship between the corrected retention volumes of thiols,  $V'_R$ , and the mobile phase pH is linear when  $[\text{H}^+] \ll K$  ( $\text{pH} > 11.0$ ), and deviates downwards for  $\text{pH} < 11.0$  (Fig. 3). The elution isotherms of thiols, taken at different pH (Fig. 2), also suggest an optimum region of pH for separation of multicomponent thiol mixtures. Thus, the mobile phase at pH 11.0 is sufficient for the separation of propanethiol from a mixture with methanethiol and ethanethiol. Analogously, at pH 11.5, butanethiol can be removed from a mixture consisting of ethanethiol, propanethiol and butanethiol. Additionally, the use of mobile phases buffered to pH 12.0 and 12.5 enables the separation of propanethiol, butanethiol and pentanethiol (Fig. 4c), and of butanethiol, pentanethiol and hexanethiol (Fig. 4d).

However, the scope of these separations at constant pH seems to be limited to binary or three-component mixtures due to the relatively low separability of the column used, compared with HPLC systems<sup>12</sup>. For this reason, the separation of more

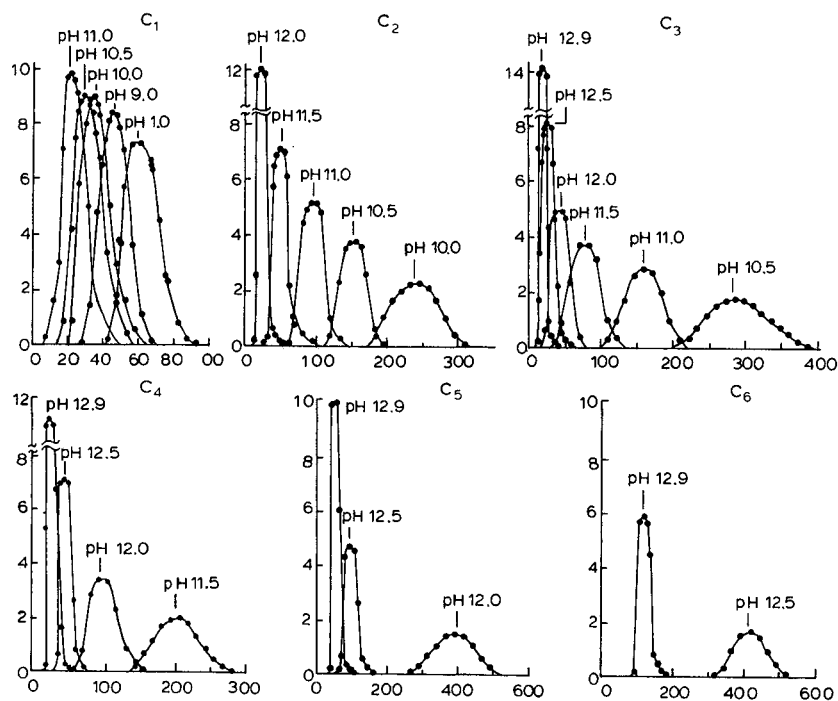


Fig. 2. Elution isotherms of thiols ( $\mu\text{mol}$  of RSH vs. ml of eluate) taken at different pH values of the mobile phase ( $20^\circ\text{C}$ ). Thiols:  $C_1$  = methanethiol;  $C_2$  = ethanethiol;  $C_3$  = *n*-propanethiol;  $C_4$  = *n*-butanethiol;  $C_5$  = *n*-pentanethiol;  $C_6$  = *n*-hexanethiol.

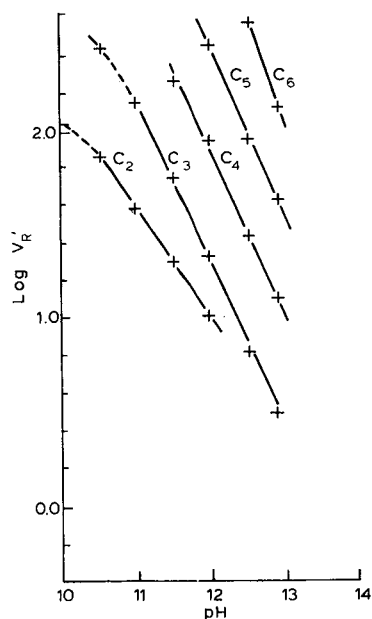


Fig. 3. Relationships of  $\log V'_R$  vs. pH for *n*-alkanethiols, determined on the basis of the elution isotherms presented in Fig. 2.

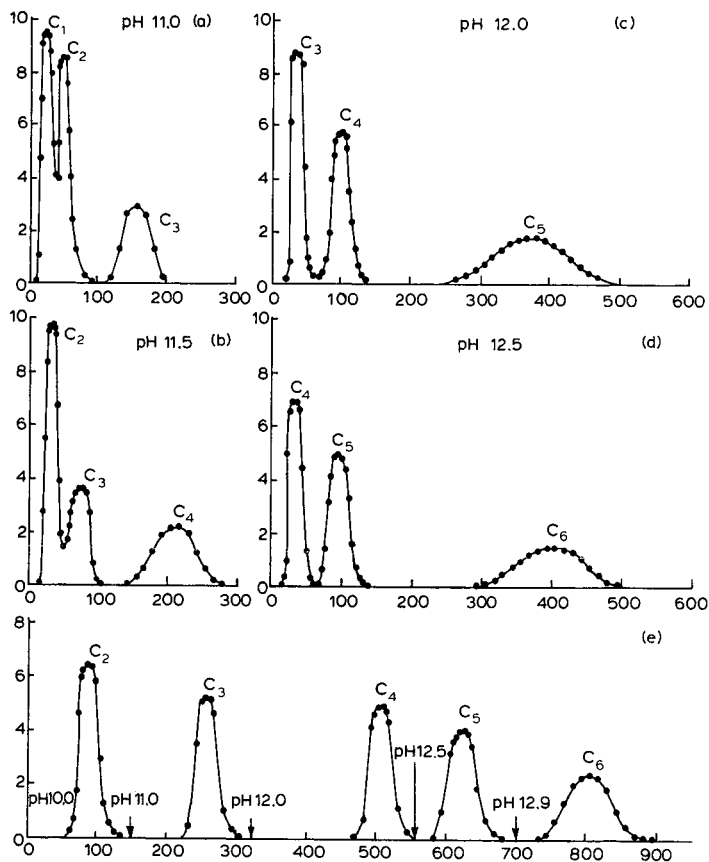


Fig. 4. Separations ( $\mu\text{mol}$  of RSH vs. ml of eluate) of thiol mixtures.

complex mixtures of alkanethiols required the further optimization of their extraction equilibria, in particular the use of a pH gradient. The elution isotherm of a five-component mixture of alkanethiols ( $C_2$ – $C_6$ ) is presented in Fig. 4e. The separation of thiols was achieved by increasing successively the pH of the mobile phase: ethanethiol was eluted at pH 10.0, propanethiol at pH 11.0, higher thiols (butanethiol, pentanethiol and hexanethiol) at pH 12.0, 12.5 and 12.9, respectively. Additionally, the high extraction capacity of the column enabled the separation of the thiols even on a millimol scale.

Further optimization of partition chromatography of high-molecular-weight alkanethiols ( $R \geq C_6H_{13}$ ) and the column capacity will be attempted.

#### ACKNOWLEDGEMENT

This project was partially supported by the Polish Academy of Sciences, National Committee of Chemistry.

## REFERENCES

- 1 E. E. Reid, *Organic Chemistry of Bivalent Sulfur*, Vol. I, Chem. Publ. Co., New York, 1958.
- 2 L. B. Ryland and M. H. Tamele, in J. H. Karchmer (Editor), *The Analytical Chemistry of Sulfur and its Compounds. The Thiols*, Vol. I, Wiley-Interscience, New York, 1970.
- 3 M. R. F. Ashworth, *Determination of Sulphur-containing Groups*, Vol. I, Academic Press, London, New York, 1976.
- 4 E. R. Cole and R. F. Bayfield, in A. Senning (Editor), *Sulphur in Organic and Inorganic Chemistry*, Vol. II, Marcel Dekker, New York, 1972, Ch. 20.
- 5 L. Blomberg, *J. Chromatogr.*, 125 (1976) 389.
- 6 C. D. Pearson, *J. Chromatogr. Sci.*, 14 (1976) 154.
- 7 M. Wroński and Z. H. Kudzin, *Chem. Anal. (Warsaw)*, 19 (1974) 1287.
- 8 M. Wroński and L. Walendziak, *J. Chromatogr.*, 211 (1981) 252.
- 9 H. W. Prinzler, D. Pape and M. Tepke, *J. Chromatogr.*, 19 (1965) 375.
- 10 K. Takashi and M. Atsushi, *Anal. Chem.*, 58 (1978) 268.
- 11 J. A. Cox and A. Przyjazny, *Anal. Lett.*, 10 (1977) 869.
- 12 H. J. Möckel, *J. Chromatogr.*, 317 (1984) 589.
- 13 S. I. Obtemperenskaya and K. C. Nguen, *Zh. Anal. Khim.*, 29 (1974) 2069.
- 14 S. L. Casco and P. K. Barrera, *Anal. Chim. Acta*, 1 (1972) 253.
- 15 M. Wroński and Z. H. Kudzin, *Chem. Anal. (Warsaw)*, 18 (1973) 577.
- 16 M. Wroński and Z. H. Kudzin, *Chem. Anal. (Warsaw)*, 19 (1974) 453.
- 17 Z. H. Kudzin, *Ph.D. dissertation*, Łódź, 1975.
- 18 M. Wroński, *Talanta*, 24 (1977) 347.
- 19 *Catalogue*, Jobling Laboratory Division, Stone, 1972.
- 20 J. C. Giddings, in E. Heftmann (Editor), *Chromatography. Theoretical Basis of Partition Chromatography*, Reinhold, New York, 1967.
- 21 E. Soczewiński, *Adv. Chromatogr. (N.Y.)*, 8 (1969) 91.

CHROM. 20 747

## Note

### Characterisation of volatile oil constituents with relatively long gas chromatographic retention times on two stationary phases

T. J. BETTS

School of Pharmacy, Curtin University of Technology, GPO Box U 1987, Perth, W. Australia 6001 (Australia)

(First received April 20th, 1988; revised manuscript received June 20th, 1988)

The new spectral-recording gas chromatographic (GC) detectors making computerised analyses of their records are the "state-of-the-art" in GC instrumentation. However, they are quite expensive, and many laboratories have to make do with cheaper, more traditional detectors. Even with these new luxury detectors it is valuable to have another method to confirm the spectral identification, especially if the computer conclusion does not have a high probability.

The flame ionisation detector is a universal, quickly set up GC detector for organic solutes, but unless molar response factors are considered, it is unable to distinguish between different chemical classes of solutes it detects.

Even before the invention of this detector attempts were made to use two stationary phases for the identification of substances. In 1956, different straight line plots for alkanes, alkanols and alkanones were obtained<sup>1</sup> by subtracting logarithmic expressions of retention times on a triethyleneglycol column from those on an ester (both polar!). Many papers appeared relating solute structure and retention values using two phases, for example that of Lewis *et al.*<sup>2</sup>. Merritt and Walsh found<sup>3</sup> that the only "very good" pairing was of two polyethyleneglycols for distinguishing homologous series. However, they then recorded<sup>4</sup> that the "only pair (of columns) which showed a change in order of elution of (five mixed) components" was polyethyleneglycol with a silicone. Smith *et al.*<sup>5</sup>, and later Ladon<sup>6</sup>, studied hydrocarbons only, on polar and non-polar (squalane) columns, and the lattermost could identify unknown peaks mathematically.

In 1970, Breckler and Betts<sup>7</sup> investigated the use of relative retention times ( $t_{R,rel}$ ) to linalol on packed columns, as a guide to such distinction for the most volatile constituents of volatile oils. Betts<sup>8</sup> reviewed this work, where substances of low polarity like limonene, cineole and menthyl acetate showed higher  $t_{R,rel}$  values on the low-polarity methyl polysiloxane column than on polar columns. More polar solutes such as anethole, citral and geraniol gave the opposite effect, with  $t_{R,rel}$  values on the low polarity column being well below the results for polar columns. It was also possible to detect an alcohol, as unlike other polar solutes it would give higher  $t_{R,rel}$  values on polyethylene glycol stationary phase (with its matching hydroxy groups) than on polyester. Five groups of volatile oil constituents with  $t_{R,rel}$  values usually in the range 0.24-4.00 could be distinguished by this method. Betts<sup>9</sup> applied this concept to capillary columns in 1984.

This work has now been extended to volatile oil constituents with relatively long retention times such as polysubstituted aromatics and sesquiterpenes. Lemberkovics and Verzar-Petri<sup>10</sup> appreciated there was a problem in identifying frequently occurring sesquiterpenes in volatile oils, but complicated their experimental situation by apparently mixing two polysiloxanes in one packed column.

Betts<sup>8</sup> found that a standard giving best results was a terpene alcohol, and as the previously used standard linalol has a short retention time, geraniol, which has the longest retention time of any monoterpenol, was here selected as standard.

## EXPERIMENTAL

### *Apparatus*

A Hewlett-Packard 5790A gas chromatograph was applied, fitted with a flame ionisation detector used at 200°C, capillary control unit and splitter injection port used at 200°C. Hewlett-Packard 3390A and 3380A recorder/integrators were used.

Two Hewlett-Packard fused-silica capillaries approximately 25 m × 0.21 mm I.D. containing: (a) Carbowax 20M (polyethylene glycol), or (b) high-performance cross-linked methyl silicone, both used isothermally at 135°C, were used.

Helium was used as the mobile phase gas at about 1 ml min<sup>-1</sup>, and as make-up gas for the detector.

### *Materials*

The materials investigated are indicated in Table I.

### *Method*

Several old volatile oils were examined on the two capillary columns using repeated injections from an initially filled and emptied microsyringe. The earlier injections gave "percentage composition" of the peaks from recorder percentage area measurements, and the subsequent injections gave shorter, more reliable retention times, particularly for the major oil components. For each capillary, the retention time of geraniol was approximately 1.45 min.

## RESULTS AND DISCUSSION

Results are given in Table I, based on the shortest retention time obtained by using traces of solutes. It is apparent that  $t_{R,rel}$  ratios for polar against non-polar phase (P/N) can give an indication of the chemical class of a volatile oil solute. From the substances studied, if the ratio is less than 0.30, it is a sesquiterpene hydrocarbon. If P/N is 0.40–0.95, the substance is most likely a terpenoid, being a sesquiterpenoid if the retention times are high. The aromatics anethole and safrole are exceptionally in this range. If the ratio is greater than 0.95, the solute is an aromatic substance, being an ether if the P/N is less than 1.6, but an aldehyde or phenol if it is greater, the lattermost being more likely with higher ratios. Although not intended as part of these studies, it was observed that the monoterpene hydrocarbon limonene had P/N 0.67 (with very short retention time). It can be concluded that methyl eugenol in terms of P/N is close in polarity to geraniol, although its retention times on both stationary phases are about 70% greater than those of this standard.

TABLE I

RELATIVE RETENTION TIMES (GERANIOL = 100) AT 135°C

Mobile phase: helium at flow-rate about 1 ml min<sup>-1</sup> at detector exit, giving  $t_R$  for geraniol (Sigma) 1.35–1.55 min on both capillaries.

Volatile oil constituent (and source)	$t_{R,rel}$ vs. geraniol		P/N	Chemical nature and comment
	Polar (P): Carbowax 20M	Non-polar (N): methyl silicone polysiloxane, cross-linked		
Caryophyllene (Koch-Light)	0.52	2.22	0.23	Sesquiterpene hydrocarbon
Zingiberene (Ginger oil Kelkar)	0.67	2.92	0.23	Sesquiterpene hydrocarbon
Curcumene (Ginger oil Kelkar)	0.76	3.31	0.23	Sesquiterpene hydrocarbon
Eudesmol (Plaimar research)	3.62	5.79	0.63	Sesquiterpenoid mixture, main peak. Very long $t_R$
Terpinen-4-ol (Dragoco)	0.52	0.80	0.65	Monoterpenoid-detected in Nutmeg oil
Carvone (Koch-Light)	0.68	0.99	0.69	Monoterpenoid
Perillal (Koch-Light)	0.82	1.09	0.75	Monoterpenoid
Anethole (Sigma)	0.88	1.15	0.76	Aromatic ether, monomethoxy
Citronellol (BDH)	0.77	0.92	0.84	Monoterpenoid
Farnesol (Aldrich)	6.92	8.14	0.85	Sesquiterpenoid (acyclic). Extremely long $t_R$
Safrrole (Fritzsche)	1.00	1.15	0.87	Aromatic ether, methylene dioxy (detected in Nutmeg oil)
Santalol (Sandawood oil Izumi)	6.04	6.46	0.93	Sesquiterpenoid. Extremely long $t_R$
Methyleugenol (Fritzsche)	1.65	1.75	0.94	Aromatic ether, dimethoxy
Elemicin (synthesised)	3.58	3.46	1.03	Aromatic ether, trimethoxy
Myristicin (Nutmeg oil Bush Boake Allen)	3.83	2.86	1.34	Aromatic ether, methylenedioxy monomethoxy (detected in Parsley seed oil)
Cinnamal (Cinnamon oil)	1.73	1.06	1.63	Aromatic aldehyde
Eugenol (Rampre)	2.82	1.50	1.88	Phenol
Thymol (Sigma)	3.15	1.14	2.76	Phenol

### Application to *Chenopodium* oil

A sample of *Chenopodium* oil (Felton, Grimwade and Bickford, Perth, Australia) exhibited a main polar phase capillary peak (67 and 62% of total peak areas determined on two runs) at  $t_R$  1.15 min or less, which if related to the main non-polar peak (60% and 59%) at  $t_R$  1.52 min gave P/N of  $0.71/1.00 = 0.71$ . This indicated a terpenoid, namely the peroxide ascaridole, present in appropriate quantity for a good specimen<sup>11</sup>. The results taken from the printouts are given in Table II.

TABLE II

RESULTS TAKEN FROM HP 3390A PRINTOUTS FROM GC RUNS OF CHENOPODIUM OIL

Run No. 23, <i>Chenopodium</i> oil (FGB) Area%, POLAR PHASE, geraniol $t_R$ 1.53 min					Run No. 3, <i>Chenopodium</i> oil (FGB) Area%, NON-POLAR PHASE, geraniol $t_R$ 1.52 min				
$t_R$	Area	Type*	AR/HT**	Area%	$t_R$	Area	Type*	AR/HT**	Area%
0.52	377080	D BB	0.023	17.587	0.42	1634	PV	0.030	0.158
0.63	7533	BP	0.045	0.351	0.47	1999	D VB	0.025	0.193
0.75	1817	PV	0.043	0.085	0.78	215720	PB	0.029	20.865
0.81	3802	VV	0.026	0.177	0.93	12353	PV	0.038	1.195
0.86	9235	VV	0.030	0.431	1.01	7885	VB	0.054	0.763
0.91	3441	VV	0.029	0.161	1.20	4346	PV	0.032	0.420
0.94	4369	D VP	0.034	0.204	1.24	6223	D VP	0.047	0.602
1.15	1433000	PB	0.057	66.834	1.40	8388	PV	0.062	0.811
1.24	1553	D BP	0.024	0.072	1.52	610280	VV	0.041	59.028
1.30	13308	PV	0.035	0.621	1.58	8470	D VV	0.030	0.819
1.39	4415	VV	0.037	0.206	1.64	6998	VV	0.033	0.677
1.46	4019	VV	0.032	0.187	1.74	25134	VV	0.038	2.431
1.51	12019	VV	0.043	0.561	1.89	74367	VB	0.037	7.193
1.66	111140	VV	0.039	5.184	2.09	2209	BP	0.035	0.214
1.71	4905	D VB	0.027	0.229	2.21	2262	PV	0.060	0.219
2.08	12695	PV	0.041	0.592	2.27	3886	VV	0.039	0.376
2.42	4072	BV	0.044	0.190	2.33	7832	VV	0.039	0.758
2.50	10832	VB	0.048	0.505	2.64	28541	PB	0.042	2.761
3.40	11239	PV	0.083	0.524	3.03	1698	BB	0.051	0.164
3.65	28914	VV	0.065	1.349	3.25	3672	PB	0.074	0.355
3.78	9245	VB	0.064	0.431					
4.90	42483	PB	0.036	1.981					
5.26	13252	BV	0.104	0.618					
6.85	13599	BB	0.105	0.634					
7.62	6144	PB	0.126	0.287					

\* The integrator provides an opinion about the type of peak recorded. B = Peak begins or ends on baseline (BB is thus the best); D = distorted peak; P = penetration of baseline (reset); V = valley between closely emerging peaks rather than baseline (VV indicates incomplete peak resolution on both sides).

\*\* AR/HT expresses the width of the peak at half its height, in min. Relatively high values indicate a less efficient match of stationary phase and solute.

Ignoring an early monoterpene hydrocarbon peak (about 20%), a polar peak was noticed at  $t_R$  1.66 min or less, giving  $t_{R,rel}$  1.06 (5 and 6%). A corresponding non-polar peak,  $t_R$  1.89 (7 and 7%) gave  $t_{R,rel}$  1.24. This yielded P/N = 0.85 and it could, from  $t_R$ , be an aromatic. Such provisional identification can assist a computerised search of spectral data on file.

A late polar peak (2 and 2%),  $t_R$  4.90 min or less with  $t_{R,rel}$  3.16, if matched with the non-polar  $t_R$  1.74 min,  $t_{R,rel}$  1.14 (2 and 3%) indicated by P/N = 2.77 a phenol, in fact thymol. This is a reported degradation product of ascaridole<sup>12</sup>. If the late polar peak was "matched" with the non-polar one at  $t_R$  2.64 min, a phenol was again indicated, although not thymol.

### *Application to Pimento oil*

A sample of "Ol Pimentae" (Faulding, Perth, Australia) gave eugenol as its major constituent, about 70% of total peak areas, an appropriate value<sup>13</sup>.

The second peak in terms of area percentage (12 and 10%) was  $t_{R,rel}$  3.07 on the polar capillary and 2.61 (11 and 11%) on the other, giving P/N = 1.18, indicating an aromatic ether which is not methyl eugenol, a reported constituent<sup>13</sup>.

The peak  $t_{R,rel}$  0.53 (4 and 6%) on polar phase, if matched with 2.18 (4 and 4%) non-polar, gave P/N = 0.24, a sesquiterpene hydrocarbon, probably  $\beta$ -caryophyllene, which has been reported at 4.2% in the oil<sup>13</sup>.

The long  $t_{R,rel}$  6.07 (1.5 and 1.3%) on the polar capillary could be related to the non-polar peak 2.99 (1.6 and 1.6%). This gave P/N of 2.03, suggesting a phenol other than eugenol. It is possibly chavicol, which has been reported<sup>13</sup>.

### *Application to Eucalyptus rudis oil*

An oil distilled from fresh leaves of *Eucalyptus rudis* in these laboratories in 1974 was examined. It was yellow and mobile, somewhat viscous. The main component cineole was present to the extent of just over 50% peak area on both columns, and some cineole had probably been lost during storage.

Another early peak at about 11% peak areas showed  $t_{R,rel}$  values of 0.65 and 0.84 on the capillaries, giving P/N of 0.77 for a monoterpene hydrocarbon. A similar peak area (10, 11, and 14%) was observed at  $t_{R,rel}$  2.12 on the polar phase, and 4.28 non-polar (12, 13 and 13%) with P/N 0.50 for a sesquiterpenoid (as retention times were large). This same substance has been detected here in oils distilled from *E. cinerea*, *E. globulus*, *E. nicholii* and *E. viminalis*.

A polar phase peak consistently of 4% total area on both capillaries was noted at  $t_{R,rel}$  of 0.54 and 2.38, giving P/N of 0.23 for a sesquiterpene hydrocarbon. Another peak on the polar phase,  $t_{R,rel}$  0.98 (3, 3 and 4%) could be related to 3.89 non-polar (2, 3 and 4%) with P/N of 0.25 indicating another sesquiterpene hydrocarbon.

Peaks of 2% total area on both capillaries with the same  $t_{R,rel}$  of 1.66 gave, of course, P/N = 1.00, suggesting an aromatic.

### REFERENCES

- 1 G. J. Pierotti, C. H. Deal, E. L. Derr and P. E. Porter, *J. Am. Chem. Soc.*, 78 (1956) 2989.
- 2 J. S. Lewis, H. W. Patton and W. I. Kaye, *Anal. Chem.*, 28 (1956) 1370.
- 3 C. Merritt and J. T. Walsh, *Anal. Chem.*, 34 (1962) 903.
- 4 C. Merritt and J. T. Walsh, *Anal. Chem.*, 34 (1962) 908.
- 5 B. Smith, R. Ohlson and G. Larson, *Acta Chem. Scand.*, 17 (1963) 436.
- 6 A. W. Ladon, *J. Chromatogr.*, 99 (1974) 203.
- 7 P. N. Breckler and T. J. Betts, *J. Chromatogr.*, 53 (1970) 163.
- 8 T. J. Betts, *Aust. J. Pharm., Suppl.*, 52 (1971) 57.
- 9 T. J. Betts, *J. Chromatogr.*, 294 (1984) 370.
- 10 E. Lemberkovics and G. Verzar-Petri, *Essential Oils and Aromatic Plants*, Martinus Nijhoff/Dr. W. Junk, Dordrecht, The Netherlands, 1985, p. 103.
- 11 E. K. Nelson, *J. Am. Chem. Soc.*, 33 (1911) 1405.
- 12 E. K. Nelson, *J. Am. Chem. Soc.*, 35 (1913) 84.
- 13 J. Nabney and F. V. Robinson, *Flav. Ind.*, 3 (1972) 50.

## Note

### Analysis of tioconazole using high-performance liquid chromatography with a porous graphitic carbon column

JOHN C. BERRIDGE

*Analytical Chemistry Department, Pfizer Central Research, Sandwich, Kent CT13 9NJ (U.K.)*

(First received March 7th, 1988; revised manuscript received June 7th, 1988)

Porous graphitic carbon (PGC) is a strong reversed-phase absorbent with retention characteristics similar to those of alkyl bonded silicas, *e.g.* octadecylsilane (ODS)<sup>1–4</sup>. However, unlike silica gel it offers a number of critically important advantages. These include the absence of residual silanol groups, which can give rise to problems with the elution of amines, insolubility in aggressive aqueous–organic mobile phases at extreme pH values, a homogeneous surface and a reproducible performance from batch to batch. Polymeric packing materials also offer some of these advantages but suffer from other problems such as limited mechanical stability and poorer mass transfer properties. PGC columns would appear, therefore, to offer unique properties which would commend them particularly to the analysis of basic compounds of pharmaceutical interest. The number of literature applications with PGC columns is still, however, very small.

The determination of tioconazole and three very closely structurally related potential impurities is the subject of a monograph in the *United States Pharmacopeia*<sup>5</sup>. However, the separation is difficult to achieve with ODS reversed-phase columns, requiring long elution times and an aggressive mobile phase (leading to short column lifetimes and requiring that a solvent conditioning pre-column be included). In addition the major hydrolysis product of tioconazole is unretained and cannot be determined. The analysis of tioconazole has been the subject of further investigation and optimisation<sup>6,7</sup> from which it was concluded that a phenyl-bonded silica with an ion-pairing mobile phase provided optimum selectivity within the constraints of a non-aggressive mobile phase. However, it was further shown that to achieve optimised resolution of the low levels expected of the potential impurities it was necessary to modify the detection wavelength from 219 nm, as specified in ref. 5, to 260 nm<sup>7</sup>. This shift to longer wavelength places increased demands upon the detector performance and makes the detection of low levels of the hydrolytic degradation product more difficult.

This paper describes the use of a PGC column to separate tioconazole from the three potential impurities and its main hydrolytic degradation product. It is also shown that the enhanced selectivity offered by the PGC column permits the use of low wavelength detection.

## EXPERIMENTAL

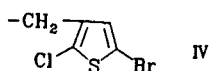
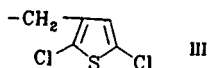
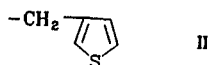
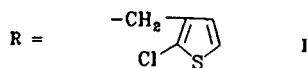
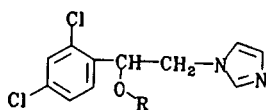
A Model 1090A liquid chromatograph (Hewlett-Packard, Wokingham, U.K.) equipped with a diode-array detector and autosampler was used for the present studies. Detection wavelengths of 220 and 260 nm were used with bandwidths of 10 nm. The column was 10 cm  $\times$  0.46 cm I.D. porous graphitic carbon of mean particle diameter 7  $\mu$ m (ChromatoGraphite; Wolfson Liquid Chromatography Unit, University of Edinburgh, Edinburgh (U.K.)). Solvents were HPLC grade (Rathburn Chemicals, Peebles, U.K.) and all other reagents were reagent grade. Tioconazole (I) and its potential impurities (II–IV) and major hydrolysis product (V) were provided by Pfizer Central Research. Solutions were prepared in mobile phase at concentrations of approximately 0.5 mg/ml. Separations were carried out with a flow-rate of 1.5 ml/min and with a column temperature of 40°C.

Comparison chromatograms result from earlier studies with tioconazole; chromatographic conditions are described on the relevant figures.

## RESULTS

The difficulties associated with achieving satisfactory resolution of tioconazole (I) from its deschloro (II) and, in particular its 2,5-dichloro (III) and 2-chloro-5-bromo (IV) analogues using the USP method are illustrated in Fig. 1.

Indeed, differentiation in the time domain (differentiating the detector signal with respect to time in order to enhance resolution) has been proposed as an adjunct to this difficult separation<sup>8</sup> to improve resolution and quantitation at low levels. The optimised separation using a phenyl column<sup>7</sup> is shown in Fig. 2. The separation is now faster and the resolution improved but, to detect levels of the impurities III and IV without interference from the tail of the tioconazole peak, it is necessary to use 260 nm



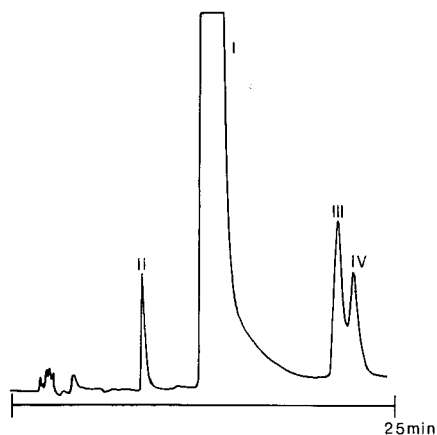


Fig. 1. Separation of tioconazole according to ref. 5. Column (25 cm  $\times$  0.46 cm I.D.) of LiChrosorb RP-18, eluted with methanol-acetonitrile-water-ammonia (220:200:190:1, v/v) at 1.5 ml/min and 40°C. Detection at 219 nm.

to capitalise upon spectral discrimination. At 260 nm the longer wavelength absorbance possessed only by compounds III and IV allows their detectability to be maintained while reducing the contribution of tioconazole. Unfortunately, compounds II and V do not possess this longer wavelength absorption and are consequently more difficult to detect. In addition, the ion-pairing mobile phase is more complex and the reproducibility of the separation, with respect to columns from different manufacturers, has not been fully evaluated.

In developing the separation on the PGC column, a simple and robust separation was desired. Retention of tioconazole and its impurities could be obtained with acidic aqueous-organic mobile phases but retention was not accompanied with

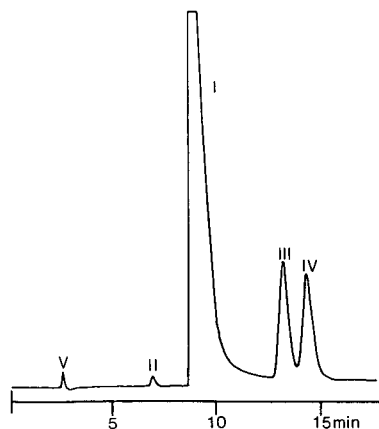


Fig. 2. Optimised separation using 15 cm  $\times$  0.46 cm I.D. (5  $\mu$ m) Hypersil phenyl column<sup>6</sup>. Mobile phase of methanol-acetonitrile-buffer (39:16:45, v/v). Buffer comprises 0.05 *M* triethylamine and 0.025 *M* 1-octanesulphonic acid adjusted to pH 4.0 with orthophosphoric acid. Flow-rate = 1.5 ml/min, column temperature = 40°C, detection at 260 nm. Compounds II-V are approximately 0.5% relative to tioconazole.

resolution. A mobile phase of 35% tetrahydrofuran in water, with 1% ortho-phosphoric acid produced a capacity factor ( $k'$ ) for tioconazole of 5. The relative ease of elution with acidic mobile phases is to be expected with the protonated compounds—tioconazole has a  $pK_a$  of 6.4. Greater retention (*i.e.* a higher  $k'$  value) and the possibility of improving the selectivity requires the use of mobile phases at pH values greater than 8.4. Unlike conventional silica based columns, PGC columns offer the possibility of working with basic mobile phases and high pH mobile phases were thus used for the remainder of the studies.

All the compounds under investigation were extremely strongly retained with basic mobile phases, neither methanol or acetonitrile being strong enough to elute the tioconazole in less than 20 column volumes of mobile phase. Tetrahydrofuran, however, proved to be a relatively strong modifier<sup>3</sup>. A mobile phase at pH 10.5 of tetrahydrofuran–water (70:30, v/v) containing 1% aqueous ammonia (sp.gr. = 0.880) produced adequate retention which was accompanied by very high selectivity for all compounds (Fig. 3) and permitted a fast separation to be achieved. Such was the selectivity between tioconazole and compounds III and IV that their detection at 0.2% (w/w) relative to tioconazole could be easily accomplished using a detection wavelength of 220 nm. Furthermore, the selectivity obtained with this simple mobile phase precluded the need to undertake a formal programme of mobile phase optimisation. The use of 220 nm also conferred the advantage of enhancing the detectability of compounds II and V, both of which were also easily detected at the 0.2% (w/w) level.

The column efficiencies were not as high as those obtained for silica-based columns, a reduced plate height of 14 being determined for the peak due to III. This lack of efficiency is the subject of further studies but potentially will reduce the ultimate detectability of the late-eluting compounds. However, because of the very high selectivity, both compounds are well resolved from each other and from tioconazole and adequate sensitivity can be maintained. Linearity of determination of all potential impurities was demonstrated over the range 0.2–1.2% (w/w) relative to the tioconazole.

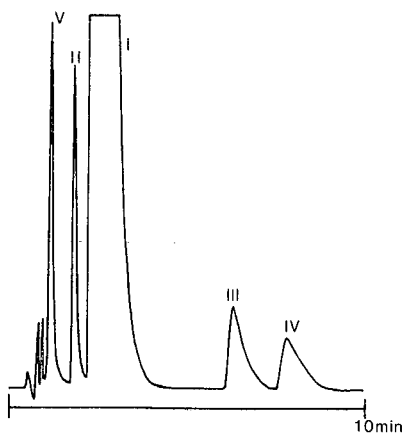


Fig. 3. Separation on 10 cm  $\times$  0.46 cm I.D. PGC column. Mobile phase of tetrahydrofuran–water (70:30, v/v) containing 1% ammonia (sp.gr. = 0.880) at 1.5 ml/min with column temperature of 40°C and detection at 220 nm. Compounds II–V are approximately 0.5% relative to tioconazole.

## CONCLUSIONS

The use of a PGC column has clearly shown advantages over the more traditional silica-based 'reversed-phase' supports. The hydrolytic stability of the support permits the use of mobile phases at pH values far exceeding those suitable for silica based columns. In the analysis of tioconazole, this stability could be exploited to permit the direct chromatographing of the unionised solutes using a basic mobile phase to obtain high selectivities. No additives were required to mask residual silanol groups and such chromatographic simplicity is likely to find widespread applicability in the separation of basic molecules. The selectivities obtained somewhat surprisingly far exceeded those obtained following extensive separation optimisation on ODS or phenyl-bonded columns. Since PGC columns by their very nature are likely to be highly reproducible, their use in pharmaceutical analysis combines all the advantages of robustness with the possibilities of straightforward method transfer to all those who may need to use it.

## ACKNOWLEDGEMENT

The author is grateful to ChromatoGraphite for kindly supplying the column used in this work.

## REFERENCES

- 1 M. T. Gilbert, J. H. Knox and B. Kaur, *Chromatographia*, 16 (1982) 138.
- 2 J. H. Knox, B. Kaur and G. R. Millward, *J. Chromatogr.*, 352 (1988) 3.
- 3 J. H. Knox, B. Kaur and H. Dias, presented at the 10th International Symposium on Column Liquid Chromatography, San Francisco, 1986.
- 4 J. H. Knox and B. Kaur, *Eur. Chromatogr. News*, 1 (1987) 12.
- 5 *United States Pharmacopeia XXI*, Supplement 2, United States Pharmacopeia Convention Inc., Rockville, MD, 1985, pp. 189-196.
- 6 A. G. Wright, A. F. Fell and J. C. Berridge, *J. Chromatogr.*, submitted for publication.
- 7 J. C. Berridge, A. F. Fell and A. G. Wright, *Analyst (London)*, submitted for publication.
- 8 J. C. Berridge and K. S. Andrews, *Analyst (London)*, 109 (1984) 287.

CHROM. 20 701

## Note

### Difference in cell surface hydrophobicity of *Halobacterium salinarum* strains

J. L. OCHOA\* and F. ASCENCIO-VALLE

Centre of Biological Research, CIB, P.O. Box 128, La Paz, B.C.S. 23000 (México)

(Received June 1st, 1988)

The cell surface of halobacteria is remarkable for its ability to support the stressing conditions conferred by the high salt concentration of the surrounding medium. This is apparently due to an excess of surface charges that counteracts external ions<sup>1–3</sup> and to the internal accumulation of osmoregulators, which contributes to compensating for the high osmotic pressure from the exterior<sup>4–7</sup>.

The balance between the charged and non-polar groups of the cell surface in halobacteria may be important in determining its degree of halo-tolerance and/or halophilism. This property necessarily varies from one species to another, and its evaluation may be an interesting approach for classification. As shown in this paper, the chromatographic behaviour on hydrophobic matrices of three well known extreme halophile strains, regarded as belonging to the same species<sup>8</sup>, is distinct. It is concluded that hydrophobic interaction chromatography (HIC), a technique which takes advantage of the high salt concentration of the medium, is a useful alternative in the study of the cell surface hydrophobicity of halobacteria.

## EXPERIMENTAL

The bacterial strains *Halobacterium halobium* (NRC 817), *H. cutirubrum* (CCM 2088) and *H. salinarum* (CCM 2148) were cultured in MH medium: 10 g/l  $\text{MgSO}_4 \cdot 7\text{H}_2\text{O}$ , 5 g/l KCl, 0.2 g/l  $\text{CaCl}_2 \cdot 6\text{H}_2\text{O}$ , 10 g/l yeast extract (DIFCO) and 2.5 g/l bacto tryptone (DIFCO), adjusted to 3.6 M NaCl at 37°C in a Lab-Line Orbit shaker at 120 rpm until the cell density reached a value of 0.45 optical units at 580 nm. Aliquots of 0.5 ml were reincubated in 50 ml as above and the bacteria from the mid-logarithmic phase were collected, washed twice with a saline solution (3.6 M sodium chloride) and kept at 4°C for chromatography. The adsorbent gels were obtained from Pharmacia (Uppsala, Sweden) and all other reagents from Sigma (St. Louis, MO, U.S.A.).

### Hydrophobic adsorption

The hydrophobicity of the selected halobacteria was determined by adsorption on 1 ml of gel in test-tubes (0.9 × 11 cm) or on chromatographic columns (33.5 × 0.8 cm bed volume). A 1-ml volume of cell suspension (about 0.45 optical units at 580 or 2.25 optical units at 280 nm, equivalent to  $6.4 \cdot 10^6$  cells when compared with a standard plot of *Halobacterium halobium*) was either mixed with the gel in the

test-tube or applied to the column at a flow-rate of 35 ml/h, collecting samples of 2 ml per tube. The absorbance of the supernatant or column effluent was determined at 280 nm in a Spectronic 2000 spectrophotometer. All experiments were run in triplicate and the mean values determined.

## RESULTS AND DISCUSSION

A number of techniques have been tried for estimating the cell surface hydrophobicity of bacteria. One example is based on its degree of aggregation at different concentrations of ammonium sulphate<sup>9-11</sup>; others utilize the distribution of microorganisms in a two-phase system of different polarity<sup>12-15</sup> or the measurement of the contact angle between the bacteria and a given solid surface<sup>16</sup>; the binding of hydrophobic probes to the cell surface has also been an approach towards this end<sup>17</sup>.

Hydrophobic interaction chromatography (HIC)<sup>18-20</sup> has been applied successfully in the study of the hydrophobicity of many bacteria<sup>9,21-23</sup> and for the separation of eukaryotic cells from various sources<sup>19</sup>. HIC is based on the interaction between an immobilized hydrophobic ligand and a hydrophobic group of the sample. The strength of interaction increases with increasing salt concentration and temperature; the nature of the hydrophobic ligand, its density on the matrix and its accessibility also determine the extent of adsorption. Hence it is possible to establish the hydrophobic character of a substance by examining its chromatographic behaviour, varying the ligand and the experimental conditions.

In general, the cell surface possesses exposed hydrophobic sites that are responsible for bacterial adsorption on hydrophobic gels<sup>24</sup>. It has been shown, for instance, that enzymatic or chemical treatments modify the hydrophobicity of various kinds of microorganisms<sup>25-27</sup>.

In this study we first chose the chromatographic approach for analysing the

TABLE I

EFFECT OF THE NATURE OF THE HYDROPHOBIC LIGAND ON THE ADSORPTION OF HALOBACTERIA ON HYDROPHOBIC GELS AT DIFFERENT SALT CONCENTRATIONS  
Values correspond to mean percentages of three replicas.

Gel	NaCl (M)														
	<i>H. cutirubrum</i>					<i>H. halobium</i>					<i>H. salinarium</i>				
	3.6	4.0	4.4	4.8	5.2	3.6	4.0	4.4	4.8	5.2	3.6	4.0	4.4	4.8	5.2
<i>Control</i>															
Agarose (4B CL)	55	49	37	41	46	80	71	76	71	71	87	89	85	86	83
<i>Aminoalkyl</i>															
Agarose-ethane	69	62	44	41	46	78	78	69	68	71	89	86	84	84	86
Agarose-butane	68	61	41	41	44	72	71	69	68	66	88	83	80	83	83
Agarose-hexane	72	52	45	36	44	84	80	76	73	66	88	81	81	79	81
<i>Alkyl</i>															
Agarose-phenyl	31	52	52	56	56	86	89	89	83	86	99	98	99	99	99
Agarose-octane	76	60	53	46	56	79	82	83	80	80	92	89	88	88	92

behaviour of extreme halophiles, which gave very low elution yields, that is, only a fraction of the cell population (about 15%) eluted from the column. This problem was first attributed to the physical entrapment of bacterial aggregates and therefore a batch-assay procedure was followed (Table I).

As shown in Table I, the percentage of adsorption of extreme halophiles (*H. halobium*, *H. salinarium* and *H. cutirubrum*) ranges from 30 to 99% according to the nature of the immobilized hydrophobic ligand and of the experimental conditions. *H. halobium*, *H. cutirubrum* and *H. salinarium* show important differences in their tendency to adsorb on the hydrophobic matrices employed in this study. This finding suggests that they possess different cell envelope properties and supports their designation as different strains of the *H. salinarium* species<sup>8</sup>. It is interesting to consider the cell surface hydrophobicity, which seems to be involved in the attachment of microorganisms to solid surfaces<sup>28-33</sup>, for classification purposes; apparently, *H. cutirubrum* shows the weakest, *H. halobium* a moderate and *H. salinarium* the strongest hydrophobicity (Table I).

There is no clear pattern of the adsorption of *H. salinarium* strains on hydrophobic gels as a function of salt concentration (Table I). In this respect they do not follow the theoretical trend of most proteins and cell particles<sup>18-20</sup>. In other words, the adsorption tendency does not increase with increasing salt concentration. This does not necessarily mean that another mechanism of adsorption (*i.e.*, avidity for the carbohydrate matrix) is involved. In fact, the strains employed here do not utilize sugars as a carbon source<sup>8</sup> and their addition to the chromatographic buffer enhances, rather than diminishes, bacterial adsorption<sup>35</sup>. Bacterial hydrophobicity is the sum of a number of cell surface characteristics and its expression may be extremely complex. As reported<sup>34</sup>, the tendency of 23 strains of *Staphylococci* to adhere to hydrophobic materials may vary within the same species; this behaviour appears to be related to the presence of capsules. Our observations, derived from the chromatographic patterns of halobacteria<sup>35</sup>, show that differences in hydrophobic character also exist among extreme halophiles. Hence it may be necessary to consider the biological significance of this property in order to interpret correctly these findings and establish their importance in bacterial classification.

## REFERENCES

- 1 H. Hara and M. Masui, *FEMS Microbiol. Ecol.*, 31 (1985) 279.
- 2 C. Pande, R. H. Callender, C.-H. Chang and T. G. Ebrey, *Photochem. Photobiol.*, 42 (1985) 549.
- 3 F. Rodriguez-Valera, G. Juez and D. J. Kushner, *System. Appl. Microbiol.*, 4 (1983) 369.
- 4 R. H. Vreeland, B. D. Mierau, C. D. Litchfield and E. L. Martin, *Can. J. Microbiol.*, 29 (1983) 407.
- 5 S. M. Henrichs and R. Cuhel, *Appl. Environ. Microbiol.*, 50 (1985) 543.
- 6 N.-K. Birkeland and S.-K. Ratkje, *Membr. Biochem.*, 6 (1985) 1.
- 7 E. A. Galinski, H.-P. Pfeiffer and H. G. Truper, *Eur. J. Biochem.*, 149 (1985) 135.
- 8 H. Larsen, in N. R. Krieg (Editor), *Bergey's Manual of Systematic Bacteriology*, Williams and Wilkins, Baltimore, London, 1984, p. 261.
- 9 T. J. Trust, W. W. Kay and E. E. Ishiguro, *Curr. Microbiol.*, 9 (1983) 315.
- 10 A. Ljungh, A. Brown and T. Wadstrom, in J. Jeljaszewicz (Editor), *The Staphylococci*, *Zbl. Bakteriol.*, Suppl. 14 (1985) 157.
- 11 F. Rozgonyi, K. R. Szitha, S. Hjerten and T. Wadstrom, *J. Appl. Bacteriol.*, 59 (1985) 451.
- 12 E. Weiss, M. Rosenberg, H. Jude and E. Rosenberg, *Curr. Microbiol.*, 7 (1982) 125.
- 13 A. H. Hogt, J. Dankert, J. Feijen and J. A. DeVries, *Antonie van Leeuwenhoek J. Microbiol. Serol.*, 48 (1982) 49.
- 14 M. Rosenberg, D. Gutnick and E. Rosenberg, *FEMS Microbiol. Lett.*, 9 (1980) 29.

- 15 D. Lichtenberg, M. Rosenberg, N. Sharfman and I. Ofek, *J. Microbiol. Methods*, 4 (1985) 141.
- 16 S. Minagi, Y. Miyake, K. Inagaki, H. Tsuru and H. Suganaka, *Infect. Immun.*, 47 (1985) 11.
- 17 J. Brunner, A. J. Franzussof, B. Luscher, C. Zugliani and G. Semenza, *Biochemistry*, 24 (1985) 5422.
- 18 J. L. Ochoa, *Biochimie*, 60 (1978) 1.
- 19 G. Halperin, M. Tauber-Finkelstein and S. Shaltiel, *J. Chromatogr.*, 317 (1984) 103.
- 20 S. Shaltiel, *Methods Enzymol.*, 104 (1984) 69.
- 21 T. Honda, M. M. A. Khan, Y. Takeda and T. Miwatani, *FEMS Microbiol. Lett.*, 17 (1983) 273.
- 22 A. Faris, M. Lindhal and T. Wadstrom, *Curr. Microbiol.*, 7 (1982) 357.
- 23 P. Johnsson and T. Wadstrom, *Curr. Microbiol.*, 8 (1983) 347.
- 24 K. Pedersen, *FEMS Microbiol. Lett.*, 12 (1981) 365.
- 25 J. H. Paul and W. H. Jeffrey, *Appl. Environ. Microbiol.*, 50 (1985) 431.
- 26 H. F. Jenkinson, *J. Gen. Microbiol.*, 8 (1983) 347.
- 27 F. Ascencio-Valle, A. Lopez-Cortes and J. L. Ochoa, *Microbios Lett.*, (1988) in press.
- 28 E. E. Ishiguro, T. Ainsworth, T. J. Trust and W. W. Kay, *J. Bacteriol.*, 164 (1985) 1233.
- 29 M. S. Hindhal and B. H. Iglewski, *J. Bacteriol.*, 159 (1984) 107.
- 30 W. J. Peros, I. Etherden, R. J. Gibbons and Z. Skobe, *J. Periodontal Res.*, 20 (1985) 24.
- 31 Y. Bar-or, M. Kessel and M. Shilo, *J. Arch. Microbiol.*, 142 (1985) 21.
- 32 N. Garber, N. Sharon, D. Shohet, J. S. Lam and R. J. Doyle, *Infect. Immun.*, 50 (1985) 336.
- 33 T. R. Tosteson, R. Revuelta, B. R. Zaidi, S. H. Imam and R. F. Bard, *J. Colloid Interface Sci.*, 104 (1985) 60.
- 34 A. H. Hogt, J. Dankert and J. Feijen, *J. Gen. Microbiol.*, 131 (1985) 2485.
- 35 F. Ascencio-Valle and J. L. Ochoa, *Rev. Latinoam. Microbiol.*, (1988) in press.

## Note

### Comparison of volatile halogenated compounds formed in the chloramination and chlorination of humic acid by gas chromatography-electron-capture detection

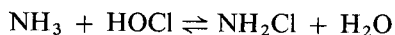
M. P. ITALIA\* and P. C. UDEN\*

*Department of Chemistry, Lederle Graduate Research Tower, University of Massachusetts, Amherst, MA 01003-0035 (U.S.A.)*

(First received March 23rd, 1988; revised manuscript received May 24th, 1988)

In recent years there has been a great deal of concern over the formation of trihalomethanes (THMs) from the chlorination of organic compounds in drinking water supplies<sup>1,2</sup>. An area of particular interest has been the chlorination of aquatic humic and fulvic acids<sup>3,4</sup>. Since Rook<sup>5</sup> first showed that THMs were formed from the chlorination of these substances, there have been hundreds of additional chlorinated compounds identified that are also formed from these humic precursors in the chlorination process<sup>6–8</sup>. The range of compounds identified includes halogenated aliphatic acids and aldehydes, haloacetonitriles, ketones and phenolic compounds. The latter aromatic compounds comprise a major non-volatile portion of the total organic chlorine content produced in the chlorination process which may also act as THM precursor material<sup>9–11</sup>.

In the search for alternate methods of water disinfection, a popular alternative to chlorination is chloramination<sup>12</sup>. Because chloramine is a less vigorous chlorinating agent, the extent of trihalomethane formation is decreased. The production of chloramine involves addition of ammonia during the chlorinating procedure, according to the following reaction<sup>13</sup>:



To determine what effect this change in the chlorinating processes had on the formation of halogenated substances from humic precursors, a comparison of the major products of chlorination and chloramination of a high-nitrogen humic acid was undertaken.

## EXPERIMENTAL

### Materials

Humic acid was obtained from Dr. Matvienko of the Universidad de Sao Paulo (Sao Carlos, Brazil), and had a composition of 35.08% carbon, 4.51% hydrogen and

\* Present address: Union Carbide Co., Bound Brook, NJ 08805, U.S.A.

7.33% nitrogen. Hypochlorous acid (as 5% sodium hypochlorite), concentrated sulfuric acid, ammonia (as 3 *M* ammonium hydroxide), and diethyl ether were obtained from Fisher Scientific (Pittsburgh, PA, U.S.A.). A pH 7 phosphate buffer was prepared and used in all humic acid solutions. A 14% boron trifluoride-methanol solution, used as a derivatizing agent, was obtained from Supelco (Bellefonte, PA, U.S.A.).

Gas chromatography (GC) was performed using a Hewlett Packard 5794 instrument equipped with an electron-capture detector and a J&W Scientific (Folsom, CA, U.S.A.) 30 m  $\times$  0.2 mm I.D. DB-5 fused-silica capillary column.

### *Methods*

Humic acid (100 mg) was added to each of two separate nitric acid washed 165-ml jars with crimp tops. To each was added 125 ml of 0.1 *M* phosphate buffer and the solutions were sonicated for 5 min to complete dissolution of the humic material.

A solution of chloramine was made by adding 25 ml of hypochlorite to 11 ml of 3 *M* ammonium hydroxide to obtain a chlorine to ammonia molar ratio of 1:1.1. This procedure minimized dichloroamine formation and mimicked typical treatment at the chlorinating plant. This mixture was then iodometrically titrated to determine the amount of chlorinating agent present. Both the chloramine and hypochlorite chlorinating agents were then added to separate vials of the previously prepared humic solutions in quantities that would add equal amounts of reactive chlorine to each sample, and give a chlorine to carbon ratio of 5:1. The samples were then crimp sealed, placed in the dark and allowed to react for 24 and 48 h.

To determine the neutral compounds present after each time period a 4-ml aliquot of the solution was removed, placed in a small vial, quenched with a few granules of sodium thiosulfate and extracted with two 2-ml portions of diethyl ether. From this extract, 1  $\mu$ l was diluted to 4 ml with diethyl ether and an injection of 2  $\mu$ l made into the gas chromatograph. When acidic compounds were to be analyzed, the procedure was modified somewhat. A 4-ml aliquot was again removed, quenched, and placed in a small vial. At this point, a few drops of concentrated sulfuric acid was added to reduce the pH to less than 1 and the mixture was extracted with 4 ml of diethyl ether. Derivatization using boron trifluoride-methanol was carried out following the procedure described by Young<sup>14</sup>. The organic layer recovered was diluted (1  $\mu$ l with 4 ml of diethyl ether) and a 2- $\mu$ l injection made to the gas chromatograph.

In all analyses the GC conditions were as follows: nitrogen carrier gas, an injection port temperature of 225°C and an electron-capture detector temperature of 320°C. For the neutral fraction, the initial temperature was 40°C with a hold of 2 min, a temperature ramp of 5°C/min to a final temperature of 180°C followed by a 1-min final hold. For acidic analyses all conditions were identical except for a 50°C initial temperature. Injections were made on a DB-5 capillary column with a 50:1 split ratio and a 1-ml/min flow-rate. All output was to a Perkin Elmer Sigma 10 recorder/integrator.

### RESULTS AND DISCUSSION

A GC comparison of the chlorination and chloramination of humic acid is shown for neutrals and acids (Figs. 1 and 2). The neutral fraction of both reactions

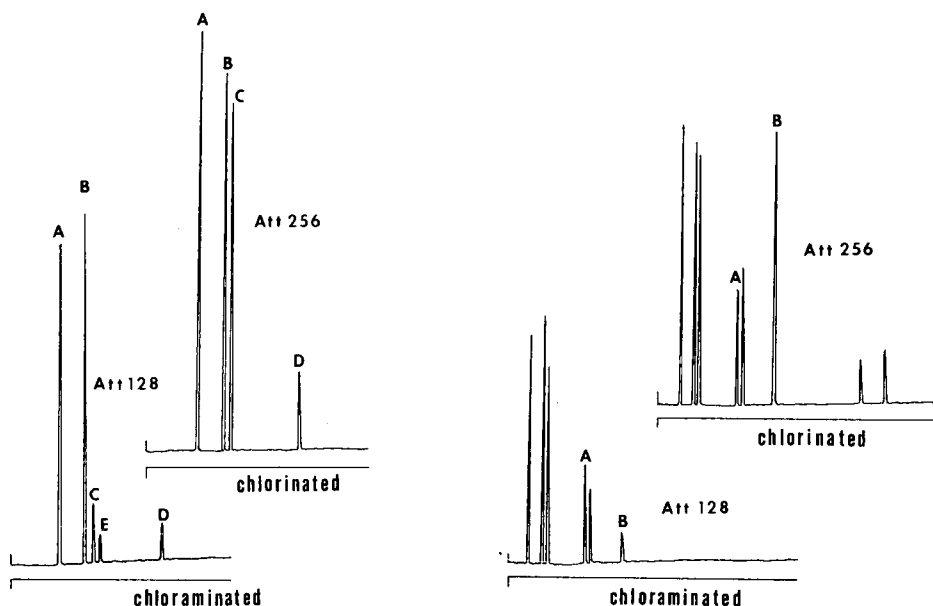


Fig. 1. GC with electron-capture detection of the neutral fraction of humic acid chlorination and chloramination. GC conditions: 40°C initial temperature, 2 min initial hold, 5°C/min temperature increase, 180°C final temperature and 1 min final hold. Column was a 30 m  $\times$  0.2 mm I.D. J&W DB-5 fused-silica capillary column with a flow-rate of 1 ml/min and a split ratio of 50:1. Attenuation of chlorinated (top) chromatogram is 256 and chloraminated (bottom) is 128. Peaks are identified as (A) chloroform, (B) dichloroacetonitrile, (C) trichloroacetaldehyde, (D) trichloroacetone and (E) unknown.

Fig. 2. GC with electron-capture detection of the acidic fraction of humic acid chlorination and chloramination after derivatization. All GC conditions are the same as in Fig. 1 with the exception of a 50°C initial temperature. Peaks are identified as methyl esters of (A) dichloroacetic acid and (B) trichloroacetic acid.

contained four chlorinated compounds formed from the chlorination of the humic material; chloroform, dichloroacetonitrile, trichloroacetaldehyde, and trichloroacetone. Upon examination of the neutral fraction (Fig. 1) it is seen that there is an overall decrease in the total halogenated material in the chloraminated sample (the attenuations were 512 for chlorination, 256 for chloramination). The most striking difference was the amount of trichloroacetaldehyde present; in the chloraminated fraction this was much reduced. It is also clear that dichloroacetonitrile is the predominant species in the chloraminated sample.

Examination of the chromatogram of the acidic fraction (Fig. 2) also shows a small amount of trichloroacetic acid (B, methyl ester), with dichloroacetic acid (A, methyl ester) as the dominant substance in chloramination. This is in contrast to the relative magnitudes of these compounds seen in chlorination. Quantitative results are given in Table I. After 24 h, chloramination has generated less than 40% of the total amount of these major halogenated compounds as produced by chlorination. This observation agrees well with the concept of chloramination; since it is a less vigorous chlorinating reagent, the multi-chlorinated species should not be produced as

TABLE I

COMPARISON OF THE AMOUNTS OF THE MAJOR CHLORINATED PRODUCTS OF HUMIC ACID CHLORINATION V/S. CHLORAMINATION AT 24 AND 48 h

Values in parentheses are percentages of respective compounds to total chlorinated organics in that fraction.

	Chlorination		Chloramination		Chlori- nation	Chlor- amination
	24 h	48 h	24 h	48 h		
<i>Neutrals</i>						
Chloroform	0.177 (44)	0.48 (27)	0.036 (24)	0.081 (23)		
Dichloroacetonitrile	0.230 (56)	1.32 (73)	0.115 (76)	0.262 (77)		
<i>Acids</i>						
Dichloroacetic acid					0.094 (27)	0.092 (81)
Trichloroacetic acid					0.244 (73)	0.021 (19)

extensively. As can be seen, the amount of highly chlorinated compounds (as evidenced by trichlorinated species) in both the acidic and neutral fraction has decreased under chloraminating conditions. Trichloroacetaldehyde was not quantified in this study, but it is clear that there is a large decrease in the amount produced under chloraminating conditions.

If the quantitation of the neutral fraction is considered in terms of the relative proportions (peak heights) of chlorinated materials, there are further interesting observations. When the chlorinated humic acid sample was examined, the relative levels of chloroform and dichloroacetonitrile showed each to be present at approximately the same level (45 and 55%, respectively of the total level of these two compounds). However, the same computations performed on the chloraminated humic acid sample showed the relative proportions of dichloroacetonitrile as 76% and chloroform 24%. After 48 h the levels of both chloroform and dichloroacetonitrile in the chlorinated sample approached that of the chloraminated sample (in terms of relative compound proportions) but this is probably due to the greater continuing persistence of the chlorinating reagent. It is significant that while the absolute level of chlorinated species is diminished with chloramination, there is an increase in the fraction of neutral chlorinated organics present as the potentially harmful dichloroacetonitrile. There are two ways to explain these results. The first is that the additional dichloroacetonitrile is produced by direct action of the chloraminating reagent functioning to reduce the generation of trichlorinated species but still producing dichlorinated compounds at the same level. The second possibility is that alternative chemical reactions occur which are making the chloramine into a source of reactive nitrogen to produce dichloroacetonitrile. This study merits further investigation fully to evaluate chloramination as an alternative to chlorination. It must be confirmed that chloramination not only reduces the level of THMs, as is apparently the case, but that it does not cause other, potentially more hazardous, halo-organics to be formed.

## ACKNOWLEDGEMENTS

This research was supported in part by the Geological Survey, US Department of the Interior through the Massachusetts Water Research Institute, by the 3M Corporation and the Dow Chemical Company.

## REFERENCES

- 1 *The Analysis of Trihalomethanes in Finished Waters by the Purge and Trap Method*, U.S. Environmental Protection Agency, Environmental Monitoring and Support Laboratory, Cincinnati, OH, September, 1977.
- 2 J. Symons, T. A. Bellar, J. K. Carswell, J. DeMarco, K. L. Kropp, G. C. Robek, D. R. Seeger, C. J. Slocum, B. L. Smith and A. A. Stevens, *J. Am. Water Works Assoc.*, 67 (1975) 634.
- 3 J. J. Rook, in R. L. Jolley, W. A. Brungs and R. B. Cumming (Editors), *Water Chlorination: Environmental Impact and Health Effects*, Vol. 3, Ann Arbor Science Publishers, Ann Arbor, MI, 1979, pp. 85-98.
- 4 B. D. Quimby, M. F. Delaney, P. C. Uden and R. M. Barnes, *Anal. Chem.*, 52 (1980) 259.
- 5 J. J. Rook, *Water Treat. Exam.*, 23 (1974) 234.
- 6 R. F. Christman, J. D. Johnson, D. I. Norwood, W. T. Liao, J. R. Hass, F. K. Pfaender, M. R. Webb and M. J. Bobenrieth, *Chlorination of Aquatic Humic Substances*; U.S. Environmental Protection Agency Project Summary, EPA-600/s2-81-016, March, 1981.
- 7 K. P. Kringstad, P. O. Ljungquist, F. deSousa and L. M. Stromberg, *Environ. Sci. Technol.*, 17 (1983) 553.
- 8 E. W. B. de Leer, J. S. Damste, C. Erkelens and L. de Galan, *Environ. Sci. Technol.*, 19 (1985) 512.
- 9 S. Onodera, N. Iino, M. Matsuda and S. Ishikura, *J. Chromatogr.*, 265 (1983) 201.
- 10 S. Onodera, K. Yamada, Y. Yamati, S. Ishikura and S. Suzuki, *J. Chromatogr.*, 354 (1986) 293.
- 11 S. Boyce and J. Hornig, *Environ. Sci. Technol.*, 17 (1983) 202.
- 12 J. M. Symons, in R. L. Jolley, H. Gorchev and D. H. Hamilton, Jr. (Editors), *Water Chlorination: Environmental Impact and Health Effects*, Vol. 2, Ann Arbor Science Publishers, Ann Arbor, MI, 1978, pp. 555-560.
- 13 S. D. Faust and O. Aly, *Chemistry of Water Treatment*, Butterworth, Boston, MA, 1983, pp. 616-632.
- 14 M. S. Young, *Ph.D. Dissertation*, University of Massachusetts, Amherst, MA, 1988.

## Note

### Detection of ligand–protein binding by direct electrophoresis of the complex

S. NOBILE\* and J. DESHUSSES

*Department of Biochemistry, University of Geneva, 30 quai E.-Ansermet, CH-1211 Geneva 4 (Switzerland)*

(First received March 22nd, 1988; revised manuscript received June 6th, 1988)

The detection of binding of a ligand to a protein is an analytical process usually accomplished by equilibrium dialysis<sup>1</sup>, ultrafiltration<sup>2</sup> or, in the case of an uncharged ligand, by isoelectric focusing in the presence of the radioactive ligand followed by autoradiography<sup>3</sup>. Other techniques such as precipitation of the complex by ammonium sulphate<sup>4</sup> or fixation of the complex on nitrocellulose membranes<sup>5</sup> have been successful in some cases, but do not allow the discrimination of the binding protein from the other unrelated proteins present in the extract. The equilibrium dialysis or ligand retention dialysis methods<sup>6</sup> are interesting since they allow the determination of the affinity constant of the protein for its ligand. However, these methods have the disadvantage of using large amounts of proteic material. Binding is the ratio between the rates of association and dissociation. For bacterial binding proteins, the rate of association has been reported to be almost diffusion controlled, while dissociation was slow but independent of association<sup>7</sup>. It is believed that isoelectric focusing or electrophoresis techniques cannot be used in the presence of charged ligands, which would dissociate and be eliminated during the analysis.

In this paper we show that complexes of radioactive ligands with bacterial periplasmic binding proteins, such as the  $\gamma$ -butyrobetaine-binding protein, leucine-binding protein and ribose-binding protein, are sufficiently stable to be detected by autoradiography after non-denaturing polyacrylamide gel electrophoresis (PAGE) using a minigel system. Thus, binding proteins can be specifically identified by their relative positions on polyacrylamide gels.

## EXPERIMENTAL

### *Bacterial strains and growth conditions*

*Agrobacterium* sp. strain HK<sub>4</sub> (DSM2938) was grown at 30°C with  $\gamma$ -butyrobetaine as a carbon and nitrogen source and to induce the transport system<sup>8</sup>. Non-induced cells were grown on 0.2% D-glucose. Strains AI271 and W1485 are derivatives of *Escherichia coli* K-12 and were grown at 37°C. Strain AI271<sup>9</sup> was grown on M9 minimum salt medium with 1% glycerol and 0.2% ribose as carbon sources. Strain W1485 was grown on minimal medium supplemented with 1% glycerol as a carbon source.

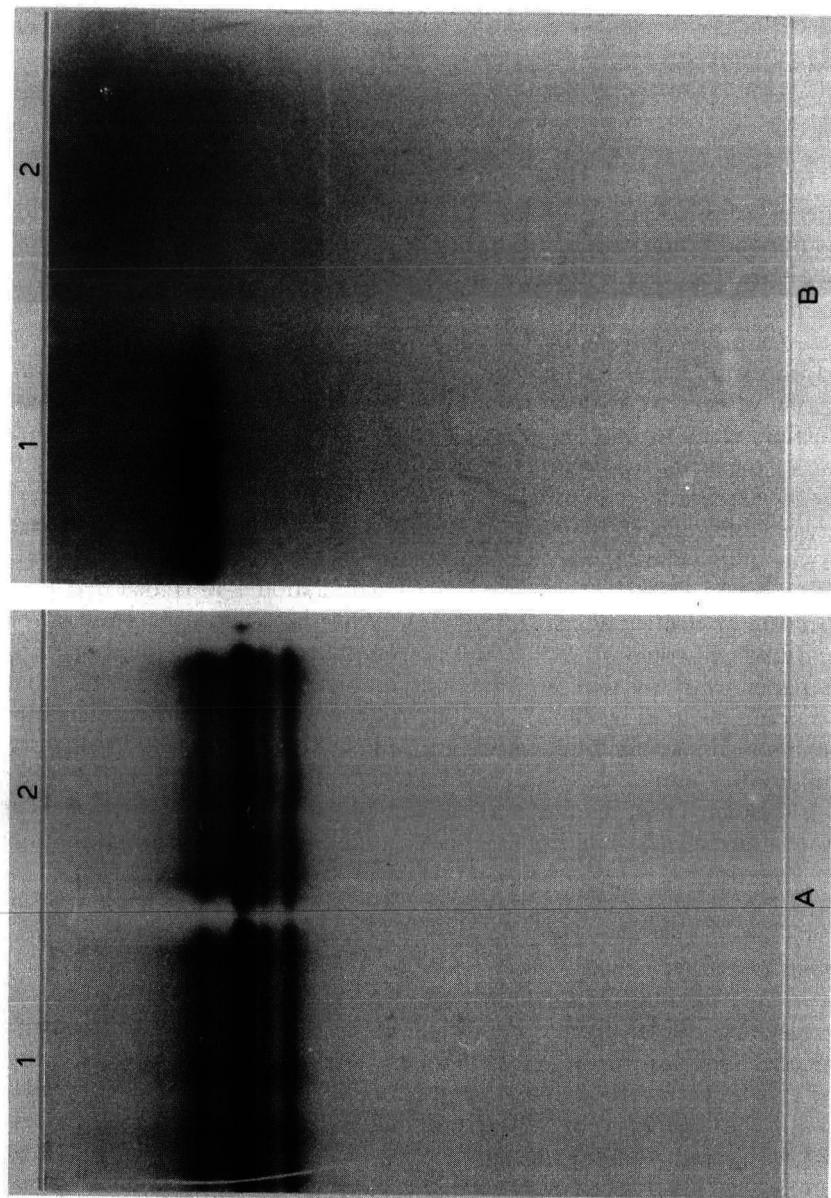


Fig. 1. 12% Non-denaturing PAGE (A) and autoradiography (B) of periplasmic proteins obtained from *E. coli* strain A1271. The periplasmic extracts (50  $\mu$ g) were incubated for 15 min with 10  $\mu$ M [ $^{14}$ C]D-ribose in the absence (lane 1) or presence (lane 2) of 500  $\mu$ M unlabelled D-ribose.

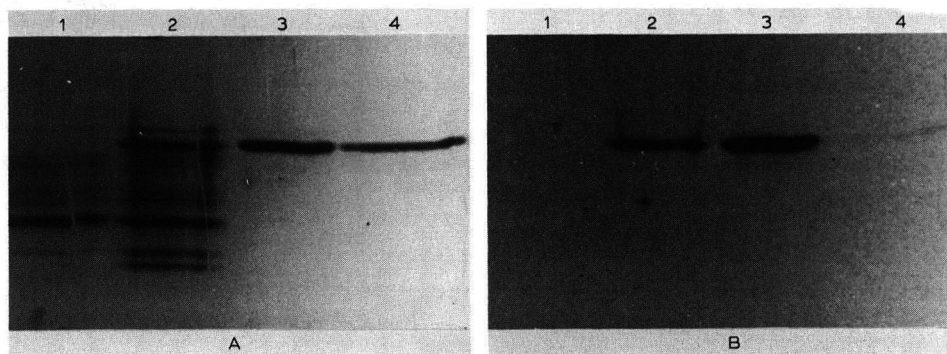


Fig. 2. 10% Non-denaturing PAGE (A) and autoradiography (B) of periplasmic proteins from non-induced *Agrobacterium sp.* HK4 cells (lane 1), periplasmic proteins from induced *Agrobacterium sp.* HK4 cells (lane 2), or purified  $\gamma$ -butyrobetaine-binding protein (lanes 3 and 4). A 50- $\mu$ g amount of the proteins was incubated for 15 min with 10  $\mu$ M [ $^{14}$ C] $\gamma$ -butyrobetaine in the absence (lanes 1, 2 and 3) or presence (lane 4) of 500  $\mu$ M unlabelled  $\gamma$ -butyrobetaine.

### Osmotic shocks

Osmotic shocks were performed according to Neu and Heppel<sup>10</sup>. The periplasmic protein extracts were filtered on membranes (Sartorius, Göttingen, F.R.G.), concentrated by ultrafiltration on YM10 Amicon membranes (Diaflo Amicon, Oosterhout, The Netherlands) to a final concentration of approximately 1 mg/ml and extensively dialyzed against 10 mM Tris-HCl buffer, pH 7.4.

### Electrophoresis and autoradiography

Aliquots of the concentrated shock fluids containing the various binding proteins (50  $\mu$ g) were mixed with the respective radioactive ligands [ $^{14}$ C] $\gamma$ -butyrobetaine (16  $\mu$ Ci/ $\mu$ mol), [ $^{14}$ C]L-leucine (330  $\mu$ Ci/ $\mu$ mol) and [ $^{14}$ C]D-ribose (58  $\mu$ Ci/ $\mu$ mol), at a final concentration of approximately 10  $\mu$ M and left at room temperature for 15 min. Laemmli's sample buffer<sup>11</sup> (without sodium dodecyl sulphate and  $\beta$ -mercaptoethanol) was then added and the samples were subjected, without denaturation and reduction, to PAGE in a discontinuous system in which sodium dodecyl sulphate was omitted. In order to shorten the time of electrophoresis, the Bio-Rad mini protean<sup>TM</sup> slab cell system (Bio-Rad Labs., Richmond, CA, U.S.A.) was used. The gels were 6 cm long, including a stacking of approximately 1 cm and the spacers were 0.75 mm thick. The analyses were performed with a constant voltage setting of 200 V, usually for approximately 45 min. The gels were then quickly dried on Whatman Nos 3MM paper and autoradiographed using Fuji X-medical films (Fuji Photo Film, Tokyo, Japan). Coomassie blue staining was performed after autoradiography by scraping the Whatman paper from the gel with ethanol.

### Protein determination

Protein concentrations were determined according to Bradford<sup>12</sup>.

### Chemicals

[ $^{14}$ C]L-Leucine and [ $^{14}$ C]D-ribose were obtained from the Radiochemical Centre (Amersham, U.K.). [ $^{14}$ C] $\gamma$ -Butyrobetaine was prepared in our laboratory by methyla-

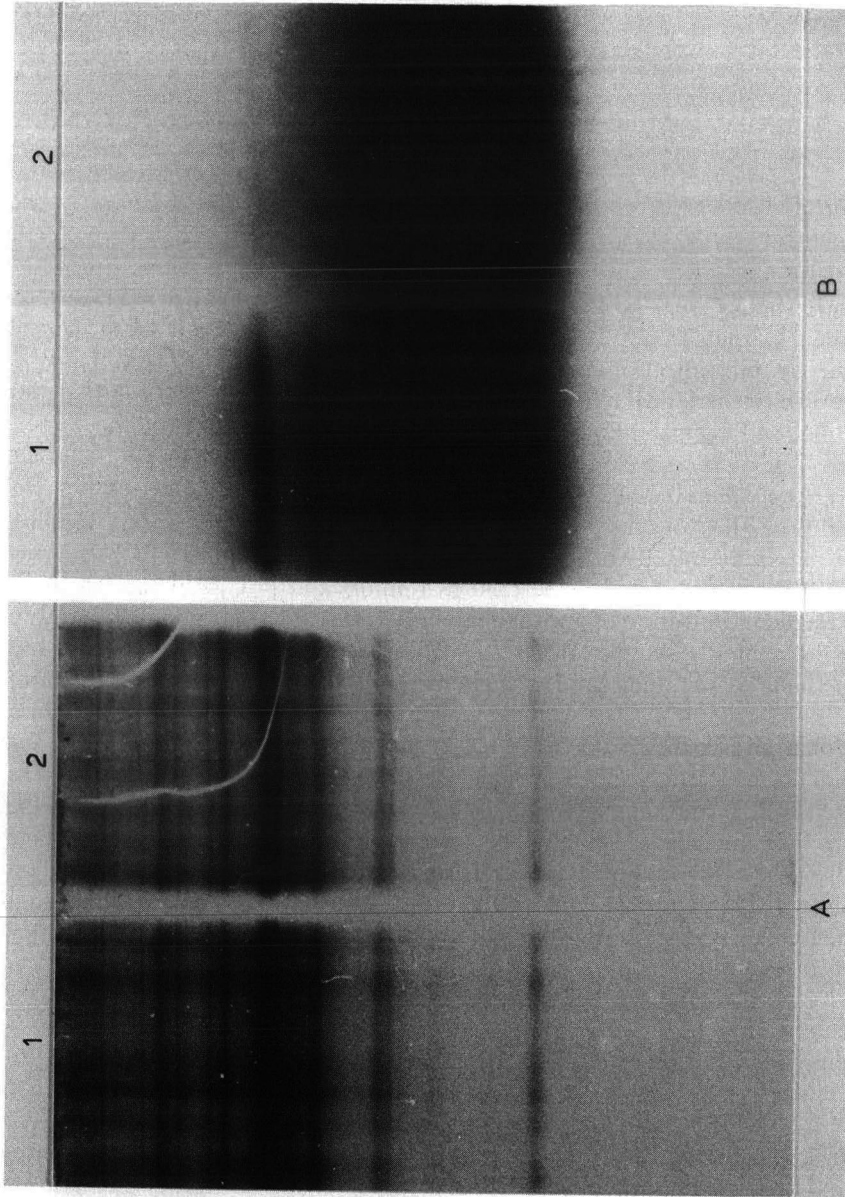


Fig. 3. 12% Non-denaturing PAGE (A) and autoradiography (B) of periplasmic proteins obtained from *E. coli* strain W1485. The periplasmic extracts (50  $\mu$ g) were incubated for 15 min with 10  $\mu$ M [ $^{14}$ C]L-leucine in the absence (lane 1) or presence (lane 2) of 500  $\mu$ M unlabelled L-leucine.

tion of [ $^{14}\text{C}$ ] $\gamma$ -aminobutyric acid (Radiochemical Centre). The other chemicals were of the highest purity available from E. Merck (Darmstadt, F.R.G.), or Fluka (Buchs, Switzerland).

## RESULTS AND DISCUSSION

In order to show that electrophoresis of complexes is a convenient method to detect the presence of a specific binding activity, crude shock fluids of bacteria induced for three different specific transport systems were used. For the detection of ribose-binding proteins, on the gel shown in Fig. 1 only one band is labelled within the mixture of the shock released proteins (lane 1). This result is in accord with the literature, indicating the involvement of one ribose-binding protein in *E. coli*<sup>13</sup>. When unlabelled D-ribose (500  $\mu\text{M}$ ) was added to the mixture a significant decrease in the labelling was observed, demonstrating the specificity of the binding phenomenon (lane 2).

Crude shock fluid obtained from an *Agrobacterium* sp. isolated from soil and able to concentrate  $\gamma$ -butyrobetaine (an highly charged molecule) through an inducible binding protein-dependent transport system<sup>8</sup> was subjected to the same procedure (Fig. 2, lane 2). Also shown is a protein preparation from non-induced cells grown on glucose (lane 1), and two samples of the purified  $\gamma$ -butyrobetaine-binding protein (lanes 3 and 4). With the crude extract as well as with the pure protein (lanes 2 and 3), a radioactive band was found at the same position, showing the presence of the label bound to the binding protein. The fact that only the  $\gamma$ -butyrobetaine-binding protein was labelled in the crude extract rules out the possibility of a non-specific binding. Finally, addition of unlabelled  $\gamma$ -butyrobetaine (500  $\mu\text{M}$ ) in the purified preparation (lane 4) resulted in a nearly complete abolition of the labelling.

L-Leucine is transported in *E. coli* by two distinct transport systems each involving distinct binding proteins (LIV-binding protein and LS-binding protein)<sup>14</sup>. Although these proteins have very similar molecular masses<sup>13</sup>, they were distinguished on our gel system despite the broad radioactive band caused by the free ligand (Fig. 3, lane 1). Here again, the addition of non-radioactive L-leucine resulted in a significant decrease in the protein labelling (lane 2).

In conclusion, we have shown that non-denaturing PAGE using a minigel system allows the detection of various bacterial binding proteins specific for neutral or highly charged molecules such as amino acids or betaines. The simplicity of the procedure should help in the detection and the purification of various proteins involved in binding phenomena.

## ACKNOWLEDGEMENTS

Financial support was provided by a grant from Lonza (Basel, Switzerland). We thank A. Iida and L. Caro for strain AI271 and W1485 respectively, M. Belet for performing the osmotic shocks and L. Poljak for her critical reading of the manuscript.

## REFERENCES

- 1 S. A. Katz, C. Parfitt and R. Purdy, *J. Chem. Educ.*, 47 (1970) 721.
- 2 H. Paulus, *Anal. Biochem.*, 32 (1969) 91.

- 3 J. Deshusses and M. Belet, *J. Bacteriol.*, 159 (1984) 179.
- 4 G. Richarme and M. Kepes, *Biochim. Biophys. Acta*, 742 (1983) 16.
- 5 J. E. Lever, *Anal. Biochem.*, 50 (1972) 73.
- 6 T. J. Silhavy, S. Szmecman, W. Boos and M. Schwartz, *Proc. Natl. Acad. Sci. U.S.A.*, 72 (1975) 2120.
- 7 D. M. Miller, J. S. Olson and F. A. Quioco, *J. Biol. Chem.*, 255 (1980) 2465.
- 8 S. Nobile and J. Deshusses, *J. Bacteriol.*, 168 (1986) 780.
- 9 A. Iida, S. Harayama, T. Iino and G. L. Hazelbauer, *J. Bacteriol.*, 158 (1984) 674.
- 10 M. Neu and L. A. Heppel, *J. Biol. Chem.*, 240 (1965) 3685.
- 11 U. Laemmli, *Nature (London)*, 227 (1970) 680.
- 12 M. M. Bradford, *Anal. Biochem.*, 72 (1976) 248.
- 13 C. E. Furlong, *Methods Enzymol.*, 125 (1986) 279.
- 14 P. M. Nazos, T. Z. Su, R. Landick and D. L. Oxender, *Microbiology*, (1984) 24.

## Note

---

### Validity of *post mortem* chest cavity blood ethanol determinations

ROBERT D. BUDD

Los Angeles County Medical Examiner-Coroner, 1104 N. Mission Road, Los Angeles, CA 90033 (U.S.A.)

(Received June 28th, 1988)

In many *post mortem* cases it is medically and/or legally important to determine whether a decedent was under the influence of ethanol at the time of his/her death. Blood specimens taken from the heart or a major artery are the specimens of choice for these laboratory ethanol concentration determinations. Occasionally, due to the massiveness and/or the nature of the decedent's injuries, blood for such an alcohol determination is unavailable or available in insufficient quantity from the heart or femoral or carotid arteries. In some of these cases the autopsy surgeon may scoop blood from the chest area for use by the toxicology laboratory to determine the concentration of ethanol present. There is no question that this scooped chest blood is a non-recommended source<sup>1-3</sup>. There is a high potential for direct contamination of this blood with ethanol from the stomach contents if the stomach and diaphragm are perforated and, with the passage of time and even if the stomach and diaphragm are not damaged, contamination may occur via *post mortem* diffusion of ethanol from the stomach contents<sup>2</sup>. Both of these factors, if operating to any extent, will yield falsely elevated ethanol determinations.

In such cases where blood cannot be obtained in sufficient quantity in any other way and, out of necessity then, scooped chest blood is used for the ethanol determination, the question arises both practically and legally as to whether this scooped chest, thorax or pleural blood is a valid specimen. The pathologist can take several steps to enhance the validity of the chest blood specimen. First, the possibility of direct contamination by ethanol from the stomach contents can be noted, *i.e.* were the stomach wall or diaphragm perforated. Second, *post mortem* diffusion can be minimized by a prompt autopsy. When the pathologist has done all that can be to verify that the chest blood has been minimally contaminated and it is deemed by him/her to be a valid specimen, the question arises as to how the ethanol concentration determined correlates with that of heart or arterial blood.

Over the years the ethanol concentrations in many body fluids and tissues have been determined and correlated with blood ethanol concentrations from the same individuals<sup>4-11</sup>. Now, to examine the validity of scooped thorax, chest or pleural blood specimens, all Los Angeles County Coroner's cases over the last eight years where both chest blood and heart or arterial bloods were obtained and submitted to the laboratory for ethanol determinations were studied. The results are correlated, summarized, and discussed.

## EXPERIMENTAL

### *Samples*

The blood specimens analyzed in this study were from persons who died in Los Angeles County between February 1, 1980 and February 9, 1988 and were from cases where a blood specimen was obtained both from the heart as well as from the thorax, chest cavity or pleural cavity.

### *Reagents*

The reagents used were 10% aqueous sodium tungstate solution and an acidic internal standard solution consisting of 0.667 *N* sulfuric acid containing 2 ml/l of *tert.*-butanol.

### *Blood analysis*

To a 12-ml centrifuge tube 1 ml of blood, 1 ml of the 10% sodium tungstate solution, and 1 ml of the internal standard solution were added. The mixture was shaken for 10 s, then the tube was centrifuged at 6000 g for 10 min.

### *Gas chromatography*

A 3- $\mu$ l volume of the supernatant was injected into the gas chromatograph: a Hewlett-Packard Model 5750 instrument with a 6-ft.  $\times$  0.85 in. I.D. metal column packed with Porapak Q, operated at 191°C. The alcohol concentration was calculated from the peak heights through the use of reference standards extracted similarly to the blood specimens.

## RESULTS AND DISCUSSION

Although blood from the heart and from the chest cavity, thorax or pleural cavity are rarely taken simultaneously from a decedent here at the Los Angeles County Medical Examiner-Coroner's Office, about 25 cases were found over the last eight years. Of these cases, fifteen showed at least one blood specimen positive for the presence of ethanol (concentration  $> 0.019\%$ , w/v).

These fifteen positive cases can be divided into two categories. Eleven cases appeared to be uncompromised (Table I). There was no evidence of stomach or diaphragm perforation; *post mortem* diffusion was minimized by performing the autopsy expediently (within three days) and by keeping the body refrigerated prior to the autopsy; and neither blood specimen was deemed suspect in any way by the pathologist or analyst. These eleven pairs of results agree quite well, have an average ratio of 1.02 (very near unity), have a correlation coefficient of 0.96, and confirm the results found by Jones and Pounder<sup>12</sup> that blood ethanol concentrations are generally independent of the part of the body from which they are taken. The standard deviation of the eleven ratios was 0.20 indicating that when the chest, thorax or pleural blood is not compromised, the ethanol concentration determined can be used to give a good estimate of the actual heart blood ethanol concentration.

Four cases, however appeared to be significantly compromised (Table II). In the first case, the stomach and diaphragm were both perforated, leading to apparent contamination of the chest blood with ethanol from the stomach contents and an

TABLE I

## HEART-CHEST ETHANOL CONCENTRATIONS (UNCOMPROMISED)

Case	Heart blood (9%) (H)	Chest/thorax/pleural blood (9%) (CTP)	Ratio (CTP/H)
1	0.22	0.19	0.86
2	0.04	0.03	0.75
3	0.13	0.14	1.08
4	0.04	0.05	1.25
5	0.12	0.13	1.08
6	0.20	0.15	0.75
7	0.05*	0.07	1.40
8	0.11	0.13	1.12
9	0.26	0.27	1.04
10	0.08	0.08	1.00
11	0.10**	0.09	0.90
Average			1.02

\* Spleen blood result.

\*\* Calculated from bile result (divided by 1.4, ref. 4).

elevated ethanol concentration. In the second case, the pathologist deemed the heart blood specimen to be suspect and, therefore, to have a falsely lowered ethanol concentration. In the third case, abdominal cavity blood, which is very readily subjected to *post mortem* ethanol diffusion by its proximity to the stomach, had a higher ethanol level despite a prompt autopsy and efforts to keep the body cold prior to the autopsy. In a fourth case, decomposition affected the chest cavity blood, causing the creation of a low concentration of ethanol. In short, none of these four compromised cases yielded accurate or consistent results.

The results of this study indicate that chest cavity blood can be a valid specimen for the determination of the decedent's blood ethanol concentration, quite representative of heart blood (Table I), when precautions are taken to minimize *post mortem* diffusion and when there was no perforation of the stomach walls or the diaphragm. The results do, however, show (Table II) that problems may occur leading to

TABLE II

## HEART-CHEST BLOOD ETHANOL CONCENTRATIONS (COMPROMISED)

Case	Heart blood (9%)	Chest/thorax/pleural blood (9%)
1	0.09	0.21*
2	0.24**	0.32
3	0.13	0.18***
4	0.00	0.03§

\* Stomach wall and diaphragm perforated.

\*\* Heart blood declared suspect and unsuitable for testing by pathologist.

\*\*\* Abdominal blood used.

§ Decomposed.

inaccurate results. In ethanol determination, if there is any question about compromise of a chest cavity, thorax or pleural cavity blood specimen, this blood should not be used or at least should be corroborated by the determination of ethanol concentrations in other body fluids and tissues.

#### REFERENCES

- 1 S. Kaye, *Am. Soc. Clin. Path.*, 74 (1980) 743-746.
- 2 V. D. Plueckhahn, *Med. J. Aust.*, 2 (1967) 118-124.
- 3 *Ethanol Determination Procedure Manual*, Los Angeles County Medical Examiner-Coroner, Los Angeles, CA, April 1988.
- 4 R. D. Budd, *J. Chromatogr.*, 252 (1982) 315-318.
- 5 P. Neil, A. J. Mills and V. M. Probhakaran, *Can. Soc. Forensic Sci. J.*, 18 (1985) 97-104.
- 6 A. Kraut and C. A. Purchase, *Can. Soc. Forensic Sci. J.*, 17 (1984) 91-97.
- 7 B. E. Stone and P. A. Rooney, *J. Anal. Toxicol.*, 8 (1984) 95-96.
- 8 R. C. Backer, R. V. Pisano and I. M. Sopher, *J. Forensic Sci.*, 25 (1980) 327-331.
- 9 R. D. Budd, *J. Chromatogr.*, 259 (1983) 353-355.
- 10 G. Christopoulos, E. R. Kirch and J. E. Gearien, *J. Chromatogr.*, 87 (1973) 455-472.
- 11 R. W. Prouty and W. H. Anderson, *J. Anal. Toxicol.*, 11 (1987) 191-197.
- 12 G. R. Jones and D. J. Pounder, *J. Anal. Toxicol.*, 11 (1987) 186-190.

CHROM. 20 725

## Note

---

### High-performance liquid chromatographic determination of loperamide hydrochloride in pharmaceutical preparations

C. P. LEUNG\* and C. Y. AU-YEUNG

*Government Laboratory, Oil Street, North Point, Hong Kong (Hong Kong)*

(Received June 6th, 1988)

Loperamide is an antidiarrhoeal used for the symptomatic relief of diarrhoeas not controlled by absorbent mixtures. Its hydrochloride salt and the capsule formulation are monographed in the *United States Pharmacopoeia* (USP)<sup>1</sup>. Other formulations of loperamide hydrochloride include tablets and syrups.

The method adopted in ref. 1 for the assay of loperamide hydrochloride capsules involves chloroform extraction, followed by the formation of a coloured complex with the indicator Tropaeolin OO and the measurement of colour intensity in toluene. This procedure, however, was found not to be applicable to syrup preparations because polyhydric alcohols such as propylene glycol, which are commonly added to syrups to retard the crystallization of sugar, would interfere with the colour formation. There are few other reports on the assay of loperamide in pharmaceutical preparations.

This paper reports a high-performance liquid chromatographic (HPLC) procedure using an adsorption column for the determination of loperamide in different pharmaceutical dosage forms. The method is rapid and simple and is free from interference from common excipients. Its reliability is demonstrated by comparing results with the official assay method and recovery tests.

## EXPERIMENTAL

### *Chromatographic conditions*

A modular system comprised of a Perkin-Elmer Series 10 pump, a Rheodyne 7125 injector with a 50- $\mu$ l loop, a Perkin-Elmer LC-15B fixed-wavelength (254 nm) detector and a Shimadzu C-R3A recording integrator was employed. A 25 cm  $\times$  4.6 mm Perkin-Elmer Analytical 10- $\mu$ m silica column was used. The mobile phase was chloroform-methanol-ammonia (95.5:4.5:0.05), the flow-rate was 2 ml/min and the detector sensitivity setting was 0.016 a.u.f.s.

### *Stock standard solution*

About 10 mg of loperamide hydrochloride were accurately weighed and dissolved in 100 ml of chloroform.

### *Internal standard solution*

A 10-mg amount of cyclizine hydrochloride was dissolved in 25 ml of chloroform.

### *Working standard solutions*

To three 25-ml volumetric flasks each containing 1.0 ml of internal standard solution, were added respectively 5, 10 and 15 ml of the stock standard solution and made up to the mark with chloroform. These working standard solutions contain respectively 0.02, 0.04 and 0.06 mg/ml of loperamide hydrochloride.

### *Procedure*

*Capsules and tablets.* An accurately weighed quantity of a powdered mixture obtained from 20 capsules or tablets equivalent to about 10 mg of loperamide hydrochloride was transferred to 1 100-ml volumetric flask and about 80 ml of chloroform were added. The flask was shaken for about 15 min and then made up to the mark with chloroform. The solution was quickly filtered through a covered filter, discarding the first 10–20 ml of the filtrate, and collecting the remainder in a glass-stoppered flask. A 5-ml volume of this solution was pipetted into a 25-ml volumetric flask, 1.0 ml of internal standard solution was added, followed by mixing and making up to the mark with chloroform. This solution was injected for HPLC using a microsyringe. The peak area ratio of loperamide hydrochloride to the internal standard was measured and the content calculated with reference to a calibration graph prepared from the working standard solutions.

*Syrup.* A quantity of sample equivalent to about 10 mg of loperamide hydrochloride was transferred to a separating funnel containing 30 ml of distilled water. The contents were extracted with four 20-ml portions of chloroform, filtering each portion through a pledget of glass wool into a 100-ml volumetric flask. After mixing and making up to the mark with chloroform, 5 ml of this solution were pipetted into a 25-ml volumetric flask. The above procedure was then employed.

## RESULTS AND DISCUSSION

When the HPLC procedure was first developed, the more commonly used reversed-phase separation was attempted. As in the case of other common basic drugs, base modifiers or ion-pair agents were used to improve the elution pattern and peak shape. However, for loperamide hydrochloride, common ion-pair agents such as hexanesulphonate and octanesulphonate were found to be of little use in improving the elution time and peak symmetry.

The procedure was repeated using an adsorption column. A 10- $\mu$ m silica column together with the mobile phase chloroform–methanol–ammonia (95.5:4.5:0.05) were found to give good separation of loperamide and the chromatographic peak could be used for quantitation. To improve the repeatability, the internal standard cyclizine hydrochloride was used throughout for peak area ratio measurements. A typical chromatogram of loperamide and the internal standard is shown in Fig. 1.

A UV detector was used for the detection of loperamide. The UV absorption maxima were in the region of 250–280 nm as shown in Fig. 2. For simplicity, a fixed wavelength (254 nm) detector was employed.

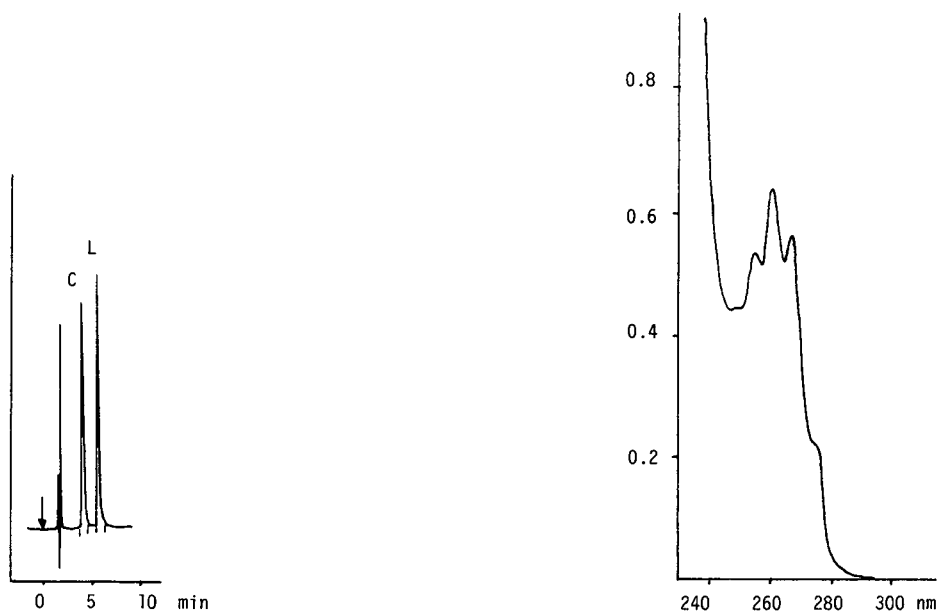


Fig. 1. Chromatogram of loperamide hydrochloride (L) and the internal standard cyclizine hydrochloride (C). See text for chromatographic conditions.

Fig. 2. Absorption spectrum of 0.05% loperamide hydrochloride in methanol (1-cm cell).

The working range of standard solutions of loperamide hydrochloride used for the preparation of the calibration graph was 0.02–0.08 mg/ml and the graph was found to be linear. The sample solutions were adjusted to similar concentrations for the determination of the loperamide hydrochloride content.

The results of the analysis of three commercial preparations of loperamide hydrochloride using both the HPLC procedure proposed and the USP colorimetric method was shown in Table I. For capsules and tablets, the results obtained by both methods were close and comparable. For syrup, the results obtained by the official method were much higher. Subsequent investigations revealed that this sample contained small amounts of propylene glycol which was partly extracted into

TABLE I

DETERMINATION OF LOPERAMIDE HYDROCHLORIDE IN PHARMACEUTICAL PREPARATIONS

Preparation	Content claimed	Percentage of labelled content found	
		HPLC method*	USP method
Capsule	2 mg	96.1 ( $\pm 0.9$ )	96.7
Tablet	2 mg	96.5 ( $\pm 1.1$ )	97.2
Syrup	2 mg/ml	102.3 ( $\pm 1.3$ )	122.5

\* Mean of three determinations, with the standard deviation in parentheses.

chloroform together with loperamide hydrochloride. This polyhydric alcohol was found to impart a yellow colour to the final toluene layer, rendering the USP method not directly applicable to this syrup preparation. The HPLC method proposed, however, was free from interference from this excipient.

To validate further the reliability of the proposed procedure, two synthetic mixtures containing known amounts of loperamide hydrochloride were prepared. The first one was a mixture containing lactose which is a common ingredient in capsules and tablets. The second one was a mixture containing syrup and small amounts of chloroform spirit and propylene glycol. The recovery from these two mixtures was found to be  $99.5 \pm 0.7$  and  $99.2 \pm 1.0\%$  respectively, indicating the applicability of the HPLC procedure to both solid and liquid formulations of loperamide hydrochloride.

#### ACKNOWLEDGEMENT

The authors thank the Government Chemist of Hong Kong for permission to publish this paper.

#### REFERENCE

- 1 *United States Pharmacopeia*, Mack Publishing Company, Easton, PA, 21st revision, 1985, p. 604.

## Letter to the Editor

---

### Use of the term “detergent” in biochemistry

Sir,

In reply to Dr. Zeman<sup>1</sup>, we would like to point out that the term “detergent” is commonly used in the biochemical literature in the sense of “micelle-forming amphiphile usually capable of solubilizing membrane lipids and integral membrane proteins” (*cf.*, refs. 2 and 3). In well known modern textbooks in biochemistry the term “detergent” is also used in this sense (see, for instance, refs. 4–6). However, we have noted that the terms “surfactant” and “surfactant micelle” are often used in the physical literature (for instance as in ref. 7).

We appreciate Dr. Zeman's comments on the industrial nomenclature in this field but we doubt that the widespread and non-ambiguous use of the term “detergent” in membrane biochemistry can be erased by the draft International Standard ISO/DIS 862. To preclude misunderstanding, the chemical name(s) of detergent(s) should always be given.

We support the use of the term “detergent” in the strict sense of “soluble amphiphile that can form micelles in water” (*cf.*, ref. 3). The term “surfactant” is wider, as some amphiphiles do not form micelles. The terminology of commercial products for laundering, washing and cleaning can hardly cause any confusion in biochemistry.

*Department of Biochemistry,  
Biomedical Centre, University of Uppsala,  
P.O. Box 576, S-751 23 Uppsala (Sweden)*

PER LUNDAHL  
ERIK MASCHER

- 1 I. Zeman, *J. Chromatogr.*, 426 (1988) 452.
- 2 A. Helenius and K. Simons, *Biochim. Biophys. Acta*, 415 (1975) 29.
- 3 J. Møller, M. Le Maire and J. P. Andersen, in A. Watts and J. J. H. M. De Pont (Editors), *Progress in Protein-Lipid Interactions* 2, Elsevier, Amsterdam, 1986, p. 147.
- 4 A. Lehninger, *Principles of Biochemistry*, Worth, New York, 4th ed., 1986.
- 5 L. Stryer, *Biochemistry*, Freeman, San Francisco, 3rd ed., 1988.
- 6 G. Zubay, *Biochemistry*, Addison-Wesley, Reading, MA, 1983.
- 7 B. Cabane and R. Duplessix, *J. Phys. (Paris)*, 48 (1987) 651.

(Received June 7th, 1988)

CHROM. 20 814

## Book Review

---

*Chromatography — Concepts and contrasts*, by J. M. Miller, Wiley, New York, 1988, 297 pp., price ca. US\$ 53.15, ISBN 0-471-84821-2.

The author believes that he presents a new approach and we quote from the preface: "This monograph attempts a unified approach to chromatography and emphasises the similarities and differences between the major divisions —GC, LC and TLC... the unified approach permits the use of one set of terms and symbols which should make learning easier".

After perusing this statement one would expect a balanced treatment of these three techniques. However the author limits the discussion of thin-layer chromatography to a 14-page chapter in which he mainly quotes review articles and books and only manages a very superficial treatment.

What he calls the Martin equation, namely

$$(R_M)_{tot} = \Sigma(R_M)_i$$

is wrong as it does not contain the system constant or "Grundkonstante". In his list of symbols and acronyms he calls the symbol  $R_M$  "Martin retention parameter", a term which he seems to have invented, as I have not encountered it before in the literature. Perhaps new terms should have been labelled as such to avoid confusion.

Also  $R_F$  is known as  $R_F$  value to workers in the field and not as retardation factor.

While the author claims a new and unified approach, but does not really present one, he seems unaware that his is certainly not the only book which gives coverage of all methods. There are at least four in my library.

Altogether the book seems to be a rather unsuccessful attempt to write a textbook on chromatography.

## Book Review

---

*Ion-exchange chromatography of proteins (Chromatographic Science Series, Vol. 43)*, by S. Yamamoto, K. Nakanishi and R. Matsuno, Marcel Dekker, New York, Basle, 1988, 401 pp., ISBN 0-8247-7903-7.

The preface to this volume states that "In this book, we describe the separation mechanism of proteins in IEC by stressing the unique characteristics of IEC of proteins. Both theoretical and experimental works concerning this method have been reviewed".

The authors, who divided their book into chapters dealing with ion-exchange equilibria, diffusion in the ion exchanger, axial dispersion and other subjects, seem to have prepared a textbook for a course on separations in biotechnology rather than a handbook on the ion exchange of proteins. There is a chapter on "Experimental Methods and Apparatus" (Chapter 6), where under the heading of apparatus one finds a block diagram of a "typical experimental setup" involving a gradient maker, a strip chart recorder, two detectors and a fraction collector. Now I am fairly certain that one could quote more than a hundred papers which dispense with all or some of these items. Nor could I find any reference to paper or thin-layer methods, so this chapter (taken as an example) seems to confirm the assumption that the authors did not feel obliged to give much consideration to reviewing theoretical and experimental work.

There seems to be no discussion of the chromatography of haemoglobins, no mention of which can be found in the index. Instead there is a statement that "synthetic ion exchange resins were not often used for protein separation because of two properties of the resin: its small pore size and its hydrophobic nature". Perhaps a discussion of the haemoglobin separations would have been more to the point, if only as an example that exceptions prove the rule.

This reviewer's opinion is that the volume can not be recommended as a reference work. It could be used as introductory reading for newcomers, but its rather unreadable style seems to make this not an option.



# journal of chromatography news section

## SYMPOSIUM PROGRAMME

8th INTERNATIONAL SYMPOSIUM ON HIGH-PERFORMANCE LIQUID CHROMATOGRAPHY OF PROTEINS, PEPTIDES AND POLYNUCLEOTIDES, COPENHAGEN, DENMARK, OCTOBER 31–NOVEMBER 2, 1988

The 8th International Symposium on HPLC of Proteins, Peptides and Polynucleotides will be held at the Hotel Scandinavian in the heart of Copenhagen, Denmark, October 31–November 2, 1988. Registration information and full details of the symposium can be obtained from the Secretariat: 8th ISPPP, c/o DIS Congress Service, Linde Allé 48, DK-2720 Vanløse/Copenhagen, Denmark. Tel. (45) 1712244, telex: 15476 dis dk, fax: (45) 1716088.

The detailed programme of the symposium is given below.

### SUNDAY, OCTOBER 30

14:00–18:00      Registration.  
18:00–19:00      Reception.

### MONDAY OCTOBER 31

#### SESSION 1: COLUMN TECHNOLOGY AND SUPPORT MATERIALS

*Chairman: M.T.W. Hearn; Co-chairman: B. Wittmann-Liebold*

08:45–09:00      Welcome and Announcements.  
09:00–09:30      Non-porous packings in interactive column liquid chromatography of biopolymers — K.K. Unger (Joh. Gutenberg University, Mainz, F.R.G.).  
09:30–10:00      Macromolecular separations in very high porosity media — F.E. Regnier (Purdue University, Lafayette, IN, U.S.A.).  
10:00–10:20      Ion-exchange chromatography supports with polymers on porous silica beads. The role of charge density and cross linking on the protein separation properties — B. Sebille, V. Housse-Ferrari and B. Chaufer (Université de Paris XII, Thiais, France).  
10:20–10:40      Fast reversed-phase chromatographic separations on non-porous micro particulate supports — G.P. Rozing and H. Goetz (Hewlett-Packard, Waldbronn, F.R.G.).  
10:40–11:15      Coffee break.

#### SESSION 2: ANALYTICAL APPLICATIONS I

*Chairman: B. Sebille; Co-chairman: B. Fournet*

11:15–11:45      Purification of ribosomal proteins for microsequence analysis of HPLC *versus* blotting techniques — B. Wittmann-Liebold and T. Choli (Max-Planck-Institut für Molekulare Genetik, Berlin, F.R.G.).

11:45–12:05	Expression, purification and characterization of a recombinant 15 000 Dalton interferon-induced human protein — D. Blomstrom, B. Cordova, D. Fahey, N. Felthan, M. Hillman and E. Knight, Jr. (DuPont, R&D, Wilmington, DE, U.S.A.).
12:05–12:25	Quantitation of free amino acids in plasma and muscle samples from uremic patients undergoing continuous ambulatory peritoneal dialysis by HPLC — G.A. Qureshi, B. Lindholm, E. Garcia and A.R. Qureshi (Karolinska Institute, Stockholm, Sweden).
12:25–12:45	Analysis of amino acids as DABS-derivatives with a sensitivity to femtomole level using RP-HPLC microbore columns — V. Stocchi, G. Piccoli, F. Palma, B. Biagiarelli and M. Magnani (Universita Studi di Urbino, Urbino, Italy).
12:45–14:00	Lunch break
14:00–16:00	Posters, Sessions 1, 2 and 3.
15:30–16:00	Coffee break

### SESSION 3: PURITY AND QC OF PROTEINS AND GLYCOPROTEINS

*Chairman: G.W. Welling; Co-chairman: W.S. Hancock*

16:00–16:30	High-performance liquid chromatography of sugars derived from glycoproteins glycans — B. Fournet (University of Science and Technology Lille Flandres Artois, Villeneuve d'Ascq, France).
16:30–17:00	Ion-exchange HPLC for the control of N-terminal and C-terminal degradation of recombinant proteins — I. Maurer-Fogy and G. Bodo (Ernst Boehringer Institute, Wien, Austria).
17:00–17:20	HPLC of polysaccharides — C. Jansen (Dionex, Idstein, F.R.G.).
17:20–17:40	Purification of recombinant gag gene product p18 [HIV-1 (Bru)] from <i>E. coli</i> by cation-exchange HPLC on polysulfoethyl aspartamide — H.V.J. Kolbe, F. Jaeger, P. Lepage, G. Lacaud, J. Sabatie, M-P. Kieny, C. Roitsch, M. Girard and J-P. Lécocq (Transgene, Strasbourg and Pasteur Vaccins, Marnes-la-Coquette, France).
17:45–18:30	Discussion session: Analytical problems in biotechnology — Chairman: I. Maurer-Fogy.
18:30–19:30	Reception.

### TUESDAY NOVEMBER 1

#### SESSION 4: PROTEIN RECOGNITION AND CONFORMATION

*Chairman: K.K. Unger; Co-chairman: E. Sulkowski*

09:00–09:30	Mechanisms of antigen–antibody recognition — C.J. van Oss (SUNY, Buffalo, NY, U.S.A.).
09:30–10:00	Investigations into the relationship between structure, retention behaviour and biological activity of peptides related to human growth hormone — A.W. Purcell, M.I. Aguilar and M.T.W. Hearn (Monash University, Clayton, Australia).
10:00–10:30	Conformational behavior of proteins adsorbed to microparticulate silica — S.S. Saavedra, A.W. Grobin and C.H. Lochmueller (Perkin-Elmer Norwalk, CT and Duke University, Durham, NC, U.S.A.).
10:30–11:00	Coffee break.

#### SESSION 5: AFFINITY CHROMATOGRAPHY

*Chairman: C. van Oss; Co-chairman: F.E. Regnier*

11:00–11:30	Immobilized metal ion affinity chromatography of proteins: Recent developments — E. Sulkowski, (RPMI, Buffalo, NY, U.S.A.).
11:30–11:50	The stereochemical resolution of enantiomeric dipeptides using an HPLC chiral stationary phase based upon immobilized $\alpha$ -chymotrypsin — P. Jadaud and I.W. Wainer (St. Jude Children's Res. Hospital, Memphis, TN, U.S.A.).

- 11:50–12:10 Single step purification of proteases from bacillus culture supernatant by high-performance liquid affinity chromatography on bacitracin–silica — V.G. Eijssink, B. van den Burg, B.K. Stulp and G. Venema (Center for Biological Sciences and Genetics, Haren, The Netherlands).
- 12:10–13:30 Lunch break.
- 13:30–15:30 Posters, Sessions 4, 5 and 6.
- 15:00–15:30 Coffee break.

## SESSION 6: PREPARATIVE CHROMATOGRAPHY

*Chairman: R.S. Hodges; Co-chairman: B.S. Welinder*

- 15:30–15:50 Isolation of recombinant hirudin by preparative HPLC — R. Bischoff, D. Clesse, O. Whitechurch and C. Roitsch (Transgene, Strasbourg, France).
- 15:50–16:10 High capacity and high resolution purification of monoclonal antibodies from ascites fluid by displacement chromatography — A.R. Torres (Bio-Fractionations, Logan, UT, U.S.A.).
- 16:10–16:30 Large-scale purification of trypsin inhibitors from plants using immobilized dye chromatography and reversed-phase chromatography — E. Algiman, S. Mills, Y. Kroviarski, S. Cochet, X. Santarelli, D. Muller, P. Boivin and O. Bertrand (Hopital Beaujon, INSERM U.160, Clichy and Université de Paris, Villetaneuse, France).
- 16:30–16:50 Process affinity chromatography using perfluorocarbon supports: An alternative strategy — S.I. Sivakoff, A.M. Ruedinger, J.W. Eveleigh, M.E. Brody and R. Arenzen (DuPont, Wilmington, DE, U.S.A.).
- 16:50–17:10 The utility of very high porosity media in preparative chromatography — N. Afeyan, I. Mazsaroff and R. Dean (Synosys Corp., Cambridge, MA, U.S.A.).
- 17:15–18:00 Discussion session: Microanalytical techniques — Chairman: J.L. Wittliff and R. Giese.
- 18:00–20:00 Free time.
- 20:00– : Danish beer fest and open discussion: The 50 questions you always wanted to ask about technical problems and practical solutions.

## WEDNESDAY NOVEMBER 2

### SESSION 7: RETENTION PROCESSES

*Chairman: C. Lochmueller; Co-chairman: S. Hjerten*

- 08:30–09:00 A novel approach to HPLC separations based on computer simulation — R.S. Hodges, J.M.R. Parker, C.T. Mant, J.W. Dolan and L.R. Snyder (University of Alberta, Edmonton, Alberta, Canada and LC Resources, Lafayette, CA, U.S.A.).
- 09:00–09:20 Application of immobilized crown ethers to the separation of proteins and nucleic acids — D. Josic, W. Reuter and J. Reusch (Freien Universität Berlin and Säulentechnik, Dr. Knauer GmbH, Berlin, F.R.G.).
- 09:20–09:40 Comparison of non-ionic detergents for extraction and ion-exchange HPLC of sendai virus integral membrane proteins — J. van Ede, S. Welling-Wester, C. Örvell and G.W. Welling (Rijksuniversiteit Groningen, Groningen, The Netherlands and National Bacteriol. Lab., Stockholm, Sweden).
- 09:40–10:00 Functional properties, in theory and practice, of novel media for high-resolution gel filtration — L. Hagel, H. Lundström, T. Andersson and H. Lindblom (Pharmacia LKB, Uppsala, Sweden).
- 10:00–10:30 Coffee break.

### SESSION 8: ANALYSIS OF NUCLEIC ACIDS

*Chairman: W. Mueller; Co-chairman: J-P. Liautard*

- 10:30–11:00 Pulsed field gel electrophoresis — C.R. Cantor and C.L. Smith (Columbia University, New York, NY, U.S.A.).

11:00–11:20	Purification of supercoiled plasmid DNA by ion-exchange chromatography — J. Flensburg, H. Lindblom and S. Eriksson (Pharmacia-LKB, Uppsala, Sweden).
11:20–11:40	The behaviour of oligonucleotides during mixed mode HPLC — I.J. Collins, M.D. Scawen, T. Atkinson and G.B. Cox (PHLS CAMR, Salisbury, U.K. and DuPont, Wilmington, DE, U.S.A.).
11:40–12:00	Determination of DNA adducts using chemical, LC and MS techniques — R. Giese and P. Vouros (Northeastern University, Boston, MA, U.S.A.).
12:00–13:00	Discussion session: Preparative separations — Chairmen: J-C. Janson and R. Bischoff.
13:00–14:00	Lunch break.
14:00–16:00	Posters, Sessions: 7, 8 and 9.
15:30–16:00	Coffee break.

## SESSION 9: ANALYTICAL APPLICATIONS II

*Chairman: D. Josic; Co-chairman: G. Rozing*

16:00–16:30	Theoretically derived conditions for optimal resolution in high-performance electrophoresis and their practical use in various applications — S. Hjerten, K. Elenbring, M. Kiessling—Johansson, F. Kilar, J. Sedzik and L. Valtcheva (University of Uppsala, Uppsala, Sweden).
16:30–16:50	Analysis of peptides by free-solution capillary zone electrophoresis (CZE) — J.C. Colburn, P.D. Grossman, S.E. Moring and H.H. Lauer (Applied Biosystems, Santa Clara, CA, U.S.A.).
16:50–17:10	RP-HPLC Analyses of the insulin biosynthesis in rat and mouse islets — S. Linde, J.H. Nielsen, B. Hansen and B.S. Welinder (Hagedorn Research Laboratories Gentofte, Denmark).
17:10–17:30	Separation of two molecular forms of human estrogen receptor (ER) by hydrophobic interaction chromatography: Gradient optimization and tissue comparison — S.M. Hyder, N.M. Heer and J.L. Wittliff (University of Louisville, Louisville, KY, U.S.A.).
17:30–17:45	Closing remarks.
18:30–19:30	Farewell party.

## PUBLICATION SCHEDULE FOR 1988

*Journal of Chromatography and Journal of Chromatography, Biomedical Applications*

MONTH	J	F	M	A	M	J	J	A	S	O	N	D
Journal of Chromatography	435/1 435/2 435/3 436/1	436/2 436/3	437/1 437/2	438/1 438/2	439/1 439/2 440 441/1	441/2 442 443	444 445/1 445/2 446	447/1 447/2 448/1	448/2 448/3 449/1	449/2 450/1 450/2 450/3 452	The publication schedule for further issues will be published later.	
Bibliography Section		460/1		460/2		460/3		460/4		460/5		460/6
Cumulative Indexes, Vols. 401–450												451
Biomedical Applications	424/1	424/2	425/1 425/2	426/1 426/2	427/1	427/2 428/1	428/2 429	430/1	430/2 431/1	431/2	432	433 434

### INFORMATION FOR AUTHORS

(Detailed *Instructions to Authors* were published in Vol. 445, pp. 453–456. A free reprint can be obtained by application to the publisher, Elsevier Science Publishers B.V., P.O. Box 330, 1000 AH Amsterdam, The Netherlands.)

**Types of Contributions.** The following types of papers are published in the *Journal of Chromatography* and the section on *Biomedical Applications*: Regular research papers (Full-length papers), Notes, Review articles and Letters to the Editor. Notes are usually descriptions of short investigations and reflect the same quality of research as Full-length papers, but should preferably not exceed six printed pages. Letters to the Editor can comment on (parts of) previously published articles, or they can report minor technical improvements of previously published procedures; they should preferably not exceed two printed pages. For review articles, see inside front cover under Submission of Papers.

**Submission.** Every paper must be accompanied by a letter from the senior author, stating that he is submitting the paper for publication in the *Journal of Chromatography*. Please do not send a letter signed by the director of the institute or the professor unless he is one of the authors.

**Manuscripts.** Manuscripts should be typed in double spacing on consecutively numbered pages of uniform size. The manuscript should be preceded by a sheet of manuscript paper carrying the title of the paper and the name and full postal address of the person to whom the proofs are to be sent. Authors of papers in French or German are requested to supply an English translation of the title of the paper. As a rule, papers should be divided into sections, headed by a caption (e.g., Summary, Introduction, Experimental, Results, Discussion, etc.). All illustrations, photographs, tables, etc., should be on separate sheets.

**Introduction.** Every paper must have a concise introduction mentioning what has been done before on the topic described, and stating clearly what is new in the paper now submitted.

**Summary.** Full-length papers and Review articles should have a summary of 50–100 words which clearly and briefly indicates what is new, different and significant. In the case of French or German articles an additional summary in English, headed by an English translation of the title, should also be provided. (Notes and Letters to the Editor are published without a summary.)

**Illustrations.** The figures should be submitted in a form suitable for reproduction, drawn in Indian ink on drawing or tracing paper. Each illustration should have a legend, all the *legends* being typed (with double spacing) together on a *separate sheet*. If structures are given in the text, the original drawings should be supplied. Coloured illustrations are reproduced at the author's expense, the cost being determined by the number of pages and by the number of colours needed. The written permission of the author and publisher must be obtained for the use of any figure already published. Its source must be indicated in the legend.

**References.** References should be numbered in the order in which they are cited in the text, and listed in numerical sequence on a separate sheet at the end of the article. Please check a recent issue for the layout of the reference list. Abbreviations for the titles of journals should follow the system used by *Chemical Abstracts*. Articles not yet published should be given as "in press" (journal should be specified), "submitted for publication" (journal should be specified), "in preparation" or "personal communication".

**Dispatch.** Before sending the manuscript to the Editor please check that the envelope contains three copies of the paper complete with references, legends and figures. One of the sets of figures must be the originals suitable for direct reproduction. Please also ensure that permission to publish has been obtained from your institute.

**Proofs.** One set of proofs will be sent to the author to be carefully checked for printer's errors. Corrections must be restricted to instances in which the proof is at variance with the manuscript. "Extra corrections" will be inserted at the author's expense.

**Reprints.** Fifty reprints of Full-length papers, Notes and Letters to the Editor will be supplied free of charge. Additional reprints can be ordered by the authors. An order form containing price quotations will be sent to the authors together with the proofs of their article.

**Advertisements.** Advertisement rates are available from the publisher on request. The Editors of the journal accept no responsibility for the contents of the advertisements.

# HIGH SPEED COUNTERCURRENT CHROMATOGRAPHY WITH ITO MULTI-LAYER COIL SEPARATOR-EXTRACTOR

Exploits Centrifugal Forces \* Uses No Solid Supports

NO EXPENSIVE COLUMNS  
INFINITE VARIETY SOLVENTS  
NO HIGH PRESSURES  
USES REGULAR SOLVENTS  
SIMPLE SYSTEM  
NO SPECIAL APPARATUS  
REQUIRED



The P.C. Inc. High Speed CCC Is Presently Being Used For:

DNP Amino Acids	Pesticides and Herbicides
Indole Plant Hormones & Abscissic Acid	Alkaloids
Xanthones	Plant Extracts
Purines and Pyrimidines	Marine Pharmaceuticals
Tannins	Glycosides
Organic Dyes	Fermentation Products
Antibiotics and Anti-tumor Agents	Metabolites
Toxins: Plant/Animal	Cortical Steroids

## **P.C. INC.**

11805 KIM PLACE  
POTOMAC, MD 20854  
(301) 299-9386

014

*Please  
mention  
this  
journal  
when  
answering  
advertisements*



## FOR ADVERTISING INFORMATION PLEASE CONTACT OUR ADVERTISING REPRESENTATIVES

USA/CANADA

### **Michael Baer**

50 East 42nd Street, Suite 504

NEW YORK, NY 10017

Tel: (212) 682-2200

Telex: 226000 ur m.baer/synergistic

GREAT BRITAIN

### **T.G. Scott & Son Ltd.**

Mr M. White or Ms A. Malcolm

30-32 Southampton Street

LONDON WC2E 7HR

Tel: (01) 240 2032

Telex: 299181 adsale/g

Fax: (01) 379 7155

JAPAN

### **ESP - Tokyo Branch**

Mr H. Ogura

28-1 Yushima, 3-chome, Bunkyo-Ku

TOKYO 113

Tel: (03) 836 0810

Telex: 02657617

REST OF WORLD

### **ELSEVIER**

### **SCIENCE**

### **PUBLISHERS**

Ms W. van Cattenburch

P.O. Box 211

1000 AE AMSTERDAM

The Netherlands

Tel: (20) 5803.714/715/721

Telex: 18582 espa/nl

Fax: (20) 5803.769